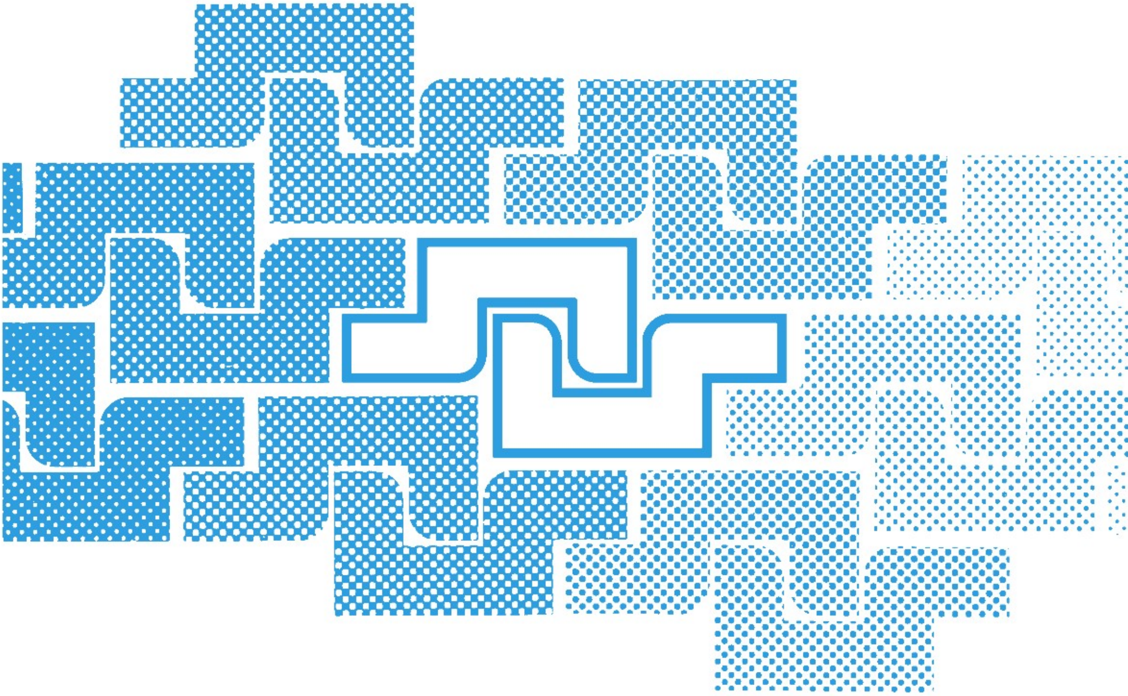

Metathesis Chemistry

From Nanostructure Design to Synthesis of Advanced Materials

Edited by

Yavuz İmamoğlu
and Valerian Dragutan

NATO Science Series

II. Mathematics, Physics and Chemistry – Vol. 243

Metathesis Chemistry

NATO Science Series

A Series presenting the results of scientific meetings supported under the NATO Science Programme.

The Series is published by IOS Press, Amsterdam, and Kluwer Academic Publishers in conjunction with the NATO Scientific Affairs Division

Sub-Series

I. Life and Behavioural Sciences	IOS Press
II. Mathematics, Physics and Chemistry	Kluwer Academic Publishers
III. Computer and Systems Science	IOS Press
IV. Earth and Environmental Sciences	Kluwer Academic Publishers
V. Science and Technology Policy	IOS Press

The NATO Science Series continues the series of books published formerly as the NATO ASI Series.

The NATO Science Programme offers support for collaboration in civil science between scientists of countries of the Euro-Atlantic Partnership Council. The types of scientific meeting generally supported are “Advanced Study Institutes” and “Advanced Research Workshops”, although other types of meeting are supported from time to time. The NATO Science Series collects together the results of these meetings. The meetings are co-organized bij scientists from NATO countries and scientists from NATO’s Partner countries – countries of the CIS and Central and Eastern Europe.

Advanced Study Institutes are high-level tutorial courses offering in-depth study of latest advances in a field.
Advanced Research Workshops are expert meetings aimed at critical assessment of a field, and identification of directions for future action.

As a consequence of the restructuring of the NATO Science Programme in 1999, the NATO Science Series has been re-organised and there are currently Five Sub-series as noted above. Please consult the following web sites for information on previous volumes published in the Series, as well as details of earlier Sub-series.

http://www.nato.int/science
http://www.wkap.nl
http://www.iospress.nl
http://www.wtv-books.de/nato-pco.htm

Series II: Mathematics, Physics and Chemistry – Vol. 243

Metathesis Chemistry

From Nanostructure Design to Synthesis of Advanced Materials

edited by

Yavuz İmamoğlu
Hacettepe University,
Beytepe, Ankara, Turkey

and

Valerian Dragutan
Romanian Academy
Bucharest, Romania

Technical Editor:

Solmaz Karabulut
Hacettepe University,
Beytepe, Ankara, Turkey

Springer

Published in cooperation with NATO Public Diplomacy Division

Proceedings of the NATO Advanced Study Institute on New Frontiers in Metathesis Chemistry: From Nanostructure Design to Sustainable Technologies for Synthesis of Advanced Materials
Antalya, Turkey
4–16 September 2006

A C.I.P. Catalogue record for this book is available from the Library of Congress.

ISBN 978-1-4020-6090-8 (PB)
ISBN 978-1-4020-6089-2 (HB)
ISBN 978-1-4020-6091-5 (e-book)

Published by Springer,
P.O. Box 17, 3300 AA Dordrecht, The Netherlands.

www.springer.com

Printed on acid-free paper

TABLE OF CONTENTS

PART I. DESIGN OF NEW GENERATIONS OF METATHESIS CATALYSTS

PART II. INTRICATE ORGANIC SYNTHESIS VIA METATHESIS CHEMISTRY

PART III. TAILORED POLYMERS BY METATHESIS POLYMERIZATION

PART IV. ADVANCED MATERIALS VIA METATHESIS AND RELATED CHEMISTRY

PREFACE

Following the fruitful tradition of the previous NATO Advanced Study Institute (ASI) meetings held on metathesis chemistry in Akcay, Turkey (1989, 1995), Polanica-Zdroj, Poland (2000), and Antalya, Turkey (2002), the new event on this fascinating topic of chemistry (Nobel Prize, 2005), organized again in Antalya during 4–16 September 2006, was devoted again to a hot subject in this field, "New Frontiers in Metathesis Chemistry: From Nanostructure Design to Sustainable Technologies for Synthesis of Advanced Materials".

Olefin metathesis, one of the most efficient transition metal-mediated C–C bond-forming reactions, asserted itself during the last few years as a powerful synthetic strategy for obtaining fine chemicals, biologically active compounds, architecturally complex assemblies, novel functionalized materials, and polymers tailored for specific utilizations (e.g. sensors, semiconductors, microelectronic devices), etc. Metathesis reactions such as ring-closing metathesis (RCM), enyne metathesis, cross-metathesis (CM), acyclic diene metathesis (ADMET), and ring-opening metathesis polymerization (ROMP) have gone far beyond 20th-century boundaries resulting in broad diversification towards sustainable technologies and perspectives for industrial applications covering a wide range, from production of smart, nanostructured materials to the manufacture of new pharmaceuticals.

As should have been expected for this timely NATO ASI meeting, seminal contributions on catalyst-related topics highlighted the newest advances in ruthenium-based complexes of high activity, selectivity, and robustness, popular for their excellent tolerance towards a variety of functional groups. A whole range of alkylidene–Ru complexes, both neutral and ionic, recoverable and recyclable, inclusive of preparation and selected applications, have been extensively illustrated by Pierre Dixneuf (University of Rennes, France). Elaborating on the essential role played by N-heterocyclic carbene (NHC) ligands in most effective Ru metathesis catalysts, Steven P. Nolan (University of Tarragona, Spain) successfully reported on the concept of incorporating this valuable moiety into other late transition metal complexes.

Deeper insights into catalyst design have been provided by Deryn Fogg (University of Ottawa, Canada) and Natalya Bespalova (United Research & Development Centre, Russia). Fogg clearly demonstrated how Ru catalysts containing electron-deficient aryloxide ("pseudohalide") ligands confer high activity at low catalyst loadings, while also expanding the structural diversity of the ligand set and the capacity for steric and electronic tuning of activity and selectivity. She pointed out that by using the matrix-assisted laser desorption ionization mass spectrometry (MALDI-MS) analysis technique distinctions in the behaviour of the Grubbs vs. pseudohalide catalysts could be revealed providing further insights into the mechanism of RCM reaction. Bespalova dwelt on modification of well-defined Ru–carbene catalysts by changing the carbenoid moiety and the imidazole ligand which allows variation of catalytic properties; a comparison of the new types of the catalysts with ill-defined catalysts based on tungsten in CM was also presented.

Further, the concept of NHC utilization in catalysis has been extensively developed by Lionel Delaude (University of Liege, Belgium), Karol Grela (Polish Academy of Sciences, Poland), Francis Verpoort (University of Ghent, Belgium), and Didier Astruc (University of Bordeaux, France). Poster presentations brought additional information in support to the role of NHC ligands in Ru-based metathesis pre-catalysts or the striking activating role of HCl in Ru complexes with O,N-bidentate ligands. The newest trends evolved in the present research on heterogeneous catalysis have been critically and selectively discussed by Hyniek Balcar (Czech Academy of Sciences).

An original topic on combining simple arene activation with Ru-catalysed olefin metathesis for the assembly and funtionalization of nano-objects has been dealt with by Didier Astruc offering convenient access to the synthesis and chemistry of supra-molecular structures. CM of vinyl-substituted organosilicon derivatives with olefins in the presence of Grubbs catalysts presented by Cesar Pietraszuk (University of Pozanan, Poland) evidenced how Ru-mediated metathesis can be fruitfully used in synthesis of a novel class of silicon-containing advanced materials. New applications of Ru-mediated metathesis reactions in tandem metathesis or non-metathesis processses have been further fully documented by Deryn Fogg in an interesting presentation on tandem ROMP-hydrogenation catalysis in tissue engineering applications, whereas the contribution on the catalytic cycloisomerization of enynes involving various activation processes by Christian Bruneau (University of Rennes, France) extended the scope of Ru-based metathesis chemistry to a variety of initiating systems of fundamental relevance for catalytic processes.

Beautiful contributions coming from Ken Wagener's group (University of Florida, USA) showed definitely how ADMET induced by Grubbs Ru catalysts can rigorously control the polymer microstructure and ultimately the product properties. Using efficient Ru-based initiators, new pathways for manufacture of high-molecular weight polymers with well-defined architectures and particular properties have been revealed. On this line, Eugene Finkelshtein (Russian Academy of Sciences, Russia) evidenced the potential of producing specialty polymers by ROMP and other ring-opening processes. Addition polymerization of selected monomers induced by the late transition metal catalysts provided new materials having special properties as it was convincingly shown in this section. Furthermore, synthesis and characterization of poly(phenylacetylene) with Schiff base end groups, polymers endowed with electrical properties, is dealt with by Christo Jossifov (Bulgarian Academy of Sciences).

Furthermore, nanostructured materials and how they could be used in nanomachines and molecular clockworks and transfer of chirality in organometallic complexes have been attractively highlighted by Lajos Bencze (Panonia University of Veszprem, Hungary), in two complementary contributions. Going beyond metathesis, but in tight correlation with this type of reaction, comprehensive presentations fully illustrated the high potential of precisely controlled macromolecular structures obtained by atom transfer radical polymerization (ATRP) to be assembled in smart materials, sensors, and various molecular devices. Finally, the successful combination of ROMP with ATRP to produce new materials with valuable properties has also been discussed.

In addition to the scientific sessions, the social programme was organized in a friendly and warm style in order to facilitate more informal scientific discussions between lecturers and young researchers, and to strengthen contacts and exchange of ideas and information between research groups of different nationalities. Overall, this outstanding international event organized under the generous sponsorship of the NATO Public Diplomacy Division successfully surveyed the latest achievements in this fascinating area of synthetic chemistry and uncovered new ways of developments for industrial-scale applications.

Yavuz İmamoğlu   Valerian Dragutan

January 2007

CO-DIRECTORS:

PROF. İMAMOĞLU YAVUZ	Department of Chemistry, Hacettepe University Beytepe, Ankara 06800, Turkey imamoglu@hacettepe.edu.tr
PROF. VALERIAN DRAGUTAN	Institute of Organic Chemistry, Romanian Academy, Bucharest, Romanıa vdragutan@yahoo.com

ORGANISING COMMITTEE:

PROF. Y. İMAMOĞLU	Department of Chemistry, Hacettepe University Beytepe, Ankara 06800, Turkey
PROF. VALERIAN DRAGUTAN	Institute of Organic Chemistry, Romanian Academy, Bucharest, Romanıa
PROF. L. BENCZE	Department of Organic Chemistry, University of Veszprem, H-8200, POB 158 Veszprem, Hungary
PROF. K.B. WAGENER	Department of Chemistry, University of Florida, POB 117200, Gainsville, FL 32611-7200, USA
DR. E. KHOSRAVI	IRC in Polymer Science and Technology, University of Durham, South Road Durham DHI 3LE, UK

LIST OF PARTICIPANTS

AFANASIEV Vladimir	United Research & Development Centre 55/1 b.2, Leninsky pr., Moscow, 119333, Russia AfanasievVV@ydr.ru
ALBERT Demonceau	Center for Education and Research on Macromolecules, Institut de Chimie (B6a), Institute of Chemistry, University of Liège, Sart-Tilman par B-4000 Liège, Belgium
ALIHANOVA Aygun	Department of Chemical Sciences Azerbaijan National Academy of Sciences Istiglaliyyet Street, 10Baku AZ 1001 Azerbaijan Republic Azerbaijan aygun81@mail.ru
ALIYEVA Ayten	Department of Chemical Sciences Azerbaijan National Academy of Sciences Istiglaliyyet Street, 10Baku AZ 1001 Azerbaijan Republic Azerbaijan ayten1@mail.ru
ANNA Michrowska	Institute of Organic Chemistry, Polish Academy of Sciences, Kasprzaka 44/52, 01-224, Warsaw, Poland
ASTRUC Didier	Nanoscience and Catalysis Group LCOO, UMR CNRS No. 5802 University Bordeaux I, 33405 Talance Cedex, France d.astruc@lcoo.u-bordeaux1.fr
AYDOĞDU Cemil	Hacettepe University, Faculty of Science, Department of Chemistry, 06800 Beytepe, Ankara, Turkey aydogdu@hacettepe.edu.tr
BALCAR Hynek	J. Heyrovsky Institute of Physical Chemistry, Academy of Sciences of the Czech Republic, Dolejskova 3, 18223 Prague 8, Czeck Republic hynek.balcar@jh-inst.cas.cz
BART Allaert	Department of Inorganic and Physical Chemistry, Organometallics and Catalysis Division, Ghent University, Krijgslaan 281 (S-3), 9000 Ghent, Belgium
BENCZE Lajos	Müller Laboratory, Department of Organic Chemistry, University of Veszprem, Egyetem utca 10, H-8200, P.O. Box 158 8201 Veszprem, Hungary ben016@almos.vein.hu
BESPALOVA Natalia	Yukos Research and Development Centre Leninsky Pr. 55 Moscow, 119333, Russia bespalovanb@yukos-rd.ru
BLACQUIERE Johanna M.	Center for Catalysis Research and Innovation, Department of Chemistry, University of Ottawa, 10 Marie Curie KZN 6N5 Ottawa, ON, Canada

BOGDAN Marciniec	Faculty of Chemistry, Department of Organometallic Chemistry, Adam Mickiewicz University, Grunwaldzka 6 60-780 Poznań, Poland
BOZ Emine	The George and Josephine Butler Polymer Research Laboratory, Center of Macromolecular Science and Engineering, Department of Chemistry, University of Florida, P.O. Box 117200 32611 Gainesville, FL 32310, USA eboz@chem.ufl.edu
BRUNEAU Christian	CNRS-Université de Rennes1, Sciences Chimie de Rennes, BAT 10C, Catalyse et Organométalliques, Campus de Beaulieu, avenue du général Leclerc, 35042 Rennes Cedex, France christian.bruneau@univrennes1.fr
BYKOV Victor I.	Topchiev Institute of petrochemical synthesis, Russian Academy of Sciences, Leninskii prospect 29, Moscow 119991, Russia bykov@ips.ac.ru
CAMM Kenneth D.	Center for Catalysis Research and Innovation, Department of Chemistry, University of Ottawa, 10 Marie Curie KZN 6N5 Ottawa, ON, Canada
CASTARLENAS Ricardo	Institut de Chimie de Rennes BAT 10C, Campus de Beaulieu 35042 Rennes Cedex, France rcastar@unizar.es
CÉDRIC Fischmeister	Catalyse et Organométalliques UMR 6226 CNRS-Université de Rennes, Institut Sciences Chimiques de Rennes BAT 10C, Campus de Beaulieu 35042 Rennes, Cedex, France
ÇETİNKAYA Sevil	Kırıkkale University, Department of Chemistry, 71450 Kırıkkale, Turkey scetinkaya@kku.edu.tr
CHRIS Stevens	Research Group SynBioC, Dept. of Organic Chemistry, Faculty of Bioscience Engineering, Ghent University, Coupure Links 653, B-9000 Ghent, Belgium
CLAUDIA Zucchi	Department of Chemistry, University of Modena and Reggio Emilia, Via Campi 183, I-41100 Modena, Italy
CONRAD Jay C.	Center for Catalysis Research and Innovation, Department of Chemistry, University of Ottawa, 10 Marie Curie KZN 6N5 Ottawa, ON, Canada
CRISTIAN-ANDI Nicolae	National Institute of Research & Development for Chemistry and Petrochemistry (ICECHIM), 202 Spl. Independentei, Sect. 6, Bucharest, Romania
DAVIDE Turrini	Department of Chemistry, University of Modena and Reggio Emilia, Via Campi 183, I-41100 Modena, Italy

DELAUDE Lionel	Center for Education and Research on Macromolecules, Institut de Chimie (B6a), Institute of Chemistry, University of Liege, Sart-Tilman par B-4000 Liege, Belgium l.delaude@ulg.ac.be
DERELI Okan	Hacettepe University, Faculty of Science, Department of Chemistry, 06532 Beytepe, Ankara, Turkey okander@hacettepe.edu.tr
DIXNEUF Pierre H.	Catalyse et Organométalliques UMR 6226 CNRS-Université de Rennes, Institut Sciences Chimique de Rennes BAT 10C, Campus de Beaulieu 35042 Rennes Cedex, France pierre.dixneuf@univ-rennes1.fr
DRAGUTAN Ileana	Institute of Organic Chemistry of the Romanian Academy, 202B Spl. Independentei, 060023 Bucharest, P.O. Box 35-108, Romania idragutan@yahoo.com
DRAGUTAN Matei	University of Agricultural Sciences, 59 Bld. Marasti, Sect 1, Bucharest, Romania mdragutan@gmail.com
DRAGUTAN Valerian	Institute of Organic Chemistry of the Romanian Academy, 202B, Spl. Independentei, 060023 Bucharest, P.O. Box 35-108, Romania vdragutan@yahoo.com
DRONOV Vitalii A.	Topchiev Institute of petrochemical synthesis, Russian Academy of Sciences, Leninskii prospect 29, Moscow 119991, Russia drvitaly@yandex.ru
DROZDZAK Renata	Department of Inorganic and Physical Chemistry, Division of Organometallic Chemistry and Catalysis, Ghent University, Krijgslaan 281 (S-3), 9000 Ghent, Belgium renatamatusiak@yahoo.fr
DÜZ Bülent	Hacettepe University, Faculty of Science, Department of Chemistry, 06800 Beytepe, Ankara, Turkey bduz@hacettepe.edu.tr
DÜZ SEVİN Fatma	Hacettepe University, Faculty of Science, Department of Chemistry, 06532 Beytepe, Ankara, Turkey sevin@hacettepe.edu.tr
ECE Abdülilah	Hacettepe University, Faculty of Science, Department of Chemistry, 06532 Beytepe, Ankara, Turkey abece@hacettepe.edu.tr
EMIL Buzdugan	National Institute of Research & Development for Chemistry and Petrochemistry (ICECHIM), 202 Spl. Independentei, Sect. 6, Bucharest, Romania

FECZKO Tivadar	Hung. Acad. Sci.Technical Chemistry Research Institute (Mszaki Kémiai Kutató Intezet) 8200 Veszprém, Egyetem utca 8. I/635, Hungary feczko@mukki.richem.hu
FINKELSHTEIN Eugene SH.	A.V. Topchiev Institute of petrochemical synthesis, Russian Academy of Sciences, Leninskii prospect 29, Moscow 119991, Russia fin@ips.ac.ru
FOGG Deryn E.	Center for Catalysis Research and Innovation, Department of Chemistry, University of Ottawa, 10 Marie Curie KZN 6N5 Ottawa, ON, Canada dfogg@science.uottawa.ca
FRANC Požgan	Laboratory “Catalyse et Organométalliques”, Institut Sciences Chimiques de Rennes, UMR 6226: CNRS- University of Rennes, Campus de Beaulieu, Av. Général Leclerc, 35042 Rennes
GEORG Fráter	Givaudan Roure Research Ltd., Überlandstrasse 138, CH-8600 Dübendorf, Switzerland
GRELA Karol	Institute of Organic Chemistry, Polish Academy of Sciences, Kasprzaka 44/52, 01-224 Warsaw, Poland grela@icho.edu.pl
GRINGOLTS Maria L.	A.V. Topchiev Institute of petrochemical synthesis, Russian Academy of Sciences, 29, Leninskii prospect, 119991 Moscow, Russia gringol@ips.ac.ru
GYULA Pályi	Department of Chemistry, University of Modena and Reggio Emilia, Via Campi 183, I-41100 Modena, Italy
HERVE Clavier	Department of Chemistry, University of New Orleans, New Orleans, 2000 Lakeshore Dr. 70148, New Orleans, Louisiana, USA; Institute of Chemical Research of Catalonia (ICIQ), Av. Països Catalans 16, 43007, Tarragona, Spain
HELMUT Fischer	Fachbereich Chemie, Universität Konstanz, Fach M 727, 78457 Konstanz, Germany
İMAMOĞLU Yavuz	Hacettepe University, Faculty of Science, Department of Chemistry, 06800 Beytepe, Ankara, Turkey imamoglu@hacettepe.edu.tr
JIŘÍ Čejka	J. Heyrovský Institute of Physical Chemistry, Academy of Sciences of the Czech Republic, Dolejškova 3, 182 23 Prague 8, Czech Republic
JOSSIFOV Christo	Institute of Polymers, Bulgarian Academy of Sciences, Acad. G. Bonchev str. 103A, 1113 Sofia, Bulgaria jossifov@polymer.bas.bg
KACZMARSKA Zuzanna	Warsaw University, Faculty of Chemistry, Pasteura 1, 02-093, Warsaw, Poland sillen@o2.pl

KALINOVA Radostina	Institute of Polymers, Bulgarian Academy of Sciences, Acad. G. Bonchev str. 103A, 1113 Sofia, Bulgaria kalinova@polymer.bas.bg
KARABULUT Solmaz	Hacettepe University, Faculty of Science, Department of Chemistry, 06800 Beytepe, Ankara, Turkey solmazk@hacettepe.edu.tr
KATOK Kseniia	Institute of Surface Chemistry of National Academy of Sciences of Ukraine, 17 General Naumov Str. 03164 Kyiv, Ukraine smpl@ukr.net
KHARLAMOV Oleksiy	Institute for Problems of Materials Science, 3, Krgiganovskogo str., 03142 Kiev, Ukraine akharlamov@ukr.net
KHOSRAVI Ezat	Interdisciplinary Research Centre in Polymer Science and Technology Department of Chemistry University of Durham DH1 3LE Durham, UK Ezat.Khosravi@durham.ac.uk
MAKOVETSKII Kiryl L.	Topchiev Institute of Petrochemical Synthesis, Russian Academy of Sciences, Leninsky prospect 29, Moscow 119991, Russia
KOVATS Nora	Pannon University, Dept. of Nature Conversation and Technology Engineering 8201 Veszprém, Egyetem utca 10 Hungary kovats@almos.vein.hu
KÖSE Dursun Ali	Hacettepe University, Faculty of Science, Department of Chemistry, 06532 Beytepe, Ankara, Turkey dkose@hacettepe.edu.tr
KURDI Robert	DELTA Electronic, Szentendrei ut 39, Budapest Wartha Vince utca 1. N /330. H-8201 Veszprém, POB 158, Hungary kurdir@chello.hu
LEDOUX Nele	Department of Inorganic and Physical Chemistry, Organometallics and Catalysis Division, Ghent University, Krijgslaan 281 (S-3) 9000 Ghent, Belgium Nele.Ledoux@ugent.be
LUCIANO Caglioti	Department of Chemistry and Technology of Biologically Active Compounds, University “La Sapienza” Roma, P. zale Moro 5, I-00185 Roma, Italy
ŁUKASZ Gułajski	Institute of Organic Chemistry, Polish Academy of Sciences, Kasprzaka 44/52, 01-224, Warsaw, Poland
MAJCHRZAK Mariusz	Department of Chemistry University of Durham DH1 3LE Durham, UK m.p.majchrzak@durham.ac.uk
MAKOVETSKII Kiryil L.	A.V. Topchiev Institute of Petrochemical Synthesis, Russian Academy of Sciences, 29, Leninskii prospect, 119991 Moscow, Russia

MAMMADALIYEVA Farah	Department of Chemical Sciences Azerbaijan National Academy of Sciences Istiglaliyyet Street, 10Baku AZ 1001 Azerbaijan Republic Azerbaijan fereh_ximik@rambler.ru
MATYJASZEWSKI Krzysztof	Department of Chemistry Carnegie Mellon University 4400 Fifth Avenue PA 15213, USA matyjaszewski@cmu.edu
MICHAŁ Bieniek	Institute of Organic Chemistry, Polish Academy of Sciences, Kasprzaka 44/52, 01-224, Warsaw, Poland
MINASYAN Gayene	Engineering Academy of Armenia, Chemical Engineering Section, 41/8 Arshakunyats, Technopark, Yerevan, 375026, Armenia armeng03@mail.ru
MONSAERT Stijn	Department of Inorganic and Physical Chemistry, Organometallics and Catalysis Division, Ghent University, Krijgslaan 281 (S-3) 9000 Ghent, Belgium Stijn.monsaert@ugent.be
MUSA Osama	Reactive Chemistry Group Leader Corporate Research Group National Starch & Chemical Co. 10 Finderne Ave., Bridgewater, NJ 08807, USA. osama.musa@nstarch.com
NENOV Nikolay	Department of Chemistry University of Durham DH1 3LE Durham, UK nikolay.nenov@durham.ac.uk
NICOLAI Dieltiens	Research Group SynBioC, Dept. of Organic Chemistry, Faculty of Bioscience Engineering, Ghent University, Coupure Links 653, B-9000 Ghent, Belgium
NICHOLAS Beach J.	Center for Catalysis Research and Innovation, Department of Chemistry, University of Ottawa, 10 Marie Curie KZN 6N5 Ottawa, ON, Canada
NIZOVTSEV Alexey V.	United Research & Development Centre, 55/1 b.2, Leninsky pr., Moscow, 11933, Russia NizovtsevAV@yrd.ru
NOLAN Steven P.	Department of Chemistry, University of New Orleans, 2000 Lakeshore Dr. 70148 New Orleans, Louisiana, USA snolan@uno.edu
OSPANOVA Gulzhan	Kazakh national technical university, Metallurgical processes & technology of special materials Department 22, Satpayev str., Almaty 050013, Kazakhstan ogulzhan@yahoo.com

ÖZDEMİR Ismail	Inönü University Faculty of Science and Arts Department of Chemistry, 44280 Malatya – Turkey iozdemir@inonu.edu.tr
ÖZTÜRK Ömer Faruk	Hacettepe University, Faculty of Science, Department of Chemistry, 06532 Beytepe, Ankara, Turkey ofo@hacettepe.edu.tr
PASCAL Van Der Voort	Department of Inorganic and Physical Chemistry, Organometallics and Catalysis Division, Ghent University, Krijgslaan 281 (S-3), 9000 Ghent, Belgium
PIETRASZUK Cezar	Faculty of Chemistry, Department of Organometallic Chemistry, Adam Mickiewicz University, Grunwaldzka 6 60-780 Poznan, Poland pietrasz@amu.edu.pl
QUILIYEV Bilal	The Y H. Mamedaliyev Institute of Petrochemical Processes Azerbaijan National Academy of Sciences N. Rafiyev Str. 30, Baku, Azerbaijan bilal_vahid@yahoo.com
QULIYEV Abas	Department of Chemical Sciences Azerbaijan National Academy of Sciences Istiglaliyyet Street, 10Baku AZ 1001 Azerbaijan Republic Azerbaijan ipoma@science.az
ROGAN Yulia V.	A.V. Topchiev Institute of petrochemical synthesis, Russian Academy of Sciences, 29, Leninskii prospect, 119991 Moscow, Russia rogan@mail.ru
ROJAS Giovanni	The George and Josephine Butler Polymer Research Laboratory, Center of Macromolecular Science and Engineering, Department of Chemistry, University of Florida, Gainesville, FL 32611, USA grojas@chem.ufl.edu
ROLAND Boese	Institute of Inorganic Chemistry, University of Essen, Universitätsstrasse 5-7, D-45117 Essen, Germany
RUFINA Alamo G.	FAMU/FSU College of Engineering, Department of Chemical and Biomedical Engineering, Tallahassee, FL 32310, USA
SAUVAGE Xavier	Center for Education and Research on Macromolecules, Institut de Chimie (B6a), University of Liège, Laboratory of Macromolecular Chemistry and Organic Catalysis, Sart-Tilman par B-4000 Liège, Belgium xsauvage@ulg.ac.be
SEBASTIEN Monfette	Center for Catalysis Research and Innovation, Department of Chemistry, University of Ottawa, 10 Marie Curie KZN 6N5 Ottawa, ON, Canada

SHISHKOVA Natalya	Donetsk Physics & Technology Institute of Ukraine National Academy of Sciences 72, R. Luxemburg st., 83114, Donetsk, Ukraine shishkov@kinetic.ac.donetsk.ua
SPURCACIU Bogdan	National Institute of Research & Development for Chemistry and Petrochemistry (ICECHIM), 202 Spl. Independentei, Sect. 6, Bucharest, Romania bogdansssss@hotmail.com
STANEVA Maia	Institute of Polymers, Bulgarian Academy of Sciences1113 Sofia, Bulgaria mstaneva@gmail.com
SZADKOWSKA Anna	Institute of Organic Chemistry, Polish Academy of Sciences, Kasprzaka 44/52, 01-224, Warsaw University, Faculty of Chemistry, Pasteura 1, 02-093, Warsaw, Poland anszad@o2.pl
TAMARAA Butenk	Topchiev Institute of Petrochemical Synthesis, Russian Academy of Sciences, Leninsky prospect 29, Moscow 119991, Russia
TUDOSE Adriana	Romanian Academy, Institute of Organic Chemistry, 202B Spl. Independentei, P.O. Box 35-108, 060023 Bucharest, Romania atudose73@yahoo.com
TÜĞSÜZ Tuğba	Hacettepe University, Faculty of Science, Department of Chemistry, 06532 Beytepe, Ankara, Turkey tugba99@yahoo.com
UBLEKOV Filip	Institute of Polymers, Bulgarian Academy of Sciences 1113 Sofia, Bulgaria ublekovphilip@gmail.com
USHAKOV Nikolai V.	A.V. Topchiev Institute of Petrochemical Synthesis, Russian Academy of Sciences, 29, Leninskii prospect, 119991 Moscow, Russia
UZGÖREN Ayşe	Hacettepe University, Faculty of Science, Department of Chemistry, 06532 Beytepe, Ankara, Turkey uzgoren@hacettepeedu.tr
VALENTIN Tertykh	Institute of Surface Chemistry of National Academy of Sciences of Ukraine, 17 General Naumov Str., 03164 Kyiv-164, Ukraine
VERPOORT Francis	Department of Inorganic and Physical Chemistry, Division of Organometallic Chemistry and Catalysis, Ghent University, Krijgslaan 281 (S-3), 9000 Ghent, Belgium francis.verpoort@ugent.be
VICTOR Yanishpolskii	Institute of Surface Chemistry of National Academy of Sciences of Ukraine, 17 General Naumov Str., 03164 Kyiv-164, Ukraine

VICTOR Martinez	Nanosciences and Catalysis Group, LCOO, UMR CNRS N°5802, Université Bordeaux I, 33405 Talence Cedex, France
VOLODYMYR Sashuk	Institute of Organic Chemistry, Polish Academy of Sciences, Kasprzaka 44/52, 01-224, Warsaw, Poland
VOVARD Chloe	Institut de Chimie de Rennes BAT 10C, Campus de Beaulieu 35042 Rennes Cedex, France chole.vovard@univ-rennes1.fr
WAGENER Kenneth B.	The George and Josephine Butler Polymer Research Laboratory, Center of Macromolecular Science and Engineering, Department of Chemistry, University of Florida, Gainesville, FL 32611, USA
YAMPOLSKII Yuri P.	A.V. Topchiev Institute of Petrochemical Synthesis, Russian Academy of Sciences, 29, Leninskii prospect, 119991 Moscow, Russia
YILDIZ Berna	Hacettepe University, Faculty of Science, Department of Chemistry, 06532 Beytepe, Ankara, Turkey yıldızb@hacettepe.edu.tr
YU Zhanru	Department of Chemistry University of Durham DH1 3LE Durham, UK zhanru.yu@durham.ac.uk
YÜKSEL Dilek	Hacettepe University, Faculty of Science, Department of Chemistry, 06532 Beytepe, Ankara, Turkey dilekyksel@yahoo.com.tr

PART I. DESIGN OF NEW GENERATIONS OF METATHESIS CATALYSTS

NEW RUTHENIUM CATALYSTS FOR ALKENE METATHESIS

CÉDRIC FISCHMEISTER, PIERRE H. DIXNEUF

Catalyse et Organométalliques UMR 6226 CNRS-Université de Rennes, Institut Sciences Chimiques de Rennes BAT 10C, Campus de Beaulieu 35042 Rennes, Cedex, France. E-mail: cedric.fischmeister@univ-rennes1.fr; pierre.dixneuf@univ-rennes1.fr

Abstract: The main developments in ruthenium catalyst design for alkene metathesis covering the last 4 years is presented. These new catalysts are essentially based on modifications brought to Grubbs- or Hoveyda-type catalysts and the generation of catalysts by activation of propargyl derivatives leading to ruthenium–allenylidene, –indenylidene, and alkenylcarbene catalysts.

Keywords: alkene metathesis, ruthenium catalysts, allenylidene, indenylidene, catalyst modification

1. Introduction

Catalytic alkene metathesis is a powerfull synthetic method with useful applications in organic synthesis and polymer fabrication. The tremendous development of olefin metathesis has only been possible thanks to the development of well-defined catalysts with enhanced activities and stability. Almost 20 years after the elucidation of the catalytic mechanism by Y. Chauvin in 1971 [1], two families of well-defined olefin metathesis catalysts have been developed. The efficient Schrock type catalyst was described in 1990 based on molybdenum alkylidene [2] and on high oxidation state, and the ruthenium alkylidene family was developed by Grubbs in 1992 [3]. Due to the relative stability of ruthenium complexes and their functional group tolerance the latter have been extensively studied by Grubbs and others in the last 10 years resulting in the disclosure of a high number of new and efficient ruthenium catalysts. Here we will review the main strategies and achievements covering the last 4 years in the design of alkene metathesis ruthenium catalysts based on the Grubbs and Hoveyda complex architectures. The first [4,5], second [6,7,8], and third-generation [9] Grubbs- and Hoveyda-type catalysts will be used as the discussion starting point. The family of catalyst precursors based on ruthenium–allenylidene [10] and ruthenium–indenylidene [11] complexes that have been developed as early as 1998, mainly by Dixneuf and Fürstner's groups will be then presented.

Y. İmamoğlu and V. Dragutan (eds.), Metathesis Chemistry: From Nanostructure Design to Synthesis of Advanced Materials, 3-27.

2. Grubbs- and Hoveyda-type catalysts

In 1992, Grubbs reported the first efficient alkylidene ruthenium catalyst $RuCl_2(=CH–CH=CR_2)(PCy_3)_2$ revealing the requirement of an alkylidene moiety linked to a neutral 16-electron system containing the electron releasing and bulky PCy_3 ligand [3]. In 1995, the benchmark Grubbs complex **1** of similar structure but more readily prepared was reported [4]. This so-called Grubbs first-generation catalyst set the bases for the development of new complexes of similar architectures. The first important breakthrough was the use of *N*-heterocyclic carbene (NHC) ligands initially introduced in alkene metathesis by Hermann in 1998 for the synthesis of $RuCl_2(=CHPh)(NHC)_2$ [12]. This led, in 1999, to the second-generation Grubbs catalysts **2** discovered by Nolan and Grubbs [6] containing only one unsaturated NHC ligand and **3** one saturated NHC ligand [7], which were followed in 2001 by the fast, initiating catalyst **4** sometimes refered as a third-generation Grubbs catalysts [9]. In the meantime, Hoveyda developed, in 1998, a recyclable catalyst with enhanced stability **5** [5]. The originality of this complex is the use of a bidentate ligand for which a release and return or boomerang mechanism is postulated [13]. The introduction of a NHC ligand led, in 2000, to complex **6** often called Hoveyda–Grubbs catalyst, which was reported almost simultaneously by Hoveyda and Blechert [8] (Figure 1).

Since the discovery of the above-mentioned complexes several improvements have been obtained by a fine-tuning of the electronic and steric properties of the ligands. We will here present the recent modifications made to the Grubbs- and Hoveyda-type complexes.

3. Recent advances in catalyst design

3.1 The modified Grubbs-type catalysts

3.1.1 Variations at the phosphine ligands

The first-generation Grubbs complex **1** with two phosphine ligands have been very little developed with respect to the NHC-based ligands due to their moderate activity and short lifetimes [14]. On the other hand, the second-generation catalysts displaying higher activity and lifetime suffer from alkene isomerization activity. Researchers at Sasol reasoned that first-generation

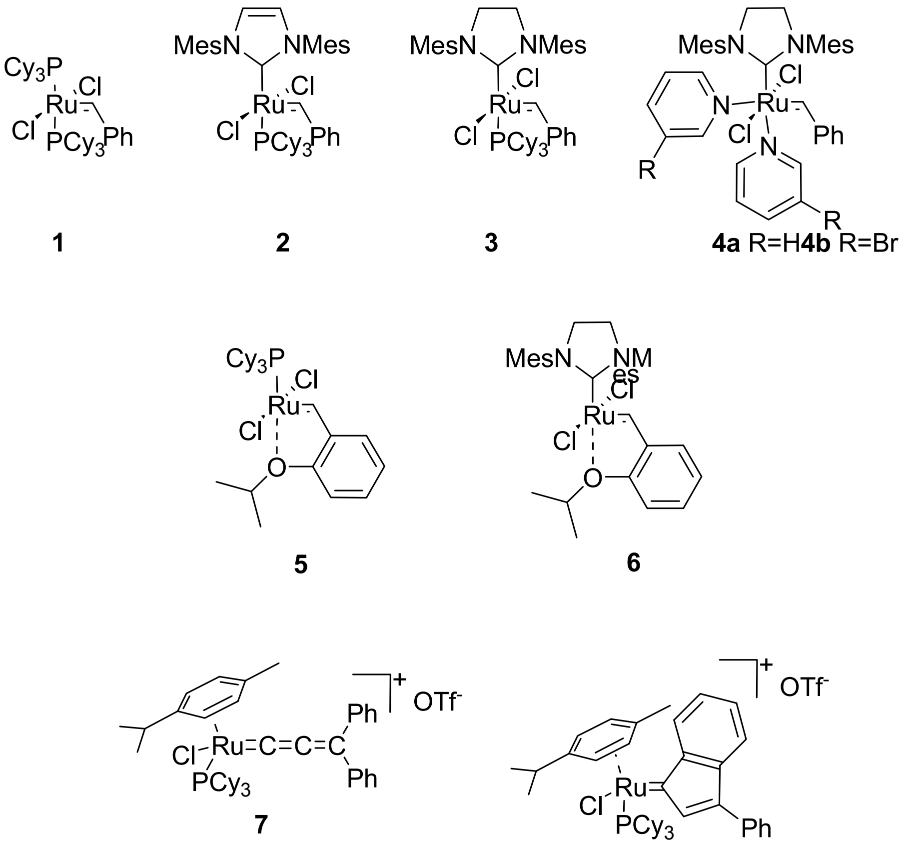

1 **2** **3** **4a** R=H**4b** R=Br

5 **6**

7 **8**

Figure 1. Ruthenium-based alkene metathesis catalysts.

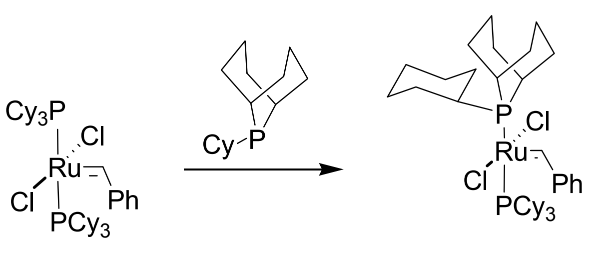

1 **9**

Scheme 1. (Sasol) Phoban-based catalyst.

catalyst with improved activity might be a good compromise between activity and selectivity. Complex **9** bearing the electron-rich Phoban ligand has been prepared and its stability and catalytic activity evaluated (Scheme 1) [15].

This complex was found to be thermally and chemically more stable than **1**. For instance, it is stable for 3 h in acetonitrile, whereas **1** decomposed after 3 min. The activity of **9** has been evaluated in transformations requiring no isomerization. The results show an increased activity of **9** with regard to **1** with an improved selectivity (less isomerization) (Table 1).

Table 1. Compared catalytic activity and selectivity of **1**, **3**, and **9**

Substrates	Process	Cat (%)	Conversion	Selectivity
1-decene[a]	Self-metathesis	**1** (0.01)	8	94
		3 (0.01)	52	63
		9 (0.01)	77	98
Methyl oleate, ethylene[b]	Ethenolysis	**1** (0.003)	14	91
		3 (0.003)	37	58
		9 (0.003)	43	98

[a] 60°C, neat 4 h; [b] 60°C, neat 4 h, 10 bar of ethylene.

A key step in the olefin metathesis mechanism using Grubbs-type catalysts is the formation of a 14-electron species by decoordination of an L ligand [16] (Scheme 2).

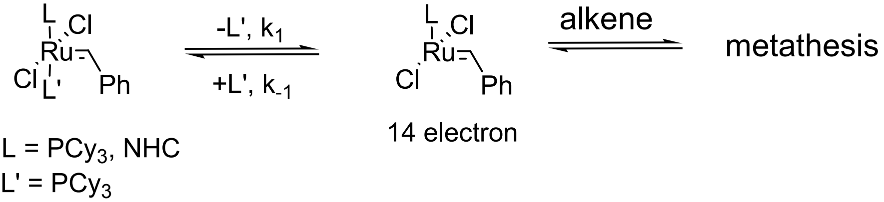

Scheme 2. Dissociative pathway leading to 14-electron catalytic species.

Several strategies involving phosphine scavenger have been used to favor the formation of the catalytically active 14-electron species [17]. Variation of the electronic and steric properties of the phosphine ligand has also been studied in details [18]. More recently Gladysz et al. reported the synthesis of the second-generation Grubbs catalyst **10** bearing a fluorinated phosphine [19] (Scheme 3).

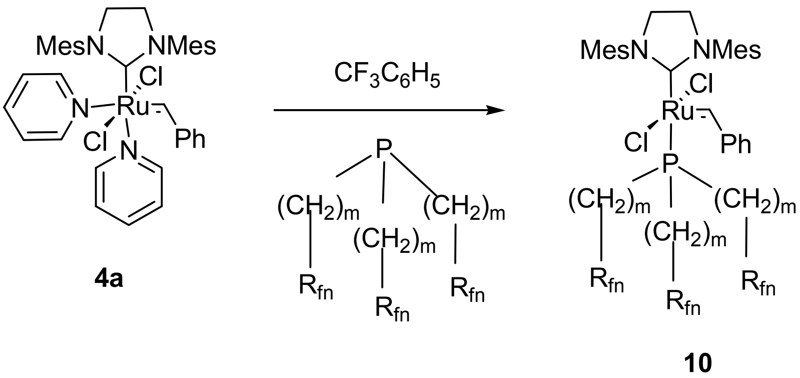

Scheme 3. Grubbs second-generation catalyst with a fluorinated phosphine ligand.

When operating under organic/fluorous liquid–liquid biphasic conditions the initiation rate of this catalyst was increased with respect to CH_2Cl_2 solvent. This is explained by the phase transfer of the fluorinated phosphine into the fluorous media hence favoring the coordination of the alkene to the 14-electron active species rather than phosphine recoordination.

3.1.2 Variations at the N-heterocyclic ligand

The second-generation catalysts have been extensively described and explored with five-membered heterocycles [20]. In 2004, Grubbs et al. reported the synthesis of the second-generation complex **11** bearing a more sterically demanding six-membered NHC [21] (Scheme 4). However this catalyst was found to operate moderately for classical ring-closing metathesis (RCM) or ring-opening metathesis polymerization (ROMP) reactions.

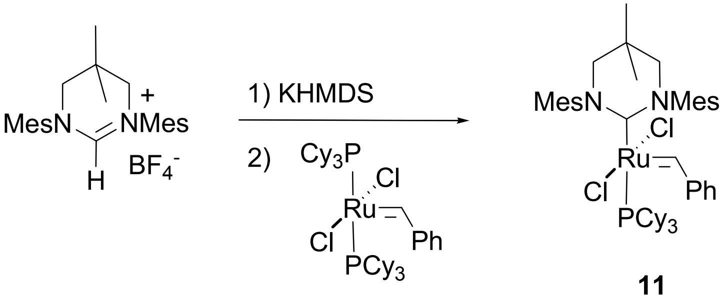

Scheme 4. Second-generation Grubbs catalyst with a six-membered NHC.

Complex **12** was prepared by Fürstner et al. where the hydroxy group served to anchor the complex onto a modified commercial silica to favor its recovery [22] (Scheme 5). The resulting immobilized complex displayed a reasonable activity and more importantly, the metal leaching was very low hence allowing the synthesis of products with very low ruthenium contents.

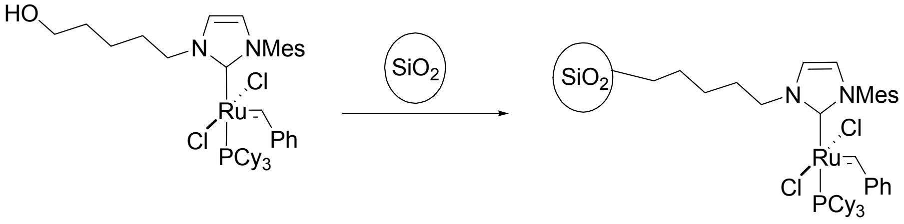

12

Scheme 5. Silica-supported catalyst.

Rate acceleration was observed with a ruthenium-based catalyst bearing a fluorinated NHC ligand [23]. Indeed, complex **13** (Figure 2) exhibits a higher activity than **3** and **6** for classical RCM reactions. This rate enhancement is believed to be due to a Ru–F interaction, which reduces the activation energy of the phosphine dissociation rate limiting step.

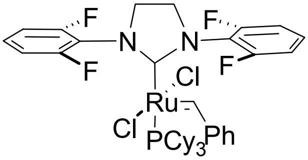

13

Figure 2. Fluorine-containing complex with enhanced activity.

3.1.3 Variations at the alkylidene ligand

The generation of the catalytically active 14-electron species is an important factor for the improvement of catalyst activity. A true 14-electron complex with no free L ligand has been reported by Piers et al. [24]. This phosphonium–alkylidene complex **14** was obtained by protonation of ruthenium carbide intermediates and isolated in 87–95% yield (Scheme 6).

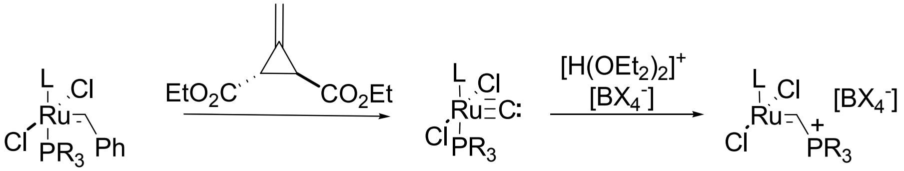

14

Scheme 6. Fast-initiating complex **14**.

The efficiency of these catalysts has been evaluated at 0°C for the RCM of diallyl diethylmalonate (Scheme 7) and compared to that of the second-generation Grubbs catalyst **3** and the fast-initiating catalyst **4b**. The results showed that catalyst **14** bearing the $ImesH_2$ ligand (L) featured an activity which outperforms the fast-initiating Grubbs catalyst **4b**. This catalyst was also found to be twice as fast as the Schrock's molybdenum catalyst for the same reaction.

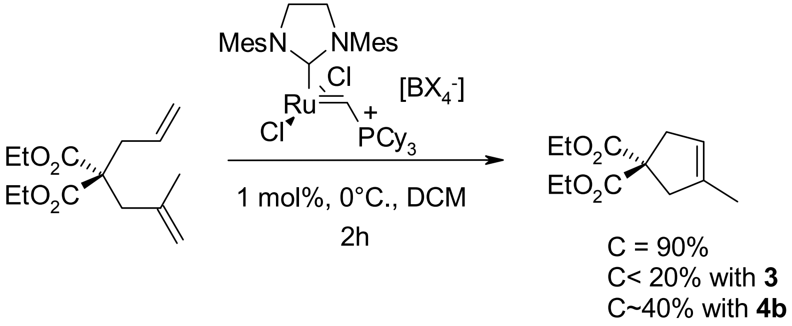

Scheme 7. RCM activity of the 14-electron complex **14**.

3.1.4 Variations at the anionic chloride ligand

Until very recently, modifications of Grubbs-type catalysts seeking for enhanced activity were uniquely performed on the L ligands (phosphines, NHC) and the alkylidene ligand. Due to the known deactivation pathways involving the chloride anion, Fogg et al. anticipated that halide-free ruthenium catalysts could be a solution to improve catalyst lifetimes. Attempts to replace chloride by alkoxide [25] or carboxylate [26] ligands were previously reported but they yielded complexes with moderate catalytic activity. Upon Upon treating complex **4a** with $TlOC_6F_5$, the pentacoordinate complex **15** was obtained in 92% yield (Scheme 8) [27].

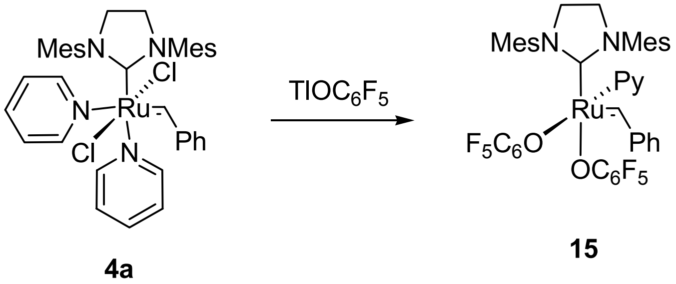

Scheme 8. Halide-free ruthenium catalyst.

Complex **15** exhibits increased catalytic activity with regard to that of the alkoxide one. It is noteworthy that this catalyst maintains a very good efficiency for the RCM of diethyl diallylmalonate even at very low catalyst/substrate ratio (Scheme 9).

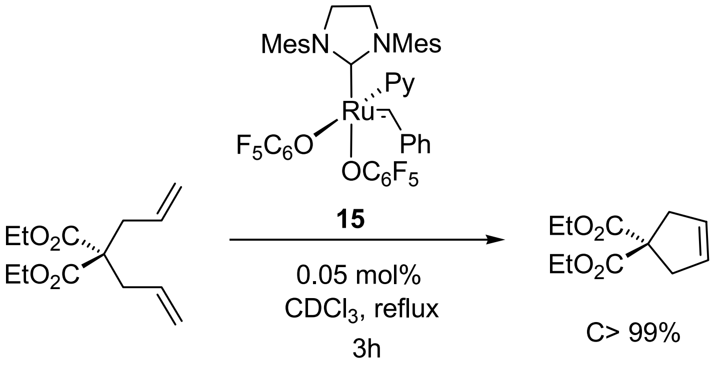

Scheme 9. Halide-free catalyst **15** for the RCM of diethyldiallylmalonate.

Complexes with chelate aryloxide have been prepared among which a cathecolate-derivative displayed high metathesis activity [28]. Two monohalide complexes have also been reported (Scheme 10) [29]. These monohalide complexes were obtained owing to the increased steric hindrance of the ArO-ligand.

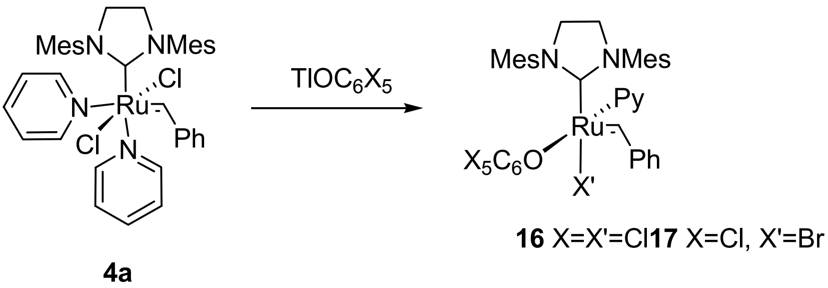

Scheme 10. Monohalide ruthenium–alkylidene complexes.

As a result, the pyridine ligand is more labile in complex **16** and **17** than in **15** resulting in higher metathesis activity. It must be noted that the presence of the aryloxide ligands increased the affinity of these complexes for silica thus allowing an efficient removal of ruthenium contaminants by a single column chromatography purification.

Nonhalide ligands were also used for the synthesis of polymer supported (PS–DVB) and nonsupported Grubbs- and Hoveyda-type complexes [30]. For instance, catalyst **18** bearing fluorinated carboxylate was prepared and exhibited a catalytic activity sometimes higher than that of the chlorinated **3** (Figure 3).

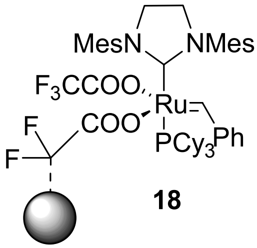

18

Figure 3. Supported halide-free Grubbs-type complex.

3.2 The modified Hoveyda-type catalysts

3.2.1 Variations at the ortho-alkoxybenzylidene ligand

Two strategies have been developed in order to increase the activity of the Hoveyda-type catalysts. Both strategies were aimed at destabilizing the ruthenium–oxygen bond of the styrenyl ether ligand.

In 2002, Blechert showed that increasing the steric bulk at the ortho position of the isopropoxy group in complex **6** resulted in an increase of the catalytic activity [31]. Thus, complex **19** was synthezised and its activity compared to that of **3** for a series of RCM test reactions (Scheme 11).

Whereas, at room temperature the RCM reaction was completed in 10 min with the catalyst **19**, 1 h was necessary under identical conditions to reach a similar yield with the Grubbs catalyst **3**. It is noteworthy that despite this increased activity, complex **19** retained a very good stability in air.

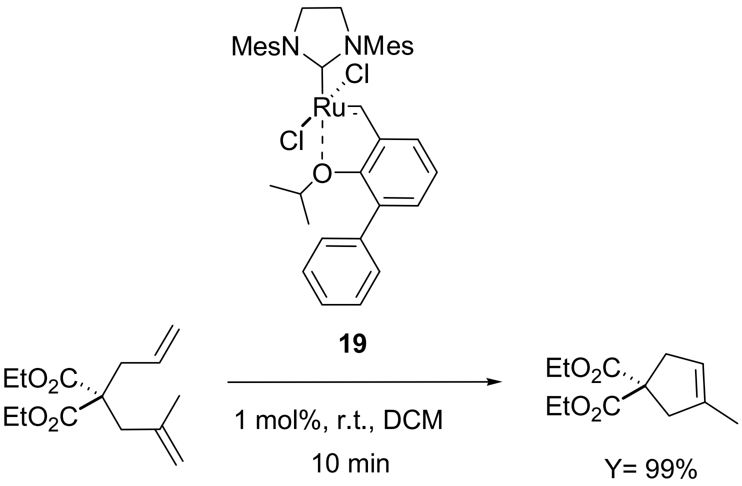

Scheme 11. Blechert catalyst.

The second strategy, implemented to increase the efficiency of Hoveyda-type catalyst, uses electronic effects to weaken the ruthenium–oxygen bond in **6**. Thus, Grela reported the synthesis of catalyst **20** bearing a nitro group in para position to the isopropoxy ligand [32] (Scheme 12).

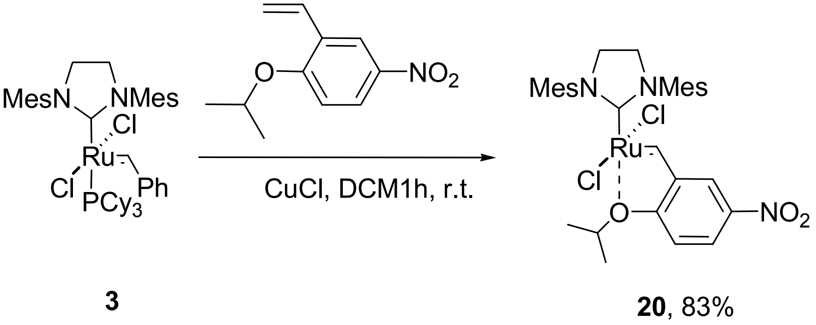

Scheme 12. Grela catalyst.

This complex was evaluated in a series of test reactions and compared to **3** and **6**. It showed in most cases a higher activity than the above-mentioned complexes with excellent stability. Catalyst **20** was found to be particularly efficient for cross-metathesis (CM) reactions involving acrylonitrile (Scheme 13).

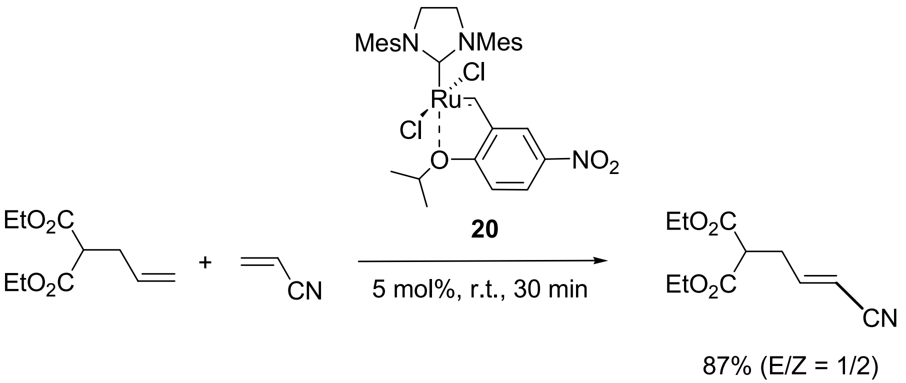

Scheme 13. Cross-metathesis activity of **20**.

Attempts to combine both the electronic and steric activations resulted in active but unstable catalysts [33]. Very recently an ammonium-activated Hoveyda-type catalyst was reported by Grela. This complex exhibited a very high efficiency associated to a very good affinity for silica, hence making catalyst removal very efficient [34].

3.2.2 Variations at the N-heterocyclic carbene ligand

Complex **21** bearing a four-membered *N*-heterocyclic carbene was reported by Grubbs et al. [35] (Scheme 14). However, its catalytic activity was found to be quite lower than that of catalysts **3** and **6**.

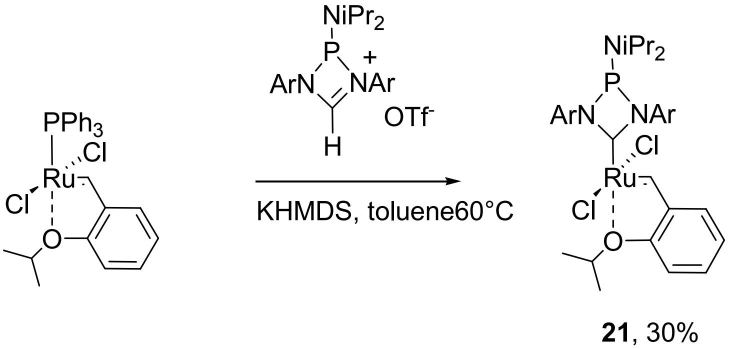

Scheme 14. Complex with a four-membered *N*-heterocyclic carbene.

Recently, complex **22** bearing a fluorinated NHC was prepared [23] (Figure 4). Contrary to the related Grubbs-type complex **13** (Figure 2), this catalyst showed a poorer activity.

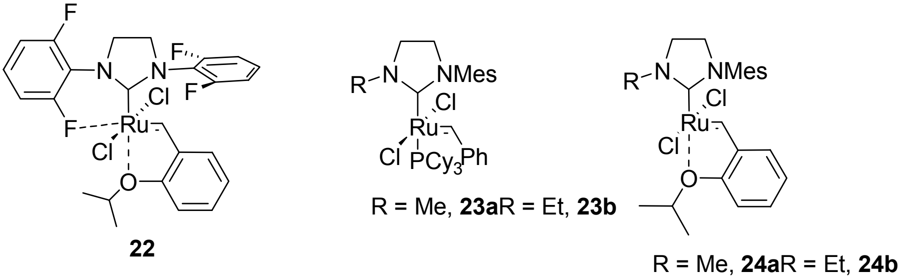

22

R = Me, **23a**R = Et, **23b**

R = Me, **24a**R = Et, **24b**

Figure 4. Catalysts bearing modified NHC ligands.

Complexes **23** and **24** bearing unsymmetrical NHC ligands have been prepared by replacing one of the mesityl substituent by a more electron-donating alkyl group [36] (Figure 4). The activity of these catalysts has been evaluated for the model RCM reaction of *N,N*-diallyl-*p*-tosylamide and found to be similar to that of **3** and **6**. Thus, the increased σ-donation of the carbene did not result in markedly enhanced catalytic activity. However, greater amounts of (Z) isomers were obtained with **23a** in comparison with **3** for a series of CM reactions. Improved diastereoselectivity was also obtained with these catalysts for a representative RCM reaction (Tables 2 and 3).

Table 2. Compared CM selectivity with catalysts **3**, **6**, **23a**, and **24a**

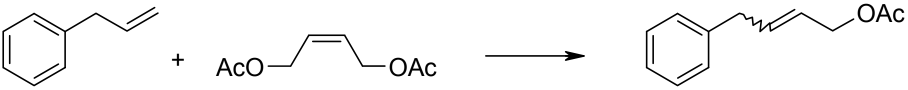

Catalyst	E:Z	Conversion %
3	6:1	79
6	6:1	72
23a	3:1	84
24a	6:1	78

Table 3. Compared diastereoselectivity with catalysts **3**, **6**, **23a**, and **24a**

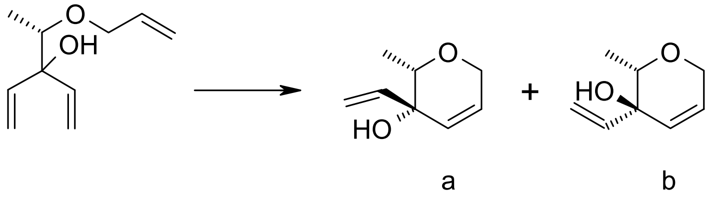

Catalyst	a:b	Conversion%
3	1.6:1	95
6	1.5:1	95
23a	1.7:1	92
24a	2.0:1	95

3.2.3 Variations at the alkylidene ligand

A series of ruthenium vinylcarbene catalysts have been prepared by Fürstner by insertion of alkynes into the ruthenium–alkylidene bond of various complexes [37]. Complexes **25**, **26**, and **27** were obtained in 72%, 59%, and 75% yields, respectively (Scheme 15).

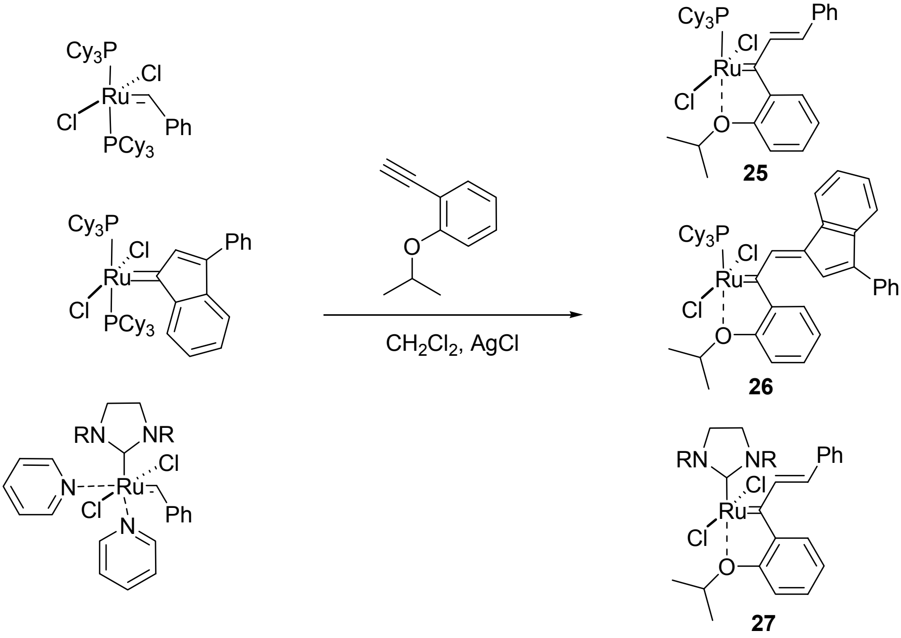

Scheme 15. Formation of vinyl carbene complexes by enyne metathesis.

Surprisingly, complex **28** was obtained when an internal alkyne bearing a silyl ether was used (Scheme 16). Due to the weak coordination of –OSiMe$_3$, this complex was found to be more active than complexes **25** and **26**. However, the catalytic activity of these four new complexes remained fairly lower than that of Grubbs or Hoveyda's catalysts.

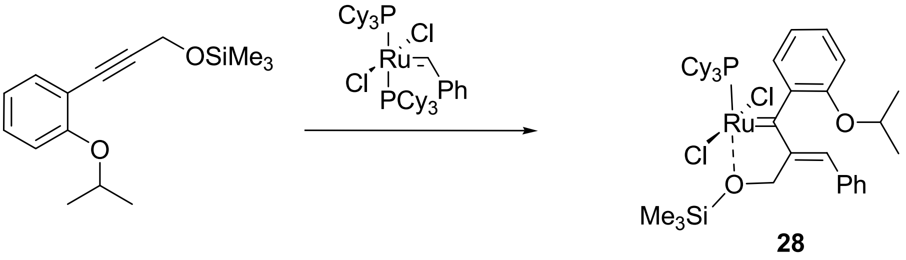

Scheme 16. Alkoxysilane ligand vs aryloxy ligand.

3.2.4 Variations at the anionic chloride ligand

Replacement of one or both chloride ligands in the phosphine-free Hoveyda complex by trifluoroacatate and trifluoromethanesulfonate groups provided complexes **29**, **30**, and **31** [38] (Scheme 17).

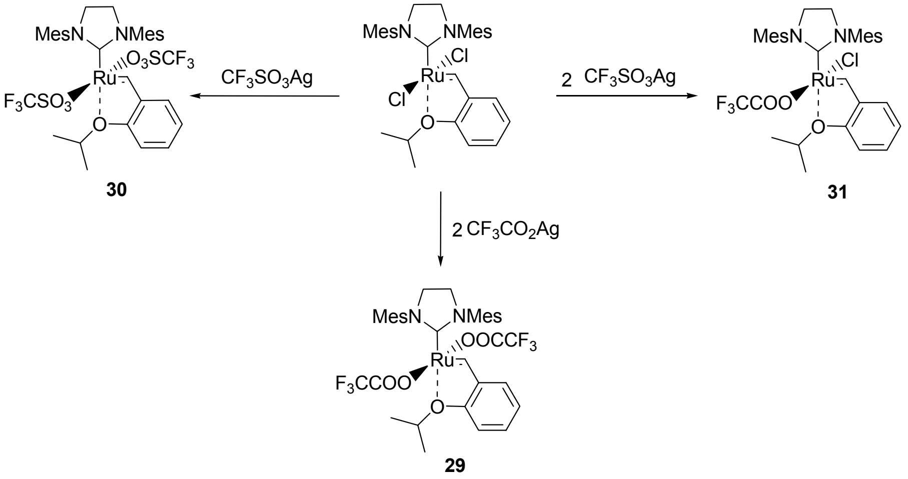

Scheme 17. Synthesis of catalysts **29**, **30**, and **31**.

These complexes have been evaluated in a series of test reactions showing that only catalyst **29** exhibited higher catalytic activity than the parent complexes **3** and **6** (Table 4).

Table 4. Compared RCM activity of catalysts **3**, **6**, and **29**

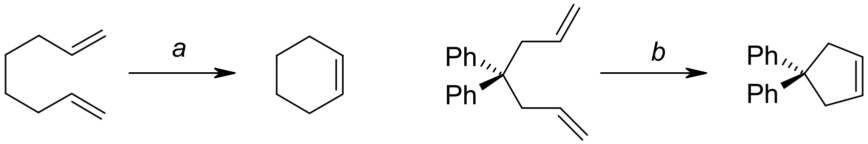

Reaction	Catalyst	Mol (%)	Tons (t)
A	**3**	0.08	1000
a	**6**	0.05	1700
a	**29**	0.05	1800
b	**3**	0.1	400
b	**6**	0.1	180
b	**29**	0.1	750

Experimental conditions: CH_2Cl_2, 2 h, 45°C.

Similar to catalyst **18**, the carboxylate ligand was used for the heterogenization of **29**. The resulting polymer supported catalyst was found to be significantly less active than its homogeneous analogue but on the other hand this supported catalyst was subject to very low ruthenium leaching.

3.3 Other ruthenium catalysts bearing bidentates ligands

Although they are not discussed in this review, a series of interesting ruthenium catalysts bearing chelating ancillary ligand have been reported in the last few years by Grubbs, Grela, and Verpoort. They involve various chelating atoms, C,N [39], C,O [40], or N,O [41] in their ligands.

4. Allenylidene–, indenylidene–, and alkenyl carbene–ruthenium catalysts

4.1 Applications of allenylideneruthenium in synthesis

As early as 1998 it was revealed that allenylidene–ruthenium complexes could behave as alkene metathesis precursors (Scheme 18) [10]. They are easy to prepare from simple propargylic alcohols and constitute the first well-defined *ionic 18-electron* catalyst precursors with respect to the neutral 16-electron Grubbs or Hoveyda catalysts [42].

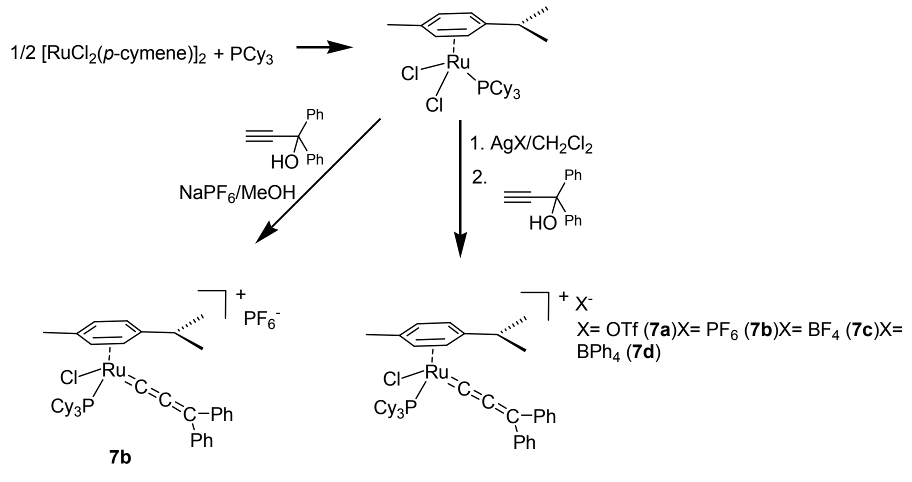

Scheme 18. Allenylidene–ruthenium synthesis.

They showed activity similar to that of the first-generation Grubbs catalyst for the production of macrocycles [10c], cyclic aminoacid derivatives (Scheme 19) [10d], and aminophosphonates analogues [10e]. It was shown that the nature of the counter-anion had a strong influence on the catalyst activity that increased with the sequence BF$_4^-$ << PF$_6^-$, BPh$_4^-$ << OTf$^-$[10c, 10g].

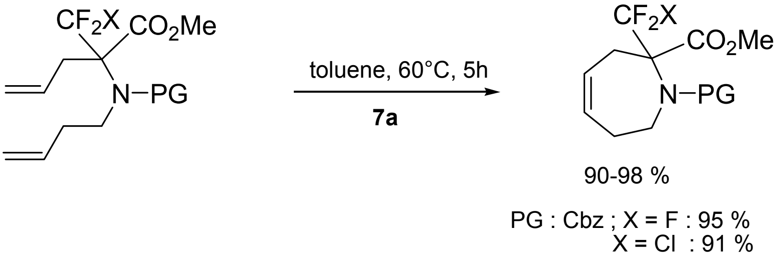

Scheme 19. Cyclic α-amino acid synthesis.

The allenylidene–ruthenium system also appeared as efficient catalyst precursors for enyne metathesis and they were applied to the preparation of fluorinated cyclic amino esters with a 1,3-diene structure allowing Diels–Alder reactions (Scheme 20) [43].

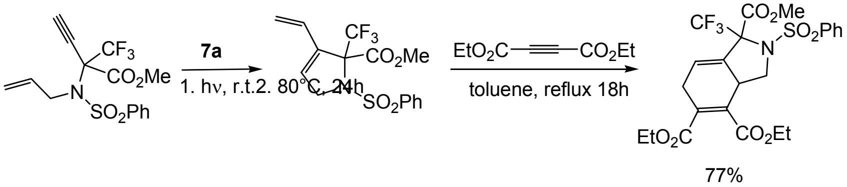

Scheme 20. Amino esters by consecutive enyne metathesis/Diels–Alder reaction.

4.2 Allenylidene–ruthenium and polymerization

The allenylidene complex **7a** was revealed to be a catalyst initiator for the polymerization of norbornene and that of cyclooctene, more resistant to ROMP, occurred at 80°C (Scheme 21).

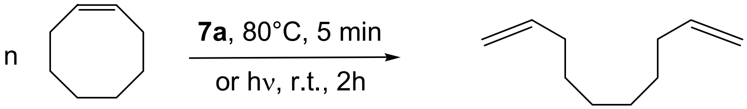

Scheme 21. ROMP of cyclooctene.

It was revealed that when the precursor **7a** was preliminarily heated in PhCl at 60°C for 25 min, the resulting system then led to polymerization of cyclooctene at room temperature [44]. This experiment suggested that precursor **7a** on thermal or UV activation led to a rearranged species acting as a polymerization initiator. The same conclusion on the existence of a catalytic species arising from complex **7a** was proposed from kinetic studies in RCM reaction [45].

The most surprising result was revealed on protonation of **7a** with five equivalents of triflic acid at room temperature in PhCl. The resulting catalytic system led to an increase of the cyclooctene polymerization TOF by three orders of magnitude. This experiment led to prove the transformation of the allenylidene complex into an indenylidene catalyst precursor.

4.3 Ionic allenylidene–ruthenium in catalysis into unusual media; ionic liquids and water

The well-defined, 18-electron, allenylidene–ruthenium complexes **7a** with ionic character offered the possibility to perform catalytic alkene metathesis in ionic liquids in which they are easily soluble.

Thus, the catalyst **7a**, highly soluble in imidazolium salt [bmim][X], performed the RCM reaction of *N,N*-diallyltosylamide at 80°C [46]. The same reaction was performed at room temperature for an 18 h period. After extraction with toluene of the metathesis product, the catalyst could be reused only once due to the slow decomposition of **7a** in this medium.

The same principle was applied to the ROMP of norbornene in C1 methylated imidazolium salt [bdmim][X] to avoid carbene formation and protonation of the catalyst [47]. Excellent polymer yield was observed for the first four catalyst recycling. This first example of ROMP in ionic liquid revealed that initiator **7a** appeared largely effective than the first and second-generation Grubbs catalysts **1** and **3** in such media.

A water-soluble allenylidene–ruthenium complex has been designed by Peruzzini's group $[\{RuCl(\mu\text{-}Cl)(=C=C=CPh_2)(TPPMS)_2]Na_4$ ($TPPMS=Ph_2P$ (m-$C_6H_4SO_3^-$))[48]. This complex promotes the ring-opening CM in water of cyclopentene and methylacrylate to give polyunsaturated esters.

4.4 Indenylidene–ruthenium complexes as catalytic precursors arising from allenylidene–ruthenium complexes

Previous studies on allenylidene–ruthenium complexes as alkene metathesis catalysts revealed that on thermal reaction they produced a new active species that was also evidenced by kinetic studies and spectroscopic observations [44]. This species was identified arising from another observation: the profitable influence of strong acid addition [11]. Thus the RCM of *N,N*-diallyltosylamide led to a TOF of 10.5/h with complex **7a** (80°C, 3 h, 70 %) and to a TOF of 53/h (room temperature, 1 h, 75 %) when five equivalent of TfOH or HBF_4 were added to complex **7a**. More drammatically, the ROMP of cyclooctene with **7a** was achieved at room temperature in 15 h (TOF = 63/h), whereas only 1 min was necessary when five equivalent of TfOH were added to **7a** (TOF=57.200/h) (Table 5). It was clear that strong acid addition promoted the generation of a new very active species.

NMR of **7a** with TfOH showed that at –40°C complex **7a** led to the formation of an alkenylcarbyne complex **32** by protonation of the allenylidene β-carbon (Scheme 22). This species was found to be catalytically inactive for a test RCM reaction. On rising the temperature to –20°C the species **32** releases its proton and afforded the indenylidene–ruthenium complex **33** that could be further isolated. The complex **33** resulted from an intramolecular rearrangement and was revealed as the active species (Scheme 22): the complex **33** was identified to the species formed from **7a** on thermal reaction.

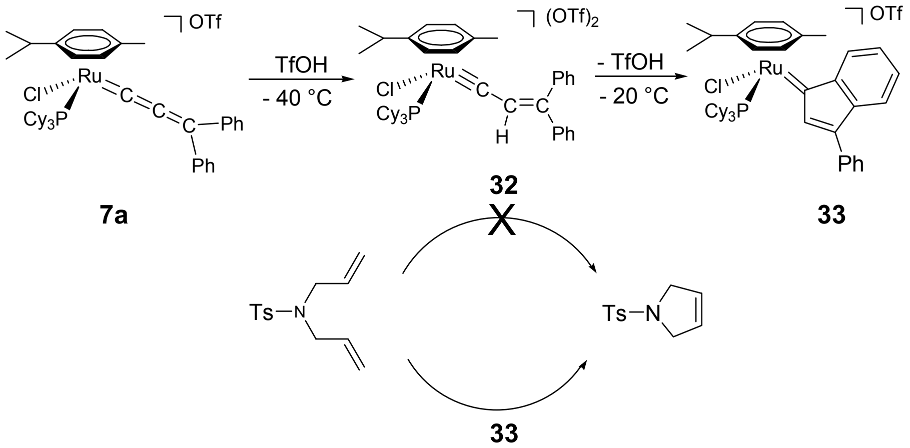

Scheme 22. Ruthenium–indenylidene formation.

On in situ generation of indenylidene species **33** high TOF for cyclooctene polymerization could be reached.

Table 5. Acid promoted cyclooctene polymerization at room temperature[a]

Entry	Cat	Ratio[b]	Acid[c]	Time	Yield	10–3 Mn	PDi	% *cis*	TOF (min^{-1})
1	**7a**	1,000	–	15 h	95%	143	1.9	27	1
2	**7a**	1,000	HBF_4 (5 eq)	1 min	92%	224	1.7	40	920
3	**7a**	1,000	HOTf (5 eq)	1 min	95%	238	1.6	38	953
4	**7a**	10,000	HOTf (5 eq)	5 min	97%	387	1.5	28	1933
5	**7a**	100,000	HOTf (100 eq)	5 min	88%	857	1.4	35	18267

[a] 4.5×10^{-3} mol of cyclooctene in 2.5 mL of PhCl. [b] [cyclooctene]/[Ru]. [c] Related to complex

The catalyst **33** was also very efficient for the ROMP of cyclopentene at –40°C and for RCM of dienes and enyne metathesis (Table 6).

Table 6. RCM and enyne metathesis reactions promoted by **33**[a]

Entry	Substrate	Product	Time	Yield
1	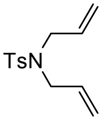	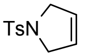	1 min	99
2	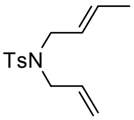	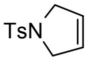	30 min	95
3	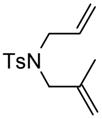	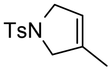	16 h	65
4	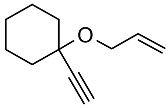	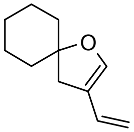	90 min	93
5	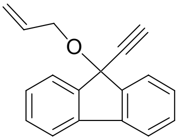	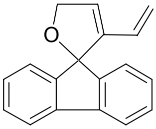	24 h	95
6	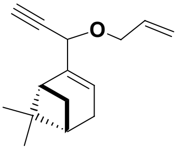	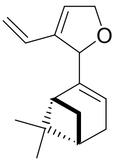	24 h	72
7	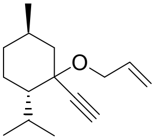	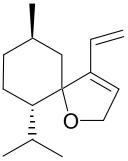	24 h	96
8	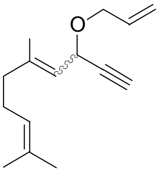	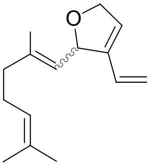	24 h	78

[a]2.5 mL of PhCl [monomer]/[Ru] = 50 at room temperature.

The transformation **7a** → **32**→ **33** offered the first direct evidence step by step of the rearrangement of an allenylidene into an indenylidene. This transformation was suggested by Nolan [49] and Fürstner [50] as on attempts to produce ruthenium–allenylidene complexes they obtained the related indenylidene system **34**, without observation of the allenylidene intermediate (Scheme 23).

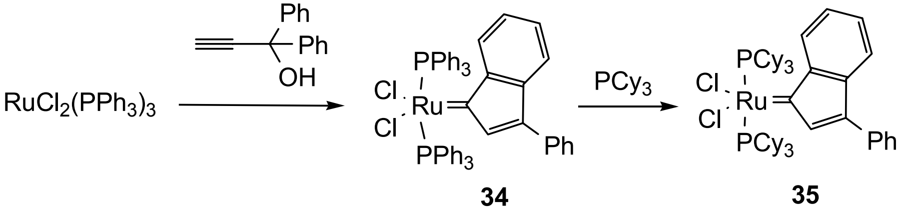

Scheme 23. Fürstner ruthenium–indenylidene.

Fürstner revealed that the PCy_3 indenylidene **35**, which is a patent-free and commercially available catalyst, is very efficient for RCM reactions [51].

Nolan prepared a second-generation type ruthenium–indenylidene complex bearing NHC ligand displaying an increased activity (Scheme 24) [49].

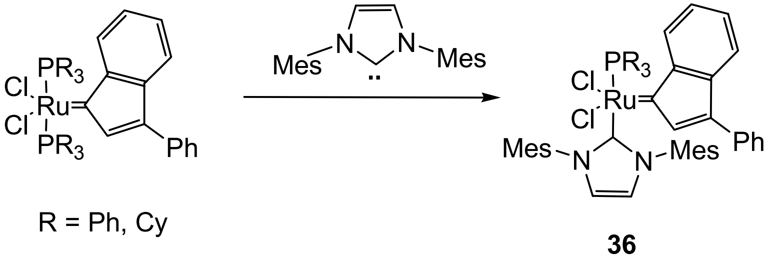

Scheme 24. Nolan ruthenium–indenylidene.

4.5 Generation of new alkene and enyne metathesis catalyst via a novel organometallic process leading to vinylcarbene

It was observed that the 16-electron complex **37** was actually an initiator to perform the enyne metathesis of propargyl allyl ether [52] although it does not possess an initiating carbene as in the Grubbs catalyst (Scheme 25).

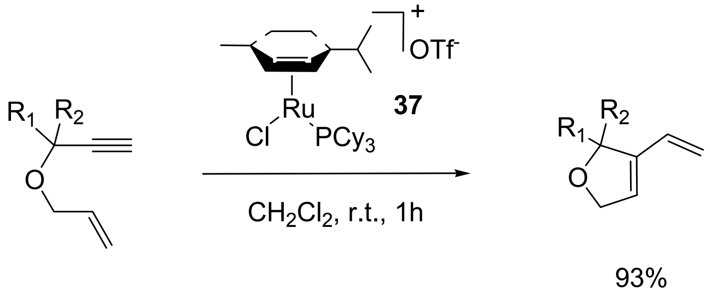

Scheme 25. Enyne metathesis initiated by the alkylidene-free complex **37**.

It was obvious that **37** and the enyne generated a enyne metathesis catalytic species. Stoichiometric reactions in the presence of $B(Ar^F)_4^-$ anion revealed by NMR the production of acrolein and the new alkenylcarbene **39**, assumed to be generated by retroene reaction from the intermediate **38** (Scheme 26).

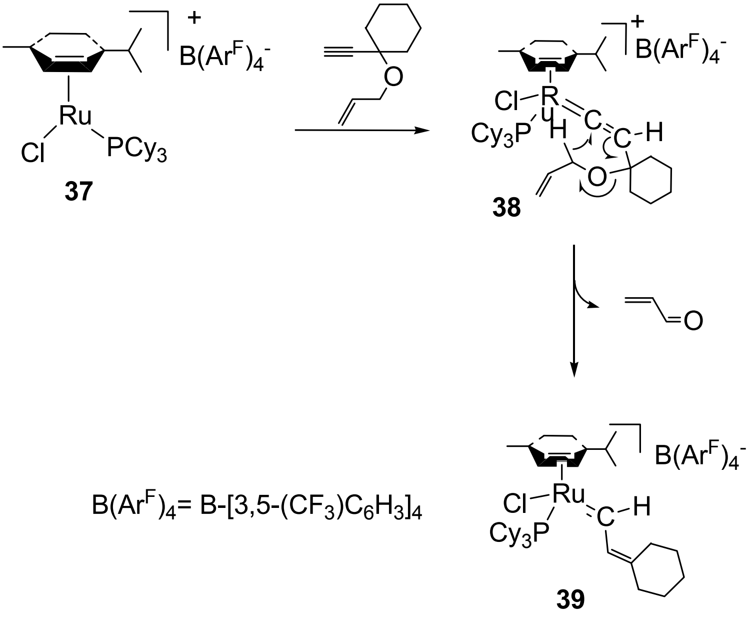

Scheme 26. Ruthenium–alkenylcarbene from propargylic enyne.

Analogously complex **37** reacted with propargyl propyl ether to generate propanal and triflate containing alkenylcarbene complex **40** that was isolable and revealed to be an excellent catalyst for both enyne metathesis and RCM of dienes (Table 7) (Scheme 27) [52].

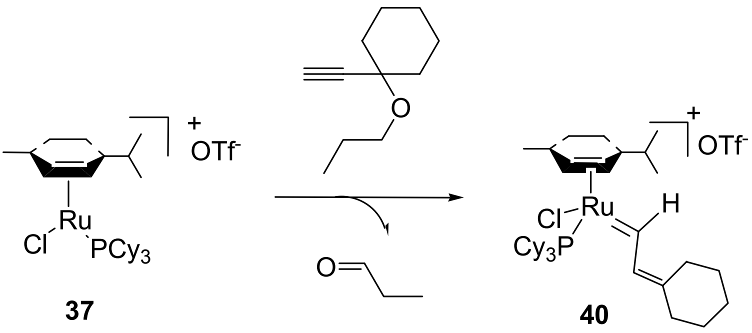

Scheme 27. Ruthenium–alkenylcarbene via activation of propyl propargyl ether.

Table 7. Diene and enyne metathesis at room temperature

Entry	**Substrate**	**Product**	**Time**	**Conv (%)**	**TOF[h^{-1}]**
1	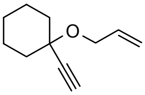	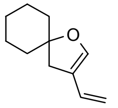	1 h	99	49
2	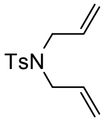	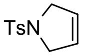	15 min	95	190
3	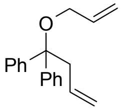	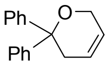	4 h	99	12
4	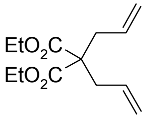	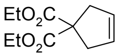	2 h	99	25
5	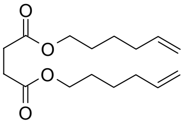	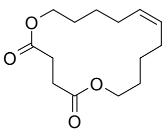	1 h	99	49

This new organometallic process should allow the synthesis of other catalysts via activation of alkyl propargylether by 16-electron metal complexes.

5. Conclusion

Over the last few years, several directions have been explored in order to improve the reactivity of the reference ruthenium–alkylidene catalysts that are the Grubbs and Hoveyda's catalysts **3** and **6**, respectively. Advances have been made in particular by Blechert and Grela who improved the reactivity of Hoveyda-type catalysts. Progress has also been made in the creation of the Piers catalyst and in the domain of nonhalide catalysts especially by Fogg, offering in some cases better activity than the reference catalysts. The Rennes group revealed several innovative processes and catalysts for alkene metathesis: the evidence that allenylidene are catalyst precursors, that they need to rearrange into indenylidene complexes to be active in catalysis as a carbene initiator, and the alkenylcarbene ruthenium systems, via intromolecular hydride transfer. Propargyl derivatives have become key molecules for the generation of catalysts: allenylidenes, indenylidenes, and alkenyl carbenes. Thanks to these recent developments in catalyst design, the chemist can draw from a broad catalyst range to answer a specific problem in terms of activity, selectivity, or functional group tolerance. This is of particular importance due to the emergence of asymmetric versions of olefin metathesis for which substrate dependent transformations will require a specific catalyst.

References

[1] Hérisson, J.L., Chauvin, Y. (1971) Makromol. Chem. 141:161.

[2] (a) Schrock, R.R., Murdzek, J.S., Bazan, G.C., Robbins, J., DiMare, M., O'Regan, M. (1990) J. Am. Chem. Soc. 112:3875; (b) Schrock, R.R. (2004) J. Mol. Catal A: Chem. 213:21.

[3] Nguyen, S.T., Johnson, L.K., Grubbs, R.H., Ziller, J.W. (1992) J. Am. Chem. Soc. 114:3974.

[4] Schwab, P., France, M.B., Ziller, J.W., Grubbs, R.H. (1995) Angew. Chem. Int. Edit. 34:2039.

[5] (a) Harrity, J.P.A., La, D.S., Cefalo, D.R., Visser, M.S., Hoveyda, A.H. (1998) J. Am. Chem. Soc. 120:2343; (b) Kingsbury, J.S., Harrity, J.P.A., Bonitatebus, P.J., Hoveyda, A.H. (1999) J. Am. Chem. Soc. 121:791.

[6] (a) Huang, J., Nolan, S.P., Petersen, J.L. (1999) J. Am. Chem. Soc. 121:2674; (b) Scholl, M., Trnka, T.M., Morgan, J.P., Grubbs, R.H. (1999) Tetrahedron Lett. 40:2247; (c) Weskamp, T., Kohl, F.J., Hieringer, W., Gleich, D., Herrmann, W.A. (1999) Angew. Chem. Int. Edit. 38:2416.

[7] Scholl, M., Ding, S., Lee, C.W., Grubbs, R.H. (1999) Org. Lett. 1:953.

[8] (a) Garber, S.B., Kingsbury, J.S., Gray, B.L., Hoveyda, A.H. (2000) J. Am. Chem. Soc. 122:8168; (b) Gessler, S., Randl, S., Blechert, S., (2000) Tetrahedron Lett. 41:9973.

[9] (a) Sanford, M.S., Love, J.A., Grubbs, R.H. (2001) Organometallics 20:5314; (b) Love, J.A., Morgan, J.P., Trnka, T.M., Grubbs, R.H. (2002) Angew.

Chem. Int. Edit. 41:4035–4037; (c) Trnka, T.M., Morgan, J.P., Sanford, M.S., Wilhelm, T.E., Scholl, M., Choi, T-L., Ding, S., Day, M.W., Grubbs, R.H. (2003) J. Am. Chem. Soc. 125:2546.

[10] (a) Fürstner, A., Picquet, M., Bruneau, C., Dixneuf, P.H. (1998) Chem. Commun. 1315; (b) Picquet, M., Bruneau, C., Dixneuf, P.H. (1998) Chem. Commun. 2249; (c) Fürstner, A., Liebl, M., Lehmann, C.W., Piquet, M., Kunz, R., Bruneau, C., Touchard, D., Dixneuf, P.H. (2000) Chem. Eur. J. 6:1847; (d) Osipov, S.N., Kobelikova, N.M., Schetnikov, G.T., Kolomiets, A.F., Bruneau, C., Dixneuf, P.H. (2001) Synlett 5:621; (e) Osipov, S.N., Artyushin, O.I., Kolomiets, A.F., Bruneau, C., Dixneuf, P.H. (2000) Synlett 7:1031; (f) Castarlenas, R., Fischmeister, C., Bruneau, C., Dixneuf, P.H. (2004) J. Mol. Catal A: Chem. 213:31; (g) Picquet, M., Touchard, D., Bruneau, C., Dixneuf, P.H. (1999) New J. Chem. 141.

[11] (a) Castarlenas, R., Dixneuf, P. (2003) Angew. Chem. Int. Edit. 42:4524; (b) Castarlenas, R., Vovard, C., Fischmeister, C., Dixneuf, P. (2006) J. Am. Chem. Soc. 128:4079.

[12] Weskamp, T., Schattenmann, W.C., Spiegler, M., Herrmann, W.A. (1998) Angew. Chem. Int. Edit. 37:2490.

[13] Kingsbury, J.S., Hoveyda, A.H. (2005) J. Am. Chem. Soc. 127:4510.

[14] Trnka, T., Grubbs, R.H. (2001) Acc. Chem. Res. 34:18.

[15] Forman, G.S., McConnell, A.E., Hanton, M.J., Slawin, A.M.Z., Tooze, R.P., Janse van Rensburg, W., Meyer, W.H., Dwyer, C., Kirk, M.M., Serfontein, D.W. (2004) Organometallics 23:4834.

[16] (a) Anderson, D.R., Hickstein, D.D., O'Leary, D.J., Grubbs, R.H. (2006) J. Am. Chem. Soc. 128:8386 and references therein; (b) Cavallo, L. (2002) J. Am. Chem. Soc. 124:8965.

[17] (a) Morgan, J.P., Grubbs, R.H. (2000) Org. Lett. 2:3153; (b) Lynn, D.M., Mohr, B., Grubbs, R.H., Henling, L.M., Day, M.W. (2000) J. Am. Chem. Soc. 122:6601; (c) Huang, J., Schanz, H.J., Stevens, E.D., Nolan, S.P. (1999) Organometallics 18:5375; (d) Rivard, M., Blechert, S. (2003) Eur. J. Org. Chem. 2225.

[18] Love, J.A., Sanford, M.S., Day, M.W., Grubbs, R.H. (2003) J. Am. Chem. Soc. 125:10103.

[19] Corrêa da Costa, R., Gladysz, J.A. (2006) Chem. Commun. 2619.

[20] Fürstner, A., Ackermann, L., Gabor, B., Goddard, R., Lehmann, C.W., Mynott, R., Stelzer, F., Thiel, O.R. (2001) Chem. Eur. J. 7:3236.

[21] Yun, J., Marinez, E.R., Grubbs, R.H. (2004) Organometallics 23:4172.

[22] Prühs, S., Lehmann, C.W., Fürstner, A. (2004) Organometallics 23:280.

[23] Ritter, T., Day, M.W., Grubbs, R.H. (2006) J. Am. Chem. Soc. 128:11768.

[24] Romero, P.E., Piers, W.E., McDonald, R. (2004) Angew. Chem. Int. Edit. 43:6161.

[25] Sanford, M.S., Henling, L.M., Day, M.W., Grubbs, R.H. (2000) Angew. Chem. Int. Edit. 39:3451.

[26] Buchowicz, W., Ingold, F., Mol, J.C., Lutz, M., Spek, A.L. (2001) Chem. Eur. J. 7:2842.

[27] Conrad, J.C., Amoroso, D., Czechura, P., Yap, G.P.A., Fogg, D.E. (2003) Organometallics 22:3634.

[28] Monfette, S., Fogg, D.E. (2006) Organometallics 25:1940.

[29] Conrad, J.C., Parnas, H.H., Snelgrove, J.L., Fogg, D.E. (2005) J. Am. Chem. Soc. 127:11882.

[30] Halbach, T.S., Mix, S., Fischer, D., Maechling, S., Krause, J.O., Sievers, C., Blechert, S., Nuyken, O., Buchmeiser, M.R. (2005) J. Org. Chem. 70:4687.

[31] Wakamatsu, H., Blechert, S. (2002) Angew. Chem. Int. Edit. 41:2403.

[32] Grela, K., Harutyunyan, S., Michrowska, A. (2002) Angew. Chem. Int. Edit. 41:4038.

[33] Michrowska, A., Bujok, R., Harutyunyan, S., Sashuk, V., Dolgonos, G., Grela, K. (2004) J. Am. Chem. Soc. 126:9318.

[34] Michrowska, A., Gulaski, L., Kaczmarska, Z., Mennecke, K., Kirschning, A., Grela, K. (2006) Green Chem. 8:685.

[35] Despagnet-Ayoub, E., Grubbs, R.H. (2005) Organometallics 24:338.

[36] Vehlow, K., Maechling, S., Blechert, S. (2006) Organometallics 25:25.

[37] Fürstner, A., Davies, P.W., Lehmann, C.W. (2005) Organometallics 24:4065.

[38] Krause, J.O., Nuyken, O., Wurst, K., Buchmeiser, MR. (2004) Chem. Eur. J. 10:777.

[39] (a) Ung, T., Hejl, A., Grubbs, R.H., Schrodi, Y. (2004) Organometallics 23:5399; (b) Barbasiewicz, M., Szadkowska, A., Bujok, R., Grela, K. (2006) Organometallics 25:3599; (c) Slugovc, C., Burtscher, C., Stelzer, F., Mereiter, K. (2005) Organometallics 24:2255.

[40] (a) Fürstner, A., Thiel, O.R., Lehmann, C.W. (2002) Organometallics 25:3599; (b) Slugovc, C., Perner, B., Stelzer, F., Mereiter, K. (2004) Organometallics 23:3622.

[41] (a) Opstal, T., Verpoort, F. (2003) Angew. Chem. Int. Edit. 42:2876; (b) Drozdak, R., Allaert, B., Ledoux, N., Dragutan, I., Dragutan, V., Verpoort, F. (2005) Adv. Synth. Catal. 347:1721.

[42] (a) Dragutan, V., Dragutan, I., Verpoort, F. (2005) Platinum Metals Rev. 49:33; (b) Dragutan, I., Dragutan, V., (2006) Platinum Metals Rev. 50:181; (c) Rigaut, S., Touchard, D., Dixneuf, P.H. (2004) Coord. Chem. Rev. 248:1585.

[43] Sémeril, D., Le Nôtre, J., Bruneau, C., Dixneuf, P.H., Kolomiets, A.F., Osipov, S.N. (2001) New J. Chem. 25:16.

[44] Castarlenas, R., Sémeril, D., Noels, A.F., Demonceau, A., Dixneuf, P.H. (2002) J. Organomet. Chem. 663:235.

[45] Basseti, M., Centola, F., Sémeril, D., Bruneau, C., Dixneuf, P.H. (2003) Organometallics 22:4459.

[46] Sémeril, D., Olivier-Bourbigou, H., Bruneau, C., Dixneuf, P.H. (2002) Chem. Commun. 146.

[47] Csihony, Sz., Fischmeister, C., Bruneau, C., Horváth, I.T., Dixneuf, P.H. (2002) New J. Chem. 26:1667.

[48] Saoud, M., Romerosa, A., Peruzzini, M. (2000) Organometallics 20:4005.

[49] Jafarpour, L., Schanz, H-J., Stevens, E.D., Nolan, S.P. (1999) Organometallics 18:5416.

[50] (a) Fürstner, A., Hill, A.F., Liebl, M., Wilton-Ely, J.D.E.T. (1999) Chem. Commun. 601; (b) Fürstner, A., Grabowski, J., Lehman, C.N. (1999) J. Org. Chem. 64:827 and references therein.

[51] Fürstner, A., Guth, O., Duffets, A., Seidel, G., Liebl, M., Gabor, B., Mynott, R. (2001) Chem. Eur. J. 7:4811.

[52] Castarlenas, R., Eckert, M., Dixneuf, PH. (2005) Angew. Chem. Int. Edit. 44:2576.

SYNTHESIS AND ACTIVITY IN RING-CLOSING METATHESIS OF PHOSPHINE AND NHC-CONTAINING RUTHENIUM–INDENYLIDENE (BIS)PYRIDINE COMPLEXES

HERVE CLAVIER[1,2], STEVEN P. NOLAN[1,2]

[1]*Department of Chemistry, University of New Orleans, New Orleans,*
2000 Lakeshore Dr. 70148, New Orleans, Louisiana, USA
[2]*Institute of Chemical Research of Catalonia (ICIQ), Av. Països Catalans 16,*
43007, Tarragona, Spain. E-mail: snolan@iciq.es, Fax: + 00 34 977 920 224

Abstract: The reactions of Cl_2–Ru–(3-phenylindenylidene) complexes with excess pyridine lead to new ruthenium (Ru)-based bis(pyridine) adducts in good yield. These thermally robust catalysts have been tested in ring-closing metathesis (RCM). In spite of promising initiation rates, only moderate to good activities have been observed in kinetic studies on several substrates.

Keywords: homogenous catalysis, metathesis, ruthenium, NHC, indenylidene

1. Introduction

Olefin metathesis is one of the most powerful and widely used reactions for forming carbon–carbon double bonds [1]. One of the major advances in this field was the discovery of well-defined homogeneous ruthenium (Ru)–benzylidene species, such as the Grubbs catalyst **1a** [2] and analogues containing *N*-heterocyclic carbenes (NHC) **1b** [3] and **1c** [4] (Figure 1). These complexes are compatible with harsh reaction conditions and extremely tolerant towards functional groups. However, lower turnover frequencies compared to catalytic systems used in hydrogenation and cross-coupling reactions [5] led to the development of novel Ru–benzylidene complexes. In 2002, Grubbs et al. reported the synthesis of substitution labile pyridine-containing complexes **2a** [6] and **2c** [7]. According to mechanistic studies on metathesis, the initiation step involves formation of the 14-electron intermediate Cl_2–Ru–(ligand)(alkylidene) [8], which is accelerated by the presence of labile ligands. Pre-catalyst **2c** showed good activity in ring-opening metathesis polymerization (ROMP), however, for both cross-metathesis (CM) and ring-closing metathesis (RCM) no significant improvement was observed when compared to previous catalysts. Activity and stability being intimately related, the active species is more easily generated when labile ligands are present, which unfortunately also translates into rapid degradation in view of slower propagation kinetics. The use of Ru–3-phenylindenylidene complexes

Y. İmamoğlu and V. Dragutan (eds.), Metathesis Chemistry: From Nanostructure Design to Synthesis of Advanced Materials, 29-37.

such as catalysts **3a** and **3b** [9,10] showing a higher thermal stability than their benzylidene counterparts appeared as an attractive alternative or at least worthy of investigation.

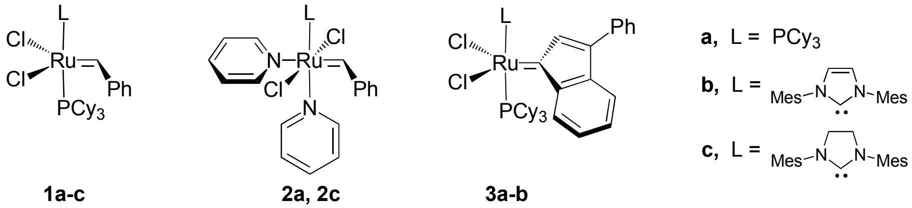

Figure 1. Well-defined ruthenium catalysts.

Herein, we report the syntheses of new metathesis catalysts: Cl_2–Ru–(py)$_2$(3-phenylindenylidene) **4a–c**. Kinetic studies enabling thorough evaluation of their stabilities and catalytic activities in RCM are also presented.

Treatment of complex **3a** with an excess of pyridine led to a rapid color change of the reaction mixture from red to black and subsequent addition of hexanes resulted in the formation of a precipitate. Further filtration at –40°C produced the bis(pyridine) adduct Cl_2–Ru–(PCy_3)(py)$_2$(3-phenylindenylidene) **4a** as an air- and moisture-sensitive brownish red solid (Scheme 1). The nuclear magnetic resonance (NMR) spectroscopic data as well as a x-ray analysis allowed to confirm the structure of the bis(pyridine) adduct **4a** [11].

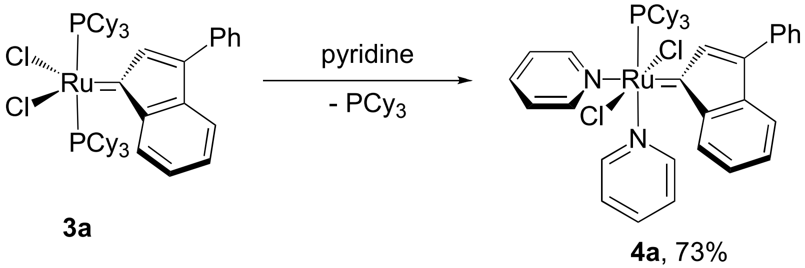

Scheme 1. Synthesis of ruthenium–bis(pyridine) adduct complex **4a**.

In order to evaluate the activity of **4a** in RCM, several kinetic studies were carried out varying the temperature and the catalyst loading. Using diethyldiallylmalonate **5** as model substrate, we performed reactions at room temperature and with low pre-catalyst loading (1 mol %) to slow the RCM reaction in order to obtain an accurate measurement of conversion (Figure 2). Under these conditions, pre-catalyst **4a** initiates RCM well, NMR conversion reached 29% after 10 min, and the color of the reaction mixture changed rapidly from red to orange. As mentioned before, the greater lability of the pyridine ligand when compared to phosphine accelerates the formation of the active species. However, the reaction rate decreased after 30 min, indicating a degradation of the 14-electron intermediate. It is noteworthy that a similar study carried out with pre-catalyst **2a** under the same conditions, showed a complete loss of activity after 15 min [6]. The authors of this study concluded that the propagating species are unstable under these reaction conditions. The RCM of **5** using complex **4a** progressed gradually reaching 44% conversion after 10 h, showing the robustness of the Ru–indenylidene architecture.

In order to obtain a total conversion, we then increased the pre-catalyst loading from 1 mol % to 5 mol %. This translated into a notable improvement of substrate conversion (35% after 10 min and 60% conversion after 10 h); nevertheless, it has to be noted that to double the conversion, we had to multiply the catalyst loading by a factor of 5. At this point, we believe that the increase of catalyst loading is associated with a higher concentration of pyridine in the reaction mixture leading to a more rapid decomposition of the catalytic species. We also studied the temperature effect and catalyst stability by performing the reaction at 40°C with 1 mol % of pre-catalyst **4a**. The reaction proceeded smoothly for the first 20 min (39% conversion); however, no further conversion was reached after 2 h. These results suggest that thermal activation should be avoided when using this pre-catalyst.

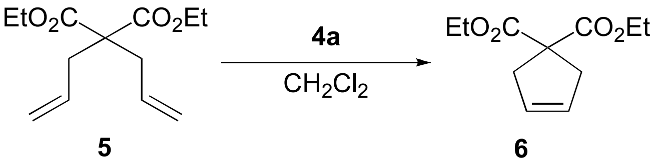

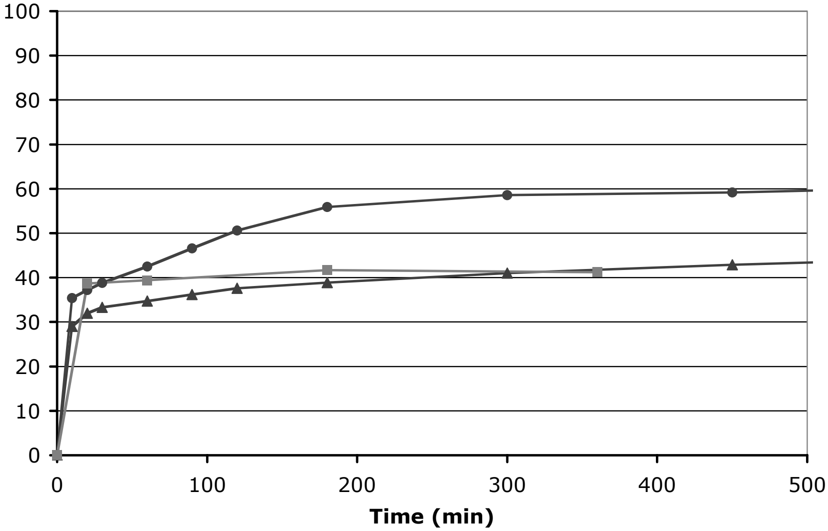

Figure 2. RCM of **5** with pre-catalyst **4a** (▲, 1 mol %, r.t.), (●, 5 mol %, r.t.) and (■, 1 mol %, 40°C).

To confirm these initial results, we carried out the same studies with a more hindered substrate **7** (Figure 3). Overall, the same trend as with **5** was observed. At 40°C, the catalytic activity is completely quenched after only 20 min (18% conversion), whereas at room temperature, the reaction progresses for 10 h (25% with 1 mol % and 29% using 5 mol % of **4a**). Again, degradation of the catalyst occurs more slowly at room temperature. Therefore, we suspect that the remainder of the unactivated initial loading of pre-catalyst acts as a reservoir of the active species.

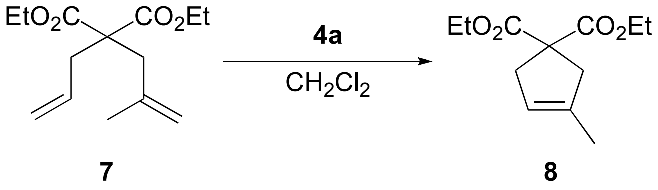

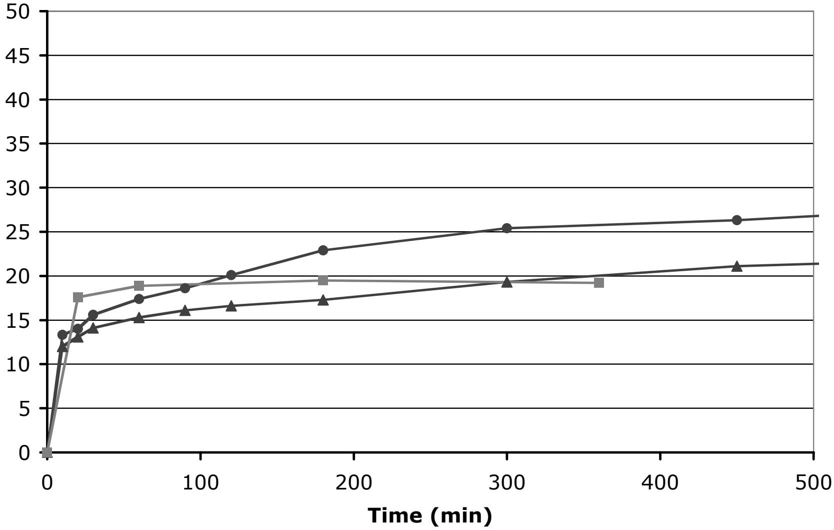

Figure 3. RCM of **6** with pre-catalyst **4a** (▲, 1 mol %, r.t.), (●, 5 mol %, r.t.), and (■, 1 mol %, 40°C).

NHC-containing complexes are known to possess an exceptional catalytic activity associated to a better stability than complexes containing phosphine units, allowing performance of many synthetic transformations under harsh conditions [12]. This improvement of the catalyst activity is mainly due to the presence of the electron-rich and sterically demanding NHC ligands. We have therefore synthesized with excellent yields new bis(pyridine) adduct complexes **4b** and **4c** containing 1,3-bis(2,4,6-trimethylphenyl)imidazol-2-ylidene (IMes) and 1,3-bis(2,4,6-trimethylphenyl)-4,5-dihydroimidazol-2-ylidene (SIMes), respectively (Scheme 2).

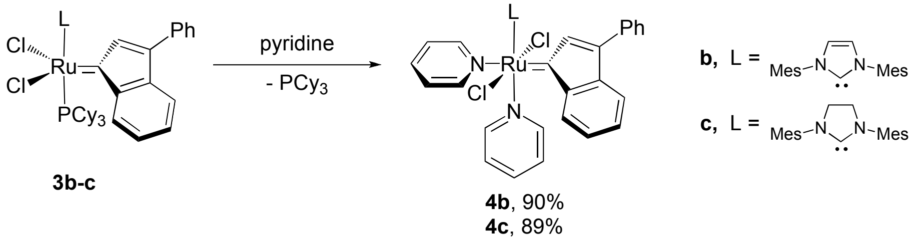

Scheme 2. Synthesis **4b** and **4c**.

As expected, the RCM of **5** carried out in presence of 1 mol % of **4b** and **4c** reached much higher conversions (respectively 72% and 90%) (Figure 4). A significant difference of activity between IMes- and SIMes-containing complexes was observed, suggesting that SIMes of **4c** allows for easier liberation of the active species. Similar conclusions have been reported recently by Jensen et al. based on quantitative structure–activity relationship model [13]. Good initiation rates were observed, but after 2 h, the reaction advancement slowed down and stopped before reaching full conversion, indicating the complete degradation of the active species. Its poor stability in pyridine-containing media cannot be totally prevented by introduction of robust ligands such as NHCs.

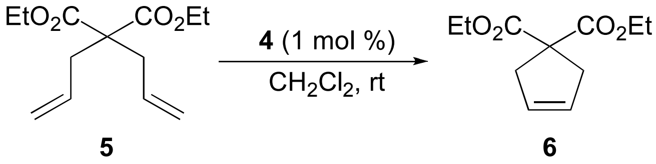

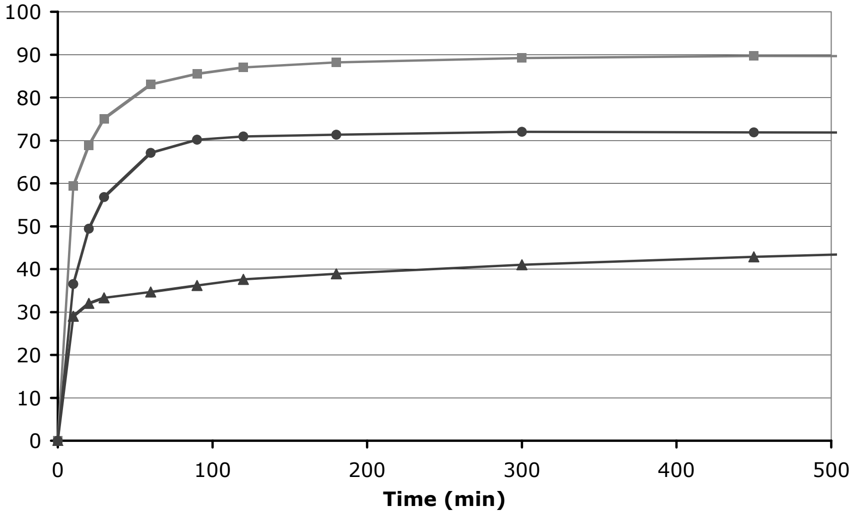

Figure 4. RCM of **5a** with pre-catalysts **4a–c** (▲, **4a**), (●, **4b**), and (■, **4c**).

To extend the scope of the pre-catalysts **4b** and **4c**, we then realized the kinetic studies on substrate **7** (Figure 5). NHC-containing complexes performed the RCM more efficiently than their phosphine analogues; nevertheless without reaching complete conversion (51% for **4b** and 66% for **4c**). This more hindered substrate highlights the problem of obtaining good activities with pyridine adducts as pre-catalysts.

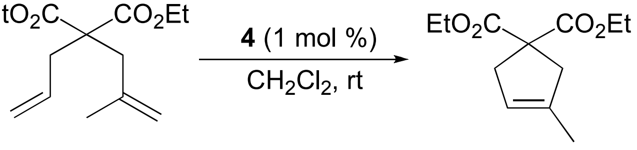

7 **8**

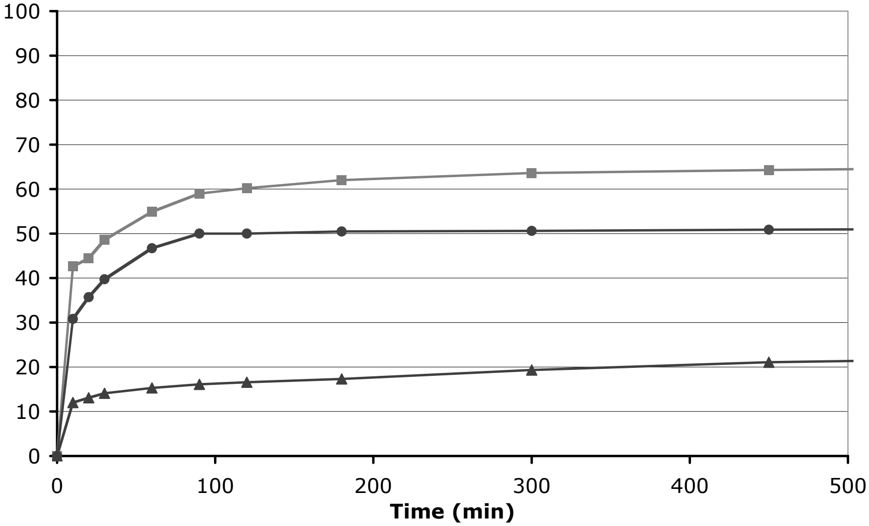

Figure 5. RCM of **7** with pre-catalysts **4a–c** (▲, **4a**), (●, **4b**), and (■, **4c**).

In conclusion, we have synthesized new bis(pyridine) Ru-based complexes **4a–c** possessing a Ru–indenylidene architecture instead of the widely used Ru–benzylidene pattern. Kinetic studies were carried out to evaluate the activity of these pre-catalysts in RCM. Despite a rapid initiation, the presence of pyridine in lieu of a better binding ligand seems to have a negative effect on the stability of the active species even when versatile NHC ligands were used and only moderate to good conversions were obtained. In view of these results and how they compare to the activity of other Ru–alkylidene fragment stability, the robustness of the Ru–indenylidene moiety appears promising. Further developments aimed at using of the Ru–indenylidene architecture are ongoing in our laboratories.

2. Experimental

General procedure for the preparation of Cl$_2$-Ru-(3-phenylindenylidene) bis(pyridine) adducts ***4a–c***: In a glove box, the starting material (500 mg) was dissolved in a minimum volume of pyridine (~1 mL). The mixture was stirred for 30 min at room temperature before adding 20 mL of hexanes. The mixture was again stirred for 30 min at room temperature before cooling at –40°C overnight. The resulting precipitate was filtered on a collection frit, washed with hexanes (3 × 10 mL), and dried under vacuum to yield the product.

Cl$_2$-Ru-(PCy$_3$)(py)$_2$(3-phenylindenylidene) ***4a***: Air-sensitive brownish red solid (310 mg, 73% yield). ^{1}H NMR (C_6D_6, 500 MHz) δ 9.32 (s, 3H), 8.64 (d, J = 7.3 Hz, 1H), 8.58 (s, 2H), 8.04 (d, J = 7.3 Hz, 1H), 7.80 (s, 1H), 7.31 (t, J = 7.3 Hz, 1H), 7.23 (d, J = 7.3 Hz, 1H), 7.02 (t, J = 7.3 Hz, 2H), 7.00 (t, J = 7.3 Hz, 1H), 6.76 (m, 3H), 6.50 (m, 1H), 6.16 (m, 2H), 3.57 (m, 3H), 2.33 (m, 3H), 2.17 (m, 6H), 2.02 (m, 6H), 1.72 (m, 6H), 1.57 (m, 3H), 1.22 (m, 6H). ^{13}C NMR (C_6D_6, 125 MHz) δ 309.3 (*C*=Ru), 159.7 (*C*), 154.5 (*C*H), 151.4 (2*C*H), 145.0 (*C*), 143.8 (*C*H), 142.5 (*C*), 138.4 (*C*), 136.5 (*C*H), 136.4 (*C*H), 130.8 (*C*H), 130.6 (*C*H), 130.1 (2*C*H), 128.9 (*C*H), 128.8 (*C*H), 128.7 (*C*H), 128.5 (*C*H), 126.7 (2*C*H), 124.0 (2*C*H), 123.3 (*C*H), 118.7 (*C*H), 37.7 (d, J_{CP} = 17.6 Hz, 3 *C*H), 30.3 (6*C*H$_2$), 29.0 (d, J_{CP} = 9.4 Hz, 6*C*H$_2$), 27.3 (3*C*H$_2$). ^{31}P NMR (C_6D_6, 121.4 MHz) δ 18.4 (s). Anal. Calculated for $C_{43}H_{53}Cl_2N_2PRu$: C, 64.49; H, 6.67; N, 3.50. Found: C, 64.22; H, 6.90; N, 3.80.

Cl$_2$-Ru-(IMes)(py)$_2$(3-phenylindenylidene) ***4b***: Air-sensitive blackish red solid (390 mg, 90% yield). ^{1}H NMR (C_6D_6, 300 MHz) δ 915 (dd, J = 7.2, 1.2 Hz, 1H), 8.63 (s, 5H), 8.38 (m, 2H), 7.89 (d, J = 8.2, Hz, 2H), 7.36 (m, 2H), 7.09 (m, 1H), 6.93 (m, 2H), 6.61 (m, 6H), 6.26 (m, 3H), 6.02 (m, 2H), 2.44 (s br, 9H) 1.90 (m, 9H). ^{13}C NMR (C_6D_6, 75 MHz) δ 301.9 (*C*=Ru), 180.8 (*C*), 152.6 (*C*H), 150.7 (4*C*), 145.1 (*C*H), 142.3 (*C*H), 140.9 (*C*H), 139.3 (*C*H), 138.4 (*C*H), 137.0 (*C*H), 136.4 (*C*H), 135.6 (2*C*), 130.1 (*C*H), 130.0 (2*C*), 129.8 (3*C*H) 129.7 (2*C*), 129.1 (2*C*H), 128.5 (2*C*), 128.1 (2*C*H), 127.2 (3*C*H), 125.3 (*C*), 123.9 (4*C*H), 123.5, (*C*H) 117.4 (*C*H), 21.6 (9*C*H$_3$).

Cl$_2$-Ru-(SIMes)(py)$_2$(3-phenylindenylidene) ***4c***: Air-sensitive blackish red solid (400 mg, 89% yield). ^{1}H NMR (C_6D_6, 300 MHz) δ 9.11 (dd, J = 6.9, 1.8 Hz, 1H), 8.54 (s, 2H), 8.04 (dd, J = 5.3, 1.8 Hz, 2H), 7.84 (d, J = 7.2, Hz, 2H), 7.31 (t, J = 7.2, Hz, 1H), 7.24 (s, 1H), 7.09 (m, 6H), 6.96 (s, 2H), 6.65 (m, 2H), 6.42 (s, 1H), 6.34 (m, 2H), 6.07 (m, 2H), 3.59 (m, 1H), 3.41 (m, 2H), 3.18 (m, 1H), 3.03 (s, 3H), 2.76 (s, 3H), 2.52 (s, 3H), 2.16 (s, 3H), 2.03 (s, 3H), 1.74 (s, 3H). ^{13}C NMR (C_6D_6, 75 MHz) δ 301.3 (*C*=Ru), 215.8 (*C*), 152.8 (*C*), 150.8 (*C*H), 144.3 (*C*), 142.1 (*C*H), 141.6 (*C*H), 141.2 (*C*H), 140.2 (*C*H), 139.9 (*C*H), 139.4 (*C*H), 138.2 (*C*H), 138.0 (*C*H), 137.8 (*C*H), 137.7 (*C*H), 137.2 (*C*H), 136.7 (*C*H), 135.6 (*C*H), 130.5 (*C*H), 130.1 (*C*H), 130.0 (2*C*), 129.8 (2*C*), 129.4 (*C*H), 129.2 (*C*H), 129.1 (*C*H), 128.9 (*C*H), 128.3 (2*C*), 127.5 (2*C*), 127.3 (2*C*), 123.9 (*C*H), 123.7 (*C*H), 117.4 (*C*H), 52.6 (CH_2), 51.0 (CH_2), 22.1 (CH_3), 21.8 (CH_3), 21.6 (CH_3), 21.5 (CH_3), 19.4 (CH_3), 19.2 (CH_3).

General procedure for kinetic studies: In a glove box, a vial was charged with the diene (1 mmol) and dichloromethane (10 mL), and then pre-catalyst **4a–c** (0.01 mmol) was added. Progress of the reaction was monitored by ^{1}H NMR by drawing aliquots from the reaction mixture and by integrating the characteristic signals for allylic proton resonance.

Acknowledgments

The National Science Foundation is gratefully acknowledged for financial support of this work. We also thank Pfizer and the Department of Chemistry of the University of Ottawa, and more specifically Professor Deryn Fogg, for hosting our group while the University of New Orleans was recovering from hurricane Katrina. Umicore AG is gratefully acknowledged for a generous gift of Cl_2–Ru–$(PCy_3)_2$(3-phenylindenylidene) and Boehringer Ingelheim Pharmaceuticals Inc. for an unrestricted grant.

References

[1] (a) Astruc, D. (2005) New J. Chem. 29:42–56; (b) Grubbs, R.H. (2003) Handbook of Metathesis, Wiley-VCH, Weinheim; (c) Schrock, R.R., Hoveyda, A.H. (2003) Angew. Chem. Int. Edit. 42:4592–4633; (d) Blechert, S., Connon, S.J. (2003) Angew. Chem. Int. Edit. 42:1900–1923; (e) Trnka, T.M., Grubbs, R.H. (2001) Acc. Chem. Res. 34:18–29.

[2] (a) Schwab, P., France, M.B., Ziller, J.W., Grubbs, R.H. (1995) Angew. Chem. Int. Edit. 34:2039–2041; (b) Sanford, M.S., Love, J.A., Grubbs, R.H. (1996) J. Am. Chem. Soc. 118:100–110.

[3] Huang, J., Stevens, E.D., Nolan, S.P., Petersen, J.L. (1999) J. Am. Chem. Soc. 121:2674–2678.

[4] Scholl, M., Trnka, T.M., Morgan, J.P., Grubbs, R.H. (1999) Tetrahedron Lett. 40:2247–2750.

[5] (a) Marion, N., Navarro, O., Mei, J., Stevens, E.D., Scott, N.M., Nolan, S.P. (2006) J. Am. Chem. Soc. 128:4101–4111; (b) Shen, Q., Shekhar, S., Stambuli, J.P., Hartwig, J.F. (2005) Angew. Chem. Int. Edit. 44:1371–1375.

[6] Trnka, T.M., Dias, E.L., Day, M.W., Grubbs, R.H. (2002) ARKIVOC xiii:28–41.

[7] (a) Sandford, M.S., Love, J.A., Grubbs, R.H. (2001) Organometallics 20:5314–5318; (b) Love, J.A., Morgan, J.P., Trnka, T.M., Grubbs, R.H. (2002) Angew. Chem. Int. Edit. 41:4035–4037.

[8] (a) Sanford, M.S., Ulman, M., Grubbs, R.H. (2001) J. Am. Chem. Soc. 123:749–750; (b) Sanford, M.S., Love, J.A., Grubbs, R.H. (2001) J. Am. Chem. Soc. 123:6543–6554.

[9] Dragutan, V., Dragutan, I., Verpoort, F. (2005) Platinum Metals Rev. 49:33–40.

[10] (a) Jafarpour, L., Schanz, H.J., Stevens, E.D., Nolan, S.P. (1999) Organometallics 18:5416–5419; (b) Fürstner, A., Hill, A.F., Liebl, M., Wilton-Ely, J.D.E.T. (1999) J. Chem. Soc., Chem. Commun. 601–602. (c) Fürstner, A., Ackermann, L., Gabor, B., Goddard, R., Lehmann, C.W., Mynott, R., Stelzer, F., Thiel, O.R. (2001) Chem. Eur. J. 7:3236–3253. (d) Fürstner, A., Thiel, O.R., Ackermann, L., Schanz, H.J., Nolan, S.P. (2000) J. Org. Chem. 65:2204–2207.

[11] Clavier, H., Petersen, J.L., Nolan, S.P. (2006) J. Organomet. Chem. doi:10.1016/j.jorchem.2006.08.07.

[12] (a) Herrmann, W.A. (2002) Angew. Chem. Int. Edit. 41:1290–1309; (b) Peris, E., Crabtree, R.H. (2004) Coord. Chem. Rev. 248:2239–2246; (c) Crudden, C.M., Allen, D.P. (2004) Coord. Chem. Rev. 248:2247–2273; (d) Díez-González, S., Nolan, S.P. (2005) Annu. Rep. Prog. Chem. Sect. B 101:171–191.

[13] Occhipinti, G., Bjorsvik, H.R., Jensen, V.R. (2006) J. Am. Chem. Soc. 128:6952–6954.

TOWARDS NEW GENERATIONS OF METATHESIS METAL–CARBENE PRE-CATALYSTS

BART ALLAERT[1], NICOLAI DIELTIENS[2], CHRIS STEVENS[2],
RENATA DROZDZAK[1], ILEANA DRAGUTAN[3],
VALERIAN DRAGUTAN[3], FRANCIS VERPOORT[1]

[1] *Dept. of Inorganic and Physical Chemistry, Division of Organometallic Chemistry and Catalysis, Ghent University, Krijgslaan 281 (S-3), 9000 Ghent, Belgium.*
E-mail: francis.verpoort@UGent.be
[2] *Research Group SynBioC, Dept. of Organic Chemistry, Faculty of Bioscience Engineering, Ghent University, Coupure Links 653, B-9000 Ghent, Belgium*
[3] *Institute of Organic Chemistry of the Romanian Academy, 202B Spl. Independentei, 060023 Bucharest, P.O. Box 35-108, Romania*

Abstract: A short general introduction combined with some historical milestones in the field of olefin metathesis is presented followed by an overview of recent representatives of metal carbene initiators. This paper attempts to relief the many superb contributions and overwhelming work invested in intelligent design and innovative synthesis in this area. Despites of recent advances there is still a great interest in the generation of new, better performing, and more environment friendly metathesis.

Keywords: Olefin metathesis, ruthenium, *N*-heterocyclic carbene, Schiff-base, alkylidene, vinylidene, allenylidene, indenylidene, immobilisation.

1. General remarks

Olefin metathesis can be thought of formally as a reaction in which the carbon–carbon double bonds in two olefins are broken and rearranged subsequently by interchange of the alkylidene residues (transalkylidenation), the process resulting in the formation of two new olefins (Scheme 1). If one of the olefin products is volatile and can be easily removed, then the reversible metathesis reaction can be driven completely to the right. The reaction needs to be catalyzed, routinely by a transition metal complex.

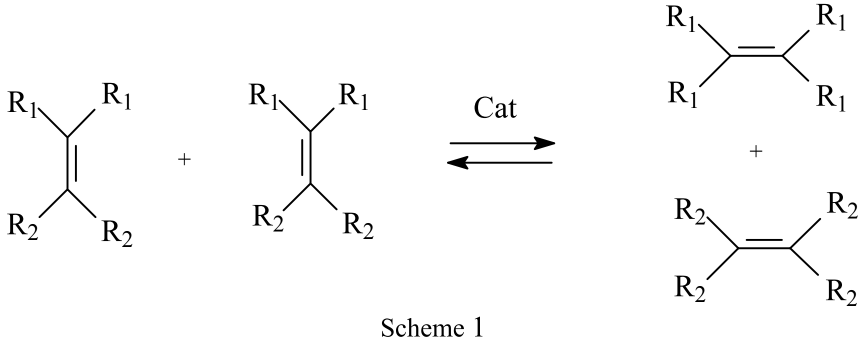

Scheme 1

Y. İmamoğlu and V. Dragutan (eds.), Metathesis Chemistry: From Nanostructure Design to Synthesis of Advanced Materials, 39-78.

Although discovered in the 1950s by researchers from industry, it was only over the last decade that olefin metathesis became one of the most prominent strategies applied for carbon–carbon bond formation in both organic and polymer synthesis, an achievement mainly due to a spectacular progress in catalyst design.[1] Presently olefin metathesis enables a whole range of industrial and pharmaceutical processes to be more efficient and environment friendly. As it allows replacement of selective atoms in one molecule with atoms from another molecule, custom-built new compounds having the desired properties can thereby be generated. Many important total syntheses of architecturally complex natural products, novel heterocyclic or macrocyclic compounds, pharmaceuticals etc., in which exquisite control is necessary, can now be achieved in less steps than previously required. Specialty polymers, caged compounds, capsules, and nanostructured materials have thus been obtained through simpler and more economic metathetic pathways starting from common and cheap raw materials.

The metathesis reaction is a versatile tool with a variety of applications in both polymer chemistry and organic synthesis. The basic metathesis reactions include ring-closing metathesis (RCM), cross-metathesis (CM), ring-opening metathesis (ROM), acyclic diene metathesis polymerization (ADMET), and ring-opening metathesis polymerization (ROMP) (Scheme 2).

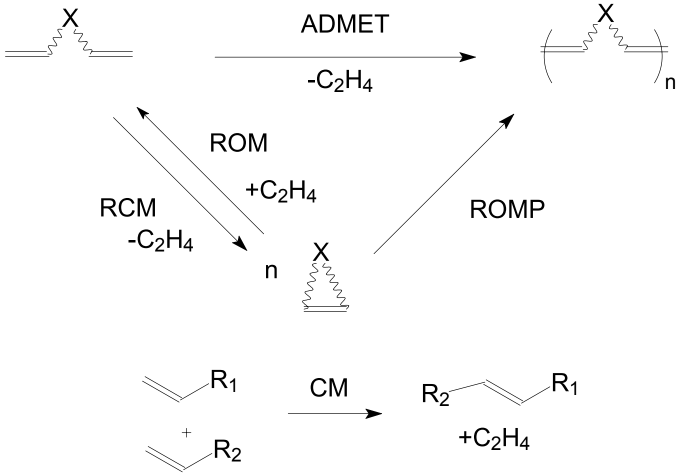

Scheme 2

The driving force in RCM and ADMET is the formation of a volatile compound and an internal olefin. To favour RCM and eliminate oligomerization through the competing ADMET process, low concentrations of substrate are recommended. Furthermore, the stability of the newly closed ring is of paramount importance in the RCM/ADMET competition, RCM being promoted in case of formation of more stable cycles. In ROM and ROMP, on the other hand, high ring strain is necessary to overcome the loss in entropy during the reaction. CM implies linear transformations and the olefin substitution pattern determines the equilibrium between homodimerization and heterodimerization. Extension of the metathesis reaction to acetylenes and enynes has also been largely developed.

According to the unanimously accepted metallacarbene–metallacyclobutane mechanism proposed by Chauvin,[2] time and again verified by later accumulation of results, the reaction is promoted by a metal–carbene complex (acting as an initiator) and then goes through a cycle of reversible steps. First, the initiating metallacarbene reacts with an olefin in a concerted mechanism to form a cyclobutane ring. The cyclobutane ring subsequently flips open either into the initiating species or, productively, into a new metal carbene fragment. Now a new olefin can react at the carbene centre to ultimately give the metathesized product and the carbene initiator, which restarts the cycle (Scheme 3). Finally, this reversible process leads to a thermodynamic equilibrium of the reaction products.

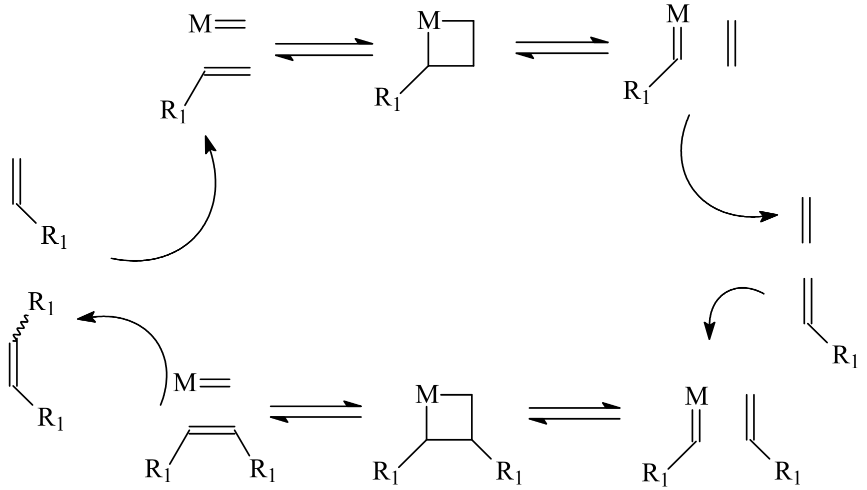

Scheme 3

In spite of its versatility, metathesis could not, until lately, be developed to its full synthetic potential because the traditional catalysts were ill-suited for application being relatively short-lived and susceptible to air, moisture, or side reactions. Schrock was the first to develop an entire family of tungsten–alkylidene and, more importantly, molybdenum–alkylidene complexes with very high activity and selectivity in olefin metathesis.[3] Further on, Grubbs discovered ruthenium (Ru) catalysts which up to now are among the most tolerant of functional groups initiators.[1a]

The first well-defined, fully characterized, complex to be active in degenerate metathesis of terminal olefins was reported by Tebbe (DuPont) in 1978 (the titanium–methylene–aluminium, $Cp_2Ti(CH_2)AlMe_2Cl$ (**1**), known as Tebbe complex); the propagating species in this reaction, a transient methylene intermediate, was also identified by Tebbe (Scheme 4).[4] Unlike the Fischer carbenes, the $Cp_2Ti(CH_2)$ fragment is polarized δ^+ on the metal and δ^- on the carbon. Furthermore, the transient methylene species could be trapped by various reagents thus supporting the metallacyclobutane intermediate formed in metathesis reactions according to the Chauvin mechanism.

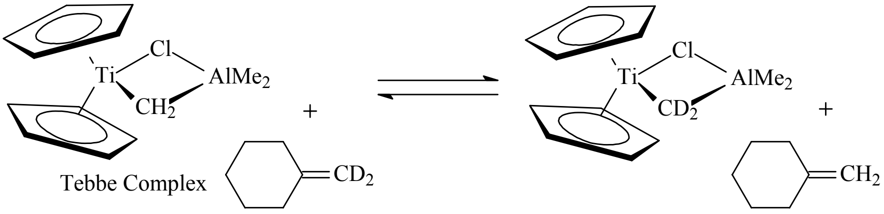

1

Scheme 4

Subsequently, other Ti–cyclobutane species were shown to be the reaction products of the Tebbe complex with olefins[5]; the analogous reaction with acetylenes gives metallacyclobutenes.[4c] Utilization of Ti–metallacycles as initiators in metathesis provides the first example of a living metathesis polymerization system.[6] Clear evidence of the intervention of metallacarbenes and metallacyclobutanes in olefin metathesis was later furnished by Kress et al.[7] through minute nuclear magnetic resonance (NMR) studies on norbornene polymerization with tungsten alkylidenes.

Tantalum–carbene complexes, originally reported by Schrock,[8] opened new paths for advancement in metal–carbene chemistry. Serendipitously, a "Ta ylide", $(Me_3CCH_2)_3Ta{=}CHCMe_3$, **2**, was obtained (along with neopentane) from $Ta(CH_2CMe_3)_3Cl_2$ upon treatment with $LiCH_2CMe_3$ (Scheme 5).[8]

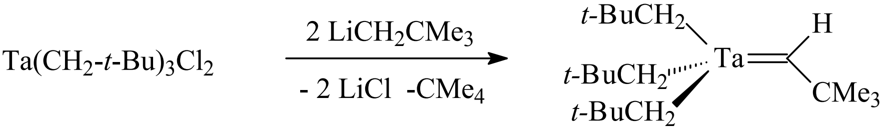

2

Scheme 5

Formation of this new "high oxidation state" metal–carbene complex was rationalized by an α-hydrogen abstraction; it was found that the process is accelerated with increasing ligand bulkiness. The complex is sensitive to oxygen, water, and a variety of functional groups and reacts with carbonyl groups in a Wittig-like manner. Later, using more sterically demanding ligands, Schrock and co-workers[9] synthesized the first isolable methylene complex, $Cp_2Ta(CH_2)Me$, with δ^+ polarization on the metal and δ^- on the carbon. Observation of tantalum–cyclobutane and –cyclopentane intermediaries in the productive metathesis of a simple olefin with a well characterized catalyst[10–12] led to better insights into the metathesis reaction mechanism. The high oxidation state is a prerequisite in the generation of this class of alkylidene complexes while the presence of alkoxides, vs chlorides, is preferable for promoting metathesis.[13]

2. Well-defined, high-oxidation state W– and Mo–alkylidene complexes

While attempting to create alkoxide carbenes a new, metathesis active, tungsten complex, $W(O)(CH\text{-}t\text{-}Bu)(PMe_3)_2Cl_2$ (**3**), was reported by Schrock (Scheme 6); nevertheless, the metathesis activity could be observed only in the presence of traces of $AlCl_3$.[14,15]

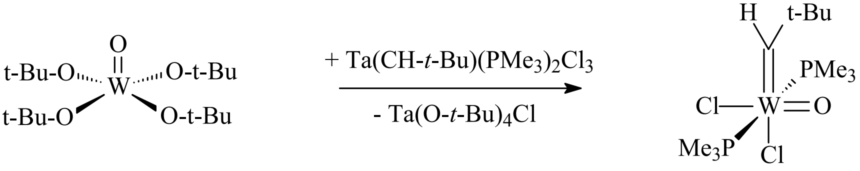

3

Scheme 6

Unlike **3**, tungsten–alkylidyne complexes of the type $(OR)_3W{\equiv}C\text{-}t\text{-}Bu$ having alkoxide ligands proved to be highly active for alkyne metathesis.[16] When the electron-withdrawing alkoxides are bulky, the expected intermediate alkylidyne and tungsten–cyclobutadiene species could be evidenced in alkyne metathesis.[16a] This lead to the introduction of the sterically demanding imido ligands that mimic the alkoxide ligands. Upon treatment of $W({\equiv}C\text{-}t\text{-}Bu)(NHAr)Cl_2(dme)$ with a catalytic amount of Et_3N, a quantitative conversion to $W({=}CH\text{-}t\text{-}Bu)(NAr)Cl_2(dme)$ (**4**)[16a,17] was attained, which subsequently, by replacement of the chloride ligands with bulky alkoxide ligands, led to $W{=}(CH\text{-}t\text{-}Bu)(NAr)(OR)_2$ (**5**) (Scheme 7). Catalysts of this type showed good activity for metathesis of internal olefins, with an optimum recorded for $R = OCMe(CF_3)_2$.

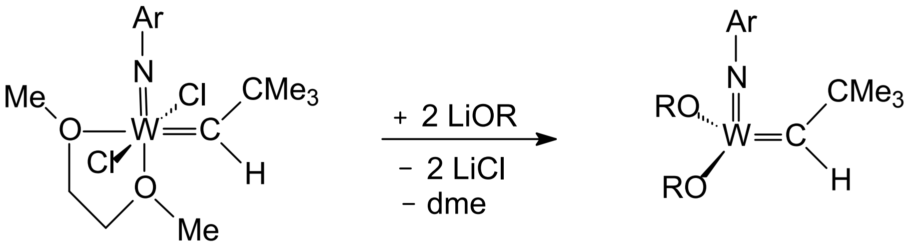

4 **5**

Scheme 7

In the quest for catalysts that are more tolerant towards functional groups, research efforts were then focused on synthesis of molybdenum analogues **6**–**8** (R = Me, Ph) (Scheme 8).[18,19]

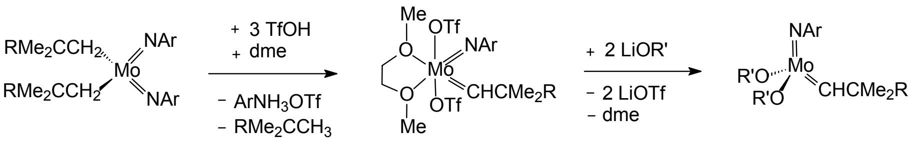

6 **7** **8**

Scheme 8

By reaction of **7** with alkoxides (e.g. LiOR′) a variety of molybdenum–imido complexes of the type $Mo(CHCMe_2R)(NAr)(OR')_2$, **8**, have been synthesized. These molybdenum complexes are stable when the alkoxide ligands are quite sterically demanding.[16a] On varying the imido group and alkoxide ligands in these complexes, fine-tuning of the catalytic activity has been achieved. This approach gave access to one of the fastest metathesis initiating molybdenum catalyst known up to this date (**9**, Scheme 9).

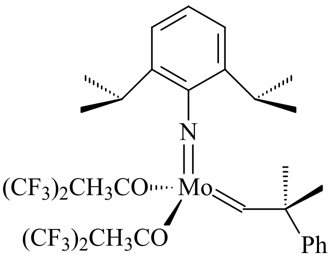

9

Scheme 9

Recent developments in the area of the W and Mo catalysts concern the incorporation of enantiomerically pure bidentate alkoxide ligands as well as of a series of different imido ligands. The resulting complexes have proved to be excellent catalysts for enantioselective RCM, ROM, and CM reactions.[1a,20–36]

3. Well-defined ruthenium–alkylidene complexes

The first ever reported well-defined Ru–carbene complex that was active in olefin metathesis (**10a**) has been prepared by Grubbs from $RuCl_2(PPh_3)_3$ and 3,3-diphenylcyclopropene (Scheme 10).[37]

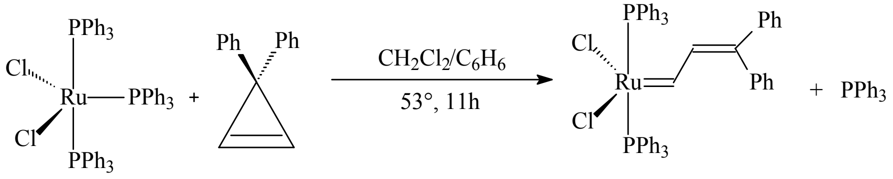

10

Scheme 10

Remarkably, in spite of the fact that **10** is stable for days in the presence of water, alcohol, acetic acid, or a diethyl ether solution of HCl and does not react with ketones or aldehydes (Wittig reaction), this catalyst is active in living ROMP of highly strained cyclic olefins (bicyclo[3.2.0]hept-6-ene, *trans*-cyclooctene) yet it is not an efficient catalyst for the ROMP of low-strain cyclic olefins or the metathesis of acyclic olefins. Substitution of the triphenylphosphine ligands in **10** with better σ-donating ligands like PCy_3 or $P(i\text{-}Pr)_3$ led to new Ru complexes (e.g. **11**) showing good functional group compatibility and a moderate stability to air. In contrast to **10**, **11** can readily catalyze ROMP of *cis*-cyclooctene, 1,5-cyclooctadiene, 7-oxanorbornene derivatives, and cyclopentene.[38]

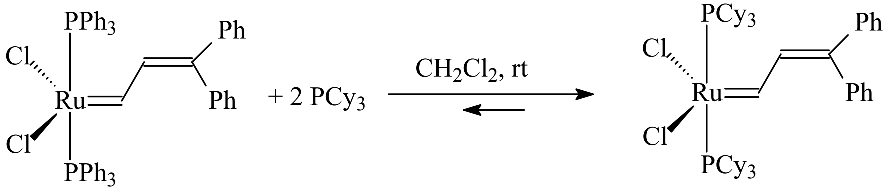

10 **11**

Scheme 11

Although **11** was a good catalyst in applications[39,40] such as RCM, ADMET, RIM of DCPD, because of its more easily scalable synthesis, the versatile series of the Ru–benzylidene complexes has been developed and became widely known as the first-generation Grubbs catalysts. The successful large-scale synthesis of the Ru complex **12** turned it into a commercially available catalyst; the synthesis is based on the reaction of $RuCl_2(PPh_3)_3$ with diazo compounds, in particular with phenyldiazomethane, yielding first $(PPh_3)_2Cl_2Ru{=}CHPh$ and subsequently, by phosphine exchange with PCy_3, the complex **12**, readily isolable in high purity due to its low solubility in acetone.[41]

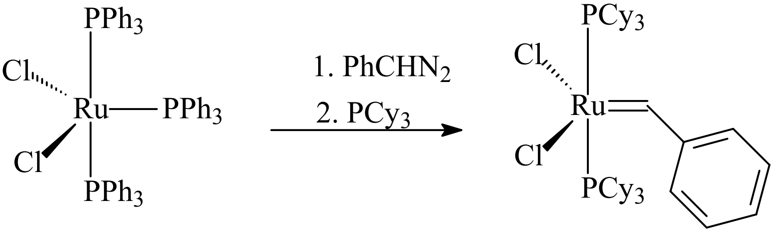

12

Scheme 12

The high k_i (initiation constant)/k_p (propagation constant) ratio (1000) of the benzylidene **12** vs the vinyl–carbene complex **11** suppresses chain transfer and the termination reaction thus allowing living polymers with narrow molecular weight distributions (PDI < 1.1) to be formed.[41] Owing to all its advantageous properties, complex **12** became a reference metathesis pre-catalyst and also got to be largely applied in numerous syntheses mainly involving RCM and CM steps. Some other synthetic methods for various Ru carbenes are also fully documented[1a,42] Incorporation of the carbene moiety is accomplished through reaction of an Ru source with dichloromethane[42a], alkynes,[42b,d] propargyl chlorides,[42b,c] vinyl chlorides,[42c] sulphur ylides,[42f] cyclopropenes,[37] dichloromethylbenzene,[42g] and propargyl alcohol.[42h–j]

4. NHC ruthenium–alkylidene catalysts

A spectacular progress in Ru–carbene pre-catalyst design was achieved when *N*-heterocyclic carbenes (NHCs) were advanced as ancillary ligands.[43] The non-labile, sterically demanding NHC ligands stabilize both the pre-catalysts and the coordinatively unsaturated, catalytically relevant intermediates. Ligands of this type show high propensity for acting as typical σ-donors, yet manifest only a slight π-back-bonding tendency, are strong Lewis bases and generate rather stable metal–carbon bonds.[44] Due to the comparatively decreased lability of NHCs, the new generation of Ru complexes bearing such ligands show improved thermal and oxidative stability, and hence make long-lived and active catalysts. Along these lines, imidazol-2-ylidene (IMes) and imidazolin-2-ylidene (SIMes) have been used to substitute phosphine in the Grubbs first-generation pre-catalysts leading to the advent of the Grubbs second-generation complexes which have superior performance in many cases.[45]

Almost at the same time, Grubbs, Herrmann, and Nolan reported on the design and synthesis of novel Ru alkylidene pre-catalysts containing nucleophilic NHCs as ancillary ligands.[46–48]

Herrmann et al.[46] published an array of NHC–Ru complexes (**13–16)** resulting from the diphosphane Ru–benzylidene complex **12** and IMes carbenes, in toluene or tetrahydrofuran, at room temperature. Products with one or two SIMes ligands, depending on the molar ratio of the complex **12** and the SIMes carbene (in practice molar ratios of 1:1.2 or 1:2.2 are used), were obtained in high yield (80–90%).

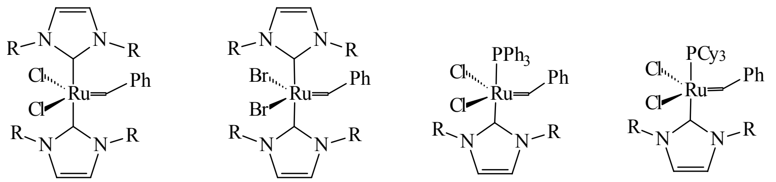

a: R = Cy, *i*-Pr
b: R = CH(Me)Ph
c: R = CH(Me)Naph

R = *i*-Pr

R = *t*-Bu

a: R = Cy
b: R = CH(Me)Ph
c: R = CH(Me)Naph

13 **14** **15** **16**

Scheme 13

A significant result of the NHC introduction, revealed by the single-crystal x-ray analysis of the bis(IMes)-*p*-chlorobenzylidene–Ru complex, indicated a lower degree of distortion of the square–pyramidal configuration as compared to the analogous diphosphane complex. In addition, several chiral IMes–Ru complexes, such as (*R,R*)-**17** and (*R,R*)-**18** (R = Ph, Cy; Ar = Ph or Naph), could be obtained by the above approach, i.e. reaction of the diphosphane Ru–benzylidene complex **12** with chiral IMes ligands (Scheme 14).[46b] Chiral compounds **17** and **18** make promising candidates for application as precursors in enantioselective metathesis starting from prochiral substrates.

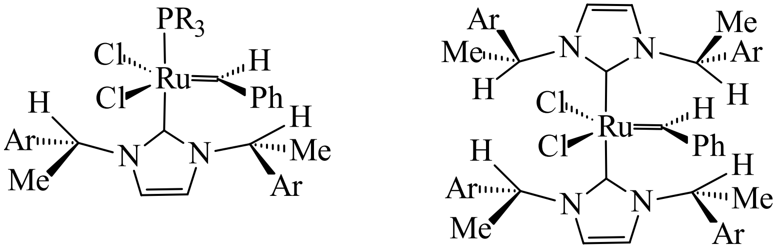

R = Ph, Cy
Ar = Ph, Naph

17 **18**

Scheme 14

By using mesityl-substituted NHCs, Grubbs[47] and Nolan[48] disclosed, practically simultaneously, the synthesis of the Ru–alkylidene complexes **19** (NHC = 1,3-dimesitylimidazol-2-ylidene); soon thereafter, the Grubbs group firther introduced complexes **20** (Cy = cyclohexyl) and **21** (Cp = cyclopentyl) containing a saturated NHC (1,3-dimesityl-4,5-dihydroimidazol-2-ylidene).

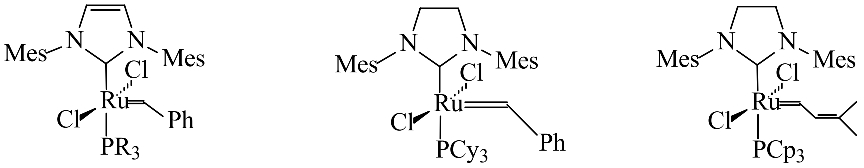

19 **20** **21**
R = Ph, Cy

Scheme 15

It should be emphasized that the metathesis activity of complexes **19**–**21** is strongly dependent on the nature of the NHC ligand, the solvent, and the substrate – with some substrates the saturated complex **20** being more active than the unsaturated one **19**. Also, it was shown that the initiation rate of second-generation catalysts **19** incorporating differently substituted phosphines is faster for the more electron-withdrawing phosphines, regardless of their steric bulk.[49] Replacement of the chloride ligands in **20** by bromide or by the even larger iodide increases the propensity for phosphine exchange in the catalyst. Surprisingly, olefin metathesis activity of these complexes follows the inverse trend leaving the chloride-substituted **20** as the most active catalyst.[50]

Detailed studies by Grubbs et al.[51] regarding the mechanism of olefin metathesis catalyzed by Ru–alkylidene complexes indicated that the initiation constant is independent of the olefin concentration over a wide range, which supports a dissociative mechanism. Furthermore, the k_{-1}/k_2 ratio for **12** was found to be four orders of magnitude higher than that of **20**; this was a first suggestion to the fact that the enhanced activity of the NHC-coordinating catalyst **20**, previously ascribed to its ability to promote phosphine dissociation (which increases k_1), could equally be assigned to an improved selectivity of the 14-electron intermediate species for binding π-acidic olefin substrates, in the presence of the σ-donating free phosphine (Scheme 16).[51]

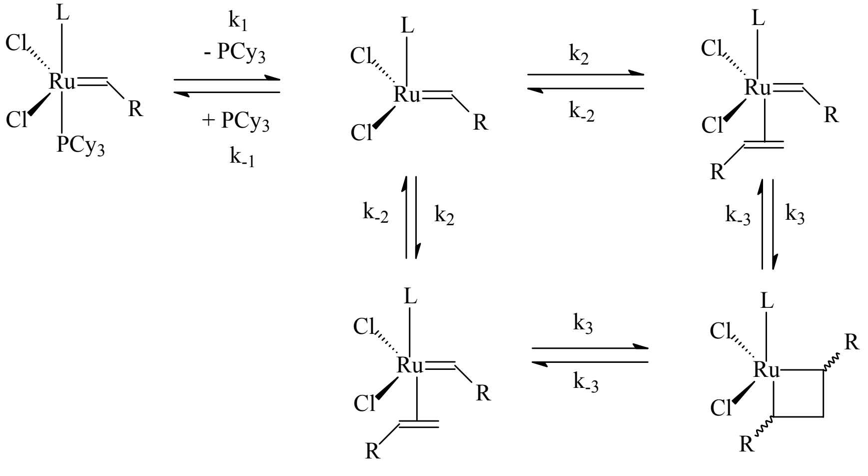

Scheme 16

In the quest for better carbene ligands Herrmann et al. explored the potential of the acyclic carbene **22**, which is a much more donating ligand than SIMes, for coordinating to the metal centre in **12**.[52] However, as in the final reaction mixture the presence of Ru–alkylidene could no longer be detected, it was concluded that attack of the free carbene **22**, in fact, occurred at the alkylidene unit.[52] Buchmeiser et al. prepared the six-membered ring analogue of SIMes whose donor capacity is comparably high to that of the acyclic carbene **22**[53]; substitution by 1,3-dimesityl-3,4,5,6-tetrahydropyrimidin-2-ylidene on complex **12** was successful, yet no comparison with SIMes on the catalytic activity was provided.[54] In a similar protocol that employed the closely related six-membered carbene **23**, Grubbs et al.[55] observed the corresponding catalyst to be slower than **20** in the polymerization of 1,5-cyclooctadiene; this drop in activity was attributed to a sterically unfavourable olefin binding.[55] A totally different four-membered NHC, **24**, was prepared by

Grubbs et al. [56]; however, the catalyst obtained with it showed lower activity than that with SIMes (**20**).[57]

Unsymmetrical NHC ligands (e.g. N,N′-substituted by one mesityl and another, different group), allowing to tailor the electronic and steric properties of NHC–Ru alkylidene complexes, have been advanced as an attractive strategy for designing new Ru catalysts as olefin metathesis initiators.[58–60] To date, there are few publications concerning unsymmetrical NHCs, referring, for example, to the large sterically encumbered mixed adamantyl and mesityl substituted NHC introduced by Mol,[61] and the bidentate asymmetric ligand developed by Hoveyda.[62]

Fürstner,[58] Blechert,[59] and Verpoort[60] have in turn reported on the synthesis and applications of such complexes. It is worth pointing out that, in the case of catalysts substituted with **25**-like ligands, Blechert concluded that the asymmetry of the NHC (**25**) is reflected in the very different E/Z ratios encountered in CM reactions and an improved selectivity in diastereoselective RCM, in comparison to the corresponding Grubbs' second-generation and Hoveyda–Grubbs complexes. Verpoort and co-workers[60] showed that Ru catalysts bearing unsymmetrical NHC ligands have a modified reactivity pattern relative to those with symmetrical NHC. In RCM a significant dependence of the reactivity on the bulkiness of the NHC was observed. For the Ru–benzylidene catalyst having NHC substituted by alkyl and mesityl groups, activity surpassed that of the Grubbs second-generation catalyst **20**, in the RCM of diethyl diallylmalonate (DEDAM).[60]

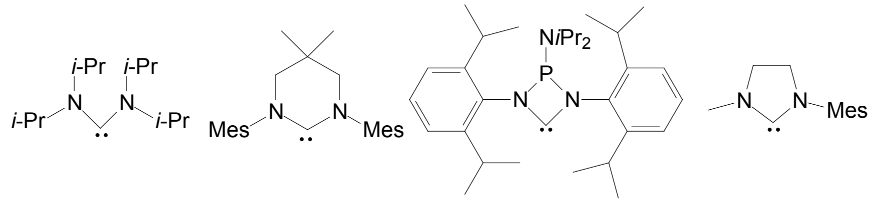

22 **23** **24** **25**

Scheme 17

Some unsymmetrically substituted complexes, e.g. **26a** (n = 1, 2, 4) possess the unique ability to metathesize their own ligands to form chelated NHC–Ru complexes in which the NHC and the "regular" carbene unit, Ru = CHR, are tethered by a variable "cyclic" structure. In one example, heating a solution of complex **26a** (n = 2) in refluxing toluene afforded the "metallacyclic" complex **26** in 75% isolated yield (Scheme 16).[58]

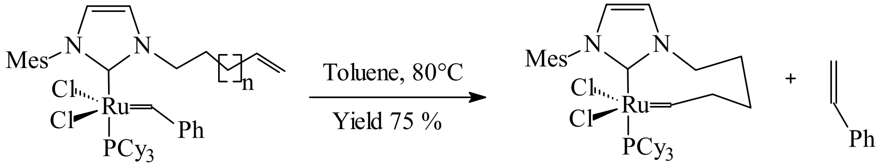

26a, n = 2 **26**

Scheme 18

It was assumed that the catalytic species are able to regenerate themselves after the productive metathesis is over and the substrate in solution has been quantitatively consumed.

Complex **27** has been prepared from the corresponding diphosphane complex **12** and 4,5-dichloroimidazol-2-ylidene, according to the procedure described above, displaying good thermal stability and catalytic activity in metathesis reactions.[58] Additionally, the unsymmetrically substituted NHC complexes **28** and **29**, containing a silylether derivative or a perfluoroalkyl chain, have been conveniently prepared by the same methodology.[58]

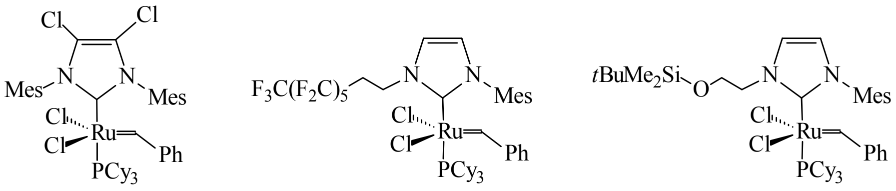

27 **28** **29**

Scheme 19

5. Grubbs–Hoveyda-type catalysts

An important advancement in the design of Ru–alkylidene pre-catalysts has been the incorporation of a bidentate chelating carbene ligand in the Grubbs first-generation complex leading to the family commonly known today as the Grubbs–Hoveyda catalysts. Hoveyda et al. were the first to disclose the preparation of **30** by reaction of (2-isopropoxyphenyl)-diazomethane, PCy_3 and $Cl_2Ru(PPh)_3$ (Scheme 20).[63] This catalyst showed excellent stability to air and moisture, and could be recycled several times.

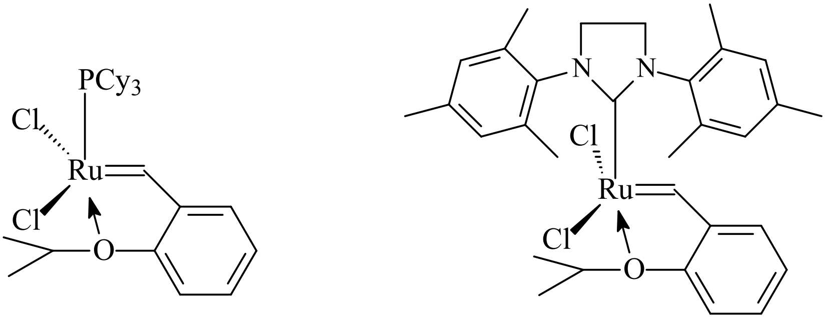

30 **31**

Scheme 20

Later, both Blechert[64] and Hoveyda[65] reported on an analogue (**31**) of the second-generation Grubbs catalyst as resulting from reaction of **20** with 2-isopropoxystyrene, in the presence of CuCl. The enhanced stability of these catalysts comes from chelation of the carbene, assisted by the donor oxygen atom, during formation of the 16-electron complex. It was postulated that with this class of catalysts olefin metathesis proceeds by a "release-return" mechanism. In the Grubbs–Hoveyda catalysts the methylidene intermediate can be trapped by the isopropoxystyrene fragment (present in the reaction medium after initiation) and thereby transformed in a very stable initiating species. The same process is responsible for the elimination of a methylidene at the end of the reaction and thus for the auto-recycling of the catalyst (Scheme 21).

Due to the slow initiation rate of **31**, implementing variations on the chelating ligand in order to improve the catalyst reactivity was still a challenge. Blechert et al.[66] obtained spectacular results in catalytic activity in RCM by changing the chelating ligands as shown in **32** and **33** (Scheme 22).

Further significant variations were introduced by Grela et al.[67] who played on the electronic properties of the isopropoxybenzylidene ligand varying substitution (nature of substituents and position) in the aromatic ring; thus, taking advantage of the electron withdrawing properties of an NO_2 substituent located in position *para* (with respect to isopropoxy group), and therefore a decreased electron density on the oxygen atom of the isopropoxy fragment, the complex **34** possessing an augmented catalytic activity could be obtained. By contrast, introduction of methoxy groups on the styrene fragment showed little rate improvement upon the parent complex **30**,[67c] as did placing the nitro group onto different positions.[67d]

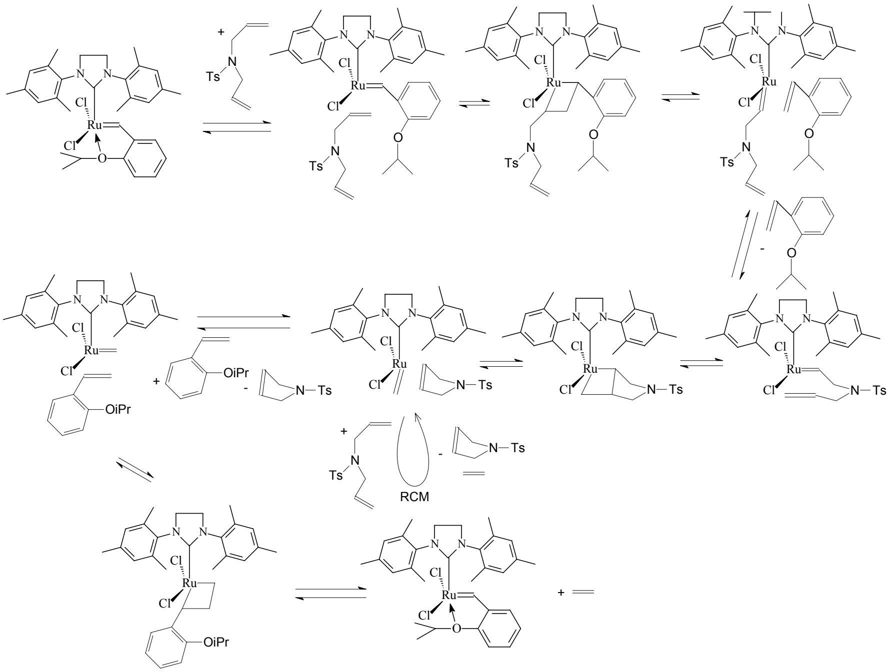

Scheme 21

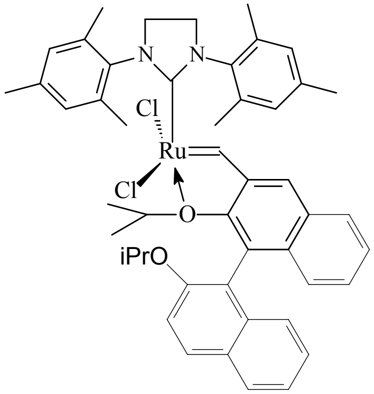

32

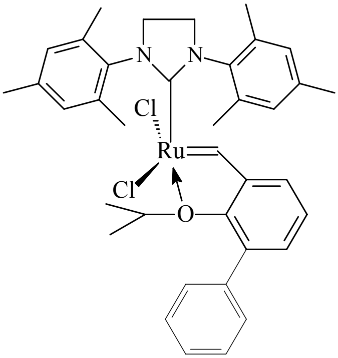

33

Scheme 22

A different system for chelating at Ru, i.e. a bidentate carbene–pyridine, was devised by Van der Schaaf et al.[68], the resulting catalyst being used in polymerization of dicyclopentadiene (DCPD); the idea was extended by Grubbs et al.[69] to yield the second-generation catalyst **35**. Fürstner et al.[70] incorporated a coordinating carbonyl ester on the bidentate carbene and

Slugovc et al.[71] implemented this group on a phenyl carbene obtaining catalyst **36** (Scheme 23).

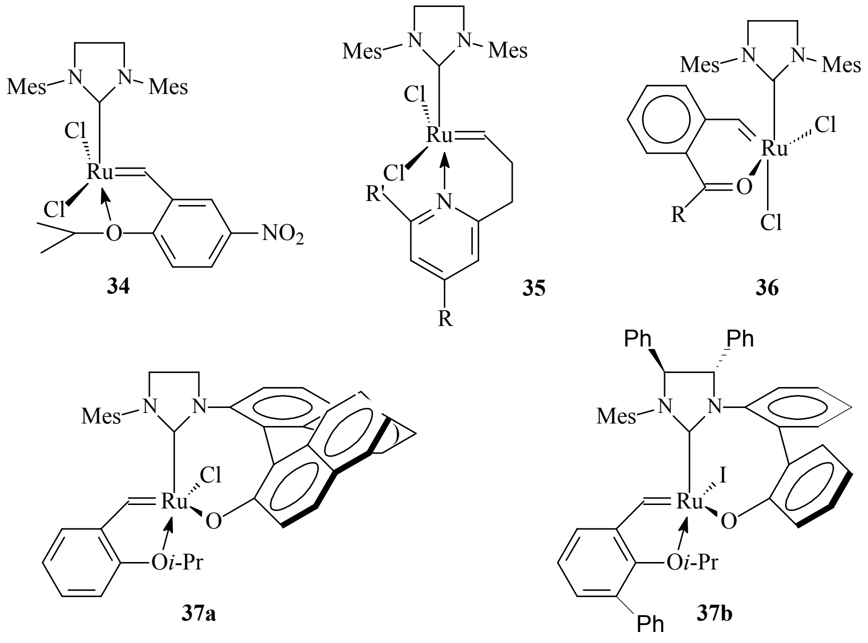

Scheme 23

Hoveyda et al.[72] also reported on the introduction of the isopropoxystyrene fragment in conjunction with chiral ligands to produce the chiral catalysts **37a**,**b** yielding high chiral resolution, and showing increased activity and selectivity (for **37b**). These chiral adjustments are important for applications of Ru catalyzed metathesis in organic synthesis paralleling results obtained with chiral Mo-based catalysts.

6. Ruthenium–vinylidene and –allenylidene complexes

While also eliminating one of the most important drawbacks of the conventional synthesis of Ru–carbene complexes that involves hazardous and toxic substituted diazomethanes or 3.3-diphenylcyclopropene, Ru–vinylidene and –allenylidene complexes, readily obtained from commercially starting materials, appeared as a promising alternative for enlarging previously existing libraries of Ru catalysts.

First, a series of neutral 16-electron Ru–vinylidene complexes, **38** (R = Ph or Cy), was efficiently prepared by Katayama and Ozawa[73] from terminal alkynes and the arene Ru dimer, $[RuCl_2(p\text{-cymene})]_2$ (Scheme 24). These complexes showed only moderate metathesis activity in the RCM of unsubstituted dienes and ROMP of highly strained norbornenes.[74]

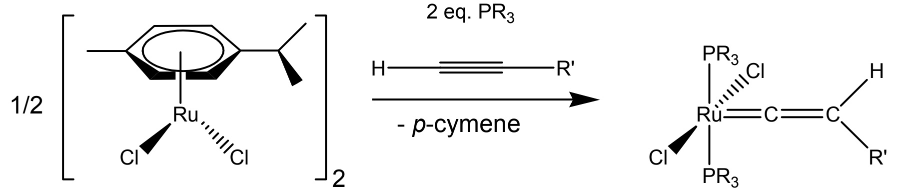

38

Scheme 24

Further on, the cationic 18-electron Ru–vinylidene complexes (e.g. **39**, **40**, and **41)**, introduced by Grubbs and co-workers[75] (Scheme 25) were screened for their catalytic properties attesting that they performed well only with a small range of olefin substrates. More effective in metathesis, several neutral and cationic 16- and 18-electron Ru–tridentate complexes, were reported by van Koten et al.[76] as obtained from reaction of $[RuCl_2(NN'N)(PPh_3)]$ (where NN'N is the 2,6-bis[(dimethylamino)methyl]pyridine ligand) with two equivalents of $Ag[BF_4]$, in the presence of an excess of phenylacetylene (isolated yield 95%).

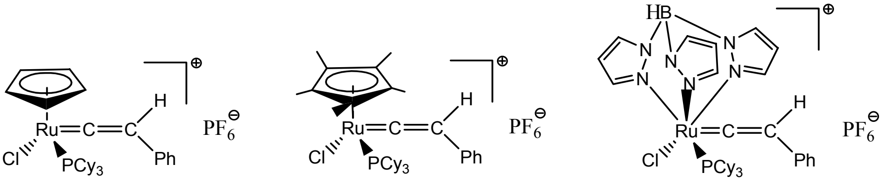

39 **40** **41**

Scheme 25

The new, very large family of Ru–allenylidene metathesis pre-catalysts, essentially involving, as in the case of Ru–vinylidenes, both neutral and cationic complexes, e.g. **42** and **43** (R = Ph or Cy, X = PF_6, BF_4, BPh_4, OTf), enjoyed considerable application profile as metathesis initiators owing to their easy accessibility and good to excellent catalytic properties (Scheme 26).[74c,77]

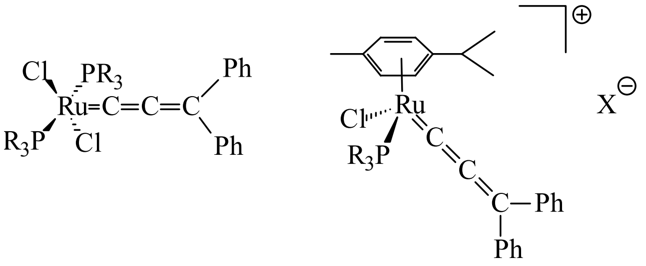

42 **43**

Scheme 26

Three neutral, coordinatively unsaturated 16-electron Ru–allenylidene complexes of different types, namely the bisphosphane complex **44**,[78] the imidazolin-2-ylidene complex **45** and the bimetallic complex **46**, are significant members of this class that have been evaluated for their catalytic behaviour showing good results in RCM.[78,79]

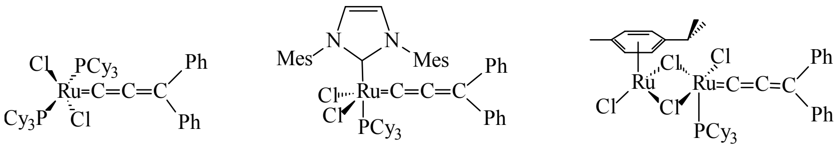

44 **45** **46**

Scheme 27

The complex, similar to **44** but having PPh_3 instead of PCy_3 groups, is rather unstable under normal conditions and was proved to rearrange readily to the corresponding indenylidene complex.[79] More stable but less active, the IMes complex **45,** which is an allenylidene analogue of the Grubbs second-generation complex, stems from complex **44** by simple ligand substitution. By contrast, the binuclear allenylidene complex **46**, related to the benzylidene complex $[Ru_2Cl_4(=CHPh)(p\text{-cymene})(PCy_3)]$[80], is a highly active metathesis Ru pre-catalyst.

Large numbers of cationic, coordinatively saturated 18-electron Ru–allenylidene complexes have been reported[81]; of these, many act as good pre-catalysts for RCM[82] and ROMP.[83] Main representatives of this group (**47**–**50**) contain η^6-arene, phosphane, and chloride ligands, in conjunction with a "non-coordinating" counterion X^-.

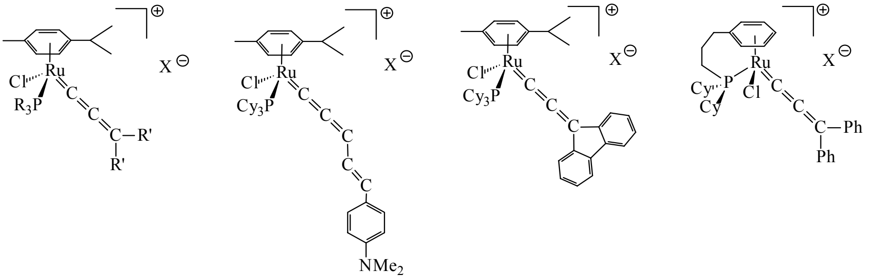

47 **48** **49** **50**

Scheme 28

By varying the substituents at the phosphine (R = Ph, Cy, *i*-Pr) and allenylidene moieties (R′ = Ph, *p*-chlorophenyl, *p*-methoxyphenyl, etc), and the nature of the counterion X^- (X^- = PF_6, BPh_4, BF_4, OTf, etc) a further array of allenylidene–Ru complexes could be obtained. As they are easily accessible, their potential as metathesis pre-catalysts has been extensively examined. Some of them allowed metathesis reactions to be performed in ionic liquids (e.g. 1-butyl-3-methylimidazolium salts) thus ensuring a high solubility of the catalytic species in the reaction medium.[84]

Capitalizing on the coordination ability of NHC, the family of Ru complexes containing NHC ligands has been rapidly expanded to the attractive Ru–vinylidene[85] and –allenylidene complexes[86] (e.g. **51–53)** as well as to the analogous Ru–indenylidene compounds **54** and **55**.

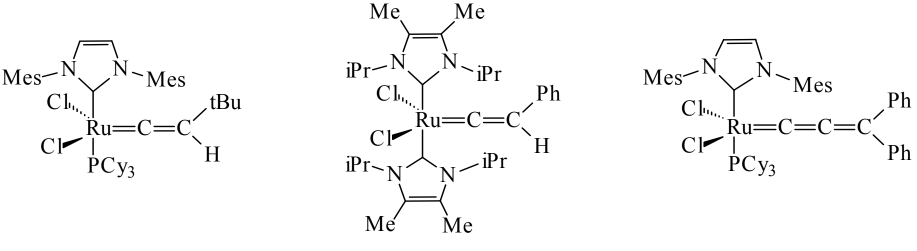

51 **52** **53**

Scheme 29

It should be outlined that incorporation of IMes as ancillary ligand in the cationic arene Ru–allenylidene complexes, e.g. **54**, provided very active initiators in ROMP of cycloolefins.[87]

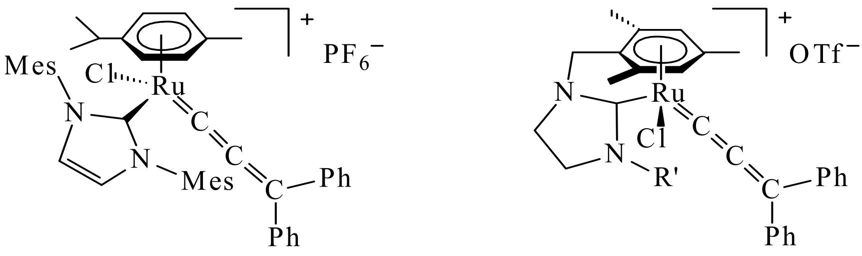

R’ = $CH_2CH_2OCH_3$, CH_2Mes

54 **55**

Scheme 30

Moreover, binding through a methylene tether the arene ligand with the dihydroimidazolin-2-ylidene unit, in a half-sandwich mode, led to the η^1:η^6–arene–carbene Ru–allenylidene complex **55**, which was highly active in RCM of 1,6-dienes.[88] This complex allowed to selectively direct metathesis of dienes either towards RCM or cycloisomerization products.

7. Ruthenium–indenylidene complexes

The widely employed in catalyst synthesis, 3-phenyl indenylidene complex **56**, has been conveniently obtained from [$RuCl_2(PPh_3)_4$] and 3,3-diphenylpropyn-3-ol as a carbene precursor. Further on, utilizing **56** as a starting material, the PPh_3 ligands could be readily replaced by the better donating ligands PCy_3, affording the parent indenylidene complex **57**, currently available commercially (Scheme 31).[78,86]

56 **57**

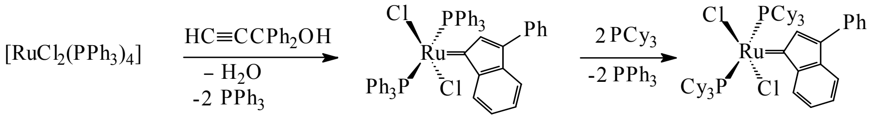

Scheme 31

This methodology can also use the trisphosphane complex [$RuCl_2(PPh_3)_3$] as the Ru source, resulting in the same indenylidene complex **56**. The rationalization behind this finding that the initially formed Ru–allenylidene complex **58** leads by intramolecular rearrangement to the more stable indenylidene complex **56** has been proved unequivocally (Scheme 32).[89]

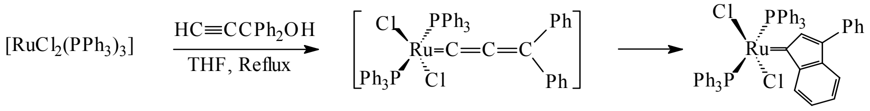

58 **56**

Scheme 32

The above indenylidene–Ru complexes showed a higher thermal stability than first-generation Grubbs catalysts and performed well in a variety of RCM reactions. It is worth mentioning that substitution of phosphane ligands in the Ru–3-phenylindenylidene complexes **56** and **57** by IMes ligands containing bulky groups in the 1 and 3 positions of the five-membered ring allowed synthesis of further 16-electron Ru–indenylidene complexes of even improved activity and stability.

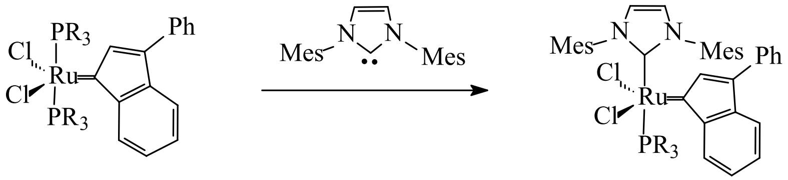

56, R = Ph
57, R = Cy

59, R = Ph
60, R = Cy

Scheme 33

Thus, addition of 1,3-dimesitylimidazol-2-ylidene to complexes **56** and **57**, in toluene at room temperature, leads readily and in high yield to complexes **59** and **60**, respectively[90] (Scheme 33).

A similar procedure starting from 1,3-bis(2,6-di-isopropylphenyl)imidazol-2-ylidene and Ru complexes **56** or **57** yielded the IMes 3-phenylindenylidene–Ru complexes **61** and **62**, respectively (Scheme 34).

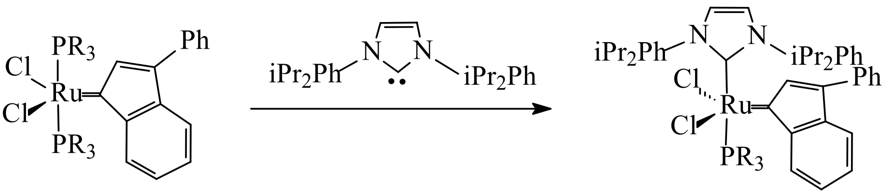

56, R = Ph
57, R = Cy

61, R = Ph
62, R = Cy

Scheme 34

Thermal stability investigations indicated that compounds **60** and **62** incorporating a PCy_3 ligand are very stable and do not decompose even after heating at 80°C for several days. RCM studies, using DEDAM and diallyl tosylamine as substrates, showed a good catalytic activity and selectivity for the Ru–indenylidene complexes of this pre-catalyst family (yield 88% and 94% in cyclic products, respectively).

Recently, the pyridine-containing Ru-based complex, $Cl_2Ru(PCy_3)(Py)_2$ (3-Ph-indenylidene), **63**, has been obtained by the broadly applied procedure of phosphine exchange from the bisphosphane analogue **57**, in the presence of excess pyridine (Scheme 35).[91] Most conveniently, complex **63** can be prepared in hot hexane affording an easier isolation of the product by simple filtration (vs evaporation of the solvent in the previous procedure), followed by washing with hexanes and drying.

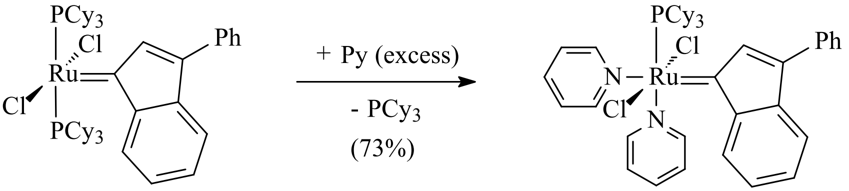

57 **63**

Scheme 35

This catalyst showed moderate activity in RCM of conventional diene substrates. As expected, the greater lability of the pyridine ligand vs phosphine enhanced the formation of the active species, but the reaction rate decreased after 30 min indicating that a degradation of the 14-electron intermediate is occurring; decomposition of the latter also augmented for higher catalyst loadings, hence is associated with a higher concentration of pyridine in the reaction mixture.

8. NHC ruthenium–arene complexes

It is worth noting that the IMes ligands have also been employed in the design and synthesis of the interesting class of arene–Ru complexes, e.g. **64–66** (Scheme 36).[92] Due to their easy accessibility from the commercially available Ru dimer [(*p*-cymene)$RuCl_2$], the last two complexes are of special importance for both radical and metathesis reactions.

64 **65** **66**

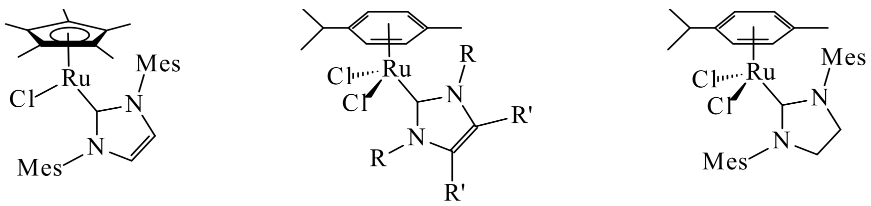

Scheme 36

Variations in the substituents of the imidazole moiety allowed an extensive exploration on the fine-tuning of the catalytic activity and selectivity. Valuable techniques, such as in situ generation of the carbene species and photo-induced metathesis processes, were applied successfully. The group of IMes–arene complexes possess high potential as precursors for further arene Ru compounds having enhanced catalytic properties for various organic reactions.

9. Schiff base–Ru complexes

Incorporation of a bidentate Schiff base ligand into Ru–benzylidene complexes has been initially performed by Grubbs et al.[93]; the resulting complexes showed high thermal stability and high tolerance towards polar solvents, yet seemed to be poor initiators in metathesis reactions, although some activity in metathesis at higher temperatures was observed.

In more extensive studies, Verpoort and co-workers[94] conveniently prepared the Schiff base –Ru–arene complexes **67a–c** (a: R = Me; b: R = *t*-Bu; c: R = 2,6-diMe-4-BrC_6H_2) following a two-step procedure starting from the commercially available Ru dimer [(*p*-cymene)RuCl_2]$_2$, which was reacted with salts of aliphatic or aromatic salicylaldimines (Scheme 37).

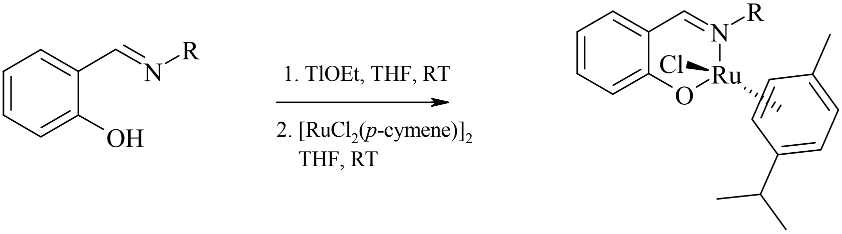

Scheme 37

Structures of these complexes have been unambiguously determined by means of infrared (IR), Raman, ^{1}H NMR, and ^{13}C NMR spectroscopy, and corroborated with data from elemental analyses. An important feature of these complexes is that the labile *p*-cymene group is present along with the better ligated bidentate Schiff base ligand. Having optimized the reaction conditions for this procedure, two new arene–Ru complexes, **68** and **69** (R_1 = *t*-Bu, R_2 = *i*-Pr), could be prepared in the same way (Scheme 38).[95]

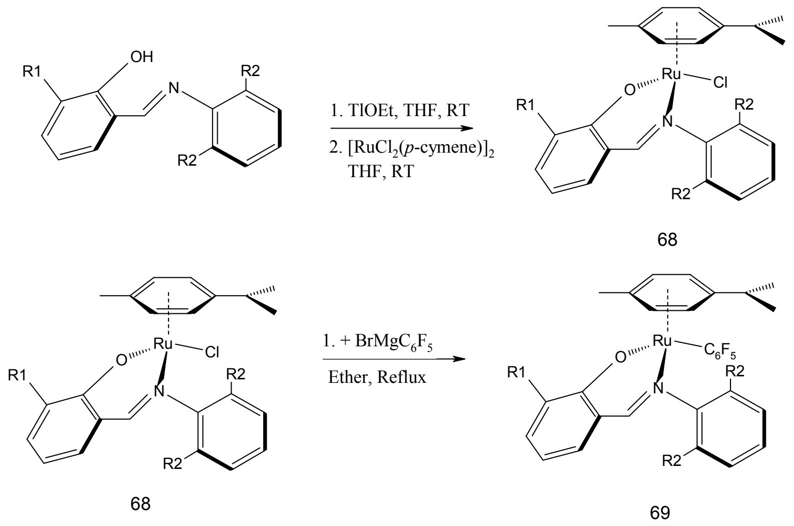

Scheme 38

The fluorinated ligand in the complex **69** could be introduced by a Grignard reaction on **68** with the appropriate reagent. In this context, the significant role of the electronic and steric effects played by both the Schiff base ligand and the other, additional ligand has been clearly evidenced in studies on ROMP and atom transfer rapid polymerization (ATRP) reactions.

Based on the bisphosphane Ru(II)complex, $RuCl_2(PCy_3)_2(CHPh)$, the above mentioned Ru dimer and different Schiff bases, a wide range of monometallic and bimetallic Ru–benzylidene complexes, **70a–f** and **71a–f**, have also been made available (Scheme 39).[95a,96]

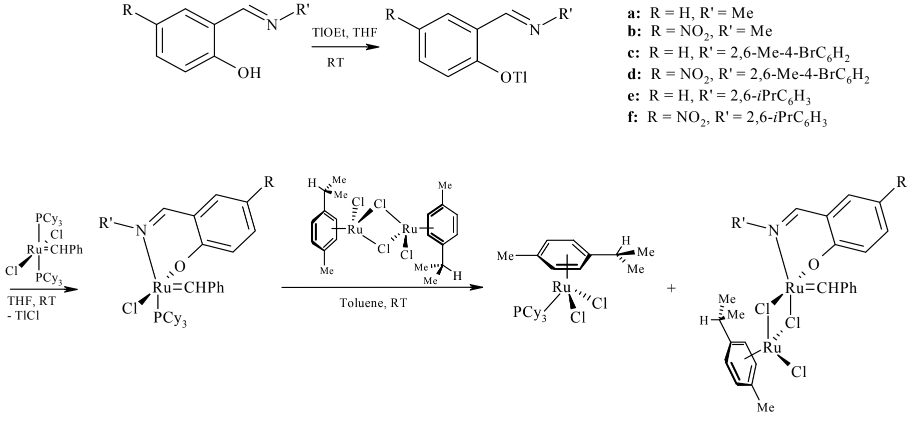

a: R = H, R' = Me
b: R = NO_2, R' = Me
c: R = H, R' = 2,6-Me-4-BrC_6H_2
d: R = NO_2, R' = 2,6-Me-4-BrC_6H_2
e: R = H, R' = 2,6-*i*PrC_6H_3
f: R = NO_2, R' = 2,6-*i*PrC_6H_3

70a–f **71a–f**

Scheme 39

This applied protocol took advantage of the facile substitution of the labile phosphane ligand from the monometallic complexes to form the bridgehead bimetallic complexes **71a–f** in a convenient way.

Of high interest for their particular activity and selectivity, the cationic Ru–benzylidene complexes **72a–f** have been prepared in situ from the corresponding Ru complexes **70a–f** by treatment with one equivalent of silver or trimethylsilyl salts (Scheme 40).[97]

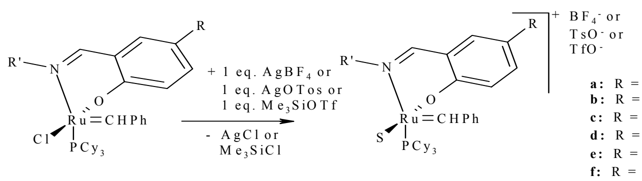

a: R = H, R' = Me
b: R = NO_2, R' = Me
c: R = H, R' = 2,6-Me-4-BrC_6H_2
d: R = NO_2, R' = 2,6-Me-4-BrC_6H_2
e: R = H, R' = 2,6-*i*PrC_6H_3
f: R = NO_2, R' = 2,6-*i*PrC_6H_3
S = solvent

70 **72**

Scheme 40

It is noteworthy that both the counterion and the solvent exert a striking effect upon the activity of these catalysts. In addition to their metathesis ability, these cationic Ru–benzylidene complexes are the first Ru–alkylidene catalysts reported so far to perform the controlled radical suspension polymerization of methyl methacrylate, methyl acrylate, and styrene in water, leading to high yields of polymer.

The activity of the Schiff base–Ru–benzylidene complexes has been further improved by Verpoort and co-workers by synthesis of NHC-containing complexes of type **73** (Scheme 41).[98,99] Herrmann et al. reported on similar bidentate pyridinyl–alcoholate ligands included in catalyst **74** that enables ROMP of cycloolefins to be performed at elevated temperatures.[100]

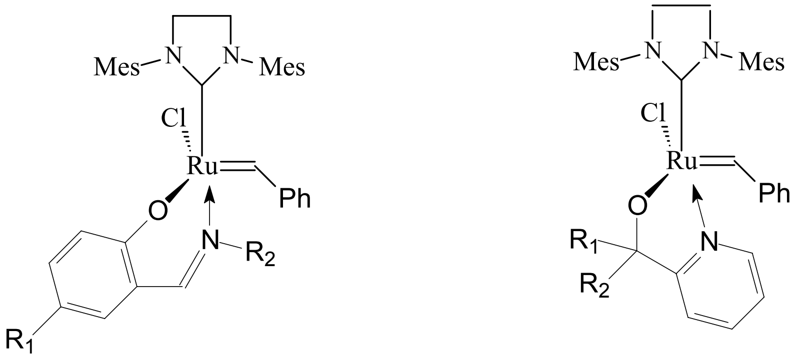

73 **74**

Scheme 41

10. Further explorations in Ru catalyst design

Although rather stable and quite compatible with functionalities, the majority of the Ru–alkylidenes that constitute the second generation of catalysts display only moderate activity in some cases, especially in RCM. A new concept that proved successful for advancement in design of Ru catalysts having an even better application profile is replacing the ligands *trans* to phosphine, IMes or SIMes, by pyridine or substituted pyridine, e.g. **75–77**. In 2001, Grubbs et al. reported on the synthesis of a pyridine functionalized second-generation catalyst, **76**,[101] recognized as an excellent initiator[102]; the same approach was also applied on the first-generation Grubbs catalyst to obtain **75**. In addition, the change to 3-bromo-pyridine, as in catalyst **77**, allowed considerably higher initiation rates and also lower polydispersity of polymers of norbornene and norbornene derivatives to be obtained.[102,103] For the pyridine-containing Ru–carbenes the term third-generation Grubbs catalysts has been coined.

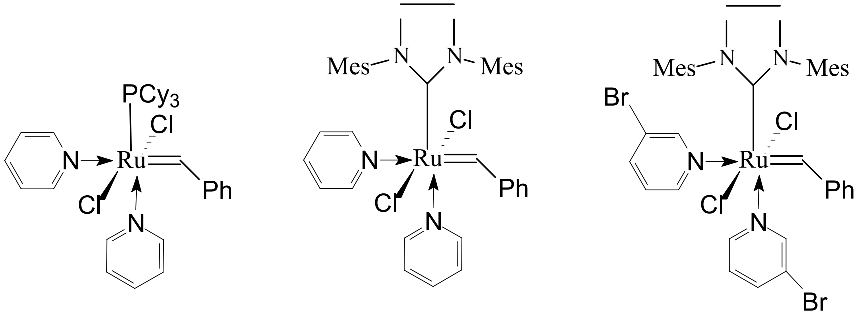

75 **76** **77**

Scheme 42

It had been long assumed that in the Ru catalytic systems, like in those of Mo or W, deactivation occurs with halide assistance. Evidence in support of this assumption came from studies by Fogg et al.[104] on dimer catalysts with bidentate chloride ligands. Furthermore, Grubbs and co-workers clearly evidenced catalyst deactivation for the methylidene analogue of **20**,[105] the key intermediate in metathesis catalyzed by Ru–alkylidenes; its thermal decomposition yielded a dinuclear Ru complex, **78**, with a bridging carbide and a hydride ligand, and methyltricyclohexylphosphonium chloride (Scheme 43). Involvement of dissociated phosphine in the decomposition was proposed. The dinuclear complex has catalytic activity for olefin isomerization, which could be responsible for the competing isomerization processes observed in certain olefin metathesis reactions.

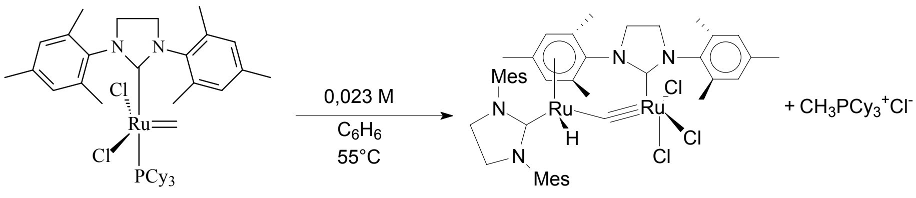

20a **78**

Scheme 43

Grubbs et al. reported on the substitution of the chloride ligands with alkoxide groups on to complex **12** to form 14-electron four coordinate species.[105,106] While the O–*t*Bu substituted complex **79** is a very poor catalyst, incorporation of more electron withdrawing groups as in **80** and **81** leads to an increased activity, however, with some loss in thermal stability.[106] Upon activation with HCl, **80** becomes more active than **12** which was ascribed to protonation of the alkoxy groups and formation of free alcohol (Scheme 44).[106]

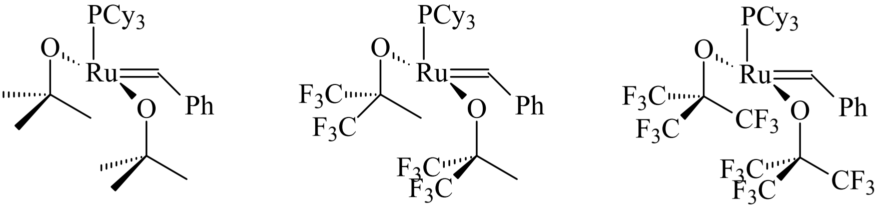

79 **80** **81**

Scheme 44

Later on, Fogg et al. reported on the reaction of **76** with two equivalents of $TlOC_6F_5$ to yield **82**; this complex exceeds in activity complexes **79–81** and even outperforms **20** for the RCM of DEDAM with turnovers up to 40,000.[107] Recently, the same group described mixed ligand systems with one "phenoxy" and one halide ligand (**83)** that show catalytic activity exceeding that of **20**, **33**, and **34**.[108] Substitution of the chloride ligands in **12** with trifluoroacetic acid or other similar groups had as effect in all cases a drop in activity for RCM of DEDAM as compared to the parent **12**.[109,110]

Continuing along these lines, Buchmeiser et al. found that the Grubbs–Hoveyda catalyst **84** with trifluoroacetic acid groups gives turnover numbers (TONs) in the same range as **12** and **20**.[111] Moreover, the complex **85**, endowed with a six-membered NHC, exhibited almost twice as high time-of-flights (TOFs) than its chloride analogue.[54]

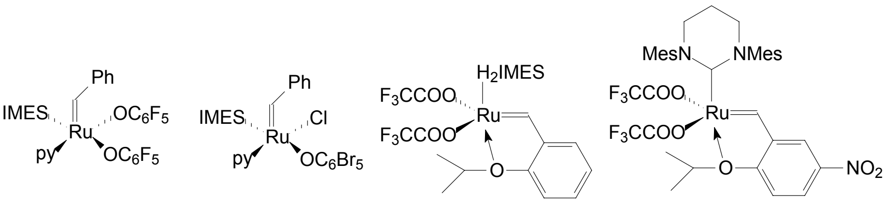

82 **83** **84** **85**

Scheme 45

An interesting Ru catalytic system, unravelled by Fröhlich et al. resulted from substitution of **12** with two equivalents of silver 2-pyridinecarboxylate; this catalyst was active for RCM, however, only after HCl activation.[112] An innovative approach was advanced by Piers et al. leading to the 14-electron species **86**, up to now the fastest initiating species reported for RCM of DEDAM (Scheme 46).[113] Therefore, induction of steric bulkiness at the carbene site of the four coordinate species **86** has proved to be more advantageous than that provided by alkoxy ligands (**79–81**).

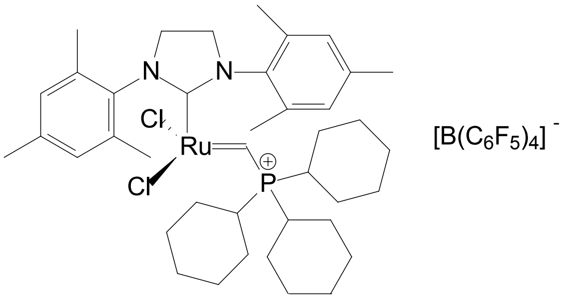

86

Scheme 46

A lasting alternative direction in Ru metathesis catalysts relating to bidentate phosphanes complexes has been introduced by Hofmann et al.[114] with the synthesis of **87** and **88** (Scheme 47)[115]; while **87** shows modest activity for the ROMP of cyclooctene, **88** clearly outperforms **12**.

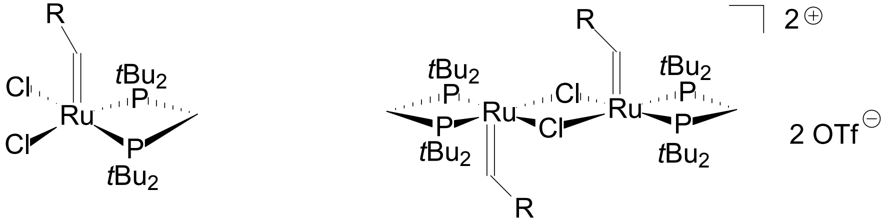

87 **88**

Scheme 47

The performance of **87** has been improved by Fogg et al.[116] by in situ replacing the dtbpm with dcypb, dppb, and 2,2′-bis(diphenylphosphino)-1,1′-binaphthyl (BINAP) (Scheme 48). Significantly, they found that all these ligands outperform the dtbpm from **87** and they even managed to achieve low polydispersity polymers. The activity increase follows the order: dcypb < dppb < BINAP.[116]

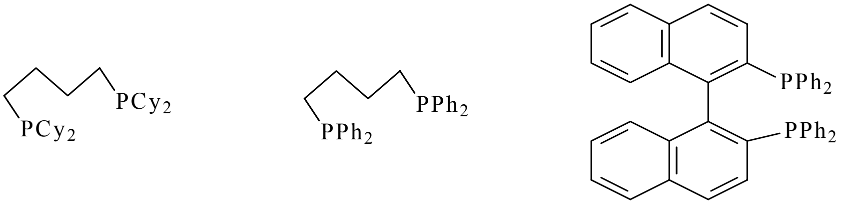

dcypb dppb BINAP

Scheme 48

Many reliable approaches to access more active Ru catalysts for metathesis reactions have been recently developed.[109,110,117–120] An appealing alternative especially for practical applications in RCM and CM, i.e. immobilization of the catalysts onto solid supports is briefly surveyed in the following section.

11. Immobilized Ru–alkylidene complexes

Immobilizing homogeneous Ru complexes onto supports offers recognized advantages for productive organic synthesis (simpler procedures, ready separation of products, recyclability of catalysts, operation in continuous flow, manageable polymer properties). Among other ligands, NHC have been employed to link metal complexes onto solid supports.[121] Blechert[122] applied this beneficial route to access a permanently immobilized and highly active

NHC Ru–benzylidene complex **89** (Scheme 49). Quite recently Grubbs[123] disclosed water-soluble NHC-Ru catalysts supported by poly(ethylene glycol), catalytically active in aqueous media.

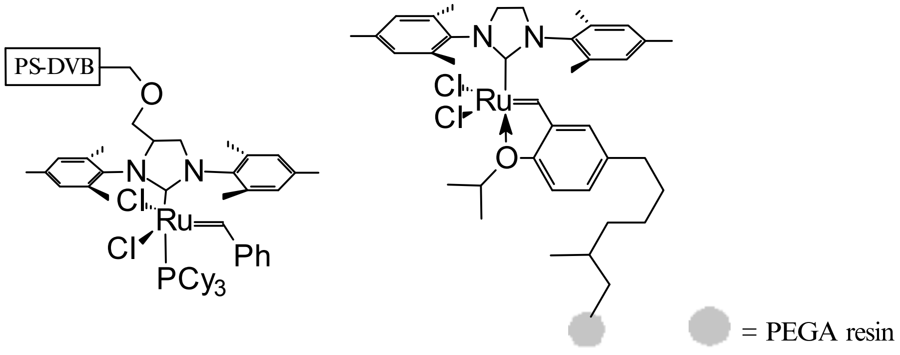

89 **90**

Scheme 49

Immobilization can be achieved not only through the NHC but also through other ligands. Thus, Blechert prepared polymer-bound catalysts of the Hoveyda–Grubbs-type, for use in either as homogeneous[124] or heterogeneous catalysis (**90**).[125] In a further variant of the above strategy, Lamaty et al.[126] introduced a polymer-bound NHC–Ru catalyst (**91**) resulting from exchange of the benzylidene unit in the Grubbs second-generation catalyst with a polyethylene glycol (PEG)-supported benzylidene ligand (Scheme 50).

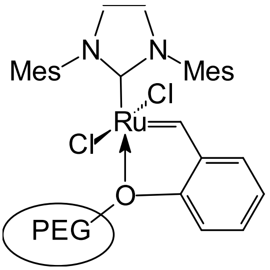

91

Scheme 50

A recently developed technique for non-covalent immobilization to soluble supports involves room temperature ionic liquids (RTILs). Thus, IL-tagged counterparts of the Hoveyda–Grubbs catalyst such as **92**[127] and **93**[128] have been used with good results in metathesis reactions conducted in ILs or IL/organic solvent mixtures (biphasic catalysis) showing an appreciable recyclability combined with high reactivity and extremely low residual Ru levels in the products (Scheme 51).

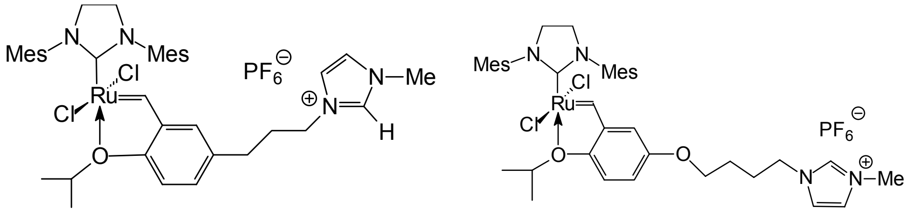

92 **93**

[BMI][PF_6]/toluene (1:3 v/v) [Bmim][PF_6]/CH_2Cl_2 (1:9 v/v)

Scheme 51

Also, novel solid-phase bound Hoveyda-type catalysts were successfully applied in RCM reactions conducted in $scCO_2$ for which very low level of leaching of Ru into the product were observed; performance of the catalysts highly depended on the nature of the support.[129] Second-generation bis-silylated Hoveyda–Grubbs-type Ru–alkylidene complexes have also been covalently bonded to the silica matrix of MCM-41.[130]

Further entries into immobilization lead to heterogeneous catalysts via anchoring NHC–Ru complexes in the pore channels of mesoporous silica,[131a] or silica gel[131b] and fluorous silica gel [131c]; this kind of immobilization resulted in a relatively high catalytic activity in olefin metathesis reactions and reusability of five or more times. In this connection, studies were conducted in the Verpoort research group to develop supported Schiff base–Ru catalysts for RCM, ROMP, Kharasch addition, ATRP, and vinylation reactions. To this purpose, two multifunctional Schiff base–Ru–carbene complexes were prepared and supported on MCM-41, providing recyclable and efficient solid catalysts (**94** and **95**). The strategy followed was to tether the organometallic compounds onto mesoporous silica surfaces by treating the inorganic support with the tris(alkoxy)silyl functionalized Ru complex. (Scheme 52).[132–134]

A new heterogeneous Ru catalyst (**96**) that exhibited excellent stability, reusability, and leaching properties has also been prepared via a similar approach by the same group (Scheme 53).[135–138]

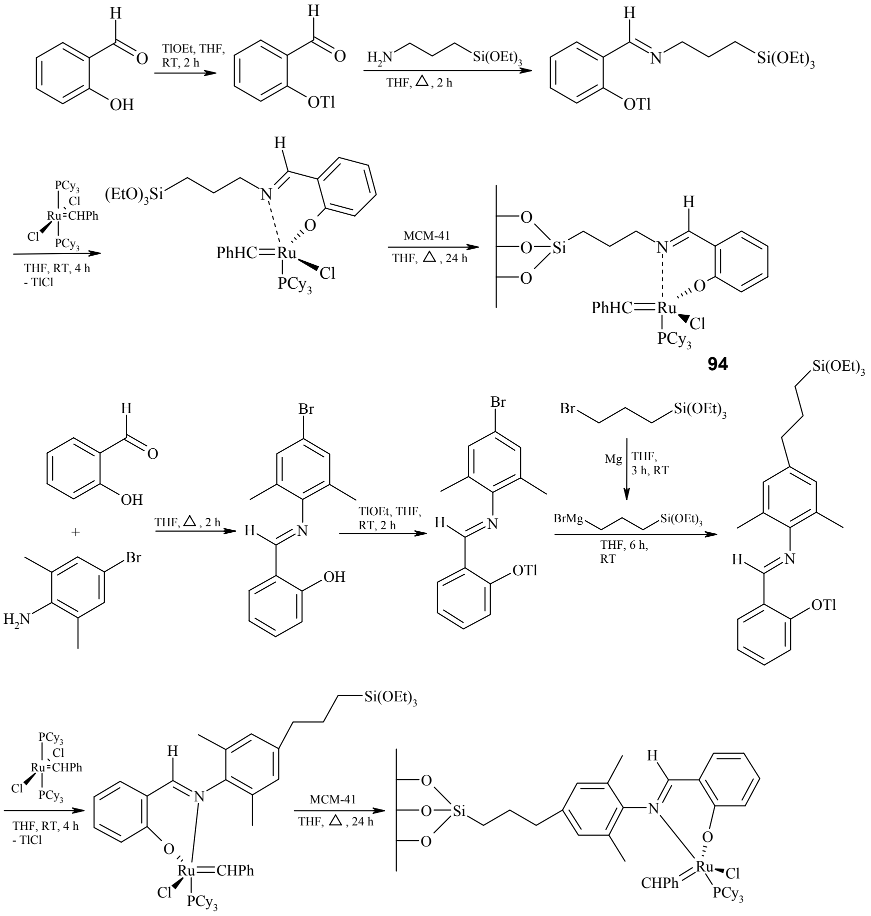

94

95

Scheme 52

By reviewing the main representatives of metal carbene catalysts, fruitfully applied in metathesis especially during the last few years, this paper has attempted to relief the many exquisite contributions and the overwhelming work invested in astute design and innovative synthesis in this area. As reflected by the abundance of references cited, to attain an even greater level of excellence in the creation of new, better performing, and more environment-friendly metathesis catalysts is still a matter of great interest.

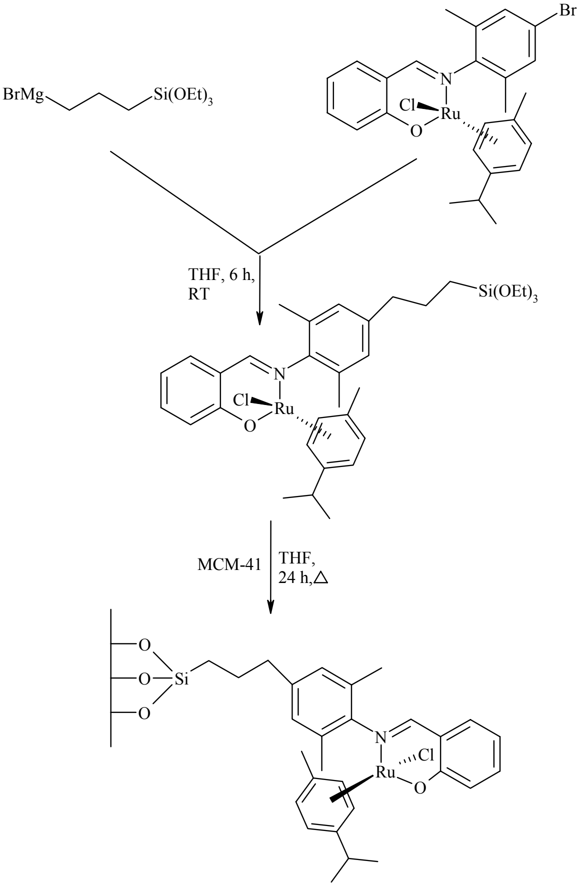

96

Scheme 53

References

[1] (a) Grubbs, R.H., (ed.), Handbook of Metathesis, Vols. 1–3, Wiley-VCH, Weinheim, 2003; (b) Astruc, D., New J. Chem. 2005, 29:42; (c) Connon, S.J., Blechert, S., Angew. Chem. Int. Edit. 2003, 42:1900; (d) Basset, J.M., Coperet, C., Soulivong, D., Taoufik, M., Thivolle-Cazat, J., Angew. Chem. Int. Edit. 2006, 45:6082.
[2] Hérisson, J.-L., Chauvin, Y., Macromol. Chem. 1971, 141:161.
[3] First synthesized by Sinn, H. and Kaminsky, W (Ref. 1a).
[4] (a) Tebbe, F.N., Parshall, G.W., Reddy, G.S., J. Am. Chem. Soc. 1978, 100:3611; (b) Tebbe, F.N., Parshall, G.W., Ovenall, D.W., J. Am. Chem. Soc. 1979, 101:5074; (c) Tebbe, F.N., Parshall, G.W., Ovenall, D.W., J. Am. Chem. Soc. 1980, 102:6149.

[5] Howard, T.R., Lee, J.B., Grubbs, R.H., J. Am. Chem. Soc. 1980, 102:6876.

[6] Gilliom, L.R., Grubbs, R.H., J. Am. Chem. Soc. 1986, 108:733.

[7] Kress, J., Osborn, J.A., Ivin, K.J., Rooney, J.J., J. Am. Chem. Soc. 1987, 109:899.

[8] Schrock, R.R., J. Am. Chem. Soc. 1974, 96:6796.

[9] Schrock, R.R., J. Am. Chem. Soc. 1975, 97:6577.

[10] McLain, S.J., Wood, C.D., Schrock, R.R., J. Am. Chem. Soc. 1979, 101:4558.

[11] Schrock, R.R., Rocklage, S.M., Wengrovius, J.H., Rupprecht, G., Feilmann, J., J. Mol. Catal. 1980, 8:73.

[12] Rocklage, S.M., Feilmann, J., Rupprecht, G., Messerle, L.W., Schrock, R.R., J. Am. Chem. Soc. 1981, 103:1440.

[13] Schrock, R.R., in: Grubbs, R.H., (ed.), Handbook of Metathesis, Vol. 1, Wiley-VCH, Weinheim, 2003.

[14] Wengrovius, J.H., Schrock, R.R., Churchill, M.R., Missert, W.J., Youngs, W.J., J. Am. Chem. Soc. 1980, 102:4515.

[15] Churchill, M.R. Rheingold, A.L., Youngs, W.J., Schrock, R.R., J. Organomet. Chem. 1981, 204:C17.

[16] (a) Schrock, R.R., J. Mol. Catal. A: Chem. 2004, 213:21–30; (b) Wengrovius, J.H., Sancho, J., Schrock, R.R., J. Am. Chem. Soc. 1981, 103:3932; (c) Churchill, M.R., Ziller, J.W., Freudenberger, J.H., Schrock, R.R., Organometallics 1984, 3:1563; (d) Freudenberger, J.H., Schrock, R.R., Churchill, M.R., Rheingold, A.L., Ziller, J.W., Organometallics 1984, 3:1563; (e) Schrock, R.R., Acc. Chem. Res. 1986, 19:342.

[17] Schrock, R.R., DePue, R., Feldman, J., Schaverien, C.J. Dewan, C.J., Liu, A.H., J. Am. Chem. Soc. 1988, 110:1423.

[18] Murdzek, J.S., Schrock, R.R., Organometallics 1987, 6:1373.

[19] Schrock, R.R., Murdzek, J.S., Bazan, G.C., Robbins, J.M., O’Regan, M., J. Am. Chem. Soc. 1990, 112:3875.

[20] Alexander, J.B., La, D.S., Cefalo, D.R., Hoveyda, A.H., Schrock, R.R., J. Am. Chem. Soc. 1998, 120:4041–4042.

[21] La, D.S., Alexander, J.B., Cefalo, D.R., Graf, D.D., Hoveyda, A.H., Schrock, R.R., J. Am. Chem. Soc. 1998, 120:9720.

[22] Zhu, S.S., Cefalo, D.R., La, D.S., Jamieson, J.Y., Davis, W.M., Hoveyda, A.H., Schrock, R.R., J. Am. Chem. Soc. 1999, 121:8251.

[23] La, D.S., Ford, J.G., Satteley, E.S., Bonitatebus, P.J., Schrock, R.R., Hoveyda, A.H., J. Am. Chem. Soc. 1999, 121:11603.

[24] Weatherhead, G.S., Ford, J.G., Alexanian, E.J., Schrock, R.R., Hoveyda, A.H., J. Am. Chem. Soc. 2000, 122:1828.

[25] Alexander, J.B., Schrock, R.R., Davis, W.M., Hultzsch, K.C., Hoveyda, A.H., Houser, J.H., Organometallics 2000, 19:3700.

[26] Dolman, S.J., Sattely, E.S., Hoveyda, A.H., Schrock, R.R., J. Am. Chem. Soc. 2002, 124:6991.

[27] Weatherhead, G.S., Houser, J.H., Ford, J.G., Jamieson, J.Y., Schrock, R.R., Hoveyda, A.H., Tetrahedron Lett. 2000, 41:9553.

[28] Hoveyda, A.H., Schrock, R.R., Chem. Eur. J. 2001, 7:945.

[29] Cefalo, D.R., Kiely, A.F., Wuchrer, M., Jamieson, J.Y., Schrock, R.R., Hoveyda, A.H., J. Am. Chem. Soc. 2001, 123:3139.

[30] Aeilts, S.L., Cefalo, D.R., Bonitatebus, P.J., Houser, J.H., Hoveyda, A.H., Schrock, R.R., Angew. Chem. Int. Edit. 2001, 40:1452.

[31] La, D.S., Sattely, E.S., Ford, J.G., Schrock, R.R., Hoveyda, A.H., J. Am. Chem. Soc. 2001, 123:7767.

[32] Hultzsch, K.C., Bonitatebus, P.J., Jernelius, J., Schrock, R.R., Hoveyda, A.H., Organometallics 2001, 20:4705.

[33] Tsang, W.C.P., Schrock, R.R., Hoveyda, A.H., 222nd ACS Meeting, Chicago, 2001, Abstract U620.

[34] Schrock, R.R., Jamieson, J.Y., Dolman, S.J., Miller, S.A., Bonitatebus, P.J., Hoveyda, A.H., Organometallics 2002, 21:409.

[35] Hultzsch, K.C., Jernelius, J.A., Hoveyda, A.H., Schrock, R.R., Angew. Chem. Int. Edit. 2002, 41:589.

[36] Kiely, A.F., Jernelius, J.A., Schrock, R.R., Hoveyda, A.H., J. Am. Chem. Soc. 2002, 124:2868.

[37] Nguyen, S.T., Johnson, L.K., Grubbs, R.H., Ziller, J.W., J. Am. Chem. Soc. 1992, 114:3974.

[38] Nguyen, S.T., Grubbs, R.H., Ziller, J.W., J. Am. Chem. Soc. 1993, 115:9858.

[39] (a) Fu, G.C., Nguyen, S.T., Grubbs, R.H, J. Am. Chem. Soc. 1993, 115:9856; (b) Fu, G.C., Nguyen, S.T., Grubbs, R.H., J. Am. Chem. Soc. 1993, 115:9858; (c) Kim, S.H., Bowden, N., Grubbs, R.H., J. Am. Chem. Soc. 1994, 116;10801; (d) Miller, S.J., Kim, S.H., Chen, Z.R., Grubbs, R.H., J. Am. Chem. Soc. 1995, 117:2108.

[40] (a) Morken, J.P., Didiuk, M.T., Visser, M.S., Hoveyda, A.H., J. Am. Chem. Soc. 1994, 116:3123; (b) Borer, B.C., Deerenberg, S., Bieraugel, H., Pandit, U.K., Tetrahedron Lett. 1994, 35:3191; (c) Huwe, C.M., Blechert, S., Tetrahedron Lett. 1995, 36:1621.

[41] (a) Schwab, P., Grubbs, R.H., Ziller, J.W., J. Am. Chem. Soc. 1996, 118:100; (b) Schwab, P., France, M.B., Ziller, J.W., Grubbs, R.H., Angew. Chem. Int. Edit. 1995, 34:2039.

[42] (a) Olivan, M., Caulton, K.G., Chem. Commun. 1997, 1733; (b) Wolf, J., Stuer, W., Grunwald, C., Werner, H., Schwab, P., Schulz, M., Angew. Chem. Int. Edit. 1998, 37:1124; (c) Wilhelm, T.E., Belderrain, T.R., Brown, S.N., Grubbs, R.H., Organometallics 1997, 16:3867; (d) van der Schaaf, P.A., Kolly, R., Hafner, A., Chem. Commun. 2000, 1045; (e) van der Schaaf, P.A., Kolly, R., Hafner, Chem. Commun. 2001, 940; (f) Gandelman, M., Rybtchinski, B., Ashkenazi, N., Gauvin, R.M., Milstein, D., J. Am. Chem. Soc. 2001, 123:5372; (g) Belderrain, T.R., Grubbs, R.H., Organometallics 1997, 16:4001; (h) Furstner, A., Guth, O., Duffels, A., Seidel, G., Liebl, M., Gabor, B., Mynott, R., Chem. Eur. J. 2001, 7:4811; (i) Harlow, K.J., Hill, A.F., Wilton-Ely, J.D.E.T., J. Chem. Soc., Dalton Trans. 1999, 285; (j) Jafarpour, L., Schanz, H.-J., Stevens, E.D., Nolan, S.P., Organometallics 1999, 18:5416.

[43] (a) Bourissou, D., Guerret, O., Gabai, F.P., Bertrand, G., Chem. Rev. 2000, 100:39; (b) Herrmann, W.A., Weskamp, T., Böhm, V.P.W., Adv. Organomet. Chem. 2001, 48:1; (c) Dragutan, V. Dragutan, I., Demonceau, A., Platinum Metals Rev. 2005, 49:123.

[44] (a) Herrmann, W.A., Kocher, C., Angew. Chem. Int. Edit. 1997, 36:2162; (b) Huang, J., Schanz, H.-J., Stevens, E.D., Nolan, S.P., Organometallics 1999, 18:2370; (c) Jafarpour, L., Nolan, S.P., Adv. Organomet. Chem. 2001, 46:181.

[45] (a) Scholl, M., Ding, S., Lee, C.W., Grubbs, R.H., Organic Lett. 1999, 1:953; (b) Weskamp, T., Kohl, F.J., Hieringer, W., Gleich, D., Herrmann, W.A., Angew. Chem. Int. Edit. 1999, 38:2416; (c) Huang, J.K., Stevens, E.D., Nolan, S.P., Petersen, J.L., J. Am. Chem. Soc. 1999, 121:2674; (d) Huang, J.K., Schanz, H.J., Stevens, E.D., Nolan, S.P., Organometallics 1999, 18:5375.

[46] (a) Weskamp, T., Schattenmann, W.C., Spiegler, M., Herrmann, W.A., Angew. Chem. Int. Edit. 1998, 37:2490; (b) Weskamp, T., Kohl, F.J., Hieringer, W., Gleich, D., Herrmann, W.A., Angew. Chem. Int. Edit. 1999, 38:2416.

[47] Scholl, M., Trnka, T.M., Morgan, J.P., Grubbs, R.H., Tetrahedron Lett. 1999, 40:2247.

[48] Huang, J., Stevens, E.D., Nolan, S.P., Petersen, J.L., J. Am. Chem. Soc. 1999, 121:2674.

[49] Love, J.A., Sanford, M.S., Day, M.W., Grubbs, R.H., J. Am. Chem. Soc. 2003, 125:10103.

[50] Sanford, M.S., Love, J.A., Grubbs, R.H., J. Am. Chem. Soc. 2001, 123:6543.

[51] Sanford, M.S., Ulman, M., Grubbs, R.H., J. Am. Chem. Soc. 2001, 123:749.

[52] Herrmann, W.A., Ofele, K., von Preysing, D., Herdtweck, E., J. Organomet. Chem. 2003, 684:235–248.

[53] Mayr, M., Wurst, K., Ongania, K.H., Buchmeiser, M.R., Chem.-Eur. J. 2004, 10:1256–1266.

[54] Yang, L.R., Mayr, M., Wurst, K., Buchmeiser, M.R., Chem.-Eur. J. 2004, 10:5761–5770.

[55] Yun, J., Marinez, E.R., Grubbs, R.H., Organometallics 2004, 23:4172–4173.

[56] Despagnet-Ayoub, E., Grubbs, R.H., J. Am. Chem. Soc. 2004, 126:10198–10199.

[57] Despagnet-Ayoub, E., Grubbs, R.H., Organometallics 2005, 24:338–340.

[58] (a) Furstner, A., Ackermann, L., Gabor, B., Goddard, R., Lehmann, C.W., Mynott, R., Stelzer, F., Thiel, O.R., Chem. Eur. J. 2001, 7:3236–3253; (b) Furstner, A., Liebl, M., Lehmann, C.W., Picquet, M., Kunz, R., Bruneau, C., Touchard, D., Dixneuf, P.H., Chem.-Eur. J. 2000, 6:1847–1857.

[59] Vehlow, K., Maechling, S., Blechert, S., Organometallics 2006, 25:25–28.

[60] Ledoux, N., Allaert, B., Pattyn, S., Van Der Mierde, H., Vercaemst, C., Verpoort, F., Chem. Eur. J. 2006, 12:4654.

[61] Dinger, M.B., Nieczypor, P., Mol, J.C., Organometallics 2003, 22:5291–5296.

[62] (a) Van Veldhuizen, J.J., Gillingham, D.G., Garber, S.B., Kataoka, O., Hoveyda, A.H., J. Am. Chem. Soc. 2003, 125:12502–12508; (b) Hoveyda, A.H., Gillingham, D.G., Van Veldhuizen, J.J., Kataoka, O., Garber, S.B., Kingsbury, J.S., Harrity, J.P.A., Org. Biomol. Chem. 2004, 2:1–16;

(c) Gillingham, D.G., Kataoka, O., Garber, S.B., Hoveyda, A.H., J. Am. Chem. Soc. 2004, 126:12288.

[63] Kingsbury, J.S., Harrity, J.P.A., Bonitatebus, P.J., Hoveyda, A.H., J. Am. Chem. Soc. 1999, 121:791.

[64] Gessler, S., Randl, S., Blechert, S., Tetrahedron Lett. 2000, 41:9973.

[65] Garber, S.B., Kingsbury, J.S., Gray, B.L., Hoveyda, A.H., J. Am. Chem. Soc. 2000, 122:8168.

[66] (a) Wakamatsu, H., Blechert, S., Angew. Chem. Int. Edit. 2002, 41:2403; (b) Wakamatsu, H., Blechert, S., Angew. Chem. Int. Edit. 2002, 41:794; (c) Dunne, A.M., Mix, S., Blechert, S., Tetrahedron Lett. 2003, 44:2733.

[67] (a) Grela, K., Harutyunyan, S., Michrowska, A., Angew. Chem. Int. Edit. 2002, 41:4038; (b) Michrowska, A., Gulajski, L., Kakzsmaeska, Z., Mennecke, K., Kirshning, A., Grela, K., Green Chem. 2006, 8:685; (c) Grela, K., Kim, M., Eur. J. Org. Chem. 2003, 963; (d) Michrowska, A., Bujok, R., Harutyunyan, S., Sashuk, V., Dolgonos, G., Grela, K., J. Am. Chem. Soc. 2004, 126:9318.

[68] van der Schaaf, P.A., Kolly, R., Kirner, H.J., Rime, F., Muhlebach, A., Hafner, A., J. Organomet. Chem. 2000, 606:65.

[69] Ung, T., Hejl, A., Grubbs, R.H., Schrodi, Y., Organometallics 2004, 23:5399.

[70] Furstner, A., Thiel, O.R., Lehmann, C.W., Organometallics 2002, 21:331.

[71] Slugovc, C., Perner, B., Stelzer, F., Mereiter, K., Organometallics 2004, 23:3622.

[72] (a) Van Veldhuizen, J.J., Garber, S.B., Kingsbury, J.S., Hoveyda, A.H., J. Am. Chem. Soc. 2002, 124:4954; (b) Van Veldhuizen, J.J., Campbell, J.E., Giudici, R.E., Hoveyda, A.H., J. Am. Chem. Soc. 2005, 127:6877.

[73] (a) Katayama, H., Ozawa, F., Organometallics 1998, 17:5190; (b) Katayama, H., Ozawa, F., Chem. Lett. 1998, 27:67; (c) Katayama, H., Ozawa, F., Coord. Chem. Rev. 2004, 248:1703.

[74] (a) Bruneau, C., Dixneuf, P.H., Acc. Chem. Res. 1999, 32:311; (b) Dragutan, V., Dragutan, I., Platinum Met. Rev., 2004, 48:148; (c) Bruneau, C., Dixneuf, P.H., Angew. Chem. Int. Edit. 2006, 45:2176.

[75] Sanford, M.S., Henling, L.M., Grubbs, R.H., Organometallics 1998, 17:5384.

[76] Del Rio, I., van Koten, G., Tetrahedron Lett. 1999, 40:1401.

[77] (a) Semeril, D., Dixneuf, P.H., in: İmamoğlu, Y., Bencze, L., (eds), Novel Metathesis Chemistry: Well-Defined Initiator Systems for Speciality Chemical Synthesis, Tailored Polymers and Advanced Material Applications, NATO Advanced Study Institute (ASI), Kluwer Academic, Dordrecht, The Netherlands, 2003; (b) Rigaut, R., Touchard, D., Dixneuf, P.H., Coord. Chem. Rev. 2004, 248:1585–1601; (c) Dixneuf, P.H., Bruneau, C., in: Helmchen, G., (ed.), Organic Synthesis via Organometallics, Viegweg, Wiesbaden, Germany, 1997, pp. 1–20.

[78] Fürstner, A., Hill, A.F., Liebl, M., Wilton-Ely, J.D.E.T., Chem. Commun. 1999, 601.

[79] (a) Schanz, H.-J., Jafarpour, L., E.D. Stevens, E.D., Nolan, S.P., Organometallics 1999, 18:5187; (b) Jafarpour, L., Schanz, H.-J., Stevens, E.D., Nolan, S.P., Organometallics 1999, 18:5416.

[80] Dias, E.L., Grubbs, R.H., Organometallics 1998, 17:2758.

[81] (a) Selegue, J.P., Organometallics 1982, 1:217; (b) Selegue, J.P, Coor. Chem. Rev. 2004, 248:1543; (c) Touchard, D., Guesmi, S., Bouchaib, M., Haquette, P., Daridor, A, Dixneuf, P.H., Organometallics 1996, 15:2579; (d) Touchard, D., Haquette, P., Daridor, A., Romero, A., Dixneuf, P.H., Organometallics 1998, 17:3844; (e) Gamasa, M.P., Gimeno, J., Gonzales-Bernardo, C., Borge, J., Garcia-Granda, S., Organometallics 1997, 16:2483; (f) Crochet, P., Demerseman, B., Valejo, M.I., Organometallics 1997, 16:5406; (g) Tenorio, M.A.J., Tenorio, M.J., Puerta, M.C., Valerga, P., Organometallics 1997, 16:5528; (h) Cadierno, V., Gamasa, M.P., Gimeno, J., Iglesias, L., Garcia-Granda, S., Inorg. Chem. 1999, 38:2874; (i) Fürstner, A., Picquet, M., Bruneau, C., Dixneuf, P.H., J. Chem. Soc. Chem. Commun. 1998, 1315.

[82] (a) Fürstner, A., Liebl, M., Lehmann, C.W., Picquet, M., Kunz, R., Bruneau, C., Touchard, D., Dixneuf, P.H., Chem. Eur. J. 2000, 6:1847; (b) Semeril, D., Le Notre, J., Bruneau, C., Dixneuf, P.H., Kolomiets, A.F., Osipov, S.N., New J. Chem. 2001, 25:16.

[83] (a) Castarlenas, R., Semeril, D., Noels, A.F., Demonceau, A., Dixneuf, P.H., J. Organomet. Chem. 2002, 663:235; (b) Csihony, S., Fischmeister, C., Bruneau, C., Horvath, I.T., Dixneuf, P.H., New J. Chem. 2002, 25:1667.

[84] (a) Semeril, D., Olivier-Bourbigou, H., Bruneau, C., Dixneuf, P.H., Chem. Commun. 2002, 146; (b) Semeril, D., Bruneau, C., Dixneuf, P.H., Adv. Synth. Catal. 2002, 344:585.

[85] (a) Louie, J., Grubbs, R.H., Angew. Chem. Int. Edit. 2001, 40:247; (b) Dragutan, I., Dragutan, V., Filip, P., Arkivoc 2005, x:105.

[86] Schanz, H.-J., Jafarpour, L., Stevens, E.D., Nolan, S.P., Organometallics 1999, 18:5187.

[87] Jafarpour, L., Huang, J., Stevens, E.D., Nolan, S.P., Organometallics 1999, 18:3760.

[88] Cetinkaya, B., Demir, S., Ozdemir, I., Toupet, L., Semeril, D., Bruneau, C., Dixneuf, P.H., New J. Chem. 2001, 25:519.

[89] Fürstner, A., Thiel, O.R., Ackermann, L., Schanz, H.-J., Nolan, S.P., J. Org. Chem. 2000, 65:2204.

[90] Jafarpour, L., Schanz, H.-J., Stevens, E.D., Nolan, S.P., Organometallics 1999, 18:5416.

[91] Clavier, H., Petersen, J.L., Nolan, S.P., J. Organomet. Chem. 2006, 691:5444.

[92] (a) Simal, F., Delaude, L., Jan, D., Demonceau, A., Noels, A.F., Polym. Prepr. (Am. Chem. Soc. Div. Polym. Chem.) 1999, 40:226; (b) Delaude, L., Demonceau, A., Noels, A.F., Chem. Commun. 2001, 986; (c) Simal, F., Delfosse, S., Demonceau, A., Noels, A.F., Denk, K., Kohl, F.J., Weskamp, T., Herrmann, W.A., Chem. Eur. J. 2002, 8:3047; (d) Delaude, L., Delfosse, S., Richel, A., Demonceau, A., Noels, A.F., Chem. Commun. 2003, 1526.

[93] (a) Chang, S., Jones, L., Wang, C.M., Henling, L.M., Grubbs, R.H., Organometallics 1998, 17:3460; (b) Ulman, M., Grubbs, R.H., J. Org. Chem. 1999, 64:7202.

[94] (a) De Clercq, B., Verpoort, F., Tetrahedron Lett. 2001, 42:8959; (b) De Clercq, B., Verpoort, F., J. Mol. Catal. A: Chem. 2002, 180:67;

(c) Drozdzak, R., Allaert, B., Ledoux, N., Dragutan, I., Dragutan, V., Verpoort, F., Coord. Chem. Rev. 2005, 249:3055.
[95] (a) De Clercq, B., Verpoort, F., Adv. Synth. Catal. 2002, 344:639; (b) Opstal, T., Couchez, K., Verpoort, F., Adv. Synth. Catal. 2003, 345:393; (c) Drozdzak, R., Allaert, B., Ledoux, N., Dragutan, I., Dragutan, V., Verpoort, F., Adv. Synth. Catal. 2005, 347:1721.
[96] De Clercq, B., Verpoort, F., Tetrahedron Lett. 2002, 43:4687.
[97] (a) Opstal, T., Verpoort, F., Angew. Chem. Int. Edit. 2003, 42:2876; (b) De Clercq, B., Verpoort, F., Macromolecules 2002, 35:8943; (c) Drozdzak, R., Ledoux, N., Allaert, B., Dragutan, I., Dragutan, V., Verpoort, F., Central Eur. J. Chem. 2005, 3:404.
[98] De Clercq, B., Verpoort, F., Tetrahedron Lett. 2002, 43:9101.
[99] De Clercq, B., Verpoort, F., J. Organomet. Chem. 2003, 672:11.
[100] Denk, K., Fridgen, J., Herrmann, W.A., Adv. Synth. Catal. 2002, 344:666.
[101] Sanford, M.S., Love, J.A., Grubbs, R.H. Organometallics 2001, 20:5314.
[102] Love, J.A., Morgan, J.P., Trnka, T.M., Grubbs, R.H., Angew. Chem. Int. Edit. 2002, 41:4035.
[103] Choi, T.L., Grubbs, R.H., Angew. Chem. Int. Edit. 2003, 42:1743.
[104] Amoroso, D., Yap, G.P.A., Fogg, D.E., Organometallics 2002, 21:3335.
[105] Hong, S.H., Day, M.W., Grubbs, R.H., J. Am. Chem. Soc. 2004, 126:7414.
[106] Sanford, M.S., Henling, L.M., Day, M.W., Grubbs, R.H., Angew. Chem. Int. Edit. 2000, 39:3451.
[107] Conrad, J.C., Amoroso, D., Czechura, P., Yap, G.P.A., Fogg, D.E., Organometallics 2003, 22:3634–3636.
[108] Conrad, J.C., Parnas, H.H., Snelgrove, J.L., Fogg, D.E., J. Am. Chem. Soc. 2005, 127:11882.
[109] Buchowicz, W., Mol, J.C., Lutz, M., Spek, A.L., J. Organomet. Chem. 1999, 588:205.
[110] Buchowicz, W., Ingold, F., Mol, J.C., Lutz, M., Spek, A.L., Chem.-Eur. J. 2001, 7:2842.
[111] (a) Krause, J.O., Nuyken, O., Wurst, K., Buchmeiser, M.R., Chem.-Eur. J. 2004, 10:777; (b) Halbach, T.S., Mix, S., Fischer, D., Maechling, S., Krause, J.O., Sievers, C., Blechert, S., Nuyken, O., Buchmeiser, M.R., J. Org. Chem. 2005, 70:4687.
[112] Hahn, F.E., Paas, M., Frohlich, R., J. Organomet. Chem. 2005, 690:5816.
[113] Romero, P.E., Piers, W.E., Mcdonald, R., Angew. Chem. Int. Edit. 2004, 43:6161.
[114] (a) Hansen, S.M., Rominger, F., Metz, M., Hofmann, P., Chem.-Eur. J. 1999, 5:557–566; (b) Volland, M. A.O., Hansen, S.M., Rominger, F., Hofmann, P., Organometallics 2004, 23:800.
[115] Hansen, S.M., Volland, M.A.O., Rominger, F., Eisentrager, F., Hofmann, P., Angew. Chem. Int. Edit. 1999, 38:1273.
[116] Amoroso, D., Fogg, D.E., Macromolecules 2000, 33:2815.
[117] Cetinkaya, B., Demir, S., Ozdemir, I., Toupet, L., Semeril, D., Bruneau, C., Dixneuf, P.H., Chem.-Eur. J. 2003, 9:2323.
[118] Six, C., Beck, K., Wegner, A., Leitner, W., Organometallics 2000, 19:4639.
[119] Gatard, S., Nlate, S., Cloutet, E., Bravic, G., Blais, J.C., Astruc, D., Angew. Chem. Int. Edit. 2003, 42:452.

[120] Baratta, W., Herrmann, W.A., Rigo, P., Schwarz, J., J. Organomet. Chem. 2000, 594, 489.

[121] (a) Ahmed, M., Arnauld, T., Barrett, A.G.M., Braddock, D.C., Procopiou, A., Synlett, 2000, 9:1007; (b) Jafarpour, L., Nolan, S.P., Org. Lett. 2000, 2:4075.

[122] Schurer, S.C., Gessler, S., Buschmann, N., Blechert, S., Angew. Chem. Int. Edit. 2000, 39:3898.

[123] (a) Gallivan, J.P., Jordan, J.P., Grubbs, R.H., Tetrahedron Lett. 2005, 46:2577; (b) Hong, S.H., Grubbs, R.H., J. Am. Chem. Soc. 2006, 128:3508.

[124] Connon, S.J., Dunne, A.M., Blechert, S., Angew. Chem. Int. Edit. 2002, 41:3835.

[125] Connon, S.J., Blechert, S., Bioorg. Med. Chem. Lett. 2002, 12:1873.

[126] Varray, S., Lazaro, R., Martinez, J., Lamaty, F., Organometallics 2003, 22:2426.

[127] (a) Clavier, H., Audic, N., Mauduit, M., Guillemin, J-C., Chem. Commun. 2004, 2282; (b) Clavier, H., Audic, N., Guillemin, Mauduit, M., J. Organomet. Chem. 2005, 690:3585.

[128] Yao, Q., Sheets, M., J. Organomet. Chem. 2005, 690:3577.

[129] Michalek, F., Madge, D., Ruhe, J., Bannwarth, W., Eur. J. Org. Chem. 2006, 577.

[130] (a) Fischer D., Blechert, S., Adv. Synth. Catal. 2006, 347:1239; (b) Elias, X., Pleixats, R., Man, M.W.C., Moreau, J.J.E., Adv. Synth. Catal. 2006, 348:751.

[131] (a) Li, L., Shi, J., Adv. Synth. Catal. 2005, 347:1745; (b) Fischer, D., Blechert, S., Adv. Synth. Catal. 2005, 347:1329; (c) Matsugi, M., Curran, D.P., J. Org. Chem. 2005, 70:1636.

[132] De Clercq, B., Lefèbvre, F., Verpoort, F., New J. Chem. 2002, 26:1201.

[133] De Clercq, B., Lefèbvre, F., Verpoort, F., Appl. Catal. A: Gen. 2003, 247:345.

[134] Melis, K., De Vos, D., Jacobs, P., Verpoort, F., J. Mol. Catal. A: Chem. 2001, 169:47.

[135] Opstal, T., Melis, K., Verpoort, F., Catal. Lett. 2001, 74:15.

[136] Opstal, T., Verpoort, F., New J Chem. 2003, 27:257.

[137] De Clercq, B., Verpoort, F., Catal. Lett. 2002, 83:9.

[138] De Clercq, B., Verpoort, F., Tetrahedron Lett. 2001, 42:8959.

RUTHENIUM–ARYLOXIDE CATALYSTS FOR OLEFIN METATHESIS

SEBASTIEN MONFETTE, JOHANNA M. BLACQUIERE,
JAY C. CONRAD, NICHOLAS J. BEACH, DERYN E. FOGG

Center for Catalysis Research and Innovation, Department of Chemistry, University of Ottawa, 10 Marie Curie K1N 6N5 Ottawa, ON, Canada

Abstract: Advances in design of ruthenium aryloxide catalysts for olefin metathesis are described. The target complexes are accessible on reaction of $RuCl_2(NHC)(py)_2$ (CHPh) (NHC – *N*-heterocyclic carbene) with electron-deficient, monodentate aryloxides, or aryloxides that yield small, rigid chelate rings. The best of these catalysts offer activity comparable to or greater than that of the parent chloride (Grubbs) systems in ring-closing metathesis (RCM). Preliminary studies of the electronic nature of the Ru–X bond suggest that the metal center is more electropositive in the aryloxide complexes than in the Grubbs systems.

Keywords: Ruthenium, catalysis, aryloxide, pseudohalide, metathesis, activity, electronics.

1. Introduction

Catalytic formation of new C=C bonds by olefin metathesis has enabled major advances in both organic synthesis and materials chemistry [1,2]. The scope of the reaction has increased dramatically with the advent of robust, functional group tolerant catalysts based on ruthenium (Ru), of which the Grubbs catalyst **1** and its "second-generation" derivatives containing an *N*-heterocyclic carbene (NHC) ligand are most prominent [1]. The commercially available complexes **1** and **2b** (Figure 1) have helped to transform olefin metathesis into a cornerstone methodology in organic synthesis, owing to their ease of handling, and – particularly for **2** – their high activity. Following the unexpected finding that the lability of the phosphine ligand in **2** is *lower* than that in the less metathesis-active complex **1** [3], intensive effort focused on synthesis of derivatives of **2** containing more labile donor ligands. While **1** and **2** remain the most widely used metathesis catalysts in organic synthesis [2], a number of more labile (and hence more reactive) derivatives of **2** have been developed, including triphenylphosphine [4] and pyridine [5,6] derivatives, and styrene ether complexes of the "Hoveyda" [7] type in which the chelated ether group is destabilized by steric or electronic factors [8,9] (e.g. **4**, Figure 1). Piers' remarkable four-coordinate phosphonium alkylidene complexes **5** [10] can be regarded as the extreme of this approach. Despite the structural distinctions between these pre-catalysts, however, it should be recognized that they converge on a single active species, $RuCl_2(NHC)(CHR)$

Y. İmamoğlu and V. Dragutan (eds.), Metathesis Chemistry: From Nanostructure Design to Synthesis of Advanced Materials, 79-90.

6, identical to that formed from **2** itself. Common decomposition routes and selectivity are thus to be anticipated [11].

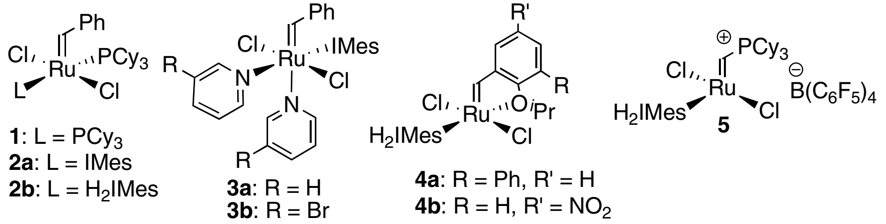

Figure 1. Key Ru metathesis catalysts converging on RuCl$_2$(L)(CHR) **6** as the active species. IMes = *N,N'*-bis(mesityl)imidazol-2-ylidene.

As these precedents illustrate, the role of the neutral donor ligands in Ru-catalyzed olefin metathesis has received much attention, owing in part to the ease of the relevant ligand exchange reactions. The role and optimum properties of the anionic ligands have been examined in much less detail. While computational studies suggest that more electron-donating neutral donors accelerate metathesis by decreasing the barrier to formation of the metallacyclobutane intermediate [12], it is unclear whether a similar rationale can be applied to the anionic ligands. Indeed, work by the Grubbs group has suggested a correlation between increased activity, and greater electron-withdrawing ability in these ligands [13,14], though a systematic study has not yet been undertaken in which steric and electronic effects can be deconvoluted. We recently summarized the work in this area, current up to 2005, and analyzed the design limitations that led to low activity for the majority of Ru–pseudohalide complexes studied [11]. These can be summed up as: (1) excessive steric crowding, which hinders the approach of substrate; (2) the absence of a labile neutral (L-donor) ligand, which impedes substrate binding, or (3) the absence of a sufficiently strong donor (such as an alkylphosphine or NHC group) among the ligands present in the active catalyst.

It is clear that none of these limitations is inherent, and that highly active RuX$_2$LL'(CHR) catalysts may therefore be accessible, if the appropriate anionic ligands can be identified. Our interest in Ru metathesis catalysts containing anionic donors other than chloride stems from the potential for tuning catalyst activity and selectivity, with added impetus coming from findings that the chloride ligands mediate catalyst deactivation, via formation of face-bridged Ru$_2$(μ-Cl)$_3$ dimers or other decomposition products [11,15–17]. We sought pseudohalide ligands that can be readily modified, and that confer minimal three-dimensional bulk. Aryloxide ligands derived from phenols satisfy both criteria. Here we describe our progress in designing Ru–pseudohalide metathesis catalysts, with a particular focus on the ring-closing metathesis (RCM) performance of the catalysts obtained, relative to their dichloride analogues.

2. Discussion

2.1 Routes to Ru–aryloxide catalysts

We have described elsewhere the challenges involved in the installation of aryloxide ligands within coordinatively unsaturated or labile Ru frameworks [11,18]. Despite the strength of the Ru–OAr bond [19], the availability of a reservoir of electron density in the aryloxide ring, in conjunction with the accessibility of three coordination sites on the metal, enables rapid σ–π isomerization, and formation of piano–stool complexes [20]. While aryloxides, that form seven-membered chelate rings, likewise undergo isomerization [21], we recently found that smaller, more rigid (five- or six-membered) chelate rings give access to stable Ru–O bonds. Catechol and *o*-sulfonato aryloxide ligands can be installed by reaction of **3a** with the appropriate thallium salts, affording complexes **7** [22]. Isomerization of monodentate aryloxides can be curbed by reducing the donor ability of the aromatic ring by functionalization with electron-withdrawing groups. Reaction of **3a** or related hydride species with thallium perfluorophenoxide yields stable, five-coordinate Ru(σ-OC_6F_5) complexes [21,23]. Perchloro- and perbromophenoxide derivatives of type **8** are likewise accessible from **3a**, but a single chloride ligand is replaced, owing to the increased bulk of these aryloxide ligands [24]. These two strategies for construction of the target Ru–aryloxide metathesis catalysts are summarized in Scheme 1. While our initial studies focused on pyridine derivatives, we subsequently undertook synthesis of 3-bromopyridine analogues, as the greater lability of this substituted pyridine ligand significantly increases catalyst activity [25]. As comprehensive screening of the bromopyridine complexes is under way, most of our discussion will focus on the pyridine catalysts **7** and **8**.

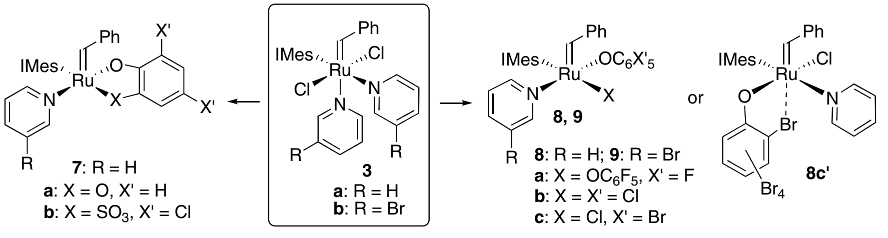

Scheme 1. Ru–pseudohalide catalysts containing aryloxide ligands.

The structure shown for the perbromoaryloxide catalysts in Scheme 1 (and, by extension, the perchloroaryloxide analogues) warrants some comment. While the apical site preference of the alkylidene ligand in such square pyramidal complexes is well established, and we were able to confirm the *cis*-disposition of the two perfluoroaryloxide ligands in **8a** by X-ray crystallography [23], the evidence for the relative positioning of the basal ligands in the mono-aryloxide derivatives is more equivocal. We originally proposed a *cis*-anionic structure [24], by analogy to that established for **8a**, and on the basis of preliminary modelling studies that suggested a push–pull interaction between *trans*-disposed pyridine and aryloxide ligands. A more detailed density functional theory (DFT) analysis of a truncated (IMe/Ru=CH_2) version of **8c** has confirmed that a five-coordinate structure in which the aryloxide and NHC ligands lie mutually *cis* is lower in energy than one in which these ligands are mutually *trans* [26]. Lower yet in energy, however, is a pseudooctahedral structure of type **8c′**, in which the anionic ligands are *trans*-disposed, and a dative Br–Ru interaction is present. Precedents exist for κ^2-coordination of aryloxide ligands bearing *ortho*-halo functionalities [27–30]. Efforts to crystallize the bromo- or chloroaryloxide complexes have not yet been successful, and experimental confirmation of this coordination mode is still pending.

2.2 Catalyst performance

Diethyldiallyl malonate (DeDAM) has been widely used as a benchmark RCM substrate for assessing the relative activity of metathesis catalysts. While its utility declines as metathesis activity increases, it provides a basis for comparison of factors such as maximum turnover numbers or solvent screening. All of the NHC-containing catalysts described herein effect quantitative RCM of DeDAM at a catalyst loading of 0.5 mol % within 15 min in refluxing $CDCl_3$, with the exception of **7b** (95%). At lower catalyst loadings, catalyst lifetime becomes increasingly important: on use of 5×10^{-4} mol % Ru, **8a** emerges as the most productive of the systems examined. A maximum turnover number (TON) of 40,000 was found (i.e. 20% conversion of 200,000 equivalent DeDAM; Table 1), vs TON values of 21,000 for **8c**, 17,000 for **2a**, and 5,100 for **3a**. In CH_2Cl_2, in contrast, the dichloride catalysts significantly outperform the aryloxide systems. In both solvents, the performance of the second-generation catalysts **2a/b** is superior to that of the more reactive, but less robust, third-generation catalyst **3a**. The improved performance of the aryloxide catalysts in $CDCl_3$ is in part due to the increase in reaction temperature, which offsets the low initiation efficiency of these catalysts.

Table 1. Performance of Grubbs and Ru–aryloxide catalysts in RCM of DeDAM at low catalyst loadings[a]

Catalyst	TON ($CDCl_3$) 200,000:1	TON (CH_2Cl_2) 5,000:1	TON ($CDCl_3$) 5,000:1	Ref.
2a	17,000	4,450	–	[31]
2b	–	4,250[b]	–	[32]
3a	5,100	3,700	–	[31]
3b	–	3,800	–	[31]
7a	–	950	1,700[c]	[31]
8a	40,000	900	2,900	[23]
8c	21,000	1,650	2,300	[31]
9a	–	900	2,350	[31]
9c	–	2,350	1,850	[31]

[a]Conditions: 100 mM DeDAM, 18 h, refluxing solvent, unless otherwise noted; [b]Substrate concentration not specified; [c]Minimum value: reaction carried out at 0.05 mol % Ru ([S]: [Ru] = 2,000:1).

The data in Table 1 illustrate the sensitivity of catalyst performance to the solvent medium. This sensitivity is explored in more detail in Figure 2, in which we retain DeDAM as substrate, in order to facilitate comparison. We note, however, that the optimum solvent is also substrate-dependent. Thus, for RCM synthesis of a 14-membered macrolactone via **8c**, the dependence of activity on solvent followed the order: benzene > CH_2Cl_2 > $CHCl_3$ [24]. The relative performance of **3a**, **8a**, and **8c** in a range of different solvents (bath temperature 75°C) is shown in Figure 2 for RCM of DeDAM; catalyst **2a** exhibited trends similar to **3a**, but generally lower activity, and is therefore not included. Most dramatic is the difference in reactivity of **8a** in CH_2Cl_2, vs 1,2-dichloroethane or $CDCl_3$. The importance of reaction temperature was noted above. We expected that the dielectric constant of the medium would also be important, but this is not borne out by the relative values for these solvents ($[ClCH_2]_2$, 10.42; CH_2Cl_2, 8.93; $CHCl_3$, 4.81 [33]). While ligand protonolysis (e.g. abstraction of the pyridine ligand) by trace acid in $CDCl_3$ could potentially account for the higher activity of **8a** in this solvent, relative to CH_2Cl_2, this would not account for the dramatic increase in reactivity in dichloroethane, vs CH_2Cl_2. Also of interest is the retention of activity by both **3a** and **8c** in coordinating solvents such as tetrahydrofuran (THF) and (albeit to a lesser extent) dimethylformamide (DMF), solvents rarely used for Ru-catalyzed RCM. This suggests opportunities for RCM of polar substrates with limited solubility in the more usual aromatic or halocarbon solvents, provided that the substrate has a strong conformational driving force for cyclization. The high activity of **3a** and **8c** in the fluorocarbon solvent FC-72 (perfluorohexane) is also of interest for the purposes of catalyst separation and recovery [34,35].

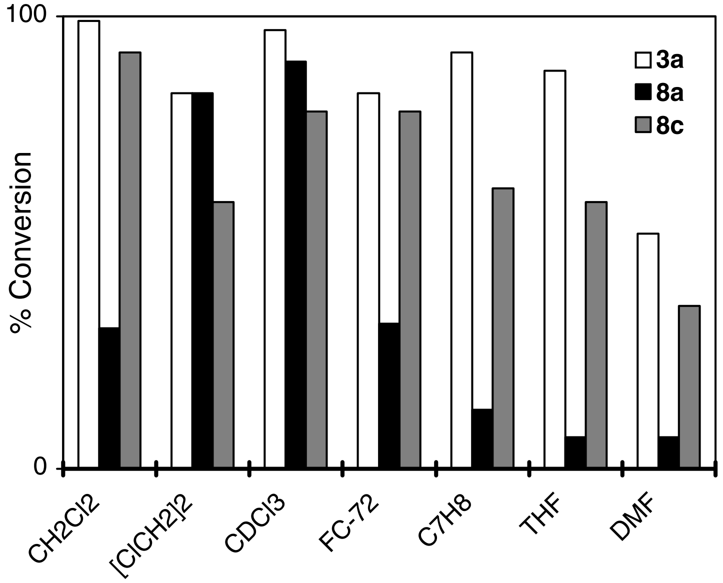

Figure 2. RCM of DeDAM at 0.5 mol % Ru (100 mM substrate, bath temp. 75°C, 4 h). Conversions by GC; average error ±2%.

Apparent from Figure 2 is the superiority of **3a** to **8a/c** for RCM of DeDAM in all solvents examined. For a number of other substrates explored, **8c** outperforms **3a**. Both **8c** and **8b** enable dramatically shorter reaction times than **3a** in RCM synthesis of macrocycles under Ziegler conditions, for example, with **8c** effecting quantitative cyclization of 14- and 16-membered macrolactones within 15 min (5 mol % Ru; refluxing CH_2Cl_2 or C_6H_6) [24]. Use of **3a** under otherwise identical conditions resulted in 63% and 30% conversion within 15 min. Complete formation of the 16-membered lactone required 3 h for **3a** (9 h for **2a**). We recently described the strong kinetic bias of **2a** and **3a** toward oligomerization of a range of dienes that are characterized by low effective molarities. This bias is unaffected by use of high substrate dilutions (5 mM) [36]. We delineated the key role of backbiting in liberating the RCM products for conformationally flexible rings of seven members and higher, including a seven-membered malonate ring, and showed that reaction times can be reduced by deliberately maximizing the initial oligomerization, then diluting to effect backbiting [36]. The much higher cyclization efficiency of the aryloxide catalysts is notable. However, it is not yet clear whether their superior performance reflects a lower kinetic bias toward oligomerization, or a faster rate of backbiting.

While the importance of concentration-dependent oligomerization–cyclodepolymerization equilibria in ring-opening metathesis polymerization (ROMP) chemistry has been known for 30 years [37], its relevance to RCM has gone largely unrecognized. Even for substrates with a strong conformational bias toward cyclization (e.g. **10**, Table 2), the proportion of oligomers formed via **2a** and **3a** (5 mol %) can be significant at high diene concentrations. At 100 mM, RCM of **10** via **2a** plateaus at 61% **11** after 45 min, the balance of material being involatile oligomers **12**. Reactions at 5 mM effect quantitative conversion to **11** within 1 h in refluxing CH_2Cl_2. In contrast, bromoaryloxide catalyst **9c** and catecholate **7a** effect complete RCM within 15 min in refluxing CH_2Cl_2 and $CDCl_3$, respectively, at 5–10 mM concentrations of diene.

Table 2. Catalytic activity of Ru–aryloxide catalysts **7–9**, vs chloride (Grubbs-class) catalysts **2**/**3**[a]

Substrate□	Product	mol % Ru	Solvent	Temp (°C)	Time□	% RCM□	Ref.
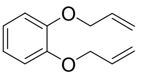 **10**	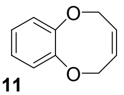 **11** + oligomer **12**	5 5	CH_2Cl_2 $CDCl_3$	40 61	30 min 45 min 15 min 1 h 30 min	**2a:** 100^b **2a**: 61 **9c**: 100^c **3b**: 100^b **7a:** 100^b	[36] [36] [31] [31] [31]
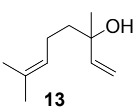 **13**	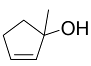 **14**	0.5 0.05	$CDCl_3$ $CDCl_3$	61 61	15 min 1 h	**2a**, **3a**, **7a**, **8a/c**: 100 **2a**: 24 **3a**: 29 **8a**: 100 **8b**: 17 **8c**: 34	[24, 31] [24] [24] [24] [24] [24]
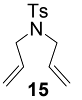 **15**	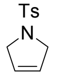 **16**	0.02 0.5□	CH_2Cl_2 $CDCl_3$ CH_2Cl_2	40 61 40	18 h□ 15 min 15 min	**2b**: 54 **3a**: 100 **7a**: 100 **9c**: 100	[32] [31] [31] [31]
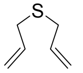 **17**	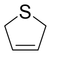 **18**	5 0.5□ □	C_7D_8 $CDCl_3$□ CH_2Cl_2	80 61 40	1 h□ 20 min	**2a:** 100 **3a**: 60^d **8a**: 40^d **8b**: 31^d **8c**, **7a**: 100	[38] [24] [24] [24] [22]
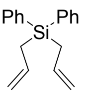 **19**	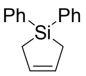 **20**	5 □	C_7H_8 $CDCl_3$	110 61	5 h□ 20 min 15 min	**2b:** 70 **2a**: 76^e **3a**, **8c**: 100 **8a**: 88^e **8b**: 94^e **7a**: 100	[39] [24] [24] [24] [24] [31]
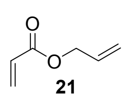 **21**	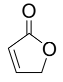 **22**	5 □ 0.5	CH_2Cl_2 $CDCl_3$ $CDCl_3$	40 61 61	1 h	**9c:** 77 **8c**: 73 **3b**: 97 **7a:** 100	[31] [31] [31] [31]
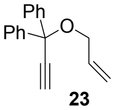 **23**	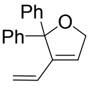 **24**	5 0.5	C_7H_8 $CDCl_3$	80 61	1 h 15 min	**2a:** 85^f **3a**: 100 **8a**: 15 **8c**: 100 **7a**: 90 **7b**: 13	[9] [31] [22] [24] [22] [22]

[a] Diene concentration ([S]) = 100 mM; conversions and yields determined by NMR and/or GC analysis; [b] [S] = 5 mM; [c] [S] = 10 mM; [d] <6% increase after 3 h; [e] 100% after 1 h; [f] isolated yield.

For the remainder of the substrates in Table 2, cyclization yields five-membered rings, and oligomerization is not observed at a standard diene concentration of 100 mM. The performance of the chloride catalyst **3a** and pseudohalide catalysts **7a** and **8c** is then generally comparable. Sulfonate **7b**, in comparison, performs poorly. Fluoroaryloxide catalyst **8a** is less active than **8b/c**, but it is potentially more robust. Illustrative of this behaviour is the performance of these catalysts in RCM of linalool **13** (which, despite the presence of a trisubstituted olefin and a potentially problematic [40] allylic alcohol, is often readily cyclized by Ru catalysts [41]). At low catalyst loadings (0.05 mol %), only **8a** effects quantitative RCM of **13** within 1 h, a reflection of the longer lifetime of the bis(aryloxide) catalyst. This distinction is lost at higher catalyst loadings (0.5 mol % Ru), at which **7a** and **8a–c**, as well as **2a** and **3a**, enable quantitative RCM within 15–20 min (refluxing $CDCl_3$). RCM of the tosylate-protected diallylamine **15** under these conditions is quantitative for catecholate **7a** and **3a** within 15–20 min. In this case, the performance of **8c** in CH_2Cl_2 is excellent, again leading to complete conversion within 15 min. At a lower catalyst loading (0.02 mol %), **2b** is reported to achieve 54% conversion after 18 h in refluxing CH_2Cl_2 [32].

Ru metathesis catalysts are widely believed to be more susceptible than the Mo catalysts to poisoning by sulphur donors [42,43]. Somewhat surprisingly, given these precedents and the evidence for a more electropositive metal center in **8c**, in particular (see below), **7a** and **8c** show good tolerance toward diallyl sulphide substrate **17**, even at catalyst loadings of 0.5 mol %. RCM is quantitative within 15–20 min in refluxing $CDCl_3$. Poorer performance is found for **3a**, suggesting that the Grubbs-class catalysts are more readily poisoned. A literature report describes complete conversion to **18** via **2a** under more forcing conditions (5 mol % **2a**, toluene, 80°C; 1 h) [38], though it is unclear whether milder conditions would suffice.

Schmidt and co-workers have proposed that RCM of diallylsilane derivative **19** is challenging because the transition state for cyclization is destabilized by the steric bulk of the diphenylsilyl group [39]. For this substrate, best performance is found for the bromoaryloxide, the catecholate, and the third-generation Grubbs catalysts (**8c**, **7a**, and **3a**), but a catalyst loading of 5 mol % is required. Chloroaryloxide catalyst **8b** is slightly less active, followed by bis(perfluoroaryloxide) catalyst **8a**. The second-generation catalyst **2a** is the least active of those we studied, although RCM proceeds to completion after 1 h. A literature report for **2b** (5 mol %) describes only 70% formation of **20** after 5 h in refluxing toluene [39], suggesting much lower activity for the H_2IMes catalyst, at least in this solvent.

Catalyst **7a** exhibits by far the highest activity for RCM of acrylate **21**, with quantitative formation of **22** within 1 h in refluxing $CDCl_3$ at a catalyst loading of 0.5 mol %. In comparison, **3b** and **8c/9c** require a catalyst loading tenfold higher, and RCM remains incomplete after 1 h (if nearly complete for **3b**). The higher conversions found for **3b,** vs. **9c,** can be partially attributed to the higher reaction temperature, but it is noteworthy that RCM via **8c/9c** plateaus at ~75% conversion. The difference in electronic properties of the catecholate catalyst, vs the bromoaryloxides, almost certainly plays a role in the greater reactivity of **7a** toward this substrate, possibly favouring metathesis over deactivation.

RCM of enyne substrate **23** is effected with greatest efficiency by catalysts **3a** and **8c**, with complete conversion to **24** within 15 min (refluxing $CDCl_3$) at catalyst loadings ten times lower than those reported for **2a** at 80°C [9]. Only slightly lower activity is found for **7a**, but **7b** is again least active of the catalysts examined.

From a mechanistic perspective, RCM studies are of limited utility in assessing relative catalyst reactivity, because the observed activity reflects the combined effect of initiation and propagation. *The true activity of a specific catalyst can thus be masked by slow initiation*. That is, a fast-initiating catalyst may outperform a more slowly-initiating catalyst of inherently higher reactivity toward a substrate of interest. For the aryloxide catalysts, ROMP studies suggest that rates of initiation are rather low relative to propagation [25], and that the observed activity reflects the operation of a low proportion of initiated species.

2.3 Electronic properties of Ru–aryloxide catalysts

Activation of the chloride and aryloxide pre-catalysts via ligand loss can be expected to be a function of the charge distribution in these complexes. Comparison of the nature and extent of the Ru–X bonding interactions is thus of keen interest, but direct experimental evaluation of these parameters is non-trivial. X-ray absorption spectroscopy (XAS) offers insight into the electronic nature of low-lying empty valence levels, and thus an element-specific experimental probe of covalent bonding [44]. XAS studies of **8c**, vs **1** and **2a**, indicated a decrease in the delocalization of the Cl 3p ligand orbital onto the empty Ru $4d_\sigma$ orbital for **8c**, and hence a reduced covalency within the Ru–Cl bond. The more electropositive nature of the Ru center in **8c**, in conjunction with the nucleophilic character of the pyridine ligand, would account for the lower lability of this ligand, and consequently the lower initiation efficiency of **8c**. Similar behaviour can be anticipated for the other haloaryloxide catalysts. The extent to which this applies to the catecholate catalyst is of compelling interest, given the high activity of this species. It cannot be assayed by the XAS method above, which is limited to ruthenium chloride complexes, and we are currently pursuing indirect methods.

3. Conclusions

The foregoing describes a new class of Ru complexes containing mono- or bidentate aryloxides as pseudohalide ligands. Monodentate aryloxides can prove excellent ligands, where the coordinating ability of the aromatic ring is attenuated by electron-withdrawing substituents. Alternatively, the Ru–OAr bond can be stabilized by incorporation into a small, rigid chelate ring. While their performance in RCM is frequently excellent, with the exception of the *o*-sulfonatoaryloxide derivative, the Ru–aryloxide catalysts suffer from low initiation efficiency relative to the first- or third-generation Grubbs catalysts. This may reflect a high positive charge on the metal center, which disfavours initiation. The high performance of these catalysts (in a number of cases, superior to that of the important Grubbs systems), *despite* their low initiation efficiency, suggests that the reactivity of the active species may be much higher than that of the chloride analogue **6**. Current work targets modification of the aryloxide ligands in order to improve initiation efficiency. Parallel studies exploit the catecholate ligand as a versatile platform for modulating electronic effects without perturbing steric parameters. Studies of the initiation efficiency and catalytic activity of a family of functionalized catecholate complexes are presently under way, and are expected to shed light on the optimum electronic properties of the anionic ligands in Ru metathesis catalysts.

References

[1] (a) Grubbs, R.H., Handbook of Metathesis, Wiley-VCH, Weinheim, 2003; (b) Nicolaou, K.C., Bulger, P.G., Sarlah, D., Angew. Chem. Int. Edit. 2005, 44:4490–4527; (c) Fürstner, A., Angew. Chem. Int. Edit. 2000, 39:3012–3043.

[2] Soderberg, B.C.G., Coord. Chem. Rev. 2006, 250:2411–2490.

[3] Sanford, M.S., Love, J.A., Grubbs, R.H., J. Am. Chem. Soc. 2001, 123:6543–6554.

[4] Huang, J., Stevens, E.D., Nolan, S.P., Petersen, J.l., J. Am. Chem. Soc. 1999, 121:2674–2678.

[5] Sanford, M.S., Love, J.A., Grubbs, R.H., Organometallics 2001, 20:5314–5318.

[6] Love, J.A., Morgan, J.P., Trnka, T.M., Grubbs, R.H., Angew. Chem., Int. Edit. 2002, 41:4035–4037.

[7] Garber, S.B., Kingsbury, J.S., Gray, B.L., Hoveyda, A.H., J. Am. Chem. Soc. 2000, 122:8168–8179.

[8] Zaja, M., Connon, S.J., Dunne, A.M., Rivard, M., Buschmann, N., Jiricek, J., Blechert, S., Tetrahedron 2003, 59:6545–6558.

[9] Michrowska, A., Bujok, R., Harutyunyan, S., Sashuk, V., Dolgonos, G., Grela, K., J. Am. Chem. Soc. 2004, 126:9318–9325.

[10] Romero, P.E., Piers, W.E., McDonald, R., Angew. Chem., Int. Edit. 2004, 43:6161–6165.

[11] Conrad, J.C., Fogg, D.E., Curr. Org. Chem. 2006, 10:185–202.

[12] Adlhart, C., Chen, P., J. Am. Chem. Soc. 2004, 126:3496–3510.

[13] Dias, E.L., Nguyen, S.T., Grubbs, R.H., J. Am. Chem. Soc. 1997, 119:3887–3897.

[14] Wu, Z., Nguyen, S.T., Grubbs, R.H., Ziller, J.W., J. Am. Chem. Soc. 1995, 117:5503–5511.

[15] Amoroso, D., Snelgrove, J.L., Conrad, J.C., Drouin, S.D., Yap, G.P.A., Fogg, D.E., Adv. Synth. Catal. 2002, 344:757–763.

[16] Amoroso, D., Yap, G.P.A., Fogg, D.E., Organometallics 2002, 21:3335–3343.

[17] Hong, S.H., Day, M.W., Grubbs, R.H., J. Am. Chem. Soc. 2004, 126:7414–7415.

[18] Conrad, J.C., Snelgrove, J., Eelman, M.D., Hall, S., Fogg, D.E., J. Mol. Catal. A 2006, 254:105–110.

[19] Holland, P.L., Andersen, R.A., Bergman, R.G., Huang, J., Nolan, S.P., J. Am. Chem. Soc. 1997, 119:12800–12814.

[20] Snelgrove, J.L., Conrad, J.C., Yap, G.P.A., Fogg, D.E., Inorg. Chim. Acta 2003, 345:268–278.

[21] Snelgrove, J.L., Conrad, J.C., Eelman, M.D., Moriarty, M.M., Yap, G.P.A., Fogg, D.E., Organometallics 2005, 24:103–109.

[22] Monfette, S., Fogg, D.E., Organometallics 2006, 25:1940–1944.

[23] Conrad, J.C., Amoroso, D., Czechura, P., Yap, G.P.A., Fogg, D.E., Organometallics 2003, 22:3634–3636.

[24] Conrad, J.C., Parnas, H.H., Snelgrove, J.L., Fogg, D.E., J. Am. Chem. Soc. 2005, 127:11882–11883.

[25] Conrad, J.C., Camm, K.D., Fogg, D.E., Inorg. Chim. Acta 2006, 359:1967–1973.

[26] Conrad, J.C., Carra, C., Fogg, D.E., Organometallics (submitted).

[27] Fries, G., Ilg, K., Pfeiffer, M., Stalke, D., Werner, H., Eur. J. Inorg. Chem. 2000, 2597–2601.

[28] Werner, H., Braun, T., Daniel, T., Gevert, O., Schulz, M., J. Organomet. Chem. 1997, 541:127–141.

[29] Darensbourg, D.J., Fontal, B., Chojnacki, S.S., Klausmeyer, K.K., Reibenspies, J.H., Inorg. Chem. 1994, 33:3526–3532.

[30] Sinha, P.K., Falvello, L.R., Peng, S.M., Bhattacharya, S., Polyhedron 2000, 19:1673–1680.

[31] Conrad, J.C., Monfette, S., Fogg, D.E., manuscript in preparation.

[32] Halbach, T.S., Mix, S., Fischer, D., Maechling, S., Krause, J.O., Sievers, C., Blechert, S., Nuyken, O., Buchmeiser, M.R., J. Org. Chem. 2005, 70:4687–4694.

[33] Lide, D.R., (ed.), CRC Handbook of Chemistry and Physics, Internet Version 2005, CRC Press, Boca Raton, FL, 2005.

[34] Yao, Q.W., Zhang, Y.L., J. Am. Chem. Soc. 2004, 126:74–75.

[35] Zhang, W., Chem. Rev. 2004, 104:2531–2556.

[36] Conrad, J.C., Eelman, M.D., Silva, J.D., Monfette, S., Parnas, H.H., Snelgrove, J.L., Fogg, D.E., J. Am. Chem. Soc. 2006 (2007), 129:1024–1025.

[37] Höcker, H., Reimann, W., Riebel, K., Szentivanyi, Z., Makromol. Chem. 1976, 177:1707–1715.

[38] Spagnol, G., Heck, M.-P., Nolan, S.P., Mioskowski, C., Org. Lett. 2002, 4:1767–1770.

[39] Schmidt, B., Pohler, M., Costisella, B., J. Org. Chem. 2004, 69:1421–1424.

[40] Werner, H., Grunwald, C., Stuer, W., Wolf, J., Organometallics 2003, 22:1558–1560.

[41] Hoye, T.R., Zhao, H., Org. Lett. 1999, 1:1123–1125.

[42] Armstrong, S.K., J. Chem. Soc., Perkin Trans. 1998, 371–388.

[43] Schrock, R.R., Hoveyda, A.H., Angew. Chem. Int. Edit. 2003, 42:4592–4633.

[44] Delgado-Jaime, M.U., Conrad, J.C., Fogg, D.E., Kennepohl, P., Inorg. Chim. Acta 2006, 359:3042–3047.

HOMOBIMETALLIC RUTHENIUM–*N*-HETEROCYCLIC CARBENE COMPLEXES FOR OLEFIN METATHESIS

XAVIER SAUVAGE, ALBERT DEMONCEAU, LIONEL DELAUDE*

Center for Education and Research on Macromolecules, Institut de Chimie (B6a),
University of Liège, Laboratory of Macromolecular Chemistry and Organic
Catalysis, Sart-Tilman par B-4000 Liège, Belgium

Abstract: In this chapter, the synthesis and catalytic activity towards olefin metathesis of homobimetallic ruthenium (Ru)–alkylidene, –cyclodiene or –arene complexes bearing phosphine or *N*-heterocyclic carbene (NHC) ligands are reviewed. Emphasis is placed on the last category of bimetallic compounds. Three representatives of this new type of molecular scaffold were investigated. Thus, [(*p*-cymene)Ru(m-Cl)$_3$RuCl (h^2-C$_2$H$_4$)(L)] complexes with L = PCy$_3$ (**15a**), IMes (**16a**), or IMesCl$_2$ (**16b**) were prepared. They served as catalyst precursors for cross-metathesis (CM) of various styrene derivatives. These experiments revealed the outstanding aptitude of complex **16a** (and to a lesser extent of **16b**) to catalyze olefin metathesis reactions. Contrary to monometallic Ru–arene complexes of the [RuCl$_2$(*p*-cymene)(L)] type, the new homobimetallic species did not require the addition of a diazo compound nor visible light illumination to initiate the ring-opening metathesis of norbornene or cyclooctene. When diethyl 2,2-diallylmalonate and *N*,*N*-diallyltosylamide were exposed to **16a**,**b**, a mixture of cycloisomerization and ring-closing metathesis (RCM) products was obtained in a nonselective way. Addition of phenylacetylene enhanced the metathetical activity while completely repressing the cycloisomerization process.

Keywords: alkylidene ligands, arene ligands, cycloisomerization, homogeneous catalysis, stilbene formation

1. Introduction

Thanks to the development of highly efficient, well-defined catalysts tolerant of many functional groups, olefin metathesis has emerged as a powerful tool for assembling unsaturated hydrocarbon backbones in organic synthesis and in polymer chemistry.[1,2] Since Grubbs and coworkers first reported on the synthesis and metathetical activity of monometallic ruthenium (Ru)–alkylidene complexes [RuCl$_2$(=CHR)(PCy$_3$)$_2$], **1a** (R = CH=CPh$_2$),[3] and **1b** (R = Ph)[4] in the mid-1990s, research groups around the world have engaged in designing further late transition–metal-based catalysts with increased

---

*To whom correspondence should be addressed. Lionel Delaude, Center for Education and Research on Macromolecules (CERM), Institut de Chimie (B6a), University of Liège, Sart-Tilman par B-4000 Liège, Belgium; e-mail: l.delaude@ulg.ac.be

Y. İmamoğlu and V. Dragutan (eds.), Metathesis Chemistry: From Nanostructure Design to Synthesis of Advanced Materials, 91-109.

robustness and proficiency, in order to reduce catalyst loading and to perform metathesis of challenging substrates under mild conditions.

In 1998, Grubbs et al. introduced a new class of well-defined, single component bimetallic catalysts, which were in some cases up to 80 times more active than their monometallic parents **1a**,**b** in the ring-opening metathesis polymerization (ROMP) of 1,5-cyclooctadiene.[5] Upon addition of 1 equivalent of $[RuCl_2(p\text{-cymene})]_2$ dimer (**2**) to a solution of either **1a** or **1b** in benzene at 45°C or at room temperature, the transformation shown in Scheme 1 took place cleanly and quantitatively. The Ru–arene dimer reacted with one phosphine ligand of complex **1a**,**b** to generate the three-legged piano–stool compound **3**, while the remaining fragment chelated the Ru–alkylidene starting material via two μ-chloro bridges. Heterobimetallic osmium–Ru and rhodium–Ru alkylidene complexes were obtained from the reaction of **1a**,**b** with $[OsCl_2(p\text{-cymene})]_2$ and $[RhCl_2(t\text{-}Bu_2Cp)]_2$, respectively, along the same lines.[5]

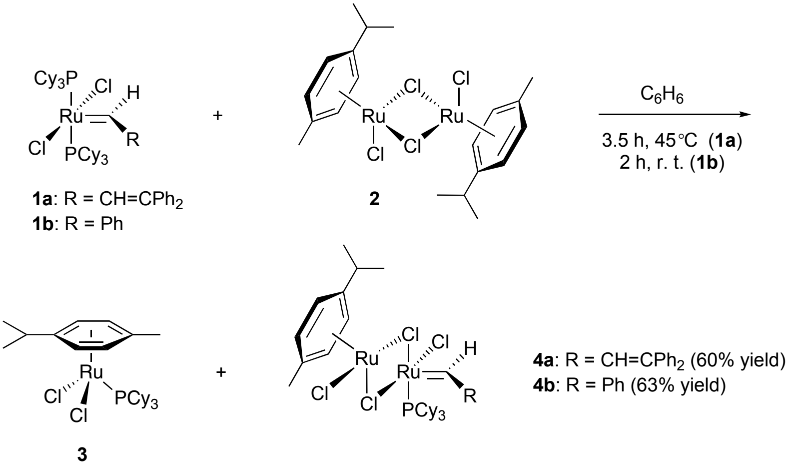

Scheme 1. Synthesis of homobimetallic ruthenium–alkylidene complexes bearing phosphine ligands.

In 1999, Herrmann and co-workers extended this procedure to the synthesis of bimetallic Ru–alkylidene complex **6** bearing a *N*-heterocyclic carbene (NHC) instead of a phosphine ancillary ligand (Scheme 2). Related heterobimetallic Ru–benzylidene complexes bearing the 1,3-dicyclohexylimidazolin-2-ylidene ligand (ICy) were also prepared using $[OsCl_2(p\text{-cymene})]_2$, $[Cp^*RhCl_2]_2$, and $[Cp^*IrCl_2]_2$ in conjunction with Ru compound **5**.[6] Density functional theory (DFT) calculations showed that a rhodium–cyclopentadienyl fragment attached to a model Ru–methylidene catalyst precursor acted as a coordinatively labile ligand and that rupture of an axial μ-chloro bridge was more favorable than phosphine dissociation, thereby populating the dissociative

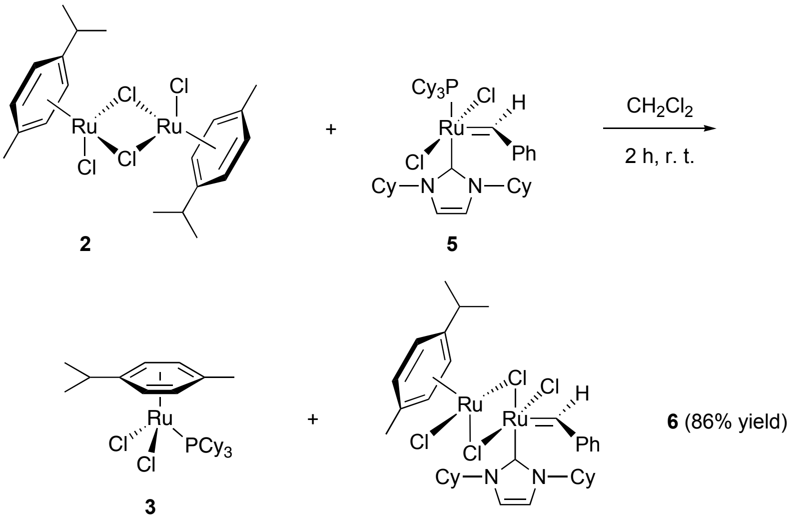

Scheme 2. Synthesis of a homobimetallic ruthenium–benzylidene complex bearing a NHC ligand.

pathway commonly accepted for olefin metathesis in the presence of Grubbs-type alkylidene complexes.[7]

Kinetic data obtained for the ROMP of 1,5-cyclooctadiene with various Ru initiators helped quantify the improvement resulting from the use of bimetallic Ru–benzylidene complexes **4b** and **6**. Thus, significantly higher rate constants were recorded with catalyst precursor **6** (k_{rel} = 13) and to a lesser extent with species **4b** (k_{rel} = 2.4) compared to the monometallic first-generation Grubbs catalyst **1b** (k_{rel} = 1).[7] Homo- and heterobimetallic Ru–alkylidene complexes were also successfully employed to promote the ROMP of cyclooctene and norbornene or norbornadiene derivatives,[8,9] the cross-metathesis (CM) of *cis*-2-pentene,[5] and the ring-closing metathesis (RCM) of a,w-dienes.[10,11] For this last application, they displayed excellent activities in the formation of tri- or even tetra-substituted cycloalkene products, a performance that could not be achieved with the monometallic complex **1b**.

Another interesting variation on homobimetallic Ru–alkylidene complexes was first investigated by Hill and Fürstner in 1999. These authors disclosed the convenient synthesis of a catalyst active in RCM by treating $[RuCl_2(PPh_3)_3]$ with 1,1-diphenylpropargyl alcohol followed by phosphine exchange with PCy_3. A structure of molecular formula $[RuCl_2(=C=C=CPh_2)(PCy_3)_2]$ containing an *allenylidene* fragment was initially proposed for this new complex. The corresponding homobimetallic adduct was obtained by reaction with $[RuCl_2(p\text{-cymene})]_2$ (**2**) and assigned the structure $[(p\text{-cymene})RuCl(m\text{-}Cl)_2$

RuCl(=C=C=CPh$_2$)(PCy$_3$)].[12,13] However, subsequent work from the groups of Nolan[14] and Fürstner[15] showed that the end products formed in these reactions were actually Ru–*indenylidene* compounds. Thus, the correct molecular representation for the synthesis of homobimetallic adduct **8** from monometallic precursor **7** is depicted in Scheme 3. In sharp contrast with the trends observed previously by Grubbs and Herrmann, bimetallic species **8** was repeatedly found to be a less efficient catalyst than its monometallic parent **7** in the RCM of several dienes.[13,15,16]

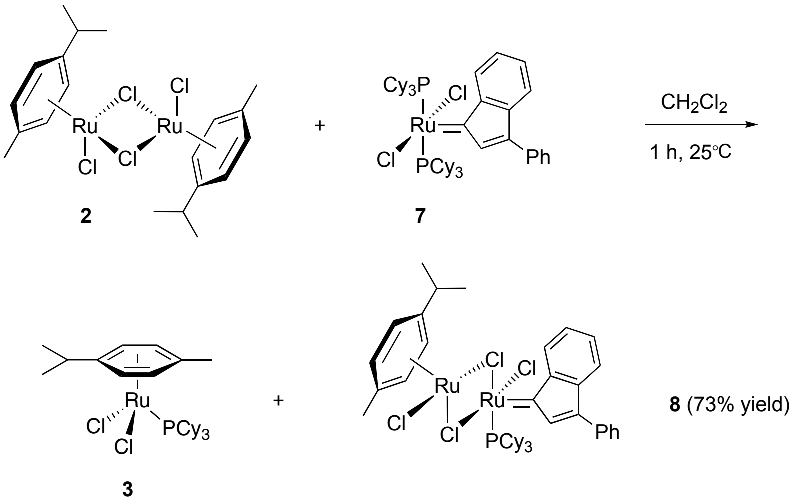

Scheme 3. Synthesis of a homobimetallic ruthenium–indenylidene complex bearing a phosphine ligand.

In 2002, Verpoort et al. prepared a series of monometallic Ru–benzylidene complexes bearing bidentate Schiff base ligands **9a–f**. By varying the nature of the R and R′ substituents on the salicylaldimine moiety, they were able to modulate the steric and electronic properties of the Schiff bases. The corresponding homobimetallic complexes **10a–f** were obtained upon opening of the Ru dimer **2** m-chloro bridges by the phosphine ligands in **9a–f** with concomitant formation of Ru–arene complex **3** (Scheme 4).[17] The catalytic activity of all these species was tested in ROMP and RCM reactions. Homobimetallic complex **10e** displayed an excellent stability combined with a very high activity for both types of olefin metathesis. In ring-closing transformations, it could be used already at 55°C, whereas monometallic complexes required a temperature of 70°C to afford satisfactory conversions. These observations were rationalized by assuming a sequential heterolytic cleavage of the (*p*-cymene)RuCl$_2$ moiety as the key step in the olefin metathesis pathway with bimetallic complexes. Hence, the presence of bulky substituents on the remaining Schiff base ligand should help protect the

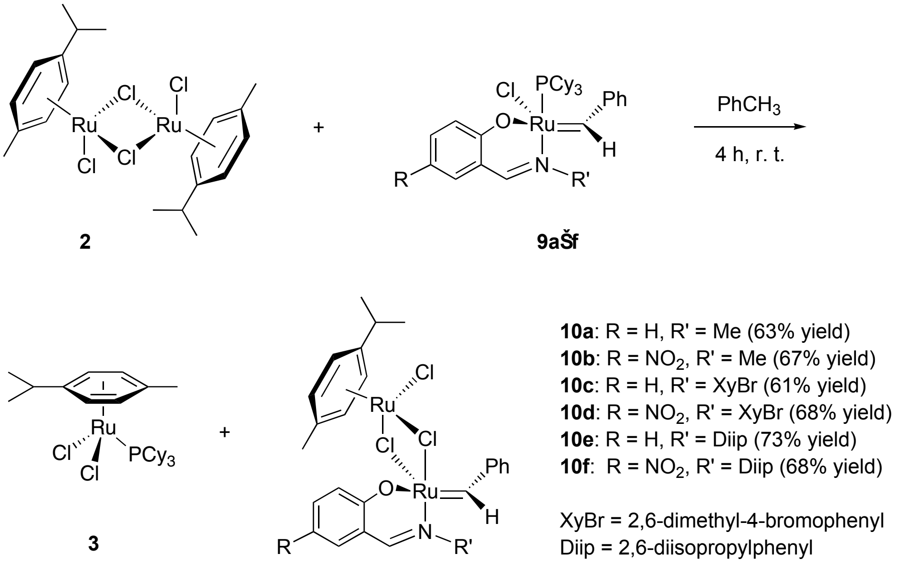

10a: R = H, R' = Me (63% yield)
10b: R = NO_2, R' = Me (67% yield)
10c: R = H, R' = XyBr (61% yield)
10d: R = NO_2, R' = XyBr (68% yield)
10e: R = H, R' = Diip (73% yield)
10f: R = NO_2, R' = Diip (68% yield)

XyBr = 2,6-dimethyl-4-bromophenyl
Diip = 2,6-diisopropylphenyl

Scheme 4. Synthesis of homobimetallic ruthenium–benzylidene complexes bearing bidentate Schiff base ligands.

coordinatively unsaturated active species, while introduction of electron-withdrawing groups such as the nitro group would destabilize them.[17]

In a follow-up work published in 2003, Verpoort and co-workers further explored the chemistry of Ru complexes bearing bidentate Schiff base ligands by exposing two metal precursors to the action of a salicylaldimine thallium salt. Thus, $[RuCl_2(NBD)]_n$ (**11a**, NBD = 2,5-norbo-ρ–nadiene) and $[RuCl_2(COD)]_n$ (**11b**, COD = 1,5-cyclooctadiene) were reacted with thallium(I) (*E*)-2-*tert*-butyl-6-((2,6-diisopropylphenylimino)methyl)phenolate (**12**) in dichloromethane at room temperature (Scheme 5). Ru–(cyclodiene) dimers **13a**,**b** bearing the O^N chelating ligand were isolated as oily products and characterized by nuclear magnetic resonance (NMR) and infrared (IR) spectroscopies. Their activity in the ROMP of norbornene was probed, but they turned out to be poorly active catalysts.[18]

In 2005, Severin and co-workers investigated the reaction of $[RuCl_2(p\text{-cymene})]_2$ with 1 equivalent of PCy_3 under an ethylene atmosphere. Under these conditions, the Ru–(*p*-cymene) dimer **2** afforded a new type of molecular scaffold **15a**, in which a $RuCl(h^2\text{-}C_2H_4)(PCy_3)$ fragment was connected via three m-chloro bridges to a Ru–arene moiety (Scheme 6).[19] Soon thereafter, the same group also synthesized the related homobimetallic complex **15b** by varying the nature of the arene ligand.[20] Complexes **15a**,**b** displayed outstanding catalytic activities in atom transfer radical reactions.

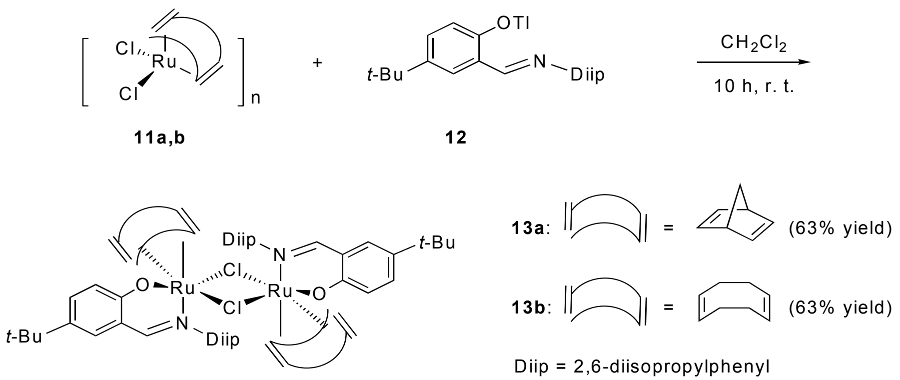

Scheme 5. Synthesis of a homobimetallic ruthenium–(cyclodiene) complex bearing bidentate Schiff base ligands.

Thus, complex **15a** catalyzed the atom transfer radical addition (ATRA) of CCl_4 and $CHCl_3$ to olefins at 0°C to 40°C with very high turnover numbers (TONs) and frequencies.[19] Replacement of the *p*-cymene ligand with 1,3,5-triisopropylbenzene enhanced the solubility of complex **15b** in hydrocarbon solvents and allowed to use it for promoting atom transfer radical poly-polymerization (ATRP) of vinyl monomers in toluene.[20]

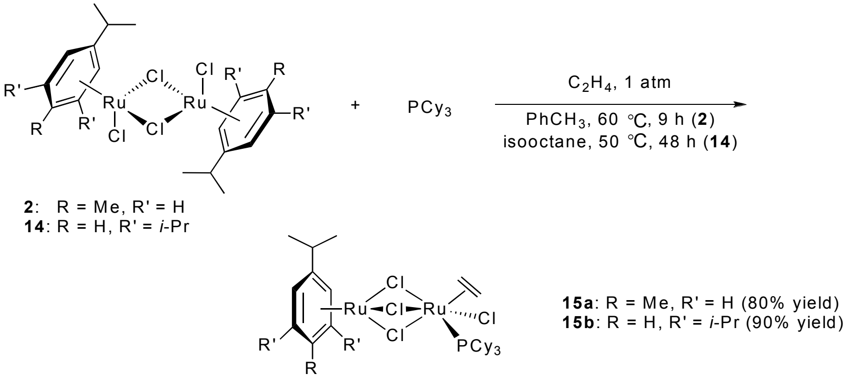

Scheme 6. Synthesis of homobimetallic ruthenium–arene complexes bearing a phosphine ligand.

Over the last decade, our group has shown in multiple instances that monometallic Ru catalysts active in olefin metathesis could also be turned into efficient promoters for atom transfer radical reactions with only minor ligand tuning.[21–26] Such a dual activity was evidenced, among others, for Grubbs catalyst **1b**,[21,22] Ru–arene complex **3**,[21,23] Herrmann bis-NHC or mixed-ligand complexes of type **5**,[24] and Verpoort–Schiff base complexes **9a** or **9c**.[27] Therefore, we decided to probe the metathetical activity of homobimetallic complex **15a**. In view of the enhancements brought by the replacement of phosphine ligands by NHCs in Ru–arene[28] or Ru–alkylidene[7,29–32] metathesis initiators, we also embarked on synthesizing and studying new homobimetallic Ru–arene complexes bearing stable carbene ligands.[33] In this contribution, we summarize the major findings that emerged from these investigations.

2. Results and discussion

2.1 Synthesis and characterization of homobimetallic Ruthenium–arene complexes bearing NHC ligands

Complexes **16a**,**b** were readily obtained by combining [RuCl$_2$(*p*-cymene)]$_2$ (**2**) with 1 equivalent of 1,3-dimesityimidazolin-2-ylidene (IMes)[34,35] or its 4,5-dichloro derivative (IMesCl$_2$)[36] under an ethylene atmosphere (Scheme 7). Both products were isolated as microcrystalline orange powders. They were stable in air for short periods of time but prolonged exposure to oxygen and moisture led to progressive color changes indicative of degradation. Under normal atmosphere, complex **16a** began to darken after a few hours, while complex **16b** resisted a few days before showing signs of decomposition. Thermogravimetric analyses (TGA) also pointed to an enhanced stability of complex **16b** compared to **16a**, since the decomposition onset occurred at 214°C for **16b** and 120°C for **16a** (Figure 1). For comparison's sake, TGA of phosphine-based complex **15a** was also carried out. Despite its remarkable stability in open air at room temperature, this complex sharply began loosing weight at 82°C.[33]

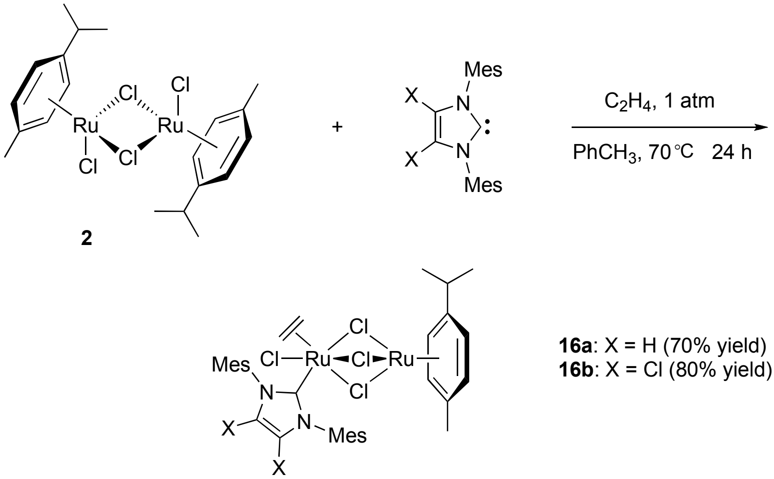

2

16a: X = H (70% yield)
16b: X = Cl (80% yield)

Scheme 7. Synthesis of homobimetallic ruthenium–arene complexes bearing NHC ligands.

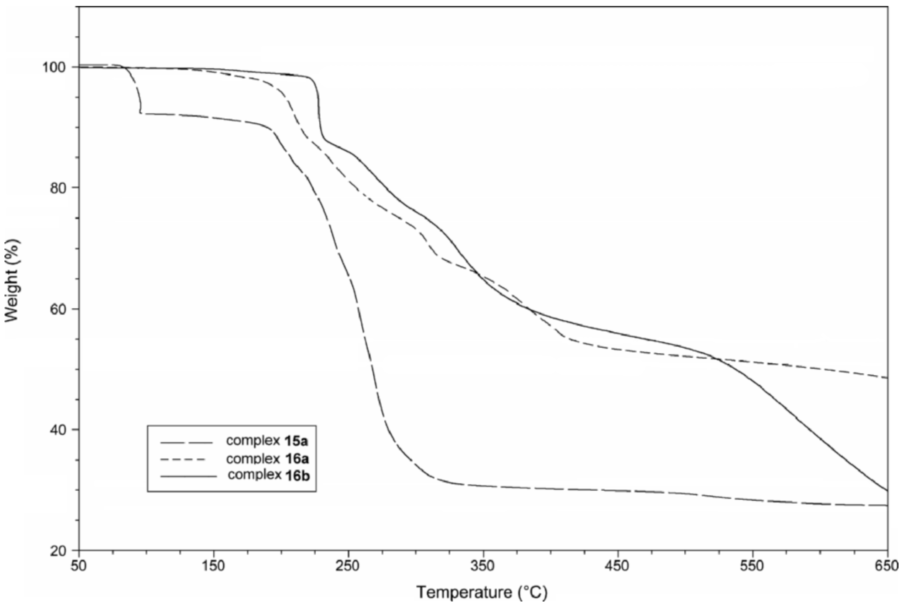

Figure 1. TGA curves of homobimetallic ruthenium–arene complexes **15a**, **16a**, and **16b**.

Complexes **16a** and **16b** displayed similar ^1H NMR features. Integration of the various signals confirmed the presence of the NHC, ethylene, and *p*-cymene ligands in 1:1:1 proportions. The h^2-C_2H_4 fragment gave rise to two multiplets centred at about 3.3 and 3.7 ppm. Only two aromatic protons from the arene ligand were visible. They resonated as two distinct multiplets forming an AB system between 5.0 and 5.1 ppm. The two other *p*-cymene ring protons were masked by the more intense absorptions of CH_2Cl_2 and free C_2H_4 at ca. 5.2 and 5.3 ppm, respectively. Yet, the nonequivalence of the four aromatic protons on the arene ligand was confirmed by $^{13}C\{^1H\}$ NMR spectroscopy that showed four distinct lines for the carbon atoms bearing these protons. The most striking difference between the NMR spectra of complexes **16a** and **16b** concerned the resonance of the imidazole C4 and C5 carbons. The replacement of hydrogen atoms by chloro substituents on these positions led to a significant decrease of their chemical shift (from 125.6 ppm in **16a** to 117.9 ppm in **16b**). The carbene centre was also affected by the modification of electron density on the heterocyclic ring, although to a lesser extent (167.8 ppm for C2 in **16a**, 172.3 ppm in **16b**). These variations are in line with NMR data previously reported for monometallic Ru–benzylidene species [$RuCl_2(=CHPh)(PCy_3)(NHC)$] when $IMesCl_2$ was substituted for IMes.[37]

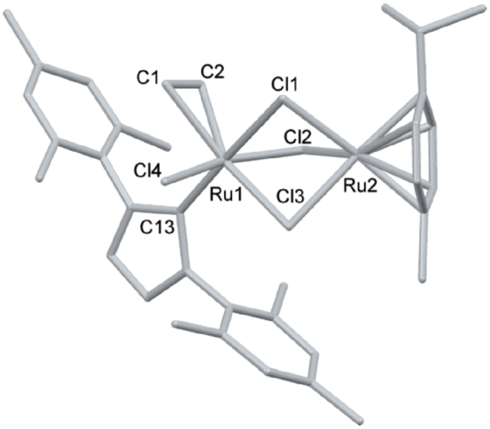

Figure 2. Molecular structure of complex **16a** in the crystal. Hydrogen atoms were omitted for clarity. Selected bond lengths (Å) and angles (°): Ru1–Cl1 2.524, Ru1–Cl2 2.472, Ru1–Cl3 2.409, Ru1–Cl4 2.383, Ru1–C1 2.327, Ru1–C2 2.188, Ru1–C13 1.980, C1–C2 1.488, Ru2–Cl1 2.416, Ru2–Cl2 2.438, Ru2–Cl3 2.445, C13–Ru1–Cl1 177.70, C13–Ru1–Cl2 100.15, C13–Ru1–Cl3 98.83, C13–Ru1–Cl4 88.59.

Crystals of **16a** were grown by slowly cooling a saturated toluene solution of the complex under an ethylene atmosphere. X-ray diffraction analysis at 120 K showed that each unit cell was made of two nonequivalent molecules of **16a** – one of them being disordered – and one molecule of solvent. Figure 2 provides a graphic rendition of the molecular structure observed, together with selected structural parameters. It should be emphasized, however, that these data are subject to caution since it was not possible to come up with a *R* parameter lower than 0.16, even when data sets were collected at low temperature on freshly synthesized crystals.

2.2 Catalytic tests

2.2.1 Cross-metathesis of styrene derivatives

To assess the metathetical activity of homobimetallic Ru–arene complexes, we first investigated the homocoupling of styrene derivatives bearing various electron-withdrawing or -donating substituents on their aromatic rings (Eq. 1). Reactions were carried out in toluene at 85°C using 0.2 mol % of catalyst and conversions were monitored by gas chromatography (GC) at regular time intervals.[33]

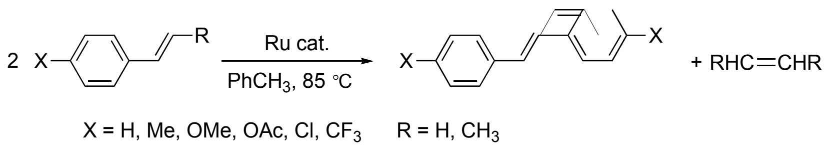

(1)

Complex **15a** was found completely devoid of metathetical activity toward styrene. Conversely, complex **16a** was highly efficient at producing (*E*)-stilbene and ethylene. A 93% conversion was achieved after 2 h and full consumption of the substrate occurred within 5 h at 85°C (Figure 3). Complex **16b** displayed a lesser activity and afforded only a 70% conversion of styrene after 2 h.

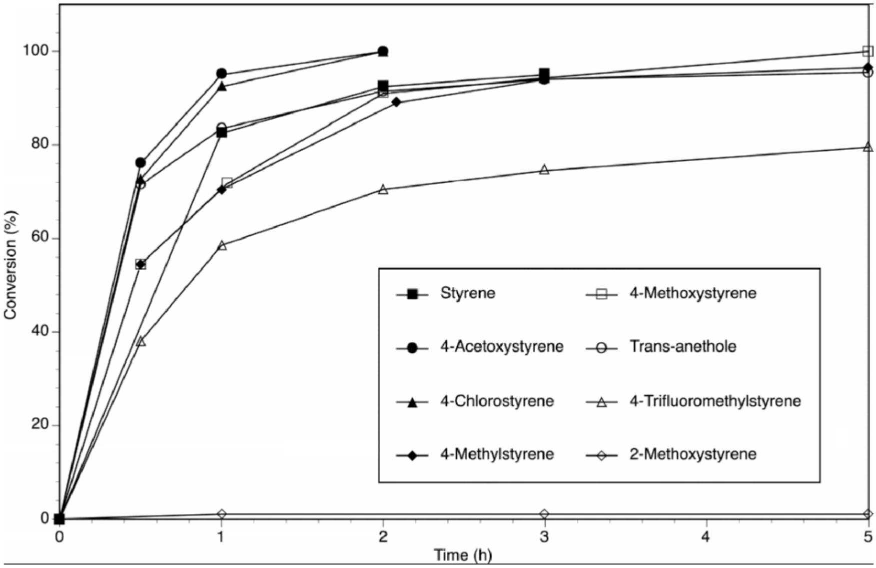

Figure 3. Cross-metathesis of styrene derivatives catalyzed by complex **16a** at 85°C. Experimental conditions: substrate (2 mmol) and catalyst (0.004 mmol) in toluene (2 mL) under Ar. Conversions were determined by GC using *n*-dodecane as internal standard.

Introduction of slightly deactivating acetoxy or chloro substituents on the *para*-position of the aromatic ring speeded up the reaction that became complete after 2 h with complex **16a** (Figure 3). Conversely, the presence of 4-methyl or 4-methoxy groups slightly reduced the reaction rate. This effect was best evidenced after 1 h and started to level off after 2 h. Eventually, almost quantitative yields of (*E*)-4,4′-dimethylstilbene or (*E*)-4,4′-dimethoxystilbene were obtained after 5 h. With the strongly deactivated 4-trifluoromethylstyrene, the reaction rate further dropped. A decent 70% conversion was reached after 2 h but did not significantly increase within the next 3 h allowed to the reaction. *trans*-Anethole (1-methoxy-4-(1-propenyl)benzene) reacted at about the same rate as styrene and was therefore more reactive than 4-methoxystyrene. It is also an inexpensive natural product, whereas 4-methoxystyrene is not widely available. Thus, *trans*-anethole is a prime starting material to access the important class of polyhydroxystilbenes via olefin metathesis.[38–40]

Attempts to homocouple a-methylstyrene with complex **16a** remained unsuccessful. This failure might be attributed to the greater steric congestion imposed to a metal–alkylidene or a metallacyclobutane intermediate by a 1,1-disubstituted double bond compared to its 1,2-disubstituted isomer or a terminal olefin. Another styrene derivative that resisted metathesis under our experimental conditions was 2-methoxystyrene. In this case, the lack of reactivity was most likely due to the formation of a stabilized Ru–benzylidene species possessing a chelated methoxy ligand.[39-47]

2.2 2 Ring-opening metathesis polymerization of cyclooctene

To further expand the scope of homobimetallic Ru–arene catalysts in olefin metathesis, we have examined the ROMP of two representative cycloalkenes, viz. norbornene and cyclooctene, in the presence of complexes **15a**, **16a**, and **16b**.[33] Polymerization of the latter, low-strain cycloolefin was carried out in chlorobenzene at 60°C for 2 h using a monomer/catalyst ratio of 250. In order to impede gelification and formation of insoluble cross-linked polymers, norbornene was reacted in more dilute solutions with 0.1 mol % of catalyst. Due to its high strain, ring-opening metathesis of this bicyclic monomer is particularly easy and occurs almost under any circumstances, provided that enough time is allowed to the reaction.[48] It was therefore not surprising to observe the full conversion of norbornene into polynorbornene with catalyst **15a**, along with **16a**,**b** (Table 1). Yet, recourse to the phosphine-based complex afforded a much broader molecular weight distribution and a lower proportion of cis double bonds in the polymer backbone, thereby underlining the influence of the ancillary ligand on the polymerization outcome.

Table 1. ROMP of norbornene catalyzed by complexes **15a**, **16a**, and **16b** at 60°C [a]

Catalyst	**Conversion (%)**[b]	**Yield (%)**	**m_n (kg mol^{-1})**[c]	**m_w/m_n**[c]	**Σ_{cis}**[d]
15a	>99	88	115	5.1	0.18
16a	>99	91	480	1.5	0.43
16b	>99	87	150	1.8	0.39

[a] Experimental conditions: Ru cat. (0.015 mmol), PhCl (12 mL), norbornene (15 mmol), 2 h at 60°C; [b]Determined by GC using norbornane as internal standard; [c]Determined by size-exclusion chromatography in THF with polystyrene calibration; [d]Fraction of *cis* double bonds in the polymer, determined by ^{13}C NMR spectroscopy.

Compared to norbornene, cyclooctene is significantly more difficult to ring open.[49] Hence, formation of polyoctenamer occurs only at a reasonable rate with highly active catalytic systems. With this monomer, a clear-cut distinction could be established between complex **15a** that did not afford any reaction after 2 h at 60°C and the NHC-containing Ru–arene species **16a** and **16b**, which led to complete conversions under the same experimental conditions (Table 2). Although the polymerizations were not controlled, almost quantitative yields of high molecular weight polymers were obtained without the need to add a diazo compound, nor to photochemically activate the catalyst precursor, as previously required with monometallic Ru–arene complexes bearing phosphine[50–52] or NHC[28,53] ligands.

Table 2. ROMP of cyclooctene catalyzed by complexes **15a**, **16a**, and **16b** at 60 controlled C[a]

Catalyst	**Conversion (%)**[b]	**Yield (%)**	m_n **(kg mol^{-1})**[c]	m_w/m_n[c]	Σ_{cis}[d]
15a	0	0	–	–	–
16a	>99	93	250	1.8	0.26
16b	>99	95	230	1.6	0.34

[a] Experimental conditions: Ru cat. (0.03 mmol), PhCl (5 mL), cyclooctene (7.5 mmol), 2 h at 60°C; [b] Determined by GC using cyclooctane as internal standard; [c] Determined by size-exclusion chromatography in THF with polystyrene calibration; [d] Fraction of *cis* double bonds in the polymer, determined by ^{13}C NMR spectroscopy.

2.2.3 Ring-closing metathesis of diethyl diallylmalonate and diallyltosylamide

In a final series of experiments, we probed the catalytic activity of complexes **15a**, **16a**, and **16b** in the RCM of two benchmark substrates, viz. diethyl 2,2-diallylmalonate (**17a**) and *N*,*N*-diallyltosylamide (**17b**). Preliminary tests were carried out in toluene at 85°C using 2 mol % of Ru catalysts (Scheme 8).[33]

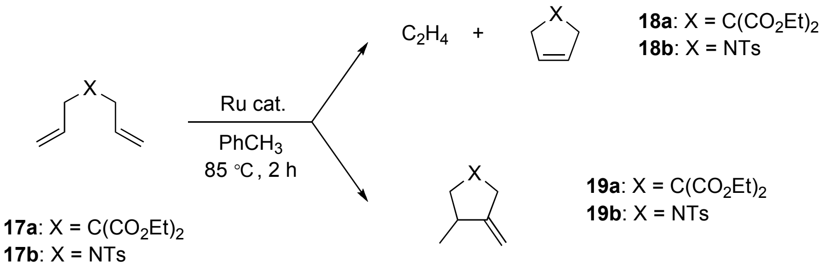

Scheme 8. Competition between RCM and cycloisomerization in the ruthenium-catalyzed reaction of diethyl diallylmalonate (**17a**) and diallyltosylamide (**17b**).

Under these conditions, no reaction occurred with the phosphine-based bimetallic species **15a** (Table 3, entries 1 and 2). With the NHC-containing catalyst precursor **16a**, full consumption of the starting materials took place within 2 h. The expected RCM cycloadducts **18a**,**b** were, however, accompanied by rearranged products **19a**,**b** formed in almost equimolar proportion (entries 3 and 4). Thus, Ru complex **16a** acted as catalyst precursor for both RCM and cycloisomerization of the acyclic a,ω-dienes. A similar twofold reaction was also observed with complex **16b** (entries 5 and 6). Yet, conversions were slightly lower and cycloisomerization took precedence over RCM, in line with the reduced metathetical activity of **16b** compared to **16a** already observed in CM and ROMP experiments.

Table 3. RCM and cycloisomerization of diethyl diallylmalonate (**17a**)[a] and diallyltosylamide (**17b**)[b] catalyzed by complexes **15a**, **16a**, and **16b** at 85°C

Entry	Substrate	Catalyst	Conversion (%)	18:19
1	**17a**	**15a**	0	–
2	**17b**	**15a**	0	–
3	**17a**	**16a**	99	53:47
4	**17b**	**16a**	98	49:51
5	**17a**	**16b**	98	40:60
6	**17b**	**16b**	96	41:59

[a] Experimental conditions: Ru cat. (0.004 mmol), substrate (2 mL of 0.1 M solution in toluene, 0.2 mmol), 2 h at 85°C. Conversions and product distributions were determined by GC using *n*-dodecane as internal standard; [b] Experimental conditions: Ru cat. (0.002 mmol), substrate (1 mL of 0.1 M solution in toluene-d_8, 0.1 mmol), 2 h at 85°C. Conversions and product distributions were determined by ^{1}H NMR spectroscopy.

Previous reports from the groups of Kurosawa[54] and Dixneuf[55,56] dealing with monometallic Ru–arene catalytic systems had shown that a,ω-dienes could be converted exclusively into metathesis products, while completely inhibiting the cycloisomerization process, by adding a small amount of terminal alkyne to the reaction media.[54–56] We have applied this strategy to homobimetallic Ru–arene complexes. Thus, substrates **17a** and **17b** were reacted with catalyst precursors **15a**, **16a**, and **16b** (2 mol %) in the presence of phenylacetylene (6 mol %). To our great satisfaction, the alkyne cocatalyst was highly effective at suppressing the cycloisomerization process altogether. At the same time, it significantly increased the rate of metathesis. Hence, with catalyst **16a** addition of phenylacetylene allowed to lower the reaction temperature from 85°C to 25°C while maintaining a quantitative

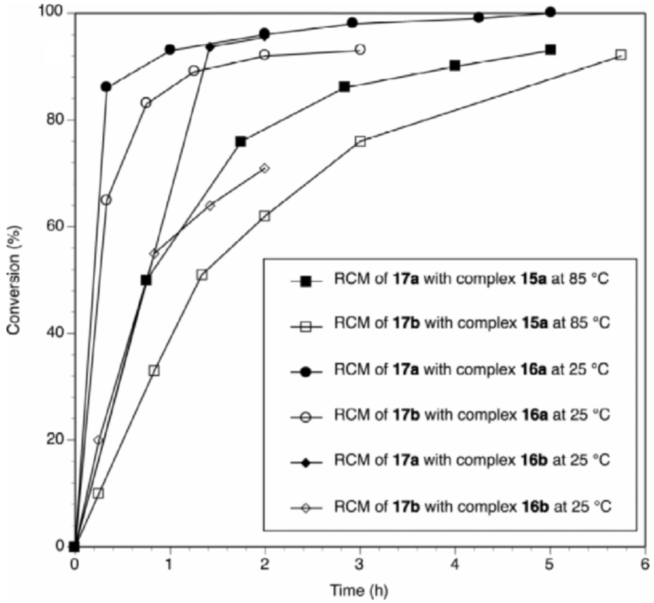

Figure 4. RCM of diethyl diallylmalonate (**17a**) and diallyltosylamide (**17b**) catalyzed by complexes **15a**, **16a**, and **16b** in the presence of phenylacetylene (6 mol %) at 25°C or 85°C. See Table 3 for experimental conditions.

conversion within 2 h (Figure 4). Replacement of the IMes ligand with its 4,5-dichloro derivative in complex **16b** once again reduced the catalytic efficiency toward metathesis, although more than satisfactory conversions were achieved already at 25°C in the presence of the alkyne cocatalyst. Complex **2a** that was completely inactive on its own (cf. Table 3) also benefited from the adjuvant and became moderately active at promoting RCM. Heating to 85°C was, however, still required to achieve satisfactory conversions within 6 h (Figure 4).

3. Conclusions

Bimetallic Ru complexes nicely complement the ubiquitous Grubbs alkylidene catalysts and related species used as initiators for olefin metathesis. Compared to their monometallic counterparts, they often display a greater propensity at releasing coordinatively unsaturated species essential for the activation of alkene substrates toward metathesis. In the case of homobimetallic Ru–arene complexes, the choice of the ancillary ligand was found crucial to achieve high metathetical activities. Thus, complexes **16a** and (to a lesser extent) **16b** bearing NHC ligands were very efficient catalyst precursors for various types of olefin metathesis reactions, whereas phosphine-based catalysts **15a**,**b** were more suited for promoting atom transfer radical additions and polymerizations.

At this stage, comprehension of the reaction mechanism is still hindered by the elusive nature of the active species generated in situ from the bulk of catalyst precursors. While thermal or photochemical arene decoordination was postulated to be the first step with monometallic Ru–(*p*-cymene) species, homobimetallic Ru complexes **16a**,**b** might be activated via an alternative pathway involving exchange of the labile ethylene ligand for a higher olefin substrate. Formation of a reactive carbene moiety could then occur through direct (albeit unfavorable) equilibration, as proposed by Bencze[57] and Mühlebach,[58] although a more complex sequence involving the intermediacy of Ru–hydride species cannot be ruled out.[59,60] Subsequent steps of metallacyclization and cycloreversion follow the mechanism commonly accepted for olefin metathesis[1,2] and complete the sequence.

Acknowledgments

We thank Prof. Bernard Tinant (Catholic University of Louvain) for the x-ray diffraction analysis of complex **16a**. The financial support of the "Fonds National de la Recherche Scientifique" (FNRS), Brussels, is gratefully acknowledged for the purchase of major instrumentation.

References

[1] Ivin, K.J., Mol, J.C., Olefin Metathesis and Metathesis Polymerization, Academic Press, San Diego, 1997.

[2] Grubbs, R.H., (ed.), Handbook of Metathesis, Wiley-VCH, Weinheim, 2003.

[3] Nguyen, S.T., Grubbs, R.H., Syntheses and activities of new single-component, ruthenium-based olefin metathesis catalysts, J. Am. Chem. Soc. 1993, 115:9858–9859.

[4] Schwab, P., France, M.B., Ziller, J.W., Grubbs, R.H., A series of well-defined metathesis catalysts—synthesis of $[RuCl_2(=CHR')(PR_3)_2]$ and its reaction, Angew. Chem. Int. Edit. 1995, 34:2039–2041.

[5] Dias, E.L., Grubbs, R.H., Synthesis and investigation of homo- and heterometallic ruthenium olefin metathesis catalysts exhibiting increased activities, Organometallics 1998, 17:2758–2767.

[6] Weskamp, T., Kohl, F.J., Herrmann, W.A., *N*-Heterocyclic carbenes: novel ruthenium–alkylidene complexes, J. Organomet. Chem. 1999, 582:362–365.

[7] Weskamp, T., Kohl, F.J., Hieringer, W., Gleich, D., Herrmann, W. A., Highly active ruthenium catalysts for olefin metathesis: the synergy of *N*-heterocyclic carbenes and coordinatively labile ligands, Angew. Chem. Int. Edit. 1999, 38:2416–2419.

[8] Frenzel, U., Weskamp, T., Kohl, F.J., Schattenmann, W.C., Nuyken, O., Herrmann, W.A., *N*-heterocyclic carbenes: application of ruthenium–alkylidene complexes in ring-opening metathesis polymerization, J. Organomet. Chem. 1999, 586:263–265.

[9] Hamilton, J.G., Frenzel, U., Kohl, F.J., Weskamp, T., Rooney, J.J., Herrmann, W.A., Nuyken, O., *N*-Heterocyclic carbenes (NHC) in olefin metathesis: influence of the NHC-ligand on polymer tacticity, J. Organomet. Chem. 2000, 606:8–12.

[10] Ackermann, L., Fürstner, A., Weskamp, T., Kohl, F.J., Herrmann, W.A., Ruthenium carbene complexes with imidazolin-2-ylidene ligands allow the formation of tetrasubstituted cycloalkenes by RCM, Tetrahedron Lett. 1999, 40:4787–4790.

[11] Ulman, M., Grubbs, R.H., Ruthenium carbene-based olefin metathesis initiators: catalyst decomposition and longevity, J. Org. Chem. 1999, 64: 7202–7207.

[12] Harlow, K.J., Hill, A.F., Wilton-Ely, J.D.E.T., The first co-ordinatively unsaturated Group 8 allenylidene complexes: insights into Grubbs' vs. Dixneuf-Fürstner olefin metathesis catalysts, J. Chem. Soc., Dalton Trans. 1999, 285–29.

[13] Fürstner, A., Hill, A.F., Liebl, M., Wilton-Ely, J.D.E.T., Coordinatively unsaturated ruthenium-allenylidene complexes: highly effective, well defined catalysts for the ring-closure metathesis of α,ω-dienes and dienynes, Chem. Commun. 1999, 601–602.

[14] Jafarpour, L., Schanz, H.-J., Stevens, E.D., Nolan, S.P., Indenylydene–imidazolylidene complexes of ruthenium as ring-closing metathesis catalysts, Organometallics 1999, 18:5416–5419.

[15] Fürstner, A., Guth, O., Düffels, A., Seidel, G., Liebl, M., Gabor, B., Mynott, R., Indenylidene complexes of ruthenium: optimized synthesis, structure elucidation, and performance as catalysts for olefin metathesis—application to the synthesis of the ADE-ring system of Nakadomarin A, Chem. Eur. J. 2001, 7:4811–4820.

[16] Reetz, M.T., Becker, M.H., Liebl, M., Fürstner, A., IR-thermographic screening of thermoneutral or endothermic transformations: the ring-closing olefin metathesis reaction, Angew. Chem. Int. Edit. 2000, 39:1236–1239.

[17] De Clerq, B., Verpoort, F., Assessing the scope of the introduction of Schiff bases as co-ligands for monometallic and homobimetallic ruthenium ring-opening metathesis polymerisation and ring-closing metathesis initiators, Adv. Synth. Catal. 2002, 344:639–648.

[18] Opstal, T., Couchez, K., Verpoort, F., Easily acessible ring opening metathesis and atom transfer radical polymerization catalysts based on arene, norbornadiene and cyclooctadiene ruthenium complexes bearing Schiff base ligands, Adv. Synth. Catal. 2003, 345:393–401.

[19] Quebatte, L., Solari, E., Scopelliti, R., Severin, K., A bimetallic ruthenium ethylene complex as a catalyst precursor for the Kharasch reaction, Organometallics 2005, 24:1404–1406.

[20] Haas, M., Solari, E., Nguyen, Q.T., Gautier, S., Scopelliti, R., Severin, K., A bimetallic ruthenium complex as a catalyst precursor for the atom transfer radical polymerization of methacrylates at ambient temperature, Adv. Synth. Catal. 2006, 348:439–442.

[21] Simal, F., Demonceau, A., Noels, A.F., Highly efficient ruthenium-based catalytic systems for the controlled free-radical polymerization of vinyl monomers, Angew. Chem. Int. Edit. 1999, 38:538–540.

[22] Simal, F., Demonceau, A., Noels, A.F., Kharasch addition and controlled atom transfer radical polymerisation (ATRP) of vinyl monomers catalysed by Grubbs' ruthenium-carbene complexes, Tetrahedron Lett. 1999, 40: 5689–5693.

[23] Simal, F., Jan, D., Delaude, L., Demonceau, A., Spirlet, M.-R., and Noels, A. F., Evaluation of ruthenium-based complexes for the controlled radical polymerization of vinyl monomers, Can. J. Chem. 2001, 79:529–535.

[24] Simal, F., Delfosse, S., Demonceau, A., Noels, A.F., Denk, K., Kohl, F.J., Weskamp, T., Herrmann, W.A., Ruthenium alkylidenes: modulation of a new clas of catalysts for controlled radical polymerization of vinyl monomers, Chem. Eur. J. 2002, 8:3047–3052.

[25] Delaude, L., Delfosse, S., Richel, A., Demonceau, A., Noels, A.F., Tuning of ruthenium N-heterocyclic catalysts for ATRP, Chem. Commun. 2003, 1526–1527.

[26] Richel, A., Delfosse, S., Cremasco, C., Delaude, L., Demonceau, A., Noels, A.F., Ruthenium catalysts bearing N-heterocyclic carbene ligands in atom transfer radical reactions, Tetrahedron Lett. 2003, 44:6011–6015.

[27] De Clerq, B., Verpoort, F., A new class of ruthenium complexes containing Schiff base ligands as promising catalysts for atom transfer radical polymerization and ring opening metathesis polymerization, J. Mol. Catal. A: Chem. 2002, 180:67–76.

[28] Delaude, L., Demonceau, A., Noels, A.F., Visible light induced ring-opening metathesis polymerisation of cyclooctene, Chem. Commun. 2001, 986–987.

[29] Weskamp, T., Schattenmann, W.C., Spiegler, M., Herrmann, W.A., A novel class of ruthenium catalysts for olefin metathesis, Angew. Chem. Int. Edit. 1998, 37:2490–2493.

[30] Huang, J., Schanz, H.-J., Stevens, E.D., Nolan, S.P., Influence of sterically demanding carbene ligation on catalytic behavior and thermal stability of ruthenium olefin metathesis catalysts, Organometallics 1999, 18:5375–5380.

[31] Scholl, M., Ding, S., Lee, C.W., Grubbs, R.H., Synthesis and activity of a new generation of ruthenium-based olefin metathesis catalysts coordinated with 1,3-dimesityl-4,5-dihydroimidazol-2-ylidene ligands, Org. Lett. 1999, 1: 953–956.

[32] Trnak, T.M., Morgan, J.P., Sanford, M.S., Wihelm, T.E., Scholl, M., Choi, T.L., Ding, S., Day, M.W., Grubbs, R.H., Synthesis and activity of ruthenium alkylidene complexes coordinated with phosphine and N-heterocyclic carbene ligands, J. Am. Chem. Soc. 2003, 125:2546–2558.

[33] Sauvage, X., Borguet, Y., Noels, A. F., Delaude, L., Demonceau, A., Homobimetallic ruthenium–*N*-heterocyclic carbene complexes: synthesis, characterization, and catalytic applications, Adv. Synth. Catal., 2006 (accepted).

[34] Arduengo, A.J., III, Rasika Dias, H.V., Harlow, R.L., Kline, M., Electronic stabilization of nucleophilic carbenes, J. Am. Chem. Soc. 1992, 114:5530–5534.

[35] Arduengo, A.J., III, Krafczyk, R., Schmutzler, R., Craig, H.A., Goerlich, J.R., Marshall, W.J., Unverzagt, M., Imidazolylidenes, imidazolinylidenes and imidazolidines, Tetrahedron 1999, 55:14523–14534.

[36] Arduengo, A.J., III, Davidson, F., Dias, H.V.R., Goerlich, J.R., Khasnis, D., Marshall, W.J., Prakasha, T.K., An air stable and mixed carbene “dimers”, J. Am. Chem. Soc. 1997, 119:12742–12749.

[37] Fürstner, A., Ackermann, L., Gabor, B., Goddard, R., Lehmann, C. W., Mynott, R., Stelzer, F., Thiel, O.R., Comparative investigation of ruthenium-based metathesis catalysts bearing *N*-heterocyclic carbene (NHC) ligands, Chem. Eur. J. 2001, 7:3236–3253.

[38] Chang, S., Na, Y., Shin, H.J., Choi, E., Jeong, L.S., A short and efficient synthetic approach to (E)-stilbenoids via solid-phase cross metathesis, Tetrahedron Lett. 2002, 43:7445–7448.

[39] Ferré-Filmon, K., Delaude, L., Demonceau, A., Noels, A.F., Stereoselective synthesis of (E)-hydroxystilbenoids by ruthenium-catalyzed cross-metathesis, Eur. J. Org. Chem. 2005, 3319–3325.

[40] Velder, J., Ritter, S., Lex, J., Schmalz, H.-G., A simple access to biologically important trans-stilbenes via Ru-catalyzed cross metathesis, Synthesis 2006, 273–278.

[41] Kingsbury, J.S., Harrity, J.P.A., Bonitatebus, P.J., Jr., Hoveyda, A.H., A recyclable Ru-based metathesis catalyst, J. Am. Chem. Soc. 1999, 121: 791–799.

[42] Garber, S.B., Kingsbury, J.S., Gray, B.L., Hoveyda, A.H., Efficient and recyclable monomeric and dendritic Ru-based metathesis catalysts, J. Am. Chem. Soc. 2000, 122:8168–8179.

[43] Gessler, S., Randl, S., Blechert, S., Synthesis and metathesis reactions of a phosphine-free dihydroimidazole carbene ruthenium complex, Tetrahedron Lett. 2000, 41:9973–9976.

[44] Wakamatsu, H., Blechert, S., A highly active and air-stable ruthenium complex for olefin metathesis, Angew. Chem. Int. Edit. 2002, 41:794–796.

[45] Wakamatsu, H., Blechert, S., A new highly efficient ruthenium metathesis catalyst, Angew. Chem. Int. Edit. 2002, 41:2403–2405.

[46] Grela, K., Harutyunyan, S., Michrowska, A., A highly efficient ruthenium catalyst for metathesis reactions, Angew. Chem. Int. Edit. 2002, 41:4038–4040.

[47] Michrowska, A., Harutyunyan, S., Sashuk, V., Dolgonos, G., Grela, K., Nitro-substituted Hoveyda–Grubbs ruthenium carbenes: enhancement of catalytic activity through electronic activation, J. Am. Chem. Soc. 2004, 126:9318–9325.

[48] Lebedev, B., Smirnova, N., Kiparisova, Y., Makovetsky, K., Thermodynamics of norbornene, of its polymerization process and of polynorbornene from 0 to 400 K at standard pressure, Makromol. Chem. 1992, 193:1399–1411.

[49] Lebedev, B., Smirnova, N., Thermodynamics of cycloalkenes, of their bulk polymerization in the presence of metathesis catalysts and of polyalkenes, Macromol. Chem. Phys. 1994, 195:35–63.

[50] Stumpf, A.W., Saive, E., Demonceau, A., Noels, A.F., Ruthenium-based catalysts for the ring-opening metathesis polymerization of low-strain cyclic olefins and of functionalised derivatives of norbornene and cyclooctene, Chem. Commun. 1995, 1127–1128.

[51] Demonceau, A., Stumpf, A.W., Saive, E., Noels, A.F., Novel ruthenium-based catalyst systems for the ring-opening metathesis polymerization of low-strain cyclic olefins, Macromolecules 1997, 30:3127–3136.

[52] Jan, D., Delaude, L., Simal, F., Demonceau, A., Noels, A.F., Synthesis and evaluation of new $RuCl_2$(*p*-cymene)(ER_2R') and (η^1:η^6-phosphinoarene) $RuCl_2$ complexes as ring-opening metathesis polymerization catalysts, J. Organomet. Chem. 2000, 606:55–64.

[53] Delaude, L., Szypa, M., Demonceau, A., Noels, A.F., New in situ generated ruthenium catalysts bearing N-heterocyclic carbene ligands for the ring-opening metathesis polymerization of cyclooctene, Adv. Synth. Catal. 2002, 344:749–756.

[54] Miyaki, Y., Onishi, T., Ogoshi, S., Kurosawa, H., Co-catalyst dependent cycloisomerisation or ring closing metathesis of α,ω-dienes catalyzed by arene ruthenium complex with side-arm alcohol, J. Organomet. Chem. 2000, 616:135–139.

[55] Çetinkaya, B., Demir, S., Özdemir, I., Toupet, L., Sémeril, D., Bruneau, C., Dixneuf, P.H., First ruthenium complexes with a chelating arene ligand as catalytic precursors for alkene metathesis and cycloisomerisation, New J. J. Chem. 2001, 25:519–521.

[56] Sémeril, D., Bruneau, C., Dixneuf, P.H., Ruthenium catalyst dichotomy: selective catalytic diene cycloisomerization or metathesis, Helv. Chim. Acta. 2001, 84:3335–334.

[57] Bencze, L., Kraut-Vass, A., Prókai, L., Mechanism of initiation of the metathesis of norbornene using W(CO)3Cl2(AsPh3)2 as catalyst, Chem. Commun. 1985, 911–912.

[58] Mühlebach, A., Bernhard, P., Bühler, N., Karlen, T., Ludi, A., Ring opening metathesis polymerization of bicyclo[2.2.1]hept-2-ene and exo,exo-5,6-bis(methoxycarbonyl)-7-oxabicyclo[2.2.1]hept-2-ene using Ru(II) and Ru(III) complexes: polymerization kinetics and ruthenium content in polymers, J. Mol. Catal. 1994, 90:143–156.

[59] Alvarez, P., Gimeno, J., Lastra, P., Catalytic synthesis of polynorbornene and polynorbornadiene of low polydispersity index by [Ru(η^5-C_9H_7)Cl(COD)] (COD = 1,5-cyclooctadiene), Organometallics 2002, 21:5678–5680.

[60] Al Samak, B., Amir-Ebrahimi, V., Corry, D.G., Hamilton, J.G., Rigby, S., Rooney, J.J., Thompson, J.M., Thompson, Dramatic solvent effects on ring-opening metathesis polymerization of cycloalkenes, J. Mol. Catal. A: Chem. 2000, 160:13–21.

PHOSPHINE-FREE EWG-ACTIVATED RUTHENIUM OLEFIN METATHESIS CATALYSTS: DESIGN, PREPARATION, AND APPLICATIONS

KAROL GRELA, ANNA MICHROWSKA, MICHAŁ BIENIEK,
VOLODYMYR SASHUK, ANNA SZADKOWSKA

Institute of Organic Chemistry, Polish Academy of Sciences, Kasprzaka 44/52, 01-224, Warsaw, Poland

Abstract: Hoveyda–Grubbs catalyst has been successfully fine-tuned by us in order to increase its activity and applicability by the introduction of electron-withdrawing groups (EWGs) to diminish donor properties of the oxygen atom. As a result, the stable and easily accessible nitro-substituted Hoveyda–Grubbs catalyst has found a number of successful applications in various research and industrial laboratories. Some other EWG-activated Hoveyda-type catalysts are commercially available. The results described herewith demonstrate that the activity of ruthenium (Ru) metathesis catalysts can be enhanced by introduction of EWGs without detriment to catalysts stability. Equally noteworthy is the observation that different Ru catalysts turned out to be optimal for different applications. This shows that no single catalyst outperforms all others in all possible applications.

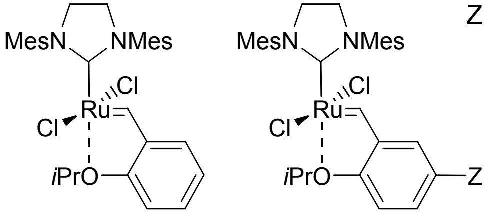

Z = NO_2, SO_2R etc

1. Introduction

Finding of a subtle balance between the stability of a catalyst (and its insensitivity to impurities), and its high activity has been called one of the "Holy Grails" of catalysis. This is especially visible in the field of olefin metathesis: a fairly old reaction that has long remained as laboratory curiosity without significance for advanced organic chemistry (Figure 1).[1]

New molybdenum and ruthenium (Ru) catalysts **1–5** (Figure 2), which combine high catalytic activity with fairly good stability, however, have revolutionized the field.[2,3] As a result, recent decades have seen a burgeoning of interest in the olefin metathesis, as witnessed by a rapidly growing number of elegant applications. Using this tool, chemists can now efficiently

Y. İmamoğlu and V. Dragutan (eds.), Metathesis Chemistry: From Nanostructure Design to Synthesis of Advanced Materials, 111-124.

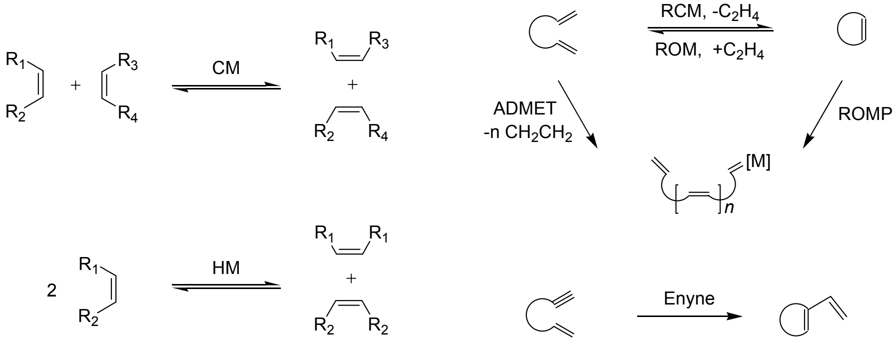

Figure 1. Olefin metatesis: RCM = ring-closing metathesis, ROM = ring-opening metathesis, ADMET = acyclic diene metathesis polymerization, ROMP = ring-opening metathesis polymerization, CM = cross-metathesis, HM = homo-metathesis.

synthesize an impressive range of molecules that only a decade ago required significantly longer and tedious routes. Especially, the development of efficient and selective Ru catalysts **2–4** has been the key to the widespread application of olefin metathesis in organic synthesis.[2–4]

1.1 Nitro-substituted Hoveyda–Grubbs ruthenium carbene: increasing the initiation ratio through electronic factors

Although the three generations of Grubbs' Ru catalyst (**2a**, **2b,** and **4**) possess in general very good application profile, combining high activity with an excellent tolerance to a variety of functional groups, the phosphine-free catalyst **3b**, introduced independently by Hoveyda and Blechert[5] displays even higher reactivity levels towards electron-deficient substrates, such as acrylonitrile, fluorinated olefins, and others.[6] Excellent air stability, ease of storage and handling, and possibility of a catalyst reuse and immobilization render additional advantages of this system.[6] In spite of the promising application profile observed in reactions of **3b**, this catalyst proved to initialize slower than **2b**, probably as a result of steric (large isopropoxy group) and electronic factors (*i*PrO→Ru electron donation).[6] Blechert and Wakamatsu have shown recently that the replacement of the isoprop-oxybenzylidene "ligand" in **3b** by BINOL- or biphenyl-based benzylidene results in large improvement in catalyst activity, as − for example − complex **5** is drastically more reactive not only than **3b** but also than the "second-generation" Grubbs' catalyst **2b** (Figure 2).[7]

At that time, we were engaged in preparation of some immobilized analogues of **3**.[8] During these studies, we have observed that the 5-bromo substituted Hoveyda catalyst reacts visibly slower then the parent catalysts **3b**. Intrigued by this result, we decided to test if tuning the electron density in the 2-isopropoxybenzylidene part of **3b** can result in the increase of catalytic activity of this complex. We surmized that strong electron-withdrawing groups (EWGs)

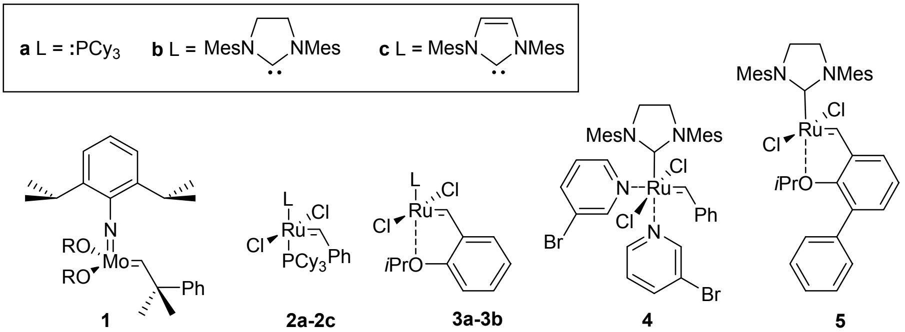

Figure 2. Modern catalysts for olefin metathesis. *i*Pr = isopropyl; Cy = cyclohexyl, Mes = 2,4,6-trimethylphenyl, R = chiral or achiral substituent [1–3].

para to the ligating *i*PrO in **3b** would weaken the *i*PrO→Ru chelation and facilitate initiation of the catalytic cycle.[9] The above hypothesis found experimental support, as we observed that the 5-nitro substituted catalyst **6** possesses a dramatically enhanced reactivity in model ring-closing metathesis (RCM), cross-metathesis (CM), and enyne-metathesis (Figure 3).[10] Interestingly, also 4-nitro isomer **7** exhibits high activity in model metathesis reactions.[10a] These complexes can be prepared in a few steps from comercially available reagents (Figure 3). It is worth to note that the air and thermodynamic stability of **6** and **7** is not reduced as compared with parent **3b**.[9,10] Later, it has been shown that the same positive effect on the catalyst activity exert other EWGs *para* (COR,[12] SO_2R,[11,12] $P(O)R_2$,[12] C_nF_{2n+2},[13] $C_5H_5N^+$,[14] and others) or *meta* (F,[15] CF_3,[15] CN,[15] NHR_2^+,[16] NR_3^+,[17] and others) to the chelating O*i*Pr group.[18]

1.2 Applications of EWG-substituted ruthenium catalysts in olefin cross-metathesis

Functionalized olefins are important building blocks for organic synthesis. Catalytic olefin CM is a convenient route to functionalized and higher olefins from simple alkene precursors. One of the most appealing facets of this

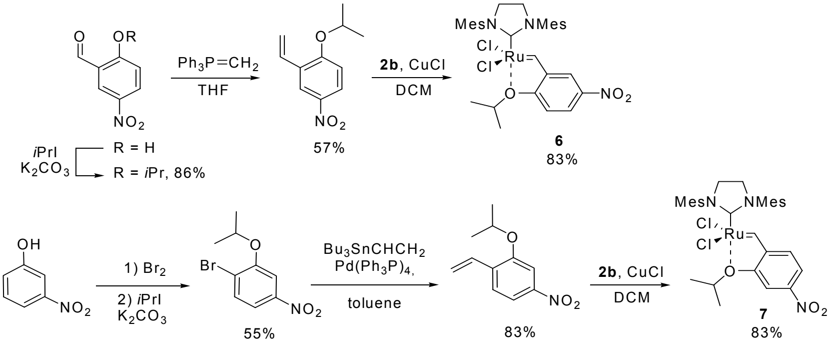

Figure 3. Preparation of nitro-substituted Hoveyda catalysts **6** and **7**.

transformation is that a carbon–carbon double bond of one of CM partners can be substituted by a heteroatom-containing or EWG.[19] Therefore, CM complements other C–C coupling methods, such as Wittig, Horner–Wadsworth–Emmons, or Heck reactions.[19] We attempted to test nitro catalysts **6** and **7** with a number of novel CM partners, such as vinyl sulfones, vinyl phosphine oxides (including a homo-metathesis – HM – variant), and vinyl azulenes. Whereas **6** was found to be catalysts of choice in most of these cases, it exhibits lower reactivity toward tetra-substituted double bonds.[10a] This shows that no single catalyst outperforms all others in all possible applications.

Vinyl sulfones. Functionalized vinyl sulfones are useful building blocks. Substituted α,β-unsaturated sulfones serve efficiently, e.g. as Michael acceptors and as 2π partners in cycloaddition reactions. In addition, the stability and ease of further transformation of sulfonyl group via elimination or either reductive or alkylative desulfonylation renders further advantages to vinyl sulfones as synthetic intermediates. Despite some previous reports,[20] we have found that the CM reaction between simple terminal alkenes and phenyl vinyl sulfone is possible using second-generation Grubbs catalyst. This transformation was later successfully applied by Evans in a stereoselective synthesis of (–)-maritolide and some other furanone natural products[21a] and by Pyne in a formal synthesis of (–)-swainsonine (Figure 4).[21b]

However, in the case of CM of more challenging alkenyl substrates, especially those bearing less available double bonds, the highest conversions and lowest catalyst loadings were achieved with **6** and **7** (Figure 5).

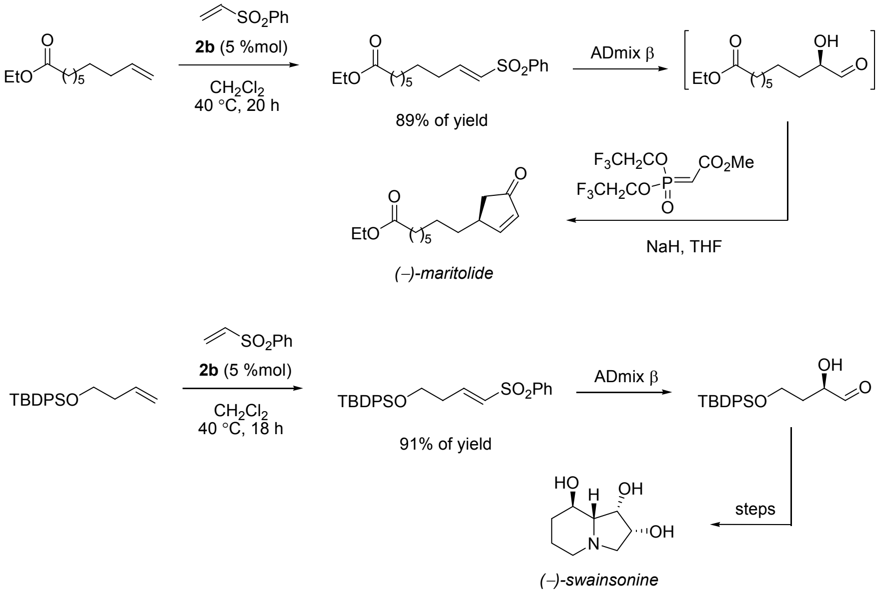

Figure 4. Application of vinyl sulfone CM in stereoselective synthesis of (–)-maritolide and (–)-swainsonine (TBDPS = *tert*-butyldiphenylsilil).

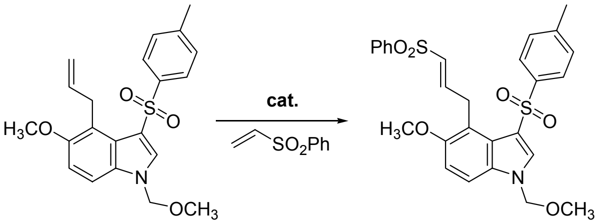

cat. (mol %)	yield
2b (10 mol %)	33%
2c (5 mol %)	44%
6 (5 mol %)	53%
7 (5 mol %)	54%

Figure 5. Comparison of catalyst **2b**, **2c**, **6**, and **7** activity in cross-metathesis of phenyl vinyl sulfone.

The commercially available divinyl sulfone $(CH_2{=}CH)_2SO_2$ and its mono and di-substituted derivatives are useful starting materials in the preparation of thiomorpholine 1,1-dioxides and other synthetically important macro- and heterocycles.[22] We have shown that divinyl sulfone can be used as a substrate for a catalytic CM, producing hitherto unreachable unsymmetrically substituted products (Figure 6).[23] The commercially available Ru complex (**2b**) and the nitro-Hoveyda catalyst (**6**) can be used in this transformation. The latter complex, in some cases revealed slightly better results with this class of compounds.[23] The presence of two double bonds in the CM products could be used for further functionalization. As an example, on Figure 6 is presented CM of divinyl sulfone followed by bis-heteronucleophilic Michael addition leading to some tiomorpholine 1,1-dioxide derivatives.[23]

Vinyl phosphine oxides. Vinyl phosphine oxides have found wide use as versatile synthetic intermediates in the preparation of various mono- and diphosphine systems.[24] The application of **2b** and **6** in CM of vinyl

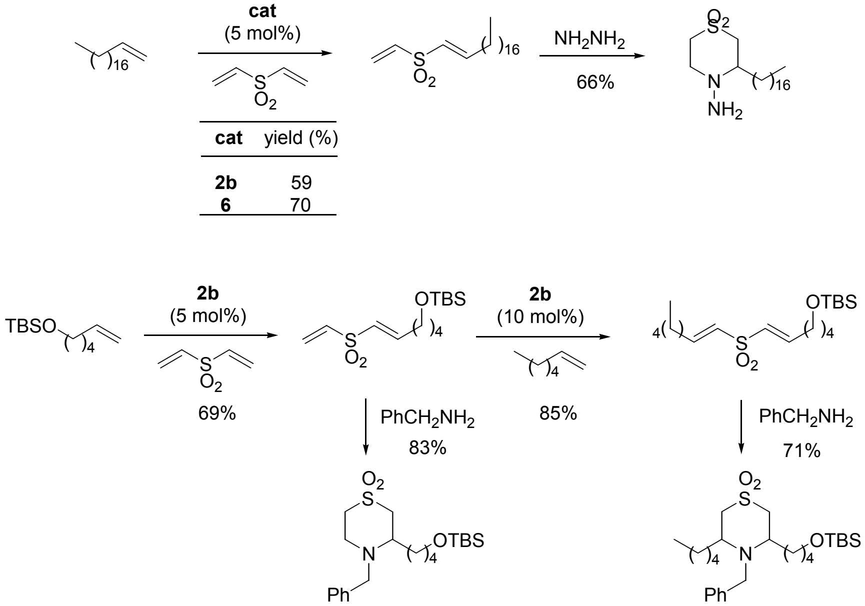

cat	yield (%)
2b	59
6	70

Figure 6. Cross-metathesis of divinyl sulfone (TBS = *tert*-butyldimethylsilil).

phosphine oxides has been reported by us (Figure 7).[25] When the CM alkene inexpensive or easily available, it can be used in excess, allowing the more economical utilization of an expensive vinylphosphine oxide partner. Olefinic substrates bearing various functionalities, including haloalkenes can be easily converted to α,β-unsaturated phosphine oxides in good yields.

In recent years, chiral, nonracemic vinyl phosphine oxides have served as convenient precursors to *P*-stereogenic ligands as well as chiral reagents for effecting *P* to *C* chirality transfer in stoichiometric addition, cycloaddition, and substitution processes. The possibility of straightforward metathetic conversion into functionalized terminally substituted analogues retaining both unsaturation and the *P*-stereogenic center has practical importance. Various substituted chiral vinylphosphine oxides can be accessed by CM reaction of enantiopure phosphine oxides catalyzed by **2a** and **6** (Figure 7).[25]

This reaction proceeds without any racemization of the chiral phosphorus center, providing easy access to functionalized enantiopure (*E*)-alkenylphosphine oxides.

Contrary to facile HM–CM of terminal olefins (Figure 1), the examples of HM between two electron-deficient olefins are rare, and good yields have only been reported for homodimerization of acrylates and enones.[26] We have found that homodimerization of some vinyl phosphine oxides proceeds with good

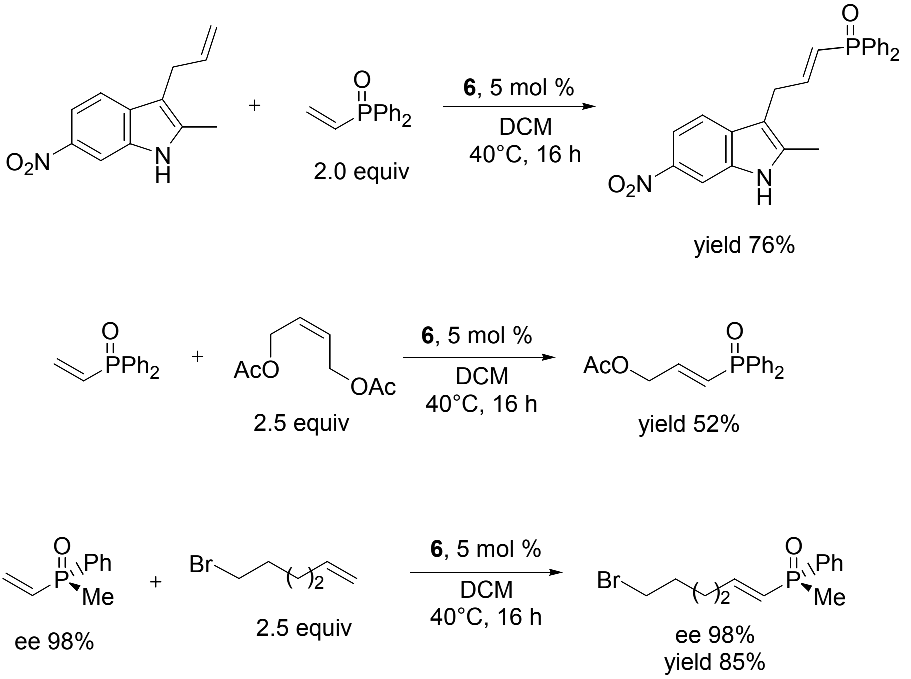

Figure 7. Cross-metathesis of vinyl phosphine oxides (Ac = $COCH_3$).

yields, leading to precursors of valuable bisphosphine ligands (Figure 8).[27] Of the Ru catalysts tested, the nitro-carbene **6** gives the best results in this transformation. The reaction proceeds under very mild conditions and chiral non-racemic products can be obtained without epimerization on a chiral-phosphorus center. A CM of vinyl phosphine oxides with other electron-deficient substrates has been also tested (Figure 8).[27]

Alkenyl and alkynyl azulenes. Azulenes, aromatic compounds with extended π-electron system, are important "organic materials" with special optical and electrical properties for the design of molecular devices. We have reported on synthesis of alkenyl-substituted azulenes utilizing metathesis reaction as a tool for functionalization of azulene core with a variety of substituents, including extending π-electron system (Figure 9).[28] According to our knowledge, this was the first example of metathesis application in the relatively unstable azulene moiety.

Vinyl chlorides. Functionalized vinyl chlorides are useful substrates in Pd-catalyzed C–C couplings and other transformations. We have found that CM reaction between substituted styrenes and *trans* or *cis*-1,2-dichloroethene used as a solvent is possible using **6** (Figure 10).[29] Further utilization of this interesting transformation is currently undergoing in our laboratory.

Applications in natural product and advanced materials synthesis. The easily accessible[30] 5-nitro substituted catalyst **6** has found a number of successful applications in various research and industrial laboratories. For

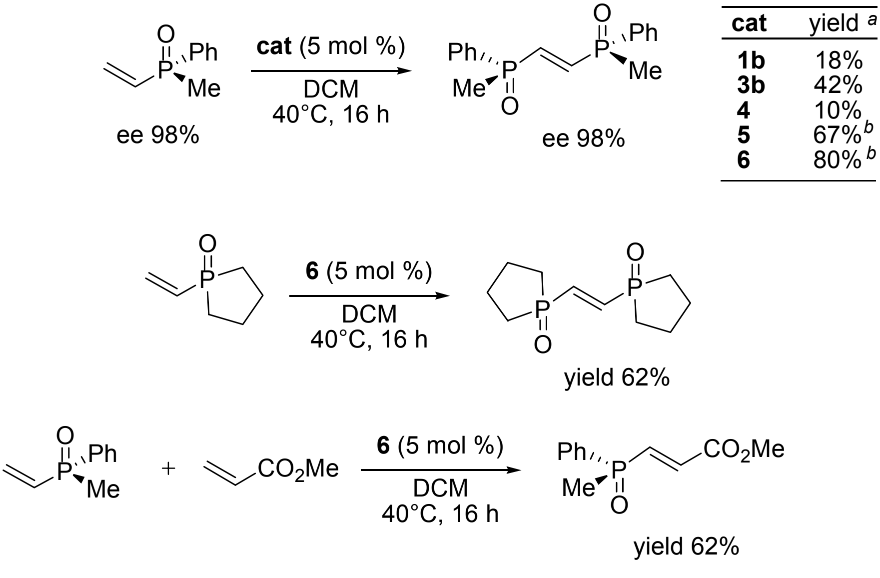

cat	yield [a]
1b	18%
3b	42%
4	10%
5	67%[b]
6	80%[b]

Figure 8. Homo- and cross-metathesis of vinyl phosphine oxides. [a]NMR yield; [b]isolated yields.

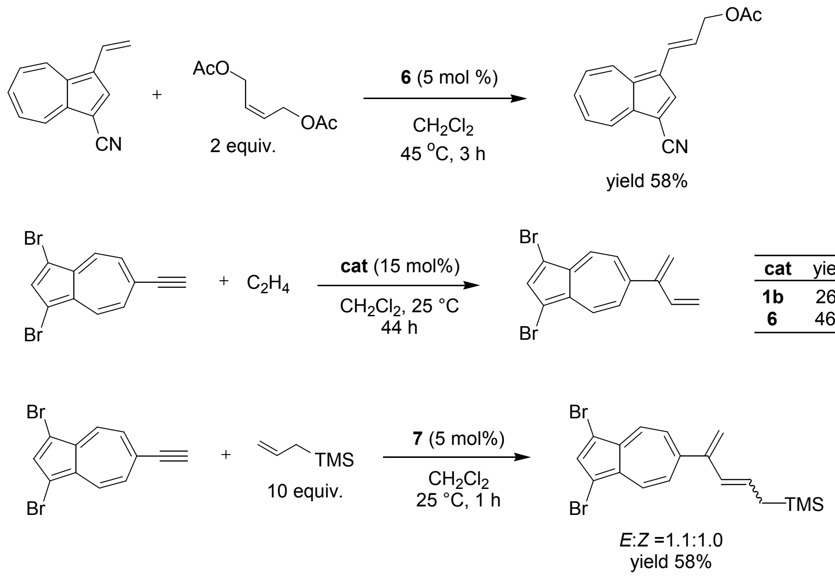

Figure 9. Preparation of substituted azulenes by cross-metathesis (TMS = Me_3Si).

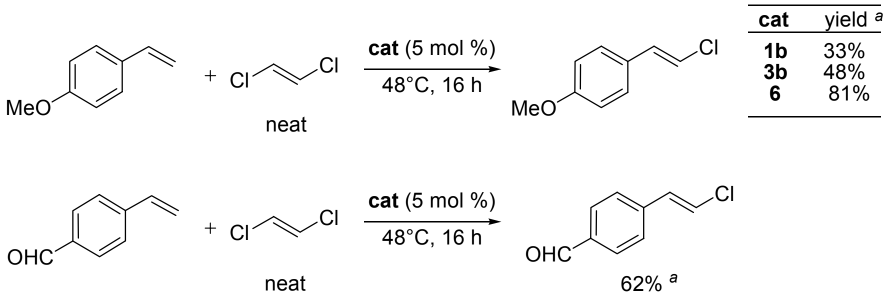

Figure 10. Preparation of substituted vinyl chlorides by cross-metathesis. [a]GC yield.

example, a very effective tandem enyne–RCM reaction using only 1 mol % of the nitro-catalyst **6** has been applied by Honda (Tokyo, Japan) as a key step in a total synthesis of a cytotoxic alkaloid (+)-viroallosecurinine (Figure 11).[31] The same research group has published a synthesis of another member of the Securinega family, (–)-securinine, utilizing similar domino reaction catalyzed by **6**.[32]

Ostrowski (Siedlce, Poland) applied **6** in preparation of some porphyrin building blocks,[33] including a porphyrin–fullerene dyad, being a new artificial photosynthetic model (Figure 12).[34]

An interesting application of the nitro-catalyst **6** has been recently published by Boehringer Ingelheim Ltd. in synthesis of BILN 2061 (Ciluprevir), the first reported hepatitis C virus (HCV) NS3 protease inhibitor to have shown

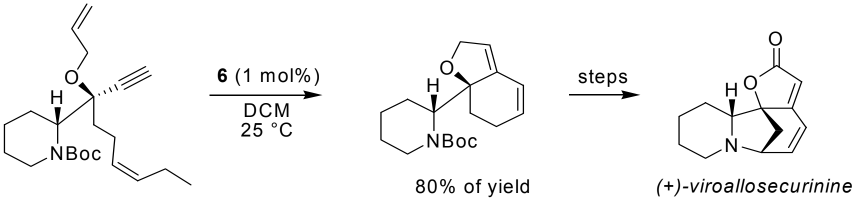

Figure 11. Application of 6 as a key step in total synthesis of (+)-viroallosecurinine (Boc = ^{t}BuOC(O))[31]

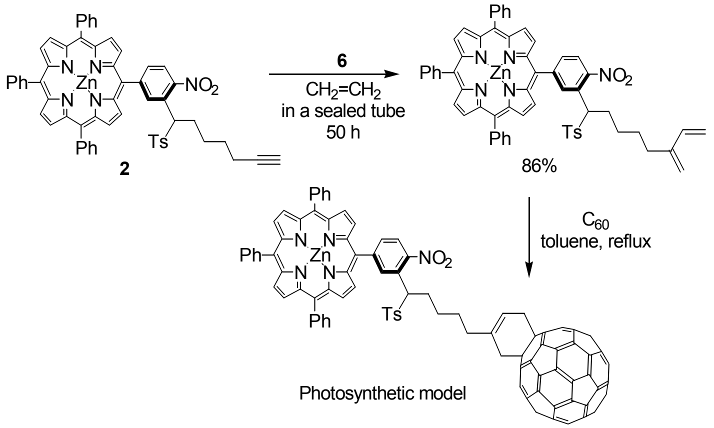

Figure 12. Preparation of a porphyrin-fullerene dyad (Ts = toluenesulfonyl)[34]

an antiviral effect in infected humans.[35] The HCV infection is a serious cause of chronic liver disease worldwide. The macrocyclic peptide, BILN 2061, is the first compound of its class to have reached clinical trials.[36] It has shown oral bioavailability and antiviral effects in humans infected with HCV.[36] The key step in the preparation of BILN 2061 is the RCM formation of the 15-membered ring.[35] Several Ru catalysts could be used in this reaction,[37] however, the nitro-substituted **6** was found to be catalyst of choice. Loadings as low as 0.6 mol % of **6** give good results in the cyclization of macrocyclic ring of BILN 2061, making this step highly effective in large-scale preparations (Figure 14).[38]

Recently, another EWG-activated catalyst obtained in Warsaw (Figure 13) have been used in the same transformation, giving similar results.[39]

A CM reaction catalyzed by **6** was used by Kalesse (Hannover, Germany) to install the conjugated ester functionality for a subsequent intramolecular Michael addition en route to antitumor hexacyclinic acid and (–)-FR182877 (Figure 15).[40]

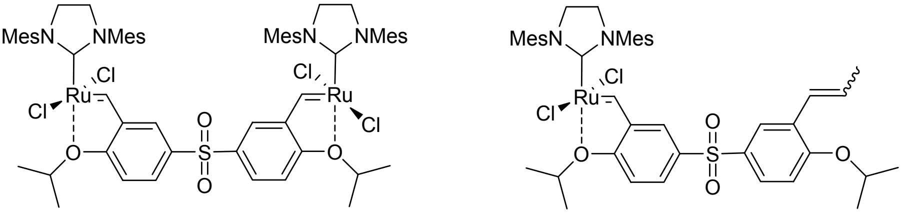

8a **8b**

Figure 13. Catalysts derived from Bisfenol – S.

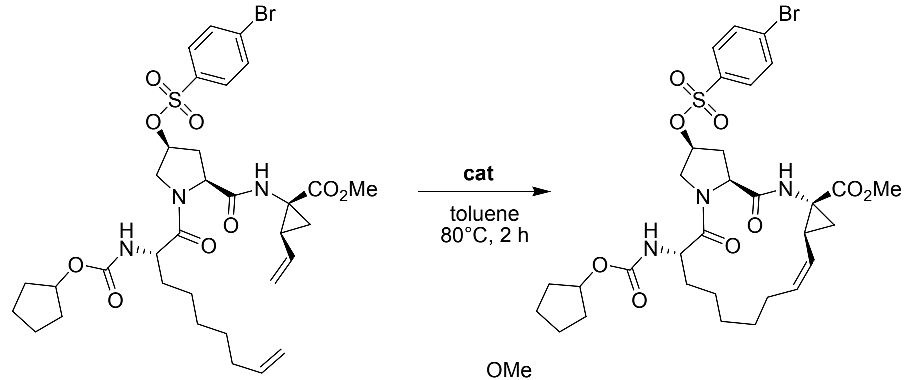

Cat (% mol)	Conversion (%)[a]
8a (0.3)	99
8b (0.4)[b]	69
8b (0.6)	89
6 (0.4)[b]	77
6 (0.6)	96

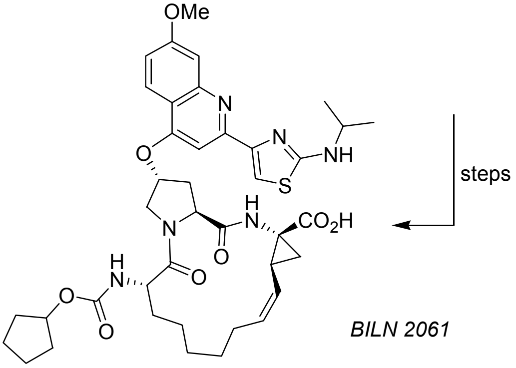

Figure 14. Preparation of the macrocyclic peptide BILN 2061. [a]Conversion calculated by HPLC; [b]conversion after 1 h.

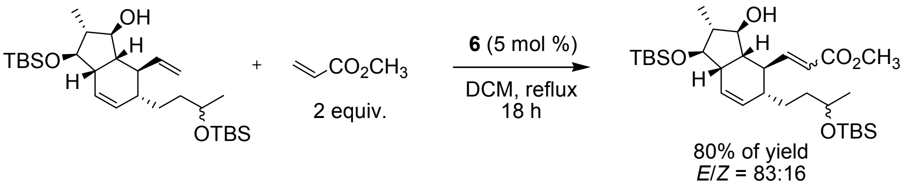

Figure 15. Preparation of an intermediate en route to hexacyclinic acid and (–)-FR182877 (TBS = *tert*-butyldimethylsilil).

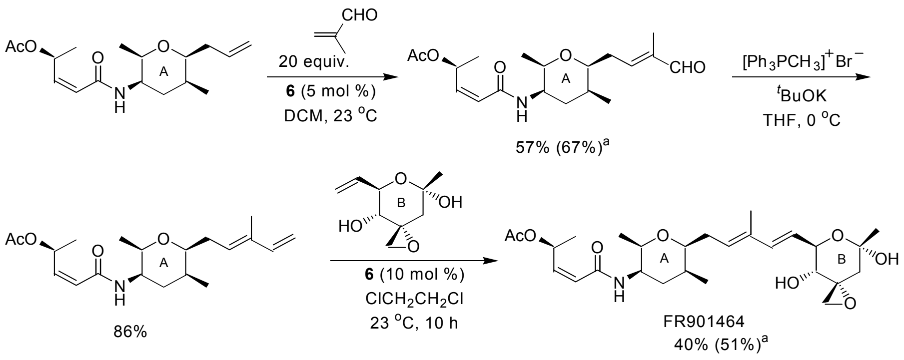

Figure 16. The final steps of FR901464 total synthesis utilizing 6 in catalytic CM. [a]Yield based on recovered substrates (Ac = $COCH_3$)[41]

Another impressive CM application of **6** was published by Koide et al. (Pittsburgh, USA) in total synthesis of FR901464, an antitumor agent that regulates the transcription of oncogenes and tumor suppressor genes (Figure 16).[41]

Especially challenging was the final connection of two fragments of this antitumor agent via diene–ene CM. The fragile nature of alkene fragment B (thermal decomposition at >47°C) precluded more forcing reaction conditions. Gratifyingly, despite the absence of *any protecting groups*,[41] application of the highly active catalyst **6** at room temperature furnished FR901464 in 40% yield (51% based on recovered diene).[41]

Recently, Barrett (Imperial College, London, UK) applied another challenging CM in the synthesis of some antibiotic viridiofungin derivatives (Figure 17).[42] The authors' statement: "In particular we focused on the use of the Grubbs II catalyst (**2b**), the Hoveyda catalyst (**3b**), the Blechert catalyst (**5**) and the Grela catalyst (**6**). In our hands, neither catalyst **2b** nor **3b** was especially effective with slow and incomplete conversions. Both catalysts **5** and **6** were superior with the Grela catalyst **6** the most effective. Although conversion by ^{1}H NMR was high (>95%), extensive chromatography was required to remove ruthenium residues from the polar acid **9**, which was isolated in 57% yield" can be a good example illustrating the fact that just a good chemical activity is not enough and also an efficient Ru removal step is equally important in a total synthesis.

A potential solution of this problem has been recently developed at Max-Planck Institut für Kohlenforschung (Mülheim an der Ruhr, Germany) in close cooperation with industrial partners.[43] Ionic liquids (IL) were used as an immobilizing matrix for catalyst **6** and the metathesis reaction was conducted in supercritical carbon dioxide. This technology can now be operated under continuous-flow conditions and used for the macrocyclization of some pharmaceutical precursors.[43]

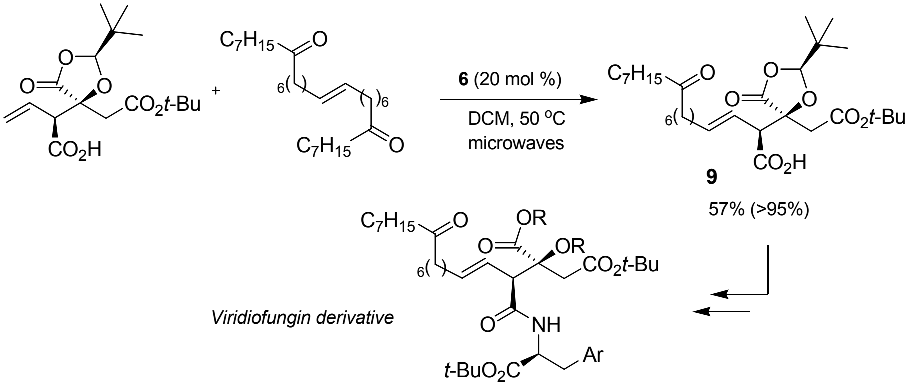

Figure 17. Preparation of viridiofungin devartivities[42]

2. Summary and outlook

Oxygen ether derivatives **3**, pioneered by Hoveyda, exhibit high activity and possess excellent functional group tolerance. Catalyst **3b** has been successfully fine-tuned by us in order to increase its activity and applicability by the introduction of EWGs to diminish donor properties of the oxygen atom. As a result, the stable and easily accessible nitro-substituted catalyst **6** has found a number of successful applications in various research and industrial laboratories. Some other EWG-activated Hoveyda-type catalysts are become commercially available. The results described herewith demonstrate that the activity of Ru metathesis catalysts can be enhanced by introduction of EWGs without detriment to catalysts stability. Equally noteworthy is the observation that different Ru catalysts turned out to be optimal for different applications. This shows that no single catalyst outperforms all others in all possible applications.

The authors are grateful to Professor Dieter Arlt (Ligand Chemie GmbH), Dr. Robert Bujok (Institute of Organic Chemistry, Warsaw) for his invaluable contribution to this work and to all coworkers, whose names appear in the references, for their enthusiastic collaboration. Financial supports from the Alexander von Humboldt Foundation, the State Committee of Scientific Research, and the Polish Academy of Sciences are gratefully acknowledged.

References

[1] Astruc, D., New, J., Chem. 2005, 29:42.
[2] Grubbs, R.H. (ed.), Handbook of Metathesis, Vols. 1–3 Wiley-VCH, Weinheim, 2003.
[3] General reviews, see [1–2] and: (a) Grubbs, R.H., Chang, S., Tetrahedron 1998, 54;4413; (b) Schrock, R.R., Top. Organomet. Chem. 1998, 1:31; (c) Fürstner, A., Angew. Chem. Int. Edit. 2000, 39:3012; (d) Trnka, T.M., Grubbs, R.H., Acc. Chem. Res. 2001, 34:18; (e) For selected key papers on achiral and chiral

molybdenum catalysts, see: Hoveyda, A.H., Schrock, R.R., Chem. Eur. J. 2001, 7:945; (f) Schrock, R.R., Hoveyda, A.H., Angew. Chem. Int. Edit. 2003, 38:4555; (g) Schrock, R.R., Pure Appl. Chem. 1994, 66:1447; (h) Murdzek, J.S., Schrock, R.R., Organometallics 1987, 6:1373.

[4] The importance of "the development of the metathesis method in organic synthesis" has been recently recognized by awarding the Nobel Prize in Chemistry for 2005 jointly to Yves Chauvin, Robert H. Grubbs and Richard R. Schrock, see: http://http://nobelprize.org/chemistry/laureates/2005/chemadv05.pdf for more details.

[5] (a) Kingsbury, J.S., Harrity, J.P.A., Bonitatebus, P.J., Hoveyda, A.H.J., Am. Chem. Soc. 1999, 121:791; (b) Garber, S.B., Kingsbury, J.S., Gray, B.L., Hoveyda, A.H.J., Am. Chem. Soc. 2000, 122:8168; (c) Gessler, S., Randl, S., Blechert, S., Tetrahedron Lett. 2000, 41:9973.

[6] (a) For a short review, see: Hoveyda, A.H., Gillingham, D.G., Van Veldhuizen, J. J., Kataoka, O., Garber, S.B., Kingsbury, J.S., Harrity, J.P.A., Org. Biomol. Chem. 2004, 2:1.

[7] (a) Wakamatsu, H., Blechert, S., Angew. Chem. Int. Edit. 2002, 41:794; (b) Wakamatsu, H., Blechert, S., Angew. Chem. Int. Edit. 2002, 41:2403; (c) For an improved synthesis of **5** and reactivity studies, see: Dunne, A.M., Mix, S., Blechert, S., Tetrahedron. Lett. 2003, 44:2733.

[8] Grela, K., Tryznowski, M., Bieniek, M., Tetrahedron Lett. 2002, 43:9055.

[9] Grela, K., Harutyunyan, S., Michrowska, A., Angew. Chem. Int. Edit., 2002, 41:4038.

[10] (a) Michrowska, A., Bujok, R., Harutyunyan, S., Sashuk, V., Dolgonos, G., Grela, K.J., Am. Chem. Soc. 2004, 126:9318; (b) Harutyunyan, S., Michrowska, A., Grela, K., in: Roberts, S. (ed.), Catalysts for Fine Chemical Synthesis, Vol. 3, Wiley Interscience, Hoboken, NJ, 2004, Chap. 9.1, pp. 169; (c) Grela, K., US Patent 6,867,303.

[11] Bieniek, M., Bujok, R., Stępowska, H., Jacobi, A., Hagenkötter, R., Arlt, D., Jarzembska, K., Woźniak, K., Grela, K., J. Organomet. Chem. (in press).

[12] Boehringer Ingelheim International GmbH, EP 03 027828.7, 2003.

[13] Bujok, R., Grela, K., unpublished data.

[14] Rix, D., Clavier, H., Gulajski, L., Grela, K., Mauduit, M., J. Organomet. Chem. 2006 (in press).

[15] Dunne, A.M., Mix, S., Blechert, S., Tetrahedron Lett. 2003, 44:2733.

[16] (a) Gułajski, Ł., Michrowska, A., Bujok, R., Grela, K., J. Mol. Catal. A: Chem. 2005, 254:118; (b) Michrowska, A., Mennecke, K., Kunz, U., Kirschning, A., Grela, K., J. Am. Chem. Soc. 2006 (in press).

[17] Michrowska, A., Gułajski, Ł., Kaczmarska, Z., Mennecke, K., Kirschning, A., Grela, K., Green Chem. 2006, 8:685.

[18] EWG-activated Hoveyda-type catalyst is available commercially from Strem Chemicals, Inc. and from Zannan Pharma.

[19] For reviews on catalytic cross-metathesis, see: (a) Blechert, S., Connon, S.J., Angew. Chem. Int. Edit. 2003, 42:1900; (b) Vernall, A.J., Abell, A.D., Aldrichimica Acta 2003, 36:93; (c) Blackwell, H.E., O'Leary, D.J., Chatterjee, A.K., Washenfelder, R.A., Bussmann, D.A., Grubbs, R.H., J. Am. Chem. Soc. 2000, 122:58; (d) For a short review on applications to commercial products, see: Pederson, R.L., Fellows, I.M., Ung, T.A., Ishihara, H., Hajela, S.P., Adv. Synth. Catal. 2002, 344:728; (e) For a general model for selectivity in olefin CM, see Chatterjee, A.K., Choi, T.-L., Sanders, D.P., Grubbs, R.H., J. Am. Chem. Soc. 2003, 125:11360.

[20] Previously, a failure in the CM reaction of vinyl sulfones was reported, see: (a) Chatterjee, A.K., Morgan, J.P., Scholl, M., Grubbs, R.H., J. Am. Chem. Soc. 2000, 122:3783; (b) Randl, S., Blechert, S., unpublished data; see Ref. 47.

[21] (a) Evans, P., Leffray, M., Tetrahedron 2003, 59:7973; (b) Au, C.W.G., Pyne S.G., J. Org. Chem. 2006, 71:7097.

[22] Teyssot, M.-L., Fayolle, M., Philouze, C., Dupuy, C., Eur. J. Org. Chem. 2003, 54, and references cited therein.

[23] Bieniek, M., Kołoda, D., Grela, K., Org. Lett. (in press).

[24] Pietrusiewicz, K.M., Zablocka, M., Chem. Rev. 1994, 94:1375.

[25] Demchuk, O.M., Pietrusiewicz, K.M., Michrowska, A., Grela, K., Org. Lett. 2003, 5:3217.

[26] (a) Choi, T.L., Lee, C.W., Chatterjee, A.K., Grubbs, R.H., J. Am. Chem. Soc. 2001, 123:10417; (b) Yao, Q., Motta, A.R., Tetrahedron Lett. 2004, 45:2447.

[27] Vinokurov, N., Michrowska, A., Szmigielska, A., Drzazga, Z., Wójciuk, G., Demchuk, O.M., Grela, K., Pietrusiewicz, K.M., Butenschön, H. Adv. Synth. Catal. 2006, 348:931.

[28] Mikus, A., Sashuk, V., Kędziorek, M., Samojłowicz, C., Ostrowski, S., Grela, K., Synlett 2005, 1142.

[29] Szadkowska, A., Grela, K., unpublished data.

[30] (a) Bujok, R., Bieniek, M., Masnyk, M., Michrowska, A., Sarosiek, A., Stępowska, H., Arlt, D., Grela, K., J. Org. Chem. 2004, 69:6894; (b) Bieniek, M., Michrowska, A., Gułajski, Ł., Grela, K., Organometallics 2006 (accepted).

[31] Honda, T., Namiki, H., Watanabe, M., Mizutani, H., Tetrahedron Lett. 2004, 45:5211.

[32] Honda, T., Namiki, H., Kaneda, K., Mizutani, H., Org. Lett. 2004, 6:87.

[33] (a) Ostrowski, S., Mikus, A., Heterocycles 2005, 65:2339; (b) Ostrowski, S., Mikus, A., Mol. Diversity 2003, 6:315.

[34] PTC Patent Application WO 2004/089974 A1, Boehringer Ingelheim International, 2004.

[35] Lamarre, D., Anderson, P.C., Bailey, M.D., Beaulieu, P., Bolger, G., Bonneau, P., Bos, M., Cameron, D.R., Cartier, M., Cordingley, M.G., Faucher, A.M., Goudreau, N., Kawai, S.H., Kukolj, G., Lagace, L., LaPlante, S.R., Narjes, H., Poupart, M.A., Rancourt, J., Sentjens, R.E., St George, R., Simoneau, B., Steinmann, G., Thibeault, D., Tsantrizos, Y.S., Weldon, S.M, Yong C.L., Llinas-Brunet, M., Nature 2003, 426:186.

[36] Faucher, A.M., Bailey, M.D., Beaulieu, P.L., Brochu, C., Duceppe, J.S., Ferland, J.M., Ghiro, E., Gorys, V., Halmos, T., Kawai, S.H., Poirier, M., Simoneau, B., Tsantrizos, Y.S., Llinas-Brunet, M., Org. Lett. 2004, 6:2901.

[37] Nicola, T., Brenner, M., Donsbach, K., Kreye, P., Org. Proc. Res. Devel. 2005, 9:513.

[38] Bieniek, M., Bujok, R., Stępowska, H., Jacobi, A., Hagenkötter, R., Arlt, D., Jarzembska, K., Woźniak, K., Grela, K., J. Organomet. Chem. 2006 (in press).

[39] Stellfeld, T., Bhatt, U., Kalesse, M., Org. Lett. 2004, 6:3889.

[40] Albert, B.J., Sivaramakrishnan, A., Naka, T., Koide, K., J. Am. Chem. Soc. 2006, 128:2792.

[41] Goldup, S.M., Pilkington, C.J., White, A.J.P., Burton, A., Barrett, A.G.M., J. Org. Chem. 2006, 71:6185.

[42] Leitner, W. in Forschungsbericht 2002–2004, Max-Planck-Institut für Kohlenforschung, Mülheim an der Ruhr, 2005, p. 60; http://www.mpi-muelheim.mpg.de/kofo/bericht2005/bereiche/alles.pdf

METATHESIS CATALYSTS STABILITY AND DECOMPOSITION PATHWAY

ALEXEY V. NIZOVTSEV[1], VLADIMIR V. AFANASIEV[1],
EGOR V. SHUTKO[1], NATALIA B. BESPALOVA[1,2]

[1]*United Research & Development center, 55/1, b.2, Leninsky pr., Moscow, 119333, Russia*
[2]*A.V. Topchiev Institute of Petrochemical Synthesis Russian Academy of Sciences, 29, Leninsky pr., Moscow, 119991, Russia*

1. Introduction

High efficiency and commercial availability of well-defined metathesis catalysts 1–3 has made olefin metathesis reaction practical for large-scale fine chemicals production.

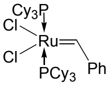

1

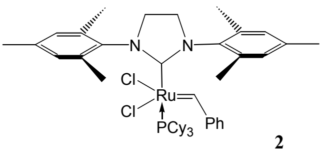

2

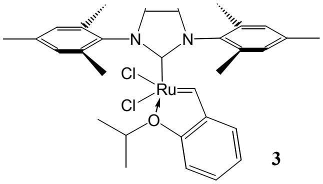

3

1.1 Mechanism of olefin metathesis reaction

The mechanism of olefin metathesis reaction catalyzed by ruthenium (Ru) carbenoids was intensively studied over last 8 years both experimentally [1] and theoretically involving calculation method [2]. It has been assumed for this reaction to proceed with participant of 14-electron–Ru complexes and

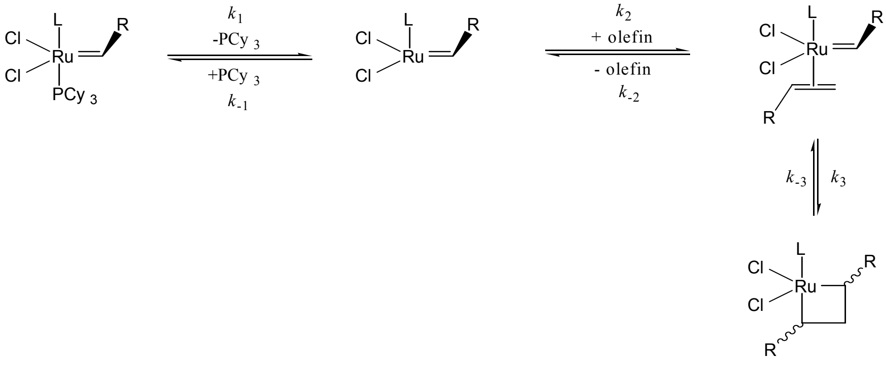

Scheme 1. A general mechanism for olefin metathesis reaction catalyzed by Grubbs catalysts [1].

Y. İmamoğlu and V. Dragutan (eds.), Metathesis Chemistry: From Nanostructure Design to Synthesis of Advanced Materials, 125-135.

ruthenocyclobutanes (Scheme 1) [1]. The formation of last species was confirmed by ^{1}H NMR recently [3].

1.2 Ligand effect on thermal stability of ruthenium olefin metathesis catalysts

Analysis of literature showed that most of information concerning thermal stability, degradation, and deactivation of Ru–carbene catalysts has been obtained for first- and second-generation Grubbs catalysts. There are only solitary reports about decomposition of Hoveyda-type catalysts without details.

1.2.1 Phosphine ligand (PR_3)

First-generation Grubbs catalyst (**1**) containing two PCy_3 substituents possess relatively high thermal stability both in solid state and in solution (half-life of (**1**) in benzene solution at 55°C is about 8 days) [4,5]. The thermal decomposition of complex (**1**) has been studied in details and it has been proposed to occur via phosphine dissociation followed by bimolecular coupling of two 4-coordinate Ru fragments [1b,4]. This process proceeds with formation of free phosphine, product of carbenoid dimerization, and inorganic products (Eq. 1). Such pathway for alkylidene decomposition was confirmed by analyzing of ^{31}P NMR and ^{1}H NMR spectra of decomposition of propylidene (**4**). ^{31}P NMR spectrum contained predominantly signals of free PCy_3 and of small amount of unidentifiable phosphine products. The most notable aspect of ^{1}H NMR spectrum of the similar reaction mixture was the initial quantitative formation of *trans*-3-hexene [4]. It has been shown that the complexes decomposition has a second-order kinetic and can be inhibited by addition of phosphine [9].

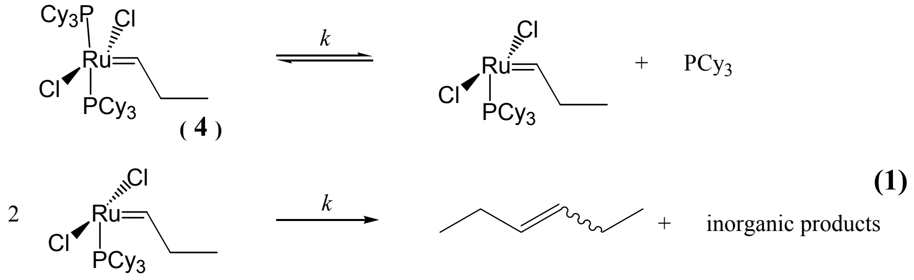

(1)

Modification of phosphine in many cases leads to changes in activity of catalyst. It has been found that the initiation step of metathesis reaction and stability of catalyst are correlated – complexes with more labile phosphines (e.g. PPh_3) exhibit high rate of Ru–P bond dissociation together with low thermal stability [1c,5,6]. Similar observations were made for second-generation Grubbs catalyst (**2a**) and its different phosphine modifications [7].

1.2.2 L-type ligand

The variation of L-type ligands is limited. It has been shown [8] that ligand for metathetically active catalyst must be electron donor and sterically blocked. Generally, it was found that the replacement of one phosphine fragment by imidazole or dihydroimidazole moiety into first-generation Grubbs catalyst (e.g. complexes **1** and **2a**, respectively) leads to significant increasing of complex stability and, at the same time, about 70-fold decrease in the rate of initiation [1b,7,8].The replacement of mesylsubstituent (2,4,6-trimethylphenyl) with *p*-tolyl or *p*-chlorophenyl significantly decrease the catalytic activity of complex [8]:

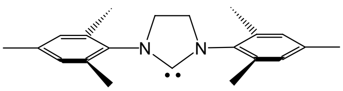

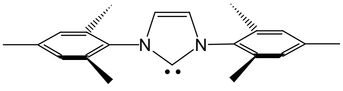

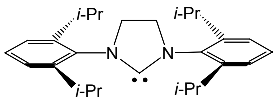

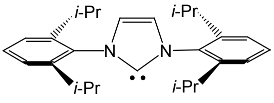

1.2.3 Carbene ligand (R_1)

It has been shown that Grubbs complexes with benzylidene group (**I**) are more stable in comparison with other carbenes (Table 1) [4]. This moiety is gradually consuming during initiation step (Scheme 1). It usually leads, especially in case of terminal olefins metathesis or ethenolysis, to the formation of methylidene carbenes (**5**) and (**6a**):

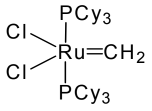

5

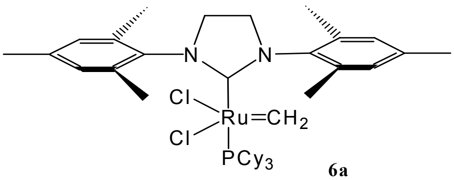

6a

From this point of view the understanding of methylidene decomposition and stability is important for designing a more stable catalytic system. Usually, the catalyst destruction was studied based only on kinetic experiments without isolation and identification of products of decomposition [8,10,11]. Recently, Grubbs and coworkers isolated the major product formed after heating of (**6a**) in benzene solution (Eq. 2) [9]. The structure of (**7**) was proved by x-ray crystallography. Complex (**7**) was isolated with yield 46%. It has been shown that this complex is responsible for the C=C double bond isomerization [9].

Table 1. Thermolytic half-lives of complexes in benzene at 55°C [1b,4,9]

Carbenoid	Half-life (h)
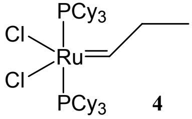 **4**	8
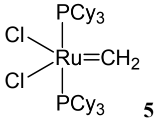 **5**	0.6
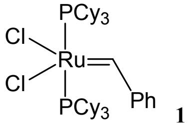 **1**	190
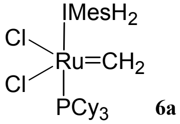 **6a**	5.6

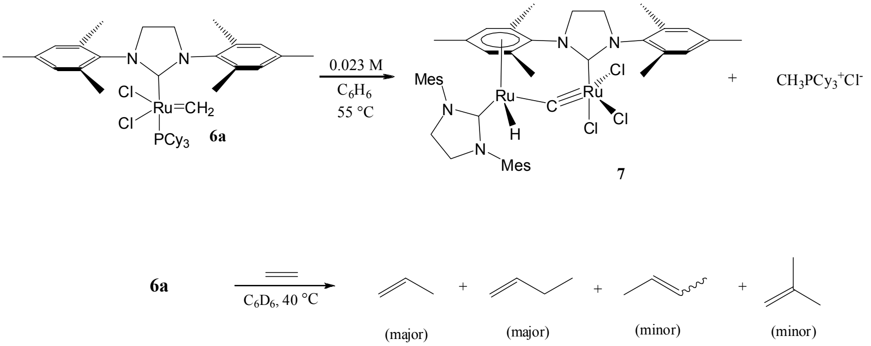

(2)

Notably the methylidene complexes (**5**) and (**6a**) appear to decompose by a different pathway than Ru alkylidenes and benzylidenes. The decomposition of both of them exhibit first-order kinetics (all other complexes have second-order kinetic) and is not inhibited by addition of free phosphines [10]. Moreover, using deuterium-labeled complexes it has been shown that phosphine takes part as a participant in this process in contrast to other alkylidenes (Scheme 2) [4].

On the other hand type of ligand (P- or N- ligand) at Ru–carbene has strong effect on the stability of methylene species: half-life time are 0.6 and 5.5 h for (**5**) (P)Ru=CH_2 and (**6a**) (N)Ru=CH_2. This fact indicates that ligand L determines the stability of the Ru–carbene catalyst.

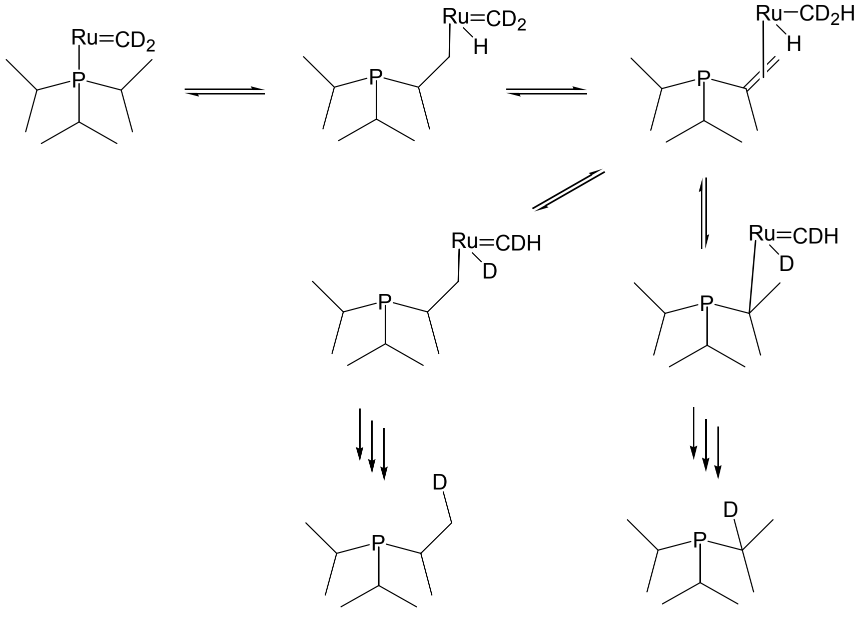

Scheme 2. Proposed pathway for deuterium incorporation on the phosphine [4].

Degradation of Grubbs catalysts both first and second generations with alcohols, water, and oxygen was studied by Mol and coworkers. Recently, they have shown that Grubbs catalyst of first generation (**1**) reacted with methanol in toluene at 70°C with formation of a monohydride species (**8**) after 2 days (Eq. 3) [13]. It has been shown that this hydride was responsible for the carbon–carbon double-bond isomerization – unwanted process in metathesis reaction [11].

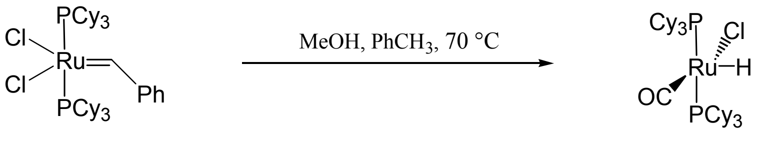

1 **8**

(3)

Addition of base as inorganic (sodium methoxide, sodium hydroxide, potassium carbonate) and organic (triethylamine) greatly facilitate the hydride-forming reaction in terms of both rate of formation and yield. Catalyst (**1**) reacts in the same manner also with ethanol and propanol, but 2-propanol remained essentially unreactive for hydride formation even in the presence of bases [11].

The reaction of (**1**) with benzyl alcohol gave the new complex (**9**) with Ru–C bond instead of (**8**) (Eq. 4) [11]. It has been shown that this compound was formed also in the reaction of (**1**) with oxygen in solvent and solid state as well. Furthermore, it was observed as a product of catalyst decomposition in solvent-free metathesis of 1-hexene in the presence of (**1**). It is necessary to note that ^{1}H NMR of decomposed catalyst showed no hydride- or metal-carbene-containing compounds [11].

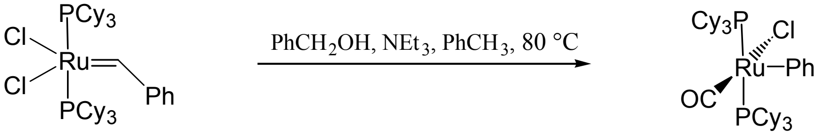

1 **9** **(4)**

Grubbs catalysts of second generation (**2a**, **b**) react with primary alcohols, benzyl alcohol, and oxygen in similar manner giving hydrides (**10a**, **b**) or Ru–C species (**11a**, **b**) [14,15]. It has been shown that the hydrides (**10a**, **b**) are also responsible for C=C double-bond isomerization in metathesis reaction [12,13].

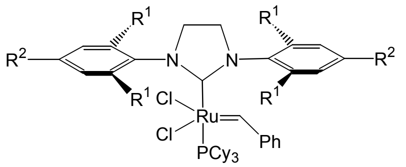

2a $R^1 = R^2 = Me$
2b $R^1 = i\text{-Pr}; R^2 = H$

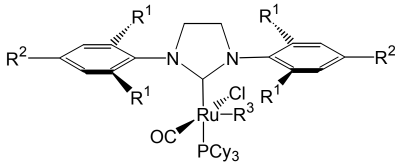

10a $R^1 = R^2 = Me; R^3 = H$
10b $R^1 = i\text{-Pr}; R^2 = H; R^3 = H$
11a $R^1 = R^2 = Me; R^3 = Ph$
11b $R^1 = i\text{-Pr}; R^2 = H; R^3 = Ph$

Poisoning effect of carbon monoxide for (**2a**) Grubbs catalyst was reported by J. Diver (Eq. 5). Reaction takes place at ambient temperature and atmospheric pressure with *N*-heterocyclic carbene (NHC) aromatic ring opening followed with benzylidene insertion [16]:

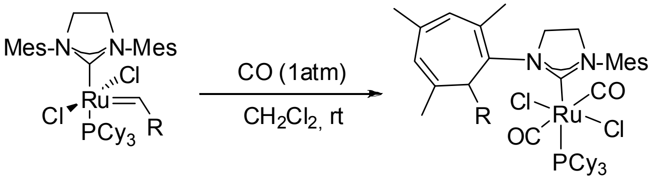

R=Ph, 90%
R=H, 63%

(5)

C–H bond activation of one ortho methyl of the mesityl group at aerobic conditions (Eq. 6) is also responsible for (**2a**) degradation [17]:

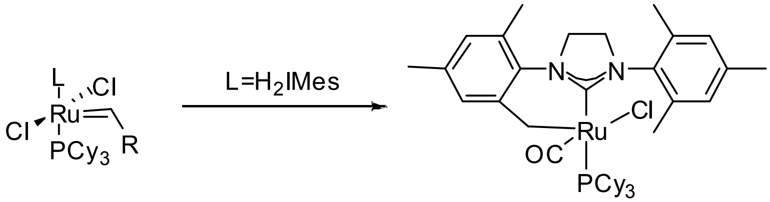

(6)

The influence of substrate. There are just a few reported experimental studies which focus on that problem [18]. All of them are concerning of the C=C double-bond isomerization process which usually was catalyzed by Ru hydride species formed in the reaction mixture after metathesis catalyst destruction. Recently, the theoretical results about substrate-induced catalyst decomposition involving β-hydride transfer from ruthenocyclobutane intermediate (Scheme 3) were published [19].

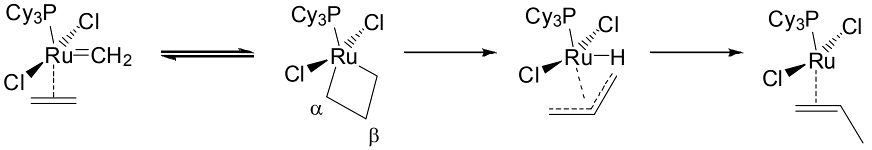

Scheme 3. A proposed metathesis catalyst decomposition route by means of β-hydride transfer [20].

This theoretical study was experimentally confirmed. In particular, it has been shown that the reaction of methylidene (**5**) with ethylene in benzene at 40°C led to the formation of mixture of products, where the propylene and 1-butene are major (Eq. 7) [19]. Similar results were obtained in reaction of methylidene (**6a**) with ethylene in the same conditions [19].

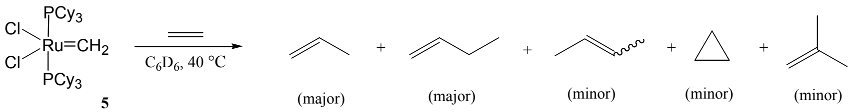

(7)

2. Results and discussion

In our investigation we tried to understand the decomposition of second-generation Hoveyda–Grubbs catalyst under ethylene atmosphere.

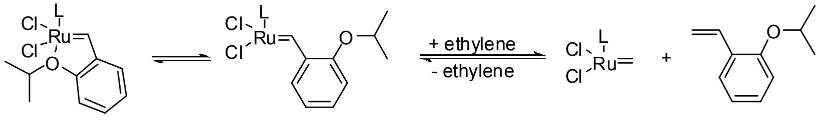

(8)

The decomposition of the same methylidene induced by ethylene was studied both as experimentally and theoretically and it has been shown that this reaction led to the formation of higher olefins (Eq. 8). [19]. We found that the substrate induced by decomposition of second-generation Hoveyda catalyst led to the similar mixture of olefins with preferable formation of propylene (Eq. 9, Table 2). According to integration of ^{1}H NMR spectrum the yield of propylene is close to amount of reacted starting complex (Figure 1)

Heating of the reaction mixture at 55°C during 24 h leads to almost full consumption of carbenoid complexes (based on analysis of low field nuclear magnetic resonance (NMR) region. No Ru hydride species were detected in the reaction mixture. In NMR olefinic region new signals were appeared which were attributed mainly to propylene as well as small amount of other alpha olefins (the major 1-butene) and internal olefins. These by-products were confirmed by global land cover (GLC) data (Figure 2).

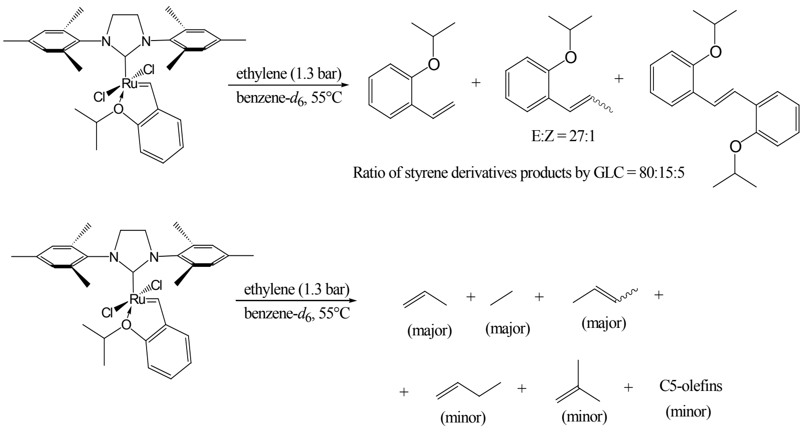

(9)

Table 2. Relative peaks area of light products observed from GC analysis after reaction of (**3**) with excess of ethylene in benzene at 55°C after 24 h (ethylene, air, and heavy compounds peaks are omitted)

Component	Area (%)
Ethane	6.93
Propylene	79.25
trans-2-Butene	7.18
1-Butene	1.19
Isobutylene	0.39
cis-2-Butene	2.50
Unidentified C5 olefins	2.56

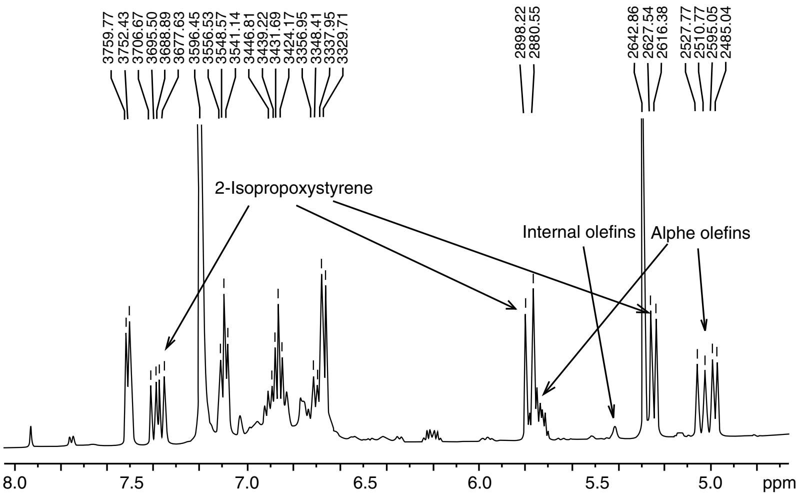

Figure 1. Olefin region of ^{1}H NMR spectrum of reaction mixture after treatment of complex (**6**) with excess of ethylene in benzene-d_6 at 55°C during 24 h.

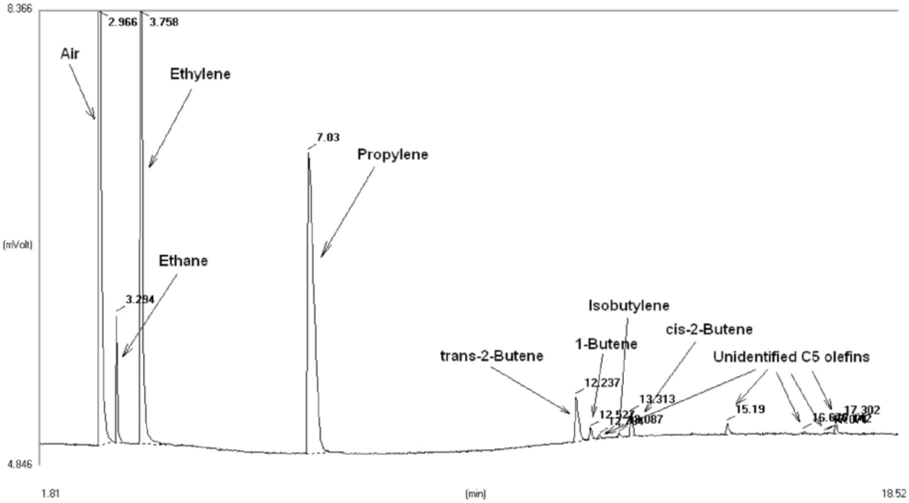

Figure 2. GLC of the reaction mixture after ethylene-induced second-generation Hoveyda catalyst decomposition in benzene-d_6 at 55°C.

As we discussed before there are possible ways for the methylidene catalyst intermediate decomposition (Scheme 4). Pathway (IV) may be omitted as the reaction was conducted in the presence of only dry purified ethylene.

Based on the observed experimental data, among all other routes we may assume that pathway (III) is preferred. Obviously only this route of catalyst decomposition depends and can be accelerated by increasing ethylene pressure.

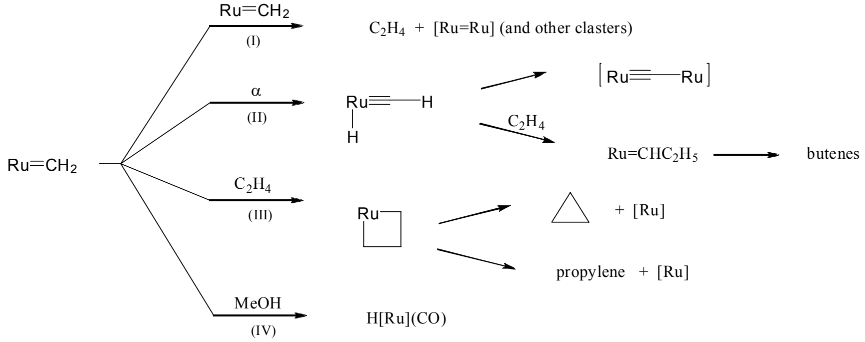

Scheme 4. Possible pathways for the decomposition of methylidene (for scheme simplification all ligands on ruthenium are omitted, except carbenoid fragment).

3. Conclusion

In this study we focused on the ethylene-promoted Hoveyda–Grubbs catalyst decomposition. The formation of large amount of propylene, butenes, and ethane was observed as well as different isopropoxystyrene derivatives. Future investigations of substrate role in olefin metathesis catalyst decomposition and the mechanism of ethane formation are in progress.

References

[1] (a) Sanford, M.S., Ulman, M., Grubbs, R.H., J. Am. Chem. Soc. 2001, 123:749–750; (b) Sanford, M.S., Love, J.A., Grubbs, R.H., J. Am. Chem. Soc. 2001, 123:6543–6554; (c) Dias, E.L., Nguyen, S.T., Grubbs, R.H., J. Am. Chem. Soc. 1997, 119:3887–3897.

[2] (a) Cavallo, L., J. Am. Chem. Soc. 2002, 124:8965–8973; (b) Adlhart, C., Chen, P., J. Am. Chem. Soc. 2004, 126:3496–3510.

[3] Romero, P.E., Piers, W.E., J. Am. Chem. Soc. 2005, 127:5032–5033.

[4] Ulman, M., Grubbs, R.H., J. Org. Chem. 1999, 64:7202–7207.

[5] Schwab, P., Grubbs, R.H., Ziller, J.W., J. Am. Chem. Soc. 1996, 118:100–110.

[6] Bielawski, C.W., Grubbs, R.H., Macromolecules 2001, 34:8838–8840.

[7] Huang, J., Stevens, E.D., Nolan, S.P., Petersen, J.L., J. Am. Chem. Soc. 1999, 121:2674–2678.

[8] Huang, J., Schanz, H.-J., Stevens, D., Nolan, S.P., Organometallics 1999, 18:5375–5380.

[9] Hong, S.H., Day, M., Grubbs, R.H., J. Am. Chem. Soc. 2004, 126:7414–7415.

[10] Furstner, A., Angew. Chem. Int. Edit. 2000, 39:3012–3043.

[11] Chatterjee, A.K., Choi, T.-L., Sanders, D.P., Grubbs, R.H., J. Am. Chem. Soc. 2003, 125:11360–11370.

[12] Ulman, M., Belderrain, T.R., Grubbs, R.H., Tetrahedron Lett. 2000, 41:4689–4693.

[13] Dinger, M.B., Mol, J.C., Organometallics 2003, 22:1089–1095.

[14] Dinger, M.B., Mol, J.C., Eur. J. Inorg. Chem. 2003, 2827–2833.

[15] Banti, D., Mol, J.C., J. Organomet. Chem. 2004, 689:3113–3116.

[16] Galan, B.R., Gembicky, M., Dominiak, P.M., Keister, J.B., Diver, S.T., J. Am. Chem. Soc. 2005, 127:15702–15703.

[17] Tmka, T., Morgan, J.P., Sanford, M.S., Wilhelm, T.E., Scholl, M., Choi, T.-L., Ding, S., Day, M.W., Grubbs, R.H., J. Am. Chem. Soc. 2003, 125:2546–2558.

[18] Bourgeois, D., Pancrazi, A., Nolan, S.P., Prunet, J., J. Organomet. Chem. 2002, 643–644:247–252.

[19] van Rensburg, W.J., Steynberg, P.J., Meyer, W.H., Kirk, M.M., Forman, G.S., J. Am. Chem. Soc. 2004, 126:14332–14333.

RUTHENIUM–VINYLIDENE COMPLEXES: AN EFFICIENT CLASS OF HOMOGENEOUS METATHESIS CATALYSTS

ILEANA DRAGUTAN[1*], VALERIAN DRAGUTAN[1],
RENATA DROZDZAK[2], FRANCIS VERPOORT[2]

[1*] *Institute of Organic Chemistry of the Romanian Academy, 202B Spl. Independentei, 060023 Bucharest, P.O. Box 35-108, Romania. E-mail: idragutan@yahoo.com*
[2]*Department of Inorganic and Physical Chemistry, Division of Organometallic Chemistry and Catalysis, Ghent University, Krijgslaan 281 (S-3), 9000 Ghent, Belgium*

Abstract: Several routes to access ruthenium (Ru)–vinylidene complexes are described, the majority of which employ alkynes and a Ru source as the starting materials. The successful application of Ru–vinylidenes as efficient pre-catalysts for the synthesis of carbocyclic and heterocyclic compounds by ring-closing metathesis (RCM) of α,ω-dienes, and in the synthesis of polymers by ring-opening metathesis polymerization (ROMP) of cyclooctene, norbornene, 5-substituted norbornene, and dicyclopentadiene is fully illustrated. Relevant aspects concerning the activity and selectivity of this type of Ru complexes in metathesis reactions are highlighted.

Keywords: ruthenium–vinylidene, metathesis, alkynes, α,ω-dienes, cycloolefins, *N*-heterocyclic carbene, Schiff base

1. Introduction

Over the past decade, the chemistry of transition metal–vinylidene complexes has become a topic of a real challenge in organometallic chemistry.[1–6] By coordination to transition metals, vinylidene ligands (:C=CHR), that are actually high-energy tautomers of alkynes (HC≡CR) and are very reactive and short-lived in the free state, can be effectively stabilized and endowed with new chemical properties useful for targeted transformations. They behave as electron-withdrawing groups and are better ligated at electron-rich metal cores. As a result of this coordination, the α-vinylidene carbon becomes highly electrophilic and prone to nucleophilic addition and the β-vinylidene carbon significantly more nucleophilic so as to induce electrophilic additions, while the M=C bond gets a pronounced metal carbene character promoting [2+2] cycloadditions to C=C and C≡C bonds with formation of metallacyclobutane and metallacyclobutene intermediates, respectively.

It has been fully documented that transition metal–vinylidene complexes play an important role in many catalytic processes.[7–9] Some relevant examples are alkene and enyne metathesis, alkyne dimerization and metathesis polymeri-

Y. İmamoğlu and V. Dragutan (eds.), Metathesis Chemistry: From Nanostructure Design to Synthesis of Advanced Materials, 137-150.

zation, cycloaromatization of conjugated enediynes, and addition of oxygen, nitrogen, and carbon nucleophiles to alkynes.[10–13]

The coordination and organometallic chemistry of ruthenium (Ru)–vinylidene complexes have been authoritatively surveyed in excellent reviews by Bruneau and Dixneuf,[14,15] by Katayama and Ozawa,[16] and other groups[17] providing important information on the preparation, structure, and reactivity of this class of transition metal complexes as well as on their wide application profile in catalysis and organic synthesis. The present paper will try to sum up new experimental data recently acquired on Ru–vinylidene complexes, including results of our research team, with emphasis on some aspects related to their synthesis and applications in metathesis chemistry.

2. Synthetic routes to ruthenium–vinylidene complexes

Several distinct routes have been applied successfully for synthesis of Ru–vinylidene complexes, the majority using as main starting materials alkynes along with a Ru source. It has been pointed out that conversion of alkynes into vinylidenes may proceed either by η^2-coordination of the triple bond, followed by 1,2-hydrogen migration, or by oxidative addition of the alkynes to the transition metal yielding an alkynyl metal intermediate which subsequently rearranges via 1,3-hydrogen migration or protonation[14] (Scheme 1).

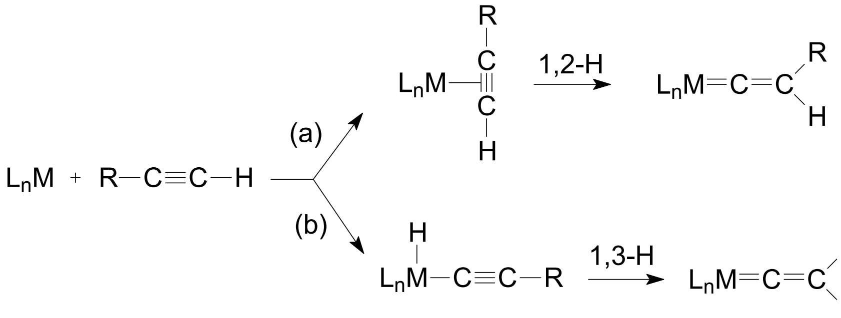

Scheme 1

Direct isomerization η^2-alkyne to η^1-vinylidene complexes by a bimolecular mechanism has also been considered.[14]

Alternately, vinylidene complexes can be produced either from Ru hydride complexes, by insertion of the triple bond to form a vinyl Ru intermediate which further undergoes α-hydrogen migration,[17] or from a Ru carbene, by a metathesis reaction with 1,2-propadiene.[18] Internal alkynes having labile substituents readily give rise to vinylidene complexes; thus, triallylsilyl, triphenylstannane, alkylthiol, and iodide groups can migrate generating vinylidene–metal complexes.

The first 18-electron, cationic Cp–Ru–vinylidene complex, [CpRu(=C=CHPh)(PPh_3)$_2$][PF_6] (**1**), was prepared by Bruce et al.[19] by reaction of CpRuCl(PPh_3)$_2$ with PhC≡CH, in the presence of NH_4PF_6 (88% yield) (Scheme 2).

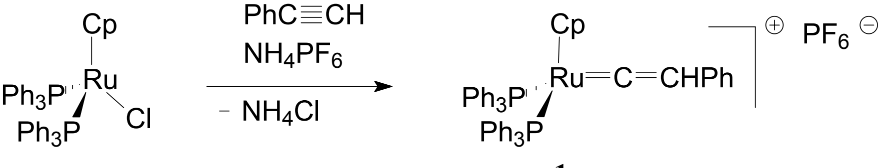

1

Scheme 2

Thereafter, coordinatively saturated, cationic Ru–vinylidene complexes have been obtained from terminal alkynes and Ru complexes, most of them containing Cp and various ancillary ligands.[14,15] Coordinatively unsaturated, 16-electron Ru–vinylidene complexes, RuX_2(=C=CHR)L_2 (X = Cl, Br, R = *t*Bu, L = PPh_3) (**2**), first reported by Wakatsuki et al.,[20] have been prepared from $RuX_2(PPh_3)_3$ and *t*BuC≡CH (Scheme 3).

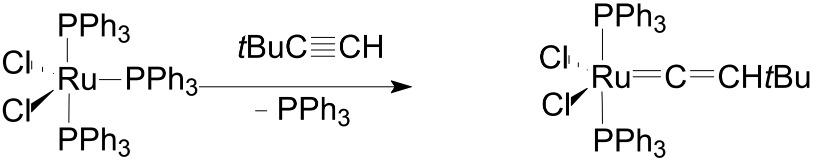

2

Scheme 3

Following these results, a variety of Ru–vinylidene complexes have been reported as obtained from terminal alkynes and different Ru sources. Thus, Werner et al.[21–24] synthesized $RuCl_2$(=C=CHPh)(P*i*Pr_3)$_2$ (**3**) from RuH_2Cl_2(P*i*Pr_3)$_2$ and PhC≡CH while Caulton et al.[25] prepared RuHCl(=C=CHPh)(PBu_2Me)$_2$ (**4**) by insertion of PhC≡CH in $RuHCl_2(H_2)(PBu_2Me)_2$ and subsequent 1,2-hydrogen migration to an intermediate styryl–Ru complex.

Two other convenient synthetic pathways to Ru–vinylidene complexes have been developed by Katayama and Osawa.[26,27] The first involves the reaction of Ru(methallyl)$_2$(COD) with P*i*Pr_3, HCl, and RC≡CH, proceeding through the intermediacy of [$RuCl_2$(P*i*Pr_3)$_2$]$_n$. The second, a more general and efficient approach, consists of heating at 80°C a toluene solution of the Ru dimer [$RuCl_2$(*p*-cymene)]$_2$, a phosphine (PR_3), and R′C≡CH; the array of neutral 16-electron Ru–vinylidene complexes **5** (R = P*i*Pr_3, PCy_3, R′ = Ph, *t*Bu, Fc, p-MeOC$_6$H$_4$, p-MeO$_2$CC$_6$H$_4$) resulted in high yield from commercially available terminal alkynes and the arene Ru dimer[26] (Scheme 4).

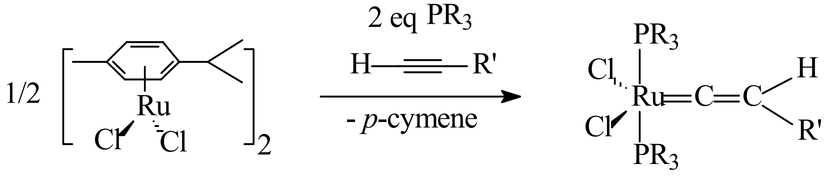

5

Scheme 4

In the case of 1,2-disubstituted alkynes such as PhC≡CSiMe$_3$, having a labile ligand, a β-silylvinylidene–Ru complex arises from 1,2-silyl migration in the coordinated η^2-alkyne intermediate. With less bulky phosphines, e.g. PMe$_2$Ph, coordinatively saturated tris(phosphane) Ru complexes are formed. Unfortunately, the latter showed only a moderate metathesis activity, e.g. in ring-closing metathesis (RCM) of unsubstituted α,ω-dienes and ring-opening metathesis polymerization (ROMP) of strained norbornenes.

By the above methodology, new cationic and neutral 18-electron Ru–vinylidene complexes **6**–**8** have been prepared by Grubbs and coworkers[28]. These complexes have been screened for metathesis activity, but their applicability remained limited to a small range of olefin substrates (Scheme 5).

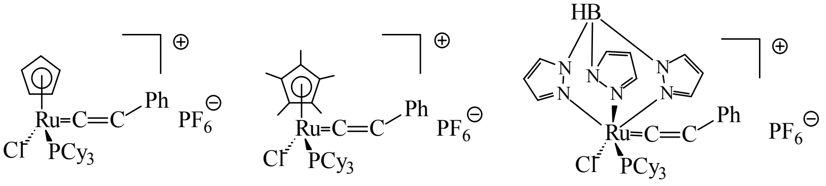

6 **7** **8**

Scheme 5

Tridentate ligands of the pincer-type (PNP, PNN, or NNN) have also been successfully employed as ancilary groups for synthesizing the Ru–vinylidene complexes, e.g. **9**–**14**.[29–32] It should be noted that some of these complexes showed good activity in ROMP of highly strained cycloolefins[29–31] (Scheme 6).

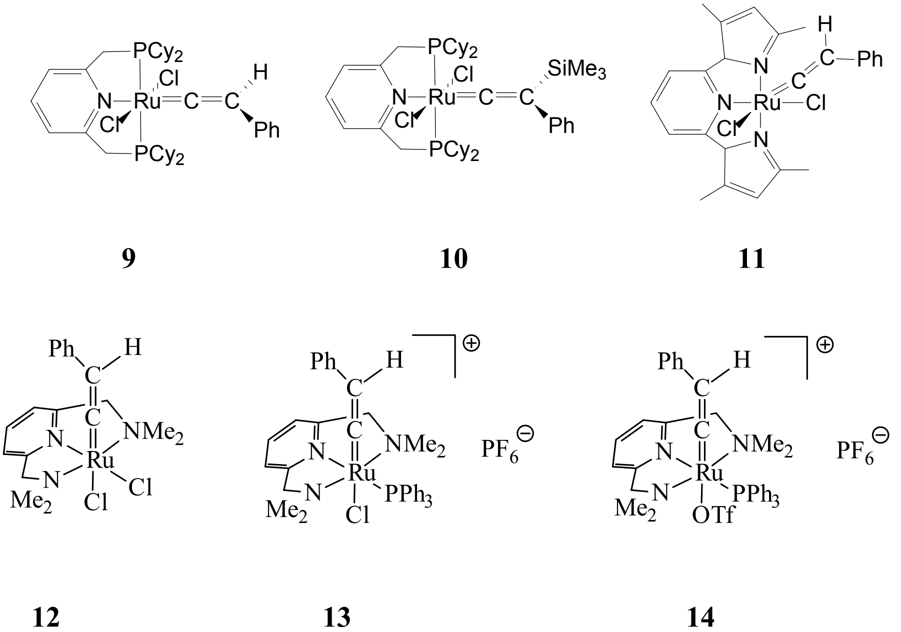

9 **10** **11**

12 **13** **14**

Scheme 6

Related tridentate N,N,O heteroscorpionate ligands provided intricate Ru–vinylidene complexes endowed with a challenging architecture.[33] This strategy was further extended to bi- and tri-metallic Ru–vinylidene complexes, obtained in high yields, but their metathesis activity has not been fully illustrated.[34]

A substantial improvement on the above-described class of Ru–vinylidene complexes has been achieved by Louie and Grubbs[35] through synthesis of a novel generation of complexes coordinating an *N*-heterocyclic carbene (NHC) ligand (e.g. imidazolylidene). This new set of Ru complexes, e.g. **15** (IMes = 1,3-(2,4,6-trimethylphenyl)imidazol-2-ylidene, R = Cy, R′ = t-Bu) and **16** (*i*PrIM = 1,3-diisopropyl-4,5-dimethyl-imidazol-2-ylidene, R = Cy, R′ = Ph) has been conveniently produced from the bisphosphane–Ru complex **9** (R = Cy) by reaction with free imidazoline carbene or its precursor salts (Scheme 7).

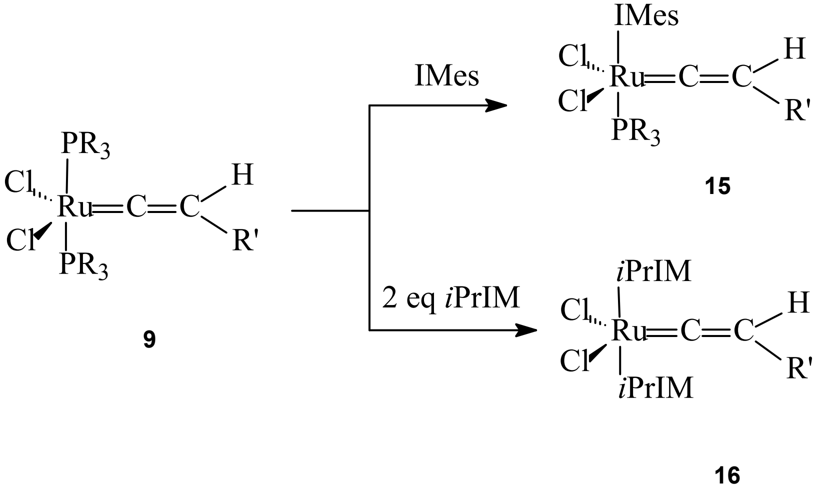

Scheme 7

3. Metathesis activity of ruthenium–vinylidene complexes

The Ru pre-catalyst **15**, with a mixed ligand system, displayed substantial metathesis activity in the standard RCM of diethyl diallylmalonate leading to the corresponding substituted cycloolefin (86% yield), though the reaction rate was slower than that with the related imidazolylidene–Ru–benzylidene complex (Scheme 8).

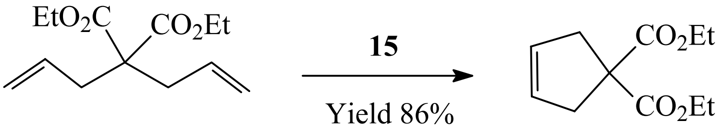

Scheme 8

Based on detailed mechanistic investigations using this type of Ru complexes, the authors concluded that increased ligand dissociation (i.e. of phosphane) is necessary to accelerate the initiation and thereby enhance the catalytic activity in metathesis. It was suggested that the coordinatively unsaturated phosphane-free Ru–vinylidene complex 17 might be directly formed in situ when starting from the Ru dimer, NHC (IMes) (as such or as its salts) and a terminal alkyne (e.g. *t*Bu–C≡CH) (Scheme 9). It is worth noting that the solvent (hexane or tetrahydrofuran) plays an important role during the in situ generation of the Ru catalyst.

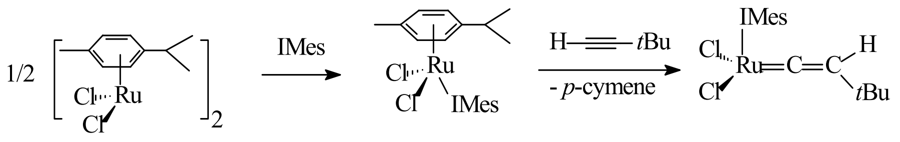

17

Scheme 9

The pathway for the generation of the actual catalytic species **18** from the catalyst precursor **17** and the olefin substrate was postulated as depicted in Scheme 10.

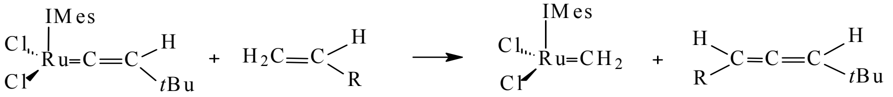

17 **18**

Scheme 10

Examination of the catalytic activity of the vinylidene complex **17** revealed this complex to be more active than **15**, pointing out to a higher unsaturation in the coordination sphere of the metal. This characteristic behaviour of **17** has been evidenced in RCM of diethyl diallylmalonate, metathesis dimerization of allyl benzene, and ROMP of 1,5-cyclooctadiene (Scheme 11).

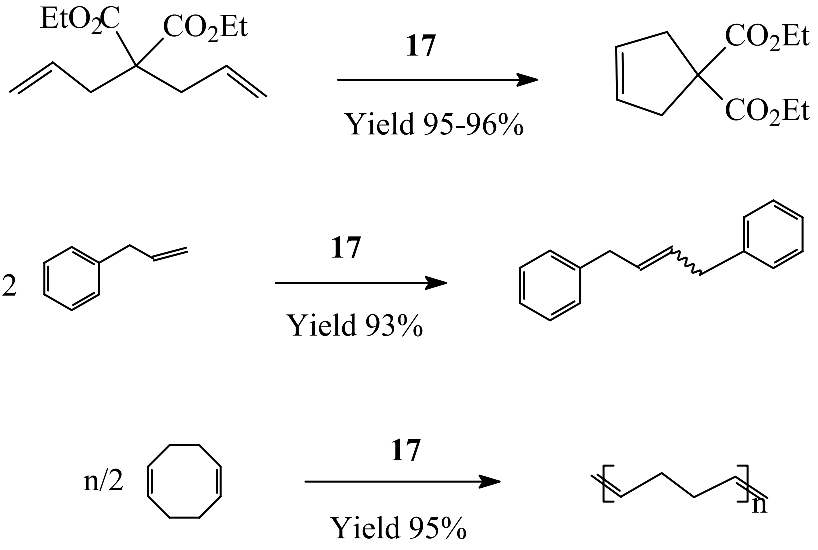

Scheme 11

A series of Ru–vinylidene complexes, **19a–f**, containing Schiff bases as chelating ligands, was prepared by Verpoort and coworkers[36–38] from the corresponding bisphosphane–Ru–vinylidene complexes, $RuCl_2(PCy_3)_2(=C=CHR')$ (R′ = Ph, $SiMe_3$ or *t*Bu), and a variety of aromatic salicylaldimines (R = H or NO_2 and R′ = Ph, $SiMe_3$ or *t*Bu) (Scheme 12).

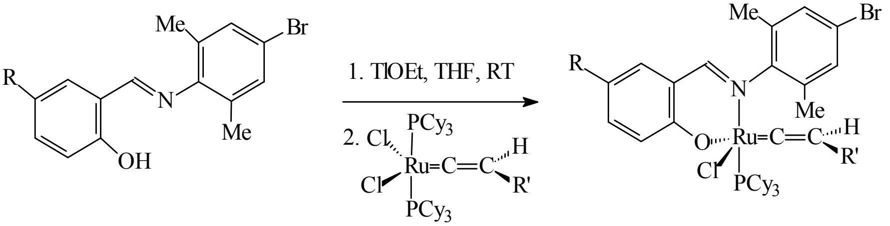

19a. R = H, R′ = Ph
19b.R = NO_2,R′ = Ph
19c. R = H, R′ = $SiMe_3$
19d. R = NO_2, R′ = $SiMe_3$
19e. R = H, R′ = *t*Bu
19f. R = NO_2, R′ = *t*Bu

Scheme 12

This easily accessible class of Ru complexes showed very high thermal stability, combined with good activity in olefin metathesis. In comparison with the parent Ru alkylidene systems, these complexes are extremely resistant to air, moisture, and heat and have been found to serve as excellent pre-catalysts in RCM of α,ω-dienes and ROMP of norbornene and 5-substituted norbornene, cyclooctene, and dicyclopentadiene.[39,40] This behaviour was assigned to the propensity for a "one-arm" *N*-decoordination of the *O*,*N*-bidentate Schiff base ligand which creates unsaturation within the metal's coordination sphere. As illustrated in Table 1, RCM of ethyl diallylmalonate, 1,7-octadiene or diallyl ether proceeds quantitatively with **19c**–**f**, under specific reaction conditions (5 mol% catalyst, 80°C, 24 h reaction time). On using variously substituted α,ω-dienes as substrates in RCM, the activity of the pre-catalysts **19** ranges in the following order: **19d** > **19c** > **19f** > **19e** > **19b** > **19a**, indicating that the catalyst activity is significantly controlled by the nature of the Schiff base and vinylidene fragment substituents. Noteworthy, the most active pre-catalyst, **19d**, contains both the electron-withdrawing NO_2 group, on the Schiff base and the labile $SiMe_3$ group, on the vinylidene.

Table 1. Isolated yields (%) in ring-closing metathesis of α,ω-dienes using Schiff base Ru–vinylidene pre-catalysts **19a–f**[a,b]

α,ω-Diene substrate	Product	Time, h	**19a**	**19b**	**19c**	**19d**	**19e**	**19f**
	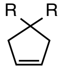	24	96	98	100	100	100	100
	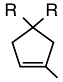	24	36	43	59	69	48	53
	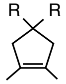	24	5	11	23	36	16	26
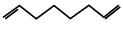	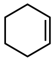	24	98	99	100	100	100	100
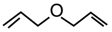		10	97	98	100	100	100	100
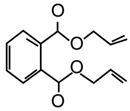	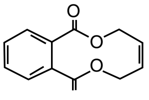	24	51	60	72	83	67	80
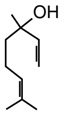	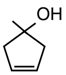	24	27	54	70	81	68	75

[a] Data from [39]

[b] Reaction conditions: catalyst loading 5 mol%, temperature 80°C, solvent C_6D_6

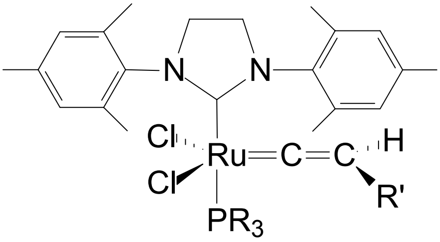

20a. R = Cy, R′ = Ph
20b. R = Cy, R′ = $SiMe_3$
20c. R = Cy, R′ = *t*Bu

Scheme 13

For a comparative study of their activity and effectiveness in olefim metathesis, related Ru–vinylidene complexes **20a–c** bearing NHC (SIMes = bis (2,4,6-trimethylphenyl)-1,3-imidazolin-2-ylidene) as ancillary ligand have also been prepared following Ozawa's procedure from the dimer [$RuCl_2$

(p-cymene)]$_2$ and two equivalents of PR$_3$ (R = Cy) which reacted with an excess of alkyne and subsequent treatment with SIMes afforded the target complex (Scheme 13).

RCM of the α,ω-dienes with complexes **20a–c** was carried out at 60°C using 5 mol% catalyst loading for 2 h reaction time. Results obtained are summarized in Table 2.

As can be observed, the most active catalyst containing SiMe$_3$ at the vinylidene fragment leads to high yields or even quantitative conversions in the examined reactions, a significant result taking into account that cyclization of diethyl diallylmalonate with the analogous Schiff base free RuCl$_2$(P*i*Pr$_3$)$_2$(=C=CH*t*Bu) reached 96% after 24 h at 60°C.

Table 2. Isolated yields (%) in ring-closing metathesis of α,ω-dienes using NHC Ruvinylidene pre-catalysts **20a**–**c**[a,b]

α,ω-Diene substrate	Product	Time, h	**20a**	**20b**	**20c**
	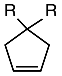	2	90	100	100
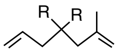	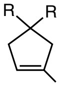	2	60	76	71
	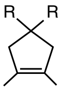	2	10	44	34
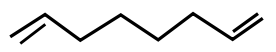	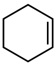	2	92	100	100
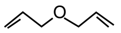		2	96	100	100
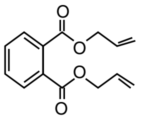	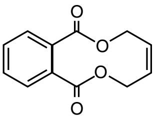	2	71	90	83
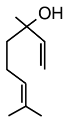	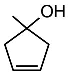	2	69	89	80

[a] Data from [39]

[b] Reaction conditions: catalyst loading 5 mol%, temperature 60°C, solvent C_6D_6

Table 3. Isolated yields (%) in ROMP of cyclooctene and dicyclopentadiene using Schiff base Ru–vinylidene pre-catalysts **19a–f** [a,b]

Substrate	Time (h)	**19a**	**19b**	**19c**	**19d**	**19e**	**19f**
Cyclooctene	15	10	15	93	100	80	88
Dicyclopentadiene	10	90	96	100	100	95	97

[a] Data from [39]

[b] Reaction conditions: monomer:catalyst = 8000, temperature 80°C, solvent toluene

ROMP of cycloolefins, a commonly encountered reaction in metathesis chemistry, provides essential mechanistic information and yields products unavailable by conventional polymerization processes. On using the pre-catalysts **19** and **20**, ROMP of a variety of cycloolefins, both low-strained (e.g. cyclooctene) and highly-strained monomers (e.g. norbornene and its derivatives), was characterized by a good to excellent reactivity, leading in substantial yields to high-molecular weight polymers (Tables 3 and 4).

Again, the most active pre-catalysts proved to be **19c** and **d** and the same order of activity as in RCM of α,ω-dienes could be observed. An interesting feature of cycloolefin polymerization with pre-catalysts **19** and **20** is that the molecular weight of the polymers are much higher than theoretically predicted from the monomer vs catalyst precursor ratios. This result implies a low initiation rate, as compared to propagation rate, in agreement with the data of Yamaguchi and Ozawa[5] who reported very low initiating efficiency in ROMP of norbornene with bisphosphane–vinylidene complexes. As a consequence, the catalyst can be mostly recovered (>90%), after monomer consumption, and resused in a new polymerization cycle showing the same level of performance.

The slow initiation step can be rationalized by a mechanism involving [2+2] cycloaddition of the olefin at the Ru=C bond of the vinylidene ligand, with generation of a new Ru carbene species able to propagate faster polymerization (Scheme 14). This mechanism has been documented by Ozawa[41] for ROMP of norbornene with $[RuCl_2(PPh_3)_2(=C=CHFc)]$ (Fc = ferrocenyl) and by Kirchner in a stoichiometric reaction using a Tp-coordinated Ru complex (Tp = tris(pyrazolyl)borohydride).[42]

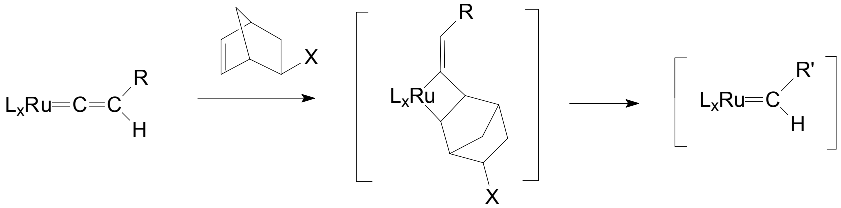

Scheme 14

The poorest pre-catalysts in polymerization of 5-substituted norbornene were **19a** and **b**, and the less reactive monomers were norbornenes bearing phenyl, cyclohexyl, and hydroxymethyl substituents (Table 4).

Table 4. Isolated yields (%) in ROMP of 5-substituted norbornene using Schiff base Ru–vinylidene pre-catalysts **19a–f** [a,b]

5-Substituted norbornene (X)	Time (h)	**19a**	**19b**	**19c**	**19d**	**19e**	**19f**
X = Hydrogen	0.5	94	98	100	100	100	100
Ethyl	4	89	100	100	100	100	100
Butyl	4	100	100	100	100	100	100
Hexyl	4	82	84	100	100	95	98
Decyl	4	83	100	100	100	100	100
Ethylidene	10	100	100	100	100	100	100
Phenyl	4	74	80	95	98	89	92
Cyclohexyl	4	73	77	87	97	79	82
Hydroxymethyl	4	10	16	59	65	34	55
Chloromethyl	4	78	89	100	100	100	100
Triethoxysilyl	4	71	79	100	100	91	99

[a] Data from [39]

[b] Reaction conditions: monomer:catalyst = 8000, temperature 80°C, solvent toluene

Microstructure determination by ^{1}H NMR spectroscopy indicated predominantly *trans*-double bond content (75–90%) in the obtained polycyclooctene and polynorbornenes, consistent with results from other Ru-catalyzed ROMP reactions. Based on the molecular weight of polynorbornenes produced with catalysts **19a–f** and the initial monomer to catalyst ratio, a initiator efficiency of ~10% was determined, which is substantially higher than the value of 2%, for the case of bisphosphane–vinylidene precursors. In spite of the high molecular weight of the polymers, the molecular weight distribution (M_w/M_n) remained narrow: 1.54–1.66 for polycyclooctene, and 1.70 for polynorbornene.

Another important characteristic, inherent to this type of pre-catalysts, is that they combine the benefit of fine-tuning the catalytic activity, through adjustments in the Schiff base unit, with a pronounced reluctance against bimolecular decomposition in solution, even at elevated temperatures; thus, they can be kept for at least 1 month in toluene solution without losing their activity. Moreover, in solid phase they are stable for over 3 months while maintaining their catalytic performance. This behaviour compares well with that of the related Ru–vinylidene complexes containing imidazolin-2-ylidene ligands displaying good stability for several days at high temperatures.

4. Conclusions

As olefin metathesis pre-catalysts, Ru–vinylidene complexes provide a convenient alternative to the classical bisphosphane–Ru alkylidenes presently widely applied in organic synthesis and polymer chemistry. An important advantage offered by Ru–vinylidenes resides in the use of commercially or easily available starting materials for their synthesis. The special design of this class of coordinatively unsaturated Ru complexes affords valuable metathesis activity. Furthermore, these pre-catalysts exhibit good stability and robustness enabling their reuse for several reaction cycles without loss of the initial activity. Combining vinylidenes with other fine-tunable ligands in the coordination sphere of the Ru (e.g. imidazolylidene and Schiff bases) opens new ways for efficiently catalyzed metathesis reactions and thereupon sustainable technologies.

References

[1] King, R.B., Coord. Chem. Rev. 2004, 248:1531.
[2] Selegue, J.P., Coord. Chem. Rev. 2004, 248:1543.
[3] Bruce, M.I., Coord. Chem. Rev. 2004, 248:1603.
[4] Cadierno, V., Gamasa, M.P., Gimeno, J., Coord. Chem. Rev. 2004, 248:1627.
[5] Herndon, J.W., Coord. Chem. Rev. 2004, 248:3.
[6] Bruce, M.I., Swincer, A.G., Adv. Organomet. Chem. 1983, 22:59.
[7] Puerta, M.C., Valerga, P., Coord. Chem. Rev. 1999, 193–195:977.
[8] Bruneau, C., Top. Organomet. Chem. 2004, 11:125.
[9] (a) Alonso, F., Beletskaya, I.P., Yus, M., Chem. Rev. 2004, 104:3079; (b) Katayama, H., Yari, H., Tanaka, M., Ozawa, F., Chem. Commun. 2005, 4336.
[10] Dragutan, V., Dragutan, I., Platinum Metals Rev., 2004, 44:148.
[11] Yi, C.S., Liu, N., Synlett 1999, 281.
[12] Wang, Y., Finn, M.G., J. Am. Chem. Soc. 1995, 117:8045.
[13] Bruneau, C., Dixneuf, P.H., Chem. Commun. 1997, 507.
[14] Bruneau, C., Dixneuf, P.H., Angew. Chem. Int. Edit. 2006, 45:2176.
[15] Bruneau, C., Dixneuf, P.H., Acc. Chem. Res. 1999, 32:311.
[16] Katayama, H., Ozawa, F., Coord. Chem. Rev. 2004, 248:1703.
[17] Werner, H., in: Grubbs, R.H. (ed.) Handbook of Metathesis, Vol. 3, Wiley-VCH, Weinheim, 2003, pp. 95–111.
[18] Schwab, P., Grubbs, R.H., Ziller, J.W., J. Am. Chem. Soc. 1996, 118:100.
[19] Bruce, M.I., Wallis, R.C., Aust. J. Chem. 1979, 32:1471.
[20] Wakatsuki, Y., Yamazaki, H., Kumegawa, N., Satoh, T., Satoh, J.Y., J. Am. Chem. Soc. 1991, 113:9604.
[21] Grunwald, C., Gevert, O., Wolf, J., Gonzales-Herrero, P., Werner, H., Organometallics 1996, 15:1960.
[22] Wolf, J., Stuer, W., Grunwald, C., Gevert, O., Laubender, M., Werner, H., Eur. J. Inorg. Chem. 1998, 1827.
[23] Wolf, J., Stuer, W., Grunwald, C., Werner, H., Schwab, P., Schulz, M., Angew. Chem. 1998, 110:1165; Angew. Chem. Int. Edit. 1998, 37:1124.

[24] Jung, S., Ilg, K., Brandt, C.D., Wolf, J., Werner, H., Eur. J. Inorg. Chem. 2004, 469.

[25] Olivan, M., Eisenstein, O., Caulton, K.C., Organometallics 1997, 16:2227.

[26] Katayama, H., Ozawa, F., Organometallics 1998, 17:5190.

[27] Katayama, H., Ozawa, F., Chem. Lett. 1998, 67.

[28] Sanford, M.S., Henling, L.M., Grubbs, R.H., Organometallics 1998, 17:5384.

[29] Del Rio, van Koten, G., Tetrahedron Lett. 1999, 40:1401.

[30] Katayama, H., Wada, C., Taniguchi, K., Ozawa, F., Organometallics 2002, 21:3285.

[31] Beach, N.J., Spivak, G.J., Inorg. Chim. Acta 2003, 343:244.

[32] Beach, N.J., Walker, J.M., Jenkins, H.A., Spivak, G.J., J. Organomet. Chem. 2006, 691:4147.

[33] Kopf, H., Pietraszuk, C., Hübner, E., Burzlaff, N., Organometallics, 2006, 25:2533.

[34] Weiss, D., Dixneuf, P.H., Organometallics 2003, 22:2209.

[35] Louie, J., Grubbs, R.H., Angew. Chem. Int. Edit. 2001, 40:247.

[36] Drozdzak, R., Allaert, B., Ledoux, N., Dragutan, I., Dragutan, V., Verpoort, F., Coord. Chem. Rev. 2005, 249:3055.

[37] Drozdzak, R., Allaert, B., Ledoux, N., Dragutan, I., Dragutan, V., Verpoort, F., Adv. Synth. Catal. 2005, 347:1721.

[38] Drozdzak, R., Ledoux, N., Allaert, B., Dragutan, I., Dragutan, V., Verpoort, F., Central Eur. J. Chem. 2005, 404.

[39] Opstal, T., Verpoort, F., J. Mol. Catal. A: Chem. 2003, 200:49.

[40] Opstal, T., Verpoort, F., Synlett 2002, 935.

[41] Katayama, H., Urushima, H., Ozawa, F., J. Organomet. Chem. 2000, 606:16.

[42] Slugovc, C., Mereiter, K., Schmid, R., Kirchner, K., J. Am. Chem. Soc. 1998, 120:6175.

MESOPOROUS MOLECULAR SIEVES AS SUPPORTS FOR METATHESIS CATALYSTS

HYNEK BALCAR, JIŘÍ ČEJKA

J. Heyrovský Institute of Physical Chemistry, Academy of Sciences of the Czech Republic, Dolejškova 3, 182 23 Prague 8, Czech Republic. E-mail: balcar@jh-inst.cas.cz

Abstract: Mesoporous molecular sieves represent a new family of inorganic oxides with regular nanostructure, large surface areas, large void volumes, and narrow pore size distribution of mesopores. These materials offer new possibilities for designing highly active and selective catalysts for olefin metathesis and metathesis polymerization. Siliceous sieves MCM-41, MCM-48, SBA-15, and organized mesoporous alumina (OMA) were used as supports for preparation of new molybdenum and rhenium oxide catalysts, as well as for heterogenization of well-defined homogeneous catalysts.

Keywords: mesoporous molecular sieves, heterogeneous catalysts, olefin matathesis, matathesis polymerization.

1. Introduction

Since their invention in 1992 mesoporous molecular sieves have attracted a high attention as new sorption material and new catalyst supports. This new kind of inorganic oxides (mainly silica and alumina) possesses unique properties such as regular structure, large surface area and void volume, and narrow pore size distribution in the range of mesopores. Large surface area endows this material with high adsorption capacity and the narrow pore size distribution represents size limits for the molecules entering and/or leaving the pores. Moreover, the sterical confinement and regularity of nanoreactors represented by these pores may positively affect the selectivity of chemical reactions proceeded in them. Therefore, the catalysts based on mesoporous molecular sieves are expected to have a very high activity and enhanced selectivity in comparison with the conventional ones.

Generally, there are two possibilities how to use mesoporous molecular sieves as supports for metathesis catalysts. First, to apply them as supports for heterogeneous metal oxide-based catalysts instead of classical silica or alumina. Second, to use them for preparation of heterogenized versions of originally homogeneous metathesis catalysts, especially for anchoring well-defined carbene complexes.

Y. İmamoğlu and V. Dragutan (eds.), Metathesis Chemistry: From Nanostructure Design to Synthesis of Advanced Materials, 151-166.

2. Mesoporous molecular sieve preparation and characteristics

Mesoporous molecular sieves represent very interesting group of periodic inorganic oxides with different chemical composition exhibiting high surface areas (up to 1500 m^2/g), large void volumes, and narrow pore size distribution in mesoporous range (from 2 to 30 nm). Their successful synthesis [1,2] substantially enlarged the possibilities of application of porous materials increasing their pore range above those providing by microporous zeolites. During recent decade, this research area was rapidly expanding to an independent field of material science.

The first materials synthesized by Mobil Oil researchers [1,2] were based on silica or aluminosilica materials of so-called M41S family including hexagonally arranged MCM-41, cubic MCM-48, and lamellar MCM-50. The synthesis is schematically depicted in Figure 1. In water solution surfactant micelles are formed, their size can control in some respect the final dimensions of the forms. Silica precursors surround the surface of the micelles, which is followed by condensation of silica building blocks into the more compact entities. Removal of surfactants carried out usually at temperatures higher than 500°C provides open structure with accessible mesopores.

In this case surfactant micelles or liquid crystal templating were employed, which means that large assemblies of organic molecules were directing the formation of the final structure instead of individual molecules or cations. The initial application of cationic surfactants by Mobil like hexadecyltrimethylammonium bromide or hydroxide has been extended to neutral or even cationic structure-directing agents. Thus, in principle three synthetic procedures exist for preparation of mesoporous molecular sieves:

1. Cationic approach – surfactants are tetraalkylammonium cations or di-*N*-quarternary cations leading to the formation of MCM-41, MCM-48, MCM-50, FSM-16, SBA-1
2. Anionic approach – utilizing long-chain alkyl carboxylic acids for the synthesis of organized mesoporous aluminas (OMAs)
3. Neutral route – various amines, triblock copolymers, and alkyl-ethylene oxides are used for preparation of different hexagonal mesoporous sieves, SBA-15, SBA-16, or OMAs.

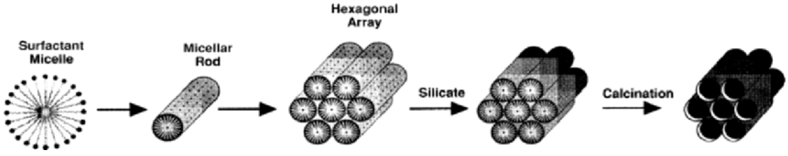

Figure 1. Scheme of the synthesis of mesoporous molecular sieves using surfactant micelles as a structure-directing agent [1].

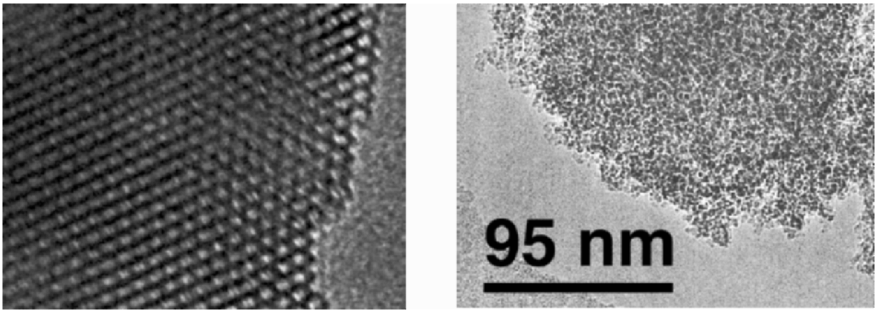

Figure 2. Scanning electron microscope (SEM) images of MCM-41 (*left*) and organized mesoporous alumina (OMA) (*right*) samples.

The individual synthetic routes lead usually to nicely ordered silica-based mesoporous molecular sieves, while in the case of OMAs worm-like channel ordering is achieved. Figure 2 presents scanning electron micrographs of siliceous MCM-41 synthesized with hexadecyltrimethylammonium hydroxide and OMA prepared with lauric acid as structure-directing agents. While in the case of MCM-41 one can see well-ordered regular hexagonal pattern, OMA exhibits worm-like motif, which is typical for this type of mesoporous materials [6].

Pore size is one of the most important parameters of mesoporous molecular sieves as it controls the accessibility of pores for bulky molecules, which has significant implications for catalysis, adsorption, or controlled desorption. Several approaches were used for pore size tuning including different length of alkyl chain in alkyltrimethylammonium cations from C_8 to C_{22}, use of auxiliary expanders by micelle swelling by solubilized organic compounds or various thermal or postsynthesis treatments. The largest pore size of about 30 nm of diameter was reported based on employing of triblock copolymers for SBA-15.

For practical applications of mesoporous molecular sieves, very important parameter is their thermal stability. In fact, this limits very much testing of these materials in the case of mesoporous titania, which can be prepared only as thin films. Purely siliceous mesoporous molecular sieves are stable up to 900–1000°C without a substantial decrease in the surface area or void volume, it means this temperature treatment is not accompanied by phase transformations. Figure 3 presents the nitrogen adsorption isotherms of OMAs showing significant changes of surface areas, void volume, and pore sizes. It is clearly seen from this picture that with increasing temperature of thermal treatment surface area and void volume of OMA are decreasing, while the apparent pore size is increasing. Further investigation of mesoporous aluminas calcined in the temperature range between 600 and 1000°C carried out by x-ray powder diffraction and transmission electron microscopy evidenced the phase transformation from amorphous alumina to crystalline one.

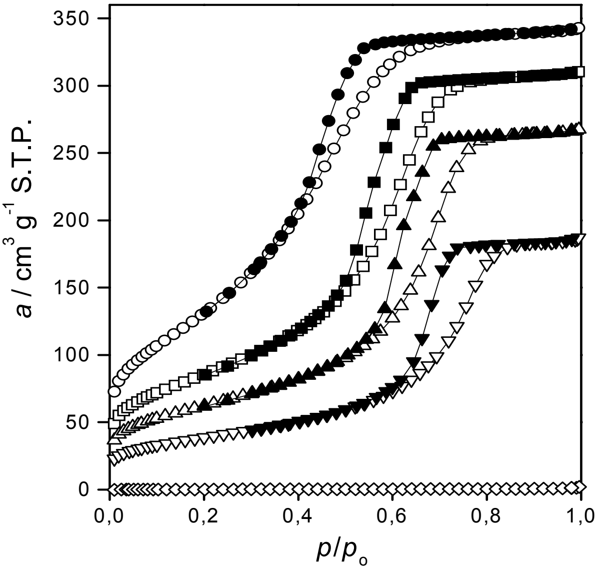

Figure 3. Nitrogen adsorption isotherms at –196°C on OMA samples: (◊) as synthetized, (○) calcined at 420°C, (□) at 600°C, (Δ) at 800°C, (∇) at 1000°C. The solid points denote desorption.

The critical issue of catalytic applications of mesoporous molecular sieve is their chemical composition. Pure siliceous materials do not practically exhibit any catalytic activity, thus, proper isomorphous substitution of other heteroatoms for silicon or various synthesis or postsynthesis treatments are needed to introduce catalytically active sites. Number of excellent papers dealing with modification of mesoporous molecular sieves for catalytic applications was published, e.g. refs. [19,20]. They clearly showed the broad field of possible catalytic applications of these materials. The relevant modifications include introduction of single metal cations via synthesis or postsynthesis treatments or introduction of transition metal oxides after the synthesis of siliceous and alumina supports. Such catalysts are highly active in SO_2 to SO_3 oxidation over Fe_2O_3/MCM-41 or metathesis of olefins over MoO_3/MCM-41 and Re_2O_7/alumina. Probably the most challenging area is the modification of mesoporous supports with organometallic complexes via grafting, anchoring, or other ways of immobilization. In this case various highly active and selective homogeneous catalysts can be heterogenized to nonactive support, which results in the formation of so-called hybrid catalysts unifying the advantages of both homogeneous and heterogeneous catalysts.

Table 1. A survey of catalyst supports

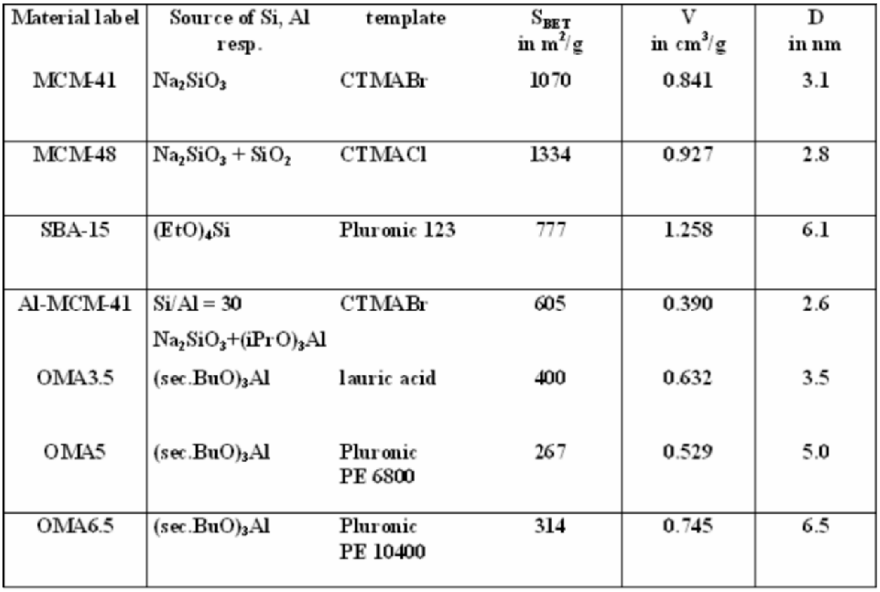

Material label	Source of Si, Al resp.	template	S_{BET} in m^2/g	V in cm^3/g	D in nm
MCM-41	Na_2SiO_3	CTMABr	1070	0.841	3.1
MCM-48	$Na_2SiO_3 + SiO_2$	CTMACl	1334	0.927	2.8
SBA-15	$(EtO)_4Si$	Pluronic 123	777	1.258	6.1
Al-MCM-41	Si/Al = 30 Na_2SiO_3+$(iPrO)_3Al$	CTMABr	605	0.390	2.6
OMA3.5	$(sec.BuO)_3Al$	lauric acid	400	0.632	3.5
OMA5	$(sec.BuO)_3Al$	Pluronic PE 6800	267	0.529	5.0
OMA6.5	$(sec.BuO)_3Al$	Pluronic PE 10400	314	0.745	6.5

CTMA = cetyltrimetylamonium, S_{BET} = surface area, V = void volume, D = pore diameter

Table 1 gives a survey of mesoporous materials prepared in the J. Heyrovský Institute and used as supports for metathesis catalyst. Detailed syntheses and texture characteristics are given elsewhere.

3. Mesoporous molecular sieves-supported metal oxide as metathesis catalysts

Heterogeneous catalysts consisting of WO_3, MoO_3, or Re_2O_7 supported on silica, silica-alumina, or γ-alumina have been used for about 3 decades, including applications in large-scale industrial processes.

In 1998, Ookoshi and Onaka reported remarkable increase in activity of MoO_3 when this was supported on hexagonal mesoporous silica instead of conventional one. With this catalyst (7 wt % Mo) they achieved high conversion of 1-octene into 7-tetradecene at 50°C. Similarly in 2002, Onaka and Oikawa found rhenium oxide dispersed on mesoporous alumina with uniform pore size (7 wt % Re) to be more active in 1-octene metathesis than rhenium oxide on conventional γ-alumina. Although both works lacked detailed characterization of supports and prepared catalysts, they clearly showed the positive effect of organized mesoporous support on catalyst activity in alkene metathesis.

In the J. Heyrovský Institute we performed a detailed study of (a) MoO_3 supported on siliceous mesoporous sieves of several types and (b) rhenium (VII) oxide supported on organized mesoporous aluminas in order to (i) verify positive effect of these supports on catalyst activity, (ii) to find out the most convenient way for catalyst preparation, (iii) to receive detailed information about their catalytic activity and selectivity, and (iv) to show the applicability of these catalysts in different types of metathesis reaction.

Thermal spreading method was used for metal oxide supporting. Calcined supports and MoO_3 and NH_4ReO_4, respectively, were carefully mixed together by hand-grinding and then were thermally treated at 500°C for 8 h in a temperature-programmed furnace (ramp 1°C/min). Following advantages of this method should be stressed: (i) it is very easy, (ii) it preserves the mesoporous structure of supports, and (iii) it quantitatively transfers Mo and Re, respectively, into the support channels and spread them on the support surface.

3.1 Properties of MoO_3 supported on siliceous mesoporous sieves

Figure 4 shows 1-octene conversion with mesoporous catalysts MoO_3/MCM-41 and MoO_3/Al-MCM-41 (Si/Al = 30), and a conventional catalyst MoO_3/SiO_2 in liquid phase at 40°C. The selectivities to 7-tetradecene are included. It is seen that (i) with MoO_3/MCM-41 the reaction proceeds about eight times rapidly than with MoO_3/SiO_2 achieving higher final conversion and high selectivity, and (ii) changing MoO_3/MCM-41 for MoO_3/Al-MCM-41, the reaction rate increases even more, but the selectivity falls considerably (probably due to the presence of acidic sites causing isomerization of starting 1-octene followed by cross-metathesis).

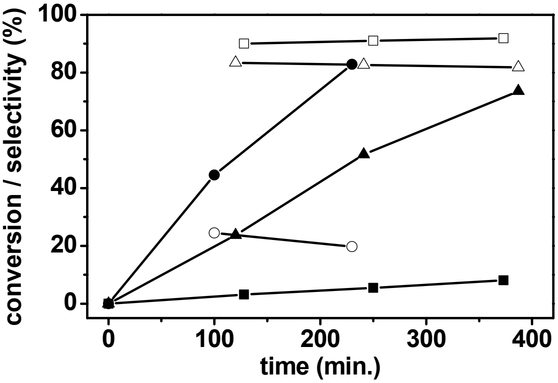

Figure 4. Conversion of 1-octene (solid symbols) and selectivity to 7-tetradecene (open symbols) dependence on time: MoO_3 supported on Al-MCM-41 with Si/Al = 30 (● ○), MCM-41 (▲ △), and SiO_2 (■ □); metathesis of neat 1-octene at 40°C, loading 8 wt % Mo.

The activity of mesoporous catalysts depends strongly on the quality of Mo species dispersion. Figure 5 shows x-ray diffraction (XRD) patterns in low θ (a) and high θ (b) regions for MCM-41 and MoO_3/MCM-41 catalysts of different loadings. The persistence of signals in the low θ region indicates the preservation of organized structure and pore size independently of catalyst loading. Very low intensity signals corresponding to MoO_3 crystallites appearing in the high θ region for high-loaded samples (from 12 wt % Mo) suggest perfect dispersion of Mo species is achieved only for low-loaded samples.

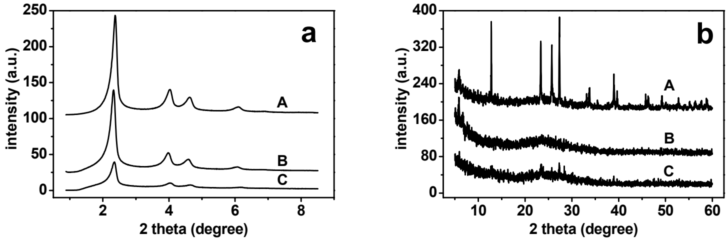

Figure 5. X-ray diffraction patterns of (a) MCM-41 (A), 8Mo/MCM-41 (B), and 16Mo/MCM-41 (C); (b) MoO_3/MCM-41: physical mixture (A), 8Mo/MCM-41 calcined 8 h at 773 K in a stream of air (B), and 16Mo/MCM-41 calcined 8 h at 773 K in a stream of air (C).

Moreover, Raman spectra of catalysts (Figure 6) showed the presence of at least three types of molybdenum species on the surface: (i) isolated molybdenum oxide species (signal at 981 cm^{-1}), (ii) surface polymolybdate (959 cm^{-1}), and bulk MoO_3 (995 and 819 cm^{-1}). The population of these individual species

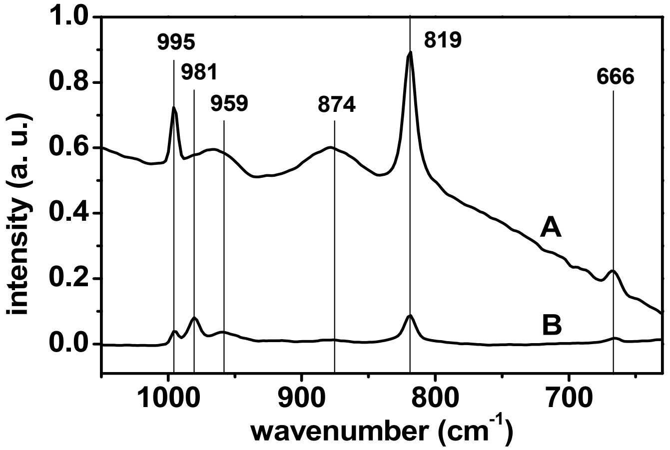

Figure 6. Raman spectra of 16Mo/MCM-41 (A) and 8Mo/MCM-41 (B) catalysts.

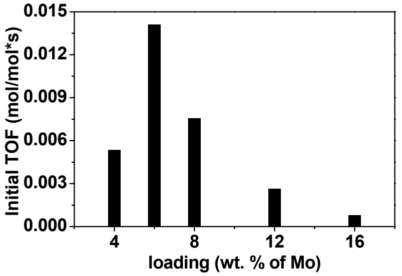

Figure 7. Specific activity (expressed as initial TOF) of MoO_3/MCM-41 catalysts; metathesis of neat 1-octene at 40°C.

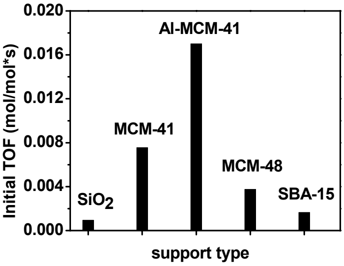

Figure 8. Specific activity (expressed as initial TOF) of MoO_3-based catalysts; metathesis of neat 1-octene at 40°C, loading 8 wt% Mo.

depends strongly on the catalyst loading and on the support type. As bulk MoO_3 is known as catalytically inactive and the activity of polymolybdate are supposed to be lower than that of isolated molybdenum oxide species, the samples with the highest population of single molybdenum oxide species would exhibit the highest catalyst activity.

For MoO_3/MCM-41 catalysts, the highest specific activity was found for catalyst with 6 wt % Mo (Figure 7). Catalysts prepared by supporting MoO_3 on MCM-48 and SBA-15 exhibited catalytic activity also higher in comparison with MoO_3/SiO_2, but significantly lower in comparison with MoO_3/MCM-41 (Figure 8). The reason for this decreased activity was found in the low population of isolated molybdenum oxide species. The selectivity of MoO_3/MCM-48 and MoO_3/SBA-15, however, was about 90%. Although the highest specific activity was found for MoO_3/Al-MCM-41, the low selectivity to the main metathesis product strongly limits its applications.

3.2. Properties of rhenium (VII) oxide on organized mesoporous aluminas

In the J. Heyrovsky Institute, OMAs with wormhole-like pore structure and narrow pore size distribution OMA3.5, OMA 5, and OMA 6.5 (number in the label corresponds with the average pore diameter) were used for supporting rhenium (VII) oxide. Two conventional commercially available γ-aluminas were used for comparison: (i) Alcoa – alumina of broad pore size distribution and large microporous fraction (S_{BET} = 342 m^2/g, V = 0.355 cm^3/g) and (ii) Condea – alumina with broad pore size distribution in mesoporous region (S = 197 m^2/g, V = 0.427 cm^3/g, average pore diameter D = 7.2 nm). Figure 9 shows the comparison of corresponding catalyst activity (all catalysts with 9 wt % of Re) in 1-decene metathesis. Catalysts are labeled as Re/support, e.g. Re/OMA3.5. It is seen that (i) OMA-based catalysts exhibited higher activity than both catalysts used conventional supports, and (ii) OMA-based catalyst with larger pores is more active than that of narrower pores. The selectivity to 9-octadecene is very high in all cases (about 95%). Similar results showing the superiority of nanostructured mesoporous aluminas supported Re (VII) oxide catalysts in alkene metathesis were obtained simultaneously by other groups [10, 11].

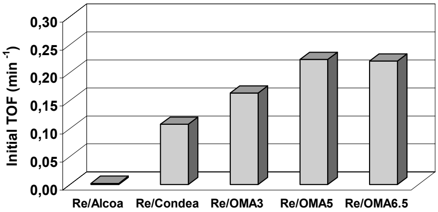

Figure 9. Activity dependence on support. Neat 1-decene, *t* = 60°C, 1-decene/Re molar.

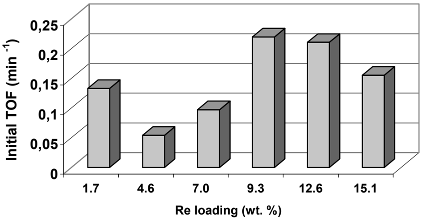

Figure 10. Activity dependence on loading. Re/OMA6.5, neat 1-decene (1.5 mL), *t* = 60°C , 50 mg catalyst.

The optimum catalyst loading found was 9 wt % Re (Figure 10). It is in agreement with ref., [11] but in contradiction with previous results obtained for rhenium (VII) oxide on conventional γ-alumina, [26] where an exponential increase of reaction rate was until approximately 14 wt % Re observed. This loading value corresponds to the formation of monolayer on the catalyst surface (Re atom per 0.35 nm^2) [26]. Contrary to the Mo, rhenium does not incline to the formation of polyanions and isolated ReO_4 species are proposed to be on the surface. Also XRD did not observe any presence of crystallites even at high loadings [9, 26]. However, for the catalytic activity of Re (VII) oxide on alumina the population of individual alumina surface OH groups (at least five differing in their acidity) seems to be essential and this population may vary with the type of alumina used.

Table 2 gives a survey of applications of Re (VII) oxide-supported catalysts in various alkene, alkadiene, and cycloalkene metathesis. In all cases, Re/OMAs exhibited higher activity in comparison with Re/Alcoa and Re/Condea. In some cases, activity of Re/OMA6.5 was found higher than that of Re/OMA3.5 (1-decene, 1,7-octadiene, 1,9-decadiene). In the case of 1,9-decadiene, the product distribution depended strongly on the catalyst pore size (Figure 11). The higher population of acyclic diene metathesis (ADMET) trimers, tetramers, and higher oligomers was obtained using catalyst with higher pores. This provides an example of pore size-controlled catalyst selectivity.

Table 2. A survey of metathesis of unsubstituted substrates with Re (VII) oxide catalysts

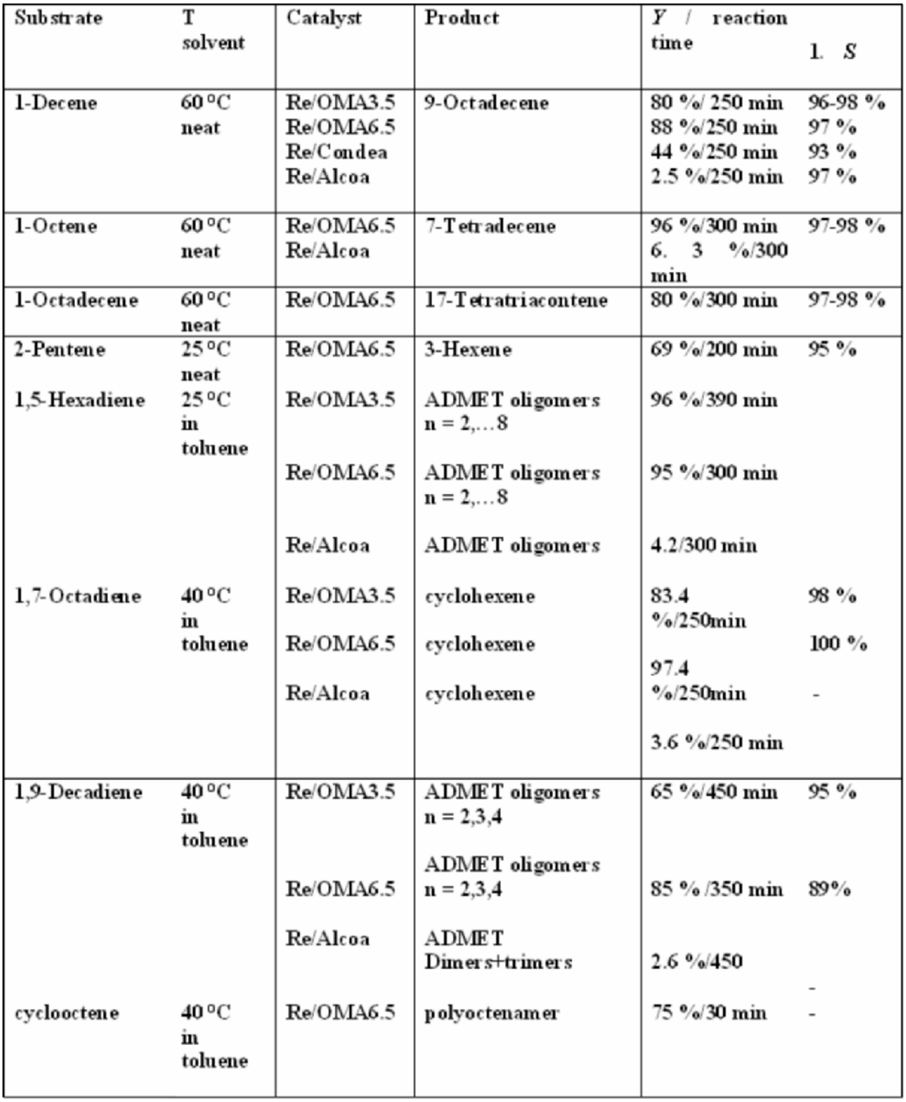

Substrate	T solvent	Catalyst	Product	*Y* / reaction time	1. *S*
1-Decene	60 °C neat	Re/OMA3.5	9-Octadecene	80 %/ 250 min	96-98 %
		Re/OMA6.5		88 %/250 min	97 %
		Re/Condea		44 %/250 min	93 %
		Re/Alcoa		2.5 %/250 min	97 %
1-Octene	60 °C neat	Re/OMA6.5	7-Tetradecene	96 %/300 min	97-98 %
		Re/Alcoa		6. 3 %/300 min	
1-Octadecene	60 °C neat	Re/OMA6.5	17-Tetratriacontene	80 %/300 min	97-98 %
2-Pentene	25 °C neat	Re/OMA6.5	3-Hexene	69 %/200 min	95 %
1,5-Hexadiene	25 °C in toluene	Re/OMA3.5	ADMET oligomers n = 2,…8	96 %/390 min	
		Re/OMA6.5	ADMET oligomers n = 2,…8	95 %/300 min	
		Re/Alcoa	ADMET oligomers	4.2/300 min	
1,7-Octadiene	40 °C in toluene	Re/OMA3.5	cyclohexene	83.4 %/250min	98 %
		Re/OMA6.5	cyclohexene	97.4 %/250min	100 %
		Re/Alcoa	cyclohexene	3.6 %/250 min	-
1,9-Decadiene	40 °C in toluene	Re/OMA3.5	ADMET oligomers n = 2,3,4	65 %/450 min	95 %
		Re/OMA6.5	ADMET oligomers n = 2,3,4	85 % /350 min	89%
		Re/Alcoa	ADMET Dimers+trimers	2.6 %/450	-
cyclooctene	40 °C in toluene	Re/OMA6.5	polyoctenamer	75 %/30 min	-

T = reaction temperature, *Y* = product yield, *S* = selectivity, catalyst loading = 9 wt % Re. Data taken from ref. [13]

Re (VII) oxide on alumina is known to catalyze metathesis of oxygen-containing substrates, however, only in combination with cocatalyst-like Me_4Sn. The presence of Me_4Sn was found to be necessary also for Re/OMA catalysts if used in metathesis of unsaturated esters and ether. Table 3 gives a survey of these experiments.

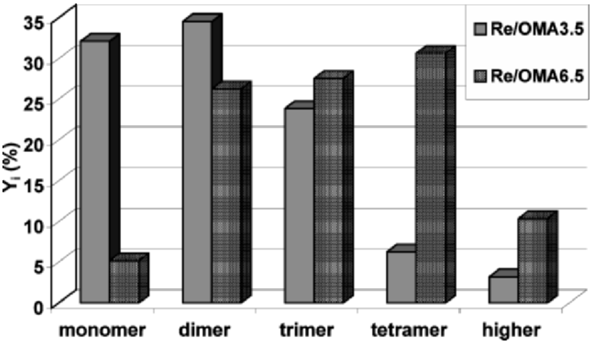

Figure 11. Products of 1,9-decadiene metathesis with Re/OMA3.5 and Re/OMA6.5. 30 mg catalyst (9 wt % Re), 0.9 mL toluene, substrate/Re = 320, 40°C, reaction time = 450 min, Y_i, yield of individual product.

Table 3. A survey of metathesis of oxygen-containing substrates with Re (VII) oxide catalysts

Substrate	Conditions	Catalyst	Product	*Y*(%)/ Reaction time (min)	*S*	TON
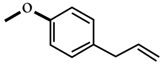	25°C Sub/Re=40	Re/OMA3.5	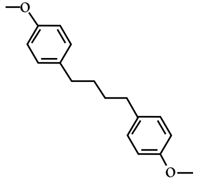	59.7/300	98.5	23.8
		Re/OMA5		91.2/300	99.3	36.5
		Re/Condea		80.3/300	99.7	32.1
		Re/Alcoa		1.5/300		0.6
	25°C Sub/Re=100	Re/OMA3.5		38.8/300	98.2	38.8
		Re/OMA5		78.5/300	99.8	78.5
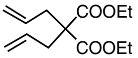	25°C Sub/Re=40	Re/OMA3.5	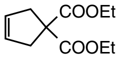	52.3/150	100	20.9
		Re/OMA5		74.5/150	100	29.8
		Re/Condea		71.5/150	100	28.6
		Re/Alcoa		1.18/150	100	0.5
Methyl-undecenoate	40°C Sub/Re=40	Re/OMA5	CH-(CH_2)$_8$$COOCH_3$? CH-(CH_2)$_8$$COOH_3$	40.2/30	100	16.1
6-hexenyl-acetate	40°C Sub/Re=25	Re/OMA5	CH-(CH_2)$_4$$OOCCH_3$? CH-(CH_2)$_4$$OOCCH_3$	43.0/30	100	10.8

Catalyst loading 9 wt % Re, Me_4Sn/Re = 1, toluene, Sub = substrate, Y = yield of given product at a given reaction time, S = selectivity to the given product

It is seen that a high selectivity to desired products were achieved with all catalysts used. The yields, however, depended on the catalyst used and considerably decreasing in the order Re/OMA5 > Re/Condea > Re/OMA3.5 > Re/Alcoa. Generally, the specific activity (turnover number [TON]) is lower in comparison with unsubstituted substrates, suggesting a competition between metathesis and catalysts deactivation by polar substrates.

4. Mesoporous molecular sieves anchored well-defined metathesis catalysts

Immobilization of well-defined metathesis catalysts on suitable supports represents an important way how to prepare highly active and selective metathesis catalysts easily separable from products, reusable, and applicable in flow systems. Several successful attempts have been made to anchor Schrock- and Grubbs-type catalysts on silica support. Very rarely, however, mesoporous molecular sieves have been used for this purpose. First-generation Grubbs catalyst was anchored on phosphinated MCM-41 and used in ring-opening metathesis polymerization (ROMP) of norbornene (NBE) and ring-closing metathesis (RCM) of diethyl diallylmalonate. Similarly, Ru–Schiff base complexes were anchored on MCM-41 and used in ROMP and RCM after activation with trimethylsilyldiazomethane.

We found that molybdenum neophylidene complexes (Schrock-type catalysts) can be immobilized on siliceous MCM-41, MCM-48, and SBA-15 via a ligand exchange reaction with surface OH groups (Scheme 1). Hybrid catalysts thus prepared exhibited high activity and selectivity in metathesis of neat 1-heptene (Figure 12). No significant differences were found in activity of individual catalysts differing in support used. Selectivity to 6-dodecene was in all cases higher than 98%.

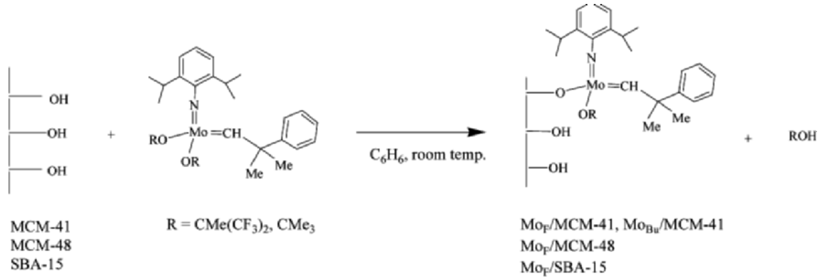

Scheme 1

The activity of hybrid catalysts approached to that of parent homogeneous system. Catalyst derived from hexafluoro-*t*-butoxy complex – $\mathrm{Mo_F}$/MCM-41 was significantly more active than that derived from *t*-butoxy complex – $\mathrm{Mo_{Bu}}$/MCM-41 (Figure 13), in accord with the well-known enhanced activity of Schrock catalysts with fluorinated alkoxo ligands. The catalysts were proved to be Mo-leaching resistant. However, in reusing experiments their activity was reduced due to inherent deactivation processes.

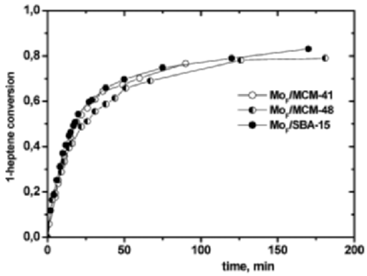

Figure 12. Metathesis of neat 1-heptene with Mo$_F$/MCM-41, Mo$_F$/MCM-48, and Mo$_F$/SBA-15. 1-heptene/Mo molar ratio = 1900, room temperature.

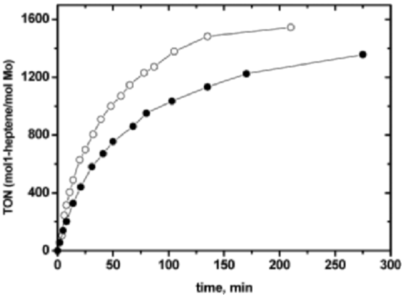

Figure 13. Metathesis of neat 1-heptene with Mo$_F$/MCM-41 (○) and Mo$_{Bu}$/MCM-41 (●). 1-heptene/Mo molar ratio = 2300, room temperature.

Hybrid catalysts prepared were also successfully used in metathesis of unsaturated esters. Thus, metathesis of 5-hexenyl acetate proceeded with Mo$_F$/MCM-41 in benzene at room temperature with 76% conversion and 100% selectivity. RCM of diethyl diallylmalonate under the same conditions gave 60% conversion and 100% selectivity.

Mo$_F$/MCM-41 and Mo$_F$/SBA-15 were also tested in ROMP of NBE and cyclooctene (COE). Corresponding polymers released into the liquid phase were isolated by precipitation in methanol and analyzed by size exclusion chromatography (SEC) and nuclear magnetic resonance (NMR). The results are summarized in Table 4. For molar ratio monomer/Mo = 100 and higher, high-molecular weigh polymers of multimodal molecular weight distribution were obtained. Especially for NBE, polymers prepared contained an extremely high-molecular weight fraction. High molecular weight of polymer can be effectively reduced using 1-heptene as a chain transfer agent (Table 4, No. 8). ^{13}C NMR confirmed the polymer structure corresponding to the ROMP mechanism and determined *cis* double bond content – 72% for poly (NBE) and 19% for poly (COE). In all cases polymers of very broad molecular weight distribution were formed, i.e. the molecular weight control (characteristic for homogeneous Schrock catalysts) was lost. The reason for it may lie in different positions of individual catalyst sites on the surface (e.g. on the external surface, in the mouth of the channels, on the walls deep in the channels) and diffusion limitations. The advantages of hybrid catalyst lie mainly in easier catalyst separation from polymers. The content of Mo in polymers was only about 6 ppm.

Table 4. A survey of ROMP experiments with hybrid catalysts

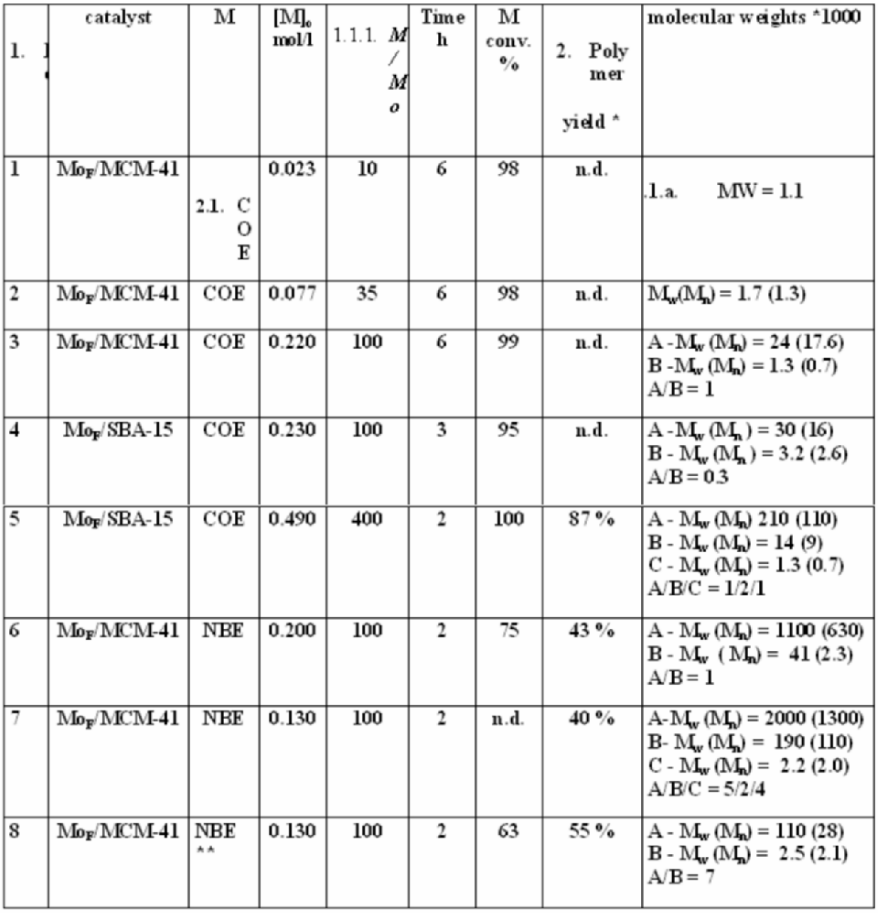

1.	catalyst	M	$[M]_o$ mol/l	1.1.1. M / Mo	Time h	M conv. %	2. Polymer yield *	molecular weights *1000
1	Mo$_F$/MCM-41	2.1. COE	0.023	10	6	98	n.d.	.1.a. MW = 1.1
2	Mo$_F$/MCM-41	COE	0.077	35	6	98	n.d.	M_w(M_n) = 1.7 (1.3)
3	Mo$_F$/MCM-41	COE	0.220	100	6	99	n.d.	A -M_w (M_n) = 24 (17.6) B -M_w (M_n) = 1.3 (0.7) A/B = 1
4	Mo$_F$/SBA-15	COE	0.230	100	3	95	n.d.	A -M_w (M_n) = 30 (16) B - M_w (M_n) = 3.2 (2.6) A/B = 0.3
5	Mo$_F$/SBA-15	COE	0.490	400	2	100	87 %	A - M_w (M_n) 210 (110) B - M_w (M_n) = 14 (9) C - M_w (M_n) = 1.3 (0.7) A/B/C = 1/2/1
6	Mo$_F$/MCM-41	NBE	0.200	100	2	75	43 %	A - M_w (M_n) = 1100 (630) B - M_w (M_n) = 41 (2.3) A/B = 1
7	Mo$_F$/MCM-41	NBE	0.130	100	2	n.d.	40 %	A-M_w (M_n) = 2000 (1300) B- M_w (M_n) = 190 (110) C - M_w (M_n) = 2.2 (2.0) A/B/C = 5/2/4
8	Mo$_F$/MCM-41	NBE **	0.130	100	2	63	55 %	A - M_w (M_n) = 110 (28) B - M_w (M_n) = 2.5 (2.1) A/B = 7

Benzene, room temperature, M = monomer, M/Mo = molar ratio monomer/Mo, *methanol-insoluble polymer, **NBE + 1-heptene in mol ratio 20/1, n.d. = not determined

5. Conclusions

1. Both silica- and alumina-type mesoporous molecular sieves are perspective supports for the preparation of new metathesis catalysts. Their mesoporous structure enables relatively bulky substrate molecules to penetrate into their channels and to employ the large inner surface for performing metathesis reactions. The mesoporous structure also enables bulky organometallic complexes to be anchored on channel walls forming effective hybrid metathesis catalysts. The tunable pore size of prepared catalysts promises the possibility to affect the reaction selectivity by choosing the catalyst of suitable pore size.

2. Molybdenum and rhenium oxide catalysts based on siliceous mesoporous sieves and OMA, respectively, proved enhanced catalytic activity in comparison with corresponding catalysts using conventional supports. The origin of this enhanced activity is not completely clear and is still a subject of discussions and continuous research. The better accessibility of catalysts site located in mesopores undoubtedly represents the essential contribution to the increased catalytic activity. Rhenium (VII) oxide on organized mesoporous alumina preserves known tolerance of Re catalysts to the polar-substituted olefins. The presence of cocatalysts like Me_4Sn is essential similarly as for conventional systems. However, the catalysts with higher pore size were found to deliver better results.
3. Siliceous mesoporous sieves are suitable for anchoring Schrock alkylidene complexes under formation of hybrid metathesis catalysts. These hybrid catalysts maintain the high activity and selectivity of parent homogeneous systems. They can be used in alkene metathesis, RCM, and ROMP including metathesis of oxygen-containing substrates. They are Mo-leaching resistant and can be easily removed from the reaction mixture delivering products free of catalyst residue.

Acknowledgments

The financial support from the Grant Agency of the Academy of Sciences of the Czech Republic (project A4040411) and from the Grant Agency of the Czech Republic (project 203/05/2194) is gratefully acknowledged.

References

[1] Beck, J.S., Vartuli, J.C., Roth, W.J., Leonowicz, M.E., Kresge, C.T., Schmitt, K.D., Chu, C.-W., Olson, D.H., Sheppard, E.W., McCullen, S.B., Higgins, J.B., Schlenker, J.L., J. Am. Chem. Soc. 1992, 114:10834–10843.

[2] Ying, J.Y., Mehnert, C.P., Wong, M.S., Angew. Chem. Int. Edit. 1999, 38:56–77.

[3] Thomas, J.M., Angew. Chem. Int. Edit. 1999, 38:3588–3628.

[4] Schüth, F., Chem. Mater. 2001, 13:3184–3195.

[5] Zhou, J., Zhou, R., Mo, L., Zhao, S., Zheng, X., J. Mol. Catal. A: Chem. 2002, 178:289–292.

[6] Čejka, J., Appl. Catal. A: General 2003, 254:327–338.

[7] Abbenhuis, H.C.L., Angew. Chem. Int. Edit. 1999, 38:1058–1060.

[8] Balcar, H., Čejka, J., Sedláček, J., Svoboda, J., Zedník, J., Bastl, Z., Bosáček, V., Vohlídal, J., J. Mol. Catal. A: Chem. 2003, 203:287–298.

[9] Balcar, H., Hamtil, R., Žilková, N., Čejka, J., Catal. Lett. 2004, 97:25–29.

[10] Oikawa, T., Ookoshi, T., Tanaka, T., Yamamoto, T., Onaka, M., Micropor. Mesopor. Mater. 2004, 74:93–103.

[11] Aguado, J., Escola, J.M., Castro, M.C., Paredes, B., Appl. Catal. A: General 2005, 284:47–57.

[12] Balcar, H., Topka, P., Žilková, N., Pérez-Pariente, J., Čejka, J., in: Jaroniec, M., Sayari, A. (eds), Nanoporous Materials IV, Studies in Surface Science and Catalysis, Vol. 156, Elsevier, Amsterdam, 2005, pp. 795–802.

[13] Hamtil, R., Žilková, N., Balcar, H., Čejka, J., Appl. Catal. A: General, 2006, 302:193–200.

[14] Topka, P., Balcar, H., Rathouský, J., Žilková, N., Verpoort, F., Čejka, J., Micropor. Mesopor. Mater. (in press).

[15] Roth, W.J., Vartuli, J.C., in: Čejka, J., van Bekkum, H., (eds) Zeolites and Ordered Mesoporous Materials: Progress and Prospects. Proceedings of 1st FEZA School on Zeolites, Prague, August 20–21, 2005, Elsevier, Amsterdam. Stud. Surf. Sci. Catal. 2005, 157:91.

[16] Zhao, D., Huo, Q., Feng, J., Chmelka, B.F., Stucky, G.D., J. Am. Chem. Soc. 1998, 120:6024–6036.

[17] Deng, W., Bodart, P., Pruski, M., Shanks, B.H., Micropor. Mesopor. Mater. 2002, 52:169–177.

[18] Čejka, J., Kooyman, P.J., Veselá, L., Rathouský, J., Zukal, A., Phys. Chem. Chem. Phys. 2002, 4:4823–4829.

[19] Corma, A., Chem. Rev. 1997, 97:2373–2420.

[20] Taguchi, A., Schüth, F., Micropor. Mesopor. Mater. 2005, 77:1–45.

[21] Čejka, J., Žilková, N., Rathouský, J., Zukal, A., Phys. Chem. Chem. Phys. 2001, 3:5076–5081.

[22] Čejka, J., Žilková, N., Rathouský, J., Zukal, A., Jagiello, J., Langmuir, 2004, 20:7532–7539.

[23] Ivin, K.J., Mol, J.C., Olefin Metathesis and Metathesis Polymerization, Academic Press, London, 1997.

[24] Ookoshi, T., Onaka, M., Chem. Commun. 1998, 2399–2400.

[25] Onaka, M., Oikawa, T, Chem. Lett. 2002, 850–851.

[26] Mol, J.C, Catal. Today 1999, 5:289–299.

[27] Balcar, H., Hamtil, R., Žilková, N., Zhang, Z., Pinnavaia, T.J., Čejka, J. (in preparation).

[28] Buchmeiser, M.R., New J. Chem. 2004, 28:549–557.

[29] Wolke, S.I., Buffon, R., J. Mol. Catal. A: Chem. 2000, 160:181–187.

[30] Preishuber-Pflügl, P., Buchacher, P., Eder, E., Schitter, R.M., Stelzer, F., J. Mol. Catal. A: Chem. 1998, 133:151–158.

[31] Mayr, M., Buchmeiser, M.R., Wurst, K., Adv. Synth. Catal. 2002, 344:712–719.

[32] Rhers, B., Salameh, A., Baudouin, A., Quadrelli, E.A., Taoufik, M., Copéret, Ch., Lefebvre, F., Basset, J.-M., Solans-Monfort, X., Eisenstein, O., Lukens, W.W., Lopez, L.P.H., Sinha, A., Schrock, R.R., Organometallics, 2006, 25:3554–3557.

[33] Melis, K., DeVos, D., Jacobs, P., Verpoort, F., J. Mol. Catal. A: Chem. 2001, 169:47–56.

[34] De Clercq, B., Lefebvre, F., Verpoort, F., New J. Chem. 2002, 26:1201–1208.

[35] Balcar, H., Žilková, N., Sedláček, J., Zedník, J., J. Mol. Catal. A: Chem. 2005, 232:53–58.

“GREENER SHADE OF RUTHENIUM”: NEW CONCEPTS OF ACTIVATION, IMMOBILIZATION, AND RECOVERY OF RUTHENIUM CATALYSTS FOR GREEN OLEFIN METATHESIS

ANNA MICHROWSKA, ŁUKASZ GUŁAJSKI, KAROL GRELA

Institute of Organic Chemistry, Polish Academy of Sciences, Kasprzaka 44/52, 01-224, Warsaw, Poland

Abstract: The results described herewith demonstrate that the activity of ruthenium (Ru) metathesis catalysts can be enhanced by introduction of electron-withdrawing groups (EWGs) without detriment to catalysts stability. This principle can be used not only to increase the catalyst activity, but also to alter its physical–chemical properties, such as solubility in given medium or affinity to silica gel. An example of novel immobilisation strategy, based on this concept is presented. The ammonium-tagged Hoveyda-type catalysts can be successfully applied in aqueous media as well as in ionic liquids (IL). Substitution of a benzylidene fragment can be used not only to immobilize the organometallic complex in such media, but also to increase its catalytic activity by electronic activation. The high stability and good application profiles of such modified catalysts in conjunction with their facile removal from organic products can be expected to offer new opportunities in green applications of olefin metathesis.

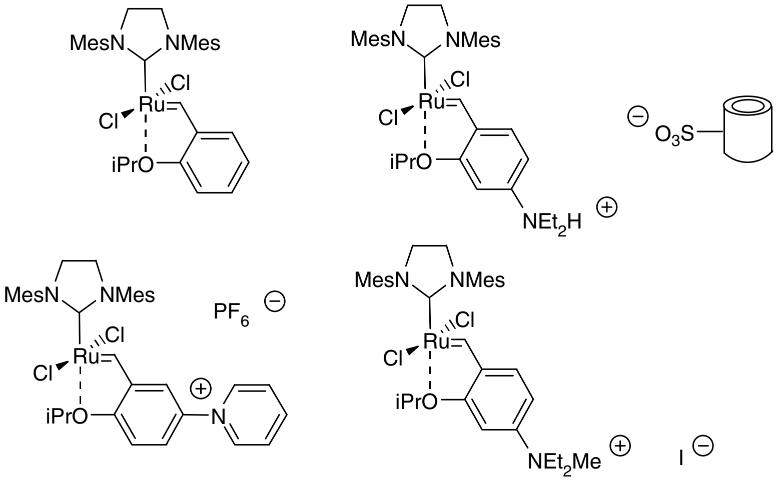

Keywords: alkene metathesis, ruthenium catalyst, Ru-removal, immobilization, water emulsions

Y. İmamoğlu and V. Dragutan (eds.), Metathesis Chemistry: From Nanostructure Design to Synthesis of Advanced Materials, 167-183.

1. Introduction

During recent years, olefin metathesis has gained a position of increasing significance. The development of modern Ru metathesis catalysts, such as Grubbs I–III (**1**, **2**, **5**) and Hoveyda–Grubbs carbenes (**3**, **4**, Figure 1) combining high activity with an excellent tolerance to a variety of functional groups has been the key to widespread applications of olefin metathesis in organic synthesis and polymer chemistry.

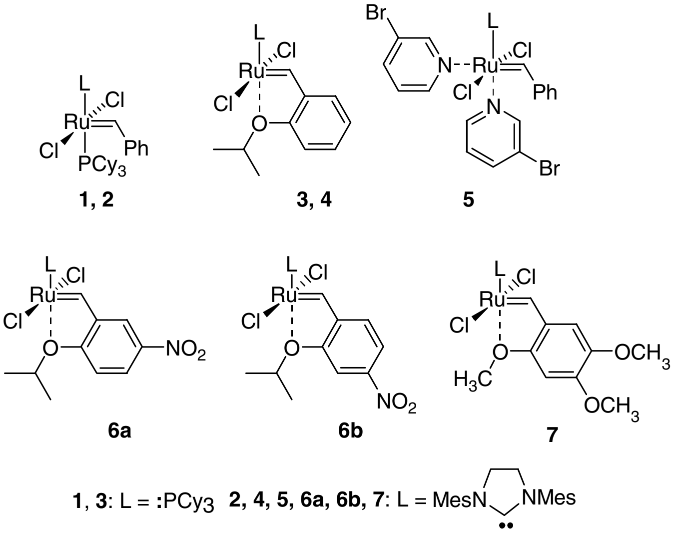

Figure 1. Ruthenium-based catalysts **1-5** for olefin metathesis (Cy = cyclohexyl, Mes = 2,4,5-trimethylphenyl).

Despite general superiority offered by this family of catalysts, they share some disadvantages. Since olefin metathesis reactions are expected to be used in pharmaceutical processes, the most undesirable feature of these complexes is that during the reaction they form Ru byproducts, which are difficult to remove from the reaction products. In many cases, Ru levels of >2000 ppm remain after chromatography of products prepared by RCM with 5 mol % of Grubbs catalysts. The Ru has to be removed prior to further processing. Several protocols to solve problems associated with Ru contamination arising during pharmaceutical or fine chemical processing, from research and development (R&D) scale through to manufacture, have been proposed.[3] Use of biphasic aqueous extraction, various scavengers, such as lead tetraacetate, dimethyl sulfoxide (DMSO), triphenylphosphine oxide,[7] and supported phosphines were reported to reduce the Ru content to between 200–1200 ppm. Alternatively, two cycles of chromatography, followed by 12 h incubation with activated charcoal, resulted in 100 ppm. Recently, special functional polymers – QuadraPure resins – were intended for heavy metal (including Ru) removal in both batch and continuous processes. Our group has recently developed a new efficient strategy for phase separation and recovery of complex **7** (Figure 1), which provides crude products containing up to 400 ppm of Ru.

From an economic point of view on the whole chemical process the catalyst's cost is another important attribute. In this respect, immobilization of homogeneous catalysts offers inherent operational and economic advantages over the parent soluble catalysts. Several attempts have been made to immobilize Grubbs-type carbenes **1–2** on solid or soluble supports either via ligand L (Figure 1) or via the carbene moiety. Hoveyda established catalysts **3–4** as remarkably robust complexes promoting olefin metathesis by a release/return mechanism. Recently, various Hoveyda–Grubbs carbenes were attached to different resins or soluble supports preferentially via the 2-alkoxybenzylidene fragment. Our group has recently presented a Hoveyda–Grubbs complex covalently bound to a polystyrene–diethylsilane (PS–DES) resin.[17b] However, for practical reasons noncovalent attachment of catalysts to a solid phase is highly desirable. The possibility of reloading the solid phase opens the door for utilizing solid supports, which have been specially designed for the individual catalytic process without considering their costs as much as would be relevant for covalently bound catalysts. Indeed, this concept should be of particular relevance in continuous-flow processes using reactors filled with heterogeneous or immobilized homogeneous catalysts. The attachment ought to be strong enough to suppress leaching of the catalyst. After inactivation of the catalyst it is beneficial if it can be removed from the solid phase and the reactor can be reactivated with fresh catalyst by simple washing protocols. Thus, this concept avoids physical removal of the fixed bed inside the reactor which can be costly.

2. On-demand activation by acids or heat

In 2002–2004 we introduced the stable 5- and 4-nitro-substituted analogues **6a**, **6b** which were shown to exhibit impressive activity in ring-closing metathesis (RCM), cross-metathesis (CM), and enyne-metathesis (Figure 1). As a result, the more easily available catalyst **6a** has found a successful application in target oriented syntheses and in the pharmaceutical industry. We proposed that the nitro group in the benzylidene fragment of **6a** and **6b** would weaken O→Ru chelation and facilitates faster initiation of the catalytic cycle. In addition, the suppression of oxygen reassociation to the Ru center caused by an electron-withdrawing group (EWG) and the increased electron deficiency at the initiating carbene species should make these complexes more active in olefin metathesis. In accordance with this assumption we observed that the very stable complex **8** (Figure 2), bearing "neutral"

-C(OH)Ph_2 substituent, in reaction with **10** exhibits similar activity to that of parent Hoveyda catalyst **4** (>70% of the conversion after 16 h; Figure 3).

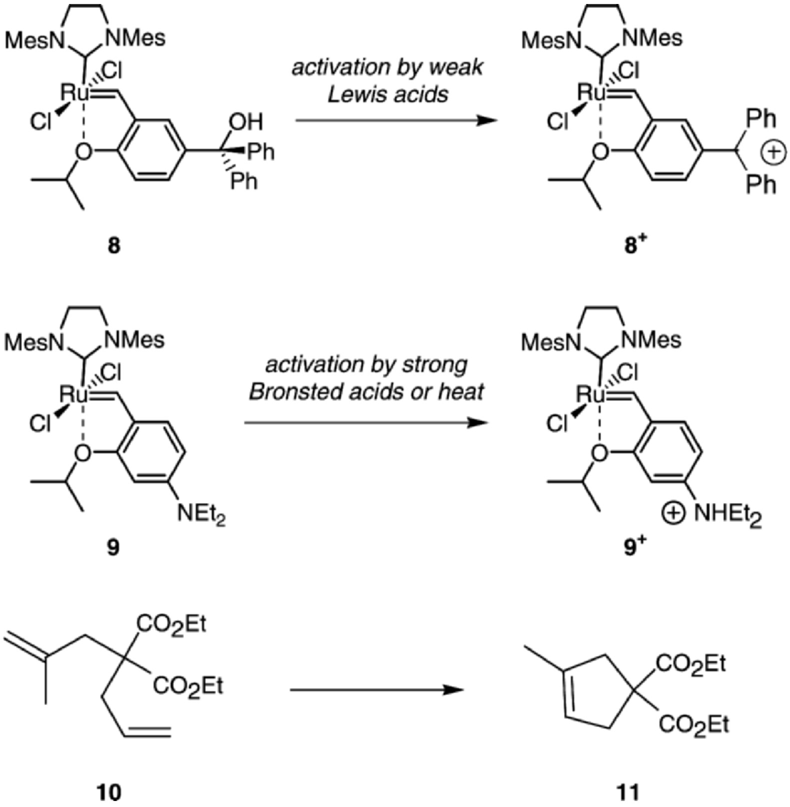

Figure 2. New ruthenium initiators.

We speculated that addition of an equimolar amount of acid can activate this complex to a much higher extent via formation (at least in some amount) highly active carbocationic species $\mathbf{8}^+$ (Figure 2). To test this possibility, the effect of various additives on complex **8** stability and activity was screened. Addition of weak acids, such as $ZnCl_2 \times HCl$ or Ph_2SnCl_2 exhibit activating effect on **8** and, at the same time, do not destroy propagating Ru species (Figure 3). The “binary” catalyst formed from **8** and Ph_2SnCl_2 was found to be of highest activity, reacting dramatically faster than parent complex **8** (Figure 3).

We also observed that the very stable (several months at +4°C in air) complex **9** (Figure 2), bearing the electron-donating diethylamino group (EDG) shows practically no activity in olefin metathesis with model substrate **10** (Figure 4).

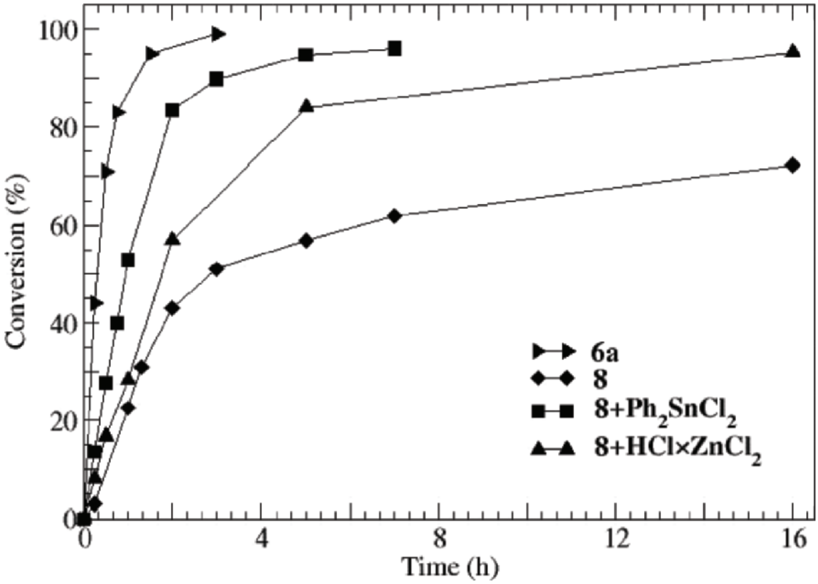

Figure 3. RCM of **10** using catalysts **8** (2.5 mol %) and **6a** (1 mol %). Conditions: CH_2Cl_2, 28°C.

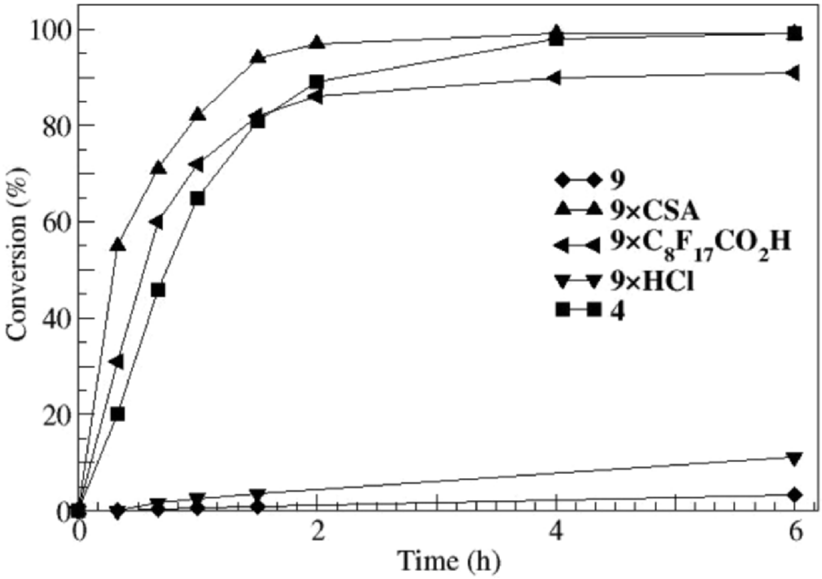

Figure 4. RCM of **10** using catalysts **4**, **9**, and in situ formed salts of **9**. CSA = (–)-camphor-10-sulfonic acid. Conditions: catalyst (5 mol. %), CH_2Cl_2, 25°C.

We envisaged that addition of one equivalent of acid can activate **9** via protonation of diethylamino group (electron donating to electron withdrawing activity switch, Figure 2) and accelerate ring-closure of **10**. In line with this expectation, the in situ formed salts obtained by treatment of **9** with organic acids are of high activity (Figure 4), in one case surpassing even the parent Hoveyda–Grubbs complex **4** in terms of initiation speed. Interestingly, different acids lead to complexes of different activity, and hydrochloric acid (used as a 2M solution in ethyl ether) produces catalyst of the lowest activity.

3. A new concept for the noncovalent binding of a ruthenium-based olefin metathesis catalyst to polymeric phases: preparation of a catalyst on Raschig rings

After reaction with polymer-supported acids, like Dowex resin, the new Ru complex **9** can be conveniently immobilized by ion exchange. In this novel strategy for the immobilization of Ru-based metathesis catalysts, the amino group plays a twofold role, being first an active anchor for immobilization (vide supra) and second, after protonation, activating the catalysts (electron donating to electron withdrawing activity switch).

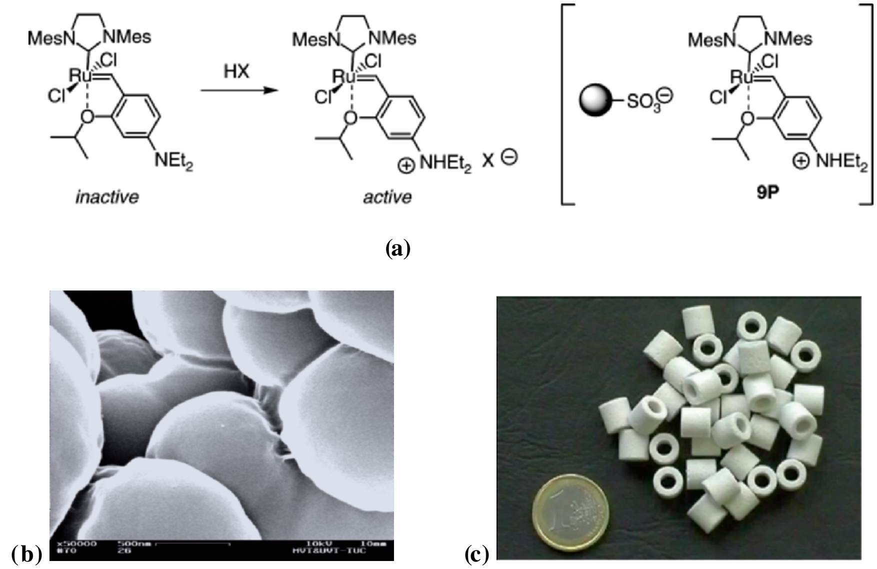

Figure 5. (a) A principle of catalyst **9** activation and non-covalent binding of a catalyst to polymeric phase; (b) Sulfonated polymer particles inside Raschig rings, as visualized by SEM; (c) Megaporous glass Raschig rings used for immobilization of **9**.

Using the above described strategy of noncovalent immobilization we prepared, in a cooperation with Kirschning group, catalyst **9P** immobilized on glass polymer composite Raschig rings (Figure 5b,c), which can be used for combinatorial chemistry and high-throughput screening.[45] Recyclability studies showed that the same ring containing catalyst **9P** can be used for up to six cycles of metathesis, however, with gradual loss of activity. Importantly, the solid phase can easily be reactivated by a washing protocol (1N HCl, H_2O, methanol then addition of fresh **9**). The contamination level of products with Ru was around 100 ppm. This is significantly lower then the Ru contamination reported for Hoveyda's catalyst on sol–gel pellets (up to 1 wt. %). Recently, another interesting report on a disk-shaped monolithic Ru catalyst for combinatorial chemistry has been published. In the case of this system the reported leaching was >3% while the average contamination of products with Ru was around 70 ppm. The catalyst was, however, designed as "one-way" discs, therefore no recycling or multiple use was attempted.[34]

Table 1. RCM and CM with catalyst **9P** bound to Raschig rings

Entry	Substrate	Product	Temp. °C, (time [h])	Conversion (%)[a]	Ru (ppm)
1	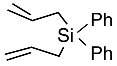	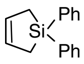	45 (18)	99	102
2	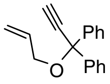	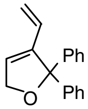	45 (4)	99	
3	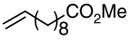	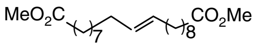	22 (18)	95 *E*:*Z* = 1.2:1	21
4	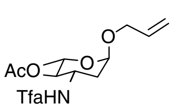	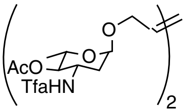	45 (24)	68[b] *E*:*Z* = 11:1	77
5	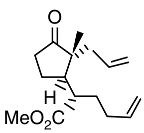	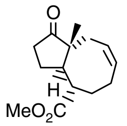	45 (16)	99	30

[a]Conditions: one Raschig ring **9P** (loading 3 μmol Ru/ring, 5 mol %) per reaction was used. [b]Two Raschig rings (loading 3 μmol Ru/ring, 10 mol %) were used.

The practicability of Raschig rings loaded with the Ru complex **9** (3 μmol Ru/ring) in high-throughput synthesis was demonstrated by the examples shown in Table 1. RCM and enyne metathesis of representative substrates proceeds cleanly, with typically high conversion, as determined by gas chromatography/mass spectroscopy (GC/MS) and ^{1}H NMR analysis, leading to various carbo- and heterocycles (entries 1, 2, 5) including the rather labile cyclopenta–cyclooctane derivative (entry 5), a potential building block in the synthesis of terpenoid natural products.[35] We have also demonstrated the ability of **9P** to perform homo CM of functionalized alkenes (entries 3, 4). Interestingly, the "dimerization" of a hexose substrate (entry 4) proceeds without double bond isomerization, although complete conversion cannot be reached after 24 h of reflux. Surprisingly, the product is formed with remarkably high E/Z-selectivity (11:1) compared to the Grubbs catalyst **1** which commonly yields dimeric spacer-linked hexoses in the E/Z ratio of 3:1 to 5:1. This excellent selectivity may be ascribed to the "bulkiness" of the solid phase. At the end of the reaction the catalyst **9P** can be simply removed with a pair of tweezers and rinsed with minimal amounts of dichloromethane, producing minimal solvent waste.[35] Usually, the resulting crude products were pure according to GC/MS and ^{1}H NMR analyses and exhibit low levels of Ru contamination: 21–102 ppm (ICP–MS analysis of Ru). We have also demonstrated for the first time that RCM can be conducted under PASSflow continuous flow conditions using a noncovalently immobilized Ru catalyst.[35]

4. Immobilization of the Grubbs III olefin metathesis catalyst with polyvinyl pyridine

Recently, Grubbs and coworkers showed that 3-bromo pyridine can form a 2:1 complex with the Grubbs II catalyst **2** to yield the active olefin metathesis catalyst **5**. Ru complex **5** is active in many types of metathesis reactions including challenging CM with acrylonitrile.[39] We found that the Grubbs III catalyst **5** can easily be immobilized through ligand exchange using polyvinyl pyridine (PVP) (obtained by precipitation polymerization) (Figure 6). The immobilization was achieved by employing PVP in tenfold excess (with reference to pyridine moieties on the polymer), which resulted in complete (96%) immobilization of catalyst **5** as was judged by ICP–MS.[4c] Grubbs III catalyst is the best choice for conducting ligand exchange reaction with polymer-bound pyridine. In terms of reusability polymer **12** behaves similar to most covalently attached examples described in the literature[4b,14a] although in selected cases longer living systems has been described.[4b] After the fifth run, activity is lost which can either be ascribed to lack of thermal stability or to the inherent problem of leaching during the catalytic cycle. The solid phase bound catalyst shows very good chemical reactivity (Figure 6) and good recyclability and importantly can easily be reactivated with fresh catalyst which opens the possibility of using catalysts of type **12** under continuous-flow conditions in flow through reactors.

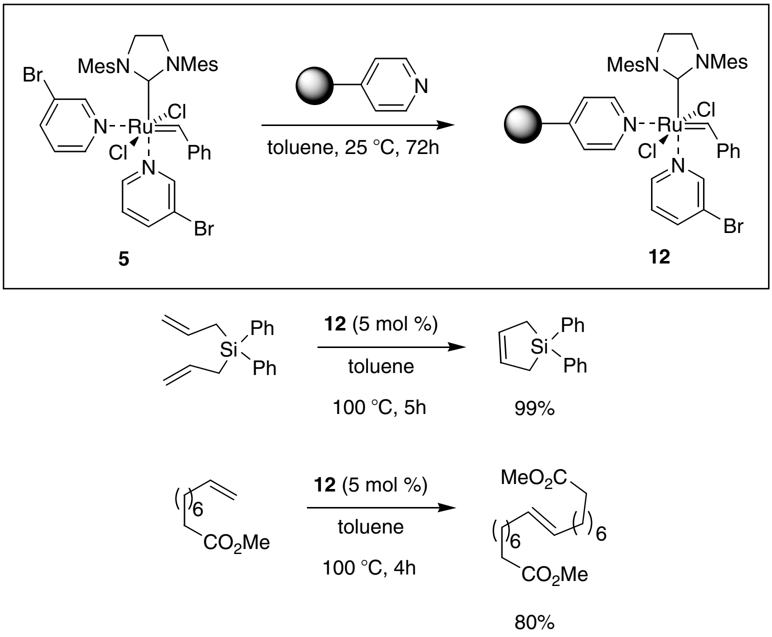

Figure 6. Preparation and activity of polymer-bound Ru complexes **12**.

5. Synthesis and application of an olefin metathesis catalyst bearing a quaternary ammonium group

Exploring further, our concept of activating a catalyst via electron donating to electron withdrawing activity switch we have obtained complex **13** bearing a quaternary ammonium group (Figure 7). This catalyst exhibits higher activity then parent Hoveyda complex **4** and have, in comparison, a high affinity for silica, enabling their efficient removal, in a single chromatographic pass. Thus, RCM of various dienes using **13**, followed by passing the reaction mixture through a short column of silica (20–60 × weight of the substrate), affords products in which the residual Ru content is typically below 100 ppm. In addition, the high efficiency of quaternary catalyst **13** in aqueous media, in conjunction with its facile removal from organic products, can be expected to offer new opportunities in green applications of olefin metathesis.

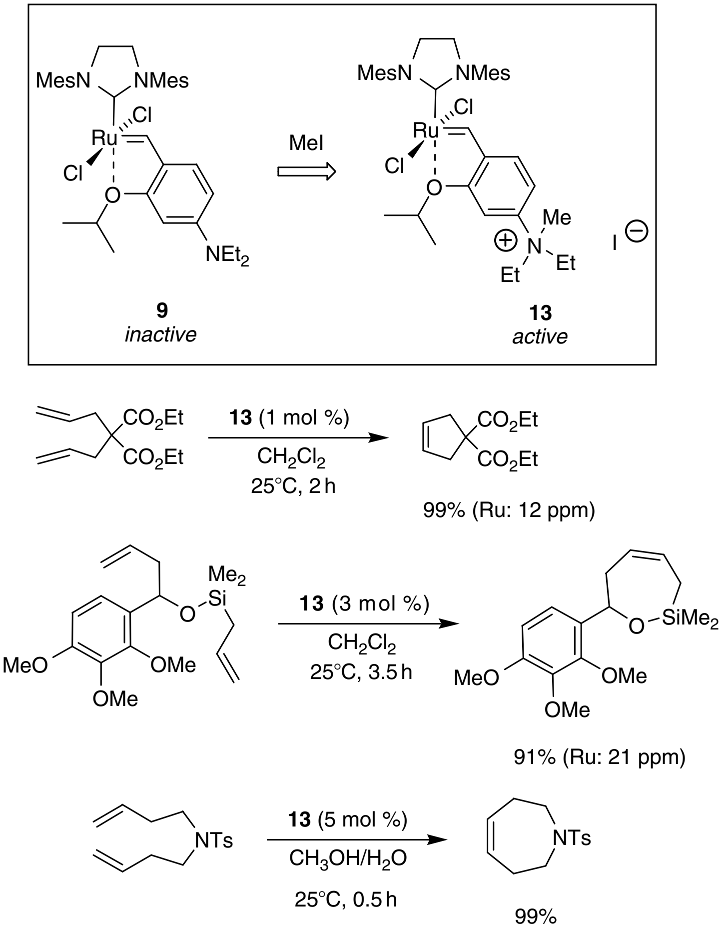

Figure 7. Applications of **13** in selected RCM reactions.

6. Activated pyridinium-tagged ruthenium complexes as efficient catalysts for ring-closing metathesis

Recently, various Hoveyda-type carbenes were attached to different resins or insoluble inorganic supports preferentially via the 2-alkoxybenzylidene fragment. An alternative method involves the use of tagged catalysts, which can be easily separated from untagged products by a phase-transfer event (precipitation or liquid-liquid partition). One particularly innovative method involves a catalyst immobilization in ionic liquids (IL). Because of their interesting properties such as ease of reuse, nonvolatility, and good ability to dissolve many kinds of organic and organometallic compounds, IL are promising candidates to replace volatile solvents traditionally used in organic chemistry. In order to develop a more environment friendly RCM process, Mauduit and Yao independently introduced IL-tagged Hoveyda-type catalysts **14a** and **14b** (Figure 8). For example, Mauduit's catalyts **14a** exhibits a high level of recyclability (the solution of catalyst in IL can be separated after the reaction and used again; this process can be repeated up to eight times) combined with a fairly good reactivity when used in a biphasic IL/toluene medium. Moreover extremely low residual ruthenium levels (average of 7 ppm) were detected in the final products.[48a,b]

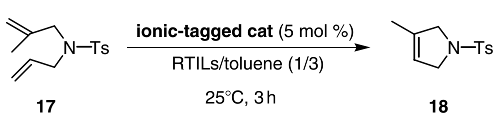

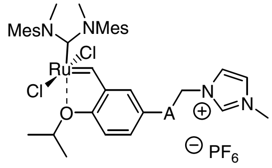

14a A=CH_2
14b A=OCH_2CH_2

Entry	Catalyst	RTILs	cycle (% conv.)[a]					
			1	2	3	4	5	6
1	**14a**	BMI.PF_6	>98	>98	>98	>98	>98	>98
2	**15**	BMI.PF_6	>98	95	65	6	-	-
3	**16**	BMI.PF_6	>98	>98	>98	>98	93	91
4	**15**	BMPy.BF_4	>98	89	26	-	-	-
5	**16**	BMPy.BF_4[b]	>98	>98	97	92	88	74

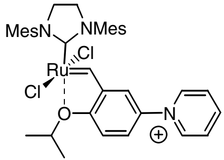

15 ⊖ PF_6

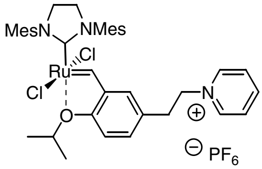

16

Figure 8. Comparative recyclability of ionic-tagged catalysts **14a**, **15**, and **16** in ionic media. [a] Determined by ^1H-NMR spectroscopic analysis at 400 MHz. [b]Reaction performed at 40°C.

Capitalizing on our efforts aimed at developing more environment friendly olefin metathesis processes, we have describe recently synthesis of new air-stable pyridinium containing Ru catalysts **15** for which the ionic tag is anchored to the styrenyl–ether benzylidene fragment (Figure 8).

In traditional solvent the ionic activated catalyst **15** showed a high activity in RCM (Table 2, entries 1, 3, 4, and 9). Nevertheless, lower activity was observed in aqueous media (EtOH/water: entry 2 or MeOH/water: entry 5) where only 40–50% of substrate reacted. The inductive coupled plasma mass

Table 2. Metathesis reactions catalyzed by **15**

Entry	Substrate	Product	Solvent	Time (h)	Conversion(%)^{a,b}	Ru (ppm)^c
1	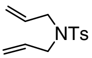	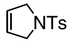	CH_2Cl_2	0.5	99	138
2			$EtOH/H_2O$	24	50	
3	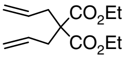	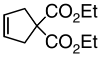	CH_2Cl_2	2	78	113
4	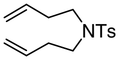	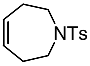	CH_2Cl_2	0.5	99	173
5			$MeOH/H_2O$	24	40	
6	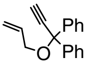	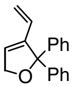	CH_2Cl_2	0.5	99	25
7			$MeOH/H_2O$	0.5	99	28
8			$EtOH/H_2O$	0.5	99	
9	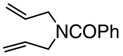	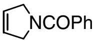	CH_2Cl_2	0.5^d	99	

[a]Conditions: 5 mol % of catalyst, CH_2Cl_2 or $MeOH/H_2O$ v/v 5:2 or $EtOH/H_2O$ v/v 5:2; c = 0.02 mol/L, 25°C; [b]Conversions were determined by analysis of ^{1}H-NMR or GC/MS of crude reaction mixture; [c]Determined by ICP-MS spectroscopy analysis and showed as parts per million; [d]With 2.5 mol % of catalyst.

spectroscopy (ICP-MS) analysis of several samples showed moderate to low levels of Ru-wastes down to 25 ppm (entry 6).

We then attempted to recycle the pyridinium-activated catalyst **15** in ionic solvents.[46,47] To evaluate the recyclability of the new activated pyridinium catalyst **15**, we performed the RCM of 2-allyl-2-methallyltosylamine **17** using 5 mol % of ionic catalyst in two different ionic solvents ($BMI.PF_6$ and $BMPy.BF_4$) with toluene as co-organic solvent (Figure 8). The activated pyridinium catalyst **15** showed a good activity in the first two cycles (>98%), but it decreases rapidly to reach 65% of conversion in the third cycle and no activity in the fourth (entry 2). As expected, the decrease of conversions was progressively obtained due to the extraction of the 14-electron catalytic species (which is unable to re-anchor its pyridinium ligand) to the organic phase during the isolation of the RCM product.

To evaluate a real effect of the pyridinium function in terms of activity and recyclability, we then prepared the complex **16**. This pyridinium-containing catalyst, equivalent to **14a**, possesses the same C3 alkyl linker between the ionic tag and the benzenylidene pattern. The direct comparison between the imidazolium-tagged catalyst **14a**, and its pyridinium-containing equivalent **16** showed similar conversions and reuses over six cycles (Figure 8, entry 3).

This result shows clearly that the nature of the cationic tag does not interfere in the activity and the recyclability of catalyst.

We then focused on the influence of the counter-anion of the ionic solvent. We therefore performed the metathesis reaction in 1-butyl-4-methyl pyridinium tetrafluoroborate ($BMPy.BF_4$) possessing the same cationic fragment but a different counter-anion. A slight decrease of activity was observed. Higher temperatures (40°C instead of 23°C) are required to obtain good results of reusability. This difference of activity could be explained by a better solubility of the ionic catalyst at this temperature, probably due to the difference of the counter-anion between the catalyst (PF_6) and the ionic solvent (BF_4).

7. Summary and outlook

Olefin metathesis is a simple and effective synthetic tool which is used to create many compounds which otherwise would require complex multistep syntheses. However, there is one disadvantage of metathesis reactions – it is not possible to remove toxic Ru-containing by-products from the end product. This is a particular problem in the pharmaceutical industry, where it is a necessity for compounds to be of high purity and contain no toxic impurities. Several attempts have been made to immobilize metathesis catalysts on solid or soluble supports. We showed some new concepts for Hoveyda-type Ru catalysts separation and reuse, either via immobilization in a liquid phase or various phase separation techniques.

The results described herewith demonstrate that the activity of Ru metathesis catalysts can be enhanced by introduction of EWGs without detriment to catalysts stability. This principle can be used not only to increase the catalyst activity, but also to alter its physical–chemical properties, such as solubility in given medium or affinity to silica gel. An example of novel immobilization strategy, based on this concept is presented. In fact, the possibility of reversibly binding catalysts to a solid phase is of major importance for industrial applications, particularly when continuous flow processes with immobilised homogeneous catalysts are pursued.

The examples presented herewith show that tagged Hoveyda-type catalysts can be successfully applied in aqueous media as well as in IL. Substitution of a benzylidene fragment can be used not only to immobilize the organometallic complex in such media, but also to increase its catalytic activity by electronic activation. The high stability and good application profiles of such modified catalysts in conjunction with their facile removal from organic products can be expected to offer new opportunities in green applications of olefin metathesis.

Studies on the use of quaternary ammonium salt in water emulsions and IL are undergoing in our laboratories. We expect exciting results in this field in the future.

Acknowledgment

The authors are grateful to the Alexander von Humboldt Foundation for financial supportss, the State Committee of Scientific Research, and the Deutsche Forschungsgemeinschaft–Polish Academy of Sciences joint project "Synthetische Nutzung von immobilisierten Ruthenium-Carben-Katalysatoren in Durchflussmikroreaktoren" (436 POL 113/109/0-1).

References and Notes

[1] General reviews: (a) Schrock, R.R., Hoveyda, A.H., Angew. Chem. Int. Edit. 2003, 42:4592; (b) Trnka, T.M., Grubbs, R.H., Acc. Chem. Res. 2001, 34:18; (c) Fűrstner, A., Angew. Chem. Int. Edit. 2000, 39:3012; (d) Grubbs, R.H., Chang, S., Tetrahedron 1998, 54:4413; (e) Schuster, M., Blechert, S., Angew. Chem. Int. Edit. 1997, 36:2037; (f) Dragutan, V., Dragutan, I., Balaban, A.T., Platinum Met. Rev. 2001, 45:155.

[2] Nicola, T., Brenner, M., Donsbach, K., Kreye, P., Org. Process Res. Dev. 2005, 9:513.

[3] (a) Conrad, J.C., Parnas, H.H., Snelgrove, J.L., Fogg, D.E., J. Am. Chem. Soc. 2005, 127:11882; (b) For example, in a crude untreated product of diethyl diallylmalonate RCM catalyzed by 5 mol % of Grubbs I-generation catalyst the theoretical amount of Ru is 90 mg per 5 mg of product (18,000 ppm). After filtration of the crude reaction mixture, the Ru level was reduced to 59.7 ± 0.50 mg per 5mg (12,000 ppm). Further purification of such crude metathesis products usually reduces ruthenium levels below 2000 ppm, see ibid, and McEleney, K., Allen, D.P., Holliday, A.E., Crudden, C.M, Org. Lett. 2006, 8:2663.

[4] Another solution to this problem might be based on the immobilization of a metathesis catalysts in a separate liquid or solid phase. For recent reviews, see: (a) Hoveyda, A.H., Gillingham, D.G., Van Veldhuizen, J.J., Kataoka, O., Garber, S.B., Kingsbury, J.S., Harrity, J.P.A., Org. Biomol. Chem. 2004, 2:1; (b) Buchmeiser, R.M., New, J., Chem. 2004, 28:549. For related systems developed in our laboratories, see: (c) Grela, K., Mennecke, K., Kunz, U., Kirschning, A., Synlett 2005, 2948; (d) Grela, K., Tryznowki, M., Bieniek, M., Tetrahedron Lett. 2002, 43:6425.

[5] Boehringer Ingelheim International GmbH, World Pat. WO 2004/ 089974 A1, 2004.

[6] Paquette, L.A., Schloss, J.D., Efremov, I., Fabris, F., Gallou, F., Mendez-Andino, J., Yang, J., Org. Lett. 2000, 2:1259.

[7] Ahn, Y.M., Yang, K., Georg, G.I., Org. Lett. 2001, 3:1411.

[8] (a) Maynard, H., Grubbs, R.H., Tetrahedron Lett. 1999, 40:4137; (b) Westhus, M., Gonthier, E., Brohm, D., Breinbauer, R., Tetrahedron Lett. 2004, 45:3141.

[9] Cho, J.H., Kim, B.M., Org. Lett. 2003, 5:531.
[10] For a technical data sheet on the application of QuadraPure resins, see: Avecia Pharmaceuticals, http://www.quadrapure.com
[11] Complex **7**, introduced recently by our group, exhibits catalytic activity comparable to the parent Hoveyda–Grubbs carbene **4**, but shows much higher affinity for silica gel when CH_2Cl_2 is used as eluent, which enables its efficient removal. See: Grela, K., Kim, M., Eur. J. Org. Chem. 2003, 963.
[12] Michrowska, A., Gulajski, L., Grela, K., Chem. Commun. 2006, 841.
[13] Reviews on polymer-bound reagents and catalysts: (a) Solodenko, W., Frenzel, T., Kirschning, A., in: Buchmeiser, M.R., (ed.), Polymeric Materials in Organic Synthesis and Catalysis, Wiley-VCH, Weinheim, 2003, pp. 201; (b) Clapham, B., Reger, T.S., Janda, K.D., Tetrahedron 2001, 57:4637–4662; (c) Baxendale, I.R., Storer, R.I., Ley, S.V., in: Buchmeiser, M.R., (ed.), Polymeric Materials in Organic Synthesis and Catalysis, Wiley-VCH, Weinheim, 2003, pp. 53; (d) Kirschning, A., Monenschein, H., Wittenberg, R., Angew. Chem., Int. Edit. 2001, 40:650; (e) Ley, S.V., Baxendale, I.R., Bream, R.N., Jackson, P.S., Leach, A.G., Longbottom, D.A., Nesi, M., Scott, J.S., Storer, R.I., Taylor, S.J., J. Chem. Soc., Perkin Trans. 2000, 1:3815; (f) Drewry, D.H., Coe, D.M., Poon, S., Med. Res. Rev. 1999, 19:97.
[14] Reviews: (a) Kingsbury, J.S., Hoveyda, A.H., in: Buchmeiser, M.R., (ed.), Polymeric Materials in Organic Synthesis and Catalysis, Wiley-VCH, Weinheim, 2003, p. 467; (b) see [Ref. 4b].
[15] (a) Kingsbury, J.S., Harrity, J.P.A., Bonitatebus, P.J., Hoveyda, A.H., J. Am. Chem. Soc. 1999, 121:791; (b) Garber, S.B., Kingsbury, J.S., Gray, B.L., Hoveyda, A.H., J. Am. Chem. Soc. 2000, 122:8168.
[16] (a) For a short review, see Hoveyda, A.H., Gillingham, D.G., Van Veldhuizen, J.J., Kataoka, O., Garber, S.B., Kingsbury, J.S., Harrity, J.P.A., Org. Biomol. Chem. 2004, 2:1.
[17] For syntheses of supported variants of **3**–**4**, see inter alia: (a) Kingsbury, J.S., Garber, S.B., Giftos, J.M., Gray, B.L., Okamoto, M.M., Farrer, R.A., Fourkas, J.T., Hoveyda, A.H., Angew. Chem., Int. Edit. 2001, 40:4251; (b) see [Ref. 4d]; (c) Connon, S.J., Dunne, A.M., Blechert, S., Angew. Chem. Int. Edit. 2002, 41:3835; (d) Dowden, J., Savovic, J. Chem. Commun. 2001, 37; (e) Yao, Q., Angew. Chem., Int. Edit. 2000, 39:3896; (f) Yao, Q., Zhang, Y., Angew. Chem., Int. Edit. 2003, 42:3395; (g) Connon, S.J., Blechert, S., Bioorg. Med. Chem. Lett. 2002, 12:1873; (h) Yao, Q., Zhang, Y., J. Am. Chem. Soc. 2004, 12:74; (i) Yao, Q., Motta, A.R., Tetrahedron Lett. 2004, 45:2447; (j) Yang, L., Mayr, M., Wurst, K., Buchmeiser M.R., Chem. Eur. J. 2004, 10:5761; (k) Krause, J.O., Nuyken, O., Wurst, K., Buchmeiser, M.R., Chem. Eur. J. 2004, 10:777; (l) Krause, J.O., Zarka, M.T., Anders, U., Weberskirch, R., Nuyken, O., Buchmeiser, M.R., Angew. Chem. Int. Edit. 2003, 42:5965; (m) Audic, N., Clavier, H., Mauduit, M., Guillemin, J.C., J. Am. Chem. Soc. 2003, 125:9248; (n) Clavier, H., Audic, N., Mauduit, M., Guillemin, J.C.G., Chem. Commun. 2004, 282.
[18] (a) Kirschning, A., Jas, G., Top. Curr. Chem. 2004, 242:209. (b) Jas, G., Kirschning, A., Chem. Eur. J. 2003, 9:5708. (c) Fletcher, P.D.I., Haswell, S.J., Pombo-Villar, E., Warrington, B.H., Watts, P., Wong, S.Y., Zhang, X.,

Tetrahedron 2002, 58:4735; (d) Kirschning, A., Solodenko, W., Mennecke, K., Chem. Eur. J. 2006, 12:5972.

[19] Kunz, U., Leue, S., Stuhlmann, F., Sourkouni-Argirusi, G., Wen, H., Jas, G., Kirschning, A., Eur. J. Org. Chem. 2004, 3601.

[20] Grela, K., Harutyunyan, S., Michrowska, A., Angew. Chem. Int. Edit. 2002, 41:4038.

[21] Michrowska, A., Bujok, R., Harutyunyan, S., Sashuk, V., Dolgonos, G., Grela, K., J. Am. Chem. Soc.1. 2004, 126:9318.

[22] Grela, K., Harutyunyan, S., Michrowska, A., in: Roberts, S.M., Whittall, J., Mather, P., McCormack, P., (eds), Catalysts for Fine Chemical Synthesis, Vol. 3, Wiley Interscience, New York, 2004, Chap. 9.1, pp. 169.

[23] Bujok, R., Bieniek, M., Masnyk, M., Michrowska, A., Sarosiek, A., Stępowska, H., Arlt, D., Grela, K., J. Org. Chem. 2004, 69:6894.

[24] (–)-Securinine: Honda, T., Namiki, H., Kaneda, K., Mizutani, H., Org. Lett. 2004, 6:87.

[25] (+)-Viroallosecurinine: Honda, T., Namiki, H., Watanabe, M., Mizutani, H., Tetrahedron Lett. 2004, 45:5211.

[26] An artificial photosynthesis model: Ostrowski, S., Mikus, A., Mol. Diversity 2003, 6:315.

[27] For a recent application of **6a** in synthesis of hepatitis C antiviral agent, BILN 2061, see: WO 2004/089974 A1, Boehringer Ingelheim International GmbH, 2004.

[28] Nicola, T., Brenner, M., Donsbach, K., Kreye, P., Org. Proc. Res. Devel. 2005, 9:513.

[29] A sample of **8** was stored in air (+4°C) for 3 years and after that time TLC analysis showed only minute decomposition. Simply passing out this sample through a Pasteur pipette with silica gel afforded 80% of the regenerated catalyst in analytically pure form.

[30] Addition of HBF_4 (0.025 equiv) to the mixture of **8** (0.025 equiv) and **10** (1 equiv) in CH_2Cl_2 caused instant color change of the solution from bright green to deep purple, however, no RCM reaction was observed. This suggests that very fast decomposition of **8** occurred after addition of such strong Brønsted acid.

[31] Michrowska, A., MSc thesis, Department of Organic Chemistry, Warsaw University of Technology, Warsaw, Poland, 2003.

[32] For an example of a catalytically active ruthenium allenylidene complex bearing a Me_2N group, see Fürstner, A., Liebl, M., Lehmann, C., Piquet, M., Kunz, R., Bruneau, C., Touchard, D., Dixneuf, P.H., Chem. Eur. J. 2000, 6:1847.

[33] Kingsbury, J.S., Garber, S.B., Giftos, J.M., Gray, B.L., Okamoto, M.M., Farrer, R.A., Fourkas, J.T., Hoveyda, A.H., Angew. Chem. Int. Edit. 2001, 40:4251.

[34] Mayr, M., Wang, D., Kröll, R., Schuler, N., Prühs, S., Fürstner, A., Buchmeiser, M.R., Adv. Synth. Catal. 2005, 347:484.

[35] Michrowska, A., Mennecke, K., Kunz, U., Kirschning, A., Grela, K., J. Am. Chem. Soc. 2006, 128:13261.

[36] For high-throughput experiments the Radleys 12 Place Heated Carousel Reaction Station (www.radleys.com) was used.

[37] Interestingly, in the case of Grubbs catalyst immobilized on polyvinyl pyridine, exclusive C–C double bond isomerization instead of CM was observed for this substrate: [Ref. 48].

[38] Chen, G.W., Kirschning, A., Chem. Eur. J. 2002, 8:2717.

[39] Love, J.A., Morgan, J.P., Truka, T.M., Grubbs, R.H., Angew. Chem. Int. Edit. 2002, 41:4035.

[40] For selected applications of 5, see inter alia: (a) Kanemitsu, T., Seeberger, P.H., Org. Lett. 2003, 5:4541; (b) Rai, A.N., Basu, A., Org. Lett. 2004, 6:2861; (c) Aggarwal, V.K., Astle, C.J., Rogers-Evans, M., Org. Lett. 2004, 6:1469; (d) Kulkarni, A.A., Diver, S.T., Org. Lett. 2003, 5:3463; (e) Giessert, A.J., Brazis, N.J., Diver, S.T., Org. Lett. 2003, 5:3819; (f) Chen, B., Sleima, H.F., Macromolecules 2004, 37:5866; (g) Rezvani, A., Bazzi, H.S., Chen, B., Rakotondradany, F., Sleiman, H.F., Inorg. Chem. 2004, 43:5112; (h) Schuehler, D.E., Williams, J.E., Sponsler, M.B., Macromolecules 2004, 37:6255; (i) Parrish, B., Emrick, T., Macromolecules 2004, 37:5863; (j) Hansen, E.C., Lee, D., Org. Lett. 2004, 6:2035.

[41] Indeed, this idea has been shown to be powerful for the immobilization of enzymes using nickel NTA-linkers on sepharose for coordinatively trapping enzymes tagged with a His-tag.

[42] Recently, Grubbs and coworkers were able to isolate a ruthenium–hydrido complex, formed as a thermal degradation product of catalyst **2** which could be made responsible for double bond migration: Hong, S.H., Day, M.W., Grubbs, R.H., J. Am. Chem. Soc. 2004, 126:7414.

[43] For Grubbs-type ruthenium alkylidenes bearing a quarternary ammonium group, see: Lynn, D.M., Mohr, B., Grubbs, R.H., Henling, L.M., Day, M.W., J. Am. Chem. Soc. 2000, 122:6601.

[44] Michrowska, A., Gułajski, Ł., Kaczmarska, Z., Mennecke, K., Kirschning, A., Grela, K., Green Chem. 2006, 685.

[45] For a review on supported variants of 4, see: (a) Garber, S.B., Kingsbury, J.S., Gray, B.L., Hoveyda, A.H., J. Am. Chem. Soc. 2000, 122:8168; (b) See [Ref. 4b].

[46] Wasserscheid, P., Welton, T., Ionic Liquids in Synthesis, 1 edn., Wiley-VHC, Weinheim, 2003.

[47] For recent reviews on ionic liquids, see: (a) Welton, T., Chem. Rev. 1999, 99:2071; (b) Holbrey, J.D., Seddon, K.R., Clean Prod. Process. 1999, 1:223; (c) Sheldon, R., Chem. Commun. 2001, 2399; (d) Olivier-Bourgbigou, H., Mogna, L., J. Mol. Catal. A: Chem. 2002, 182–183, 419; (e) Wasserscheid, P., Keim, W., Angew. Chem. Int. Edit. 2000, 39:3772; (f) Dupont, J., De Souza, R.F., Suarez, P.A., Chem. Rev. 2002, 102:3667; (g) Jain, N., Kumar, A., Chauhan, S., Chauban, S.M.S., Tetrahedron 2005, 55:1015.

[48] (a) Clavier; H., Audic, N., Mauduit, M., Guillemin, J.C., Chem. Commun. 2004, 2282; (b) Clavier, H., Audic, N., Mauduit, M., Guillemin, J.C., J. Organomet. Chem. 2005, 690:3585; (c) Yao. Q.J., J. Organomet. Chem. 2005, 690:3577.

[49] Rix, D., Clavier, H., Coutard, Y., Gulajski, L., Grela, K., Mauduita, M., J. Organomet. Chem., 2006, 691:5397.

RING-OPENING METATHESIS ACTIVITY OF RUTHENIUM-BASED OLEFIN METATHESIS CATALYST COORDINATED WITH 1,3-BIS(2,6-DIISOPROPYLPHENYL)-4,5-DIHYDROIMIDAZOLINE

SOLMAZ KARABULUT[1], FRANCIS VERPOORT[2]

[1]*Hacettepe University, Department of Chemistry, 06800 Beytepe, Ankara, Turkey*
[2]*Department of Inorganic and Physical Chemistry, Division of Organometallic Chemistry and Catalysis, Ghent University, Krijgslaan 281 (S-3), 9000 Ghent, Belgium*

Abstract: A 1,3-bis-(2,6-diisopropylphenyl)-4,5-dihydroimidazol-2-ylidene substituted ruthenium (Ru)-based complex **(4)** has been prepared starting from $(PCy_3)_2(Cl)_2Ru{=}CHPh$ **(2)**. The catalytic performance of catalyst **(4)** is checked on ring-opening metathesis polymerization (ROMP) of the low strain monomer, cycloocta-1,5-diene (COD), and also compared with catalyst **(2)** and **(3)**.

Keywords: ruthenium; *N*-heterocyclic carbene (NHC) ligands, ring opening metathesis, cyclooctadiene

1. Introduction

The advent of well-defined catalysts for olefin metathesis has revolutionized in organic synthesis and polymer chemistry in the last few years [1]. Many catalyst systems are active in olefin metathesis [2], but most of them are ill-defined, multicomponent mixtures consisting of transition-metal compounds, cocatalysts, and promoters [3]. Recently, well-defined single-component metal carbene complexes have been utilized as catalyst precursors in olefin metathesis. Among these systems, well-characterized tungsten, molybdenum, and ruthenium alkylidene complexes have been prepared. Schrock developed tungsten- and molybdenum-based catalysts that have proven to be very active. The most recognized and most impressive one is the catalyst with general formula $Mo(CHR)(NAr)(OR)_2$, also known as the Schrock catalyst **(1)** [4]. This catalyst exhibits the higher reactivity of the two toward a broad range of substrates with many steric or electronic variations; however, it also suffers from extreme sensitivity to air and moisture as well as decomposition upon storage. The synthesis of relatively stable ruthenium (Ru)-based alkylidene complexes was introduced by Grubbs and has been improved [5]. The Grubbs first generation catalyst $(PCy_3)_2(Cl)_2Ru{=}CHPh$ **(2)** shows a good reactivity towards olefins in the presence of functional groups but is less active than the Schrock catalyst [6]. Recently, a new family of ruthenium-based

Y. İmamoğlu and V. Dragutan (eds.), Metathesis Chemistry: From Nanostructure Design to Synthesis of Advanced Materials, 185-192.

olefin metathesis catalysts such as catalyst **(3)** have been prepared by the substitution of a single PCy_3 ligand of **(2)** with a *N*-heterocyclic carbene (NHC). These new alkylidenes not only exhibit high reactivity in a variety of olefin metathesis reactions but also are highly tolerant of many different organic functional groups [7]. Although catalyst **(2)** and **(3)** are powerful tools in organic synthetic strategies, the relatively high cost of Ru, coupled with the relatively high catalyst loading generally employed, render these systems disadvantageous for use in large-scale reactions.

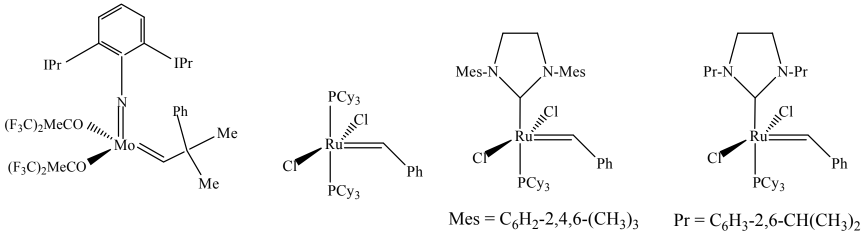

(1) (2) (3) (4)

Scheme 1

While these points are especially pertinent for potential industrial applications for these catalysts, they are also relevant when relatively inexpensive substrates are to be reacted. Mol and coworkers reported improved turnovers during the cross-metathesis (CM) of terminal olefins with a modified version of the imidazolylidene ligand, catalyst $(IPrH_2)(PCy_3)(Cl)_2Ru{=}CHPh$ **(4)**, first synthesized by Fürstner [9,10]. Also, Wagener and coworkers reported the activity of catalyst **(4)** against other catalysts for CM, ADMET, and RCM [11–13]. In this study, synthesis and characterization of catalyst **(4)** is reported. The catalytic performance of catalyst **(4)** is checked on ring-opening metathesis polymerization (ROMP) of the less strained 1,5-cyclooctadiene (COD). Yet, there is no report on $(IPrH_2)(PCy_3)(Cl)_2Ru{=}CHPh$ **(4)** as a catalyst for the ROMP of cycloolefins.

2. Experimental

2.1 General remarks

All syntheses were performed under inert atmospheres of argon on a vacuum line using standard Schlenk tube techniques. Liquids were transferred by syringe and introduced into the Schlenk flasks through rubber septa or through a stopcock under positive argon pressure while air- and/or moisture-sensitive solids were transferred using a glove bag. Solvents were dried, distilled and degassed under argon prior to use. The catalyst $(PCy_3)_2(Cl)_2Ru{=}CHPh$ **(2)** was prepared according to literature. Potassium tert-butoxide (KOtBu) and potassium hexamethyldisilazide (KHMDS) (Aldrich) were used as received. COD was dried over CaH_2, distilled and degassed by three standard freeze-pump-thaw cycles. NMR spectra were recorded with a Varian Unity-300 spectrometer, chemical shifts were recorded in parts per million (δ) and referenced to TMS.

2.2 Catalyst preparation

The carbene ligands 1,3-bis-(2,4,6-trimethylphenyl)-4-5-dihydroimidazolium chloride (H_2IMes), 1,3-bis-(2,6-diisopropylphenyl)-4-5-dihydroimidazolium chloride (H_2IPr) were prepared according to literature procedure [14].

2.2.1 Synthesis of (IMesH$_2$)(PCy$_3$)(Cl)$_2$Ru=CHPh (3)

A flame-dried Schlenk flask was charged with 1.32 g (1.60 mmol) of **(2)**, 0.658 g (19.20 mmol) of (H_2IMes), and 3.84 mL of a 0.5 M sol. KHMDS in toluene. This initially purple, turbid reaction mixture was stirred for 1 h at ambient temperature, during which time the solution turned dark red. After evaporation of solvent the residue was stirred in methanol and filtered resulting in clean pinkish complex **(3)** in good yield (94%).

2.2.2 Synthesis of (IPrH$_2$)(PCy$_3$)(Cl)$_2$Ru=CHPh (4)

A solution of 0.176 g potassium *tert*-butoxide (KOtBu, 1.57 mmol) in 15 mL THF was slowly added under Ar atmosphere at room temperature to a solution of 0.904 g 1,3-bis-(2,6-diisopropylphenyl)-4-5-dihydroimidazolium chloride (H_2IPr, 2.12 mmol) in 15 mL THF. The suspension was stirred at room temperature for 15 min and added to a solution of 0.5 g compound $(PCy_3)_2(Cl)_2$Ru=CHPh **(2)** (0.61 mmol) in 30 mL toluene. The mixture was stirred for 30 min. at 80°C under Ar atmosphere. The solvent was then removed in vacuo, and residue was washed with methanol (2 × 10 mL). The brown suspension was filtered and finally dried under Ar to afford a pinkish powder in (85%) yield. The solid precipitate was analyzed using ^1H and ^{13}C NMR. ^1H NMR ($CDCl_3$, 300 MHz): δ = 19.40; 7.94; 7.35-7.05; 7.04; 6.76; 4.14; 4.07–3.87; 3.54; 2.18–2.00; 1.50–1.37; 1.49; 1.37; 1.35–1.30; 1.21; 1.11; 0.95. ^{13}C NMR ($CDCl_3$, 300 MHz): δ = 296.63; 222.45; 151.53; 149.89; 147.35; 138.54; 136.37; 131.90; 130.56; 129.43; 124.87; 124.34; 55.21; 32.46; 32.34; 29.89; 29.76; 28.45; 28.36; 28.28; 27.86; 27.13; 26.82; 24.23; 24.14.

2.3 Activity studies

Small oven-dried glass vials with septum were charged with a stir bar and the appropriate amounts of catalyst (taken from a CH_2Cl_2 stock solution). The dichloromethane was subsequently evaporated, and the glass vials with solid catalyst were kept under argon atmosphere. To start the ROMP test, 200 μL of toluene was added in order to dissolve the catalyst. The COD was then transferred to the vial containing the catalyst via syringe under vigorous stirring at room temperature. After a certain time span, a small quantity of the reaction mixture, which had become viscous, was taken out of the vial and solved in $CDCl_3$. The yield could then easily be determined by ^1H NMR spectroscopy.

3. Results and discussion

For the synthesis of the catalysts **(3)** and **(4)** we first tried to exchange the phosphine with the imidazole ligand (H_2IMes and H_2IPr) from the first-generation Grubbs' parent catalyst **(2)** using the more steric base potassium hexamethyldisilazide (KHMDS). Synthesis of **(3)** could then be achieved following the well established in situ generation of the free carbene using KOtBu [8]. In addition we found it possible and less time and energy (at ambient temperature) consuming to obtain complex **(3)** in a one-pot synthesis by employing the KHMDS. Surprisingly all of our attempts for synthesis of **(4)** using KHMDS were unsuccessful and the best results were mixtures of **(2)** (25%) and small amounts of **(4)** (75%) with considerable destruction of Ru–carbene during the synthesis. The catalyst **(4)** has been synthesized and characterized by Fürstner and coworkers [9]. But its catalytic activity has not been reported in this study because of the fact that this catalyst has had some dihydride complex $(PCy_3)_2Ru(H)_2(Cl)_2$ as a by-product. We have successfully optimized Fürstner's procedure and synthesized, isolated this catalyst from the crude reaction residue following procedure (Scheme 2). The NMR spectra of obtained catalyst **(4)** in this study is consistent with the literature [9, 10].

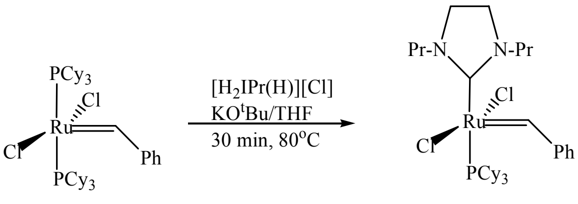

(2) **(4)**

Scheme 2

COD, a typical low-strained olefin, was polymerized at room temperature with the catalyst system **(4)**. The polymerization process is illustrated in Scheme 3.

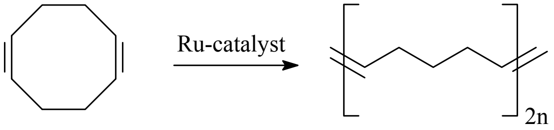

Scheme 3

The polymerization reaction was monitored as a function of time at ambient temperature by integrating olefinic ^1H signals of the formed polymer and the disappearing monomer. As shown in Figure 1, this made it possible to compare catalytic activities of the various olefin metathesis initiating systems. The well-known Grubbs' catalysts **(2)** and **(3)** show logical ROMP-activities (Figure 1). The catalyst **(3)** is typified by a slower initiation compared to **(2)** but shows a higher overall activity. The catalyst **(4)** is clearly very active and reaches full conversion slowly. At room temperature, catalyst **(2)** gives a maximum yield 61%. The second-generation catalysts, in particular **(4)**, performed significantly better. The catalyst **(3)** gave an optimal yield 94%, while the yield achieved with catalyst **(4)** achieved 100%. The reason for the appreciably higher yield of the catalyst **(4)** relative to **(3)** is not entirely clear, but could conceivably be attributed to a faster initiation rate due to the increased steric bulk of the $IPrH_2$ ligand relative to $IMesH_2$. This confirms that generally replacement of one of the two phosphine ligands with a more electron donating NHC ligand substantially improves metathesis activity. Insertion of an NHC-ligand leads to greater electron density at the metal centre as a consequence of strong σ-donation coupled with a reduced π-back bonding. In addition the significant increase in steric effect of $IPrH_2$ relative to $IMesH_2$, together with its superior electron donating properties relative to unsaturated analague, IPr [15] might give rise to a highly active metathesis initiator [16,17]. This results in a greater preference for olefin binding and thereupon higher metathesis activity.

For a quantitative estimation of polymer yield, a series of polymerizations were carried out by varying the catalyst/monomer ratio. Under these experimental conditions, the polymerization of COD is monitored in Table1. At first a set of experiments was performed by varying catalyst/monomer ratio 1/300 and 1/30000.

Conversion to polymer was obtained in maximum yield when the catalyst/monomer ratio was 1/300 and 1/3000. The dependence of the catalyst/monomer ratio on the polymerization yield was analyzed. The polymerization yield increases with catalyst/monomer ratio and the yield after 24 h reaches 90% when the catalyst/monomer ratio is 1/300.

Table 1. Ring-opening metathesis polymerization of COD with catalyst (4)

Entry	catalyst/monomer	time (s)	Yield (%)
1	1/300	1800	100
2	1/3000	1800	100
3	1/10 000	1800	57
			63
		3600	68
		overnight	
4	1/30 000	3600	42
		overnight	49

General reaction conditions: Ar atmosphere, room temperature, toluene as solvent, yield determined by ^{1}H NMR spectroscopy. Catalyst = **(4)**

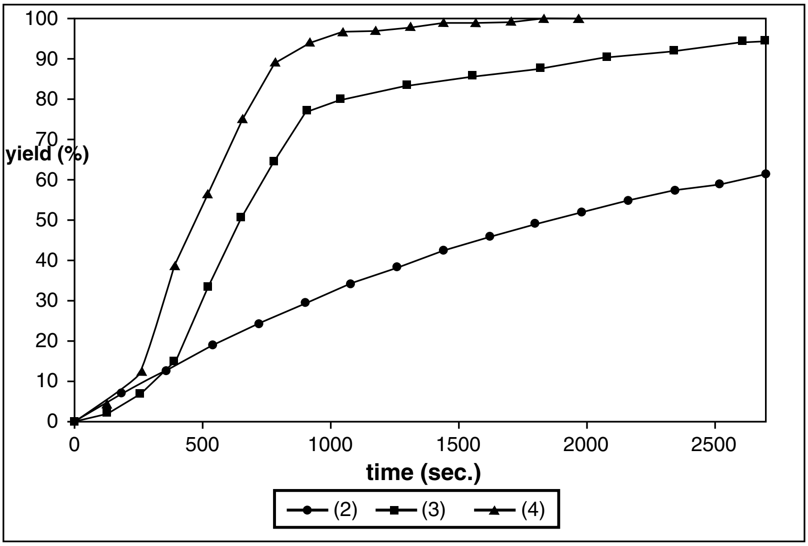

Figure 1. Ring-opening metathesis polymerization of COD with catalyst **(4)** (Reaction conditions: catalyst/monomer = 1/300, room temperature, toluen).

4. Conclusion

We have shown that the 1,3-bis-(2,6-diisopropylphenyl)-4,5-dihydroimidazol-2-ylidene substituted Ru-based complex **(4)** are active catalyst precursor in the ROMP of COD. This air and water tolerant complex was shown to exhibit higher ROMP activity compared to that of the parent complex **(2)** and previously developed complex **(3)**. In the future, we aim to further broaden the scope of this catalyst, to prepare a variety of Schiff base-substituted complexes of **(4)**.

Acknowledgments

S. Karabulut would like to express thanks to Professor Francis Verpoort (Ghent University) for his invaluable help, professional advice and support throughout this study. He also gratefully acknowledges the Turkish Scientific and Technical Research Council and NATO for a research grant (TUBITAK-BAYG NATO-A2).

References

[1] Grubbs, R.H. (ed.), Handbook of Metathesis, Wiley-VCH, Weinheim, 2003.

[2] (a) Ivin, K.J., Mol, J.C., Olefin Metathesis and Metathesis Polymerization, Academic Press, London, 1997; (b) Schrock, R.R., J. Organometallic Chem. 2003, 684:56–67; (c) Schrock, R.R. Jamieson, J.Y., Araujo, J.P., Bonitatebus, P.J., Sinha, A., Lopez, L.P.H., J. Mol. Catal. A: Chem. 2004, 213:21–30; (d) Trnka, T.M., Grubbs, R.H., Acc. Chem. Res. 2001, 34:18; (e) Grubbs, R.H., Chang, S., Tetrahedron 1998, 54:4413; (f) Furstner, A., Angew. Chem. Int. Edit. 2000, 39:3012–3043; (g) Opstal, T., Verpoort, F., Angew. Chem. Int. Edit. 2003, 42:2876; (h) Dieltiens, N., Stevens, C.V., De Vos, D., Allaert, B., Drozdzak, R., Verpoort F., Tetrahedron Lett. 2004, 45:8995–8998.

[3] Ivin, K.J., Mol., J.C., Catal. A: Chem. 1998, 133:1–16.

[4] Schrock, R.R., Murdzek, J.S., Bazan, G.C., Robbins, J., Dimare, M., O'Regan, M.J., Am. Chem. Soc.1990, 112:3875.

[5] Warwel S., Seikermann V., Macromol. Chem. Rapid Commun. 1983, 4:423.

[6] Nguyen, S.T, Johnson, L.K., Grubbs, R.H., J. Am. Chem. Soc. 1992, 114: 3974–3975.

[7] Schwab, P., France, M.B., Ziller, J.W., Grubbs, R.H., Angew. Chem. Int. Edit. 1995, 34:2039.

[8] Fu, G.C., Nguyen, S.T, Grubbs, R.H., J. Am. Chem. Soc. 1993, 115:9856–9857.

[9] Früstner, A., Ackermann, L., Gabor, B., Goddard, R., Lehmann, C.W., Mynott, R., Stelzer, F., Theil, O.R., Chem. Eur. J., 2001, 7:3236–3253.

[10] Dinger, B.D., Mol J.C., Adv. Synt. Catal. 2002, 344:671–677.

[11] Courchay, F.C., Sworen, J.C., Wagener, K.B., Polym. Prepr. 2003, 44:940.

[12] Courchay, F.C., Sworen, J.C., Wagener, K.B., Macromolecules 2003, 36:8231–8239.

[13] Oakley, G.W., Wagener, K.B., Macromol. Chem. Phys. 2005, 206:15–24.

[14] Arduengo, A.J., Krafczyk, R., Schmutzler, R., Tetrahedron 1999, 55:14523–14534.

[15] Scholl, M.C.W., Lee, R.H., Grubbs, Org. Lett. 1999, 1:953–956.

[16] Jafarpour, L., Stevens, E.D., Nolan S.P., J. Organometal. Chem. 2000, 606:49–54.

[17] Sanford, M.S., Love, J.A., Grubbs, R.H., J. Am. Chem. Soc. 2001, 123: 6543–6554.

PART II. INTRICATE ORGANIC SYNTHESIS VIA METATHESIS CHEMISTRY

RECENT APPLICATIONS OF ALKENE METATHESIS FOR FINE CHEMICAL AND SUPRAMOLECULAR SYSTEM SYNTHESIS

FRANC POŽGAN, PIERRE H. DIXNEUF*

Laboratory "Catalyse et Organométalliques", Institut Sciences Chimiques de Rennes, UMR 6226: CNRS-University of Rennes, Campus de Beaulieu, Av. Général Leclerc, 35042 RENNES, France. E-mail: Pierre.dixneuf@univ-rennes1.fr

Abstract: Alkene metathesis has become a synthetic method that has strongly modified approaches in the building of complex molecules. The review will concentrate on the recent applications of ring-closing metathesis (RCM) and cross-metathesis (CM) reactions for the design of useful molecules and architectures: new functional macrocycles (RCM) and multifunctional linear alkenes (CM), but also cyclic ligands, rotaxanes, catenanes, and supramolecular systems.

Keywords: alkene metathesis, ruthenium catalysts, macrocycles, supramolecular systems, cross-metathesis

Ac, acetyl; Ar^F, 3,5-bis(trifluoromethyl)phenyl; Boc, *tert*-butoxycarbonyl; Bn, benzyl; cat, catalyst; *t*-Bu, *tert*-butyl; Cbz, benzyloxycarbonyl; Cy, cyclohexyl; Mes, 2,4,6-trimethylphenyl; Fmoc, 9-fluorenylmethoxycarbonyl; MOM, methoxymethyl; Piv, pivaloyl; *i*-Pr, isopropyl; TBAF, tetrabutylammonium fluoride; TBDPS, *tert*-butyldiphenylsilyl; Tf, triflyl; Tfa, trifluoroacetyl; Tos, tosyl

1. Introduction

Alkene metathesis is a catalytic reaction that has brought revolutions during the last 15 years, not only in catalysis and organic synthesis but also in polymer and material science. This is due to the discovery of the catalytic mechanism based on metal–carbene by Chauvin [1] and of well-defined, efficient catalysts from 1990 based on coordinatively unsaturated alkylidene–metal complexes mainly derivatives of molybdenum by Schrock [2] and of ruthenium (Ru) by Grubbs [3]. The increasing importance of alkene metathesis and its catalysts by the scientific community has led to the award of 2005 chemistry Nobel Prize to the main pioneers in this field, Chauvin, Grubbs, and Schrock [1–3].

Y. İmamoğlu and V. Dragutan (eds.), Metathesis Chemistry: From Nanostructure Design to Synthesis of Advanced Materials, 195-222.

Alkene metathesis has become one of the best tools to make carbon–carbon bond affording a large variety of functional macrocycles via ring-closing metathesis (RCM) [4], but also introducing functional groups in alkenes via cross-metathesis (CM) [5]. Such a way to make C–C bonds alkene metathesis is often preferred to nucleophilic substitutions, requiring protections and deprotections of functional groups, and even to catalytic cross-coupling reactions. In material science the control of ring-opening metathesis polymerization (ROMP) [6] and acyclic diene metathesis (ADMET) [7] polymerization has led to the production of a variety of new functional polymers and of recoverable catalysts.

During the last 10 years several reviews have, step by step, shown the development of alkene metathesis [4–8].

The objective of this review is to show some recent examples of alkene metathesis, not covered by the above reviews, used for the production of fine chemicals, ligands, rotaxanes, catenanes, and supramolecular systems mainly via RCM and CM reactions performed with Ru catalysts that tolerate functional groups.

The most commonly used Ru catalysts are described in Scheme 1, the Grubbs first-generation catalyst **1** [9], the Nolan **2** [10], and Grubbs second-generation catalyst **3** [11], the Hoveyda catalyst **4** [12], the phosphine-free Hoveyda catalyst **5** [13], the allenylidene precursor **6** [14] leading to active indenylidene catalyst **7** [15], and the indenylidene complex **8** [16].

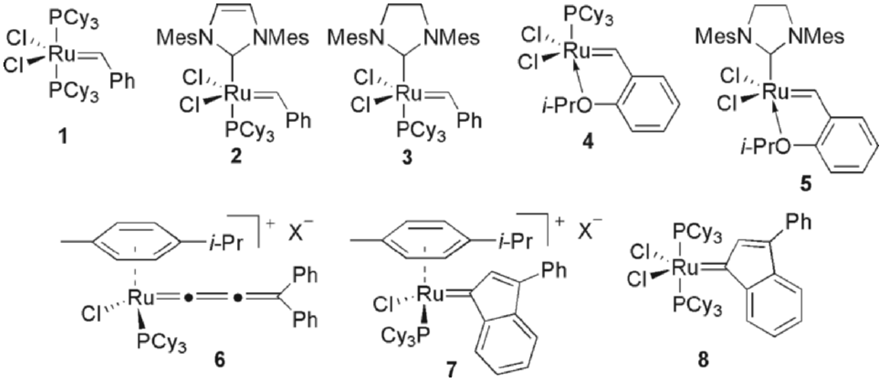

Scheme 1. Ruthenium–alkylidene complexes as catalyst precursors for alkene metathesis.

The following aspects will be discussed.

- Synthesis of new macrocycles via RCM reaction
- RCM in the synthesis of new ligands, rotaxanes, catenanes, and supramolecular systems
- CM in synthesis and supramolecular system formation

2. Synthesis of new macrocycles via RCM reaction

2.1 A diversity of examples

In order to produce functional macrocycles the RCM, using the efficient Grubbs catalysts and related catalysts, is a method of choice as these catalysts tolerate a large number of functional groups.

A variety of macrocyclic crown diamides **9** have been produced with the first-generation Grubbs catalyst **1** from dienes readily obtained by allylation of salicylamides (Scheme 2) [17]. This strategy was also used for the synthesis of BINOL derivatives [18].

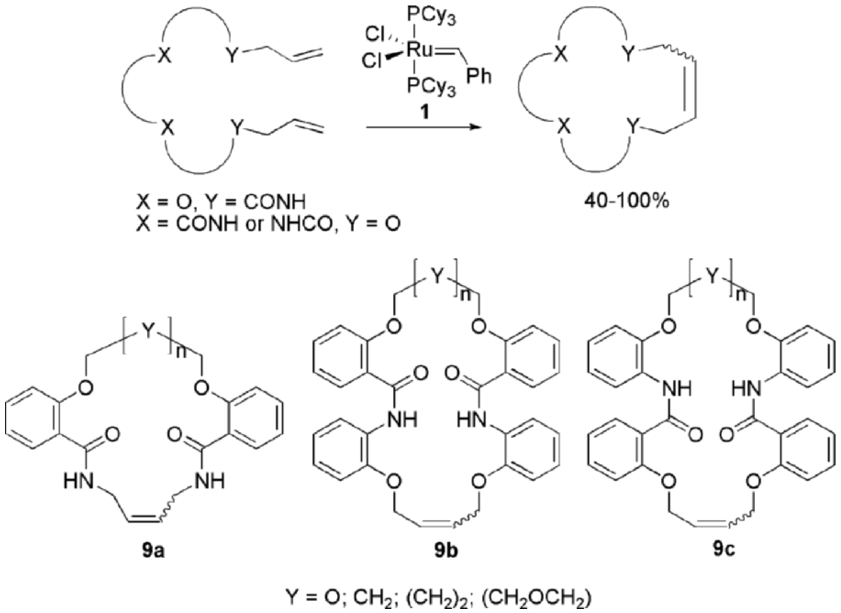

Scheme 2. Macrocyclic crown diamides obtained via RCM.

The RCM reaction is now currently used to improve the synthesis of known drugs and create new ones. This is the case of the synthesis of resorcinylic macrocycles with lactone or lactam functionality (Scheme 3) [19]. Thus, the dienes **10** are transformed with catalyst **1** (CH_2Cl_2, reflux) into **11** and the hydrogenation of the cyclized products (Pd/C) affords quantitatively the hydrogenated and deprotected macrocycles **12**.

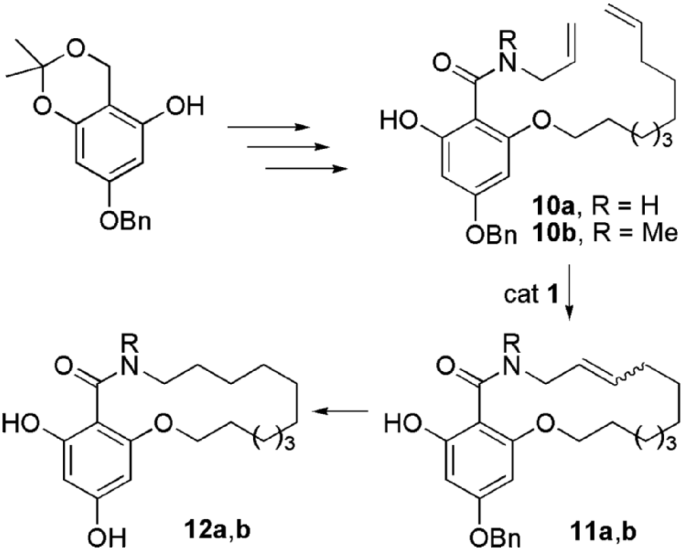

Scheme 3. Synthesis of resorcinylic macrocycles.

Another example is the synthesis of (–)-microcarpalide **15** that was generated by RCM reaction of **13** with **1** (CH_2Cl_2, reflux), followed by deprotection of the hydroxy groups with $TiCl_4$ (Scheme 4) [20].

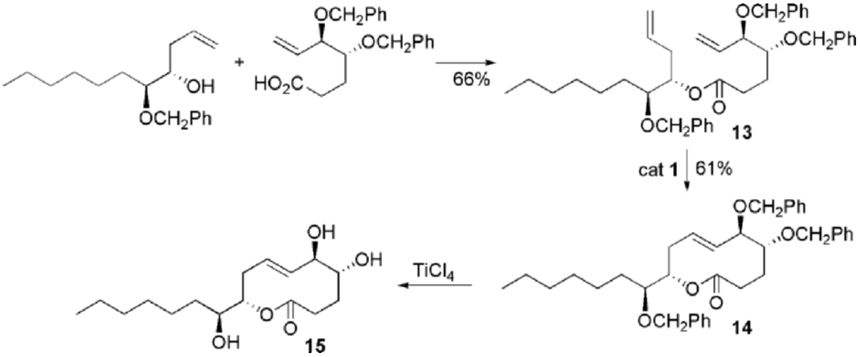

Scheme 4. Synthesis of (–)-microcarpalide **15** via RCM reaction.

The tolerance of Grubbs catalyst **1** for carbonates in spite of Ru Lewis acidity has been used by Grela to produce macrocyclic carbonates, analogous of musks [21]. Thus, the carbonate **16** with terminal olefinic branches led with **1** to the macrocyclic carbonate isomers **17** (5:1) in 80%

yield (Scheme 5). It is noteworthy that *N*-heterocyclic carbene (NHC)-containing catalysts such as **3** and **5** are not so active for carbonate-containing macrocycle synthesis.

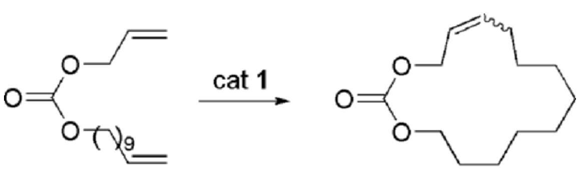

16 **17**

Scheme 5. Formation of cyclic carbonates.

Medium size macrocycles were made by two successive RCM reactions, followed by a ring expansion resulting from an opening of N–N bond. Thus, the macrocycle **18** was produced by classical RCM with catalyst **3** and was transformed into a second diene **19** according to scheme 6 [22]. A second RCM reaction with catalyst **3** followed by opening of N–N bond led to the macrocycle **20**.

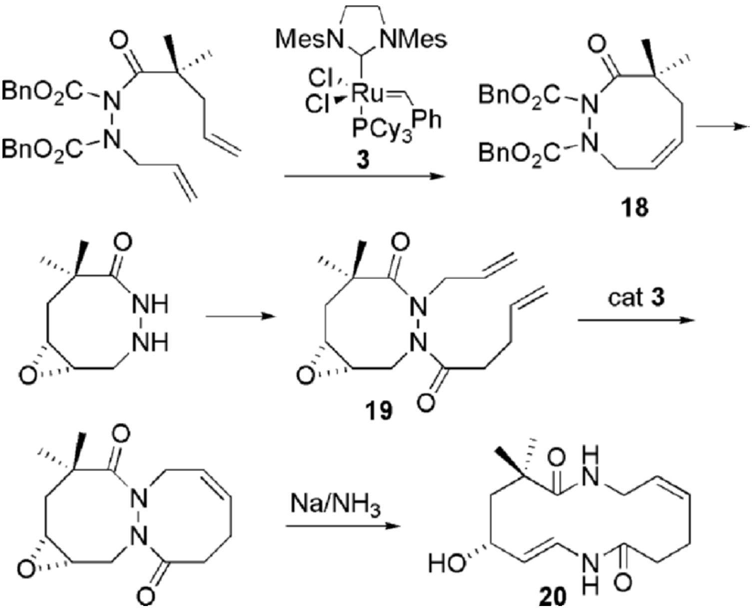

Scheme 6. Medium size macrocycle synthesis via successive RCM reactions.

The Ru–allenylidene complexes **6** have been revealed as early as 1998 as alkene metathesis catalyst precursors [14]. Since then it has been demonstrated that they become a catalyst by intramolecular rearrangement into an indenylidene–Ru intermediate **7** [15]. Catalyst precursor **6** (X = OTf) has been used for a variety of applications [23] and especially for the formation of macrocycles (Scheme 7) [24].

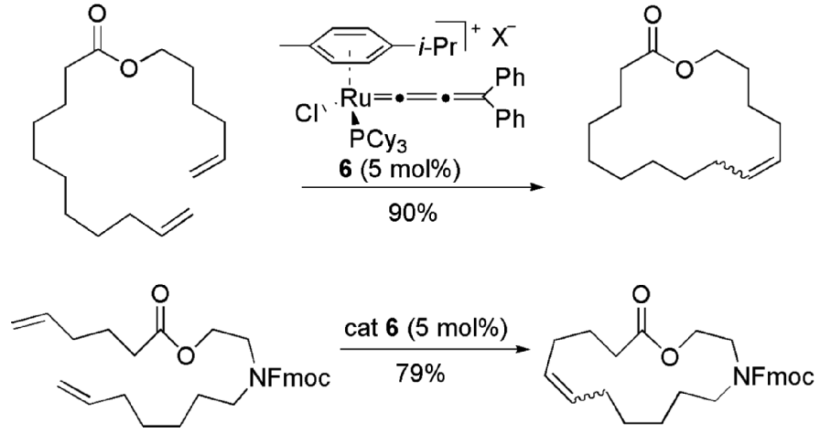

Scheme 7. Macrocycle synthesis with ruthenium–allenylidene **6**.

2.2 Peptide- and carbohydrate-containing macrocycles

Cyclic amino acid and fluorinated amino acid derivatives and their phosphonate analogues have been readily obtained via RCM reaction using catalyst **1** [25] and allenylidene **6** [26]. Medium size cyclic amino esters have been obtained using catalyst **6** (Scheme 8) [27].

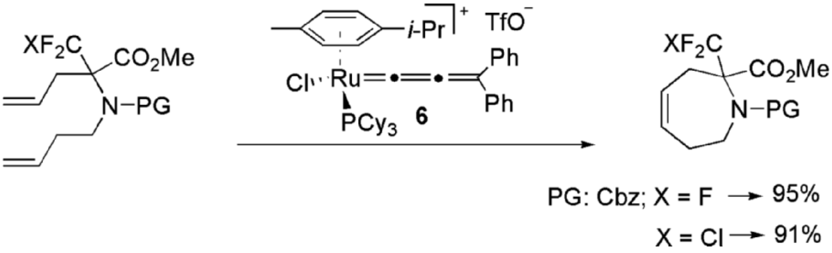

Scheme 8. Synthesis of medium size cyclic amino esters with catalyst **6**.

The Ru-catalyzed RCM reaction can be used for the direct access to macrocycles containing peptide or carbohydrate. For the synthesis of macrocyclic peptidomimetics by RCM, the nature of Ru catalysts is important to obtain an *E* CH=CH bond configuration. The transformation of **21**→**22** was achieved with catalyst **3** and the only *E* isomer was obtained in 51% yield, whereas catalyst **1** led to 69% yield of a isomer mixture *E*/*Z* (3/1) (Scheme 9) [28].

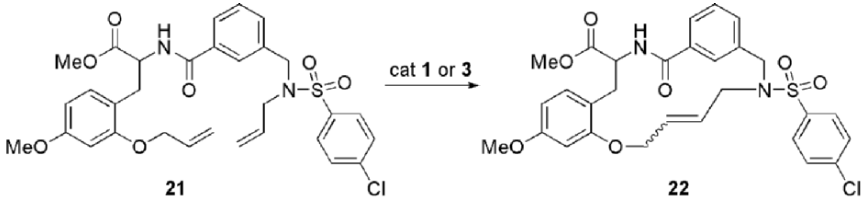

Scheme 9. Amino ester-containing macrocycle.

Carbohydrate-containing macrocycles such as cyclic glycolipides possess a variable number of linked carbohydrates tied up with a lipophilic aglycon. Several cyclic glycolipides and analogues were first prepared by RCM reaction by Fürstner using a first-generation Grubbs catalyst $RuCl_2(=CH–CH=CPh_2)(PCy_3)_2$ [3b] analogous to catalyst **1**, the allenylidene **6** [24], or the indenylidene catalyst **8** [4a,29] (Scheme 10).

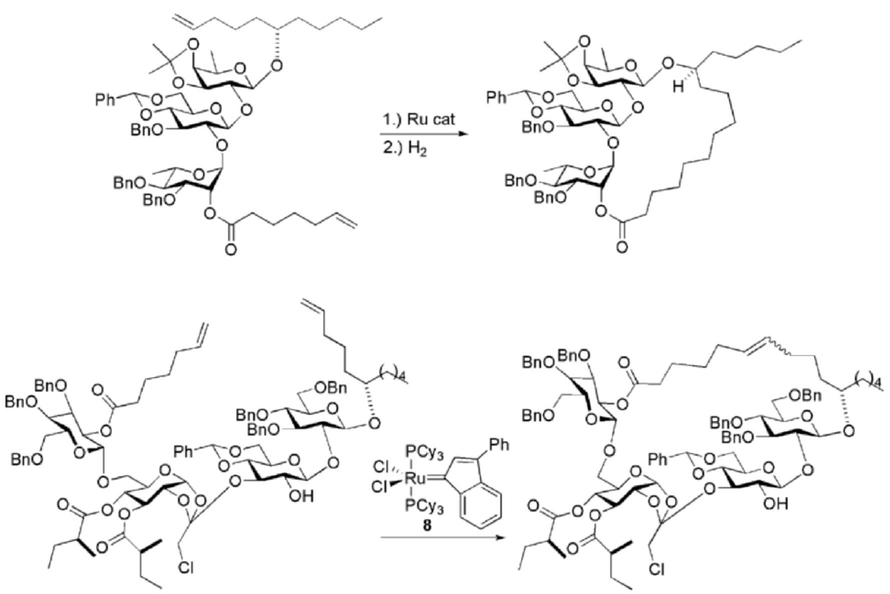

Scheme 10. Synthesis of carbohydrate-containing macrocycles.

Recently, this methodology has been used for the preparation of a variety of structurally related macrocycles such as spacer-linked aminoglycosides [30] or cyclic multivalent scaffolds [31]. For example, it is shown that the preorganization by a bis-tertiary amide linkage of a sugar-containing diene is essential to achieve the RCM reaction (Scheme 11) [31]. The tertiary bis-amide **23** with Grubbs catalyst **1** gives the macrocyclic compound in 96% yield (*E*/*Z* = 3/1) that after deprotection leads to the scaffold **24**.

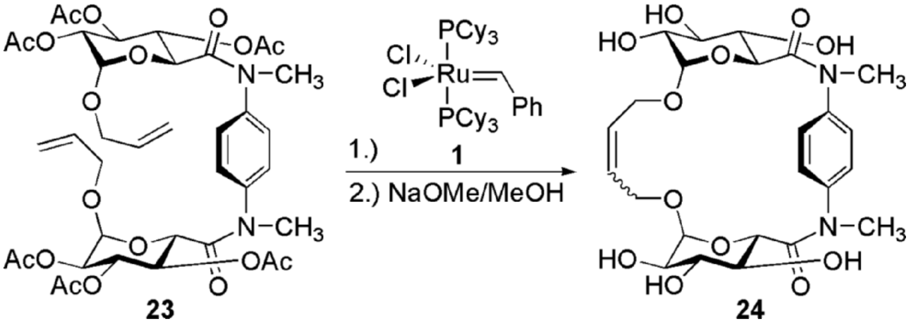

Scheme 11. Preorganized intermediate for selective macrocycle synthesis.

Another type of carbohydrate-containing macrocycles was produced by combining click-dimerization and RCM reaction (Scheme 12). The click reaction is first achieved on treatment of a carbohydrate azide containing an alkene chain (R^1) with 1,7-octadiyne in the presence of a copper(II) salt. A carbohydrate dimer is first obtained. Thus, starting with the azide **25** the click reaction followed by RCM reaction with catalyst **1** affords the macrocycle **26** which on hydrogenation ($Pd(OH)_2/C$) leads to **27** (Scheme 12) [32].

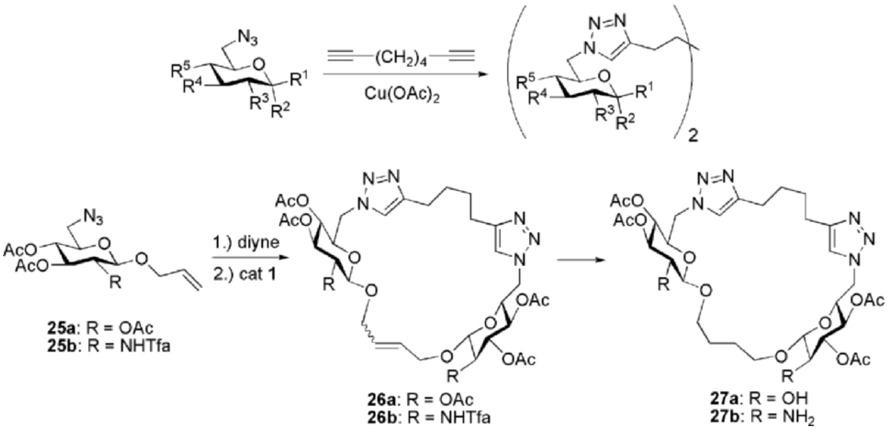

Scheme 12. Tandem click–RCM reactions.

2.3 Brief indications of RCM reaction in the synthesis of macrocyclic natural products or biologically active compounds

A tremendous advantage of catalytic alkene metathesis deals with new approaches to make carbon–carbon bonds and especially cycles and macrocycles with catalysts tolerating functional groups. This is a reason why this reaction has brought a revolution in organic synthesis by reducing the number of steps in multiple step synthesis and the protection or deprotection steps. The discovery of efficient well-defined catalysts for RCM reaction has very early led to new synthesis of natural products or drugs in which alkene metathesis is a crucial step. Several reviews have been produced by Fürstner [4], Nicolaou [8a], Lebreton [8d], or Prunet [8e]. This aspect involving multistep synthesis will not be developed here although recent, important contributions based on RCM reactions have been found. A number of examples can be cited among natural products: macrosphelides [33], (+)-pinnatoxin A [34], macrolactam (–)-isooncinotine [35], (–)-norsecurinine alkaloid [36], (–)-kendomycin with bioregulatory properties [37], feigrisolide C [38], and a family of coleophomones B, C, D [39], but also as biologically active or drug intermediates such as thrombin inhibitors [40], binding macrocycle inhibitors [41], or ansamycin antibiotics [42].

3. RCM reaction in the synthesis of new ligands, rotaxanes, catenanes, and supramolecular systems

New developments of the RCM reactions involve easy modification of ligands to be used in catalysis, the building of supramolecular systems, host–guest systems or molecular materials. These examples show that alkene metathesis also strongly improves these new fields and allows to create new molecular and supramolecular objects.

3.1 Modification and creation of ligands

RCM has been used recently for the modification of a well-known and used ligand BINOL and its incorporation into a macrocycle that can be used as a quite different ligand [18].

2,2′-Bipyridine is a commonly used ligand to favour electron transfers in metal complexes or to significantly modify photochemical properties. It has been included into a macrocycle ($E/Z = 9/1$) that can be hydrogenated and still offer the coordination properties of both nitrogen atoms (Scheme 13) [43].

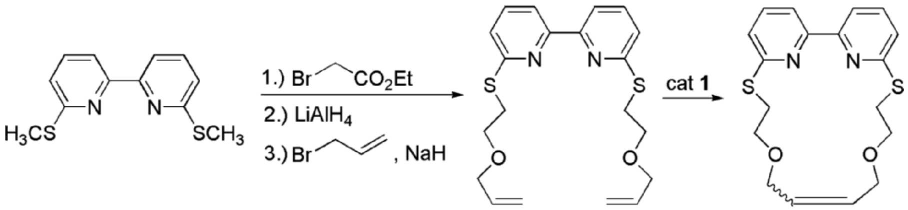

Scheme 13. Synthesis of macrocyclic bipyridines.

Potential multidentate ligands have also been created by serendipity. Whereas the terpene derivative **28** had been prepared to build the AB rings of taxane **29** its treatment with the Grubbs catalyst **3** has led to its unexpected cyclotrimerization and the production in 70% of the multifunctional system of C_3 symmetry **30** (Scheme 14) [44].

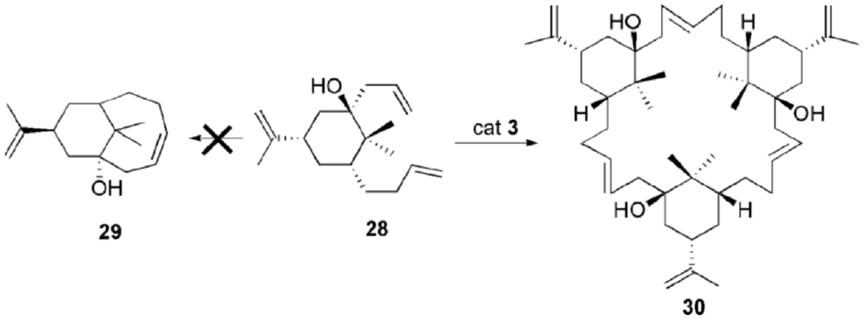

Scheme 14. Unexpected synthesis of macrocycle by cyclotrimerization.

The RCM reaction has been used for the synthesis of macrocyclic molecules offering cavity with potential as a host molecule or artificial receptor for ions and small molecules. Thus, the multifunctional molecule **31** has been designed to produce a polymacrocycle **32**. On treatment with Grubbs catalyst **1** it affords 66% of **32** that was further hydrogenated (Pd/C) to afford the corresponding system (86%) with all hydrogenated double bonds. The success of this reaction is based on the easiness of RCM reaction between the alkene chains of two branches rather than within one branch: the formation of 11-membered ring being disfavoured (Scheme 15) [45].

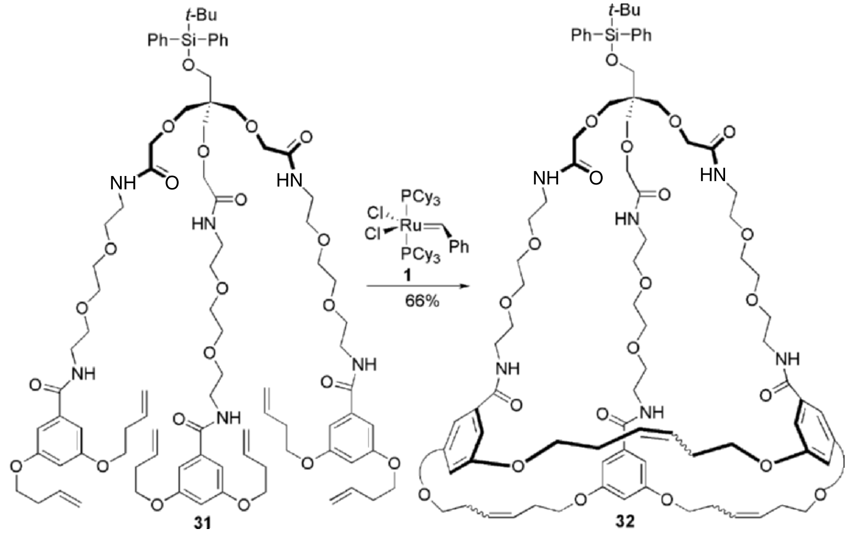

Scheme 15. Synthesis of a polymacrocycle **32**.

Rotaxanes are mechanically interlocked molecules constituted of a trapped macrocycle around a suitable sterically hindered molecule at both ends. Thus, the macrocycle **34** can be easily prepared from **33** by RCM, but in the presence of ammonium salt **35**, the same RCM reaction affords 73% of the rotaxane **36** in which the ammonium ion with two bulky end groups is trapped into the macrocycle (Scheme 16, left-hand route) [46].

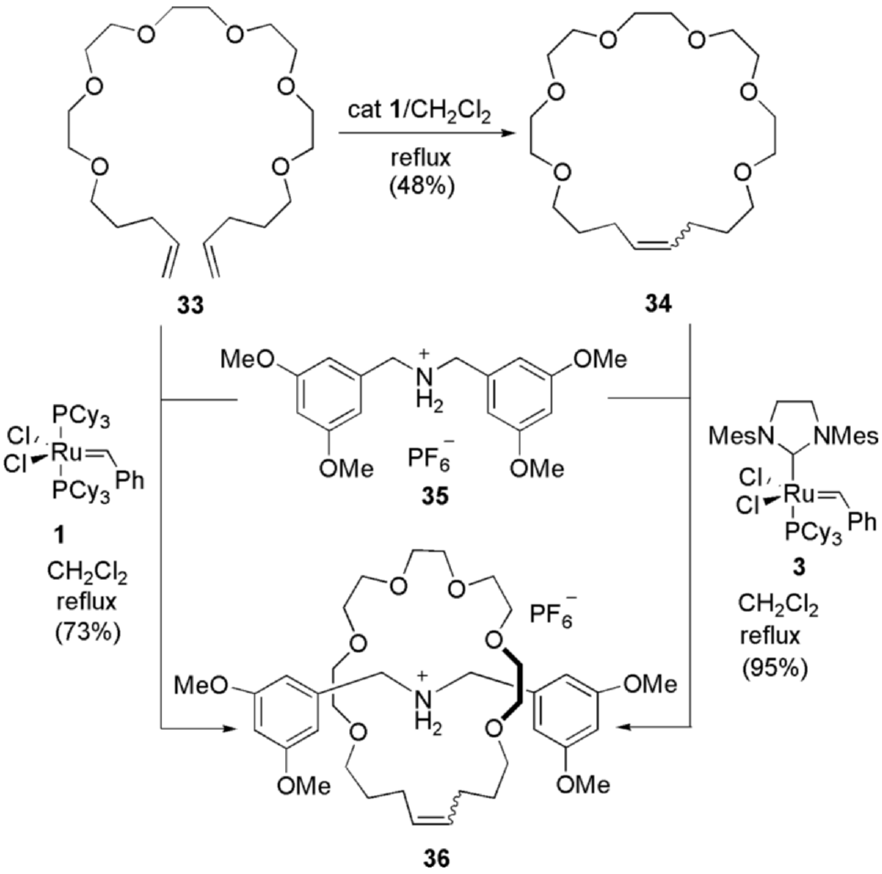

Scheme 16. Preparation of a rotaxane based on ammonium polyether interaction.

Because of the reversibility of the RCM process the same type of rotaxane can be produced from the macrocycle containing a CH=CH bond that can be opened and closed reversibly. The macrocycle **34** with the salt **35** in the presence of catalyst **3** affords the catenane **36** in 95% yield, thus offering an example of a "*magic ring*" allowing the introduction of an ionic molecule **35** that can not mechanically enter the ring (Scheme 16, right-hand route) [47].

Catenanes are molecules constituted of two interlocked rings. Very early the RCM reaction was used by Sauvage and Grubbs to produce catenanes using the coordination properties of phenanthroline derivatives to assemble together the ring A with the opened molecule B with two terminal olefin ends before RCM reaction (Scheme 17) [48].

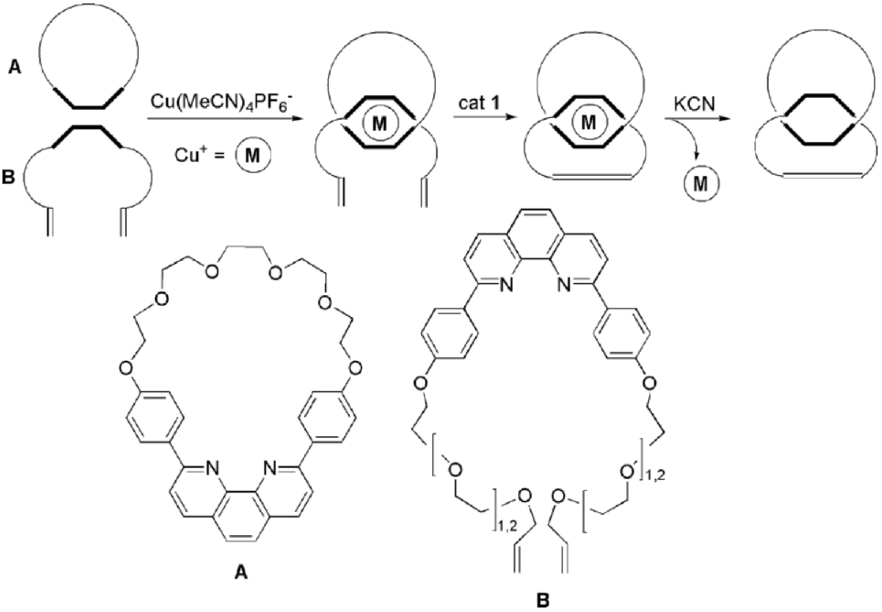

Scheme 17. RCM application to catenane synthesis via phenanthroline–Cu complex.

New catenanes are now produced by interaction of a macrocycle containing an ammonium salt **37** with either the macrocycle precursor **33** or the macrocycle **34** in the presence of catalyst **3** (Scheme 18) [47]. Thus, the catenane **38** was produced in good yield. In order to avoid the process reversibility, the hydrogenation of **38** (PtO_2) affords the stable catenane **39**. The direct transformation of two macrocycles **34** and **37** into the interlocked macrocycle molecule **38** illustrates "*magic rings*" *interlocking* [47].

New catenanes containing terpyridine ligands have been produced using Ru^{2+} ion, arising from $RuCl_2(dmso)_4$, to assemble in tail-to-tail, orthogonal positions, both coordinating terpyridines each of them with two alkene branches. Thus, the resulting Ru complex **40** on reaction with catalyst **1** led

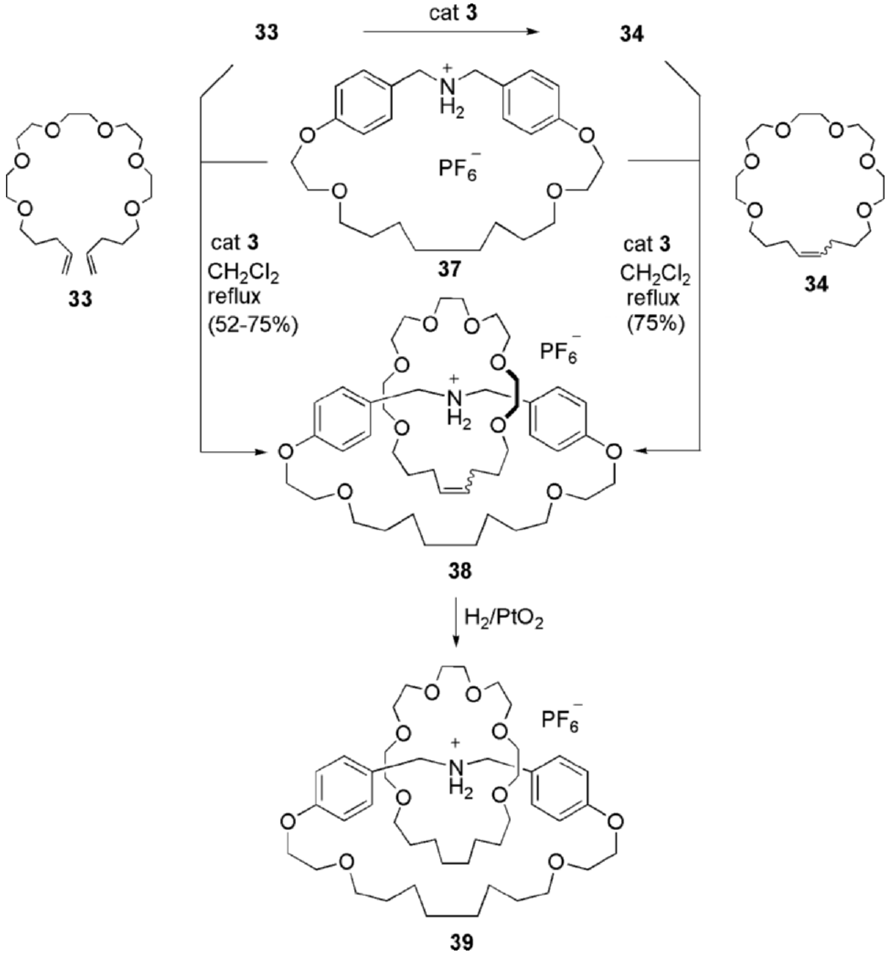

Scheme 18. RCM application to catenane synthesis with the help of ammonium–ether interaction.

to the formation of catenanes that were hydrogenated (Pd/C) to afford the catenane **41** and the unexpected non-catenane product **42** in a 1:2 ratio, corresponding to the coupling of intramolecular and intermolecular branches, respectively (Scheme 19) [49]. Thus, the elimination of the Ru^{2+} cation affords catenane from **41** and very large macrocycle from **42**.

RCM has allowed the synthesis of a catenane consisting of a large ring threaded through both cyclic units as in a handcuff-like structure. The synthesis is based on the model shown in Scheme 20 [50].

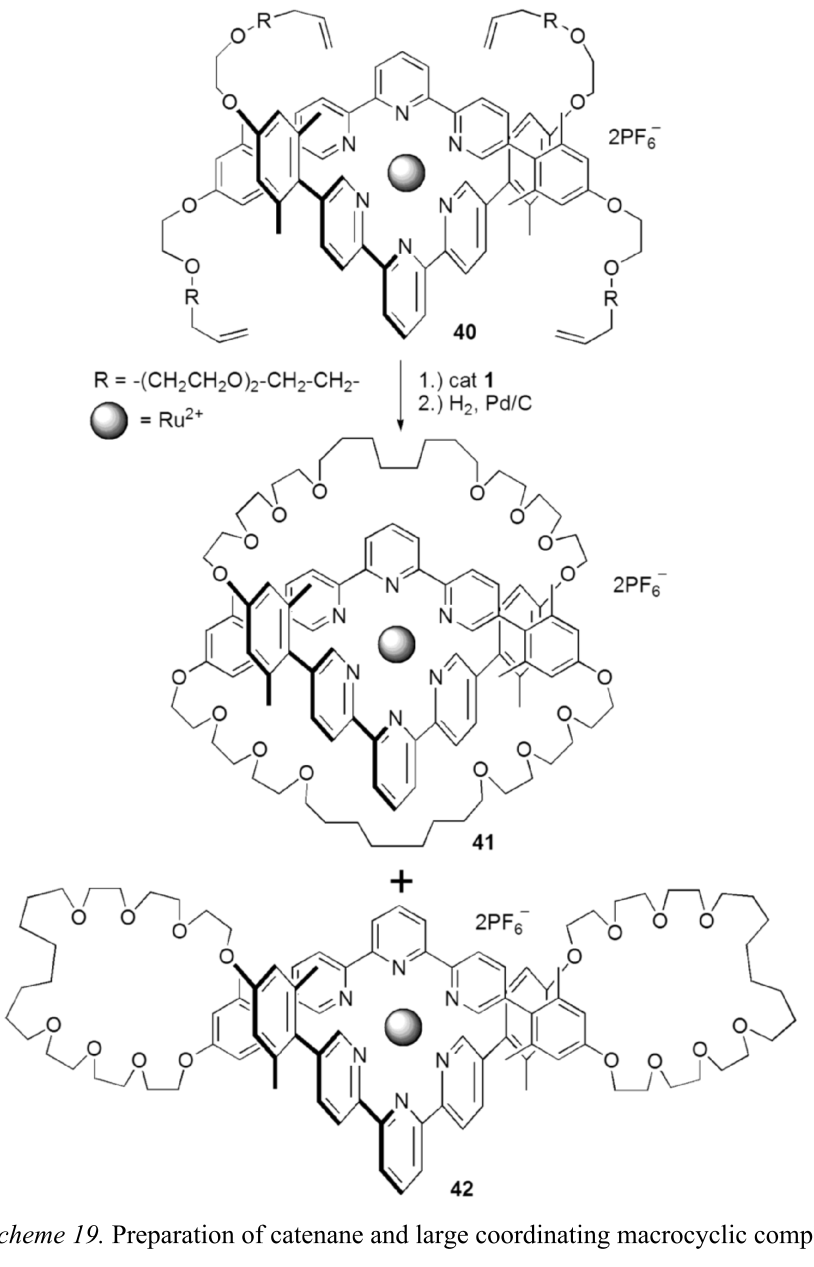

Scheme 19. Preparation of catenane and large coordinating macrocyclic complex.

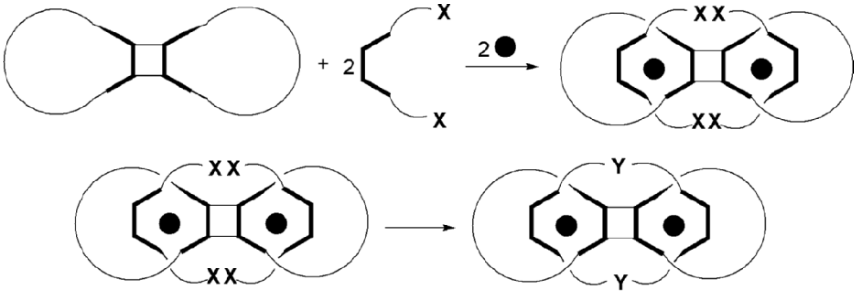

$X = CH{=}CH_2$, $Y = CH{=}CH$

Scheme 20. Model for the synthesis of handcuff structure catenanes.

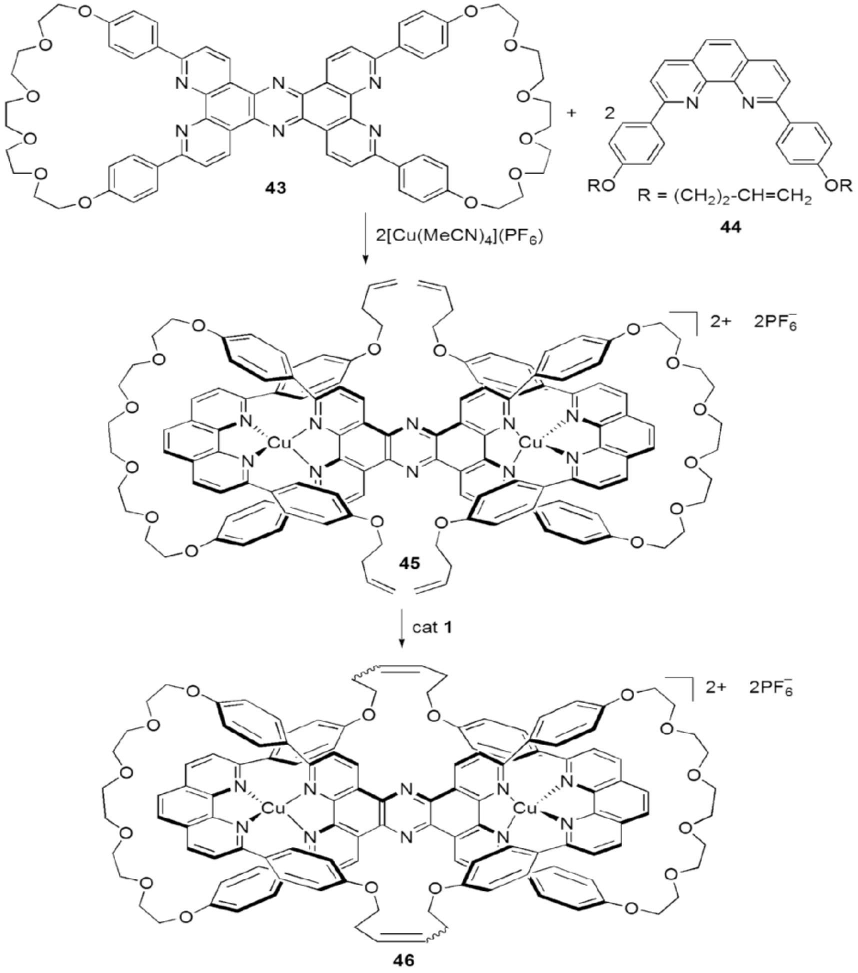

Scheme 21. Synthesis of handcuff structure catenane.

It was achieved by Sauvage et al. [50] starting from the bicyclic molecule **43** with two phenanthroline moieties each of them associated with the help of a Cu(I) salt with the diene **44**. RCM with Grubbs catalyst **1** of complex **45** led to the catenane **46** that can be hydrogenated (Scheme 21).

3.2 Cooperation of templates and RCM reactions to selectively build large macrocycles

Calixarenes have been used as templates to favour the suitable arrangement of pendant terminal CH=CH_2 bonds of another calixarene to selectively produce large macrocycles [51]. The calixarene **47** containing four chains, each with two pendant alkene branches, in the presence of the simple calixarene **48** gives a heterodimer **47–48**, **47** being a truncated cone above **48**, allowing the slow preorganization of the terminal alkene bonds (2 days room temperature) in suitable position and vicinity for RCM couplings. Then the treatment of the resulting supramolecular system **47–48** with Grubbs catalyst **1** (40%, 2–6 days) followed by catalytic hydrogenation (PtO_2) leads to the cyclized, hydrogenated heterodimer **48–49** which is separated into components **48** and **49** by chromatography. The urea links of the resulting compound **49** can be cleaved with acetic acid and the large macrocycle **50** can be obtained (Scheme 22) [51a]. Various macrocycles have been made, based on this method.

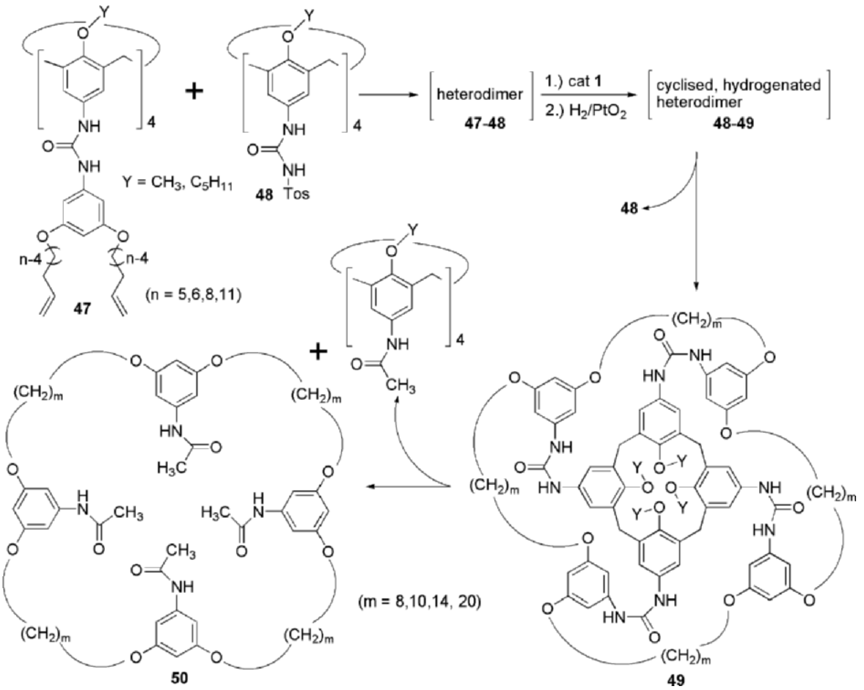

Scheme 22. Synthesis of huge macrocycles using a calixarene as template.

A triplatinum template has been used by the van Koten team to build a large macrocycle by mean of RCM reaction [52]. The triplatinum complex **51** has persistent relative positions of the three Pt atoms, and each of them can coordinate a pyridine by displacement of the chloride. A variety of pyridines with long 2,6-dialkene substituents were reacted with **51** and the resulting complexes **52** were reacted with the Grubbs catalyst **1**, or the Schrock catalyst $Mo(=CHCMe_2Ph)(=N\text{-}2,6\text{-}(i\text{-}Pr)_2C_6H_3)(OCMe(CF_3)_2)_2$ [2b] to give the macrocyclic triplatinum complex **53**. On treatment of **53** with NaCl the macrocycle was displaced from the platinum atoms to give back **51** and the large macrocycle **54** that was further hydrogenated (Pd/C) to give **55** (Scheme 23) [52a].

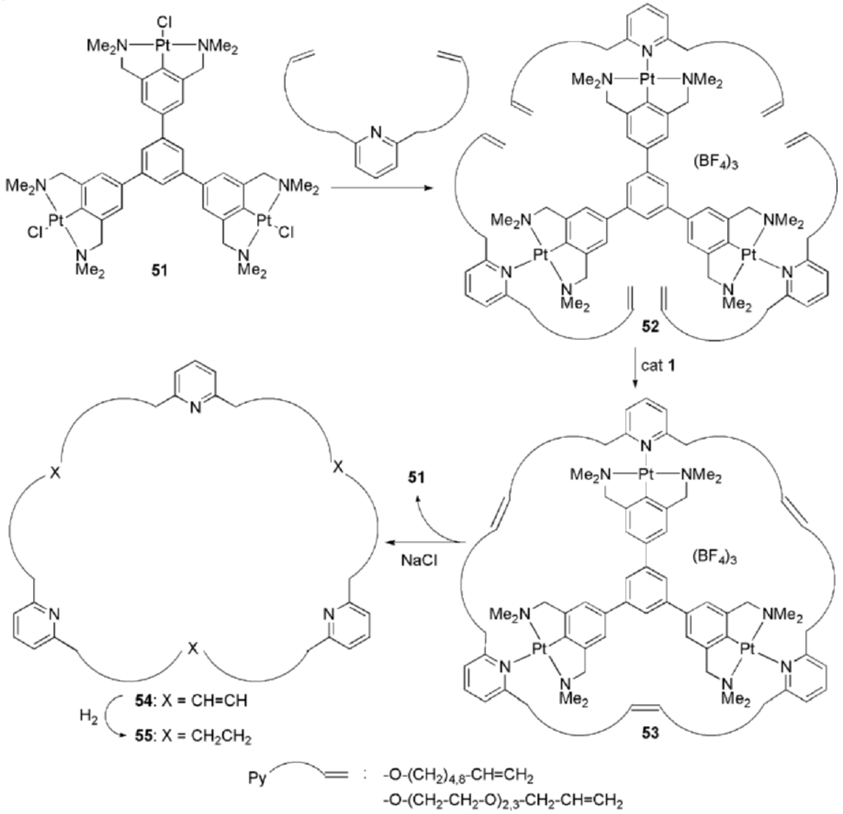

Scheme 23. Template-directed synthesis of large macrocycles.

4. Cross-metathesis in synthesis and supramolecular system formation

Alkene CM consists in the synthesis of a difunctional alkene from two different functional alkenes with formation of ethylene or simple alkene. It is a bimolecular reaction by comparison with the previous intramolecular RCM reaction which involves the formation of a cyclic olefin from two different functional olefins contained in the same molecule.

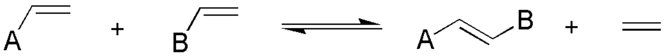

Thus, CM is often difficult to perform and the suitable catalyst for a given reaction has often to be selected from different experiments performed with a box of catalysts.

Several reviews have been more dedicated to CM [5]. Here are selected CM applications reported within the last 3 years.

Functional electron-withdrawing alkenes have key utilizations for instance in Diels–Alder reactions. The unsaturated β-ketonic phosphonates **57** can be obtained by CM with ethyl acrylate in the presence of Ru catalyst **3** or **5** (Scheme 24) [53].

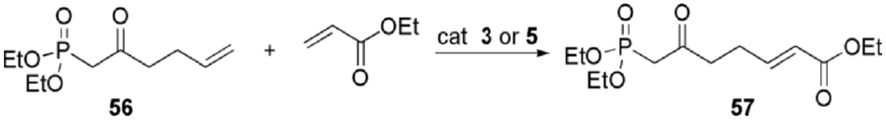

Scheme 24. Cross-coupling reaction of β-ketonic phosphonates.

This study shows that the Hoveyda phosphine-free catalyst **5** is more efficient than the second-generation Grubbs catalyst **3**. In addition, the microwave irradiation, by offering fast heating and increased pressure, allowed catalyst **5** to afford complete conversion and excellent product yield. It is noteworthy that the CM of the β-ketoester **58** with **5** ($ClCH_2CH_2Cl$, reflux only) leads to similar yields (~60%) as **56**, whereas that of **60**, with only one carbonyl group, affords **61** with **5** at room temperature in 83% (Scheme 25) [53].

It was assumed that the reduced activation of β-dicarbonyl compounds is due to the formation of bidendate Ru intermediate (**I**). Indeed, attempts to disfavour coordination of a carbonyl by addition of Ti(*i*-PrO)$_4$ led to complete conversion of both **56** and **58** at room temperature.

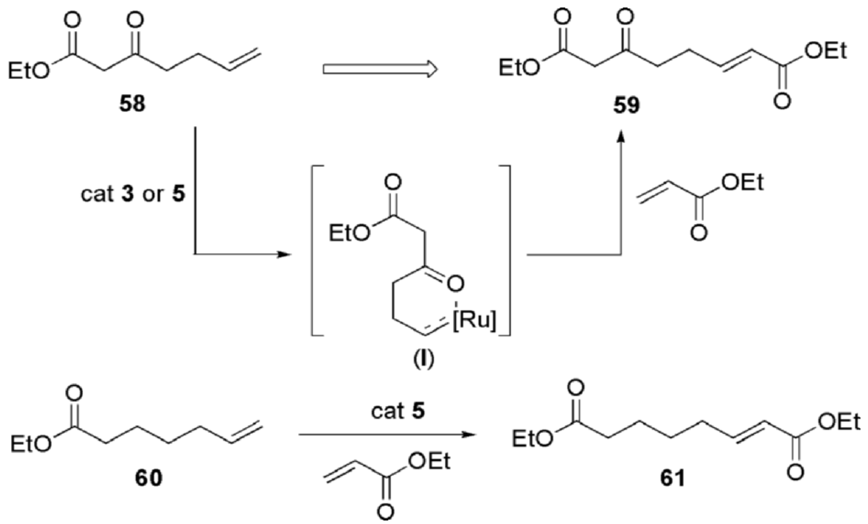

Scheme 25. Cross-metathesis of unsaturated β-ketoester.

Non-racemic allylic hydroxy phosphonates are usually produced by enzymatic kinetic resolution [54] or enantioselective catalysis [55]. They can be now produced by CM of allylic hydroxy phosphonates **62** with Grubbs catalyst **3** (Scheme 26) [56]. CM compounds **63** are the main products with respect to the self-metathesis product **64**.

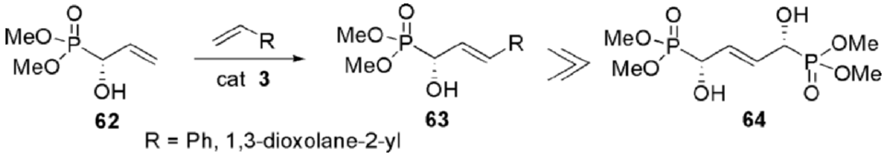

Scheme 26. Synthesis of substituted optically active allylic hydroxy phosphonates.

(*S*)-Lysine and (*S*)-arginine homologues were prepared via CM according to scheme 27 followed by hydrogenation (Pd/C) [57].

C-Glycosyl amino acids of type **68**, for example, are robust to degradation by glycosidases with respect to *O*-glycosides. They can be obtained directly by CM of *C*-allyl glycosides with unsaturated amino esters [58]. They were recently produced by CM of vinylcarbohydrate **65** with the amino ester **66**. The mercury(II)-mediated cyclization of **67** affords the *C*-glycosyl amino esters **68** (Scheme 28) [59].

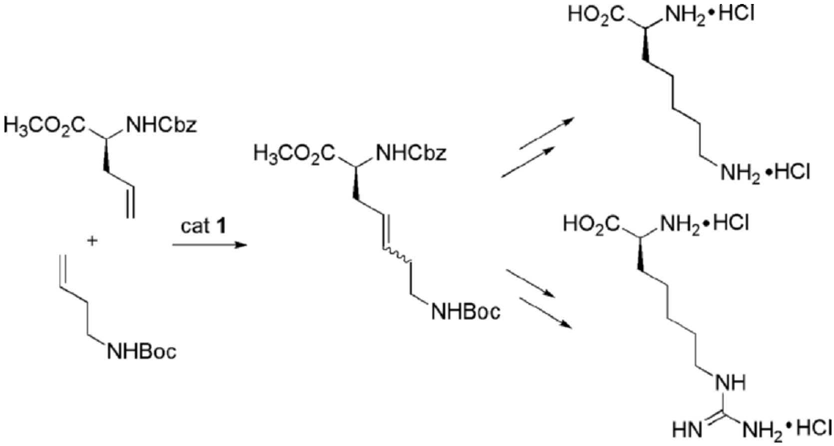

Scheme 27. Synthesis of (*S*)-lysine and (*S*)-arginine homologues.

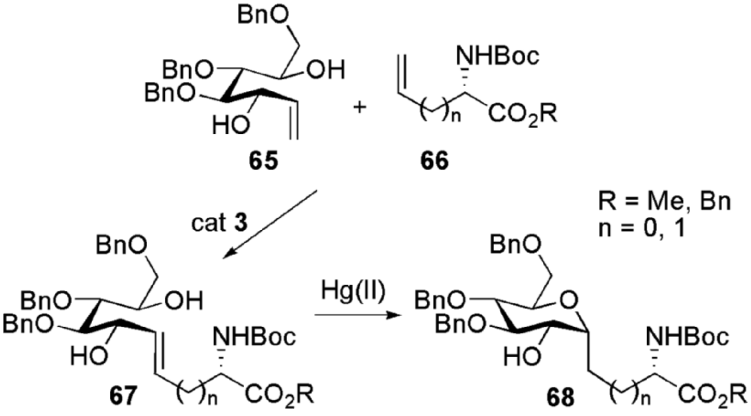

65 **66** **67** **68**

Scheme 28. *C*-glycosyl amino ester synthesis.

CM has also become a key reaction for the development of drugs or the improvement of natural products synthesis.

Viridiofungin A **71** is a natural product offering a broad spectrum of antifungal activity. It was produced by CM of **69** and **70** with either Grubbs **3** or Hoveyda **5** catalysts (Scheme 29) [60].

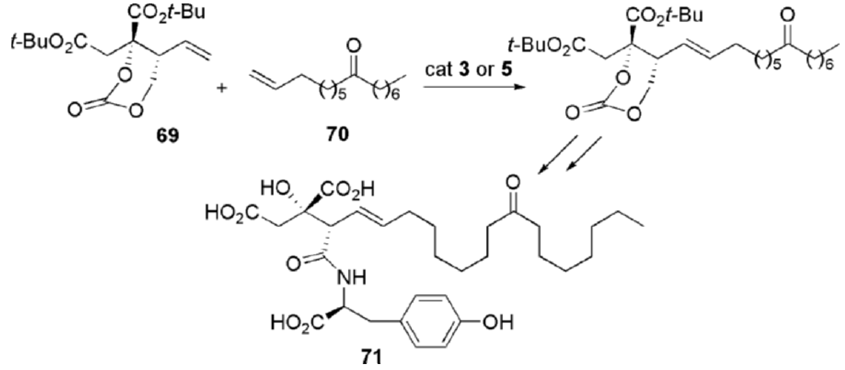

Scheme 29. A short synthesis of viridiofungin A.

(+)-Carpamic acid **74** is a member of natural piperidine alkaloids displaying important biological activity [61]. It has all-cis-configuration of its substituents and was made recently by CM of **72** and **73** with Grubbs catalyst **3** (Scheme 30) [62].

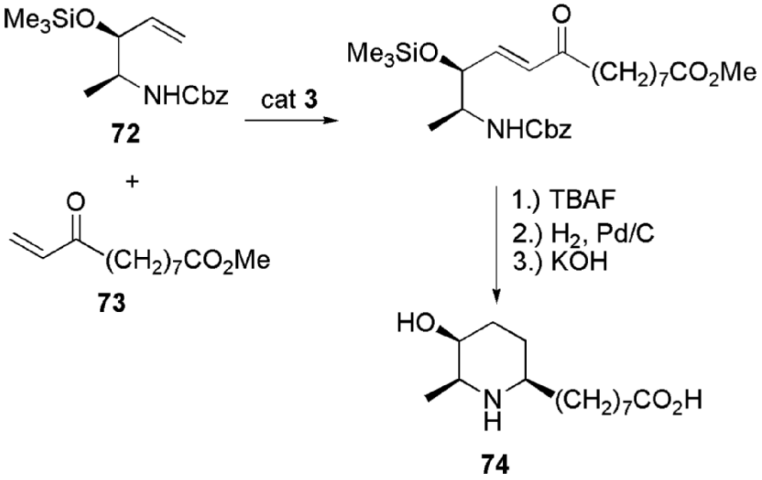

Scheme 30. A short synthesis of (+)-carpamic acid.

The synthesis of γ,δ-unsaturated-β-keto lactones was achieved by tandem CM or lactonization reactions [63]. A 16-membered macrolide antibiotic (–)-A26771B **79** was prepared by such a way (Scheme 31). The key reaction step involved the CM of **75** and **76** to give **77** in the presence of Hoveyda catalyst **5**. The lactonization led to the macrocycle **78** which was transformed into the macrolid **79** [63].

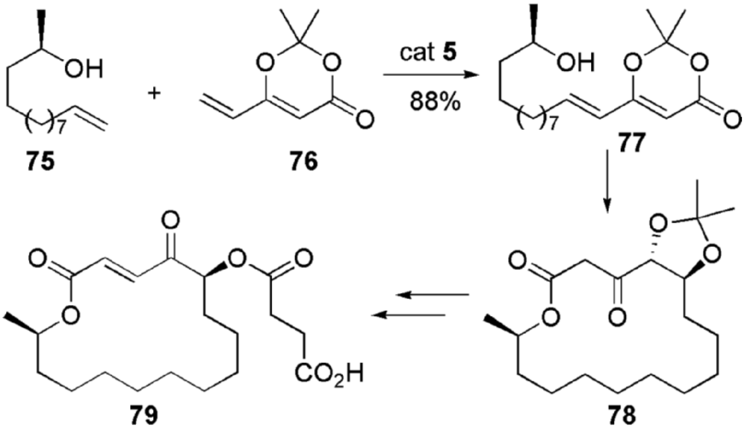

Scheme 31. Key cross-metathesis step in the synthesis of macrolide **79**.

The antitumour activity of tetrahydrofuran (THF) containing acetogenins has led to development of new functional THFs and non-adjacently linked bis-THF derivative synthesis. Bullatanocin **84** is one of the latter and was recently prepared by CM [64] (Scheme 32). Treatment of **80** and **81** in the presence of Grubbs catalyst **3** led to the bridged derivative **82**. Subsequent hydrogenation (Pd/C) and Wittig reaction with **83** led to the natural product bullatanocin **84**.

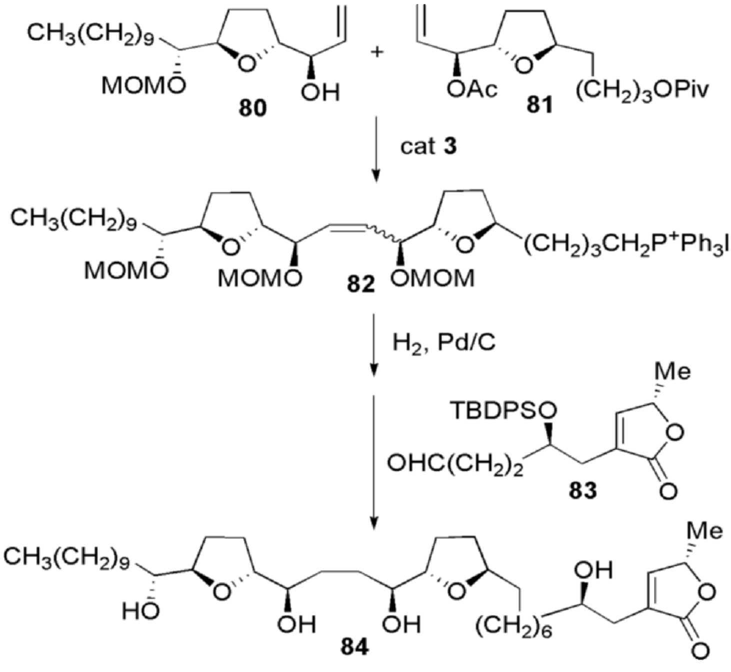

Scheme 32. Fast synthesis of bullatanocin.

CM also constitutes a useful reaction to attach a suitable functionality to a substrate. An example is given for the functionalization of a macrocyclic lactam by an amino ester functionality. *N*-allyl macrocycle was reacted with *O*-allylamino acid derivative in the presence of catalyst **3** and led to the macrocycle **85** with amino acid chain in 48% yield (Scheme 33) [65].

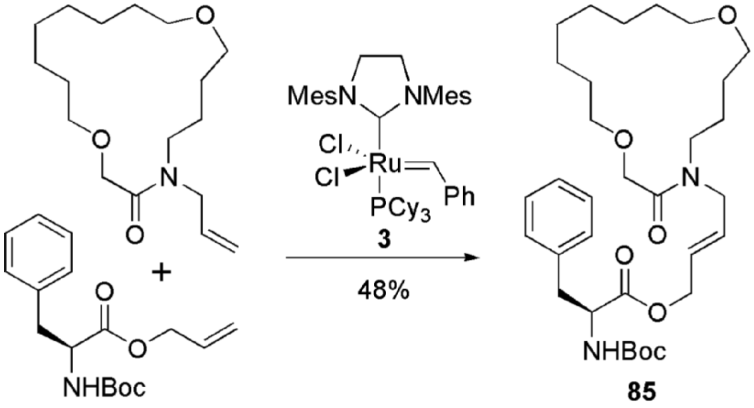

Scheme 33. Synthesis of amino ester-linked macrocycle.

A template has been used to promote self-metathesis of a macrocycle with pendant one or two alkene chains by bringing two C=C double bonds in suitable positions. As ammonium salts interact with macrocyclic polyethers, the macrocycle **86** with a lateral alkene chain leads, with Grubbs catalyst **3**, to the homo CM product **88** in 35% yield. The presence of half an equivalent of the diammonium ion **87** favours the transformation of **86** and rises the yield of **88** formation to 72% under the same conditions (Scheme 34) [66].

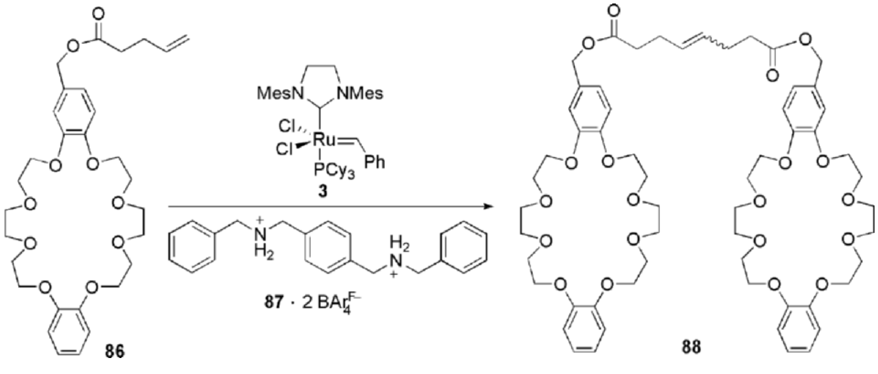

Scheme 34. Template-promoted cross-metathesis.

This yield increasing effect can be explained by the threading of the diammonium salt **87** into two macrocycles to give the supramolecular system **A** favouring the CM leading to the supramolecular system **B** (Scheme 35) [66].

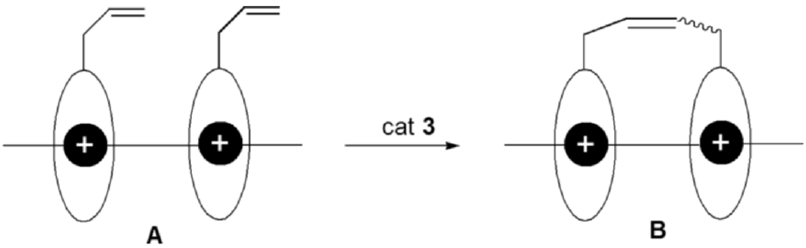

Scheme 35. Model for a template-promoted cross-metathesis.

Several examples illustrate this concept.

5. Conclusion

The above recent examples of RCM reactions leading to new macrocycles, natural products, and drugs but also to new ligands, rotaxanes, catenanes, and supramolecular systems show how alkene metathesis has become unavoidable to produce rapidly useful fine chemicals and new molecular and supramolecular architectures. The high usefulness of this reaction is confirmed by CM allowing the access to highly functionalized monomers and molecules that can not be easily reached by classical catalytic transformations of olefins: cross-coupling or Heck-type reactions. But alkene metathesis has also been shown to bring revolutions in various other fields such as in enantioselective catalysis [67], catalysis in ionic liquids [68,69], green chemistry, renewable resources [70], and functional dendrimer and polymer production [6,71].

The growing interest and potential of catalytic alkene metathesis calls for creativity in the design of more efficient and robust, but also recyclable alkene metathesis catalysts. There is still the need to develop organometallic processes leading to the creation of novel and active alkene metathesis catalysts and innovation in synthesis and new architecture building.

References

[1] (a) Chauvin, Y. (2006) Angew. Chem. Int. Edit. 45:3741; (b) Hérisson, J.-L., Chauvin, Y. (1971) Makromol. Chem. 141:161.

[2] (a) Schrock, R.R. (2006) Angew. Chem. Int. Edit. 45:3748; (b) Schrock, R.R., Murdzek, J.S., Bazan, G.C., Robbins, J., DiMare, M., O’Regan, M. (1990) J. Am. Chem. Soc. 112:3875.

[3] (a) Grubbs, R.H. (2006) Angew. Chem. Int. Edit. 45:3760; (b) Nguyen, S.T., Grubbs, R.H. (1993) J. Am. Chem. Soc. 115:9858; (c) Nguyen, S.T., Johnson, L.K., Grubbs, R.H., Ziller, J.W. (1992) J. Am. Chem. Soc. 114:3974.
[4] (a) Fürstner, A. (2004) Eur. J. Org. Chem. 943; (b) Fürstner, A. (ed.) (1998) Topics in Organometallic Chemistry: Alkene Metathesis in Organic Synthesis, Vol. 1, Springer, Berlin.
[5] (a) Connon, S.J., Blechert, S. (2004) In: Bruneau, C., Dixneuf, P.H. (eds) Topics in Organometallic Chemistry: Ruthenium Catalysts and Fine Chemistry, Vol. 11, Springer, Berlin, p. 93; (b) Connon, S.J., Blechert, S. (2003) Angew. Chem. Int. Edit. 42:1900.
[6] Buchmeiser, M.R. (2000) Chem. Rev. 100:1565.
[7] Smith, J.A., Brzezinska. K.R., Valenti. D.J., Wagener. K.B. (2000) Macromolecules 33:3781.
[8] (a) Nicolaou, K.C., Bulger, P.G., Sarlah, D. (2005) Angew. Chem. Int. Edit. 44:4490; (b) Brenneman, J.B., Stephen, M.F. (2005) Curr. Org. Chem. 9:1535; (c) Grubbs, R.H. (2004) Tetrahedron 60:7117; (d) Felpin, F.-X., Lebreton, J. (2003) Eur. J. Org. Chem. 3693; (e) Prunet, J. (2003) Angew. Chem. Int. Edit. 42:2826; (f) Trnka, T.M., Grubbs, R.H. (2001) Acc. Chem. Res. 34:18; (g) Fürstner, A. (2000) Angew. Chem. Int. Edit. 39:3012; (h) Maier, M.E. (2000) Angew. Chem. Int. Edit. 39:2073; (i) Mol, J.C. (1999) Catal. Today 289; (j) Armstrong, S.K. (1998) J. Chem. Soc. Perkin. Trans. 1:371; (k) Grubbs, R.H., Chang, S. (1998) Tetrahedron 54:4413; (l) Ivin, J.K. (1998) J. Mol. Catal. A: Chem. 133:1; (m) Randall, M.L., Snapper, M.L. (1998) J. Mol. Catal. A: Chem. 133:29.
[9] (a) Schwab, P., France, M.B., Ziller, J.W., Grubbs, R.H. (1995) Angew. Chem. Int. Edit. 34:2039; (b) Schwab, P., Grubbs, R.H., Ziller, J.W. (1996) J. Am. Chem. Soc. 118:100.
[10] Huang, J., Stevens, E.D., Nolan, S.P., Petersen, J.L. (1999) J. Am. Chem. Soc. 121:2674.
[11] Scholl, M., Ding, S., Lee, C.W., Grubbs, R.H. (1999) Org. Lett. 1:953.
[12] Kingsbury, J.S., Harrity, J.P.A., Bonitatebus, P.J. Jr., Hoveyda, A.H. (1999) J. Am. Chem. Soc. 121:791.
[13] Garber, S.B., Kingsbury, J.S., Gray, B.L., Hoveyda, A.H. (2000) J. Am. Chem. Soc. 122:8168.
[14] (a) Fürstner, A., Picquet, M., Bruneau, C., Dixneuf, P.H. (1998) J. Chem. Soc. Chem. Commun. 1315; (b) Picquet, M., Bruneau, C., Dixneuf, P.H. (1998) J. Chem. Soc. Chem. Commun. 2249.
[15] (a) Castarlenas, R., Dixneuf, P.H. (2003) Angew. Chem. Int. Edit. 42:4524; (b) Castarlenas, R., Vovard, C., Fischmeister, C., Dixneuf, P.H. (2006) J. Am. Chem. Soc. 128:4079.
[16] (a) Fürstner, A., Grabowski, J., Lehmann, C.W. (1999) J. Org. Chem. 64:8275; (b) Jafarpour, L., Schanz, H.-J., Stevens, E.D., Nolan, S.P. (1999) Organometallics 18:5416; (c) Fürstner, A., Guth, O., Düffels, A., Seidel, G., Liebl, M., Gabor, B., Mynott, R. (2001) Chem. Eur. J. 7:4811.
[17] (a) Ibrahim, Y.A. (2006) J. Mol. Catal. A: Chem. 254:43; (b) Ibrahim, Y.A., Behbehani, H., Ibrahim, M.R., Malhas, R.N. (2003) Tetrahedron 59:7273.
[18] Ibrahim, Y.A., John, E. (2006) Tetrahedron 62:1001.

[19] Cooper, T.S., Atrash, B., Sheldrake, P., Workman, P., McDonald, E. (2006) Tetrahedron Lett. 47:2241.

[20] Davoli, P., Fava, R., Morandi, S., Spaggiari, A., Prati, F. (2005) Tetrahedron 61:4427.

[21] Michrowska, A., Wawrzyniak, P., Grela, K. (2004) Eur. J. Org. Chem. 2053.

[22] Kim, Y.J., Lee, D. (2004) Org. Lett. 6:4351.

[23] Castarlenas, R., Fischmeister, C., Bruneau, C., Dixneuf, P.H. (2004) J. Mol. Catal. A: Chem. 213:31.

[24] Fürstner, A., Liebl, M., Lehmann, C.W., Picquet, M., Kunz, R., Bruneau, C., Touchard, D., Dixneuf, P.H. (2000) Chem. Eur. J. 6:1847.

[25] Osipov, S.N., Bruneau, C., Picquet, M., Kolomiets, A.F., Dixneuf, P.H. (1998) J. Chem. Soc. Chem. Commun. 2053.

[26] Osipov, S.N., Artyushin, O.I., Kolomiets, A.F., Bruneau, C., Dixneuf, P.H. (2000) Synlett 7:1031.

[27] Osipov, S.N., Artyushin, O.I., Kolomiets, A.F., Bruneau, C., Picquet, M., Dixneuf, P.H. (2001) Eur. J. Org. Chem. 20:3891.

[28] Barret, A.G.M., Hennessy, A.J., Le Vézouët, R., Procopiou, P.A., Seale, P.W., Stefaniak, S., Upton, R.J., White, A.J.P., Williams, D.J. (2004) J. Org. Chem. 69:1028.

[29] Fürstner, A., Müller, T. (1999) J. Am. Chem. Soc. 121:7814.

[30] (a) Jaunzems, J., Oelze, B., Kirschning, A. (2004) Org. Biomol. Chem. 2:3448; (b) Kirschning, A., Chen, G.W., Jaunzems, J., Jesberger, M., Kalesse, M., Lindner, M. (2004) Tetrahedron 60:3505; (c) Chen, G.W., Kirschning, A. (2002) Chem. Eur. J. 8:2717.

[31] Velasco-Torrijos, T., Murphy, P.V. (2004) Org. Lett. 6:3961.

[32] Dörner, S., Westermann, B. (2005) Chem. Commun. 2852.

[33] Matsuya, Y., Kawaguchi, T., Nemoto, H. (2003) Org. Lett. 5:2939.

[34] Sakamoto, S., Sakazaki, H., Hagiwara, K., Kamada, K., Ishii, K., Noda, T., Inoue, M., Hirama, M. (2004) Angew. Chem. Int. Edit. 43:6505.

[35] Scheiper, B., Glorius, F., Leitner, A., Fürstner, A. (2004) PNAS 101:11960.

[36] Alibés, R., Bayón, P., de March, P., Figueredo, M., Font, J., García-García, E., González-Gálvez, D. (2005) Org. Lett. 7:5107.

[37] (a) Smith, A.B. III, Mesaros, E.F., Meyer, E.A. (2006) J. Am. Chem. Soc. 128:5292; (b) Smith, A.B. III, Mesaros, E.F., Meyer, E.A. (2005) J. Am. Chem. Soc. 127:6948.

[38] Kim, W.H., Jung, J.H., Sung, L.T., Lim, S.M., Lee, E. (2005) Org. Lett. 7:1085.

[39] Nicolaou, K.C., Montagnon, T., Vassilikogiannakis, G., Mathison, C.J.N. (2005) J. Am. Chem. Soc. 127:8872.

[40] Nantermet, P.G., Selnick, H.G. (2003) Tetrahedron Lett. 44:2401.

[41] Oishi, S., Shi, Z.-D., Worthy, K.M., Bindu, L.K., Fisher, R.J., Burke, T.R. (2005) Chem. Bio. Chem. 6:668.

[42] Peng, W., Blagg, B.S.J. (2006) Org. Lett. 8:975.

[43] Branowska, D., Buczek, I., Kalińska, K., Nowaczyk, J., Rykowski, A. (2005) Tetrahedron Lett. 46:8539.

[44] Srikrishna, A., Dethe, D.H. (2005) Tetrahedron Lett. 46:3381.

[45] Fang, S., Bergstrom, D.E. (2004) Tetrahedron Lett. 45:8501.

[46] Kilbinger, A.F.M., Cantrill, S.J., Waltman, A.W., Day, M.W., Grubbs, R.H. (2003) Angew. Chem. Int. Edit. 42:3281.

[47] Guidry, E.N., Cantrill, S.J., Stoddart, J.F., Grubbs, R.H. (2005) Org. Lett. 7:2129.

[48] Mohr, B., Weck, M., Sauvage, J.-P., Grubbs, R.H. (1997) Angew. Chem. Int. Edit. 36:1308.

[49] Loren, J.C., Gantzel, P., Linden, A., Siegel, J.S. (2005) Org. Biol. Chem. 3:3105.

[50] Frey, J., Kraus, T., Heitz, V., Sauvage, J.-P. (2005) Chem. Commun. 5310.

[51] (a) Cao, Y., Wang, L., Bolte, M., Vysotsky, M.O., Böhmer, V. (2005) Chem. Commun. 3132; (b) Vysotsky, M.O., Bogdan, A., Wang, L., Böhmer, V. (2004) Chem. Commun. 1268.

[52] (a) Chuchuryukin, A.V., Chase, P.A., Dijkstra, H.P., Suijkerbuijk, B.M.J.M., Mills, A.M., Spek, A.L., van Klink, G.P.M., van Koten, G. (2005) Adv. Synth. Catal. 347:447; (b) Chuchuryukin, A.V., Dijkstra, H.P., Suijkerbuijk, B.M.J.M., Klein Gebbink, R.J.M., van Klink, G.P.M., Mills, A.M., Spek, A.L., van Koten, G. (2003) Angew. Chem. Int. Edit. 42:228.

[53] Bargiggia, F.C., Murray, W.V. (2005) J. Org. Chem. 70:9636.

[54] (a) Hammerschmidt, F., Wuggenig, F. (1999) Tetrahedron: Asymmetry 10:1709; (b) Wuggenig, F., Hammerschmidt, F. (1998) Monatsh. Chem. 129:423; (c) Drescher, M., Hammerschmidt, F. (1997) Tetrahedron 53:4627; (d) Eidenhammer, G., Hammerschmidt, F. (1996) Synthesis 748; (e) Drescher, M., Hammerschmidt, F., Kahlig, H. (1995) Synthesis 1267; (f) Drescher, M., Li, Y.-F., Hammerschmidt, F. (1995) Tetrahedron 51:4933; (g) Li, Y.-F., Hammerschmidt, F. (1993) Tetrahedron: Asymmetry 4:109; (h) Heisler, A., Rabiller, C., Douillard, R., Goalou, N., Hägele, G., Levayer, F. (1993) Tetrahedron: Asymmetry 4:959.

[55] (a) Rowe, B.J., Spilling, C.D. (2001) Tetrahedron: Asymmetry 12:1701; (b) Ward, C.V., Jiang, M., Kee, T.P. (2000) Tetrahedron Lett. 41:6181; (c) Duxbury, J.P., Cawley, A., Thorton-Pett, M., Wantz, L., Warne, J.N.D., Greatrex, R., Brown, D., Kee, T.P. (1999) Tetrahedron Lett. 40:4403; (d) Groaning, M.D., Rowe, B.J., Spilling, C.D. (1998) Tetrahedron Lett. 39:5485; (e) Yokomatsu, T., Yamagishi, T., Shibuya, S. (1997) J. Chem. Soc. Perkin. Trans. 1:1527; (f) Sasai, H., Bougauchi, M., Arai, T., Shibasaki, M. (1997) Tetrahedron Lett. 38:2717; (g) Arai, T., Bougauchi, M., Sasai, H., Shibasaki, M. (1996) 61:2926; (h) Rath, N.P., Spilling, C.D. (1994) Tetrahedron Lett. 35:227; (i) Yokomatsu, T., Yamagishi, T., Shibuya, S. (1993) Tetrahedron: Asymmetry 4:1779; (j) Yokomatsu, T., Yamagishi, T., Shibuya, S. (1993) Tetrahedron: Asymmetry 4:1783.

[56] He, A., Yan, B., Thanavaro, A., Spilling, C.D., Rath, N.P. (2004) J. Org. Chem. 69:8643.

[57] Boyle, T.P., Bremner, J.B., Coates, J.A., Keller, P.A., Pyne, S.G. (2005) Tetrahedron 61:7271.

[58] Dondoni, A., Giovannini, P.P., Marra, A. (2001) J. Chem. Soc. Perkin. Trans. 1:2380.

[59] Nolen, E.G., Kurish, A.J., Potter, J.M., Donahue, L.A., Orlando, M.D. (2005) Org. Lett. 7:3383.

[60] Morokuma, K., Takahashi, K., Ishihara, J., Hatakeyama, S. (2005) Chem. Commun. 2265.

[61] (a) Bailey, P.D., Millwood, P.A., Smith, P.D. (1998) Chem. Commun. 633; (b) Schneider, J.M. (1996) In: Pelletier, S.W. (ed.) Alkaloids: Chemical and Biological Perspectives, Vol. 10, Wiley, New York, p. 155 (c) Fodor, G.B., Colasanti, G. (1985) In: Pelletier, S.W. (ed.) Alkaloids: Chemical and Biological Perspectives, Vol. 3, Wiley, New York, p. 1.

[62] Randl, S., Blechert, S. (2004) Tetrahedron Lett. 45:1167.

[63] Gebauer, J., Blechert, S. (2006) J. Org. Chem. 71:2021.

[64] (a) Zhu, L., Mootoo, D.R. (2004) J. Org. Chem. 69:3154; (b) Zhu, L., Mootoo, D.R. (2003) Org. Lett. 5:3475.

[65] Enholm, E., Low, T. (2006) J. Org. Chem. 71:2272.

[66] Cantrill, S.J., Grubbs, R.H., Lanari, D., Leung, K.C.-F., Nelson, A., Poulin-Kerstien, K.G., Smidt, S.P., Stoddart, J.F., Tirrell, D.A. (2005) Org. Lett. 7:4213.

[67] (a) Funk, T.W., Berlin, J.M., Grubbs, R.H. (2006) J. Am. Chem. Soc. 128:1840; (b) Gillingham, D.G., Kataoka, O., Garber, S.B., Hoveyda, A.H. (2004) J. Am. Chem. Soc. 126:12288; (c) Costabile, C., Cavallo, L. (2004) J. Am. Chem. Soc. 126:9592; (d) Van Veldhuizen, J.J., Garber, S.B., Kingsbury, J.S., Hoveyda, A.H. (2002) J. Am. Chem. Soc. 124:4954; (e) Seiders, T.J., Ward, D.W., Grubbs, R.H. (2001) Org. Lett. 3:3225; (f) Hoveyda, A.H., Schrock, R.R. (2001) Chem. Eur. J. 7:945.

[68] (a) Clavier, H., Audic, N., Guillemin, J.-C., Mauduit, M. (2005) J. Organomet. Chem. 690:3585; (b) Clavier, H., Audic, N., Mauduit, M., Guillemin, J.-C. (2004) Chem. Commun. 2282; (c) Audic, N., Clavier, H., Mauduit, M., Guillemin, J.-C. (2003) J. Am. Chem. Soc. 125:9248; (d) Yao, Q., Zhang, Y. (2003) Angew. Chem. Int. Edit. 42:3395; (e) Csihony, S., Fischmeister, C., Bruneau, C., Horváth, I.T., Dixneuf, P.H. (2002) New J. Chem. 26:1667; (f) Sémeril, D., Olivier-Bourbigou, H., Bruneau, C., Dixneuf, P.H. (2002) Chem. Commun. 146.

[69] (a) Thuriez, C., Olivier-Bourbigou, H., Dixneuf, P., Hillion, G. (2006) European Patent EP 1698686 A1; (b) Thuriez, C., Olivier-Bourbigou, H., Dixneuf, P., Hillion, G. (2006) US Patent US 0079704 A1.

[70] (a) Zhu, Y., Patel, J., Mujcinovic, S., Jackson, W.R., Robinson, A.J. (2006) Green Chem. 8:746; (b) Patel, J., Mujcinovic, S., Jackson, W.R., Robinson, A.J., Serelis, A.K., Such, C. (2006) Green Chem. 8:450; (c) Patel, J., Elaridi, J., Jackson, W.R., Robinson, A.J., Serelis, A.K., Such, C. (2005) Chem. Commun. 5546; (d) Mol, J.C. (2004) Top. Catal. 27:97.

[71] (a) Liang, C.O., Fréchet, J.M.J. (2005) Macromolecules 38:6276; (b) Gatard, S., Nlate, S., Cloutet, E., Bravic, G., Blais, J.-C., Astruc, D. (2003) Angew. Chem. Int. Edit. 42:452.

THE OLEFIN METATHESIS REACTIONS COMBINED WITH ORGANO-IRON ARENE ACTIVATION TOWARDS DENDRIMERS AND POLYMERS

DIDIER ASTRUC, VICTOR MARTINEZ

Nanosciences and Catalysis Group, LCOO, UMR CNRS N°5802, Université Bordeaux I, 33405 Talence Cedex, France; E-mail: d.astruc@lcoo.u-bordeaux1.fr

Abstract: The subjects treated in the two lectures of the North Atlantic Treaty Organization (NATO) summer course are (1) the combination of arene activation and perfunctionalization using organo-iron chemistry with olefin metathesis incuding metathesis of dendritic polyolefin molecules; (2) the synthesis of metallodendritic benzylidene complexes that catalyse ring-opening metathesis polymerization (ROMP) under ambient conditions and the formation of dendritic stars; (3) the use of stoichiometric and catalytic electron-transfer processes with standard reservoirs of electrons (reductants) or electron holes (oxidants) iron complexes to achieve noteworthy metathesis reactions or synthesize compounds that are useful in metathesis. Only the two first topics are treated in this chapter, and interested readers can find references concerning the third aspect called in the introduction and subsequently cited in the reference list.

Keywords: metathesis, polymerization, dendrimer, arene, iron, olefin

1. Introduction

Here we combine, for the summer school, basic principles of organometallic chemistry in the field of olefin and alkyne metathesis[1–5] with research results obtained in our group in this area.[6–15] Emphasis is given to metathesis processes yielding or dealing with nano-sized molecules such dendrimers and polymers. First, metathesis is carried out with metallocarbenic dendrimers. Metallodendritic catalysts combine the advantages of homogeneous and heterogeneous catalysts: they are soluble and perfectly well defined on the molecular level, and yet they can be recovered by precipitation, ultrafiltration, or ultracentrifugation (as biomolecules) and recycled several times. We describe a ring-opening metathesis polymerization (ROMP) process herewith yielding dendritic stars, a research project carried out in our group by Sylvain Gatard and Sylvain Nlate[8] with the collaboration of Jean-Yves Saillard and Samia Kahlal in Rennes for density functional theory (DFT) calculations, Eric Cloutet in Bordeaux for polymer studies, and George Bravic in Bordeaux for

Y. İmamoğlu and V. Dragutan (eds.), Metathesis Chemistry: From Nanostructure Design to Synthesis of Advanced Materials, 223-236.

crystallographic studies.[9] The second aspect concerns the combination of arene actition using $CpFe^+$ with olefin metathesis, these reactions being detailed for dendronic and dendritic substrates. This work was started by the PhD thesis of Victor Martinez[12,13,15] and was later continued by Denise Méry and Catia Ornelas with dendrimers (see the last section).[16] Chemio-, regio-, and steoselectivity is especially looked for.

Other points have been discussed during our two lectures at this North Atlantic Treaty Organization (NATO) summer course but will not be detailed here. Interested readers may find the appropriate quoted references below. These aspects concentrate on the implications of stoichiometric and catalytic electron-transfer processes achieved using electron–reservoir complexes[14] in metathesis reactions and related problems. The first of these aspects deals with the chemical engineering of the electron-transfer-catalyzed ligand substitutions. It can for instance be applied to very cleanly decorate phosphine dendrimers with triruthenium carbonyl clusters by catalyzing carbonyl substitution with each phosphino group of the dendrimer with Fe^I, a project performed by Ester Alonso.[6] It can also be applied to metathetic alkyne polymerization. We have indeed shown that combining rational electron-transfer-catalyzed ligand (alkyne) substitution with metathetic alkyne polymerization leads to a considerable acceleration of the reaction (r.t. instead of 100°C). In this latter area, the contribution was that of Marie-Hélène Desbois (married Delville).[17] Interestingly, chemical engineering can also control the way terminal alkynes are metathesized. Indeed, whereas the metahesis of terminal alkynes is known to provide polymers according to the Chauvin–Katz mechanism,[18] Mortreux has shown that the metathetic carbyne exchange of standard terminal alkynes can also be obtained with high selectivity.[19] The second aspect involves the synthesis of functional *N*-heterocyclic carbenes (NHC) that can be formed by deprotonation of an imadazolium salt, for instance when *t*-BuOK is not efficient, using air together with a standard electron-reservoir Fe^I complex. This very recent work is that of Denise Méry together with Jaime Ruiz Aranzaes.[20]

2. Dendritic ruthenium benzylidene catalysts that form dendrimer-cored stars with norbornene by ROMP

A few metal–carbene metallodendritic catalysts with four branches were known before our study and metathesis activity had been recorded,[2] but good recyclability was still a challenge. The difficulty resides in the need to sustain both metathesis activity and stability of the metallodendrimer. Thus, we selected the ruthenium (Ru) family of catalysts, and designed metallodendrimers containing Ru–benzylidene fragments located at the dendrimer periphery and chelating phosphine ligands on the branch termini. The choice of chelating phosphines may seem counterintuitive, because the activity of Grubbs' catalysts involves the decoordination of a phosphine from these *trans*-bis-phosphine complexes.[3] Studies by the groups of Hofmann, Fog, and Leitner, however, have shown the metathesis activity of *cis*-bis-phosphine–Ru–benzylidene catalysts.[4] We therefore used Reetz's bis-phosphines derived from the commercial polyamine DSM dendrimers.[5] These dendritic bis-phosphines are useful and versatile in metalodendritic catalysis and provided the first recyclabable metallodendritic catalysts.[5] They also very cleanly yielded, with two phenyl groups on each phosphorus atom, the first dendrimers decorated with clusters at the periphery by an efficient electron-transfer-chain reaction with [$Ru_3(CO)_{12}$)] catalyzed by [$Fe^ICp(\eta^6-C_6Me_6)$], **1**, leading to the substitution of a carbonyl by a dendritic phosphine on each tether.[6] Related dendritic bis-phosphines with two cyclohexyl groups on each phosphorus were decorated with Ru–benzylidene metathesis using Hoveyda's Ru–benzylidene metathesis catalyst[7] as a starting point. These reactions provided the four generations of new, stable metallodendrimers containing Ru–benzylidene fragments at the periphery (Scheme 1).[8] The fourth-generation metallodendrimer containing 32 Ru–benzylidene fragments, however, was found to have a rather low solubility in common organic solvents, unlike the three first-generation complexes that respectively contained 4, 8, and 16 Ru–benzylidene moieties. This weak solubility of the 32 Ru dendrimer is presumably due to steric congestion at its periphery. The x-ray crystal structure of the model mononuclear complex in which the dendritic branch was replaced by a benzyl group showed the distorted square pyramidal geometry and the classic geometric features of a Ru=C double bond (Scheme 2). The oxygen atom of the isopropyl aryl ether group is not coordinated unlike in Hoveyda's complex. The fundamental organometallic chemistry of this monomeric model complex was also original and was reported elsewhere.[9,10]

The three first generations of metallodendrimers **2** and the model complex were efficient catalysts for the ROMP of norbornene under ambient conditions, giving dendrimer-cored stars (Scheme 2).[23] Analysis of the molecular weights by size exclusion chromatography (SEC) gave data that were close to the theoretical ones, which indicated that all the branches were efficiently polymerized (yet, given the PDI that is modest around 2 as usual, polymer stars contain large defects on branches). Dendritic-cored stars with an average of about 100 norbornene units on each dendritic branch were synthesized with the three first generations of Ru–carbene dendrimers containing respectively 4, 8, and 16 Ru=C bonds.

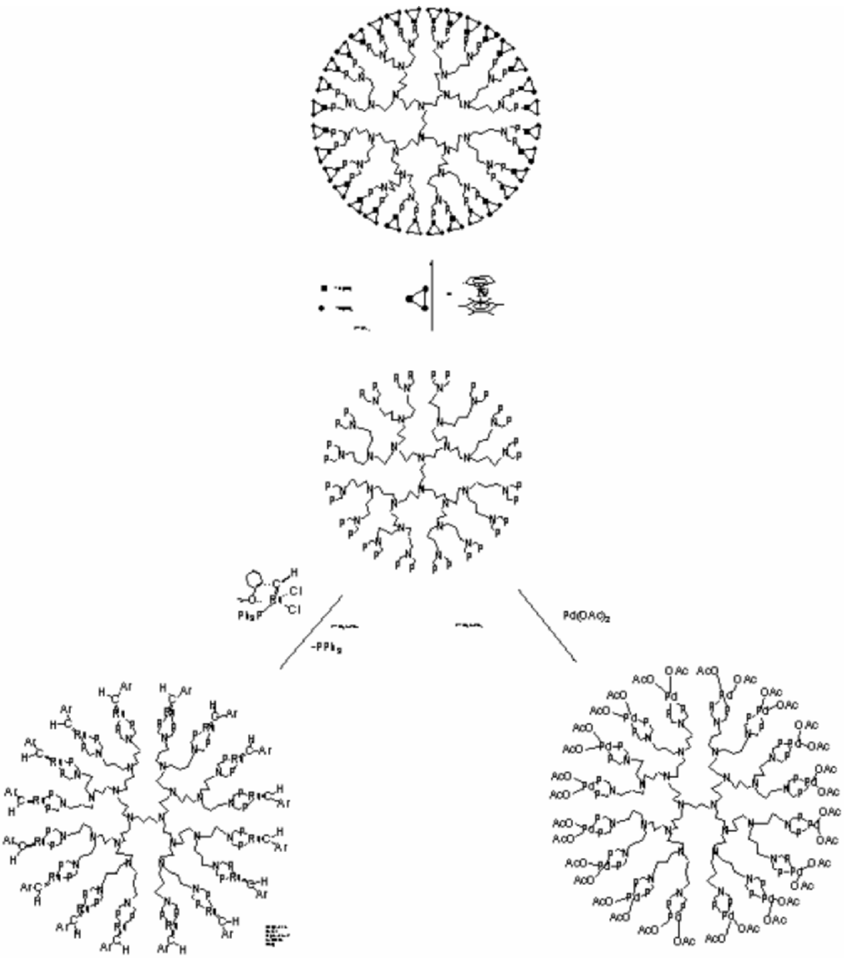

Scheme 1. Synthesis of various third-generation metallodendrimers from dendritic bis-phosphines.

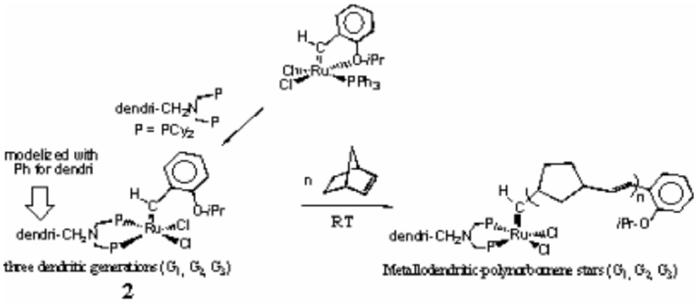

Scheme 2. Strategy for the ROMP of norbornene by Ru–benzylidene dendrimers to form dendrimer-cored stars.

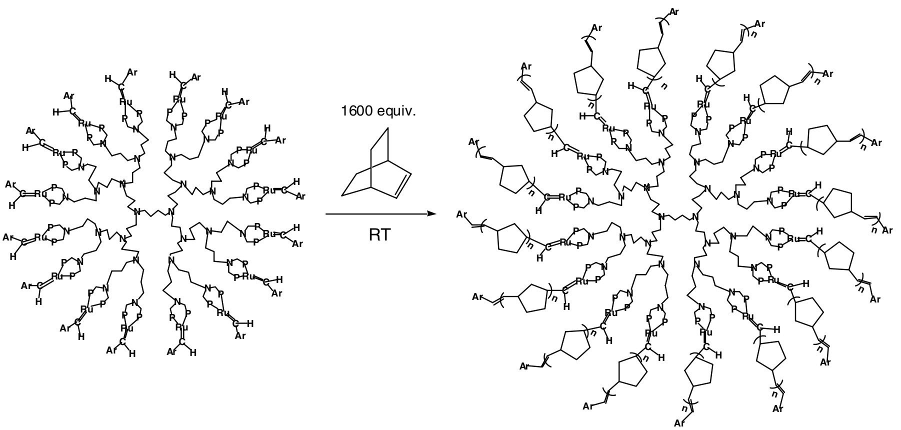

Equation 1. Third-generation (16 Ru atoms) ruthenium–benzylidene dendrimer that catalyzes the ROMP of norbornene at 25°C to form dendrimer-cored stars. With 100 norbornene units on each branch, the polymerization is living (i.e. can be continued by adding more norbornene)

Two kinds of dendritic effect were found upon analysis of the kinetic data[23,24]:

1. The dendrimers were more efficient catalysts than the monomeric model complex. This could possibly be due to labilization of metal–phosphine bonds that is facilitated in dendrimers as compared to the monomer for entropic reasons. Indeed, DFT calculation showed that the catalytic process must involve decoordination of a phosphorus atom, since the interaction of the olefin with the diphosphine complex is nonbonding.[24] The dendritic Ru–benzylidene dendrimers were air-sensitive contrary to the monomer model complex, consistent with more rapid dissociation of the alkyl phosphine in the dendrimers than in the monomer.
2. The efficiency of catalysis decreased upon increasing the dendrimer generation. This second dendritic effect is thus a negative one, and it is probably related to the more difficult access to the metal center due to the increasing steric effect at the dendrimer periphery when the generation increases.

The analogous Ru–benzylidene dendrimers were very recently synthesized with two tertiobutyl groups on each phosphorus and they were slightly more reactive ROMP catalysts for the polymerization of norbornene than those involving the cyclohexyl substituents.[10] These new dendritic ligands proved very efficient in palladium catalysis.

3. Combining $CpFe^+$-induced arene perfunctionalization with olefin metathesis

The hexahapto complexation of arenes by the cationic group $CpFe^+$ considerably increases the acidity of its benzylic protons (the *p*Ka's of the arenes in DMSO are lowered upon complexation with $CpFe^+$ by approximately 15 units, for instance from **43** to **28** for C_6Me_6).[11] Therefore, deprotonation of the $CpFe(arene)^+$ complexes is feasible under mild conditions with KOH. Deprotonated $CpFe(arene)^+$ complexes are good nucleophiles and reaction with electrophiles such as the alkylhalides leading to the formation of new C–C bonds. Coupling the deprotonation and the nucleophile attack reactions in situ in the presence of excess substrates leads to perfunctionalized in casacade multistep reactions. When the electrohile is allyl bromide, polyolefin compounds are produced, and these compounds are ideal substrates for ring-closing metathesis (RCM) and cross-metathesis (CM) as exemplified below.

RCM of iron complexes containing two allyl groups per benzylic position. The diallyl ethylbenzene complex **4** was obtained from **3** using allyl bromide in KOH/DME. Upon metathesis, **4** yields **5** using the catalyst **1** in dichloromethane at room temperature. Separation of the catalyst was very easy, because of the cationic character of the $CpFe(arene)^+$ complex.

Similarly, perallylation of **6** gave **7** whose metathesis reaction catalyzed by **1** yielded the dicyclopentenyl complex **8**.[12]

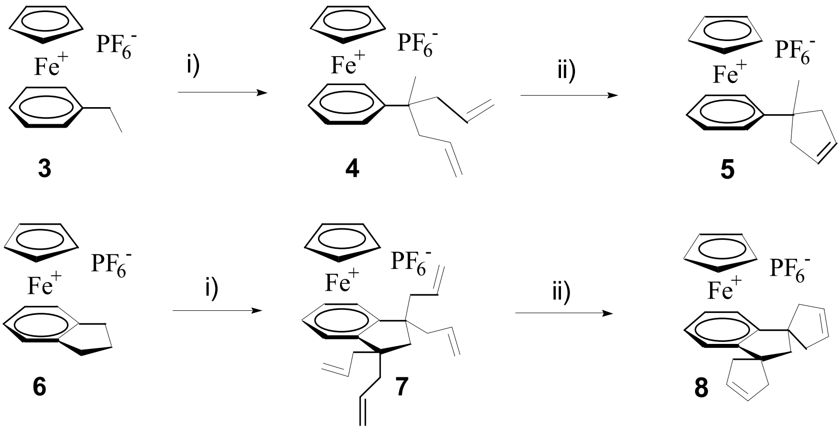

Scheme 3. (i) Allyl bromide, KOH, DME; (ii) $[Ru(PCy_3)_2Cl_2(=CHPh)]$, **1**, CH_2Cl_2, r.t.

The $[\text{CpFe(octaallyldurene)}^+][\text{PF}_6^-]$ 10 complex was obtained in one-pot octaallylation using **9**, allyl bromide, and KOH in THF instead of DME. The allyl groups of **10** were cyclized in dichloromethane giving **11**. The iron-free organic compound **12** was obtained by photolysis of **10** using visible light in the presence of PPh_3. The RCM was successfully applied to **12** yielding **13**. In order to obtain **13**, it was more convenient, however, to use the photolysis of the cationic iron complex **11**, because the metathesis product was easily separated from the catalyst **1** at the level of the cationic compound **11**.

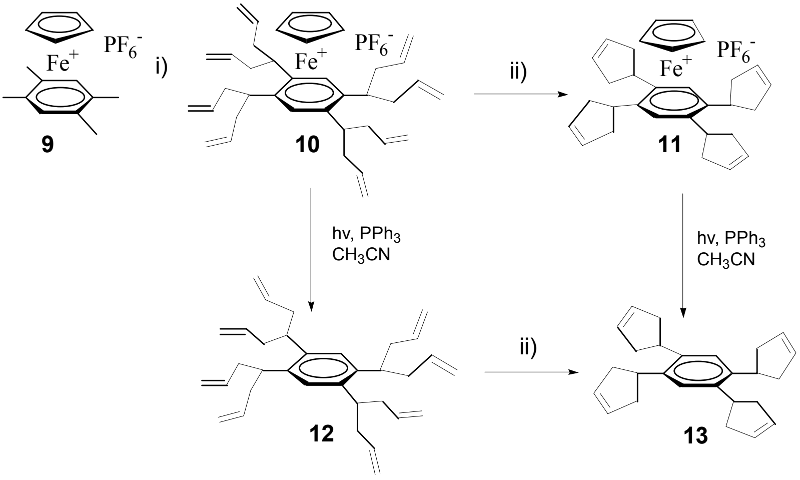

Scheme 4. (i) Allyl bromide, KOH, DME; (ii) $[\text{Ru(PCy}_3)_2\text{Cl}_2(\text{=CHPh})]$, **1**, CH_2Cl_2, r.t.

Reactions of metathesis over hexaallyl-*p*-xylene derivates. The complex [CpFe(triallyltoluene)+][PF6⁻] **15** complex was easily obtained by CpFe+ induced perallylation of **14** using KOH and allyl bromide in DME. The RCM of the triallylated compound **15** catalyzed by **1** in dichloromethane yielded **16** at room temperature. Only by heating at 60°C, **1** could catalyze the CM of **16** to form **17**. On the other hand, metathesis reaction of the decomplexed triallylated compound **18** catalyzed by **1** at room temperature produced mixtures of **19** and **20** (corresponding RCM and CM products). In order to avoid the formation of the dimeric compound **20** and easily isolate **19**, we decomplexed the organometallic RCM product **16**.[12]

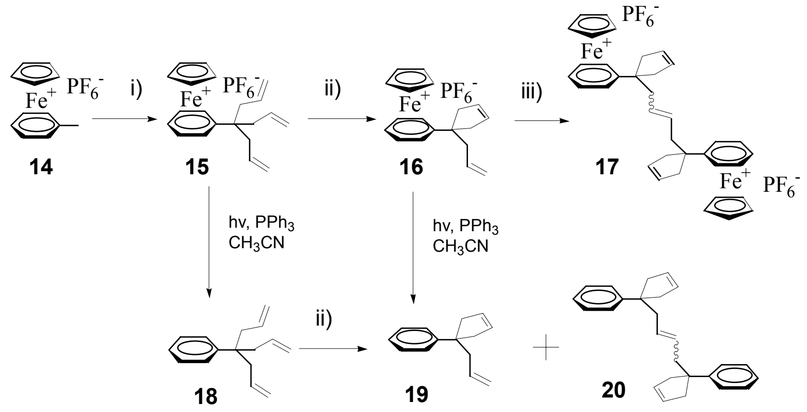

Scheme 5. (i) Allyl bromide, KOH, DME; (ii) $[Ru(PCy_3)_2Cl_2(=CHPh)]$, **1**, CH_2Cl_2, r.t.; (iii) $[Ru(PCy_3)\{C(N(mesityl)CH)_2\}Cl_2(=CHPh)]$, **2**, $C_2H_4Cl_2$, 60°C.

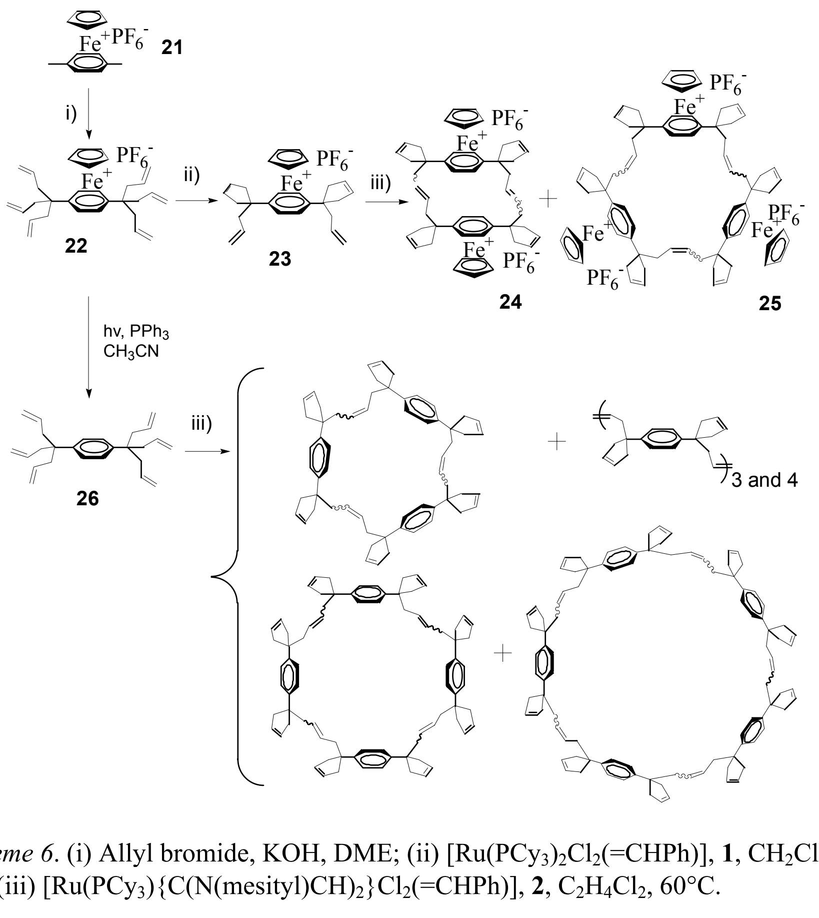

Scheme 6. (i) Allyl bromide, KOH, DME; (ii) $[Ru(PCy_3)_2Cl_2(=CHPh)]$, **1**, CH_2Cl_2, r.t.; (iii) $[Ru(PCy_3)\{C(N(mesityl)CH)_2\}Cl_2(=CHPh)]$, **2**, $C_2H_4Cl_2$, 60°C.

Reactions of metathesis over hexaallyl-*p*-xylene derivates. The complex [CpFe(hexaallyl-*p*-xylene)$^+$][PF$_6^-$] 22 was also obtained by perallylation of [CpFe(*p*-xylene)$^+$][PF$_6^-$] 21. Its metathesis reaction catalyzed by **1** at room temperature gave the RCM product **23** selectively that keeps two terminal olefins in *para,* too far away to interreact. However, by heating at 60°C and using **2** as CM catalyst, these two olefins led to the formation of oligomers. Due to the reversibility of the metathesis reaction that works under thermodynamic control, the final products of CM were **24** and **25**. Metathesis of **26** with **1** at room temperature afforded **27** and a mixture of cyclic and linear oligommers. In order to obtain **27**, an organometallic route was necessary; from decomplexation of oligomer-free **23** was obtained pure.[13]

Metathesis of nonaallylmesitylene derivatives. The activation of mesitylene by the CpFe$^+$ moiety followed by a one-pot perallylation yielded [CpFe(nonaallylmesitylene)$^+$][PF$_6^-$], **29**. After its triple RCM reaction catalyzed by **1**, **30** was isolated. Furthermore and interestingly, when the metathesis reaction was carried out in refluxing dichloroethylene and upon adding catalyst **2**, the cage compound **31** was formed. Similarly, the iron-free nonaallylated compound **32** gave **33** by metathesis and the organic cage **34**. After hydrogenation with H_2/Pd/C in CH_2Cl_2 of this tripled-briged cage, the single product **35** is isolated. The ^{1}H NMR signals of the β-hydrogens are shifted upfield at 0.64 ppm.

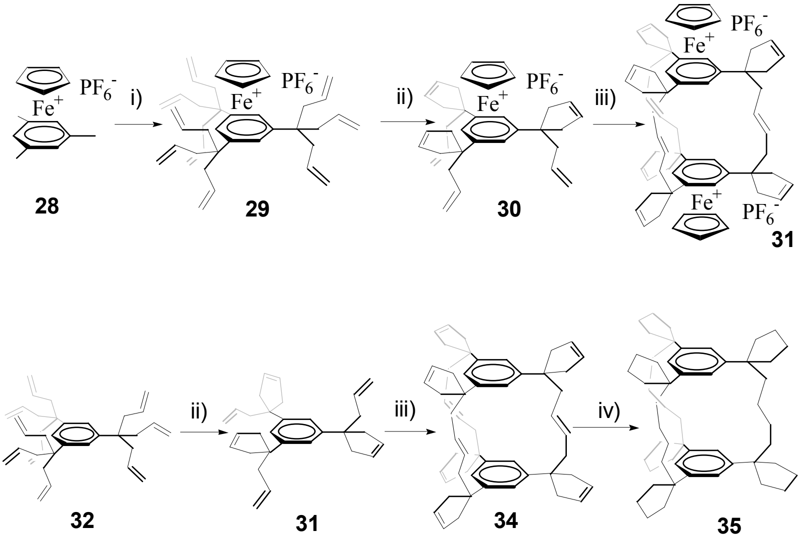

Scheme 7. (i) Allyl bromide, KOH, DME; (ii) [Ru(PCy$_3$)$_2$Cl$_2$(=CHPh)], 1, CH_2Cl_2, r.t.; (iii) [Ru(PCy$_3$){C(N(mesityl)CH)$_2$}Cl$_2$(=CHPh)], 2, $C_2H_4Cl_2$, 60°C; (iv) H_2 Pd/C CH_2Cl_2.

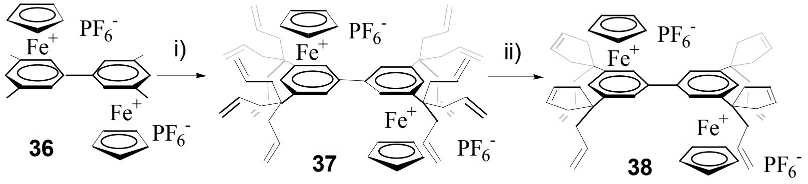

Scheme 8. (i) Allyl bromide, KOH, DME; (ii) [Ru(PCy$_3$)$_2$Cl$_2$(=CHPh)], **1**, CH$_2$Cl$_2$, r.t.

RCM of a dodecaallylated bimetallic complex. 3,3′,5,5′-tetramethylbyphenyl was coordinated to two CpFe$^+$ groups by reaction of this arene with ferrocene using the standard conditions yielding the bimetallic complex **36**. The perallylation reaction of **36** gave the dodecaallylated derivate **37**. Finally, RCM of **37** catalyzed by **1** yielded the tetrapentenyl compound **38**.

RCM of a decallylated cobalticinium. Pentamethylcobalticinium **39** was perallylated to yield a decaallylated cobalticinium **40**, then RCM of the organometallic complex proceeded to afford **41** using the catalyst **1**.[12]

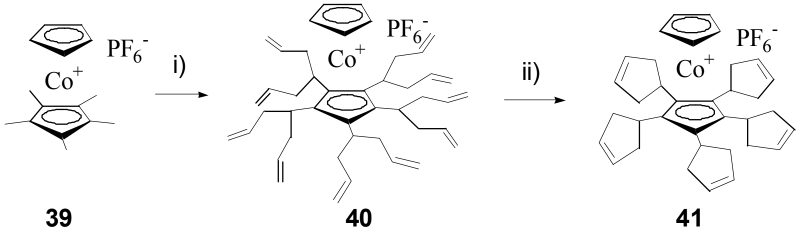

Scheme 9. (i) Allyl bromide, KOH, DME; (ii) [Ru(PCy$_3$)$_2$Cl$_2$(=CHPh)], **1**, CH$_2$Cl$_2$, r.t.

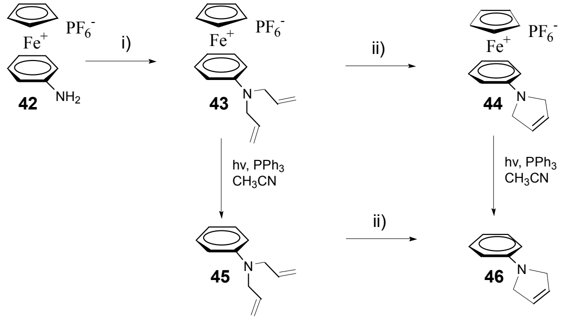

Scheme 10. (i) Allyl bromide, KOH, DME; (ii) [Ru(PCy$_3$)$_2$Cl$_2$(=CHPh)], **1**, CH$_2$Cl$_2$, r.t.

RCM of an iron complex containing an *N* heteroatom. The complex [CpFe(aniline)$^+$][PF$_6^-$] 42 may be obtained by direct ligand exchange from aniline, but the yields is low (10%). An alternative method is the synthesis from [CpFe(chlorobenzene)$^+$][PF$_6^-$] by amination with ammonia in dichloromethane, or even better ("greener"), in water at 60°C. The diallylated product **43** was obtained by reaction of **42** with allyl bromide and KOH in THF. The metathesis with **1** yielded the cyclopenteneaniline iron complex **44**. Decomplexation of **42** or **43** is not possible by photolysis; it is necessary to use an exergonic single-electron reduction with one equivalent of the 19-electron complex [CpFe^I(hexamethylbenzene)].[14] Metathesis of the iron-free diallylaniline **45** yielded the *N*-phenyl–pyrroline derivate **46** using **1**.[12]

Macrocycles. The complex [CpFe(*p*-isopropylbenzenze)$^+$][PF$_6^-$] **47** is ideal for building a family of *p*-dialkenylaryl derivatives. In order to obtain organometallic [*n*] paracyclophanes, dialkenylcomplex were synthesized with longer chains. Dialkenylation of the *p*-diisopropylbenzene complex **47** with a ω-alkenyl halide allowed the preparation of a large variety of paradisubstituted substrates and intramolecular metathesis may led to the desired paracyclophanes. Dialkenylation with 5-bromopentene or 6-bromohexene gave **48** and **49**, respectively. Using **1** as catalyst in chloroform at room temperature, the substrate **48** led to a mixture of linear oligomers (2 to 6 units) and mono-, bi-, and trimetallic paracyclophanes identified by their molecular peaks in the MALDI TOF mass spectrum. On the other hand, **49**, containing alkenyl chains that are one methylene unit longer than in **48**, selectively led to the cyclophane product **50**. In the ^{1}H NMR spectra of **19**, the signals of the β-hydrogens of the cyclophanes are shifted at 0.51 ppm because of the aromatic anisotropy.[13]

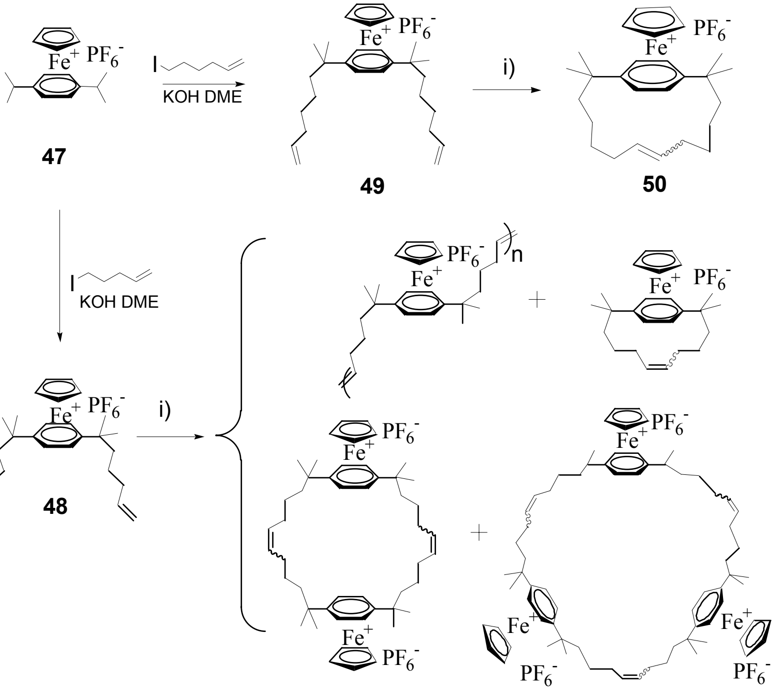

Scheme 11. (i) [Ru(PCy$_3$)$_2$Cl$_2$(=CHPh)], **1**, CH$_3$Cl, r.t.

The preparation of the hexabutenyl complex **52** by selective hexaallylation of [CpFe(hexamethylbenzenze)$^+$][PF$_6^-$], **51**, was easily carried out using KOH and allyl bromide in THF. The metathesis of the terminal olefins of **52** in dichloromethane led to a yellow precipitate that was insoluble in all solvents. The MALDI TOF spectra of the soluble intermediates during the reaction, shows the formation of **53**. Nevertheless, its concentration was low and the equilibrium was always displaced towards the irreversible formation of insoluble polymeric products. CM of **52**, as well as ROMP of **53** may indeed form reticulated polymers.[15]

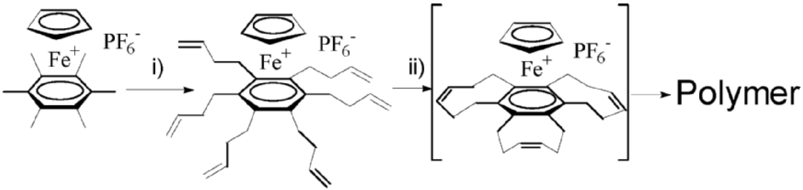

51 **52** **53**

Scheme 12. (i) Allyl bromide, KOH, DME; (ii) [Ru(PCy$_3$)$_2$Cl$_2$(=CHPh)], **1**, CH$_2$Cl$_2$, r.t.

4. Chemio-, regio-, and streospecific cross metathesis of terminal double bonds of dendritic tethers

As shown by Bechert's and Grubbs' groups,[16,17] it is possible to cross metathesize terminal olefins with olefins bearing a strongly electron-withdrawing substituent such as CO$_2$H or CO$_2$Me. This selectivity can be usefully applied to functionalize polyolefin dendrimers and even solubilize them in water using the carboxylate substituent. For this purpose, it is necessary to use the second-generation ruthenium metathesis catalyst (Scheme 13).[18,19]

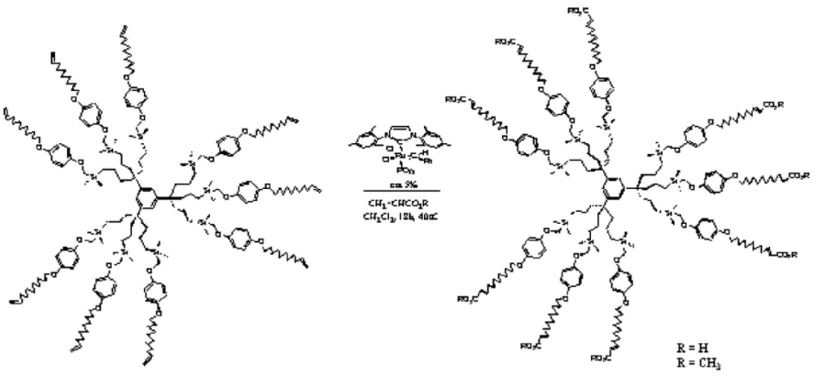

Scheme 13. Selective cross-metathesis of polyolefin dendrimers using acrylic acid or methyl acrylate.

Acknowledgment

Contributions to ideas and efforts by our colleagues and students who have collaborated to this chemistry are gratefully acknowledged (see text and references) as is financial support from the Institut Universitaire de France, the CNRS, and the University Bordeaux I.

References

[1] Grubbs, R.H. (ed.), Handbook of Metathesis, Wiley-VCH, Weinheim, 2002.
[2] (a) Wijkens, P., Jastrzebski, J.T.B.H., van der Schaaf, P.A., Kolly, R., Hafner, A., van Koten, G., Org. Letters 2000, 2:1621; (b) Garber, S.B., Kingsbury, J.S., Gray, B.L., Hoveyda, A.H., J. Am. Chem. Soc. 2000, 122:8168; (c) Beerens, H., Verpoort, F., Verdonck, L., J. Mol. Cat. 2000, 151:279; 159:197; (d) Sanford, M.S., Ulman, M., Grubbs, R.H., J. Am. Chem. Soc. 2001, 123:749.
[3] Trnka, T.M., Grubbs, R.H., Acc. Chem. Res. 2001, 34:18.
[4] (a) Hansen, S.M., Volland, M.A.O., Rominger, F., Eisenträger, F., Hofmann, P., Angew. Chem. Int. Edit. 1999, 38:1273; (b) Hansen, S., Rominger, F., Metz, M., Hofmann, P., Chem. Eur. J. 1999, 5:557; (c) Adlhart, C., Volland, M.A.O., Hofmann, P., Chen, P., Helv. Chim. Acta 2000, 83:3306; (d) Amoroso, D., Fogg, D.E., Macromolecules 2000, 33:2815; (e) Six, C., Beck, K., Wegner, A., Leitner, W., Organometallics 2000, 19:4639.
[5] Reetz, M.T., Lohmer, G., Schwickardi, R., Angew. Chem. Int. Edit. 1997, 36:1526.
[6] Alonso, E., Astruc, D., J. Am. Chem. Soc. 2000, 122:3222.
[7] Kingsbury, J., Harrity, J.P.A., Bonitatebus, P.J., Hoveyda, A.H., J. Am. Chem. Soc. 1999, 121:791.
[8] Gatard, S., Nlate, S., Cloutet, E., Bravic, G., Blais, J.-C., Astruc, D., Angew. Chem. Int. Edit. 2003, 42:452.
[9] Gatard, S., Kahlal, S., Méry, D., Nlate, S., Cloutet, E., Saillard, J.-Y., Astruc, D., Organometallics 2004, 23:1313.
[10] Méry, D., Astruc, D., J. Mol. Cat. A. 2005, 227:1.
[11] (a) Astruc, D. (ed.), Modern Arene Chemistry, Wiley-VCH, Weiheim, 2002; (b) Astruc, D., Nlate, S., Ruiz, J., in ref. 11a, p. 400.
[12] Martinez, V., Blais, J.-C., Astruc, D., Org. Letters 2002, 4:651.
[13] Martinez, V., Blais, J.-C., Angew. Chem. Int. Edit. 2003, 42:4366.
[14] Astruc, D., Electron Transfer and Radical Processes in Transition Metal Chemistry, VCH, New York, Chapters 3, 6, 1995.
[15] Martinez, V., Blais, J.-C., Bravic, G., Astruc, D., Organometallics 2004, 23:861.
[16] Ornelas, C., Méry, D., Ruiz, J., Blais, J.-C., Cloutet, E., Astruc, D., Angew. Chem. Int. Edit. 2005, 44:7399.
[17] (a) Desbois, M.-H., Astruc, D., J. Chem. Soc. Chem. Commun. 1988, 472; (b) Desbois, M.-H., Astruc, D., New J. Chem. 1989, 13:595; (c) Astruc, D. Acc. Chem. Res. 1991, 24:36.

[18] Katz, T.J., Lee, S.J., J. Am. Chem. Soc.1980, 102:422.

[19] (a) Mortreux, A., Petit, F., Petit, M., Szymanska-Buzar, T., J. Mol. Catal. A: Chem. 1995, 96:95; (b) Mortreux, A., Coutelier, O., J. Mol. Cat. A.: Chem. 2006, 254:96.

[20] Méry, D., Aranzaes, J., Astruc, D., J. Am. Chem. Soc. 2006, 128:5602–5603.

OLEFIN METATHESIS WITH RUTHENIUM–ARENE CATALYSTS BEARING *N*-HETEROCYCLIC CARBENE LIGANDS

LIONEL DELAUDE,* ALBERT DEMONCEAU

Center for Education and Research on Macromolecules, Institut de Chimie (B6a), Institute of Chemistry, University of Liège, Sart-Tilman par B-4000 Liège, Belgium

Abstract: In this chapter, we summarize the main results of our investigations on the ring-opening metathesis polymerization (ROMP) of cyclooctene catalyzed by various ruthenium (Ru)–arene complexes bearing imidazolin-2-ylidene, imidazolidin-2-ylidene, or triazolin-5-ylidene ligands. Three major findings emerged from this study. First, we underscored the intervention of a photochemical activation step due to visible light illumination. Second, we established that the presence of an endocyclic double bond in the carbene ligand central heterocycle was not crucial to achieve high catalytic efficiencies. Third, we demonstrated that *ortho*-metallation of the *N*-heterocyclic carbene (NHC) ligand by the Ru center led to inactive catalysts.

Keywords: cyclooctene, homogeneous catalysis, imidazole, *ortho*-metallation, ring-opening metathesis polymerization (ROMP), triazole

1. Introduction

Ruthenium (Ru)–arene complexes[1–4] are versatile and efficient catalyst precursors for various important organic transformations.[5–10] This is due in part to the lability of the h^{6}-arene ligand that can be easily removed upon thermal[11] or photochemical[12–14] activation to release highly active, coordinatively unsaturated species. During the 1990s, we demonstrated that [RuCl$_2$(*p*-cymene)(PR$_3$)] complexes bearing basic and bulky phosphine ligands, such as tricyclohexylphosphine (PCy$_3$, see structure **1**), were highly effective pre-catalysts for the ring-opening metathesis polymerization (ROMP) of both strained and low-strain cycloolefins when activated by a suitable carbene precursor such as trimethylsilyldiazomethane (TMSD).[15,16] Although we were not able to isolate the active species formed upon addition of the cocatalyst and monomer to the Ru–arene starting material, ^{1}H NMR and ^{31}P NMR analyses of the reaction

---

[*] To whom correspondence should be addressed. Lionel Delaude, Center for Education and Research on Macromolecules (CERM), Institut de Chimie (B6a), University of Liège, Sart-Tilman par B-4000 Liège, Belgium. E-mail: l.delaude@ulg.ac.be

Y. İmamoğlu and V. Dragutan (eds.), Metathesis Chemistry: From Nanostructure Design to Synthesis of Advanced Materials, 237-250.

media supported the intermediacy of Ru–alkylidene complexes of the Grubbs type as actual ROMP initiators (Scheme 1).[16]

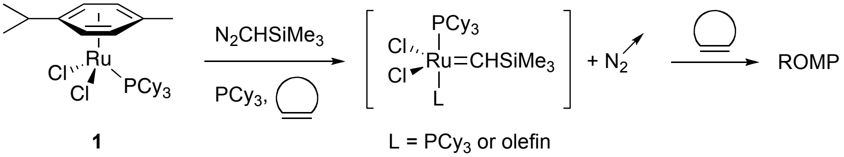

Scheme 1. Possible mechanism for the formation of metathetically active alkylidene species from ruthenium–arene complexes in the presence of TMSD.

The past decade also witnessed the experimental reality of stable nucleophilic *N*-heterocyclic carbenes (NHCs), which were first isolated and characterized by Arduengo and coworkers in 1991.[17–20] These divalent carbon species are neutral, two-electron ligands with only little π-back-bonding tendency.[21] They behave as phosphine mimics, yet they are better σ-donors and they form stronger bonds to metal centers than most phosphines. Their electronic and steric properties are liable to ample modifications simply by varying the substituents on the heterocyclic ring. Therefore, NHCs have become ubiquitous ligands in organometallic chemistry and catalysis.[22–25] They have also acquired a place on their own as reagents and catalysts in organic synthesis, since they behave as powerful nucleophilic agents.[26–28]

Most NHCs investigated so far derive from imidazole or triazole (Figure 1). These five-membered electron-rich heterocycles provide a suitable framework that stabilizes the carbene center located between two nitrogen atoms. An extensive range of imidazolin-2-ylidene or imidazolidin-2-ylidene derivatives has already been prepared by varying the nature of the substituents on the heterocyclic ring and/or by adding or removing the C4–C5 endocyclic double bond.[29] Triazole-based compounds are less common. Only a few representatives of this class of stable carbenes have been described so far by Enders and coworkers.[30,31] Noteworthily, introduction of a chiral R^1 group on the triazolin-5-ylidene ring system proved a successful strategy to induce asymmetry in various organic or organometallic catalytic processes.[32]

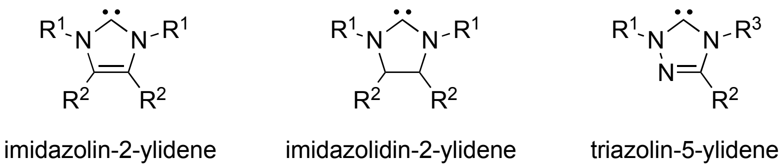

Figure 1. Stable *N*-heterocyclic carbenes derived from imidazole or triazole.

To further expand the scope of Ru–arene catalyst precursors in olefin metathesis, we have investigated the replacement of phosphine ligands by NHC species, either preformed or generated in situ, in monometallic dichlororuthenium complexes of the [$RuCl_2$(*p*-cymene)(L)] type.[33] In this contribution, we summarize the main results that were obtained with both imidazole- or triazole-based ancillary ligands for the ROMP of cyclooctene.

2. Ruthenium–arene catalysts bearing imidazolin-2-ylidene and imidazolidin-2-ylidene ligands

2.1 Preformed catalysts

Complexes **2**–**10** bearing a variety of imidazolin-2-ylidene ligands were prepared from [$RuCl_2$(*p*-cymene)]$_2$ and the corresponding unsaturated NHCs according to literature procedures (Eq. 1).[34,35] The free carbene ligands were obtained from the parent imidazole-2(3*H*)-thiones (in the case of **2**, **3**, **5**, **7**)[36] or from imidazolium chlorides (for **4**, **6**, **8**, **10**)[18,19] by reduction with potassium or deprotonation with potassium *tert*-butoxide or hydride, respectively. The dichlorocarbene in **9** was the adduct of 1,3-dimesitylimidazolin-2-ylidene and CCl_4.[37] Complex **11** sporting the saturated imidazolidin-2-ylidene ligand commonly referred to as SIMes (or H_2IMes)[17,19] was obtained in a similar way by reacting [$RuCl_2$(*p*-cymene)]$_2$ with a stoichiometric amount of the free carbene ligand (Eq. 2).

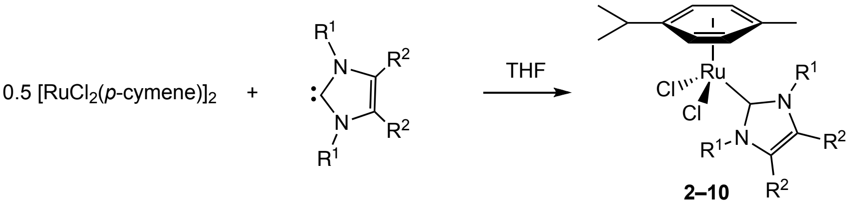

2–10

(1)

2 $R^1 = R^2 =$ Me
3 $R^1 =$ *i*-Pr, $R^2 =$ Me
4 $R^1 =$ *i*-Pr, $R^2 =$ H
5 $R^1 =$ Cy, $R^2 =$ Me
6 $R^1 =$ Cy, $R^2 =$ H
7 $R^1 =$ Mes, $R^2 =$ Me
8 $R^1 =$ Mes, $R^2 =$ H
9 $R^1 =$ Mes, $R^2 =$ Cl
10 $R^1 =$ Diip, $R^2 =$ H

Cy = cyclohexyl Diip = 2,6-diisopropylphenyl Mes = 2,4,6-trimethylphenyl

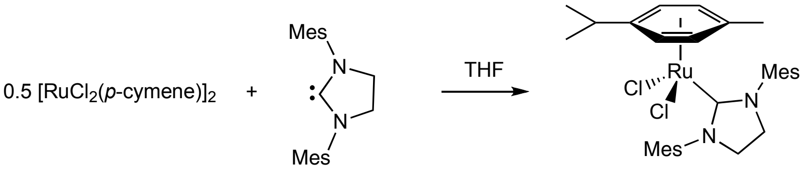

11

(2)

Polymerization of cyclooctene in chlorobenzene for 4 h at 60°C was elected as a test reaction for our catalytic screening. These experimental conditions, complemented by TMSD initiation, were found optimal in our previous studies with the phosphine-based complex **1**.[15,16] Transposed to the case of Ru–NHC catalyst precursors, they led to dichotomous results. Complexes **2**–**6** bearing alkyl-substituted imidazolin-2-ylidene ligands were devoid of any significant activity for the ROMP of cyclooctene, even in the presence of the TMSD carbene precursor. With the 250:1 monomer to Ru ratio adopted for our study, conversions stagnated below 16% and no polymer was isolated after 4 h at 60°C. Aryl-substituted ligands, on the other hand, afforded polyoctenamer in moderate to high yields (Table 1). Complexes **7** and **11** were only poorly active and led to high-molecular weight polymers that remained insoluble in tetrahydrofuran (THF) and could not be subjected to gel permeation chromatography (GPC) analysis. With complexes **8**–**10**, gelation of the reaction mixtures occurred within a few minutes and a near quantitative yield of polyoctenamer was obtained within 4 h at 60°C. When the reaction temperature was lowered to ~20°C, this remarkable high activity was maintained.[38]

Table 1. ROMP of cyclooctene using complexes **7**–**11** as catalyst precursors[a]

Catalyst precursor	Temperature (°C)	Isolated yield (%)	s_{cis}[b]	$10^{-3}\ M_n$[c]	M_w/M_n[c]
7	60	12	0.48	Insoluble polymer	
8	60	85	0.19	429	2.02
9	60	91	0.22	624	1.29
10	60	88	0.20	462	1.82
11	60	62	0.47	Insoluble polymer	
8	20	84	0.27	625	2.00
10	20	76	0.26	550	2.22

[a] Experimental conditions: cyclooctene (7.5 mmol) and a catalyst precursor (0.03 mmol) were reacted in PhCl (5 mL) under inert atmosphere for 4 h
[b] Fraction of *cis* double bonds within the polyoctenamer, determined by ^{13}C NMR
[c] Determined by GPC in THF vs. monodisperse polystyrene standards

Most interestingly, we found that the polymerization of cyclooctene with catalysts **8**–**10** performed equally well in the absence of TMSD, whereas the addition of a diazo compound was a requisite with complex **1**.[15,16] Conversely, the presence of light played a key role in the nucleophilic carbene-based system. Indeed, the intervention of a photochemical activation step was evidenced from the results gathered in Table 2. In the darkness, a mere 20% yield of polymer was obtained after 2 h at room temperature. Normal lighting in the laboratory, a combination of daylight and of fluorescent light, was sufficient to raise the conversion to 93% within the same period of time. More intense visible light sources brought the reaction to completion while ensuring reproducible conditions. Thus, recourse to an ordinary 40 W "cold white" fluorescent tube or to a 250 W incandescent light bulb standing 10 cm away from the standard Pyrex reaction flasks afforded quantitative yields of polyoctenamer. The differences in the emission spectra of the two light sources did not have any incidence on the polymer microstructure. In both cases, the polyoctenamer obtained was mainly *trans* and had a relatively narrow molecular weight distribution.[38]

Table 2. Effect of light on the ROMP of cyclooctene at room temperature using complex **8** as catalyst precursor[a]

Lighting conditions	Monomer conversion[b] (%)	Isolated yield (%)	s_{cis}[c]	$10^{-3}\ M_n$[d]	M_w/M_n[d]
Darkness	22	20	0.36	21	1.53
Normal	93	84	0.27	625	2.00
Neon tube	99	93	0.17	553	1.33
Light bulb	>99	91	0.18	537	1.33

[a] Experimental conditions: cyclooctene (7.5 mmol) and complex **8** (0.03 mmol) were reacted in PhCl (5 mL) at room temperature for 2 h under inert atmosphere
[b] Determined by GC
[c] Fraction of *cis* double bonds within the polyoctenamer, determined by ^{13}C NMR
[d] Determined by GPC in THF vs. monodisperse polystyrene standards

2.2 Catalysts generated in situ

We next examined the possibility of generating Ru–arene catalysts bearing aryl-substituted NHC ligands in the presence of cycloalkene monomers instead of having to synthesize and isolate them prior to ROMP experiments. We found that a 1:2:4 molar association of $[\text{RuCl}_2(p\text{-cymene})]_2$, 1,3-dimesitylimidazolium chloride, and potassium *tert*-butoxide was almost as effective as the preformed complex **8** in the polymerization of cyclooctene at 60°C. Because only stable and readily available commercial reagents were needed to release the active catalytic species in situ, such a polymerization procedure was very simple and straightforward to implement.[38] Recourse to a similar three-component catalytic system to activate the [RuCl$_2$(*p*-cymene)]$_2$ dimer had already been reported by Dixneuf and coworkers for the enyne metathesis reaction,[39,40] while Nolan et al. have used NHCs produced in situ by deprotonation of imidazolium salts to act as ancillary ligands in various palladium-catalyzed coupling reactions.[41–45]

We have taken advantage of the ease of generating Ru–NHC complexes in situ to help define structure–activity relationships for imidazolin-2-ylidene and imidazolidin-2-ylidene derivatives used as ancillary ligands in metathesis catalysts. For this purpose, a wide range of new imidazolium and imidazolinium chlorides bearing aromatic substituents was synthesized. These ionic precursors were deprotonated with potassium *tert*-butoxide or sodium hydride and combined with [RuCl$_2$(*p*-cymene)]$_2$ in chlorobenzene at 60°C. Cyclooctene was then added and its polymerization was allowed to proceed for 2 h under visible light illumination (Eq. 3).[46]

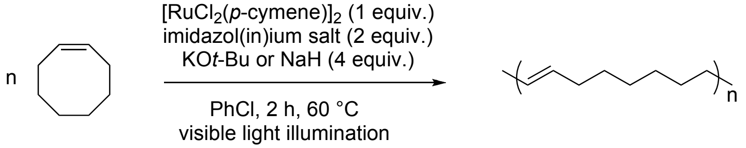

(3)

In a first part of our screening, we probed the catalytic activity of imidazolium chlorides **12**–**16** in the presence of potassium *tert*-butoxide. With the 4-biphenyl derivative **12**, monomer conversion reached 24% but the ring-opening probably stopped at the oligomerization stage and no polymer was isolated. In the presence of the *ortho*-tolyl-substituted salt **13**, no reaction at all occurred after 2 h at 60°C. As previously noted, a mixture of 1,3-dimesitylimidazolium chloride **15**, [RuCl$_2$(*p*-cymene)]$_2$ and KO*t*-Bu was almost as efficient as the preformed complex **8** under the experimental conditions adopted. Within the time allowed for the reaction to proceed, monomer conversion was essentially quantitative and a high-molecular weight polymer containing mostly *trans* double bonds was formed in almost quantitative yield (Table 3). The absence of the *para*-methyl groups in compound **14** did not alter its catalytic activity compared to **15**. This result did not come as a surprise, since the structural change between the two ligands affects only a position remote from the metal center. Switching from methyl to isopropyl groups on both ortho positions of the aryl substituents by replacing **14** or **15** with **16** caused a much more significant change in terms of steric occupancy around the Ru atom. A rather high catalytic activity was, however, maintained.

Further insight into the influence of the NHC ligand structure on the polymerization of cyclooctene came from the study of imidazolinium salts **17**–**24** in a second series of ROMP experiments. Compounds **17**–**19** bearing, respectively, phenyl, 1-naphthyl, and 3,5-dimethylphenyl units on their nitrogen atoms did not afford any polyoctenamer. In all three cases, monomer consumption stagnated below 10% after 2 h at 60°C. The *N,N′*-di(4-biphenyl) derivative **20** and the *N,N′*-di(2-tolyl) salt **21** were slightly more active, with conversions now in the 20–30% range, but oligomers – and no polymers – still accounted for these figures. In sharp contrast with these results, satisfactory to quantitative conversions were achieved with imidazolinium chlorides **22**–**24** (see Table 3).

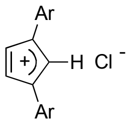

12–16

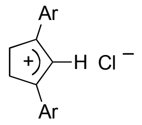

17–24

12, **20** Ar = 4-biphenyl
13, **21** Ar = 2-methylphenyl (2-tolyl)
14, **22** Ar = 2,6-dimethylphenyl (xylyl)
15, **23** Ar = 2,4,6-trimethylphenyl (mesityl)
16, **24** Ar = 2,6-diisopropylphenyl (diip)
17 Ar = phenyl
18 Ar = 1-naphthyl
19 Ar = 3,5-dimethylphenyl

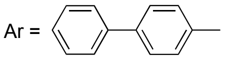

12, **20**

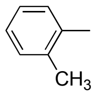

13, **21**

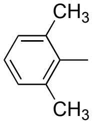

14, **22**

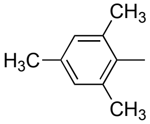

15, **23**

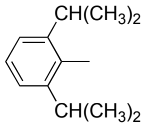

16, **24**

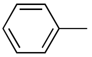

17

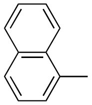

18

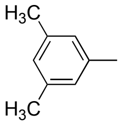

19

As far as the nature of the aryl substituents is concerned, the same trends were therefore observed for both the unsaturated imidazolium salts and their saturated imidazolinium analogues. The presence of alkyl groups on both ortho positions of the phenyl rings was much more critical to reach high catalytic efficiencies. Compounds **12**, **17**, **18**, or **20** bearing phenyl, 1-naphthyl, and 4-biphenyl groups did not meet this criterion and were devoid of any significant catalytic activity. The absence of polymerization with compounds **13** and **21**, which possessed only one methyl group blocking an ortho position was even more revealing, as was the test reaction carried out with the *meta*-disubstituted imidazolinium salt **19**.

Table 3. ROMP of cyclooctene catalyzed by ruthenium–arene complexes generated in situ from $[RuCl_2(p\text{-cymene})]_2$ and a NHC precursor in the presence of potassium *tert*-butoxide[a]

NHC precursor	Monomer conversion (%)	Isolated yield (%)	s_{cis}[b]	10^{-3} M_n[c]	M_w/M_n[c]
14	>99	89	0.19	742	2.08
15	99	92	0.20	659	2.02
16	99	60	0.20	398	3.09
22	99	93	0.19	641	2.40
23	99	93	0.23	512	2.19
24	57	44	0.51	838	2.13

[a] Experimental conditions: cyclooctene (7.5 mmol), $[RuCl_2(p\text{-cymene})]_2$ (0.015 mmol), KO*t*-Bu (0.06 mmol), and an imidazol(in)ium salt (0.03 mmol) were reacted in PhCl (5 mL) under inert atmosphere for 2 h at 60°C

[b] Fraction of *cis* double bonds within the polyoctenamer, determined by ^{13}C NMR

[c] Determined by GPC in THF vs. monodisperse polystyrene standards

3. Ruthenium–arene catalysts bearing triazolin-5-ylidene ligands

This section focuses solely on the use of a commercially available triazolin-5-ylidene carbene, viz. 1,3,4-triphenyl-4,5-dihydro-1*H*-1,2,4-triazol-5-ylidene.[30,31] When the stoichiometric reaction between this ligand and $[RuCl_2(p\text{-cymene})]_2$ was carried out in THF, a mixture of product and starting dimer was obtained. NMR analysis showed that coordination of the incoming carbene to the Ru center was accompanied by an *ortho*-metallation of the phenyl substituent in position 1, thereby releasing one equivalent of HCl in solution. Addition of a base (EtN*i*-Pr_2 in excess) drove the reaction to completion and prevented side reactions between the protic acid and the highly reactive free carbene species. Thus, a single adduct could be obtained selectively and quantitatively (Eq. 4).[47]

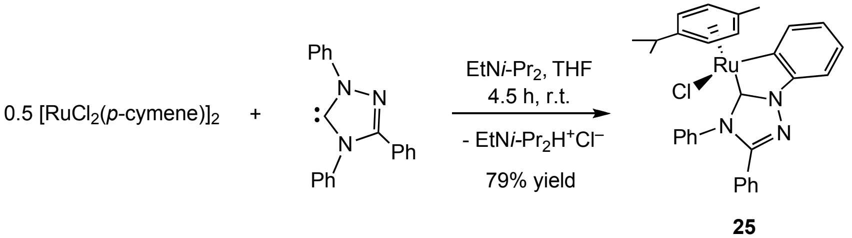

25

(4)

Complex **25** was isolated as a yellow, air- and water-stable crystalline powder and subjected to x-ray diffraction analysis (Figure 2). Its structure in the solid state closely matched the one reported by Enders and coworkers for a related Ru–(*p*-cymene) complex bearing a chiral triazolin-5-ylidene ligand.[48] The Ru atom lies in a pseudo-tetrahedral environment, and the C(1)–Ru–C(30) angle formed between the metal and the two carbon atoms from the chelating ligand equals 76.11(11)° (see Figure 2 for atom numbering). The triazolin-5-ylidene ring is planar and the interatomic distances are in agreement with those observed in other Ru–NHC complexes.[49,50] *Ortho*-metallation takes place with the phenyl ring located at N(3) rather than N(1). At 2.071(3) Å the Ru–carbon σ bond to the phenyl ring (Ru–C(30)) is comparable to the values obtained for other *ortho*-metallated *N*-arylcarbenes.[48] Furthermore, the *para*-cymene ligand is tilted, the distances Ru–C(3), Ru–C(4), and Ru–C(8) [2.267(3)–2.300(3) Å] are longer than the distances Ru–C(5), Ru–C(6), and Ru–C(7) [2.185(3)–2.207(3) Å]. This distortion is attributed to a relatively important *trans* effect of the *ortho*-metallated carbene ligand.

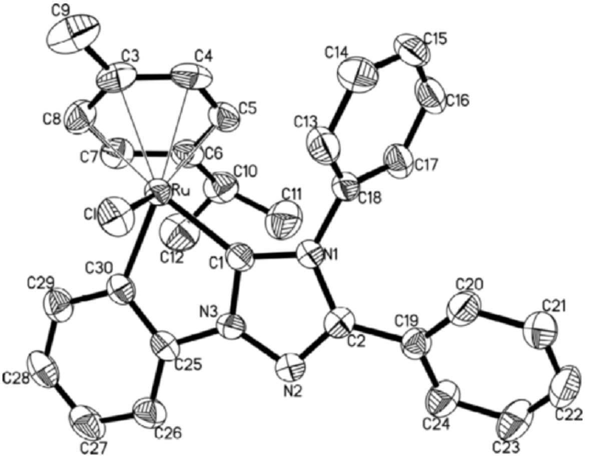

Figure 2. ORTEP drawing of complex **25** in the solid state, thermal ellipsoids set at 50% probability.

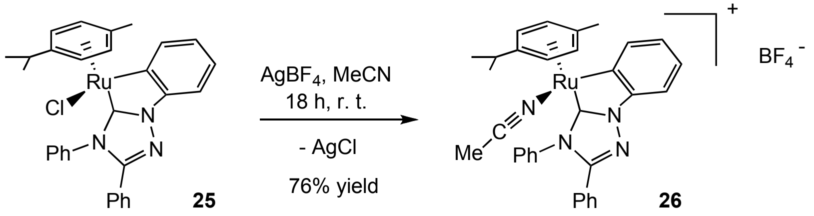

(5)

Addition of 1 equivalent of silver tetrafluoroborate to the neutral complex **25** led to the corresponding cationic species **26** ligated to an extra molecule of acetonitrile solvent (Eq. 5).[47]

Both complexes **25** and **26** were tested as catalyst precursors in the ROMP of cyclooctene, but they did not afford any polymer. After 4 h at 60°C, no monomer conversion was detected by GC even when TMSD was added as a cocatalyst.[51] These negative results clearly demonstrated the adverse effect of *ortho*-metallation on the metathetical activity of Ru–arene complexes bearing a triazolin-5-ylidene ligand. Although the in situ procedure that was adopted for generating imidazolin-2-ylidene or imidazolidin-2-ylidene species precluded the isolation and characterization of chelate complexes, we are confident that metallation of a phenyl C–H bond adjacent to the imidazole ring is highly probable when these NHCs are exposed to $[RuCl_2(p\text{-cymene})]_2$. This assumption is further supported by related work from the group of Lappert that presented undisputable evidence for the spontaneous *ortho*-metallation of imidazolidin-2-ylidene ligands bearing phenyl, *para*-tolyl, or *para*-anisyl substituents when the corresponding carbene dimers were reacted with $[RuCl_2(PPh_3)_3]$.[52,53]

3. Conclusion

A major advantage of employing transition metal complexes as catalysts is the possibility to fine-tune their electronic and steric properties through a rational design of their ligands. Our research on the ROMP of cyclooctene catalyzed by various Ru–arene complexes bearing imidazolin-2-ylidene, imidazolidin-2-ylidene, or triazolin-5-ylidene ligands nicely illustrates this concept. Two main structure–activity relationships emerged from this study. First, we established that the presence of a C4–C5 double bond in the carbene ligand central heterocycle was not crucial to achieve high catalytic efficiencies. Second, we underscored the existence of an *ortho*-effect. Blocking all the *ortho* positions of the NHC phenyl rings with alkyl groups was required for obtaining efficient catalysts. These findings pave the way for future developments in catalytic engineering with Ru–arene or Ru–alkylidene complexes in olefin metathesis and related reactions.

Acknowledgments

This work was partly supported by the EU through contracts HPRN-CT-2000-00010 “Polycat” and G5RD-CT-2001-00554 “Dentalopt”. The financial support of the “Fonds National de la Recherche Scientifique” (FNRS), Brussels, is gratefully acknowledged for the purchase of major instrumentation.

References

[1] Le Bozec, H., Touchard, D., Dixneuf, P.H., Organometallic chemistry of arene ruthenium and osmium complexes, Adv. Organomet. Chem. 1989, 29:163–247.

[2] Bennett, M.A., Recent advances in the chemistry of arene complexes of ruthenium(0) and ruthenium(II), Coord. Chem. Rev. 1997, 166:225–254.

[3] Pigge, F.C., Coniglio, J.J., Stoichiometric applications of η^6-arene ruthenium(II) complexes in organic chemistry, Curr. Org. Chem. 2001, 5:757–784.

[4] Rigby, J.H., Kondratenko, M.A., Arene complexes as catalysts, Top. Organonomet. Chem. 2004, 7:181–204.

[5] Küçükbay, H., Çetinkaya, B., Guesmi, S., Dixneuf, P.H., New (carbene)ruthenium-arene complexes: preparation and uses in catalytic synthesis of furans, Organometallics 1996, 15:2434–2439.

[6] Çetinkaya, B., Özdemir, I., Dixneuf, P.H., Synthesis and catalytic properties of N-functionalized carbene complexes of rhodium(I) and ruthenium(II), J. Organomet. Chem. 1997, 534:153–158.

[7] Fürstner, A., Müller, T., Efficient total synthesis of resin glycosides and analogues by ring-closing olefin metathesis, J. Am. Chem. Soc. 1999, 121:7814–7821.

[8] Castarlenas, R., Dixneuf, P.H., Highly active catalysts in alkene metathesis: first observed transformation of allenylidene into indenylidene via alkenyl-carbyne-ruthenium species, Angew. Chem. Int. Edit. 2003, 42:4524–4527.

[9] Castarlenas, R., Eckert, M., Dixneuf, P.H., Alkenylcarbene ruthenium arene complexes as initiators of alkene metathesis: an enyne creates a catalyst that promotes its selective transformation, Angew. Chem. Int. Edit. 2005, 44: 2576–2579.

[10] Yiğit, M., Yiğit, B., Özdemir, I., Çetinkaya, E., Çetinkaya, B., Active ruthenium-(N-heterocyclic carbene) complexes for hydrogenation of ketones, Appl. Organomet. Chem. 2006, 20:322–327.

[11] Quebatte, L., Haas, M., Solari, E., Scopelliti, R., Nguyen, Q.T., Severin, K., Atom-transfer radical reactions under mild conditions with $[\{RuCl_2(1,3,5\text{-}C_6H_3iPr_3)\}_2]$ and PCy_3 as the catalyst precursors, Angew. Chem. Int. Edit. 2005, 44:1084–1088.

[12] Hafner, A., Mühlebach, A., van der Schaaf, P.A., One-component catalysts for thermal and photoinduced ring opening metathesis polymerization, Angew. Chem. Int. Edit. 1997, 36:2121–2124.

[13] Fürstner, A., Ackermann, L., A most user-friendly protocol for ring closing metathesis reactions, Chem. Commun. 1999, 95–96.

[14] Fürstner, A., Liebl, M., Lehmann, C.W., Picquet, M., Kunz, R., Bruneau, C., Touchard, D., Dixneuf, P.H., Cationic ruthenium allenylidene complexes as catalysts for ring closing olefin metathesis, Chem. Eur. J. 2000, 6:1847–1857.

[15] Stumpf, A.W., Saive, E., Demonceau, A., Noels, A.F., Ruthenium-based catalysts for the ring-opening metathesis polymerization of low-strain cyclic olefins and of functionalised derivatives of norbornene and cyclooctene, Chem. Commun. 1995, 1127–1128.

[16] Demonceau, A., Stumpf, A.W., Saive, E., Noels, A.F., Novel ruthenium-based catalyst systems for the ring-opening metathesis polymerization of low-strain cyclic olefins, Macromolecules 1997, 30:3127–3136.

[17] Arduengo, A.J. III, Harlow, R.L., Kline, M., A stable crystalline carbene, J. Am. Chem. Soc. 1991, 113:361–363.

[18] Arduengo, A.J. III, Rasika Dias, H.V., Harlow, R.L., Kline, M., Electronic stabilization of nucleophilic carbenes, J. Am. Chem. Soc. 1992, 114:5530–5534.

[19] Arduengo, A.J. III, Krafczyk, R., Schmutzler, R., Craig, H.A., Goerlich, J.R., Marshall, W.J., Unverzagt, M., Imidazolylidenes, imidazolinylidenes and imidazolidines, Tetrahedron 1999, 55:14523–14534.

[20] Arduengo, A.J. III, Looking for stable carbenes: the difficulty in starting anew, Acc. Chem. Res. 1999, 32:913–921.

[21] Bourrisou, D., Guerret, O., Gabbaï, F.P., Bertrand, G., Stable carbenes, Chem. Rev. 2000, 100:39–91.

[22] Jafarpour, L., Nolan, S.P., Transition-metal systems bearing a nucleophilic carbene ancillary ligand: from thermochemistry to catalysis, Adv. Organomet. Chem. 2001, 46:181–222.

[23] Herrmann, W.A., Weskamp, T., Böhm, V.P.W., Metal complexes of stable carbenes, Adv. Organomet. Chem. 2002, 48:1–69.

[24] Herrmann, W.A., N-heterocyclic carbenes: a new concept in organometallic catalysis, Angew. Chem. Int. Edit. 2002, 41:1290–1309.

[25] Dragutan, I., Dragutan, V., Delaude, L., Demonceau, A., N-Heterocyclic carbenes as highly efficient ancillary ligands in homogeneous and immobilized metathesis ruthenium catalytic systems, Arkivoc (x) 2005, 206–253.

[26] Nair, V., Bindu, S., Sreekumar, V., N-heterocyclic carbenes: reagents, not just ligands!, Angew. Chem. Int. Edit. 2004, 43:5130–5135.

[27] Enders, D., Balensiefer, T., Nucleophilic carbenes in asymmetric organocatalysis, Acc. Chem. Res. 2004, 37:534–541.

[28] César, V., Bellemin-Laponnaz, S., Gade, L.H., Chiral N-heterocyclic carbenes as stereodirecting ligands in asymmetric catalysis, Chem. Soc. Rev. 2004, 33:619–636.

[29] Herrmann, W.A., Köcher, C., N-heterocyclic carbenes, Angew. Chem. Int. Edit. 1997, 36:2162–2187.

[30] Enders, D., Breuer, K., Raabe, G., Runsink, J., Teles, J.H., Melder, J.-P., Ebel, K., Brode, S., Preparation, structure, and reactivity of 1,3,4-triphenyl-4,5-dihydro-1*H*-1,2,4-triazol-5-ylidene, a new stable carbene, Angew. Chem. Int. Edit. 1995, 34:1021–1023.

[31] Enders, D., Breuer, K., Kallfass, U., Balensiefer, T., Preparation and application of 1,3,4-triphenyl-4,5-dihydro-1*H*-1,2,4-triazol-5-ylidene, a stable carbene, Synthesis 2003, 1292–1295.

[32] Enders, D., Gielen, H., Synthesis of chiral triazolinylidene and imidazolinylidene transition metal complexes and first application in asymmetric catalysis, J. Organomet. Chem. 2001, 617–618:70–80.

[33] Delaude, L., Demonceau, A., Noels, A.F., Synthesis and application of new N-heterocyclic carbene ruthenium complexes in catalysis: a case study, Curr. Org. Chem. 2006, 10:203–215.

[34] Herrmann, W.A., Köcher, C., Goossen, L.J., Artus, G.R.J., Heterocyclic carbenes: a high-yielding synthesis of novel, functionalized N-heterocyclic carbenes in liquid ammonia, Chem. Eur. J. 1996, 2:1627–1636.

[35] Jafarpour, L., Huang, J., Stevens, E.D., Nolan, S.P., (*p*-cymene)RuLCl_2 (L = 1,3-bis (2,4,6-trimethylphenyl)imidazol-2-ylidene and 1,3-bis(2,6-diisopropylphenyl)imidazol-2-ylidene) and related complexes as ring closing metathesis catalysts, Organometallics 1999, 18:3760–3763.

[36] Kuhn, N., Kratz, T., Synthesis of imidazol-2-ylidenes by reduction of imidazole-2(3*H*)-thiones, Synthesis 1993, 561–562.

[37] Arduengo, A.J. III, Davidson, F., Dias, H.V.R., Goerlich, J.R., Khasnis, D., Marshall, W.J., Prakasha, T.K., An air stable and mixed carbene "dimers", J. Am. Chem. Soc. 1997, 119:12742–12749.

[38] Delaude, L., Demonceau, A., Noels, A.F., Visible light induced ring-opening metathesis polymerisation of cyclooctene, Chem. Commun. 2001, 986–987.

[39] Ackermann, L., Bruneau, C., Dixneuf, P.H., Simple new three-component catalytic system for enyne metathesis, Synlett 2001, 397–399.

[40] Sémeril, D., Cléran, M., Bruneau, C., Dixneuf, P.H., New *in situ* generated ruthenium catalyst for enyne meathesis: access to novel cyclic siloxanes, Adv. Synth. Catal. 2001, 343:184–187.

[41] Zhang, C., Huang, J., Trudell, M.L., Nolan, S.P., Palladium-imidazol-2-ylidene complexes as catalysts for facile and efficient Suzuki cross-coupling reactions of aryl chlorides with arylboronic acids, J. Org. Chem. 1999, 64:3804–3805.

[42] Huang, J., Nolan, S.P., Efficient cross-coupling of aryl chlorides with aryl Grignard reagents (Kumada reaction) mediated by a palladium/imidazolium chloride system, J. Am. Chem. Soc. 1999, 121:9889–9890.

[43] Grasa, G.A., Nolan, S.P., Palladium/imidazolium salt catalyzed coupling of aryl halides with hypervalent organostannates, Org. Lett. 2001, 3:119–122.

[44] Viciu, M.S., Grasa, G.A., Nolan, S.P., Catalytic dehalogenation of aryl halides mediated by a palladium/imidazolium salt system, Organometallics 2001, 20:3607–3612.

[45] Grasa, G.A., Viciu, M.S., Huang, J., Nolan, S.P., Amination reactions of aryl halides with nitrogen-containing reagents mediated by palladium/imidazolium salt systems, J. Org. Chem. 2001, 66:7729–7737.

[46] Delaude, L., Szypa, M., Demonceau, A., Noels, A.F., New in situ generated ruthenium catalysts bearing N-heterocyclic carbene ligands for the ring-opening metathesis polymerization of cyclooctene, Adv. Synth. Catal. 2002, 344:749–756.

[47] Simal, F., Jan, D., Delaude, L., Demonceau, A., Spirlet, M.-R., Noels, A.F., Evaluation of ruthenium-based complexes for the controlled radical polymerization of vinyl monomers, Can. J. Chem. 2001, 79:529–535.

[48] Enders, D., Gielen, H., Raabe, G., Runsink, J., Teles, J.H., Diastereoselective synthesis of the first enantiomerically pure (triazolinylidene)ruthenium(II) and -rhodium(III) chelate complexes, Chem. Ber./Recl. 1997, 130:1253–1260.

[49] Huang, J., Stevens, E.D., Nolan, S.P., Petersen, J.L., Olefin metathesis-active ruthenium complexes bearing a nucleophilic carbene ligand, J. Am. Chem. Soc. 1999, 121:2674–2678.

[50] Weskamp, T., Schattenmann, W.C., Spiegler, M., Herrmann, W.A., A novel class of ruthenium catalysts for olefin metathesis, Angew. Chem. Int. Edit. 1998, 37:2490–2493.

[51] Jan, D., Organometallic engineering of new ruthenium and chromium complexes. Applications to olefin polymerization, Ph.D. thesis, University of Liège (2000).

[52] Hitchcock, P.B., Lappert, M.F., Pye, P.L., Spontaneous N-aryl (rather than P-aryl) orthometallation in the system $[RuCl_2(PPh_3)_3(NHC)]$ (Ar = C_6H_4Me-4); X-ray crystal and molecular structure of a stereochemically rigid 5-coordinate Ru(II) complex, with a short (2.2 A) Ru...H contact, Chem. Commun. 1977, 196–198.

[53] Hitchcock, P.B., Lappert, M.F., Pye, P.L., Thomas, S., Carbene complexes. Part 16. Synthesis and properties of NN′N″N‴-tetra-aryl-substituted electron-rich olefin-derived carbeneruthenium(II) complexes containing a spontaneously formed *ortho*-metallated-N-arylcarbene ligand, J. Chem. Soc., Dalton Trans. 1979, 1929–1942.

OLEFIN METATHESIS MEDIATED BY: - SCHIFF BASE Ru-ALKYLIDENES - Ru-ALKYLIDENES BEARING UNSYMMETRICAL NHC LIGANDS

STIJN MONSAERT, NELE LEDOUX, BART ALLAERT, RENATA DROZDZAK, PASCAL VAN DER VOORT, FRANCIS VERPOORT

Department of Inorganic and Physical Chemistry, Organometallics and Catalysis Division, Ghent University, Krijgslaan 281 (S-3), 9000 Ghent, Belgium

Abstract: The classic Grubbs second-generation complex **2** was modified through

1. The introduction of a bidentate Schiff base ligand
2. Changes in the amino side groups of the NHC ligand

Representative olefin metathesis test reactions show the effects induced by the ligand modifications and demonstrate some interesting new properties of the described catalysts. catalysts.

Keywords: Olefin metathesis, ruthenium, asymmetrical *N*-heterocyclic carbene, Schiff-base, alkylidene, DCPD.

1. Introduction

Metathesis has evolved during the last decades from black-box polymerizations to well-defined catalysts as versatile tools for organic and polymer chemists. Its main protagonists have recently been rewarded the Nobel Prize.[1] The revolution in this chemistry was induced by the understanding of the catalysts mechanism[2] and the development of active tungsten[3], molybdenum,[4] and ruthenium (Ru)[5] complexes. Grubbs et al. presented the first well defined Ru–carbene active for metathesis[5] in 1992 and soon thereafter optimized it to the catalyst now known as Grubbs' first-generation catalyst **1**.[6–8] The introduction of an *N*-heterocyclic carbene (NHC) to replace a phosphine increased its activity[9–12] and lead to the development of the Grubbs' second-generation catalyst **2**.[13] This activity enhancement is caused by a higher selectivity of the catalyst for olefins[14], a lower barrier for the formation of the cyclobutane intermediate[15,16] and the benefits of twofold symmetry.[17] Optimization of the NHC ligand through variation of the amino sidegroups and backbone substituents has been under great investigation but improvement on the catalyst activity was found very challenging.[18–23] On the other hand, enhanced activity and control in asymmetric metathesis has been demonstrated by varying one side of the H_2 IMES ligand by our group[24,] and others.[25,26]

Y. İmamoğlu and V. Dragutan (eds.), Metathesis Chemistry: From Nanostructure Design to Synthesis of Advanced Materials, 251-263.

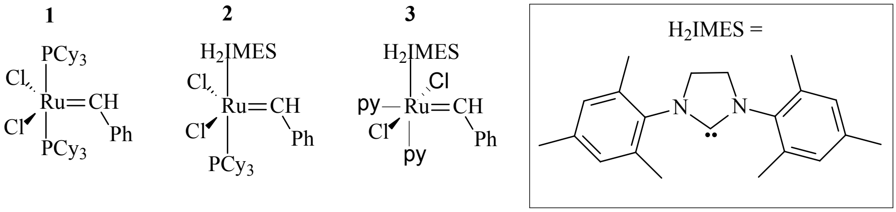

Scheme 1. Grubbs catalysts.

The ingenious introduction of a chelating carbene by Hoveyda et al. has increased the stability of the Grubbs catalyst, making purification by column chromatography, recycling, and stabilization of the methylidene species in ring-closing metathesis (RCM) possible.[27–29] A great deal of approaches have been successfully explored to improve the initiation of this chelating carbene fragment.[26,30–36]

Various other approaches have been applied in changing the Grubbs catalysts, such as the introduction of electron-withdrawing phosphines,[14] bidentate Schiff bases,[37,38] piridinyl–alcoholate ligands,[39] pyridines[40–42] (with formation of bis(pyridine) complex **3**), pyridinecarboxylate,[43] different halides,[44] alkoxides,[40–45] phenoxides,[46,47] and substituted acetic acid groups.[48–51] Indenylidene has been successfully introduced as a substitute for benzylidene.[52,53] Furthermore, the benzylidene has been successfully altered by Piers et al. through introduction of a phosphonium salt which created a highly active and stable 14-electron initiator.[54]

In this contribution, we wish to highlight our introduction of bidentate Schiff base ligands with formation of **4**,[38] which is an extremely stable catalyst type. We will show that this extreme stability is concomitant with lower activity. On the other hand, it will also be demonstrated that bypassing this lack of reactivity by simple heating and the introduction of acid additives[55,56] is simple and provides a catalyst system with extra features such as storage of the catalyst in the monomer without undesired reaction.

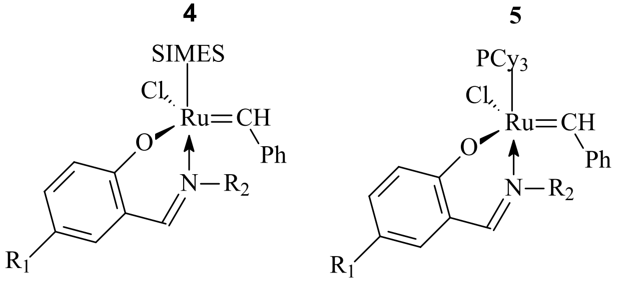

Scheme 2. Schiff base catalysts.

Furthermore we will describe some subtleties in the modification of the NHC unit. We will show how the retaining of one mesityl group is essential for catalyst preparation and how changes in the other side chain may lead to catalysts with a substantial activity increase.[24]

2. Results and discussion

2.1 Schiff base Ru–alkylidenes

In 1998, Grubbs et al. published on the introduction of bidentate Schiff base ligands for olefin metathesis initiators **5**, which showed remarkable stability.[37] Our group was able to extend this stability through the incorporation of H_2IMES as a substitute for the phosphine.[57–59] Recently, we rectified a previous methodology of reacting the first-generation Schiff base complex **5** with an in situ generated carbene.[38,58] We found that the previously reported methodology was ineffective in preparing the new catalyst. However, addition of a Schiff base thallium salt to the pyridine functionalized second-generation catalyst led smoothly to **4a–d**.[38] (Scheme 3)

4

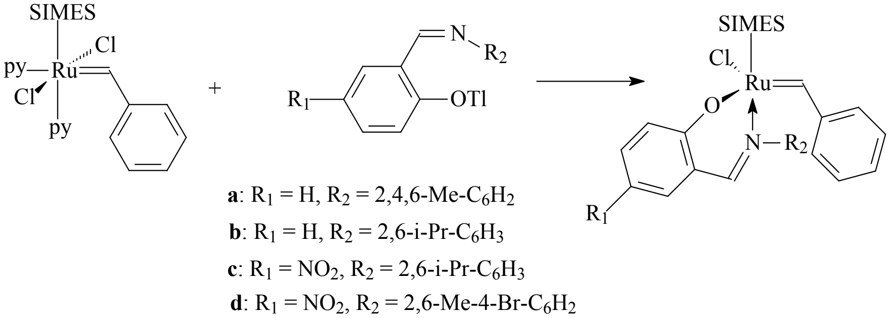

a: $R_1 = H, R_2 = 2,4,6\text{-Me-}C_6H_2$
b: $R_1 = H, R_2 = 2,6\text{-i-Pr-}C_6H_3$
c: $R_1 = NO_2, R_2 = 2,6\text{-i-Pr-}C_6H_3$
d: $R_1 = NO_2, R_2 = 2,6\text{-Me-4-Br-}C_6H_2$

Scheme 3. Preparation of the second-generation Schiff base catalyst.

In addition we were able to grow a single-crystal which confirmed the structure of complex **4c**[38] (Figure 1).

The Ru–N bond in **4c** (2.125 (2) Å) is somewhat longer than in **5c** (2.106 (4) Å), which was ascribed to the enhanced *trans* influence of the H_2IMES ligand. The Ru–C(NN) bond in **4c** (2.035 (3) Å) is shorter than in the second-generation catalyst **2** (2.085 (2) Å), which can be attributed to the decreased *trans* influence in **4c** of the nitrogen. However, other factors could also facilitate this. The π–π stacking of both mesityl substituents, one with the benzylidene, the other with the phenoxy fragment clearly have an impact on the H_2IMES geometry. It seems that the Ru–C(H_2IMES)-N_1 (117.1°) and C(H_2IMES)-N_1-C(Mesityl) (122.4°) angles show low values due to this π–π

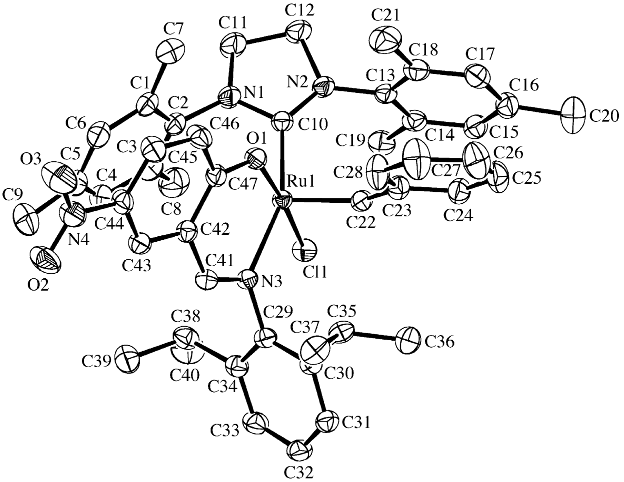

Figure 1. ORTEP plot of **4c**.

stacking, while accordingly a shorter Ru–C(NN) distance might have a similar effect. Furthermore the π–π stacking fixes the phenoxy fragment and thereby controls the position of the *N*-donor. This causes a small C(NN)-Ru–N (157.2 (1)) angle and places the H_2IMES ligand less *trans* to the *N* atom. Still, this effect does not seem to influence the Ru–N distance.

The catalysts **4a–d** show no activity at room temperature but are stable for months in solution. We tested their activity in the ring-opening metathesis polymerization (ROMP) of 1,5-cyclooctadiene (COD) at 90°C in toluene-d8 (Figure 2). The Schiff base catalysts **4a–d** and **5c** are clearly less active than

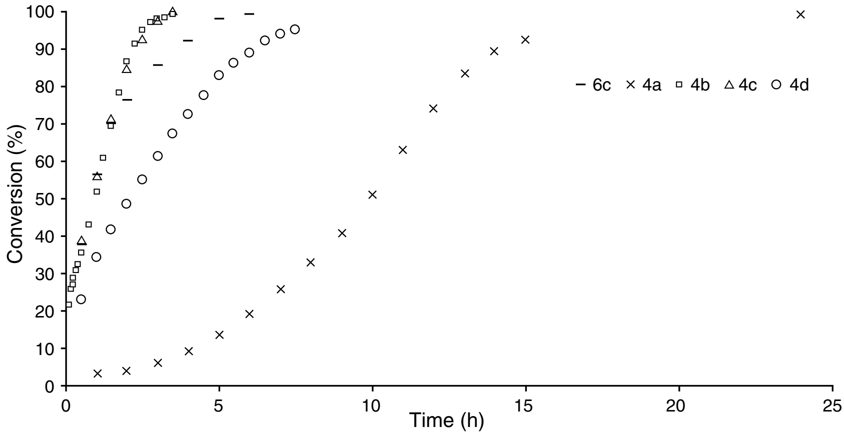

Figure 2. ROMP of 1,5-cyclooctadiene in toluene-d8 at 90°C with **4a–d** and **5c**. [Ru]:[COD] = 1:300.

their phosphine analogues **1** and **2**, which is likely caused by the bidentate effect. The H_2IMES substituted **4c** is only a slightly better initiator than its phosphine analogue **5c**. **4b–c** with $^{i-}$Pr groups in the ortho position are the fastest initiators which can be explained by increased steric hindrance. Surprisingly, incorporation of a NO_2 group (**4c**) has no effect on catalyst activity in contrast to our expectation of a weakened Ru–N bond.

Additionally, the ROMP of 20,000 equiv of dicyclopentadiene (DCPD) using catalysts **4c** and **5c** was followed while the reaction mixture was heated up to 150°C (Figure 3). The reaction with **4c** shows a sharp exotherm at 130°C which is not present in the reaction with its phosphine analogue **5c**. With **5c** only a gelated polymer was obtained.

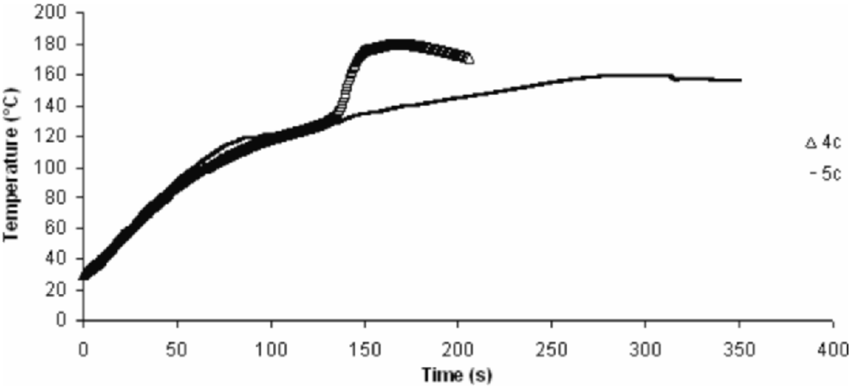

Figure 3. Thermal analysis of the ROMP of dicyclopentadiene with catalysts **4c** and **5c**. [Ru]:[DCPD] = 1:20 000.

This truly demonstrates the potential of catalyst **4c**. While it is inactive for weeks in DCPD at room temperature, it needs 4 h to polymerize 300 equivalent of COD at 90°C, and it can easily be activated thermally to convert 20,000 equivalent of DCPD in less than 3 min.

Acid activation is – next to thermal activation – another well-documented activation technique. The scope of a two-component system, where the stable catalyst and the catalyst activator can placed in two separate monomer streams, prompted us to do research in this direction. First, we investigated the potential of this activation strategy for the Schiff base catalysts **4d** and **5d** in the ROMP of COD (Figure 4).

Figure 4 summarizes the catalytic activities of complexes **4d** and **5d** and depicts their activity versus the Grubbs catalysts **1**, **2,** and **3**. Both Schiff base catalysts show negligible activity but the addition of hydrochloric acid

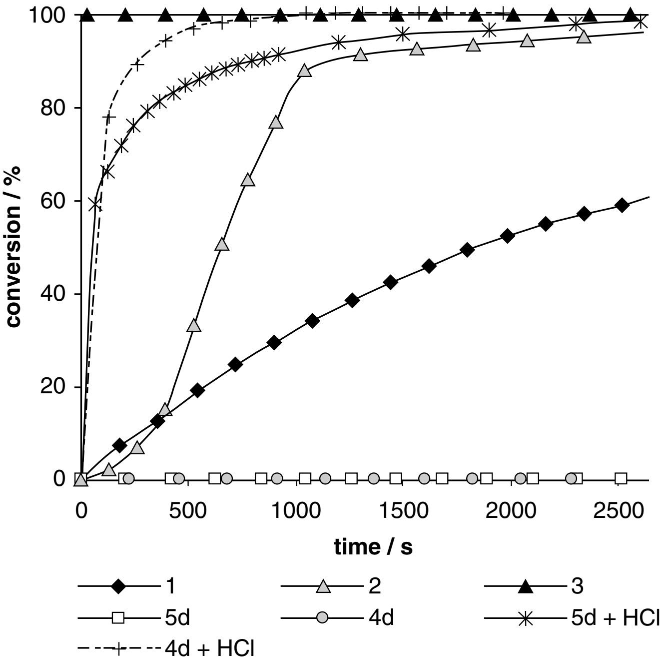

Figure 4. Monitoring ROMP of COD via ^{1}H NMR spectroscopy, $CDCl_3$, 20°C, COD/catalyst = 300, catalyst concentration = 4.52 mM. Acid addition: 0.05 mL of 1N HCl in ether.

substantially enhanced their activity. Both acid activated catalysts show complete conversion within one hour. These observations demonstrate the high potential of this acid activation technique and stimulated us to further explore the potential of the activated catalyst **4d** (Table 1). Some data obtained from polymerization reactions using Grubbs catalyst **2** were included for comparison. It is noteworthy that HCl did not activate catalyst **2**, but induced catalyst decomposition.

The Schiff base catalyst **4d** shows no activity towards 300 equivalent COD, while the addition of an excess of HCl allowed for high turnover numbers (TONs) within 1 h. TONs up to 90,000 were found within the reach of this catalyst system.

Also in the ROMP of DCPD, the HCl activation of catalyst **4d** turned out very interesting. Figures 5, 6 and 7 show the thermograms from the polymerization of different amounts of DCPD and different amounts of HCl. High exotherms were recorded, which indicates a high conversion of monomer. It is illustrated that TONs up to 30,000 and 40,000 were easily achieved. The thermograms show a clear bend between 60°C and 80°C, which we ascribe to the catalyst activation kinetics.

Table 1. Ring-opening metathesis polymerization of COD

Entry	Catalyst	Acid	Cat./monomer/acid	Time (min)	Conversion (%)
1	**2**	-	1/300/0	30	100
2	**2**	-	1/3,000/0	30	100
3	**2**	-	1/30,000/0	overnight	24
4	**2**	HCl[a]	1/30,000/10	overnight	0[b]
5	**2**	HCl[a]	1/30,000/70	overnight	0[b]
6	**4d**	-	1/300/0	60	0
7	**4d**	HCl[a]	1/30,000/70	30	100
8	**4d**	HCl[a]	1/90,000/140	30	100
9	**4d**	HCl[a]	1/120,000/210	60	81
10	**4d**	HCl[a]	1/150,000/210	overnight	0.5[b]

General reaction conditions: Ar atmosphere, room temperature, toluene as solvent, conversion determined by ^{1}H NMR spectroscopy. [a]HCl (1N in Et_2O); [b]due to decomposition of catalyst.

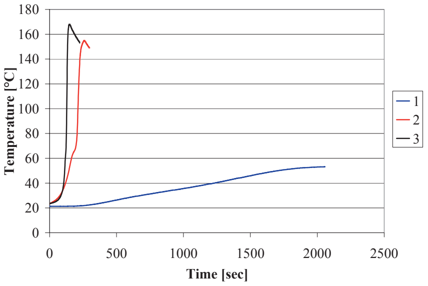

Figure 5. Conditions: **4d**/DCPD = 1/30,000.
Entry 1: **4d**/HCl = 1/10
Entry 2: **4d**/HCl = 1/20
Entry 3: **4d**/HCl = 1/40

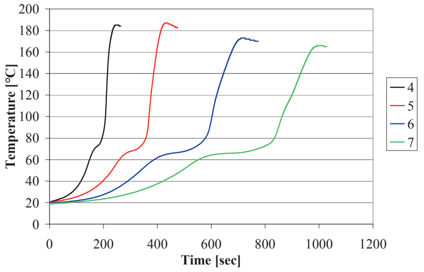

Figure 6. Conditions: **4d**/HCl = 1/30.
Entry 4: **4d**/DCPD = 1/30,000
Entry 5: **4d**/DCPD = 1/40,000
Entry 6: **4d**/DCPD = 1/50,000
Entry 7: **4d**/DCPD = 1/60,000

It is common to use Brønsted acids as phosphine scavengers in olefin metathesis phosphine bearing catalysts.[60] On the other hand, it is obvious that HCl plays a different role in catalyst **4d**, since this complex does not carry a phosphine ligand. To understand more about the activation mechanism, an NMR study was undertaken.

From spectral analysis, we were able to detect protonated (broad signal at δ 8.72 ppm) and decondensated imine (aldehyde peak at δ 10.01 ppm), as well as two new signals in the alkylidene region (δ 16.91 and δ 17.62 ppm). Furthermore, we observed the formation of a peak at δ 11.61 ppm (Ar–O*H*), which witnessed the breaking of the Ru–O bond and the presumed formation of a new Ru–Cl bond. After 2 h, the addition of an amount of cyclooctene

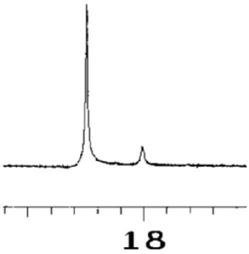

Figure 7. Selected part of the ^{1}H NMR spectrum after addition of cyclooctene. The benzylidene proton of catalyst **4d** is at 18.5 ppm. The propagating species is observed as an alkylidene peak at 18.0 ppm.

led to the observation of the propagating species as an alkylidene peak at δ 18.0 ppm (Figure 7).

From these observations, we have a strong tendency to believe that first the imine is protonated and hydrolyzed – an event catalyzed by HCl – while in a second step the Ru–O bond is protonolyzed, liberating the 14-electron active species which is responsible for the metathesis activity.

2.2 Ru–alkylidenes bearing unsymmetrical NHC ligands

A second part of the current research carried out by our group involves a study on the effect of new NHCs in Grubbs' second-generation catalysts.[24] A few reports describing modified dihydro NHC ligands for Grubbs complexes have witnessed some interesting new properties.[61–65] Hereby inspired, we attempted further catalyst tuning through the variation of the NHC's amino side groups. The introduction of aliphatic amino groups was expected to induce a substantially altered catalytic behavior of the corresponding Grubbs' second-generation analogues as a consequence of steric and electronic effects.

The symmetrical dihydro NHC ligands shown in Scheme 4 were prepared by condensation of glyoxal with the appropiate amines, followed by reduction, treatment with HCl, and ring closure with triethyl orthoformate.[66] These NHC chloride salts were deprotonated with base and reacted with the Grubbs catalyst **1**, implying that free carbenes were generated during reaction. Despite several persistent attempts, we were unable to achieve isolation of pure complexes of type **6**. Since this is likely due to obstruction caused by the aliphatic amino side groups which are steric in three dimensions, we anticipated that more success would be accessible through unsymmetrical NHCs bearing one planar aromatic amino group. Unsymmetrical chloride salts were conveniently synthesized following a synthetic strategy outlined by Grubbs et al. (Scheme 4).[67] Upon reaction with base and complex **1**, exchange of a phosphine ligand was acquired under normal reaction conditions which allowed for successful isolation and characterization of complexes **7a–e**. X-ray analysis revealed that the aromatic benzylidene and mesidine moieties are roughly coplanar, indicating that π–π interactions might be of significant importance for the stability of Grubbs second-generation complexes.[24,62] The lack of such a stabilizing interaction for complexes of type **6**, is likely responsible for the difficult coordination of NHCs ligands bearing two aliphatic amino side groups.

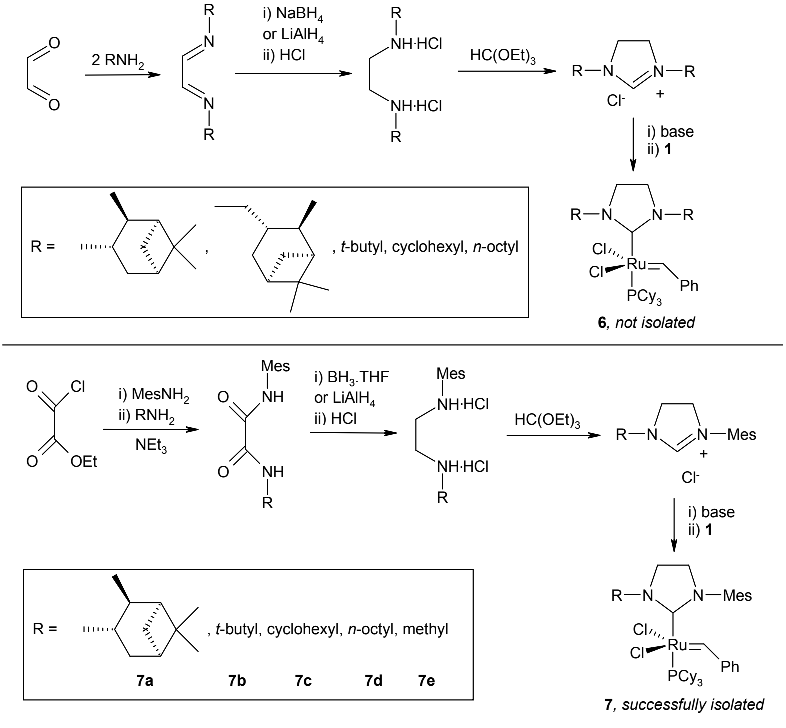

Scheme 4. Synthetic pathway towards complexes **6** and **7**.

To explore the catalytic potential of the new complexes, they were tested for the ROMP of *cis*,*cis*-cycloocta-1,5-diene (COD), Figure 8, and the RCM of diethyl diallylmalonate Figure 9. Catalyst **7e**, bearing the least steric NHC ligand was found to outperform the classic Grubbs complex **2**. On the other hand, catalyst **7b** with a bulky *tert*-butyl group on the NHC ligand, was found to be virtually inactive at room temperature. It is therefore obvious that the steric bulk of the amino side groups is an important factor determining catalyst activity.

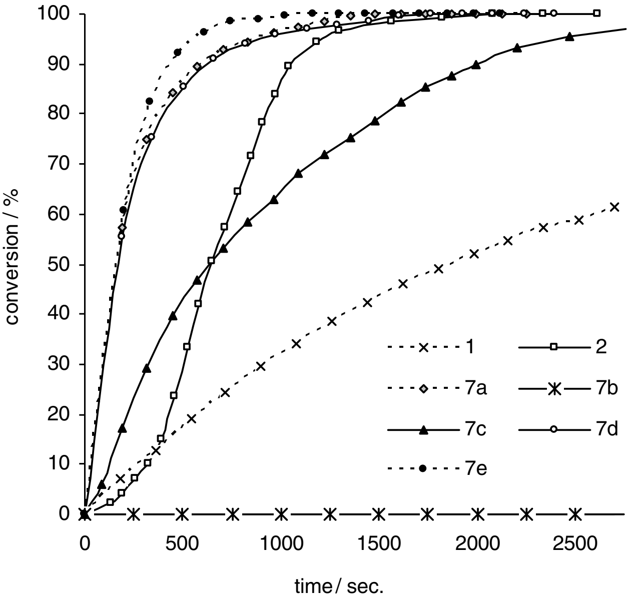

Figure 8. Monitoring ROMP of COD via ^{1}H NMR spectroscopy, 20°C, COD/catalyst = 300, catalyst conc. = 4.52 mM, solvent = $CDCl_3$.

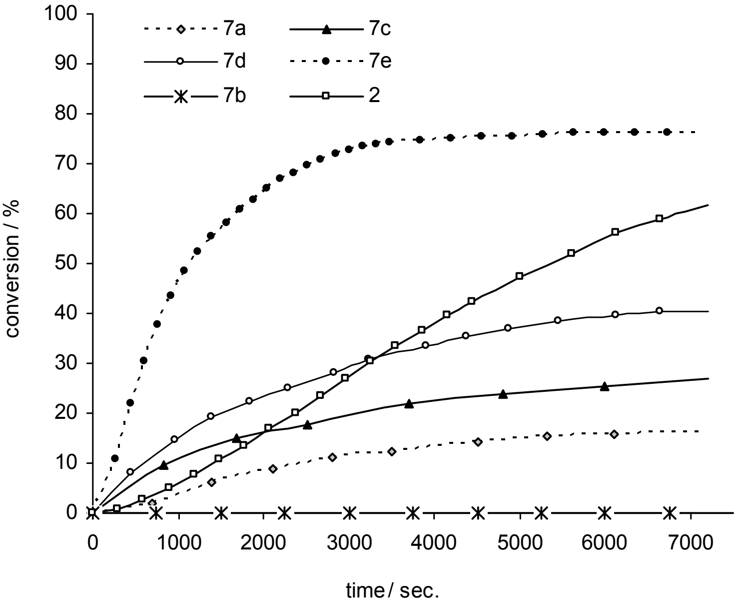

Figure 9. Monitoring RCM of diethyl diallylmalonate via ^{1}H NMR spectroscopy, 20°C, diethyl diallylmalonate/catalyst = 200, catalyst conc.= 4.52 mM, solvent = CD_2Cl_2.

In addition, Blechert et al. demonstrated that complex **7e** provides significantly different E:Z ratios in cross–metathesis (CM) reactions and an improved selectivity in diastereoselective ring closing metathesis reactions.[25] These observations encourage us to continue our investigation of modified NHC ligands, in order to gain a better understanding of the catalytic activity determining factors and selectivity effects. Studies aimed at altering the steric bulk of the aromatic amino side group are currently ongoing.

3. Conclusion

This report demonstrates that ligand modifications in Grubbs complexes induce substantial changes in the reactivity patterns of the corresponding catalysts. The introduction of a Schiff base was found to generate very stable complexes which require thermal or chemical activation in order to obtain olefin metathesis activity. At first glance, inactivity at room temperature might be interpret as a huge disadvantage but the catalyst activation strategies allow for interesting applications such as acid-initiated reaction injection molding (RIM). Furthermore, modification of the NHC ligand in Grubbs' second-generation complexes revealed the importance of the steric bulk of the amino side groups. Noteworthy is also that the presence of at least one aromatic amino side group seems to be necessary to generate a stable catalyst.

Acknowledgments

The authors gratefully acknowledge the FWO-Flanders (Research Foundation – Flanders), the research Fund of Ghent University and IWT-Flanders (Institute for the Promotion of Innovation through Science and Technology) for generous financial support during the preparation of this manuscript.

References

[1] http://nobelprize.org/chemistry/laureates/2005/chemadv05.pdf
[2] Hérisson, J.-L., Chauvin, Y., Macromolecular Chem. 1971, 141:161.
[3] Schrock, R.R., DePue, R., Feldman, J., Schaverien, C.J., Dewan, C.J., Liu, A.H., J. Am. Chem. Soc. 1988, 110:1423.
[4] Schrock, R.R., Murdzek, J.S., Bazan, G.C., Robbins, J., Dimare, M., O'Regan, M., J. Am. Chem. Soc. 1990, 112:3875.
[5] Nguyen, S.T., Johnson, L.K., Grubbs, R.H., Ziller, J.W., J. Am. Chem. Soc. 1992, 114:3974–3975.
[6] Nguyen, S.T., Grubbs, R.H., Ziller, J.W., J. Am. Chem. Soc. 1993, 115: 9858–9859.
[7] Schwab, P., France, M.B., Ziller, J.W., Grubbs, R.H., Angew. Chem. Int. Edit. 1995, 34:2039.

[8] Schwab, P., Grubbs, R.H., Ziller, J.W., J. Am. Chem. Soc. 1996, 118:100–110.

[9] Jafarpour, L., Schanz, H.J., Stevens, E.D., Nolan, S.P., Organometallics 1999, 18:5416–5419.

[10] Huang, J.K., Schanz, H.J., Stevens, E.D., Nolan, S.P., Organometallics 1999, 18:5375–5380.

[11] Weskamp, T., Schattenmann, W.C., Spiegler, M., Herrmann, W.A., Angew. Chem. Int. Edit. 1998, 37:2490–2493.

[12] Weskamp, T., Kohl, F.J., Hieringer, W., Gleich, D., Herrmann, W.A., Angew. Chem. Int. Edit. 1999, 38:2416–2419.

[13] Bielawski, C.W., Grubbs, R.H., Angew. Chem. Int. Edit. 2000, 39:2903–2906.

[14] Love, J.A., Sanford, M.S., Day, M.W., Grubbs, R.H., J. Am. Chem. Soc. 2003, 125:10103–10109.

[15] Cavallo, L., J. Am. Chem. Soc. 2002, 124:8965–8973.

[16] Adlhart, C., Chen, P., J. Am. Chem. Soc. 2004, 126:3496–3510.

[17] Adlhart, C., Chen, P., Angew. Chem. Int. Edit. 2002, 41:4484–4487.

[18] Despagnet-Ayoub, E., Grubbs, R.H., J. Am. Chem. Soc. 2004, 126:10198–10199.

[19] Despagnet-Ayoub, E., Grubbs, R.H., Organometallics 2005, 24:338–340.

[20] Herrmann W.A., Ofele, K., von Preysing, D., Herdtweck, E., J. Organometallic Chem. 2003, 684:235–248.

[21] Mayr, M., Wurst, K., Ongania, K.H., Buchmeiser, M.R., Chem. -A Eur. J. 2004, 10:1256–1266.

[22] Yang, L.R., Mayr, M., Wurst, K., Buchmeiser, M.R., Chem. -A Eur. J. 2004, 10:5761–5770.

[23] Yun, J., Marinez, E.R., Grubbs, R.H., Organometallics 2004, 23:4172–4173.

[24] Ledoux, N., Allaert, B., Pattyn, S., Vander Mierde, H., Vercaemst, C., Verpoort, F., Chem. -A Eur. J. 2006, 12:4654–4661.

[25] Vehlow, K., Maechling, S., Blechert, S., Organometallics 2006, 25:25–28.

[26] Van Veldhuizen, J.J., Garber, S.B., Kingsbury, J.S., Hoveyda, A.H., J. Am. Chem. Soc. 2002, 124:4954–4955.

[27] Kingsbury, J.S., Harrity, J.P.A., Bonitatebus, P.J., Hoveyda, A.H., J. Am. Chem. Soc. 1999, 121:791–799.

[28] Garber, S.B., Kingsbury, J.S., Gray, B.L., Hoveyda, A.H., J. Am. Chem. Soc. 2000, 122:8168–8179.

[29] Gessler, S., Randl, S., Blechert, S., Tetrahedron Lett. 2000, 41:9973–9976.

[30] Grela, K., Harutyunyan, S., Michrowska, A., Angew. Chem. Int. Edit. 2002, 41:4038–4040.

[31] Grela, K., Kim, M., Eur. J. Org. Chem. 2003, 963–966.

[32] Michrowska, A., Bujok, R., Harutyunyan, S., Sashuk, V., Dolgonos, G., Grela, K., J. Am. Chem. Soc. 2004, 126:9318–9325.

[33] Gulajski, L., Michrowska, A., Bujok, R., Grela, K., J. Mol. Catal. A: Chem. 2006, 254:118–123.

[34] Wakamatsu, H., Blechert, S., Angew. Chem. Int. Edit. 2002, 41:2403–2405.

[35] Wakamatsu, H., Blechert, S., Angew. Chem. Int. Edit. 2002, 41:794.

[36] Ung, T., Hejl, A., Grubbs, R.H., Schrodi, Y., Organometallics 2004, 23: 5399–5401.

[37] Chang, S., Jones, L., Wang, C.M., Henling, L.M., Grubbs, R.H., Organometallics 1998, 17:3460–3465.

[38] Allaert, B., Dieltiens, N., Ledoux, N., vercaemst, C., Van der Voort, P., Stevens, C.V., Linden, A., Verpoort, F., J. Mol. Catal. A: Chem. 2006, 260:221–226.
[39] Denk, K., Fridgen , J., Herrmann, W.A., Adv. Synth. Catal. 2002, 344:666–670.
[40] Sanford, M.S., Love, J.A., Grubbs, R.H., Organometallics 2001, 20:5314–5318.
[41] Love, J.A., Morgan, J.P., Trnka, T.M., Grubbs, R.H., Angew. Chem. Int. Edit. 2002, 41:4035–4037.
[42] Choi, T.L., Grubbs, R.H., Angew. Chem. Int. Edit. 2003, 42:1743–1746.
[43] Hahn, F.E., Paas, M., Frohlich, R., J. Organomet. Chem. 2005, 690:5816–5821.
[44] Sanford, M.S., Love, J.A., Grubbs, R.H., J. Am. Chem. Soc. 2001, 123: 6543–6554.
[45] Sanford, M.S., Henling, L.M., Day, M.W., Grubbs, R.H., Angew. Chem. Int. Edit. 2000, 39:3451.
[46] Conrad, J.C., Amoroso, D., Czechura, P., Yap, G.P.A., Fogg, D.E., Organometallics 2003, 22:3634–3636.
[47] Conrad, J.C., Parnas, H.H., Snelgrove, J.L., Fogg, D.E., J. Am. Chem. Soc. 2005, 127:11882–11883.
[48] Buchowicz, W., Ingold, F., Mol, J.C., Lutz, M., Spek, A.L., Chem. - A Eur. J. 2001, 7:2842–2847.
[49] Buchowicz, W., Mol, J.C., Lutz, M., Spek, A.L., J. Organomet. Chem. 1999, 588:205–210.
[50] Krause, J.O., Nuyken, O., Wurst, K., Buchmeiser, M.R., Chem. - A Eur. J. 2004, 10:777–784.
[51] Halbach, T.S., Mix, S., Fischer, D., Maechling, S., Krause, J.O., Sievers, C., Blechert, S., Nuyken, O., Buchmeiser, M.R., J. Org. Chem. 2005, 70:4687–4694.
[52] Furstner, A., Guth, O., Duffels, A., Seidel, G., Liebl, M., Gabor, B., Mynott, R., Chem. - A Eur. J. 2001, 7:4811–4820.
[53] Harlow, K.J., Hill, A.F., Wilton-Ely, J.D.E.T., J. Chem. Soc. -Dalton Trans. 1999, 285–291.
[54] Romero, P.E., Piers, W.E., Mcdonald, R., Angew. Chem. Int. Edit. 2004, 43:6161–6165.
[55] Monsaert, S., Ledoux, N., Schaubroeck, D., Allaert, B., Drozdak, R., van der Voort, P., verpoort, F., Adv. Synth. Catal. 2006 (submitted).
[56] Ledoux, N., Allaert, B., Schaubroeck, D., Monsaert, S., van der Voort, P., verpoort, F., J. Organomet. Chem. 2006, 691:5482–5486.
[57] De Clercq, B., Verpoort, F., Tetrahedron Lett. 2002, 43:9101–9104.
[58] De Clercq, B., Verpoort, F., J. Organomet. Chem. 2003, 672:11–16.
[59] Opstal, T., Verpoort, F., Angew. Chem. Int. Edit. 2003, 42:2876–2879.
[60] Lynn, D.M., Mohr, B., Grubbs, R.H., J. Am. Chem. Soc. 1998, 121:1627–1628.
[61] Dinger, M.B., Mol, J.C., Adv. Synth. Catal. 2002, 344:671–677.
[62] Dinger, M.B., Nieczypor, P., Mol, J.C., Organometallics 2003, 22:5291–5296.
[63] Seiders, T.J., Ward, D.W., Grubbs, R.H., Org. Lett. 2001, 3:3225–3228.
[64] Funk, T..W., Berlin, J.M., Grubbs, R.H., J. Am. Chem. Soc. 2006, 128: 1840–1846.
[65] Ritter, T., Day, M.W., Grubbs, R.H., J. Am. Chem. Soc. 2006, 128:11768–11769.
[66] Arduengo III, A.J., Krafczyk, R., Schmutzler, R., Tetrahedron 1999, 55:14523–14534.
[67] Waltman, A.W., Grubbs, R.H., Organometallics 2004, 23:3105–3107.

CROSS-METATHESIS OF VINYL-SUBSTITUTED ORGANOSILICON DERIVATIVES WITH OLEFINS AND DIENES IN THE PRESENCE OF GRUBBS CATALYSTS

CEZARY PIETRASZUK[1], HELMUT FISCHER[2],
BOGDAN MARCINIEC[1]

[1]*Faculty of Chemistry, Department of Organometallic Chemistry, Adam Mickiewicz University, Grunwaldzka 6 60-780 Poznań, Poland*
[2]*Fachbereich Chemie, Universität Konstanz, Fach M 727, 78457 Konstanz, Germany*

Abstract: A short overview on the reactivity modes and on efficient synthetic routes based on metathesis transformations of vinylsilanes in the presence of Grubbs catalysts is presented. Efficient cross-metathesis of various olefins with vinylsilanes, carrying a large spectrum of different substituents at silicon, in the presence of the first- and second-generation Grubbs catalyst and Hoveyda–Grubbs catalyst is described. Moreover, recent results on the reactivity of a variety of (di)vinyl-substituted silanes and siloxanes are presented. On the basis of the results of equimolar reactions of vinylsilanes and of experiments with deuterium-labelled reagents, a general carbene mechanism for the cross-metathesis of trisubstituted vinylsilanes with olefins is suggested. The reactions constitute a novel valuable method for the synthesis of unsaturated organosilicon derivatives.

Keywords: cross-metathesis, alkylidene complexes, vinylsilanes, ruthenium, Grubbs catalysts

1. Introduction

Olefin metathesis has evolved into an important synthetic tool in organic and polymer chemistry. The family of ruthenium (Ru)-based catalysts (e.g. **I**, **II**, or **III**, Figure 1), tolerant of normal organic and polymer-processing conditions and preserving their catalytic properties in the presence of the majority of functional groups has allowed a great number of new applications [1].

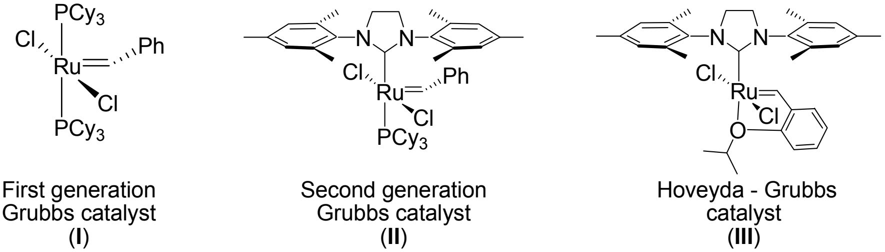

Figure 1. Grubbs-type ruthenium–alkylidene complexes.

Y. İmamoğlu and V. Dragutan (eds.), Metathesis Chemistry: From Nanostructure Design to Synthesis of Advanced Materials, 265-281.

Metathesis transformations have also found many applications in organosilicon chemistry [2]. A number of papers appeared on the metathesis of vinylsilanes as they constitute a class of unsaturated organosilicon compounds of prospective wide applicability in organic synthesis [3], especially in the fast developing palladium-catalysed coupling of vinylsilanes with organic derivatives [4]. Stereoelectronic properties of substituents at silicon in vinylsilanes strongly affect the reactivity of C=C double bond, therefore different reactivity modes are observed in their metathesis transformations.

In this contribution, we will overview reactivity modes and efficient synthetic routes based on metathesis transformations of vinylsilanes in the presence of Grubbs catalysts. The efficient cross-metathesis of vinylsilanes, carrying a large spectrum of different substituents at silicon, with various olefins in the presence of the first- and second-generation Grubbs catalyst and Hoveyda–Grubbs catalyst is described (Eq. 1).

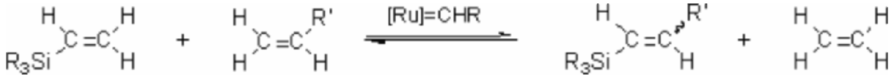

(1)

The effect of substituents at silicon on the reaction is outlined. We discuss advantages and drawbacks of cross-metathesis of vinylsilanes with olefins as a general method for the synthesis of vinyl-trisubstituted silanes and finally present a general mechanistic scheme that explains the processes taking place in the studied systems. Moreover, recent results on the cross-metathesis of a variety of (di)vinyl-substituted silanes, disiloxanes, and monovinyl-substituted siloxanes with olefins are reported [5].

2. Cross-metathesis of vinylsilanes with olefins

The reactions of trialkoxy- or trisiloxy-substituted vinylsilanes with styrene in the presence of Grubbs-type Ru–carbene complex (II) proceed stereoselectively giving trans-β-(silyl)styrenes with high yield (Eq. 2) [6].

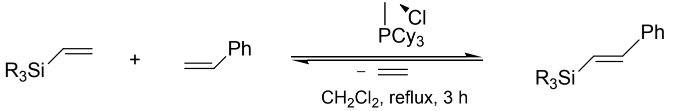

SiR_3	yield [%]
$Si(OMe)_3$	95
$Si(OEt)_3$	94
$Si(OSiMe_3)_3$	95

(2)

Vinylsilsesquioxanes react similarly with pent-4-en-1-on and 5-brompent-1-ene in the presence of Schrock catalyst [7]. We found that Grubbs catalyst **I** exhibits high activity in the cross-metathesis of octavinylsilsesquioxanes with olefins (Eq. 3) [8]. The reaction offers possibilities for the synthesis of highly functionalized silsequioxane and spherosilicate frameworks but it can also be a model for vinylsiloxanes and for vinyl-functionalized surface modification.

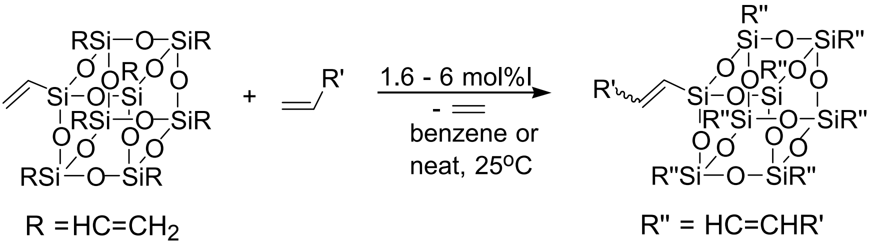

R'	yield [%]	E/Z
Bu	100	85/15
Ph	81	E
$CH_2Si(OMe)_3$	100	88/12
$(CH_2)_3Br$	76	94/6
$(CH_2)_8COOEt$	100	80/20

(3)

The process can be extended efficiently to reactions of trialkoxy- and trisiloxy-substituted vinylsilanes with substituted styrenes, 1-alkenes, and selected allyl derivatives (Eq. 4) [9].

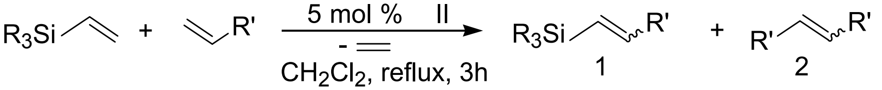

SiR3	R'	yield of 1 [%]	E/Z 1	yield of 2 [%]
$Si(OEt)_3$	Ph	95	E	traces
$Si(OEt)_3$	$p-C_6H_4Cl$	95	E	traces
$Si(OEt)_3$	$p-C_6H_4OMe$	95	E	traces
$Si(OEt)_3$	Bu	75	9/1	10
$Si(OMe)_3$	Bu	60	10/1	8
$Si(OSiMe_3)_3$	Bu	72	10/1	7
$Si(OEt)_3$	CH_2SiMe_3	95	E	traces
$Si(OEt)_3$	$CH_2Si(OEt)_3$	71	15/1	traces
$Si(OEt)_3$	CH_2Ph	68	10/1	traces
$Si(OEt)_3$	CH_2OPh	72	5/1	traces

(4)

Grubbs-type Ru–carbene complexes were found to catalyse the stereoselective cross-metathesis of trialkoxy- and trisiloxy-substituted vinylsilanes with allyl alkyl ethers (Eq. 5) [10] and allyl esters (Eq. 6) [11]. The reaction is accompanied by olefin homo-metathesis.

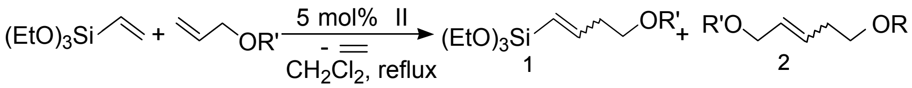

R'	yield of 1 [%]	E/Z 1	yield of 2 [%]
Bu	95	6/1	5
Ph	72	5/1	8
CH_2Ph	86	12/1	14
$SiMe_3$	65	9/1	10

(5)

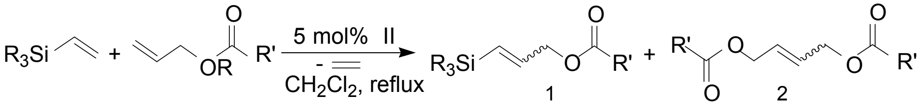

SiR_3	R'	yield of 1 [%]	E/Z 1	yield of 2 [%]
$Si(OEt)_3$	Me	90	12/1	10
$Si(OEt)_3$	Et	94	14/1	5
$Si(OEt)_3$	Pr	93	13/1	2
$Si(OSiMe3)_3$	CH_2CH_2Cy	90	8/1	6

(6)

High yields and selectivities were obtained when some other functionalized olefins underwent cross-metathesis with vinylsilanes [12,13].

The cross-metathesis of 1,9-octadiene with an excess of trialkoxy- and trisiloxy-substituted vinylsilanes results in the formation of bis(silyl)dienes (Eqs. 7 and 8) [14].

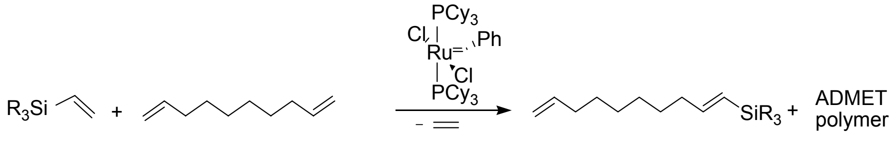

(7)

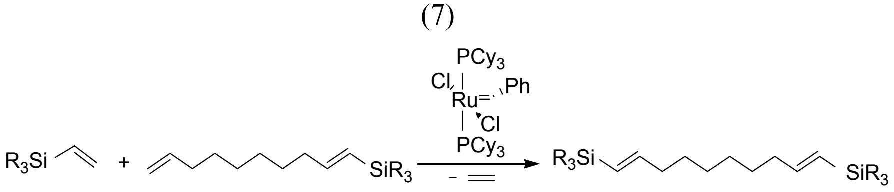

SiR3	yield [%]
$Si(OMe)_3$	73
$Si(OEt)_3$	58
$Si(OSiMe3)_3$	45

(8)

The efficient and stereoselective cross-metathesis of vinylsilanes carrying electron-withdrawing substituents with various olefins has likewise been described (Eq. 9) [15].

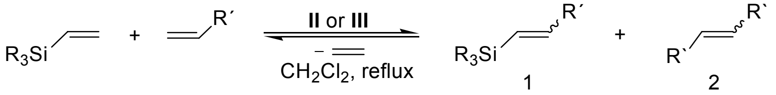

SiR_3	R'	cat.	yield of 1 [%]	E/Z 1	yield of 2 [%]
$SiCl_3$	Ph	**II**	83	E	2
$Si(OAc)_3$	Ph	**II**	75	E	5
$SiCl_2Me$	Ph	**II**	78	E	traces
$SiCl_2(OSiMe_3)$	Ph	**II**	95	E	traces
$SiCl_2Ph$	Ph	**III**	98	E	traces
$SiCl_3$	Ph	**III**	85	E	15
$SiCl_3$	C_4H_9	**III**	100	20/1	0
$SiCl_3$	C_4H_9	**II**	97	20/1	traces
$Si(OAc)_3$	C_4H_9	**II**	100	20/1	0
$SiCl_2Me$	C_4H_9	**II**	100	20/1	0
$SiCl_2(OSiMe_3)$	C_4H_9	**II**	97	20/1	traces
$SiCl_2Ph$	C_4H_9	**II**	95	25/1	traces
$SiCl_3$	CH_2SiMe_3	**II**	100	25/1	0
$SiCl_3$	CH_2OBu	**II**	92	8/1	8

(9)

3. Homo-metathesis of vinylsilanes

It was found that vinylsilanes containing two chloro-substituents at silicon underwent highly stereoselective homo-metathesis in the presence of **I** or **II**. The reactions allows for the complete conversion of vinylsilanes and led to moderate to high yields of *E*-1,2-bis(silyl)ethenes (Eq. 10) [16].

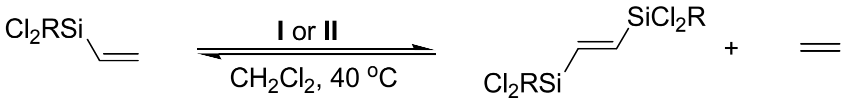

R	cat.	yield [%]
Me	**I**	95
$OSiMe_3$	**I**	93
$OSiMe_3$	**II**	99
C_6H_5	**I**	80
C_6H_4Me-4	**I**	80

(10)

Homo-metathesis of dichloro-substituted vinylsilanes occurring in the presence of **I** or **II** offers an attractive route to *E*-1,2-bis(silyl)ethenes. These reactions are the first examples of vinylsilane homo-metathesis in the presence of the well-defined catalysts.

4. Cross-metathesis of divinyl-substituted silanes and disiloxanes with olefins

A series of divinylsilanes (Figure 2a) and divinyldisiloxanes (Figure 2b) containing electron-withdrawing groups were tested with respect to their reactivity in olefin metathesis [5].

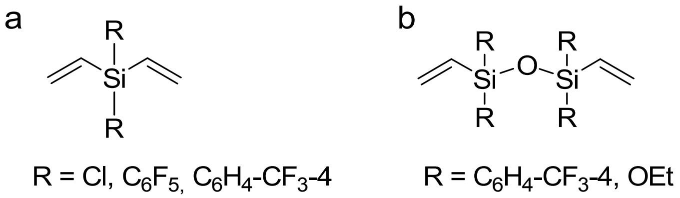

R = Cl, C_6F_5, C_6H_4-CF_3-4

R = C_6H_4-CF_3-4, OEt

Figure 2. Divinyl-substituted silanes and disiloxanes.

Treatment of a mixture of divinylsilane and olefin in the presence of 5–10 mol % of catalyst I, II, or III in boiling CH_2Cl_2 gave rise to the stereoselective formation of monosubstituted and disubstituted vinylsilanes (Eq. 11).

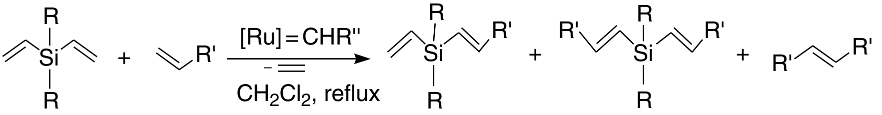

R = Cl, C_6F_5, $C_6H_4CF_3$-4

R' = C_8H_{17}, C_6H_4Cl-4, C_6H_4OMe-4

(11)

The reactions were accompanied by competitive olefin homo-metathesis. On the contrary no divinylsilane homo-metathesis was observed. Selected results are summarized in Table 1.

Similarly, the cross-metathesis of divinyl-substituted disiloxanes with olefins proceeds in the presence of 5–10 mol % of catalyst I, II, or III in boiling CH_2Cl_2 proceeded stereoselectively producing a mixture of monosubstituted and disubstituted vinylsilanes and ethene and a products of competitive olefin homo-metathesis (Eq. 12). Under the optimum conditions the products were obtained with moderate to high yields. Selected results are summarized in Table 2.

Table 1. Cross-metathesis of divinylsilanes with olefins [5]

Divinylsilane R =	Olefin R′ =	Catalyst	Yield of 1 (%)	1 E/Z	Yield of 2 (%)	2^a E,E/E,Z
Cl	C_8H_{17}	**II**	0	E	99	15/1
	C_6H_4Cl-4	**II**	0	E	98	E
C_6H_4-CF_3-4	C_8H_{17}	**I**	63	25/1	0	E
	C_8H_{17}	**II**	4	E	96	15/1
	C_6H_4Cl-4	**III**	2	E	96	E
C_6F_5	C_8H_{17}	**I**	38	25/1	0	E
	C_8H_{17}	**II**	2	E	98	15/1
	C_6H_4Cl-4	**III**	1	E	98	E

Reaction conditions: CH_2Cl_2, reflux; 5 h, catalyst conc. 5 mol %
[a]Isomer Z,Z was not observed

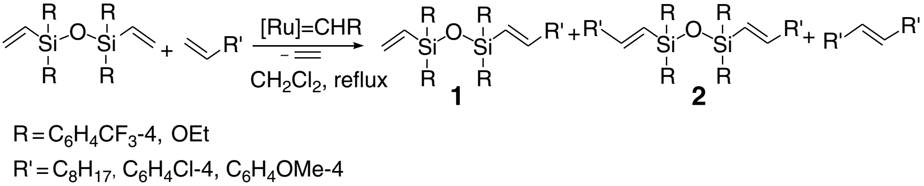

(12)

Table 2. Cross-metathesis of divinyldisiloxanes with olefins [5]

Disiloxane R =	Olefin R′ =	Catalyst	Yield of C (%)	C E/Z	Yield of D (%)	D E,E/E,Z
Ph	C_8H_{17}	**II**	12	E	0	E
	C_6H_4Cl-4	**II**	4	E	0	15/1
C_6H_4-CF_3-4	C_8H_{17}	**II**	8	E	92	15/1
	C_6H_4Cl-4	**III**	12	E	87	E
OEt	C_8H_{17}	**I**	54	25/1	5	E
	C_6H_4Cl-4	**II**	2	E	95	E

Reaction conditions: CH_2Cl_2, reflux; 5 h, catalyst conc. 5 mol %
[a]Isomer Z,Z was not observed

5. ADMET copolymerization of divinyl-substituted silicon compounds with dienes

The reaction proved to be a valuable method for the synthesis of unsaturated organosilicon derivatives and a model for the study of synthesis of oligo and polymeric products via acyclic diene metathesis (ADMET) copolymerization of divinyl-substituted silanes and disiloxanes with dienes. We previously also reported ADMET of $H_2C{=}CH{-}Si(OEt)_2OSi(OEt)_2CH{=}CH_2$ with 1,9-decadiene (Eq. 13) [17] and 1,4-divinylbenzene (Eq. 14) [18].

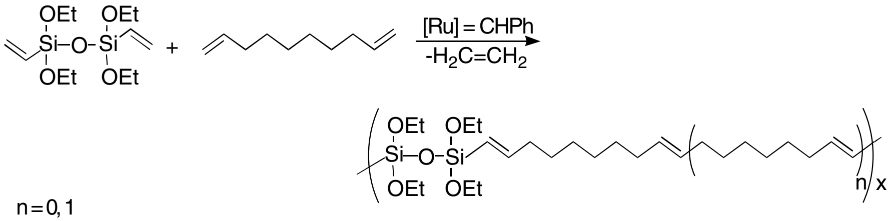

(13)

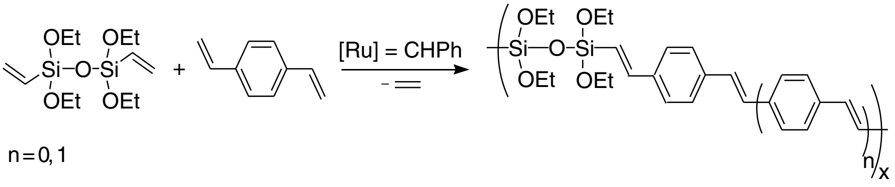

(14)

Accordingly, preliminary experiments showed that ADMET (co)polymers are formed in the reaction of divinyldichlorosilane with diene (Eq. 15) and divinylbenzene (Eq. 16). Some other organosilicon divinyl derivatives were also found to exhibit reactivity in these processes [19].

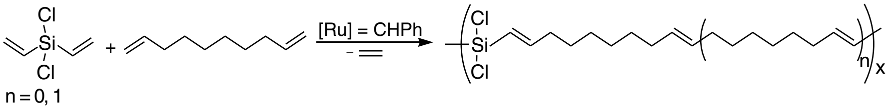

(15)

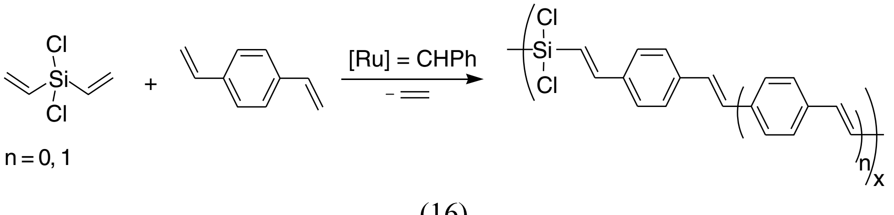

(16)

6. Reactivity of vinylsiloxanes: the model study for modification and cross-linking of poly(vinyl)siloxans via metathesis

Despite the fast development in the metathesis of unsaturated organosilicon compound, the area of vinylsiloxanes is relatively unexplored. Effective cross-metathesis was reported for vinyltris(trimethylsiloxy)silane in the presence of the first- [6] and second-generation [20] Grubbs catalyst and for chloro-substituted vinylsiloxysilanes in the presence of the second-generation [20] Grubbs catalyst.

Vinylsiloxanes of the type illustrated in Figure 3 are model compound for poly(vinyl)siloxanes. Therefore, a series of vinylsiloxanes (Figure 3) was synthesized and the reactivity of these compounds in cross-metathesis with styrenes and 1-decene was studied [21].

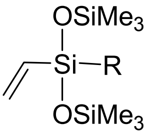

R = Me, $OSiMe_3$, Cl, C_6H_5,
C_6H_4OMe-4, C_6H_4Me-4

Figure 3. Vinylsiloxanes tested in cross metathesis with olefins.

The reaction of vinylsiloxane with olefins in the presence of 5 mol % of catalyst I, II, or III in boiling CH_2Cl_2 produced ethene, substituted vinylsiloxane, and products of competitive olefin homo-metathesis (Eq. 17). Under optimized conditions the products were formed in moderate to high yields. Selected results are summarized in Table 3 [21].

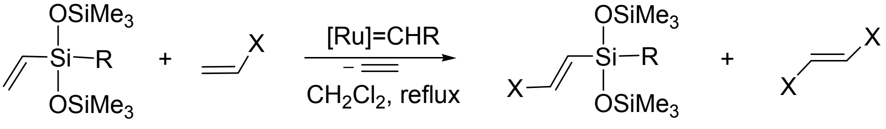

R = Me, $OSiMe_3$, C_6H_5, C_6H_4OMe-4
X = Ph, C_8H_{17}

(17)

The reactivity of vinylsiloxanes provided important clues concerning the functionalization and cross-linking of poly(vinyl)siloxanes. Preliminary investigations showed a limited reactivity of poly(vilyl)siloxanes in the functionalization via cross-metathesis [21]. A pronounced influence of the properties of the substituents at silicon on the metathesis of vinylsilanes was observed (Eq. 18) [21].

Table 3. Cross-metathesis of divinylsilanes with olefins [21]

Siloxane R =	Olefin X =	Catalyst	Yield of vinylsiloxane (%)	E/Z
Me	C_8H_{17}	**II**	5	E
	C_6H_5	**II**	5	E
$OSiMe_3$	C_6H_5	**I**	95	E
	C_8H_{17}	**II**	95	15/1
	C_6H_5	**II**	94	E
	C_6H_4OMe-4	**II**	98	E
Ph	C_8H_{17}	**II**	35	15/1
	C_6H_5	**II**	40	E
	C_6H_4OMe-4	**II**	45	E
C_6H_4OMe-4	C_8H_{17}	**II**	60	15/1
	C_6H_5	**II**	75	E
	C_6H_5	**III**	78	E

Reaction conditions: CH_2Cl_2, reflux, 5 h, catalyst conc.: 5 mol %

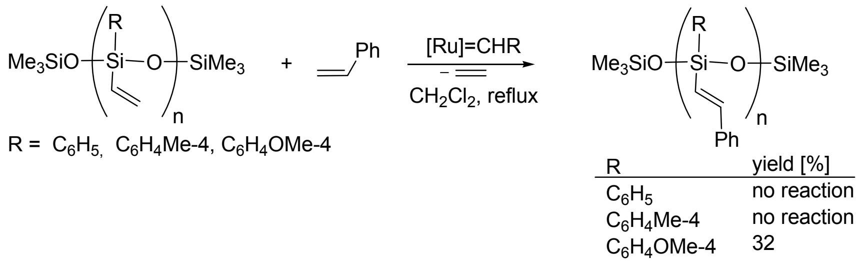

R	yield [%]
C_6H_5	no reaction
C_6H_4Me-4	no reaction
C_6H_4OMe-4	32

(18)

7. Modes of vinylsilanes metathesis

On the basis of substantial differences in the reactivity in metathesis, vinylsilanes can be divided into four general classes (Scheme 1) [20].

Class **1** consists of vinylsilanes containing three identical or different electron-withdrawing substituents such as Cl, OR, OC(O)R, $OSiMe_3$ C_6H_4-(CF_3)-4 at silicon. The cross-metathesis of olefin with the aforementioned vinylsilanes provides the products with high yields and selectivities. Vinylsilanes $H_2C{=}CHSi(OAc)_3$ or $H_2C{=}CHSiCl_3$ undergoes effective cross-metathesis in the presence of **II** and **III** but not **I**. Those vinylsilanes that contain one or two electron-withdrawing groups at silicon and the remaining substituent have no electron-donating properties are substantially less active

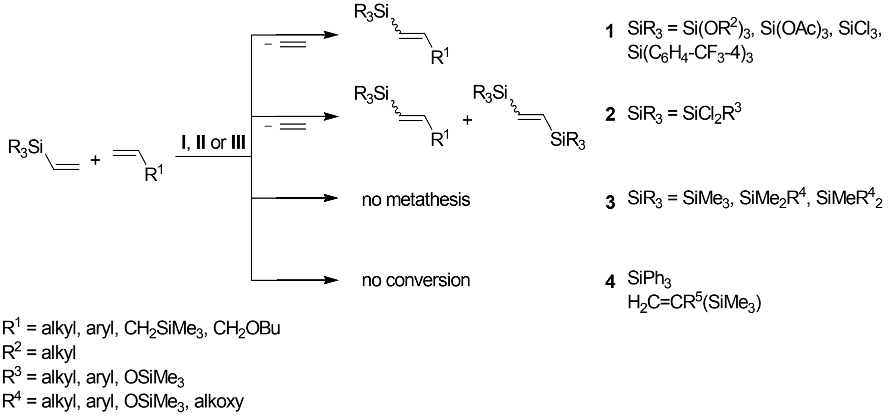

Scheme 1. Reactivity of vinylsilanes in the presence of ruthenium–alkylidene complexes.

in cross-metathesis with olefins. $H_2C{=}CHSiF_2Ph$ in the presence of catalysts **I**, **II**, or **III** and $H_2C{=}CHSi(OEt)_2Ph$ or $H_2C{=}CHSiClPh_2$ in the presence of catalysts **II** or **III** effectively react with styrene or 1-hexene, however, require extended reaction times. $H_2C{=}CHSi(OEt)Ph_2$ and $H_2C{=}CHSiFPh_2$ undergo cross-metathesis with styrene in the presence of **II** or **III**, but afford the products with lower yields and selectivities.

Class **2** consists of vinylsilanes that exhibit activity both in *homo*-metathesis and cross-metathesis with olefins. Only one "substituent motif", that is $H_2C{=}CHSiCl_2R$ (where R = alkyl, aryl, $OSiMe_3$) was found to be characteristic of this class. Cross-metathesis of $H_2C{=}CHSiCl_2R$ with olefins catalysed by **II** or **III** gives cross-metathesis products with high yields and selectivities. For these silanes, care must be taken to choose the proper reaction conditions as well as the vinylsilane to olefin ratio because cross-metathesis is accompanied by competitive homo-metathesis of vinylsilane and olefin.

Class **3** consists of trimethylvinylsilane, all tested dimethyl-substituted and most monosubstituted vinylsilanes. These compounds do not react with olefins by cross-metathesis in the presence of **I**, **II**, or **III** but rather by decomposition [22].

Class **4**, finally, consist of vinylsilanes containing substituents at C_α, e.g. $H_2C{=}C(SiMe_3)_2$ and $H_2C{=}C(Ph)(SiMe_3)$. They do not react with the catalyst. Presumably, a ruthenacyclobutane intermediate cannot be formed because of the steric properties of these 1,1-disubstituted olefins. Similarly, $H_2C{=}CHSiPh_3$ does not react the conditions used.

8. Stoichiometric reactions of ruthenium complexes with vinylsilanes

Both complexes, **I** and **II**, underwent equimolar metathesis with trialkoxy- and tris(trimethylsiloxy)vinylsilane. The reactions led to the selective formation of a methylidene complex and E-1-phenyl-2-(triethoxysilyl)ethene (Eq. 19) [6]. Analogously, the reaction of catalyst **III** with $H_2C{=}CHSi(OEt)_3$ afforded E-1-[(2-isopropoxy)phenyl]-2-(triethoxysilyl)ethene.

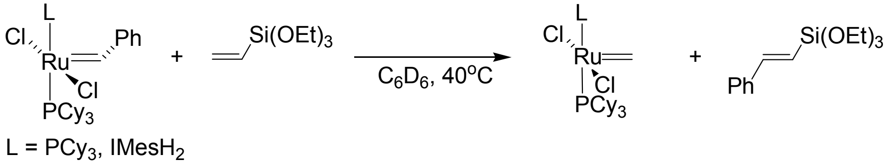

(19)

The reaction of **II** with trichlorovinylsilane $H_2C{=}CHSiCl_3$ gave styrene, silylstyrene, ethylene, and unidentified Ru complexes (Eq. 20) [20].

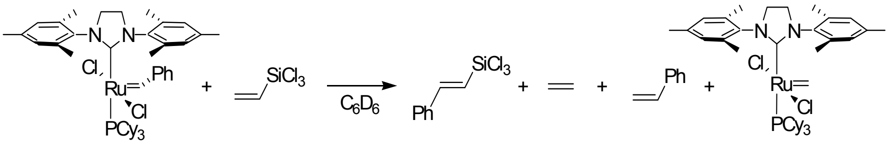

(20)

Chloro-substituted vinylsilanes reacted readily with complex **I** to form unidentizfied non-alkylidene complexes [13]. In contrast, catalysts **II** and **III** were more stable than **I** towards these reagents.

The equimolar reactions of dichloro-substituted vinylsilanes, $H_2C{=}CHSiCl_2R$ (where R = Me, $OSiMe_3$, Ph), with **II** gave styrene, silylstyrene ethylene, and methylidene complexes (Eq. 21) [20].

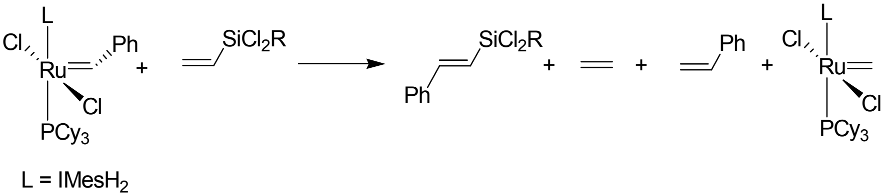

(21)

The identification of styrene among the reaction products suggested the formation of silylcarbene complex. However, all efforts to detect the silylcarbene complex by spectroscopic means or to trap it at low temperature have failed. Obviously, such complexes are thermally or, more likely, kinetically unstable under the conditions used.

The equimolar reaction of trimethylvinylsilane with Grubbs catalyst **I** undergoes yielded substituted propenes and non-alkylidene Ru complexes (Eq. 22).

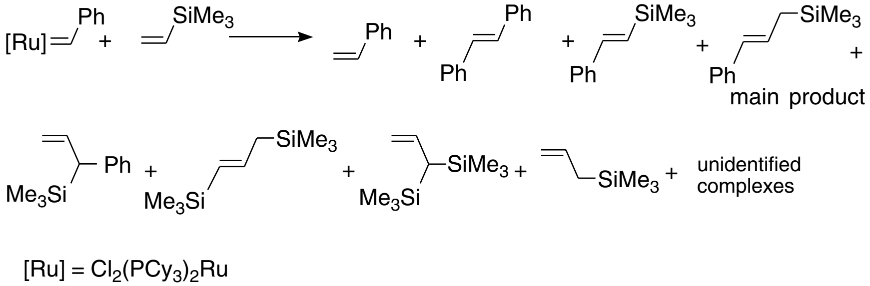

(22)

To accounts for these observations formation of a β-(trimethyylsilyl) ruthenacyclobutane intermediate and subsequent β-elimination of the silyl group was proposed (Scheme 2) [22]. The same process presumably also applies to the reactions of catalyst **II**.

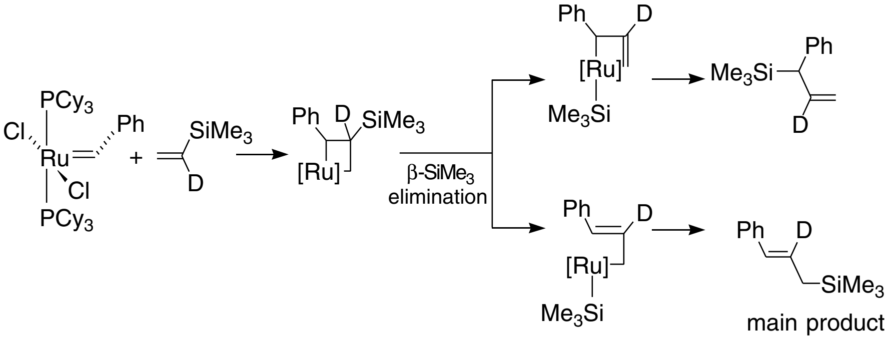

Scheme 2. Proposed mechanism for the decomposition of catalyst I in the presence of trimethylvinylsilane [22].

9. Mechanistic implications

For the catalytic transformantion of vinylsilanes and olefins into silylolefins and ethene two different mechanisms are conceivable namely

(a) Silylative coupling, a non-carbene mechanism established for $[RuHCl(CO)(PPh_3)_3]$- and $[RuCl(SiR_3)(CO)(PPh_3)_2]$-catalysed reactions (Eq. 23)
(b) Cross-metathesis via metalacarbenes (Eq. 24) [2]

Addition of carbene complexes to mixtures of vinylsilanes and olefins does not necessarily mean that their transformations proceed exclusively by the carbene mechanism since alkylidene complexes can decompose to form catalytically active hydride species [23]. Conversely, alkylidene complexes can be formed in the presence of hydride complexes [24].

To distinguish between the non-carbene mechanism of silylative coupling and the carbene mechanism the reactions of a number of vinylsilanes with styrene-d_8 in the presence of I, II, or III were investigated. In the case of the non-carbene mechanism the formation of silylstyrene-d_7 and ethylene-d_1 is to be expected (Eq. 23). In contrast, the carbene mechanism should afford silylstyrene-d_6 and ethylene-d_2 (Eq. 24).

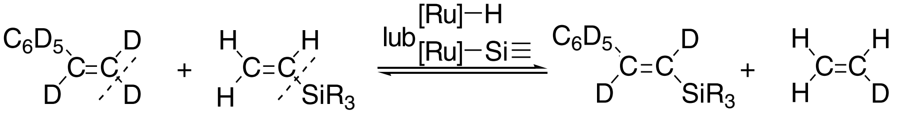

(23)

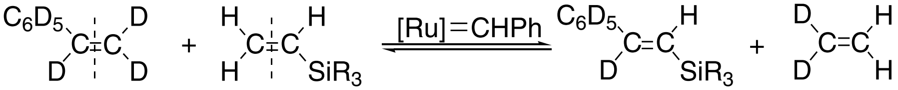

(24)

Analysis of the products formed in the reactions of styrene-d_8 with $H_2C{=}CHSi(OEt)_3$ in the presence of **I** [6], $H_2C{=}CHSiCl_2Me$ in the presence of **II**, and $H_2C{=}CHSiCl_3$ in the presence of **II** and **III** revealed that exclusive *E*-1-phenyl-2-(silyl)ethene-d_6, is formed. This observation strongly supports the metalacarbene mechanism [6,20].

Based on the results of all equimolar and catalytic reactions of vinylsilanes in the presence of Ru–alkylidene complexes, a general mechanistic scheme can be proposed (Scheme 3) [20].

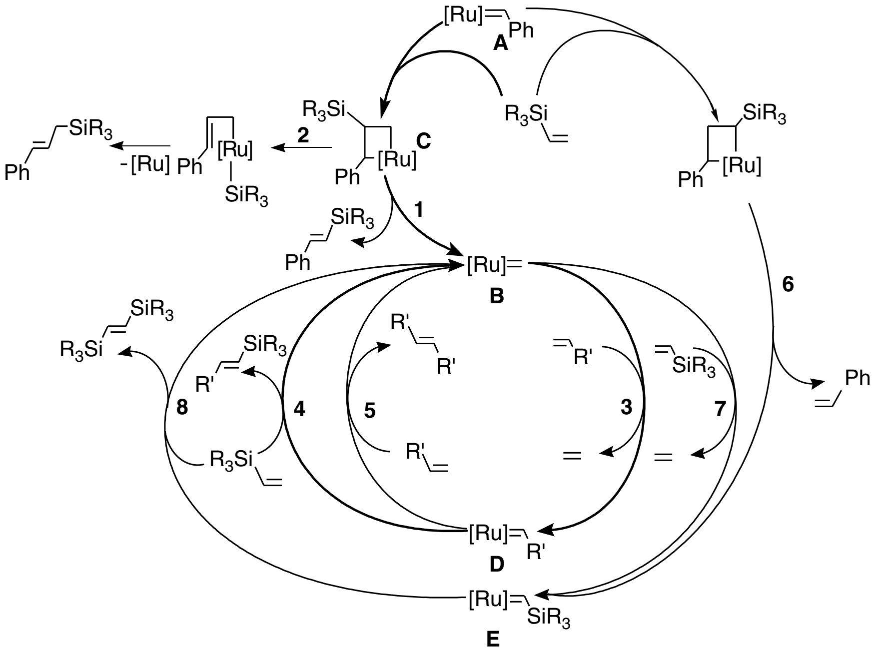

Scheme 3. General scheme of reactivity in the system containing Grubbs catalyst, vinylsilane, and metathetically active olefins [20].

The reaction of vinylsilanes with coordinatively unsaturated benzylidene complex **A** produces methylidene complex **B** and *E*-1-phenyl-2-(silyl)ethene (path 1). This metathesis exchange proceeds by a formal 2 + 2 cycloaddition of the C=C to the Ru=C bond to form the β-(silyl)ruthenacyclobutane intermediate **C** followed by ring opening and dissociation of *E*-1-phenyl-2-(silyl)ethane. When methyl-substituted vinylsilanes are employed, opening of the β-(silyl)ruthenacyclobutane ring **C** and β-silyl elimination in **C** are competing reactions. Silyl elimination is followed by reductive elimination (path 2) thus leading to the loss of the alkylidene moiety and to the formation of complexes inactive in metathesis [22]. The methylidene complex **B** reacts with olefins to form alkylidene complex **D** and ethene (path 3). Alternatively, reaction of B with vinylsilanes could yield ethene and silylcarbene E (path 7). Vinylsilanes and olefins compete for coordination to alkylidene complex **D**. Reaction of **D** with vinylsilanes affords cross-metathesis products and regenerates methylidene complex **B** (path 4), while reaction with olefins affords olefin homo-metathesis products and **B** (path 5). By using the vinylsilanes in excess formation of olefin homo-metathesis products can be avoided in most cases.

The putative (silyl)methylidene complex **E** is formed either by reaction of dichloro-substituted vinylsilanes with benzylidene complex **A** (path 6) or with methylidene complex **B** (path 7). Subsequent reaction of **B** with dichlorovinylsilane yields the homometathesis product 1,2-bis(silyl)ethene and again regenerates methylidene complex **B** (path 8).

10. Conclusions

The investigation of the reactivities of a series of vinylsilanes in the presence of equimolar and catalytic amounts of Grubbs catalysts of the first and second generation and of the Hoveyda–Grubbs catalysts (second generation) provides comprehensive information on the reactivity of a wide range of vinylsilanes. The carbene mechanism of the cross-metathesis of vinylsilanes and styrene has been established on the basis of experiments with deuterium-labelled reagents. The lack of methyl-substituted vinylsilane activity in metathesis processes can readily be explained. The dependence of the vinylsilane reactivity in metathesis transformations on the nature of the substituents at the silicon atom is now understood. A general mechanistic scheme of the reactivity of vinylsilanes in metathesis transformations explains the formation of all products observed and all the processes taking place in the system.

The cross-metathesis of a variety of (di)vinyl-substituted silanes, disiloxanes, and monovinyl-substituted siloxanes with olefins has proved to be a valuable method for the synthesis of unsaturated organosilicon derivatives and a model for the study of the synthesis of oligo and polymeric products via ADMET copolymerization of divinyl-substituted silanes and disiloxanes with dienes. Furthermore, differently substituted vinylsiloxanes are valuable model compounds for studying poly(vinyl)siloxanes modification and cross-linking.

Acknowledgement

We thank the European Commission (Contract numbers ICA1-CT-2002-70001 and ICA1-CT-2002-70002) and Ministry of Science and Higher Education (Project number PBZ-KBN-118/T09/17) for the financial support of this investigation.

References

[1] Grubbs, R.H. (ed.) Handbook of Metathesis, Wiley-VCH, Weinheim, 2003.
[2] (a) Marciniec, B., Pietraszuk, C., Metathesis of silicon-containing olefins, in: Grubbs, R.H. (ed.) Handbook of Metathesis, Wiley-VCH, Weinheim, 2003, Chapter 2.13; (b) Marciniec, B., Pietraszuk, C., Curr. Org. Chem. 2003, 7:691.

[3] (a) Chan, T.H., Fleming, I., Synthesis 1979, 761; (b) Weber, W.P., Silicon Reagents for Organic Synthesis, Springer, Berlin, 1983, Chapter 7; (c) Colvin, E.W., Silicon Reagents in Organic Synthesis, Academic Press, London, 1988, Chapter 3; (d) Luh, T.-Y., Liu, S.-T., in: Rappoport, Z., Apeloig, Y. (eds) The Chemistry of Organosilicon Compounds, Wiley, Chichester, 1998, Chapter 30.

[4] For recent reviews on the use of silyl olefins in cross-coupling reactions see (a) Hiyama, T., in: Diederich, F., Stang, P., (eds) Metal Catalysed Cross-coupling Reactions, Wiley-VCH, Weinheim, 1998, Chapter 10; (b) Denmark, S.E., Sweis, R.F., Acc. Chem. Res. 2002, 35:835; (c) Hiyama, T., J. Organomet. Chem. 2002, 653:58.

[5] Pietraszuk, C., Rogalski, S., Majchrzak, M., Marciniec, B., J. Organomet. Chem. 2006 (in press).

[6] Pietraszuk, C., Marciniec, B., Fischer, H., Organometallics 2000, 19:913.

[7] Feher, F.J., Soulivong, D., Eklund, A.G., Wydham, K.D., Chem. Commun. 1997, 1185.

[8] Itami, Y., Marciniec, B., Kubicki, M., Chem. Eur. J. 2004, 10:39.

[9] Pietraszuk, C., Fischer, H., Kujawa, M., Marciniec, B., Tetrahedron Lett. 2001, 42:1175.

[10] Kujawa-Welten, M., Pietraszuk, C., Marciniec, B., Organometallics 2002, 21:840.

[11] Kujawa-Welten, M., Marciniec, B., J. Mol. Catal. A: Chem. 2002, 190:79.

[12] (a) Marciniec, B., Jankowska, M., Pietraszuk, C., Chem. Commun. 2005, 663; (b) Jankowska, M., Pietraszuk, C., Marciniec, B., Zaidlewicz, M., Synlett 2006, 1965.

[13] Marciniec, B., Chadyniak, D., Krompiec, S., J. Mol. Catal. A: Chem. 2004, 224:111.

[14] Pietraszuk, C., Marciniec, B., Jankowska, M., Adv. Synth. Catal. 2002, 344:789.

[15] Pietraszuk, C., Marciniec, B., Fischer, H., Tetrahedron Lett. 2003, 44:7121.

[16] Pietraszuk, C., Marciniec, B., Rogalski, S., Fischer, H., J. Mol. Catal. A: Chem. 2005, 690:5912.

[17] Malecka, E., Marciniec, B., Pietraszuk, C., Church, A.C., Wagener, K.B., J. Mol. Catal. A: Chem. 2002, 190:27.

[18] Marciniec, B., Majchrzak, M. J., Organomet. Chem. 2003, 686:228.

[19] Pietraszuk, C., Rogalski, S., Majchrzak, M., Marciniec, B. (not published results).

[20] Pietraszuk, C., Fischer, H., Rogalski, S., Marciniec, B., J. Organomet. Chem. 2005, 690:5912.

[21] Pietraszuk, C., Wrzesniak, P., Rogalski, S., Marciniec, B. (2006) (prepared for publication).

[22] Pietraszuk, C., Fischer, H., Chem. Commun. 2000, 2463.

[23] For review see: Schmidt, B., Eur. J. Org. Chem. 2004, 1865.

[24] (a) Nguyen, S.T., Trnka, T.M., The discovery and development of well-defined, ruthenium based olefin metathesis catalysts, in: Grubbs, R.H. (ed.) Handbook of Metathesis, Wiley-VCH, Weinheim, 2003, Chapter 1.6; (b) Werner, H., Wolf, J., Synthesis of rhodium and ruthenium carbene complexes with a 16-electron count, in: Grubbs, R.H. (ed.) Handbook of Metathesis, Wiley-VCH, Weinheim, 2003, Chapter 1.8.

PART III. TAILORED POLYMERS BY METATHESIS POLYMERIZATION

FROM DRUG COCKTAILS TO TISSUE ENGINEERING: SYNTHESIS OF ROMP POLYMERS FOR BIOMEDICAL APPLICATIONS

KENNETH D. CAMM, DERYN E. FOGG

Center for Catalysis Research and Innovation, Department of Chemistry, University of Ottawa, 10 Marie Curie K1N 6N5 Ottawa, ON, Canada

Abstract: Challenges and advances in the synthesis of ring-opening metathesis polymerization (ROMP) polymers bearing biologically relevant functionalities are examined. The impact of various initiators, monomer platforms, and reaction conditions on control over polymer chain lengths and architectures, is discussed. Particular attention is given to the level of control currently attainable in Ru-promoted ROMP of unprotected monomers in aqueous or protic media, vs. ROMP of protected monomers in organic solvents.

Keywords: olefin metathesis, polymerization, aqueous, ROMP, biological, drug

1. Introduction

Synthetic polymers and polymer composites have long been deployed in biomedical applications as prostheses, dental materials, and medical devices [1,2], as supports for the fabrication of engineered tissues [3], and, more recently, as “polymer therapeutics” or drug-delivery agents [4]. Success in such applications rests on the biocompatibility of the materials, as well as their ability to serve the required function. The advent of materials that can be designed, rather than modified, for service in biological contexts is opening up new possibilities in this area. Of particular interest are living polymerization strategies that permit synthesis of well-defined materials, with specification of polymer chain lengths, molecular weight distributions, block architectures, and the composition of pendant and end-group functionalities. The target polymer properties may be a function of any or all of these parameters, and the capacity to specify and vary structure, and hence to develop structure–property relationships, is essential in order to identify which parameters are important. Of the available living polymerization techniques, ruthenium (Ru)-catalyzed ring-opening metathesis polymerization (ROMP) is attractive for its exceptional versatility and synthetic convenience [5,6]. Recent advances in catalyst (or “initiator”) design expand opportunities further, bringing within reach straightforward methods for the molecular-level design of macromolecular materials. Such methods are likely to have a

Y. İmamoğlu and V. Dragutan (eds.), Metathesis Chemistry: From Nanostructure Design to Synthesis of Advanced Materials, 285-303.

transformative impact on the design of materials for an enormous range of applications, among which biological contexts present a particularly stringent challenge. In the following review, we highlight advances in the synthesis of ROMP polymers for biomedical applications, with a particular focus on the accessibility of polymers with precise control over chain lengths, polydispersities (PDIs), and block architectures. Much of this work was influenced by Kiessling's pioneering studies of the construction and deployment of ROMP neoglycopolymers as probes of receptor interactions and function [7, 8]. While the area of application is outside the scope of this review, synthetic issues relevant to the present topic will be discussed.

2. Synthesis of ROMP polymers bearing biologically relevant groups

2.1 General considerations

2.1.1 Monomer platform

The majority of "designer" ROMP polymers prepared to date are 5-functionalized polynorbornenes (Eq. 1; **A**, X = CH_2). A key advantage of norbornene monomers is the ring strain present in the bicyclic structure, which confers high reactivity toward ring-opening, and renders the reaction irreversible. The increase in steric bulk relative to, (e.g.) polyoctenes, also constitutes a steric impediment to backbiting and interchain metathesis. Living ROMP can be achieved with many norbornene monomers on use of appropriate initiators and reaction conditions, enabling precise control over polymer chain lengths and block architectures. A further advantage is the very wide range of norbornenes accessible by Diels-Alder [9] or S_NAr [10] reactions, or by modification of norbornenes bearing suitable functionalities, such as acid chloride or alcohol groups. Oxanorbornenes (e.g. **A**, X = O) are also readily accessible by Diels–Alder reactions with furan. While retro-Diels–Alder reactions are a potential drawback [9], these monomers offer added opportunities in biological contexts: the furan ring improves water solubility, and the structural resemblance to the furanose sugars may improve biocompatibility [11].

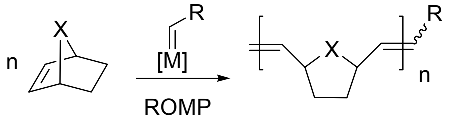

(1)

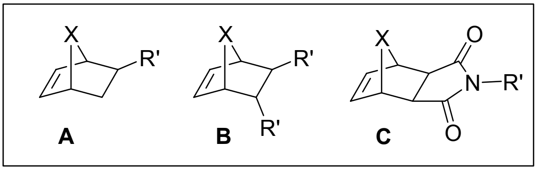

In comparison to norbornene (or oxanorbornene) monomers bearing biologically relevant substituents at the 5-position, 5,6-disubstituted monomers containing independent pendant groups (**B**) have been little explored. The increased density of functional groups may be valuable in improving solubility, in masking the potentially bioincompatible polymer backbone, and in providing additional sites for interaction. Given the steric bulk associated with many biologically relevant functionalities, however, such monomers can impose considerable demand on the reactivity of the ROMP initiator. More common are succinimide monomers such as **C**, readily accessible from himic anhydride (2-norbornene-5,6-dicarboxylic anhydride). For all of these monomers, *endo* and *exo* isomers are possible, of which the latter are more reactive.

A potential challenge in using functionalized polymers in biological environments is the hydrolytic sensitivity of the ester or anhydride functionalities commonly used to tether pendant functionalities to the norbornene ring [9]. In model studies, Weck and coworkers reported hydrolysis of ester, acetal, and β-amino ester groups at different pH ranges; saccharide monomers were also affected [12].

2.1.2 ROMP initiators

Controlled ROMP of norbornene monomers bearing biologically relevant substituents has been achieved using a range of initiators, of which most important are the molybdenum (Mo) and Ru complexes pioneered by Schrock and Grubbs, respectively (Figure 1). The Mo initiators require greater care in handling, owing to their thermal sensitivity and their susceptibility to decomposition by air, water, and protic or oxygen-donor functionalities, such as hydroxyl or aldehyde groups. Initiator **1a** is most commonly used of the Schrock catalysts, as the progressively higher reactivity of **1b** and **1c** can enable backbiting and chain-transfer reactions. While ROMP of monomers of Classes **A** and **C**, in particular, is typically faster than ring-closing metathesis (RCM) reactions, much greater care must be taken to ensure pristine conditions when using the Group 6 initiators for ROMP. Side-reactions such as hydrolysis or oxidation limit catalyst efficiency in any metathesis reaction, but are particularly detrimental in ROMP because they also compromise control over polymer chain lengths, and thus polymer properties. Development of the more robust, easily-handled Ru initiator **2** was thus a major advance, despite its much lower reactivity relative to **1a**. The greater functional-group tolerance of the Ru systems, though frequently highlighted, tends in practice to be less significant: similar protecting-group strategies are generally required for **2** as for **1**, as aqueous ROMP is not routinely compatible with controlled polymerization for sterically encumbered monomers (see Section 2.2.).

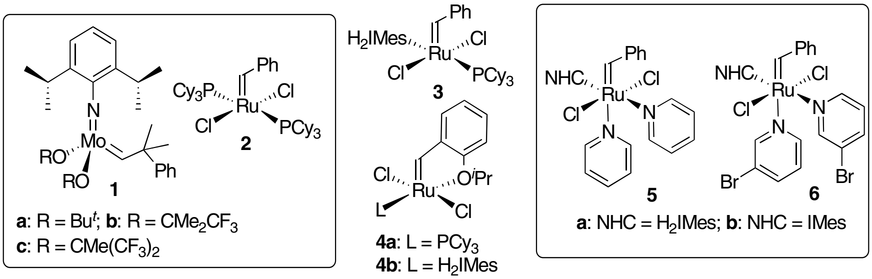

Figure 1. Well-defined metathesis catalysts. Initiators capable of controlled ROMP are enclosed in boxes. IMes = *N,N'*-bis(mesityl)imidazol-2-ylidene.

Much of the work discussed below involves use of the Grubbs catalyst **2**. The "second-generation" catalysts of type **3** are of limited use in ROMP applications. While such catalysts have had an enormous impact on organic chemistry, in which their amplified reactivity has helped to transform RCM and cross-metathesis (CM) into cornerstone synthetic methodologies, their low initiation efficiency is a major drawback in ROMP. Because only a small proportion of these initiators contributes to polymerization, polydispersities are high, and molecular weights are uncontrolled (often double or triple the values expected from the reaction stoichiometry). Similar limitations are found for the "Hoveyda" catalysts **4**: these initiate slowly, owing to the high thermodynamic stability of the five-membered chelate ring, but propagate very rapidly following removal of the ether donor from the coordination sphere. The pyridine complexes **5** and **6** [13], justly regarded as "third-generation" Ru initiators, combine high ROMP activity with excellent control over chain lengths (including, in some cases, living ROMP [14]). Their higher reactivity, however, also translates into a generally higher sensitivity, and these complexes are, for example, more susceptible to decomposition in aerobic solutions.

2.1.3 Polymer architecture and topology

Fundamental to many biological applications of ROMP polymers is the multivalent effect, a strategy brought to prominence in context of ROMP by Kiessling and coworkers [7,8,15]. Presentation of multiple recognition elements on a polymer to multiple binding sites on a target can significantly increase binding affinities, relative to monovalent species, if the spacing of the recognition elements permits multiple docking interactions. Reinforcing this "chelate" effect, high local concentrations of recognition elements around a target also increase the probability of encounter, and thus replacement of a recognition element following a dissociation event. The ease of specifying functionality and valency (through functional group density and chain length) has been a significant advantage in use of ROMP polymers as probes of multivalent effects in biological processes, as well as in the design of materials to exploit the phenomenon [7,8].

The most common multivalent ROMP array is a polynorbornene bearing multiple pendant functional groups, typically a homopolymer (Figure 2a), but sometimes a block copolymer. In aqueous media, amphiphilic block copolymers may form micelles. A multivalent array may be presented on the surface (Figure 2b); alternatively, such entities may act as artificial liposomes in which the exterior coat confers merely water-solubility, and "Trojan horse" strategies enable release of guest compounds held in the lipophilic core. End-functionalization strategies can also be useful (Figure 2c), either as a means of modifying multivalent polymers, or in their own right. End-groups can be installed during ROMP, by use of an appropriately functionalized alkylidene group on the initiator, or by post-polymerization modification. Other post-polymerization reactions can also be valuable: of particular importance is hydrogenation, which eliminates the unsaturation of the polymer backbone, and hence cross-linking or other degradation reactions that exploit the latent reactivity of the olefinic sites.

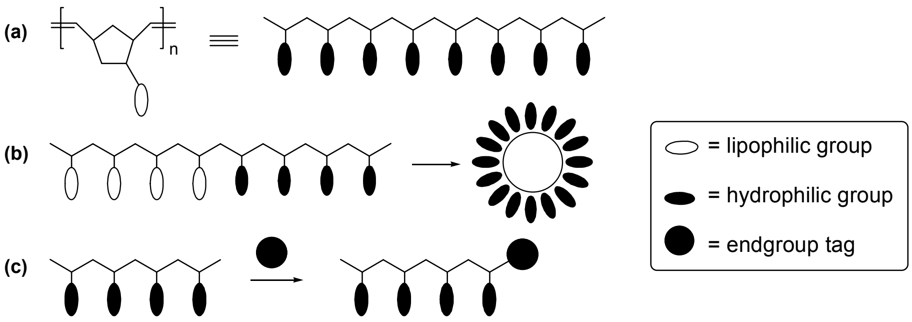

Figure 2. Common architectural motifs in ROMP polymers designed for biological applications.

2.2 Synthetic challenges and approaches

Solubility is a major issue in ROMP of biologically relevant monomers, the majority of which bear hydrophilic functionalities. In rare cases, the unprotected monomers are soluble in relatively polar, non-protic organic solvents. Gibson and coworkers found that norbornenes bearing small amino acid groups were sufficiently soluble in tetrahydrofuran (THF) to support ROMP in this solvent (**7**, Figure 3) [16]. Reaction with **2** (50–100 equiv **7**; 4 h, r.t.) afforded polymer in 65–96% yield after workup. No correlation between yield and steric bulk was noted. Agreement between calculated and experimental (GPC) M_n values ranged from excellent to 50% higher than expected. High PDI values (1.3–1.4) may indicate preferential binding of THF to the initiating, vs the propagating species. Precipitation of the growing polymer chain was not reported, but is a common hazard where organic solvents are used for ROMP of monomers bearing polar substituents, especially where chain lengths extend beyond the oligomeric. ROMP of penicillin-functionalized **8** (10 equiv) in acetone solution was accompanied by precipitation within minutes at ambient temperature [17]. Electrospray ionization–mass spectroscopy (ESI–MS) analysis indicated the presence of oligomers of up to 17 repeat units, but quantitative analysis was precluded by their low solubility.

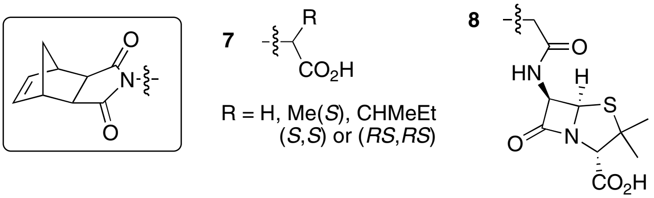

Figure 3. Representative unprotected monomers subjected to ROMP in polar organic solvents.

The relative robustness of the Ru initiators opens the possibility of metathesis in water. Degassed water is attractive as an inexpensive, nontoxic solvent that offers the potential for ROMP of hydrophilic monomers without need for protecting groups. While much less aggressive toward Ru than, e.g., Mo catalysts, water is not an innocuous medium for this chemistry and success is determined by the kinetics of polymerization vs catalyst decomposition. Best results are achieved with highly reactive monomers, in conjunction with initiators in which reactivity can be tuned to maximize the kinetic discrimination between ROMP and deleterious side-reactions. Stoichiometric quantities of HCl have been used to increase the rate of ROMP relative to deactivation in polymerization of Class C monomers by water-soluble Grubbs-class catalysts [18]. A number of these initiators have been reported [5], but methodologies for controlled polymerization of demanding substrates have not yet been perfected, and few monomers relevant to the present discussion have been explored.

More extensive are studies involving reaction of a well-defined Ru catalyst (typically **2**) with the unprotected monomers in water or methanol. As **2** is insoluble in these media, it is usually predissolved in a chlorocarbon solvent. For reactions in water, intimate contact between monomer and catalyst is then promoted by use of methanol as co-solvent, or by use of an emulsifying agent such as dodecyltrimethylammonium bromide (DTAB). The impact of the conditions chosen on polymer chain length and polydispersity is discussed below. A note concerning characterization is warranted, however. Analysis of the molecular weights of the resulting water-soluble ROMP polymers is almost invariably carried out by NMR evaluation of the average degree of polymerization (DP_{av}), as many of the research groups active in this area have limited access to aqueous GPC capabilities. In ROMP via **2**–**4**, integration of the ^1H NMR signals due to the phenyl end-group against the olefin signals enables estimation of the average chain length, but does not report on the polymer polydispersity. The accuracy of integration will be highest for relatively short chain lengths, and for systems in which chain transfer or backbiting reactions are minimal.

2.2.1 ROMP in the presence of methanol

We consider metathesis in the presence of methanol separately, in view of work from the Mol group describing decomposition of **2** and **3** by methanol at 70°C. Multiple products were obtained, including $RuHCl(CO)(L)(PCy_3)$ ($L = PCy_3$, NHC) [19,20].

In a rare example of ROMP in methanol alone, the sterically demanding vancomycin monomer **9a** (Figure 4) was polymerized via **2**, following purification of the monomer by reverse-phase chromatography using 1% trifluoroacetic acid (TFA) in 1:2 $MeCN:H_2O$ [21]. ROMP of 7–10 equivalents of the monomer was incomplete after 1.5 days at room temperature. Purification as before yielded the polymer in 60% yield. Gel electrophoresis showed the presence of four distinct molecular weight fractions, ranging from ~8 to >20 kDa, vs the theoretical value of 10.5 kDa. Observation of distinct molecular weight fractions is consistent with the operation of multiple Ru species of different activity, though the insolubility of the initiator in methanol will also increase polydispersity.

Low yields in ROMP of carbohydrate-functionalized monomers in chlorocarbon–methanol mixtures were attributed to low solubility, though initiator decomposition may also contribute. Thus, Fraser and Grubbs found that ROMP of glucose-functionalized **10** (55 equiv; Figure 4) by $RuCl_2(PCy_3)_2(=CHCH{=}CPh_2)$ in 2:3 $CH_2Cl_2:MeOH$ afforded only trace polymer even after 2 days at 50°C [22]. Likewise, Kiessling and coworkers reported that ROMP of 15 equivalents of sulfated galactose monomer **11a** via **2** in 1.5:1 $CH_2Cl_2:MeOH$ proceeded to only 25% yield after 2 days at 65°C. Some improvement was found where a single sulfate group was present on the monomer (**12a**), but yields were still limited to ~50% [23]. Addition of water (5:6:1 dichloroethane:$MeOH:H_2O$) enabled near-quantitative ROMP of 7 equivalents of mannose-functionalized **9b** at room temperature, yielding an oligomer with a DP_{av} of 10 [24]. High conversions were retained on use of 50 equivalents of **9b**, but dropped to 50% on use of 100 equivalents: this may reflect a decrease in solubility, or termination becoming increasingly competitive

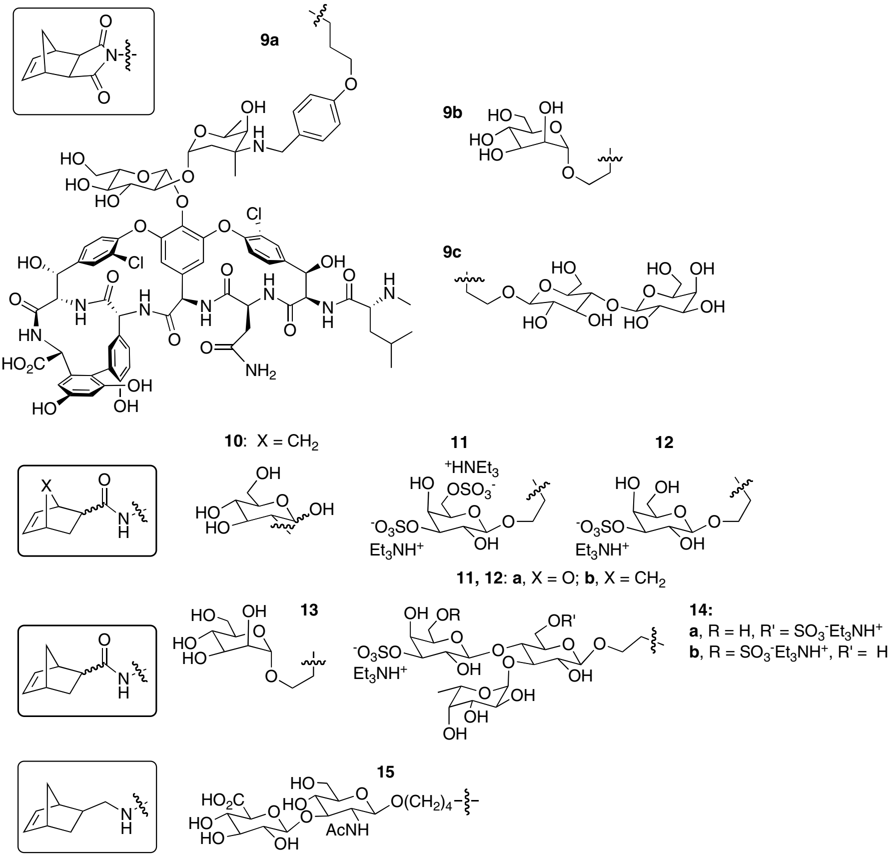

Figure 4. Summary of unprotected carbohydrate-containing monomers discussed.

with propagation as the proportion of monomer increases. ROMP of sterically encumbered lactose monomer **9c** (10 equiv, r.t.) under similar conditions gave polymers with a DP_{av} of 20 [25].

Nguyen and coworkers undertook synthesis of ROMP polymers bearing the chemotherapeutic drug doxorubicin in chlorocarbon–methanol mixtures [26]. Homopolymers of **16** (Figure 5) proved insoluble in 9:1 $CDCl_3$–CD_3OD, but solubility was improved by copolymerization with hexaethylene oxide monomer **17a**. Thus, sequential ROMP of **17a** and **16** using initiator **2** (15 equiv of each, 2 h, r.t.) gave a dark red copolymer, isolated in 76% yield. Gel permeation chromatography (GPC) analysis in THF indicated an M_n

value of 12.5 kDa, vs a theoretical value of 17.8 kDa (PDI 1.3). The discrepancy was attributed to the low hydrodynamic radius of the copolymer relative to the polystyrene GPC standards. ^{1}H NMR integration values suggested incorporation of ~80% **16** into the copolymer, while ultraviolet–visible (UV–Vis) absorption studies suggested complete incorporation.

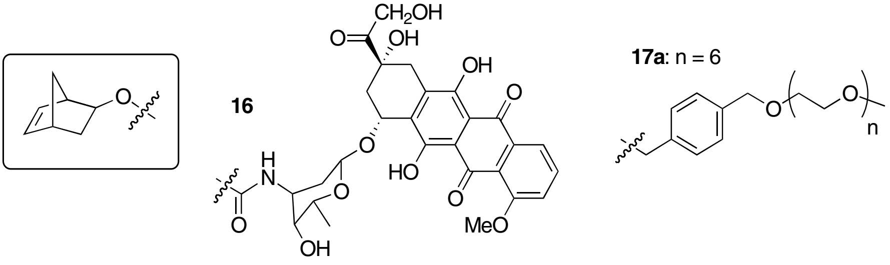

Figure 5. Monomers used to prepare a potentially chemotherapeutic polymer via ROMP in the presence of methanol.

Grubbs and coworkers reported that monomers bearing GRGD and SRN peptide sequences, of interest for their potential cell adhesion properties, exhibit low solubility in organic media, even when protected [27]. Use of **2** to effect random copolymerization of **18a**,**b** (Figure 6) with ethylene glycol monomer **17b** (CH_2Cl_2, r.t.) resulted in low polymer yields (<26%) and bimodal molecular weight distributions if more than 10% of either peptide monomer was present. Incorporation of a higher proportion of peptide groups was sought by using **3** as initiator, in CH_2Cl_2–MeOH. Copolymers of **18a** and **18b** were obtained in only ~30% yield in 1:1 CH_2Cl_2–MeOH (55°C, 2 h; total 20 equiv monomer). Copolymerization with **17b** increased yields to 74–92%. Homopolymers of **18a** or **18b**, prepared by reaction of 10 equivalents of monomer with **3** or closely related catalysts, were 2–3 times longer than expected (M_n values measured by aqueous GPC following deprotection). Analogous monomers bearing GRGDS, PHSRN, or GRGES peptide sequences gave homo- and diblock copolymers in 64–90% yields (10 equiv monomer), with similarly high M_n values [28]. While poor control over chain lengths is a characteristic feature of **3**, reflecting the low initiation efficiency noted above, bond scission during deprotection may also be an issue. Removal of *tert*-butyl protecting groups by treatment with HF resulted in polymers with considerably higher PDI values than those obtained on TFA deprotection of trityl- or Pbf-protected polymers (1.7, vs a range of 1.13–1.3).

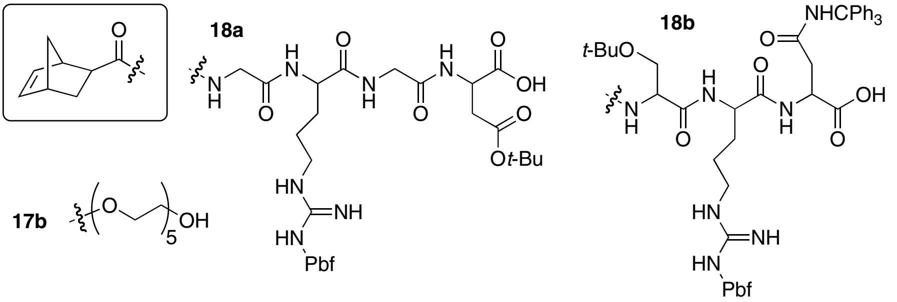

Figure 6. Representative monomers used to prepare polymers bearing peptide sequences via ROMP in the presence of methanol. Pbf = 2,2,4,6,7-pentamethyldihydrobenzofuran-5-sulfonyl.

In attempts to synthesize related peptide-functionalized polymers via **2** or **3** in 3:1 CH_2Cl_2:MeOH, the Sampson group noted that precipitation limited chain lengths to ~10 repeat units, even on use of 25–50 equivalents of monomer [29]. Addition of HCl gave no improvement, but addition of LiCl yielded polymers with DP_{av} values in good agreement with theoretical ratios, in 64–88% yield. The additive was proposed to inhibit monomer aggregation. Use of **6a** to effect ROMP of the protected peptide monomers was less successful [30]. GPC analysis at successive stages of assembly of a triblock copolymer suggested decomposition over the course of reaction. The heightened reactivity of the pyridine initiators increases their susceptibility to decomposition, as noted above. The correlation between high metathesis activity and short catalyst lifetime is now well recognized: it is particularly problematic in context of ROMP, as it has a direct impact on chain lengths, rather than simply affecting catalytic efficiency.

A common theme in the examples described above is the limited control over polymer chain lengths found for ROMP in the presence of methanol. Catalyst decomposition (particularly at elevated temperatures) provides a partial explanation. An added complication, for longer polymer chains or large monomers, is the insolubility of the growing polymer chains. In some cases, addition of water to the reaction mixture resulted in higher yields and improved agreement between observed and calculated DP_{av} values.

2.2.2 ROMP in aqueous emulsion

For ROMP in organic–aqueous solvent mixtures, emulsifying agents such as DTAB can facilitate interphase exchange of initiator and monomer, obviating the need for methanol. This can improve yields, and enable preparation of longer polymer chains [31,32]. While ROMP of glucose-functionalized **10** by **2** in 2:3 CH_2Cl_2–MeOH afforded only trace polymer, as noted above, reaction under emulsion conditions gave quantitative yields (35 equiv **10**, 3 equiv DTAB, 1:6 CH_2Cl_2–H_2O, 50°C, 1 day) [22]. Control over chain lengths is not improved, however: Grubbs and coworkers have proposed that this is due to exchange of the chloride ligands on **2** with the bromide groups of DTAB [18]. Thus, polymers of mannose monomer **13** (Figure 4; 10–50 equiv) prepared via **2** were double the expected lengths [33], as were those prepared by ROMP of 10–15 equiv of galactose monomers **11/12** under similar conditions, but at 40–55°C. Isolated yields were lower where two sulfate groups were present on the monomer (32% and 65% for **11a** and **11b**; 74% and 70% for **12a** and **12b**, respectively). However, yields for **11a** and **12a** were higher than in chlorocarbon–methanol [23,34]. Long chains could also be obtained: ROMP of 100 equiv of mannose monomer **9b** via **2** in 1:2 dichloroethane-H_2O (1.6 equiv DTAB, 20 h, r.t.) proceeded to 98% conversion, affording polymer with a DP_{av} of 143 [24]. In contrast with the usual observations, ROMP of the hyaluronan monomer **15** via **3** (20 equiv **15**, 20 equiv DTAB, 1:1.5 dichloroethane–H_2O; 5 h, 60°C) gave a DP_{av} value of ~15, lower than expected [35].

Building on the observation that Brønsted acids can improve conversions and reduce PDI values for ROMP via **2** in water, Kiessling and co-workers carried out emulsion ROMP of trisaccharide monomers at pH 6 (15 equiv **14a** or **14b**; 30 equiv DTAB, 1:2 dichloroethane: 2,2-bis(hydroxymethyl)-2,2′,2″-nitrilotriethanol, 60°C, 14 h) [36]. Isolated yields ranged from 70% to 84%, with DP_{av} values of 15. ROMP of 15 equivalents of **11b** under similar conditions proceeded more rapidly (40°C, 30 min), again affording polymers with a DP_{av} value in excellent agreement with the theoretical value, in 60–80% isolated yield [37].

In order to circumvent the limitations associated with ROMP in aqueous or protic media, the Kiessling group sought a general synthetic route involving post-ROMP modification [33] (Figure 7). Polymerization of succinimide monomer **19** via **2** in dichloroethane gave efficient, high-yield access to a ROMP platform in which the succinimide groups can be subjected to nucleophilic exchange with, for example, primary amines, in DMF or DMSO solvent. Application of this strategy to synthesis of a mannose-functionalized polymer is shown. Using 10 equivalents of **19**, a polymer with a DP_{av} of 18 was obtained in 71% yield. Efficient access to longer polymer chains is possible on ROMP via **6a**, though the high reactivity of this initiator requires reaction to be carried out at low temperature in order to maintain control over chain lengths (100 equiv **19**, CH_2Cl_2, –20°C, 30 min) [38]. Nucleophilic exchange afforded the mannose-functionalized polymers in quantitative yields; GPC analysis showed good agreement between theoretical and experimental M_n values (34.5 and 30.8 kDa, respectively; PDI 1.07). These

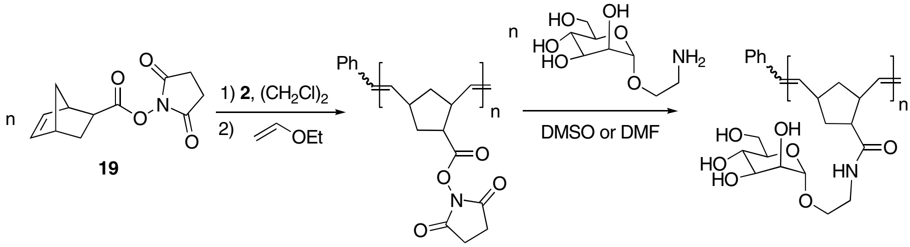

Figure 7. Synthesis of ROMP neoglycopolymers by post-ROMP modification.

strategies may provide more general routes to ROMP polymers bearing unprotected biologically active substituents.

2.2.3 ROMP in organic media

As the preceding sections suggest, use of aqueous or protic media to effect ROMP of monomers bearing biologically relevant, polar functionalities often limits control over polymer chain lengths. Use of organic solvents can give significantly improved results, where polar functionalities can be masked with lipophilic groups. Key issues in choosing a protecting group are the impact on the steric demand of the monomer, and the severity of the deprotection methods required. Both Schrock and Grubbs-class catalysts have been employed with excellent results. While the majority of studies to date involve use of the Grubbs catalyst **2**, several recent reports describe excellent results with the third-generation pyridine or bromopyridine initiators **5** and **6**.

Routes to neoglycopolymers have been most extensively examined. Grubbs and coworkers investigated the effect of different protecting groups (**20a**–**c**, Figure 8), using $RuCl_2(PCy_3)_2(=CHCH=CPh_2)$ as initiator [22]. ROMP of 40 equivalents of acetate-protected **20a** (50°C, CH_2Cl_2, 1 h) afforded polymers in 71% isolated yield, with M_n values of 13.4 kDa (calculated 19.3 kDa), and a PDI of 2.25. Use of higher monomer/initiator ratios resulted in insoluble gels. ROMP of 20 equivalents of benzyl-protected **20b** (C_6H_6, 50°C, 10 h) was slow, but isolated yields reached 91%, with M_n values of 16.9 kDa (calculated 13.5 kDa). Reaction in CH_2Cl_2 led to lower yields and higher PDI values. Low conversions of the sterically encumbered, silyl-protected **20c** over 3 days in CH_2Cl_2 were attributed to competing decomposition of the initiator. ROMP in benzene (35 equiv **20c**; 50°C, 2 days) was also slow, but the polymers were obtained in nearly 80% isolated yield, with a M_n value of 40.1 kDa (calculated 27.0 kDa; PDI 1.10). While this monomer was most challenging to polymerize, deprotection by treatment with tetrabutylammonium fluoride in THF was straightforward. In comparison, removal of the acetate protecting groups using NaOMe in MeOH/THF was inefficient, while attempts at hydrogenolysis of the benzyl ether groups using Pd/C/H_2 were unsuccessful.

The Schrock group demonstrated the efficacy of Mo initiator **1a** for ROMP of acetal-protected galactose-, ribose-, or mannofuranose-functionalized monomers in toluene (**21a**–**c**, respectively; Figure 8) [39]. Homopolymers were obtained within <1 h at room temperature; for block copolymers, one hour per block was generally sufficient. Isolated yields were near-quantitative, and M_n values ranged from 1.1 to two times the calculated values (PDI 1.03–1.25). ROMP of 30 equivalents of the sterically demanding di-galactose monomer **22** required 1.5 h, and gave polymers with the largest discrepancy between observed and calculated M_n values (~2.5 times), with a PDI value of 1.21. TFA deprotection was successful only for the galactose-functionalized polymers. Nomura and coworkers compared the efficacy of **1a**, **2**, and **3** in ROMP of acetyl-protected glucose and maltose-functionalized monomers (**21d**,**e**) [40,41]. ROMP initiated by **1a** in toluene or **2** in CH_2Cl_2 at ambient temperature afforded homopolymers and block copolymers in >90% isolated yield, with good agreement between calculated and observed M_n values. Living polymerization was demonstrated for both **1a** and **2**, but **1a** enabled considerably faster polymerization, with slightly greater control over chain lengths. For example, ROMP of 20 equiv **21d** via **1a** was complete within 15 min, giving polymer with an M_n value of 9.4 kDa (calculated 9.4 kDa; PDI 1.17). Use of **2** required 2 h, and afforded polymer with a significantly higher M_n value (11.3 kDa; PDI 1.16). ROMP of **21d** or **21e** by **3** in CH_2Cl_2 at ambient temperature afforded polymers in >90% yield within 1 h, but chain lengths were double the theoretical values, as typically found for this initiator.

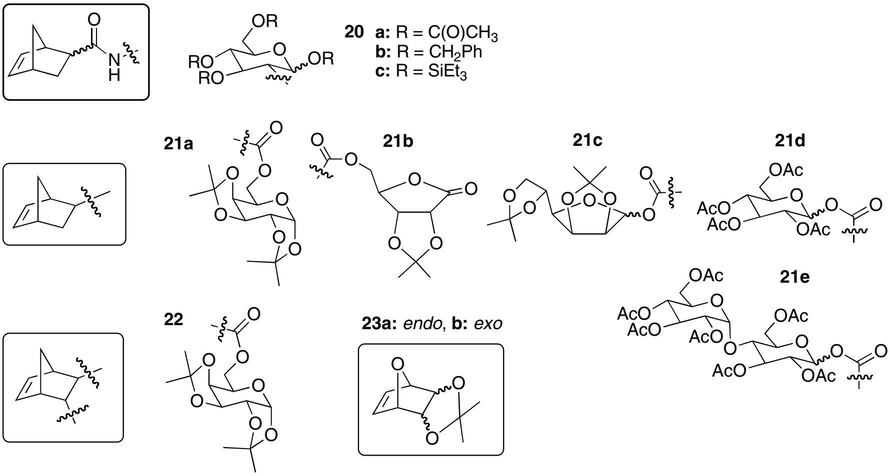

Figure 8. Protected carbohydrate monomers subjected to ROMP in organic solvents.

On use of **1a** to prepare diblock copolymers from **21a** and norbornene in toluene (25 equiv each; total 40 min at r.t.), the Nomura group found that M_n values measured by GPC were higher than expected (M_n 15.6 kDa, calculated 11.9 kDa; PDI ~1.1), but that values measured by endgroup analysis (^{1}H NMR) suggested good agreement [42]. Polymer yields of 94% or higher were obtained. By quenching ROMP with a silyl-functionalized aldehyde, and hydrolyzing with aqueous HCl, they obtained hydroxy-terminated polymers, which were treated with a mesylated poly(ethylene glycol) to afford amphiphilic copolymers with well-defined block architectures. In a subsequent elaboration of this approach, the hydroxy-terminated copolymers were treated with 5-norbornene-2-carboxylic acid chloride, and ROMP of this "macroinitiator" via an analogue of **1c** was carried out to obtain very regular, highly branched polymers. The corresponding, ribose-functionalized materials were obtained by use of **21b** in place of **21a** [43]. Most recently, Paton, Nomura, and coworkers prepared xylose-, glucose-, or mannose-functionalized norbornenes by 1,3-dipolar cycloaddition of glycosyl nitrile oxides and norbornadiene [44]. High yields were obtained in ROMP of these monomers via **1a** or **2** in toluene or CH_2Cl_2, respectively, with good control over polymer chain lengths (**1a**: PDI <1.2; **2**: PDI 1.1–1.35). In striking contrast, ROMP via **3** under identical conditions gave 75% yield of very high molecular weight material (M_n 470.5 kDa, calculated 11.8 kDa; PDI 1.64).

Mülhaupt, Stelzer and co-workers described synthesis of polyribofuranose analogues via ROMP. Polymerization of the unprotected oxanorbornene-5,6-diol in water via $RuCl_2(PCy_2CH_2CH_2NMe_3Cl)_2(=CHPh)$ failed [11], but acetal-protected **23** was polymerized by **2** in THF in 80–90% yield. M_n values determined by GPC were higher than calculated by 1.5–2.3 times, with control being poorer for the *exo* monomer. PDI values were also high (1.4–1.5). Catalytic dihydroxylation of the olefinic groups in the polymer backbone, followed by TFA deprotection of the carbohydrate groups, afforded polyhydroxylated polyribofuranose analogues.

Tethering small drug molecules to polymeric supports offers potential to enhance drug potency by increasing water-solubility, improving selectivity (by, e.g., incorporating recognition elements on the support), and reducing drug clearance rates [4]. A number of recent studies describing the synthesis of ROMP polymers bearing drug molecules (Figure 9) are discussed below. Control over chain lengths is important in order to ensure a consistent dose, and may be critical if multivalent interactions are important. Random, amphiphilic ROMP copolymers with antibacterial activity were explored by Coughlin and coworkers [45]. Initiators **1c, 2, 3** and **6a** were applied to ROMP of *t*Boc-protected monomers **24** in CH_2Cl_2. Only **6a** enabled ROMP at room temperature, with high yields, low PDI values (1.08–1.20), and good to excellent agreement between observed (GPC) and calculated M_n values (e.g. 25 equiv **24a**: M_n 8.6 kDa, calculated 8.8 kDa; 17 equiv **24b**: M_n 7 kDa, calculated 5.9 kDa). TFA deprotection afforded amphiphilic polymers active for disruption of phospholipid membranes. Random copolymers with varying degrees of hydrophilic and hydrophobic character, prepared similarly, gave highly selective, nonhemolytic antibacterial agents [46].

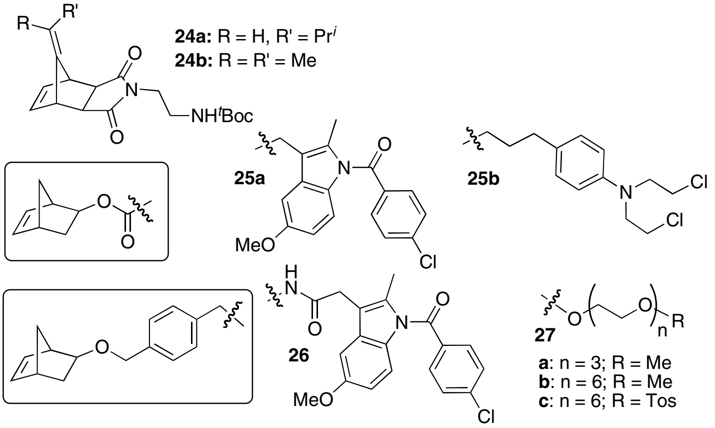

Figure 9. ROMP monomers used for assembly of polymers bearing drug molecules.

Nguyen and coworkers prepared polymer-bound "drug cocktails" consisting of homo-, block and random copolymers bearing chemotherapeutic agents such as indomethacin **25a**, a nonsteroidal anti-inflammatory with tumour-regressive activity, and chlorambucil **25b**, an alkylating agent used in the treatment of chronic lymphatic leukaemia and malignant melanomas, including Hodgkin's disease [47]. ROMP of 40 equivalents of **25a** via **2** (CH_2Cl_2, r.t.) afforded the homopolymer in 92% yield, with M_n values in good agreement with calculated values (M_n 19.4 kDa, calculated 18.1 kDa; PDI 1.25). ROMP of **25b** (26 equiv) under similar conditions likewise proceeded with excellent yields, though chain lengths were ~1.5 times longer than expected (M_n 16.8 kDa, calculated 10.3 kDa; PDI 1.26). Block copolymers were also prepared (M_n 27.6 kDa, calculated 21.4 kDa). A random copolymer of **25a** with ethylene oxide monomer **27a**, prepared in the hope of increasing the water-solubility of the material, exhibited a chain length more than double that expected, with a PDI value of greater than 2. Better control was attained in copolymerization of the related indomethacin monomer **26** with **27b** via **2** in CH_2Cl_2 [48]. PDI values ranged from 1.07 to 1.34, and chain lengths were in good agreement with theoretical values, except for a 100-mer, for which the M_n value was very low (~35 kDa, calculated 53 kDa). Aggregation of these amphiphilic polymers in water gave micelles or "nanoparticles", with a hydrophilic ethylene oxide sheath, and a drug-laden core. Acid hydrolysis of the amide group by which the drug molecule is tethered enabled release of indomethacin on incubation at pH 3 and 37°C in vitro (~20% release over 48 h). Finally, block copolymers of **26** and **27c** (35 equiv **26**, 15 equiv **27c**) were obtained within 1 h in ROMP via **2** in CH_2Cl_2. Control over chain lengths was excellent (M_n 30 kDa, calculated 29 kDa; PDI 1.14). The tosyl groups present on **27c** enabled post-ROMP modification of the polymer to introduce DNA and tumour-targeting antibodies associated with a breast cancer cell line. Micelles functionalized with fluorescein-labeled DNA and the antibodies were found to diffuse into breast cancer cells, whereas polymers without antibodies remained outside the cells [49].

As the foregoing suggests, many recent biomedical applications of ROMP polymers focus on drug design and delivery. An emerging application of ROMP materials is tissue engineering. Fogg and coworkers have prepared saturated ROMP polymers for use as biocompatible collagen cross-linking agents relevant to corneal tissue engineering [50,51]. Use of **5b** to effect ROMP of acetal-protected galactose monomer **22** in CH_2Cl_2 enabled rapid reaction (~3 h, vs 3 days for ROMP via **2**; Figure 10) with excellent control over chain lengths (M_n 33.2 kDa, calculated 33.3 kDa; PDI 1.03). Polymer hydrogenation was undertaken in order to maximize the in vivo stability of the replacement corneas, using new tandem ROMP-hydrogenation methodologies [51], which expand on those previously established for **2** [52]. Addition of PCy_3 proved valuable in stabilizing the Ru end group on the unsaturated polymer. Quantitative hydrogenation of 50-mers was achieved within 3 h at 1000 psi H_2 and 60°C, without adverse effects on polymer molecular weights or polydispersity. Subsequent TFA deprotection afforded the water-soluble, saturated neoglycopolymers.

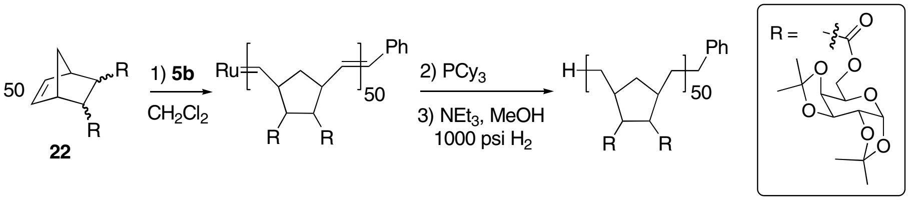

Figure 10. Saturated neoglycopolymers for tissue engineering, prepared via tandem ROMP-hydrogenation.

3. Conclusions

ROMP has emerged as a versatile and powerful tool for preparation of complex polymeric materials. A key area of opportunity centers on construction of well-defined ROMP polymers bearing functionalities of biological relevance. Control over polymer chain lengths is an important aspect of this research area, because of the impact on polymer properties, and because high reproducibility is essential for quantitative evaluation of structure/property correlations. While some excellent results have been reported in ROMP of simple, highly reactive monomers in water, the greater complexity of many of the biologically relevant monomers discussed presents a challenge for controlled ROMP of the unprotected monomers in aqueous media. While materials prepared via emulsion ROMP, or ROMP in the presence of methanol, have led to major advances, control over polymer chain lengths is often limited, particularly at elevated temperatures. Improved precision is attainable by polymerization of protected monomers in organic solvents, in which the monomer and initiator are present in a homogeneous solution. While considerably less convenient, owing to the need to develop and implement appropriate protection/deprotection strategies, this enables living ROMP, and hence high control over polymer chain lengths and architecture, if appropriate initiators and reaction conditions are used. Suitable initiators are the Schrock catalyst **1a**, or the Grubbs-class catalysts **2**, **5**, or **6**. The “third-generation” Ru initiators **5** and **6**, in particular, offer a near-ideal combination of high activity, ease of handling, and excellent control. These factors can be expected to significantly expand opportunities in the application of ROMP polymers in biomedical applications, and to enable further advances in the use of ROMP materials as probes of biological processes.

References

[1] Ramakrishna, S., Mayer, J., Wintermantel, E., Leong, K.W., Composite Sci. Tech. 2001, 61:1189–1224.
[2] Moszner, N., Salz, U., Prog. Polym. Sci. 2001, 26:535–576.
[3] Lee, K.Y., Mooney, D.J., Chem. Rev. 2001, 101:1869–1879.
[4] Haag, R., Kratz, F., Angew. Chem. Int. Edit. 2006, 45:1198–1215.
[5] Fogg, D.E., Foucault, H.M., Transition metal catalysts in organic synthesis: ring-opening metathesis polymerization, in: Crabtree, R.H., Mingos, M.P. (eds) Comprehensive Organometallic Chemistry III, Elsevier, Oxford, 2006.
[6] Black, G., Maher, D., Risse, W., Living ring-opening metathesis polymerization, in: Grubbs, R.H. (ed) Handbook of Metathesis, Vol. 3, Wiley-VCH, Weinheim, 2003, pp. 2–71.
[7] Kiessling, L.L., Owen, R.M., Synthesis and applications of bioactive polymers generated by ring-opening metathesis polymerization, in: Grubbs,

R.H. (ed) Handbook of Metathesis, Vol. 3, Wiley-VCH, Weinheim, 2003, pp. 180–225.
[8] Kiessling, L.L., Gestwicki, J.E., Strong, L.E., Angew. Chem. Int. Edit. 2006, 45:2348–2368.
[9] Ivin, K.J., Mol, J.C., Olefin Metathesis and Metathesis Polymerization, Academic Press, New York, 1997.
[10] Abd-El-Aziz, A.S., May, L.J., Edel, A.L., Macromol. Rapid Commun. 2000, 21:598–602.
[11] Meier, S., Stelzer, F., Reisinger, H., Haag, R., Mecking, S., Mulhaupt, R., Chem. Commun. 2001, 855–856.
[12] Carlise, J.R., Kriegel, R.M., Rees, W.S., Jr., Weck, M., J. Org. Chem. 2005, 70:5550–5560.
[13] Sanford, M.S., Love, J.A., Grubbs, R.H., Organometallics 2001, 20:5314–5318.
[14] Choi, T.-L., Grubbs, R.H., Angew. Chem., Int. Edit. 2003, 42:1743–1746.
[15] Mortell, K.H., Gingras, M., Kiessling, L.L., J. Am. Chem. Soc. 1994, 116:12053–12054.
[16] Biagini, S.C.G., Gareth Davies, R., Gibson, V.C., Giles, M.R., Marshall, E.L., North, M., Polymer 2001, 42:6669–6671.
[17] Biagini, S.C.G., Gibson, V.C., Giles, M.R., Marshall, E.L., North, M., Chem. Commun. 1997, 1097–1098.
[18] Lynn, D.M., Mohr, B., Grubbs, R.H., Henling, L.M., Day, M.W., J. Am. Chem. Soc. 2000, 122:6601–6609.
[19] Dinger, M.B., Mol, J.C., Organometallics 2003, 22:1089–1095.
[20] Dinger, M.B., Mol, J.C., Eur. J. Inorg. Chem. 2003, 2827–2833.
[21] Arimoto, H., Nishimura, K., Hayakawa, I., Kinumi, T., Uemura, D., Chem. Commun. 1999, 1361–1362.
[22] Fraser, C., Grubbs, R.H., Macromolecules 1995, 28:7248–7255.
[23] Manning, D.D., Strong, L.E., Hu, X., Beck, P.J., Kiessling, L.L., Tetrahedron 1997, 53:11937–11952.
[24] Kanai, M., Mortell, K.H., Kiessling, L.L., J. Am. Chem. Soc. 1997, 119: 9931–9932.
[25] Pohl, N.L., Kiessling, L.L., Synthesis 1999, 1515–1519.
[26] Bertin, P.A., Smith, D., Nguyen, S.T., Chem. Commun. 2005, 3793–3795.
[27] Maynard, H.D., Okada, S.Y., Grubbs, R.H., Macromolecules 2000, 33: 6239–6248.
[28] Maynard, H.D., Okada, S.Y., Grubbs, R.H., J. Am. Chem. Soc. 2001, 123:1275–1279.
[29] Roberts, K.S., Sampson, N.S., J. Org. Chem. 2003, 68:2020–2023.
[30] Baessler, K.A., Lee, Y., Roberts, K.S., Facompre, N., Sampson, N.S., Chem. Biol. 2006, 13:251–259.
[31] Claverie, J.P., Soula, R., Prog. Polym. Sci. 2003, 28:619–662.
[32] Claverie, J.P., Viala, S., Maurel, V., Novat, C., Macromolecules 2001, 34: 382–388.
[33] Strong, L.E., Kiessling, L.L., J. Am. Chem. Soc. 1999, 121:6193–6196.
[34] Manning, D.D., Hu, X., Beck, P., Kiessling, L.L., J. Am. Chem. Soc. 1997, 119:3161–3162.
[35] Iyer, S., Rele, S., Grasa, G., Nolan, S., Chaikof, E.L., Chem. Commun. 2003, 1518–1519.

[36] Sanders, W.J., Gordon, E.J., Dwir, O., Beck, P.J., Alon, R., Kiessling, L.L., J. Biol. Chem. 1999, 274:5271–5278.
[37] Gordon, E.J., Gestwicki, J.E., Strong, L.E., Kiessling, L.L., Chem. Biol. 2000, 7:9–16.
[38] Pontrello, J.K., Allen, M.J., Underbakke, E.S., Kiessling, L.L., J. Am. Chem. Soc. 2005, 127:14536–14537.
[39] Nomura, K., Schrock, R.R., Macromolecules 1996, 29:540–545.
[40] Nomura, K., Sakai, I., Imanishi, Y., Fujiki, M., Miyamoto, Y., Macromol. Rapid Commun. 2004, 25:571–576.
[41] Miyamoto, Y., Fujiki, M., Nomura, K., J. Polym. Sci. A 2004, 42:4248–4265.
[42] Murphy, J.J., Kawasaki, T., Fujiki, M., Nomura, K., Macromolecules 2005, 38:1075–1083.
[43] Murphy, J.J., Nomura, K., Chem. Commun. 2005, 4080–4082.
[44] Murphy, J.J., Nomura, K., Paton, R.M., Macromolecules 2006, 39:3147–3153.
[45] Ilker, M.F., Schule, H., Coughlin, E.B., Macromolecules 2004, 37:694–700.
[46] Ilker, M.F., Nusslein, K., Tew, G.N., Coughlin, E.B., J. Am. Chem. Soc. 2004, 126:15870–15875.
[47] Watson, K.J., Anderson, D.R., Nguyen, S.T., Macromolecules 2001, 34: 3507–3509.
[48] Bertin, P.A., Watson, K.J., Nguyen, S.T., Macromolecules 2004, 37:8364–8372.
[49] Bertin, P.A., Gibbs, J.M., Shen, C.K.-F., Thaxton, C.S., Russin, W.A., Mirkin, C.A., Nguyen, S.T., J. Am. Chem. Soc. 2006, 128:4168–4169.
[50] Fogg, D.E., Liu, Y., Griffiths, M., US Patent App. 11/442,755, 2006.
[51] Camm, K.D., Castro, N.M., Liu, Y., Czechura, P., Snelgrove, J.L., Fogg, D.E., J. Am. Chem. Soc. 2007, 129:4168–4169.
[52] Drouin, S.D., Zamanian, F., Fogg, D.E., Organometallics 2001, 20:5495–5497.

PRECISION POLYOLEFIN STRUCTURE: MODELING POLYETHYLENE CONTAINING METHYL AND ETHYL BRANCHES

GIOVANNI ROJAS, KENNETH B. WAGENER*

The George and Josephine Butler Polymer Research Laboratory, Center of Macromolecular Science and Engineering, Department of Chemistry, University of Florida, Gainesville, FL 32611, USA. *Phone: (352) 392-4666; Fax: (352) 392-9741; *E-mail: wagener@chem.ufl.edu*

Abstract: Sequenced copolymers of ethylene and diverse species have been created using acyclic diene metathesis (ADMET) polymerization, a step growth, condensation-type polymerization driven to high conversion by the removal of ethylene. ADMET permits control over branch content and branch length, which can be predetermined during the monomer synthesis, allowing sequence control in the resultant unsaturated polymer. Monomers are symmetrical α,ω-dienes with a pendant functionality. Diverse functional groups are compatible with ADMET polymerization when Schrock's or first-generation Grubb's catalysts are used. Saturation with hydrogen after ADMET polymerization affords a polyethylene (PE) backbone bearing specific functionalities in precise places. Varying both the pendant functional group and the spacing between functionalities alters the physical and chemical properties of the polymer. Incorporation of alkyl chains into the PE backbone via ADMET leads to the study of perfect structures modeling the copolymerization of ethylene with α-olefins such as 1-propene, 1-butene, 1-hexene, and 1-octene.

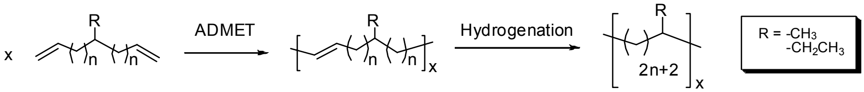

Keywords: acyclic diene metathesis, ADMET, polymerization

1. Introduction

Polyethylene (PE) is the largest volume polymer produced in the last decade,[1,2] and an average annual growth rate of 5.2% in terms of demand-production during 2000–2010 is expected.[3] Its synthesis started in the 1930s when Friedrich and Marvel reported the first low-molecular weight polymer arising by accident during high-pressure experiments with ethylene; in 1933 the British chemical company Imperial Chemical Industries (ICI) reported the first existence of PE and later in 1937 obtained the patent for its massive

Y. İmamoğlu and V. Dragutan (eds.), Metathesis Chemistry: From Nanostructure Design to Synthesis of Advanced Materials, 305-324.

production.[4] This methodology produces polymer with no control over the primary structure via chain propagation chemistry using free-radical initiation, which generates PE with a high content of long and short branches.[4]

A significant contribution to polymer chemistry was made by Karl Ziegler at the Max Planck Institute in West Germany at the end of the 1950s with the synthesis of high-density polyethylene (HDPE) at low pressure and temperature using a heterogeneous titanium catalyst. Inspired by Dr. Ziegler, Giulio Natta in 1954 applied this technology to obtain polypropylene. The importance of these contributions led to the Nobel Prize in 1963 for both Karl Ziegler and Giulio Natta, based on their work in ethylene and propylene polymerization and the development of new catalysts, today known as Ziegler–Natta catalysts.[5,6] Polymerization of ethylene using Ziegler–Natta[5–10] and homogenous metallocene-based catalysts[11,12] produces highly crystalline materials, 62–80% by density, which can be controlled by the copolymerization of ethylene with α-olefins, producing linear low-density polyethylene (LLDPE). The incorporation of the comonomer, typically 1-propene, 1-butene, 1-hexane, and 1-octene, produces long-run lengths of unbranched linear PE with random branched regions. These branched PEs have gained attention for their enhanced mechanical properties and industrial importance. Diverse types of materials can be obtained by controlling the mode of polymerization, catalyst nature, pressure, and temperature, all of which have studied for the last 60 years.[7,10–24]

Physical properties of PE obtained via α-olefin copolymerization depend on the branch content which is directly related to the amount of comonomer incorporated into the PE backbone. More important is the interaction between polymer chains.[17–19,24–29] Physical properties of LLDPE can vary depending on the molecular weight, molecular weight distribution, and branch content. Control over its physical properties can be achieved using diverse methods based on catalyst, initiator, polymerization type, monomer types, temperature, and pressure variations.

Synthesis of commercial LLDPE is usually performed via Ziegler–Natta or metallocene chemistry. Ziegler–Natta systems produce heterogeneous primary structures with low-molecular weight and high-molecular weight distribution, which originates from their multisite initiation on the heterogeneous catalyst. However, metallocenes provide LLDPEs with narrower molecular weight distributions and higher levels of comonomer incorporation because of the single-site initiation on the homogeneous catalyst. Unfortunately, in both cases random errors are introduced in the main backbone, causing defects or heterogeneity in the primary structure. Experiments have shown that the average defect content in metallocene-based PE is narrower than in Ziegler–Natta systems. The addition of these defects is widely used to manipulate the main backbone, obtaining polymers with desired physical properties. However, attempts to produce model structures fail in both Ziegler–Natta and metallocene chemistry.[19,24,27,30–32] Modeling-branched PE can lead to a better understanding of the polymer processing, the overall microstructural effect produced by branch perturbations on PE-based materials,[16,33,34] but inevitable chain transfer and/or chain walking can occur if the model PE is made by free-radical, Ziegler–Natta, or metallocene chemistry.[16,21,22,35] Most of the PE research focuses on the study of short chain branching (SCB) as well as short chain branch distribution (SCBD).[2,16,18,19,24,27–34,36–39] More recently, the use of acyclic diene metathesis (ADMET) chemistry followed by exhaustive hydrogenation of its product has offered a new approach in the synthesis of PE backbones with no branches,[40] or specific branches precisely placed on the main backbone.[41,42] This chemistry is controlled by the organic synthesis, instead of indirect catalyst or comonomer adjustment. Contrary to the copolymerization of ethylene with α-olefins, polymerization of one kind of symmetric macromonomer produces low-density polyethylene (LDPE) with a perfectly known primary structure.[40–44]

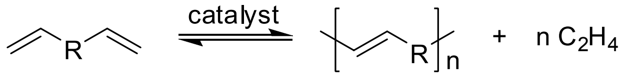

1 **2** **3**

Figure 1. The ADMET reaction.

ADMET is a step growth polycondensation reaction, with ethylene a usual by-product. Elimination of ethylene, the driving force of the reaction, is easily accomplished applying vacuum under normal polymerization conditions between 25°C and 55°C. Figure 1 shows the formation of an unsaturated high-molecular weight polymer with the concomitant releasing of ethylene. ADMET has been used to produce functionalized unsaturated polyolefins[45] as well as saturated PE models with perfect primary strutures.[41,42,44] The first synthetic and thermal studies were developed on methyl and ethyl branches; these are models of ethylene/1-propene and ethylene/1-butane random copolymers obtained via Zielger–Natta or metallocene chemistry. Herein, we review the synthesis and thermal behavior of the family of perfectly sequenced and statistically random ethylene/1-propene and ethylene/1-butane copolymers.

2. Linear ADMET polyethylene

Synthesis of perfectly linear PE with no branches or undesired defects on the main backbone is of considerable interest. More important is the behavior of this polymer during crystallization, which is intimately related with thermal response of the material during differential scanning calorimetry (DSC) studies.[19] Polymerization of ethylene using Ziegler–Natta or metallocene chemistry does not allow the formation of perfect PE structures. Model studies have been conducted on large *n*-paraffins (monodisperse PE oligomers) up to 390 carbons long.[36,46] Extrapolation to high-molecular weight PE is required in these studies since defect-free high-molecular weight PE is the ultimate objetive.[1,37,38] Paraffin models allow the study of perfect primary structures, but the presence of methyl end groups leads to nonoptimal results when morphological behavior of these models are extrapolated to a high-molecular weight systems. These methyl end groups can be thought as defects that at some extent impede crystallization. Comparisons between these two systems are useful, mostly from the point of view of the primary structure, but ambiguous results can be obtained.[1,36–38]

Introduction of ADMET polymerization leads to the synthesis of perfect PE with absence of undesired SCB and SCBD. The polymer also known as ADMET PE is obtained via bulk polymerization of 1,9-decadiene in presence of first-generation Grubb's or Schrock's catalyst. The resulting polyoctenamer is exhaustively hydrogenated producing a completely saturated linear PE, as is shown in Figure 2.

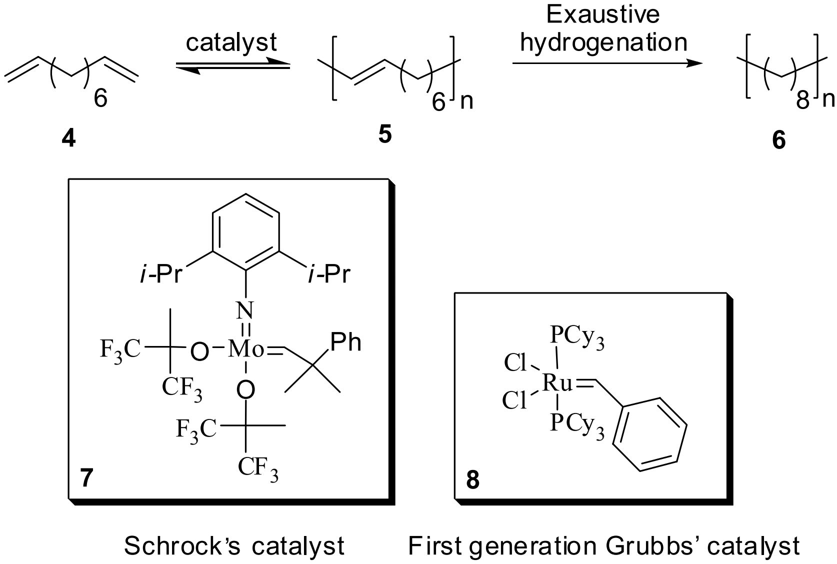

Figure 2. ADMET polymerization of 1,9-decadiene followed by hydrogenation.

Table 1. Effect of molecular weight on thermal behavior in linear ADMET PE

M_n	Polydispersity index (PDI)	T_m (°C) (peak)	Δh_m (J/g)
2400	2.4	130.7	252
7600	2.4	131.3	213
11,000	1.9	132.0	221
15,000	2.6	133.9	204

Regardless of the difference in molecular weight, ADMET PE exhibits similar thermal behavior to that of HDPE. However, the molecular weight of ADMET PE can be controlled by regulating reaction time, temperature, and monomer to catalyst ratio. Table 1 shows the melting temperature (T_m) of ADMET PE with different molecular weights from 2000 to 15,000 g/mol. Despite the low molecular weight all samples show sharp T_m by DSC above 130°C. Small increment on the peak melting temperature is observed when the molecular weight increases; however, when the number average molecular weight becomes 15,000 g/mol the melting transition seems to be the same that HDPE. Based on this melting behavior, it is obvious that regardless of the low molecular weight ADMET PE is useful for model studies.[40,47]

3. Precise models of ethylene/α-olefin copolymers

Polymers obtained by copolymerization of ethylene with α-olefins display diverse physical and chemical properties. Applications of these materials are directed related with extent of comonomer incorporated into the final polymer. More important is their thermal behavior which is dependent of the comonomer content and distribution.[16,18,19,24,26–34,39] Synthesis of precisely placed methyl-branched PE was the first attempt in these modeling studies.[41,42,44,47,48] Continuation of this research led to the development of ethyl-branched PE.[41,47] These polymers are ideal models in comparison with those obtained by Ziegler–Natta or metallocene chemistry using ethylene/1-propylene and ethylene/1-butene, respectively.

Synthesis of these previous methyl- and ethyl-branched PEs has been successful using different approaches in the preparation of the respective α,ω-diene monomers. However, an easy and very productive pathway for these monomers is based on the double alkylation of ethyl acetoacetate[41,42,44,47,48] or diethylmalonate.[47,49]

4. Precise models of ethylene/1-propylene copolymers

Copolymers of ethylene with propylene (EP) are one of the members in the big family of statistically random alpha olefin copolymers.[1,28,47] Perfectly sequenced EP copolymers can be obtained via ADMET polymerization of a symmetrical α,ω-diene monomer bearing a pendant methyl group. The indispensable α,ω-diene monomer was first prepared by alkylating ethyl acetoacetate[42,47]; however, a modified synthesis can be applied to the preparation of α,ω-diene monomers starting from diethylmalonate.[47,49] Figure 3 shows the synthetic scheme employed for preparation of diverse methyl α,ω-diene monomers, first alkylation of ethyl acetoacetate with alkenyl bromide produces a β-alkenyl-β-ketoester. The β-ketoester is then deacylated via retro-Claisen condensation. The resulting ester is further reduced to alcohol. Tosylation of the alcohol followed by displacement by hydride produces the required methyl branched diene monomers.

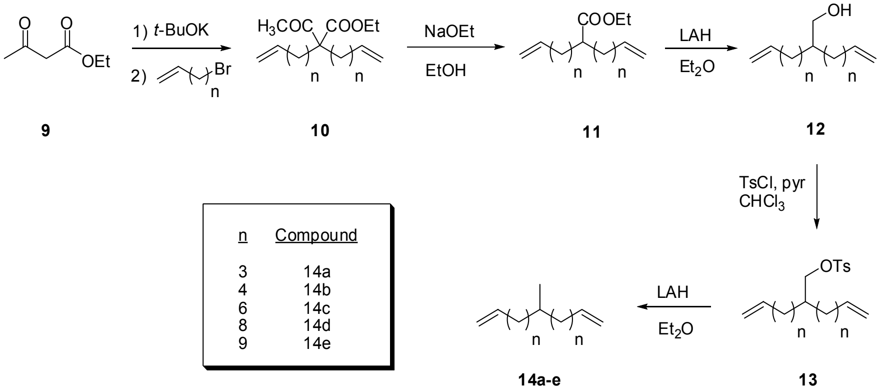

n	Compound
3	14a
4	14b
6	14c
8	14d
9	14e

Figure 3. Synthesis of diverse methyl monomers.

Polymerization of methyl α,ω-diene monomers 14a–e are carried out with first-generation Grubbs' or Schrock's catalyst. The produced unsaturated ADMET polymer is then exhaustively hydrogenated yielding ADMET PE with methyl groups precisely placed along the PE backbone. This strategy has been used to synthesize a pool of ADMET PE materials containing methyl groups on every 9th, 11th, 15th, 19th, and 21st carbon along the polymer backbone (Figure 4).[42,47]

Thermal analysis of five ADMET polymers EP9–EP21 was performed using DSC. Table 2 summarizes the thermal behavior of such polymers. The endothermic transitions of each polymer are sharp and defined, as is shown in Figure 5,[42,47] rather than broad and bimodal transitions usually observed for EP copolymers obtained via chain polymerization.[28] Peak melting

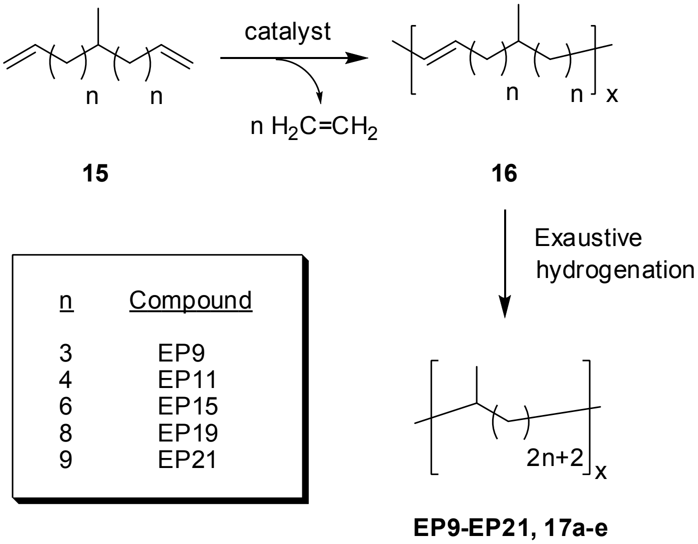

n	Compound
3	EP9
4	EP11
6	EP15
8	EP19
9	EP21

Figure 4. General synthetic scheme for synthesis of symmetrical methyl-branched polyethylene models by ADMET.

temperature of ADMET EPs increases when the branch content decreases, an increment on the melting enthalpies when longer ethylene run lengths are present indicates a more crystalline structure.[42,47]

Table 2. Precise short chain branch distribution and its effect on thermal behavior

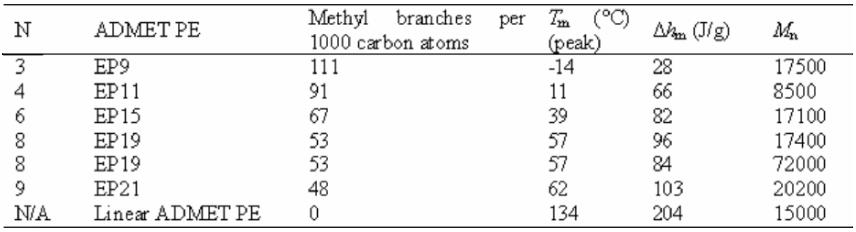

N	ADMET PE	Methyl branches per 1000 carbon atoms	T_m (°C) (peak)	Δh_m (J/g)	M_n
3	EP9	111	-14	28	17500
4	EP11	91	11	66	8500
6	EP15	67	39	82	17100
8	EP19	53	57	96	17400
8	EP19	53	57	84	72000
9	EP21	48	62	103	20200
N/A	Linear ADMET PE	0	134	204	15000

EP copolymers obtained via Ziegler–Natta exhibit a broad and indistinct melting behavior when the percentage of propylene incorporated in the final material exceeds 15%.[50,51] While ADMET PE shows very distinct and sharp endotherms comparable with PE obtained by commercial routes, T_m of 134°C with Δh_m of 204 J/g, the precisely placed methyl group on every ninth carbon EP9 shows a melting transition at –14°C with a Δh_m of 28 J/g. This polymer melts about 150°C lower than linear ADMET PE. Also, melting enthalpy has shown a decrement of 176 J/g indicating a highly amorphous

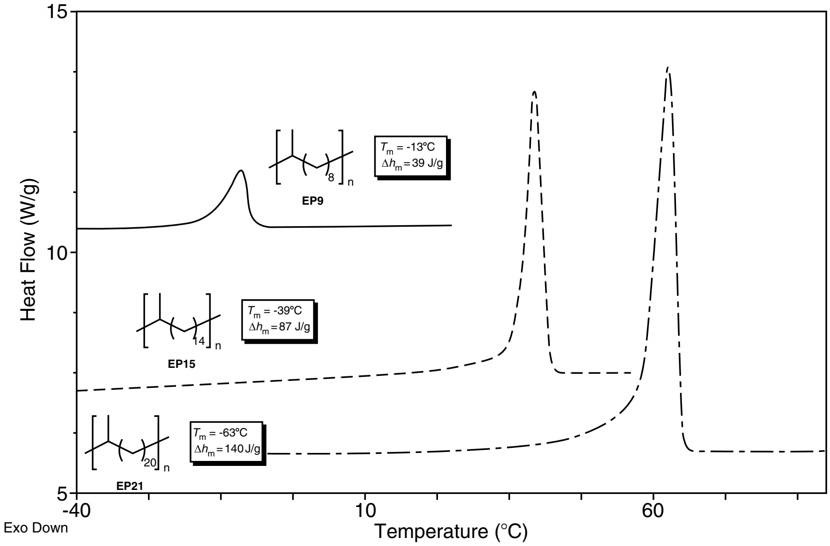

Figure 5. DSC profiles for EP9, EP15, and EP21 copolymers.

behavior. As the methylene spacing increases along the methyl-branched ADMET PE series, melting temperatures, and heats of fusion increase up to 64°C and 103 J/g for EP21, PE containing a methyl group on every 21st carbon. All these ADMET PE models exhibited sharp and distinct melting behavior product of their semicrystalline behavior.[42,47] Given that the series of methyl-branched ADMET PE exhibits a highly amorphous content, glass transition temperature of these materials becomes easy to measure. Three ADMET PE were analyzed, EP9, EP11, and EP21, all displaying a T_g of, –44°C and ΔC_p of 27–29 J/g °C, regardless of the branch frequency along the polymer backbone.

It is evident that a molecular weight dependence of the melting behavior exists in polymeric materials.[46,52] However, this study demonstrates that ADMET polymers posses sufficient high molecular weight capable of modeling EP copolymers. Two versions of ADMET EP copolymers were prepared containing a methyl branch on every 19th carbon, both possessing dramatically different number average molecular weight M_n = 17,400 and M_n = 72,000 g/mol.[42,47] A sharp melting endotherm of 57°C is observed for both polymers, which implies that a minimum number average molecular weight of approximately 15,000 is sufficient for comparison of this model with commercial EP copolymers.[40,42,47]

5. Effects of short ethylene run lengths

Modeling ADMET EP copolymers based on perfectly symmetrical monomers has been the approach for the preparation of EP9 through EP21.[42] Because ring-closing metathesis is observed if the reaction is carried out with 1,6-heptadiene-based structures, synthesis of shorter branch run lengths, highly branched copolymers, requires polymerization via ADMET of "dimers" containing two methyl groups on each monomer unit. Figure 6 shows the general approach for synthesizing ADMET monomers containing two precisely placed methyl groups as part of the monomer unit.[53]

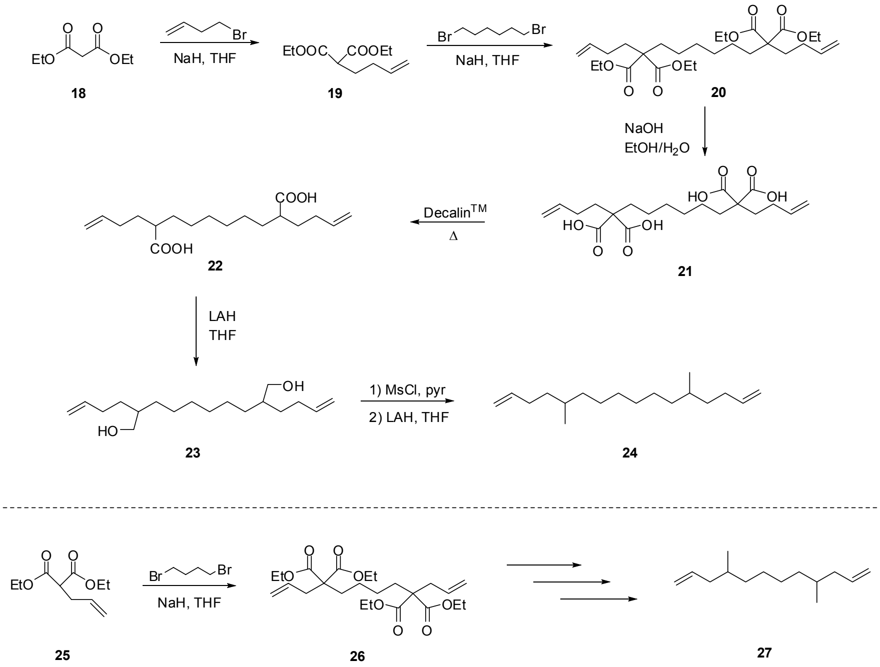

Figure 6. General synthetic scheme for short ethylene run length monomers for ADMET.

Synthesis of monomers 24 and 27 is based on diethyl malonate chemistry. Dialkylation of a dibromide with diethyl alkenyl malonate yields a tetraester diene. Diacid diene is obtained after saponification and decarboxylation of the respective tetraester diene. Reduction to the diol is achieved with lithium aluminum hydride. Subsequently, dimesylation of the respective diol followed by reductive cleavage with hydride yields the desired monomer 24 and 27.[53]

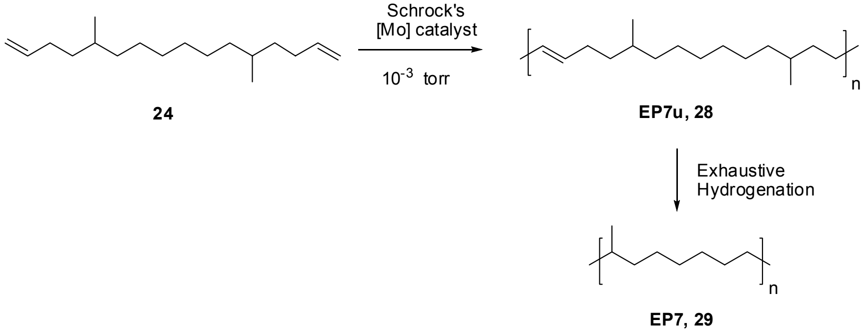

Figure 7. Synthesis of EP7 copolymer.

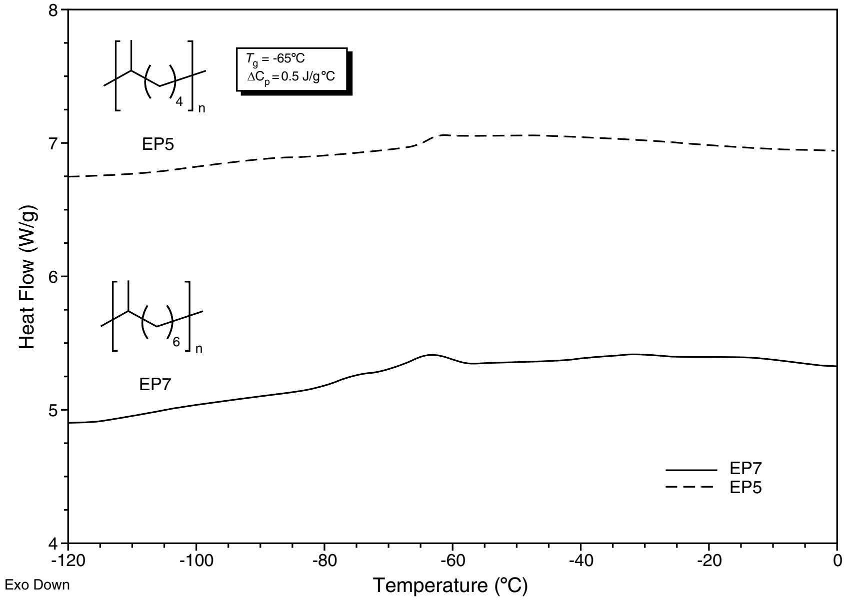

Figure 8. DSC profiles of EP5 and EP7.

Polymerization of monomers 24 and 27 was carried out in the bulk with Schrock's catalyst under high vacuum. High-molecular weight unsaturated polymers EP5u M_n = 26,000 g/mol and EP7u M_n = 12,700 g/mol were isolated, and exhaustive hydrogenation yielded EP5 and EP7, respectively. Figure 7 shows polymerization/hydrogenation of 24 yielding unsaturated polymer EP7u and PE bearing methyl groups on every seventh carbon EP7.

DSC of these ADMET EP copolymers was performed to determine the effects of short exact run length on thermal response. As was mentioned before, all previously ADMET EP copolymers from EP9 to EP21 exhibit semicrystalline behavior. Increment of the peak melting temperature and heat of fusion is observed while decreasing branch content along the PE backbone. However, EP5 and EP7 in contrast to polymers with lower branch content or higher ethylene run length exhibit fully amorphous behavior. While a β glass transition temperature for semicrystalline ADMET EP copolymers has been reported at –43°C from EP9 to EP21 regardless of branch content, for EP5 a relaxation at –65°C with a ΔC_p of 0.5 J/g °C has been recorded. This relaxation transition assigned as the glass transition temperature is about 22°C lower than previously reported EP9 throughout EP21. Figure 8 shows the DSC profiles of these two fully amorphous sequenced EP copolymers EP5 and EP7. The dramatic shift to a lower temperature of the observed T_g is attributed to the highly methyl content along the polymer chain, which inhibits chain flexibility imparted by the ethylene run length along the backbone.[20]

PE bearing methyl groups on shorter ethylene run length such as EP5 represents the first example of fully amorphous precisely structured EP copolymer. The branch content necessary to avoid crystallization in this type of EP copolymers has become known, where the smallest crystallizable ethylene run length is six carbons.

6. Precise models of ethylene/1-butene copolymers

Copolymers of ethylene with α-olefins also known as LLDPE are an important topic due to their enhanced mechanical properties, structural simplicity, and industrial importance. Copolymers of ethylene with 1-butene, 1-hexene, and 1-octene, have been obtained by copolymerization via Ziegler–Natta and metallocene chemistry.[16,33,34] While many studies deal with modification of the catalyst and optimization of the reaction's conditions, thermal behavior of LLDPE is more important for understanding the morphology of these materials.[19,24,27,29–32,39] Inspired by the success obtained modeling EP copolymers via ADMET polymerization, extension of this investigation led us to the synthesis of PE with only ethyl branches precisely placed along the main backbone, or precisely sequenced ethylene/1-butene (EB) copolymers.[41,47] In an effort to extend our LLDPE library to longer branch identities, a synthetic methodology based on our experience with EP copolymers was explored.[41] The synthesis of monomers needed for modeling EB copolymers was challenging despite the apparent structural simplicity. Multiple synthetic procedures were attempted in order to obtain perfectly ethyl-branched LLDPE materials, our ultimate goal. The first synthetic strategy to produce ethyl-branched α,ω-diene monomers is based on alkenylation of ethyl acetoacetate, as is shown in Figure 9; however, some problems during reduction of tosylate impede the application of this methodology to longer chain length. The preferred synthetic approach for these longer branch spacers is shown in Figure 10, where diethyl malonate is alkenylated in presence of base. Saponification of compound 37, decarboxylation, reduction to the respective alcohol, followed by bromination yielded bromo alkyl α,ω-diene 40. A single carbon homologation was then performed by addition of CO_2 to the respective Grignard of 40.[41,47]

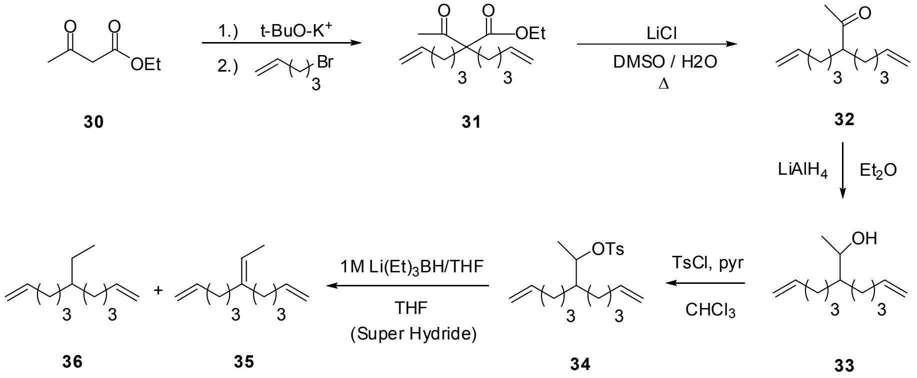

Figure 9. Ethyl-branched monomer synthesis via acetoacetate route.

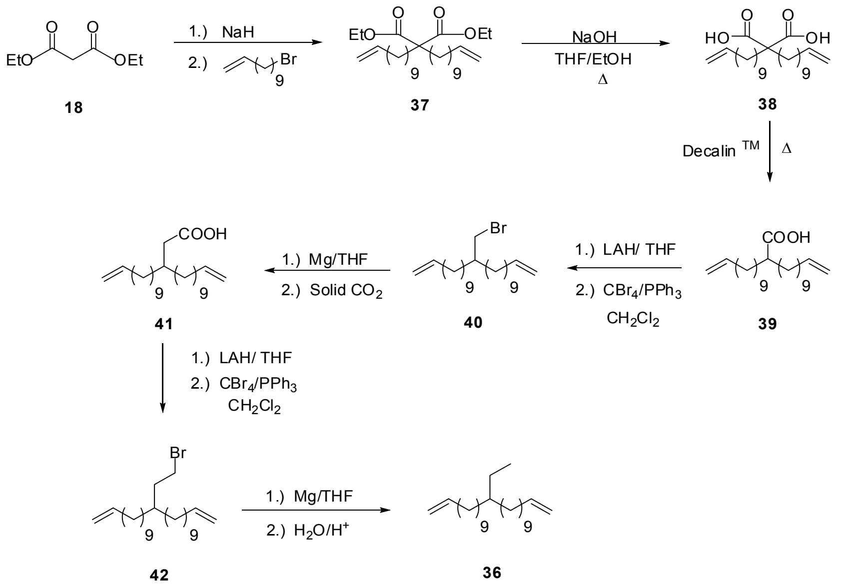

Figure 10. Synthetic pathway to ethyl-branched monomer via malonate modification.

Similar to the results obtained for EP copolymers, precisely sequenced EB copolymers increase the peak melting temperature, enthalpy, and crystallinity with increasing run length. Like EP copolymers, SCB influences the melting behavior of ADMET EB copolymers; however, the most determinant factor on the final physical properties seems to be the SCB distribution.[41] A direct comparison between these two classes of copolymers, EP9 and EB9, shows a dramatic effect as is shown in Figure 11. PE containing a methyl branch on every ninth carbon shows a peak melt at –14°C, while the ethyl branch version shows only a glass transition temperature of –76°C with no apparent melting behavior.

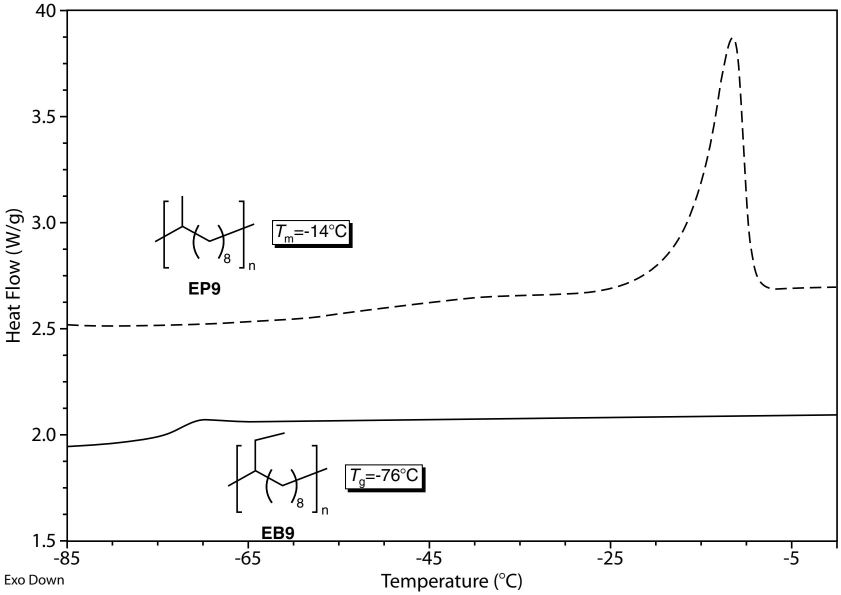

Figure 11. Comparison of EP9 (*top*) and EB9 (*bottom*) DSC traces.

The only viable explanation for this thermal behavior difference results from the difference in branch content. While crystallization is observed when methyl branches are present on every ninth carbon, the analogous polymer with ethyl branches only shows amorphous behavior. In the case of EP9, the pendant methyl branches are too small for inhibiting crystallization. Although it has not proved, it is possible that methyl groups can fit within the crystal lattice in small concentration.[41,42,44,47] On the other hand, ethyl branches on EB9 copolymer are big enough for blocking crystallization. An increment of one carbon unit over the branch identity results in such dramatic change in the thermal behavior, this phenomenon suggests the inability of ethyl branches to reside within the crystalline lattice at such high concentrations producing a fully amorphous material.

In a similar manner of EP copolymers, the crystal formation and crystallization kinetics of EB copolymers is directly affected when the overall branch content is increased. For example, increasing the branch content in EB copolymers produces diverse thermal behavior, from fully amorphous EB9

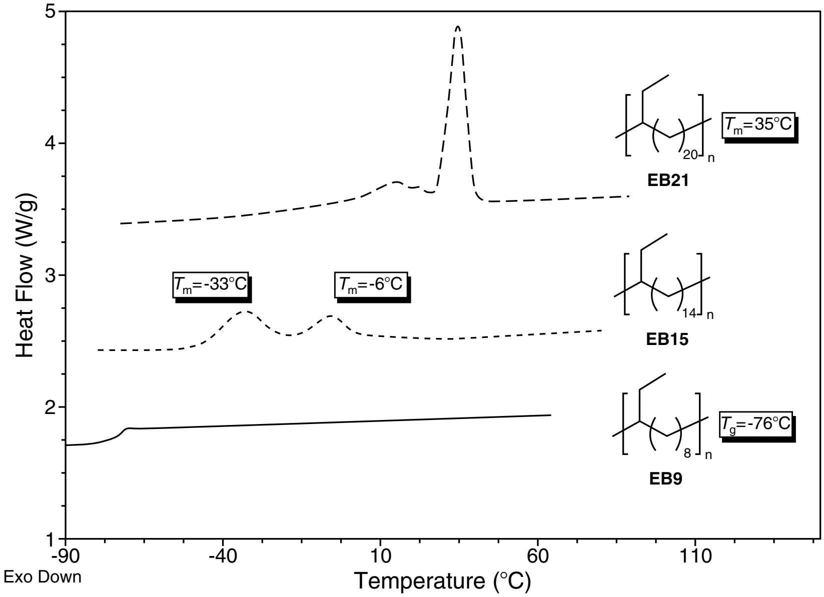

Figure 12. DSC profiles of EB9, EB15, and EB21.

to semicrystalline EB21. Figure 12 shows the DSC profiles of EB9, EB15, and EB21. While EB9 showed only a glass transition temperature at –76°C with no apparent melting transition, EB21 showed a sharp and defined melting transition at 35°C. However, decreasing the run length from 20 to 14 carbons produces a bimodal profile with a melting temperature of –33°C and –6°C.

7. Random models of ethylene/α-olefins copolymers

7.1 Random methyl branching

While previous studies containing precisely placed methyl- and ethyl-branched PE copolymers via ADMET are perfectly sequenced models of EP and EB materials, copolymers of ethylene with α-olefins are obtained in a statistically random fashion using Ziegler–Natta or metallocene chemistry. Although these materials can be obtained totally randomized, imperfections over the branch identity are usually incorporated into the PE backbone due to the chain nature of this chemistry. Randomly branched copolymers with only one kind of branch identity can be created using ADMET, copolymerization followed by exhaustive hydrogenation of a methyl-branched α,ω-diene with an unbranched α,ω-diene yields statistically random EP copolymers.[44,47] Randomness in the final material is assured since copolymerization of both diene monomers is carried out, and no electronically or sterically major differences are present promoting transmetathesis of the monomer units. Figure 13 shows six statistical copolymers bearing different methyl comonomer content, which models their industrial EP copolymers analogs.

The melting temperatures for model random EP copolymers follow a similar pattern to commercial materials obtained via chain chemistry. As the methyl branch content increases, the peak melting temperature, percent crystallinity, and heat of fusion decrease.[44,47] A decline in the melting temperature when methyl branches are incorporated into the PE backbone is observed, starting from perfectly linear PE with T_m of 133°C, to PE with 55.6 methyl branches per 1000 carbon atoms with T_m of 52°C.[44] Table 3 shows the peak melting temperature, heat of fusion, and percent crystallinity of all six materials obtained via ADMET copolymerization.

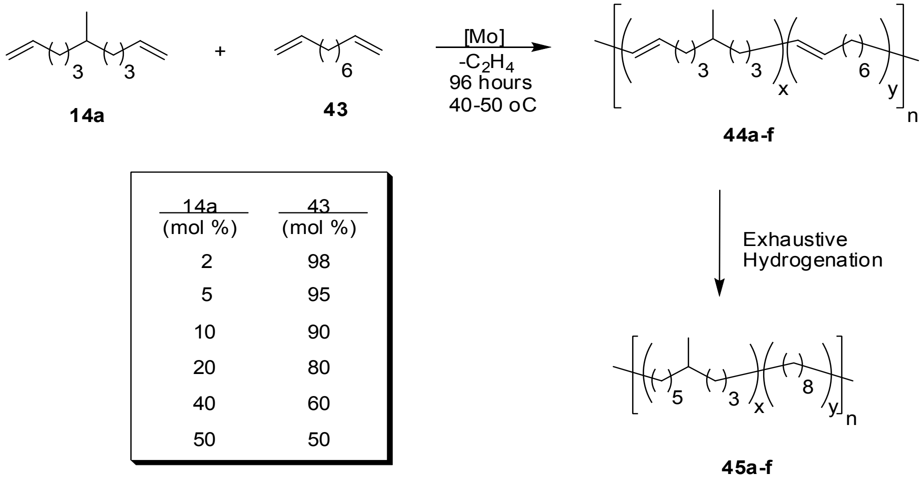

14a (mol %)	43 (mol %)
2	98
5	95
10	90
20	80
40	60
50	50

Figure 13. Synthesis of statistical EP copolymers by varying diene comonomer ratios.

Polymers with the highest amount of propylene incorporation (43.3 and 55.6 branches per 100 carbons) show broad and indistinct DSC profiles similar to commercial materials; however, lower amount of propylene is reflected as sharp and well-defined endotherms similar to those obtained in perfectly sequenced EP copolymers. Polymers with perfectly placed methyl branches containing 45 methyl branches per 1000 carbons have shown sharp, well-defined distinct melting temperatures, while randomized analog systems have shown broad, ill-defined melting transitions, which is attributed to the lower microstructural order due to randomization of the methyl branches along the main PE backbone. Figure 14 illustrates the difference in thermal behavior when PE containing 45 methyl branches per 1000 carbons are placed in a precisely (top) and randomly (bottom) fashion along the backbone.[44,47]

Table 3. The effect of increasing branch content on thermal behavior and crystallinity in random EP copolymers

Polymer	Methyl branches per 1000 carbon atoms	T_m (°C) (peak)	Δh_m (J/g)	Crystallinity (%)
Linear ADMET PE	0	133.0	230.0	78.5
45a	1.5	129.0	207.6	71.3
45b	7.1	123.2	183.4	62.1
45c	13.6	119.0	165.8	56.3
45d	25.0	111.6	137.3	47.6
45e	43.3	80.7	87.0	29.6
45f	55.6	52.1	85.0	29.0

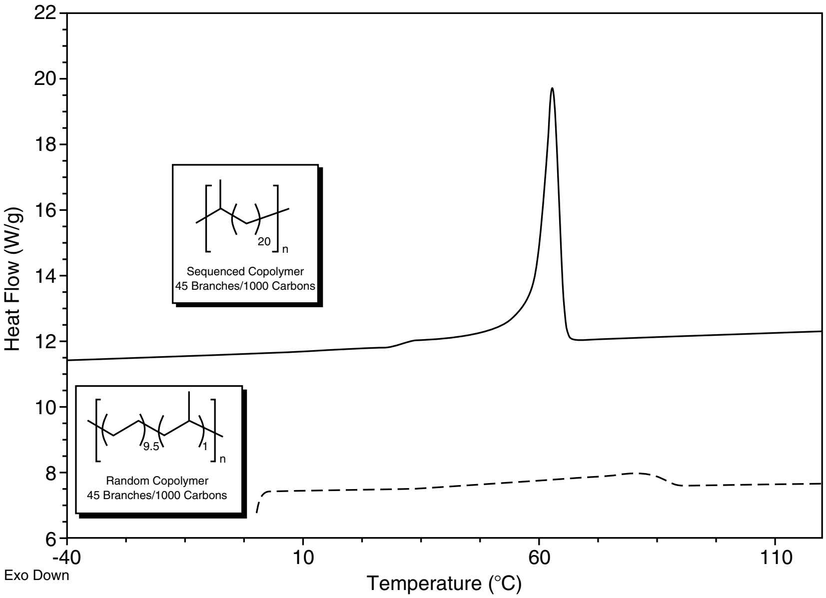

Figure 14. DSC traces of precise methyl (*top*) and random methyl (*bottom*) polymers having similar branch content.

Thermal analyses of EP copolymers have shown interesting thermal behavior due to the precise microstructural control, unique lamellar thicknesses are observed since control of the methyl branch frequency is imparted along the polymer backbone. While precisely branched systems present sharp well-defined endotherms due to exact run length between branches, random systems exhibit broad thermal responses due to variable lamellar thickness imparted by the uneven ethylene run length. In contrast to the precisely placed methyl branched EP copolymer, the random EP material exhibits a higher peak melting temperature and a lower enthalpy of fusion, which is attributed to longer ethylene run length and lower crystallinity due to the variable lamellar thickness imparted by those sections. These facts illustrate the effect of random and uniform SCB on EP copolymers. ADMET is proven to impart control over the branch content and more importantly branch identity, allowing formation of model polymers unobserved before in any EP copolymerization via conventional chain chemistry.[44,47]

8. Conclusions

ADMET polymerization has been proven useful in modeling precisely sequenced and random ethylene/α-olefin copolymers. PE materials produced via ADMET polymerization have shown unique properties in terms of their thermal response and morphology. In contrast to commercial LLDPE obtained by chain-growth polymerization, materials obtained with step-growth ADMET polymerization show perfectly known primary structures. Sequenced ethylene copolymers containing only one kind of branch identity along the backbone have shown to produce model materials with precise microstructure, useful for a better understanding of commercial PE. Sequenced ethylene copolymers produced using ADMET exhibit unique properties not seen before using chain-growth chemistry.

References

[1] Gedde, U.W., Mattozzi, A., Polyethylene morphology, long-term properties of polyolefins, Adv. Polym. Sci. 2004, 169:29–73.

[2] Knuuttila, H., Lehtinen, A., Nummila-Pakarinen, A., Advanced polyethylene technologies – controlled material properties, long-term properties of polyolefins, Adv. Polym. Sci. 2004, 169:13–27.

[3] Univation Technologies – Market Information, http://www.univation.com

[4] Fawcett, E.W., Gibson, R.Q., Perrin, M.H., Patton, J.G., Williams, E.G., Brit. Pat. 2, 816, 883, Sept. 6, Imperial Chemical Industries Ltd., 1937.

[5] Ziegler, K., Belg. Pat. 533,326, May 5, 1955 (Patent).

[6] Ziegler, K., Kunststoffe 1955, 45:506.

[7] Forte, M.M.D., da Cunha, F.O.V., dos Santos, J.H.Z., Zacca, J.J., Ethylene and 1-butene copolymerization catalyzed by a Ziegler–Natta/metallocene hybrid catalyst through a 23 factorial experimental design, Polymer 2003, 44:1377–1384.

[8] Usami, T., Gotoh, Y., Takayama, S., Generation mechanism of short-chain branching distribution in linear low-density polyethylenes, Macromolecules 1986, 19:2722–2726.

[9] Mirabella, F.M., Correlation of the elution behavior in temperature rising elution fractionation and melting in the solid-state and in the presence of a diluent of polyethylene copolymers, J. Polym. Sci. Part B: Polym. Phys. 2001, 39:2819–2832.

[10] Dias, M.L., Barbi, V.V., Pereira, R.A., Mano, E.B., Morphology and thermal properties of polyethylenes made by metallocene and Ziegler–Natta catalysts, Mater. Res. Innov. 2001, 4:82–88.

[11] Villar, M.A., Ferreira, M.L., Co- and terpolymerization of ethylene, propylene, and higher alpha-olefins with high propylene contents using metallocene catalysts, J. Polym. Sci. Part A: Polym. Chem. 2001, 39:1136–1148.

[12] Vanden Eynde, S., Mathot, V., Koch, M.H.J., Reynaers, H., Thermal behaviour and morphology of homogeneous ethylene-propylene and ethylene-1-butene copolymers with high comonomer contents, Polymer 2000, 41:3437–3453.

[13] Al-Hussein, M., Strobl, G., Strain-controlled tensile deformation behavior of isotactic poly(1-butene) and its ethylene copolymers, Macromolecules 2002, 35:8515–8520.

[14] DesLauriers, P.J., Rohlfing, D.C., Hsieh, E.T., Quantifying short chain branching microstructures in ethylene 1-olefin copolymers using size exclusion chromatography and Fourier transform infrared spectroscopy (SEC-FTIR), Polymer 2002, 43:159–170.

[15] Fernyhough, C.M., Young, R.N., Poche, D., Degroot, A.W., Bosscher, F., Synthesis and characterization of polybutadiene and poly(ethylene-1-butene) combs, Macromolecules 2001, 34:7034–7041.

[16] Gates, D.P., Svejda, S.K., Onate, E., Killian, C.M., Johnson, L.K., White, P.S., Brookhart, M., Synthesis of branched polyethylene using (alpha-diimine) nickel (II) catalysts: Influence of temperature, ethylene pressure, and ligand structure on polymer properties, Macromolecules 2000, 33:2320–2334.

[17] Hadjichristidis, N., Xenidou, M., Iatrou, H., Pitsikalis, M., Poulos, Y., Avgeropoulos, A., Sioula, S., Paraskeva, S., Velis, G., Lohse, D.J., Schulz, D.N., Fetters, L.J., Wright, P.J., Mendelson, R.A., Garcia-Franco, C.A., Sun, T., Ruff, C.J., Well-defined, model long chain branched polyethylene. 1. Synthesis and characterization, Macromolecules 2000, 33:2424–2436.

[18] Haigh, J.A., Nguyen, C., Alamo, R.G., Mandelkern, L., Crystallization and melting of model polyethylenes with different chain structures, J. Therm. Anal. Calorim. 2000, 59:435–450.

[19] Jokela, K., Vaananen, A., Torkkeli, M., Starck, P., Serimaa, R., Lofgren, B., Seppala, J., Differential scanning calorimetry, small-angle X-ray scattering, and wide-angle x-ray scattering on homogeneous and heterogeneous ethylene-alpha-copolymers, J. Polym. Sci. Part B: Polym. Phys. 2001, 39:1860–1875.

[20] Mader, D., Heinemann, J., Walter, P., Mulhaupt, R., Influence of n-alkyl branches on glass-transition temperatures of branched polyethylenes prepared by means of metallocene- and palladium-based catalysts, Macromolecules 2000, 33:1254–1261.

[21] Mattice, W.L., Complex branch formation in low-density polyethylene, Macromolecules 1983, 16:487–490.

[22] Mattice, W.L., Stehling, F.C., Branch formation in low-density polyethylene, Macromolecules 1981, 14:1479–1484.

[23] Rangwala, H.A., Lana, I.G.D., Szymura, J.A., Fiedorow, R.M., Copolymerization of ethylene and 1-butene using a Cr-silica catalyst in a slurry reactor, J. Polym. Sci. Part A: Polym. Chem. 1996, 34:3379–3387.

[24] Zhang, F.J., Song, M., Lu, T.J., Liu, J.P., He, T.B., The polydispersity of ethylene sequence in metallocene ethylene/alpha-olefin copolymers III: crystallization and melting behavior of short ethylene sequence, Polymer 2002, 43:1 453–1460.

[25] Ungar, G., Zeng, K.B., Learning polymer crystallization with the aid of linear, branched and cyclic model compounds, Chem. Rev. 2001, 101:4157–4188.

[26] Bracco, S., Comotti, A., Simonutti, R., Camurati, I., Sozzani, P., Low-temperature crystallization of ethylene-ran-propylene copolymers: conformational rearrangement of sequences during the formation of the aggregates, Macromolecules 2002, 35:1677–1684.

[27] Starck, P., Malmberg, A., Lofgren, B., Thermal and rheological studies on the molecular composition and structure of metallocene-and Ziegler–Natta-catalyzed ethylene-alpha-olefin copolymers, J. Appl. Polym. Sci. 2002, 83:1140–1156.

[28] Wright, K.J., Lesser, A.J., Crystallinity and mechanical behavior evolution in ethylene-propylene random copolymers, Macromolecules 2001, 34: 3626–3633.

[29] Pak, J., Wunderlich, B., Melting and crystallization of polyethylene of different molar mass by calorimetry, Macromolecules 2001, 34:4492–4503.

[30] Adisson, E., Ribeiro, M., Deffieux, A., Fontanille, M., Evaluation of the heterogeneity in linear low-density polyethylene comonomer unit distribution by differential scanning calorimetry characterization of thermally treated samples, Polymer 1992, 33:4337–4342.

[31] Alamo, R.G., Mandelkern, L., Crystallization kinetics of random ethylene copolymers, Macromolecules 1991, 24:6480–6493.

[32] Starck, P., Rajanen, K., Lofgren, B., Comparative studies of ethylene-alpha-olefin copolymers by thermal fractionations and temperature-dependent crystallinity measurements, Thermochim. Acta 2003, 395:169–181.

[33] Johnson, L.K., Killian, C.M., Brookhart, M., New Pd(Ii)-based and Ni(Ii)-based catalysts for polymerization of ethylene and alpha-olefins, J. Am. Chem. Soc. 1995, 117:6414–6415.

[34] Quijada, R., Rojas, R., Bazan, G., Komon, Z.J.A., Mauler, R.S., Galland, G.B., Synthesis of branched polyethylene from ethylene by tandem action of iron and zirconium single site catalysts, Macromolecules 2001, 34:2411–2417.

[35] Roedel, M.J., The molecular structure of polyethylene 1. Chain branching in polyethylene during polymerization, J. Am. Chem. Soc. 1953, 75:6110–6112.

[36] Tracz, A., Ungar, G., AFM study of lamellar structure of melt-crystallized n-alkane C390H782, Macromolecules 2005, 38:4962–4965.

[37] Ungar, G., Keller, A., Effect of radiation on the crystals of polyethylene and paraffins 1. Formation of the hexagonal lattice and the destruction of crystallinity in polyethylene, Polymer 1980, 21:1273–1277.

[38] Vaughan, A.S., Ungar, G., Bassett, D.C., Keller, A., On hexagonal phases of paraffins and polyethylenes, Polymer 1985, 26:726–732.

[39] Mirabella, F.M., Correlation of the melting behavior and copolymer composition distribution of Ziegler–Natta-catalyst and single-site-catalyst polyethylene copolymers, J. Polym. Sci. Part B: Polym. Phys. 2001, 39:2800–2818.

[40] O'Gara, J.E., Wagener, K.B., Acyclic diene metathesis (Admet) polymerization – synthesis of perfectly linear polyethylene, Makromol. Chem. Rapid Commun. 1993, 14:657–662.

[41] Sworen, J.C., Smith, J.A., Berg, J.M., Wagener, K.B., Modeling branched polyethylene: copolymers possessing precisely placed ethyl branches, J. Am. Chem. Soc. 2004, 126:11238–11246.

[42] Smith, J.A., Brzezinska, K.R., Valenti, D.J., Wagener, K.B., Precisely controlled methyl branching in polyethylene via acyclic diene metathesis (ADMET) polymerization, Macromolecules 2000, 33:3781–3794.

[43] Baughman, T.W., Wagener, K.B., Recent advances in ADMET polymerization, metathesis polymerization, Adv. Polym. Sci. 2005, 176:1–42.

[44] Sworen, J.C., Smith, J.A., Wagener, K.B., Baugh, L.S., Rucker, S.P., Modeling random methyl branching in ethylene/propylene copolymers using metathesis chemistry: synthesis and thermal behavior, J. Am. Chem. Soc. 2003, 125:2228–2240.

[45] Baughman, T.W., van der Aa, E., Lehman, S.E., Wagener, K.B., Circumventing the reactivity ratio dilemma: synthesis of ethylene-co-methyl-vinyl ether copolymer, Macromolecules 2005, 38:2550–2551.

[46] Wunderlich, B., Czornyj, G., Study of equilibrium melting of polyethylene, Macromolecules 1977, 10:906–913.

[47] Berda, E.B., Baughman, T.W., Wagener, K.B., Precision branching in ethylene copolymers: synthesis and thermal behavior, J. Polym. Sci. Part A: Polym. Chem. 2006, 44:4981–4989.

[48] Wagener, K.B., Valenti, D., Hahn, S.F., ADMET modeling of branching in polyethylene. The effect of a perfectly-spaced methyl group, Macromolecules 1997, 30:6688–6690.

[49] Hopkins, T.E., Wagener, K.B., ADMET Synthesis of polyolefins targeted for biological applications, Macromolecules 2004, 37:1180–1189.

[50] Mirabella, F.M., Ford, E.A., Characterization of linear low-density polyethylene –cross-fractionation according to copolymer composition and molecular-weight, J. Polym. Sci. Part B: Polym. Phys. 1987, 25:777–790.

[51] Wunderlich, B., Poland, D., Thermodynamics of crystalline linear high polymers 2. Influence of copolymer units on thermodynamic properties of polyethylene, J. Polym. Sci. Part A 1963, 1:357.

[52] Wilski, H., Grewer, T., Specific heat of poly-1-butene, J. Polym. Sci. Part C 1964, 33.

[53] Baughman, T.W., Sworen, J.C., Wagener, K.B., Sequenced ethylene-propylene copolymers: effects of short ethylene run lengths, Macromolecules 2006, 39:5028–5036.

MODELING LOW DENSITY POLYETHYLENE WITH PRECISELY PLACED BUTYL BRANCHES

GIOVANNI ROJAS, KENNETH B. WAGENER*

*The George and Josephine Butler Polymer Research Laboratory, Center of Macromolecular Science and Engineering, Department of Chemistry, University of Florida, Gainesville, FL 32611, USA. Phone: (352) 392-4666; Fax: (352) 392–9741 *E-mail: wagener@chem.ufl.edu*

Abstract: Polyethylene (PE) is a commodity produced on a massive scale and also is one of the most studied macromolecules. Crystallinity can be controlled by copolymerizing ethylene with α-olefins, producing a wide range of material responses. Physical properties of PE, obtained via α-olefin copolymerization, depend on the branch content that is directly related to the comonomer incorporation into the PE backbone. Materials with unknown primary structures are produced via chain-growth chemistry, because unwanted side reactions generate defects in the main backbone that alter the morphological behavior and thermal response. Acyclic diene metathesis (ADMET) polymerization/hydrogenation methodology produce perfect sequenced copolymers of ethylene with α-olefins. Synthesis and thermal properties of PE with butyl branches precisely placed along the polymer backbone using ADMET chemistry is described within.

Keywords: acyclic diene metathesis, ADMET, polymerization, butyl branches

1. Introduction

Polyethylene (PE) is the most widely utilized thermoplastic polymer today. In the next 5 years its worldwide demand is forecast to grow about 5% annually.[1] Its synthesis was first reported in the 1930s when Friedrich and Marvel reported low molecular weight PE by accident during high-pressure experiments with ethylene.[2] Later in 1933, the British chemical company Imperial Chemical Industries reported the first high molecular weight PE obtained by free-radical polymerization. The patent for its large-scale production was obtained in 1937.[3]

The free-radical polymerization of ethylene produces low-density PE (LDPE). The reaction is carried out by chain propagation radical chemistry producing a high branching content where 30% are usually butyl groups.[3] PE obtained by free-radical polymerization presents little control over the primary polymer structure. While free-radical polymerization of ethylene produces highly branched architectures, polymerization of ethylene using

Y. İmamoğlu and V. Dragutan (eds.), Metathesis Chemistry: From Nanostructure Design to Synthesis of Advanced Materials, 325-332.

Ziegler–Natta[4–9] and homogenous metallocene-based catalysts[10,11] produces highly crystalline, more linear, materials ranging from 62% to 80% crystallinity by density measurements. A wide range of material responses based on their crystallinity can be achieved by copolymerization of ethylene with α-olefins. The incorporation of a comonomer, typically 1-propylene, 1-butene, 1-hexane, or 1-octene, produces long-run lengths of unbranched linear PE with random insertion of comonomer yielding pendant alkyl branches. Diverse types of materials can be obtained by controlling the mode of polymerization, catalyst nature, pressure, and temperature, all of which have been studied for the last 60 years.[4,7,10–23] Physical properties of PE obtained via α-olefin copolymerization depend on the branch content that is directly related to the comonomer incorporation into the PE backbone. More important is the interaction between polymer chains.[16–18,23–28] However, synthetic methodologies used in the preparation of branched PE produce materials with unknown primary structures, because unwanted side reactions produce defects in the main backbone that alter the morphological behavior and thermal response.

A different approach of modeling ethylene-based copolymers is presented using acyclic diene metathesis (ADMET) polymerization. Monomer synthesis dictates final polymer structure due to step-growth chemistry yielding only to olefin metathesis. While copolymerization of ethylene with α-olefins produces random distribution of alkyl branches along the PE backbone, polymerization of one kind of symmetric macromonomer produces PE with a perfectly known primary structure, as seen in Figure 1.

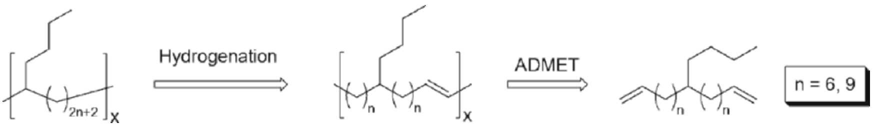

Figure 1. Retrosynthesis of sequenced ethylene-co-1-hexene.

ADMET is a step-growth condensation polymerization, where ethylene is the condensed product. Elimination of ethylene gas is the driving force of the reaction, producing an unsaturated high molecular weight polymer in the bulk. Figure 1 shows the retrosynthesis of these copolymers, with butyl branches precisely placed along the polymer backbone. The first attempt in these modeling studies was performed on PE containing methyl branches on each and every 9th, 11th, 15th, 19th, and 21st carbon along the backbone,[29] continuation of this research led to the development of ethyl-branched PE, or sequenced ethylene-co-1-butene.[30] In comparison of PE obtained by Ziegler–Natta or metallocene chemistry, polymers obtained via ADMET are ideal models of PE copolymers of sequenced ethylene/1-propylene and ethylene/1-butene respectively.

2. Experimental

ADMET polymerization was conducted in the bulk on 1.0 g scale. A Schlenk flask equipped with a high-vacuum Teflon valve and a magnetic stir bar was placed in an argon-filled dry box. The monomer was transferred to the polymerization flask and first-generation Grubbs' catalyst (monomers/[Ru] = 250/1) was added. The polymerization was moved out of the box and onto a high vacuum line for 3 days. Quenching with ethyl vinyl ether and precipitation from toluene into methanol yielded a white solid. Hydrogenation was performed using a 150 mL Parr high-pressure stainless steel reaction vessel equipped with a glass liner and a Teflon stir bar. The unsaturated polymer was dissolved into 100 mL of toluene and added a glass liner with 5 w/w % of $RuHCl(CO)(PCy_3)_2$. The glass liner was placed into the vessel, and the bomb was sealed. The Parr vessel was purged three times with 150 psi of hydrogen gas. The bomb was charged to 700 psi and the mixture was stirred for 24 h at 50°C followed by 96 h at 80°C (120 h total). The resultant polymer was filtered and precipitated into acidic methanol to obtain a colorless and viscous oil.

3. Results and Discussion

This study reports the synthesis and characterization of butyl-branched PE as a model for a sequenced copolymer of ethylene and 1-hexene. The ADMET polymerization of the symmetrical butyl-substituted diene monomer, followed by exhaustive hydrogenation, yielded a copolymer containing a butyl branch on each 15th and 21st carbon. The product polymer obtained by this polymerization/hydrogenation methodology has linear PE backbone without unwanted branch content and homogeneous branch distribution. Within this report, we describe a new universal synthetic pathway to yield pure alkyl branched α, ω-diene monomers using commercially available alkenyl bromides, as is shown in Figure 2.

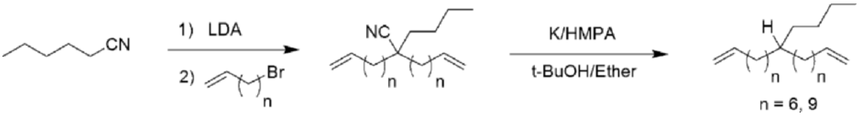

Figure 2. Synthesis of α,ω-olefins via dialkylation of hexanenitrile.

ADMET produces polymers from a metal mediated coupling of two terminal olefins driven by the condensation of ethylene, as is shown in Figure 3. The controlled polymerization allowed by ADMET produces polymers with perfect branch identity and distribution along the polymer backbone.

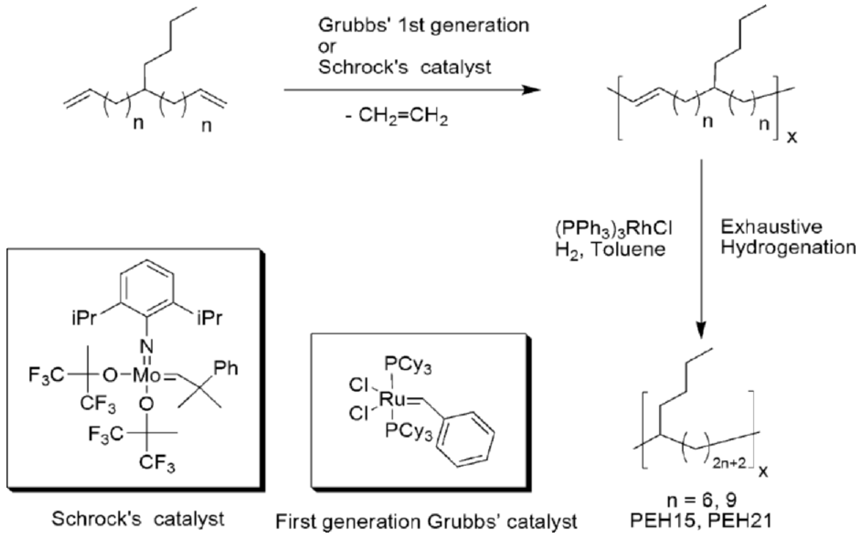

Figure 3. Synthesis of PEH15 and PEH21 via ADMET polymerization and its further hydrogenation.

This chemistry yields a linear, unsaturated polymer, which is formed by only one type of repeat unit. The polymerization is carried out using Schrock's or first-generation Grubbs' catalyst,[31–36] followed by hydrogenation. The nomenclature of our metathesis generated copolymers is based on the parent chain-addition copolymer. All copolymers begin with the prefix E (PE) followed by the comonomer type (H, 1-hexene) and the precise branch frequency (21); for example, EH21 is designated as the ethylene/1-hexene copolymer, which contains a butyl branch on every 21st carbon.

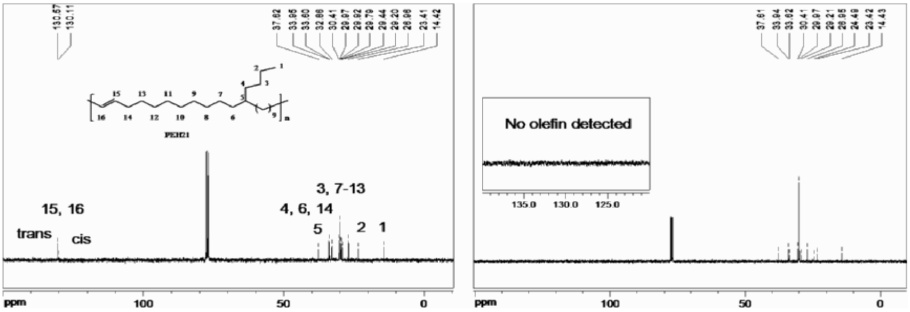

Figure 4. ^{13}C NMR of unsaturated and saturated PEH21.

The primary structure of all polymers has been fully characterized by ^{1}H NMR and ^{13}C NMR. Figure 4 shows the ^{13}C NMR spectrum of EH21 before and after exhaustive hydrogenation as an indication of complete saturation of the hydrocarbon chain. The olefin region illustrates the conversion of monomer to unsaturated polymer with the disappearance of the terminal olefin signal and the subsequent growth of internal olefin. Upon exhaustive hydrogenation, these olefin resonances completely disappear showing a simple and clean spectrum proper of a saturated PE structure.

Differential scanning calorimetry (DSC) has been used to examine the morphology and structure of PE. Numerous investigations are available concerning the structure and thermal properties of branched PE, particularly for LDPE and HDPE made by chain-addition chemistry.[18,23,25–28,37]

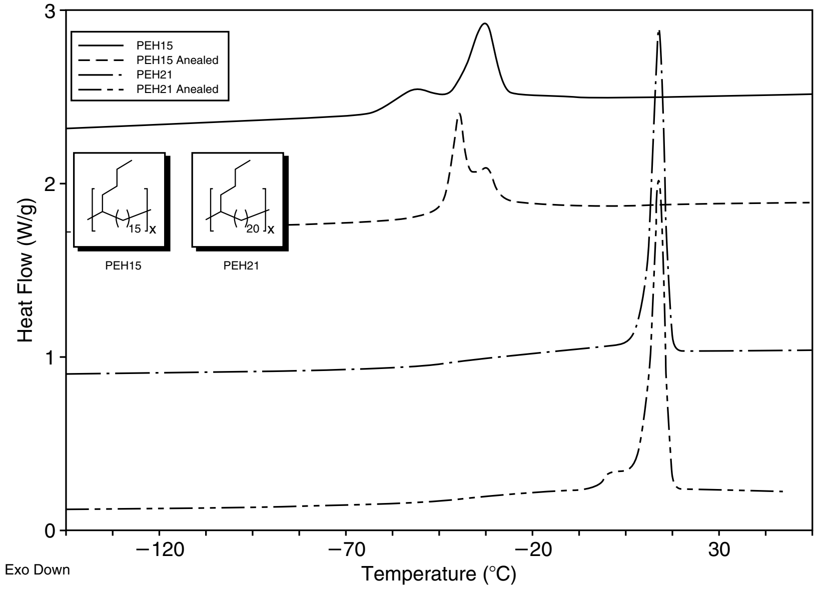

Figure 5. DSC plot of PEH15 and PEH21 obtained by ADMET.

Figure 5 shows the DSC plot obtained by the analysis of EH15 and EH21. Endothermic transitions of each polymer are sharp and defined rather than broad transitions usually observed for copolymers obtained via chain polymerization.[27] Peak melting temperature of ADMET EHs increases when the branch content decreases, an increment on the melting enthalpies when longer ethylene run lengths are present indicates a more crystalline structure.

4. Conclusions

A new and universal synthetic methodology in the preparation of alkyl branched α,ω-olefins is reported. Dialkylation followed by decyanation produces monomers in two steps in quantitative yields, making this route a cost effective and efficient synthesis. Using this new monomer synthesis, the production of PE with precisely placed butyl branches was explored via ADMET. Sequenced ethylene-co-1-hexene, or precisely butyl-branched PE, obtained is interesting in terms of its thermal response and crystallization as it sheds light on structure–property relationships are a widely produced material.

Acknowledgment

We would like to thank the Army Research Office, National Science Foundation, and Sumitomo Chemical Company for financial support.

References

[1] Univation Technologies – Market Information, http://www.univation.com
[2] Friedrich, M.E.P., Marvel, C.S., The reaction between alkali metal alkyls and quaternary arsonium compounds, J. Am. Chem. Soc. 1930, 52:376–384.
[3] Fawcett, E.W., Gibson, R.Q., Perrin, M.H., Patton, J.G., Williams, E.G., Brit. Pat. 2, 816, 883, Sept. 6, Imperial Chemical Industries, Ltd, 1937.
[4] Forte, M.M.D., da Cunha, F.O.V., dos Santos, J.H.Z., Zacca, J.J., Ethylene and 1-butene copolymerization catalyzed by a Ziegler-Natta/Metallocene hybrid catalyst through a 23 factorial experimental design, Polymer 2003, 44:1377–1384
[5] Usami, T., Gotoh, Y., Takayama, S., Generation mechanism of short-chain branching distribution in linear low-density polyethylenes, Macromolecules 1986, 19:2722–2726.
[6] Mirabella, F.M., Correlation of the elution behavior in temperature rising elution fractionation and melting in the solid-state and in the presence of a diluent of polyethylene copolymers, J. Poly. Sci. Pol. Phy. 2001, 39:2819–2832.
[7] Dias, M.L., Barbi, V.V., Pereira, R.A., Mano, E.B., Morphology and thermal properties of polyethylenes made by metallocene and Ziegler-Natta catalysts, Mat. Res. Innov. 2001, 4:82–88.
[8] Ziegler, K., Belg. Pat. 533,326, May 5, 1955.
[9] Ziegler, K., Kunststoffe 1955, 45:506.
[10] Villar, M.A., Ferreira, M.L., Co- and terpolymerization of ethylene, propylene, and higher alpha-olefins with high propylene contents using metallocene catalysts, J. Poly. Sci. Pol. Chem. 2001, 39:1136–1148.
[11] Vanden Eynde, S., Mathot, V., Koch, M.H.J., Reynaers, H., Thermal behaviour and morphology of homogeneous ethylene-propylene and ethylene-1-butene copolymers with high comonomer contents, Polymer 2000, 41:3437–3453.
[12] Al-Hussein, M., Strobl, G., Strain-controlled tensile deformation behavior of isotactic poly(1-butene) and its ethylene copolymers, Macromolecules 2002, 35:8515–8520.

[13] DesLauriers, P.J., Rohlfing, D.C., Hsieh, E.T., Quantifying short chain branching microstructures in ethylene 1-olefin copolymers using size exclusion chromatography and Fourier transform infrared spectroscopy (SEC-FTIR), Polymer 2002, 43:159–170.

[14] Fernyhough, C.M., Young, R.N., Poche, D., Degroot, A.W., Bosscher, F., Synthesis and characterization of polybutadiene and poly(ethylene-1-butene) combs, Macromolecules 2001, 34:7034–7041.

[15] Gates, D.P., Svejda, S.K., Onate, E., Killian, C.M., Johnson, L.K., White, P.S., Brookhart, M., Synthesis of branched polyethylene using (alpha-diimine)-nickel(II) catalysts: Influence of temperature, ethylene pressure, and ligand structure on polymer properties, Macromolecules 2000, 33:2320–2334

[16] Hadjichristidis, N., Xenidou, M., Iatrou, H., Pitsikalis, M., Poulos, Y., Avgeropoulos, A., Sioula, S., Paraskeva, S., Velis, G., Lohse, D.J., Schulz, D.N., Fetters, L.J., Wright, P.J., Mendelson, R.A., Garcia-Franco, C.A., Sun, T., Ruff, C.J., Well-defined, model long chain branched polyethylene. 1: synthesis and characterization, Macromolecules 2000, 33:2424–2436.

[17] Haigh, J.A., Nguyen, C., Alamo, R.G., Mandelkern, L., Crystallization and melting of model polyethylenes with different chain structures, J. Ther. Anal. Calorim. 2000, 59:435–450.

[18] Jokela, K., Vaananen, A., Torkkeli, M., Starck, P., Serimaa, R., Lofgren, B., Seppala, J., Differential scanning calorimetry, small-angle X-ray scattering, and wide-angle X-ray scattering on homogeneous and heterogeneous ethylene-alpha-copolymers, J. Polym. Sci. Pol. Phy. 2001, 39:1860–1875.

[19] Mader, D., Heinemann, J., Walter, P., Mulhaupt, R., Influence of n-alkyl branches on glass-transition temperatures of branched polyethylenes prepared by means of metallocene- and palladium-based catalysts, Macromolecules 2000, 33:1254–1261.

[20] Mattice, W.L., Complex branch formation in low-density polyethylene, Macromolecules 1983, 16:487–490.

[21] Mattice, W.L., Stehling, F.C., Branch Formation in Low-Density Polyethylene, Macromolecules 1981, 14:1479–1484.

[22] Rangwala, H.A., Lana, I.G.D., Szymura, J.A., Fiedorow, R.M., Copolymerization of ethylene and 1-butene using a Cr-silica catalyst in a slurry reactor, J. Polym. Sci. A1 1996, 34:3379–3387.

[23] Zhang, F.J., Song, M., Lu, T.J., Liu, J.P., He, T.B., The polydispersity of ethylene sequence in metallocene ethylene/alpha-olefin copolymers III: crystallization and melting behavior of short ethylene sequence, Polymer 2002, 43:1453–1460.

[24] Ungar, G., Zeng, K.B., Learning polymer crystallization with the aid of linear, branched and cyclic model compounds, Chem. Rev. 2001, 101:4157–4188.

[25] Bracco, S., Comotti, A., Simonutti, R., Camurati, I., Sozzani, P., Low-temperature crystallization of ethylene-ran-propylene copolymers: Conformational rearrangement of sequences during the formation of the aggregates, Macromolecules 2002, 35:1677–1684.

[26] Starck, P., Malmberg, A., Lofgren, B., Thermal and rheological studies on the molecular composition and structure of metallocene-and Ziegler-Natta-catalyzed ethylene-alpha-olefin copolymers, J. Appl. Polym. Sci. 2002, 83:1140–1156.

[27] Wright, K.J., Lesser, A.J., Crystallinity and mechanical behavior evolution in ethylene-propylene random copolymers, Macromolecules 2001, 34:3626–3633.

[28] Pak, J., Wunderlich, B., Melting and crystallization of polyethylene of different molar mass by calorimetry, Macromolecules 2001, 34:4492–4503.

[29] Smith, J.A., Brzezinska, K.R., Valenti, D.J., Wagener, K.B., Precisely controlled methyl branching in polyethylene via acyclic diene metathesis (ADMET) polymerization, Macromolecules 2000, 33:3781–3794.

[30] Sworen, J.C., Smith, J.A., Berg, J.M., Wagener, K.B., Modeling branched polyethylene: Copolymers possessing precisely placed ethyl branches, J. Am. Chem. Soc. 2004, 126:11238–11246.

[31] Schrock, R.R., Murdzek, J.S., Bazan, G.C., Robbins, J., Dimare, M., Oregan, M., Synthesis of molybdenum imido alkylidene complexes and some reactions involving acyclic olefins, J. Am. Chem. Soc. 1990, 112:3875–3886.

[32] Bazan, G.C., Khosravi, E., Schrock, R.R., Feast, W.J., Gibson, V. C., Oregan, M.B., Thomas, J.K., Davis, W.M., Living ring-opening metathesis polymerization of 2,3-difunctionalized norbornadienes by Mo(Ch-Tert-Bu)(N-2,6-C6h3-Iso-Pr2)(O-Tert-Bu)2, J. Am. Chem. Soc. 1990, 112:8378–8387.

[33] Bazan, G.C., Oskam, J.H., Cho, H.N., Park, L.Y., Schrock, R.R., Living ring-opening metathesis polymerization of 2,3-difunctionalized 7-oxanorbornenes and 7-oxanorbornadienes by Mo(Chcme2r)(N-2,6-C6h3-Iso-Pr2)(O-Tert-Bu)2 and Mo(Chcme2r)(N-2,6-C6h3-Iso-Pr2)(Ocme2cf3)2, J. Am. Chem. Soc. 1991, 113:6899–6907.

[34] Fox, H.H., Schrock, R.R., Living cyclopolymerization of diethyl dipropargylmalonate by Mo(Ch-T-Bu)(Nar)[Ocme(Cf3)2]2 in dimethoxyethane, Organometallics 1992, 11:2763–2765.

[35] Feldman, J., Murdzek, J.S., Davis, W.M., Schrock, R.R., Reaction of neopentylidene complexes of the type M(Ch-T-Bu)(N-2,6-C6h3-I-Pr2)(or)2(M = W, Mo) with methyl acrylate and N,N-dimethylacrylamide to give metallacyclobutane complexes, Organometallics 1989, 8:2260–2265.

[36] Oskam, J.H., Schrock, R.R., Rate of interconversion of Syn and antirotamers of Mo(Chcme2ph)(Nar)(or)2 and relative reactivity toward 2,3-bis(trifluoromethyl)norbornadiene, J. Am. Chem. Soc. 1992, 114:7588–7590.

[37] Ke, Ke., Characterization of polyolefins by differential thermal analysis, J. Polym. Sci. 1960, 42:15–23.

CORRELATING PRECISELY DEFINED PRIMARY STRUCTURE WITH CRYSTALLINE PROPERTIES IN HALOGEN CONTAINING POLYOLEFINS

EMINE BOZ[1], RUFINA G. ALAMO[2], KENNETH B. WAGENER[1]*

[1]*The George and Josephine Butler Polymer Research Laboratory, Center for Macromolecular Science and Engineering, Department of Chemistry, University of Florida, Gainesville, FL 32611*
[2]*FAMU/FSU College of Engineering, Department of Chemical and Biomedical Engineering, Tallahassee, FL 32310, USA. *E-mail: wagener@chem.ufl.edu*

Abstract: Polyethylene (PE) and poly(vinyl chloride) (PVC) are among the most important polymers produced in industry, although other halogen-containing derivatives of PE, such as poly(tetrafluorethylene) (PTFE) have also found wides pread use. A related class of polymers is the ethylene-co-vinyl-halide family. Such copolymers are expected to show distinct properties relative to their better known industrial analogues. For example, much interest has focused on ethylene vinyl chloride (EVC) polymers based on their potential for improved thermal stability relative to PVC. Various techniques have been used to synthesize these ethylene vinyl halide (EVH) copolymers and the simplest approach is halogenation of PE, which results in an irregular distribution of halogens along the polymer backbone and poorly defined materials. Direct copolymerization of ethylene/vinyl-halide monomers using free radical techniques results in polymers that contain numerous structural defects, and Ziegler–Natta conditions prove difficult for controlling the copolymer composition. Conversely, acyclic diene metathesis polymerization (ADMET) has been successfully employed for the synthesis of precisely defined EVC polymers, with a chlorine atom on each and every 19th carbon (PE19Cl). With ADMET, variation in the monomer structure gives rise to a broad range of precisely defined polymers, allowing easy correlation of structure–property relationships. Here we discuss a family of precision fluorine, chlorine, and bromine containing polyolefins synthesized via ADMET. These polymers are analyzed in order to establish how the halogen size affects the crystalline structure. The level of structural control achieved via ADMET in these halogen-containing polyolefins surpasses that previously reported in the literature for EVH polymers. Detailed thermal and crystalline analysis reveals a strong effect of the nature of the halogen substituent on the polymer properties.

Keywords: Olefin metathesis, ADMET polymerization, ethylene/vinyl halide, polyethylene

1. Introduction

Polyolefins are perhaps the most important large volume polymers produced today.[1] Modification of the parent structure through halogen incorporation,

Y. İmamoğlu and V. Dragutan (eds.), Metathesis Chemistry: From Nanostructure Design to Synthesis of Advanced Materials, 333-345.

as in the case of poly(vinyl chloride) (PVC) or poly(tetrafluorethylene) (PTFE), extends the range of applications as a result of changes in polymer structure at all levels.[2] The copolymer ethylene vinyl halide (EVH) analogues are also of interest as, for example, ethylene vinyl chloride (EVC) copolymers offer improved thermal stability relative to PVC.[3] Similarly, ethylene vinyl fluoride (EVF) polymers, such as poly(vinyl fluoride) (PVF), poly(vinylidene fluoride) (PVF_2), and poly(ethylene-*alt*-tetrafluorethylene) are of value.[4] Comparatively less known are the ethylene vinyl bromide copolymers and partially brominated polyethylene (PE).[5,6]

As is relevant to EVH polymers, it has been known for decades now, that random incorporation of relatively small amounts (<10 mol %) of a structural irregularity in PE generates copolymers possessing thermal properties that adhere to thermodynamic principles of phase transitions in two-component systems.[7] The large amount of experimental data that exists demonstrates that large side groups such as ethyl, propyl, vinyl acetate, and styrene are not incorporated into the copolymer crystal lattice.[8] Their solid–liquid transition follows the basis of Flory's equilibrium theory derived on the assumption of formation of a pure crystalline phase.[9] On the other hand, smaller side groups such as methyl, chlorine, and oxygen can be partially incorporated into the crystalline lattice.[7] Differences in partitioning of the side groups has a strong impact on the thermodynamic and physical properties of these copolymers. Thus, melting temperatures of random copolymers with Cl pendant groups and CH_3 branches are significantly higher than those of copolymers with matched compositions of side groups excluded from the crystal.[10] The differences reflect the fraction of longer continuous crystallizable sequences present in the former type.

A more complex problem is the analysis of the thermodynamic behavior of random ethylene copolymers with > ~10 mol % branch points in the main chain. At these high-branching levels, the melting temperatures and degrees of crystallinity usually deviate upward from the linear trends observed at the lower branching contents,[11,12] and divergences are accentuated for copolymers with side groups that can be accommodated in the crystal.[13,14] In reference to thermodynamic principles, the branching distribution in highly branched systems is of concern as it relates to how closely the crystallization behavior follows models based on selection of crystallizable sequences. A decreased length of continuous methylene sequences might cause a different crystallization mode,[13] consistent with observations of a change in crystallographic packing with increasing comonomer content.[13,14,15,16] Understanding the details of the crystallization behavior for these highly branched systems can only be accomplished via model polymers with well-defined microstructures.

Acyclic diene metathesis polymerization (ADMET)[17] polymerization leads to polymers with precisely defined microstructures and, hence, to excellent models to study the crystallization behavior of highly branched ethylene copolymers. With ADMET, variation in the monomer structure gives access to a broad range of precisely defined polymers, allowing direct correlation of structure-property relationships.[18] This “clean polycondensation” chemistry is used here to produce a branched architecture characterized by the precise branch placement every “n” fixed methylene units according to the following structural repeating unit:

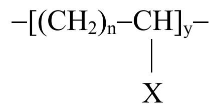

$$-[(CH_2)_n-\underset{X}{\underset{|}{C}}H]_y-$$

The unique characteristics of these systems permit the study of ideal models of functionalized PE with precisely placed substituents in which *n* and *X* can be varied independently. Here we discuss the crystalline properties of a series of precision ADMET PE structures containing fluorine, chlorine, and bromine located on each and every 19th carbon (n = 18) along the polymer backbone. The effect of the substituent on the crystallographic packing is studied using infrared (IR) spectroscopy and wide angle x-ray diffraction (WAXD), while the partitioning of the substituent between crystalline and noncrystalline regions is inferred from solid-state nuclear magnetic resonance (NMR) spectroscopy and from the polymer’s thermal behavior. The systematic increase of van der Waals radius of the substituents in the series allows quantitative data of the degree to which the orthorhombic PE lattice can tolerate atomic hydrogen substitution. The thermodynamic properties of these model systems is directly correlated to substituent radius and bond lengths to establish fundamental grounds for strategies to modify structural and thermal behavior of PEs.

2. Results and discussion

The synthesis of fluorine, chlorine, and bromine substituted EVH polymers with a halogen on each and every 19th carbon required the preparation of $\alpha-\omega$ diene monomers, followed by ADMET polymerization and subsequent exhaustive hydrogenation as described previously.[19] The primary structure for these well-defined halogenated polyolefins was established using a combination of ^{1}H NMR, ^{13}C NMR, thermogravimetric analysis (TGA), IR spectroscopy, and elemental analysis. The precise structure of the polymers is supported by NMR, while TGA results prove the composition of the polymer through the clearly observed thermal decomposition and release of exact masses of HX (calculated HF = 7.0% and HBr = 23.5%, found HF = 7.3 %, and HBr = 22.7%), followed by catastrophic decomposition. The mass loss in all cases is in accord with the theoretically calculated value.

Figure 1 shows the IR spectra for thin films of the three halogenated polymers, which support the expected primary structure. Here the absence of a peak at 967–969 cm^{-1}, corresponding to the out-of-plane C–H wag (γ_w) of an alkene,[20] indicates complete hydrogenation of the polymer backbone. Further, the IR spectra support the presence of each of the expected halogens on the polymer backbone. For **PE19F (**PE19X indicates a PE backbone with a halogen substituent (X) on every 19th carbon), the sharp peak at 1068 cm^{-1} protruding from a broader underlying peak is characteristic of the C–F stretch.[21] The peaks observed at 611, 660, and 802 cm^{-1} in **PE19Cl** are characteristic of C–Cl stretching vibrations,[22] while for **PE19Br**, the peak at 612 cm^{-1} is assigned to the vibrations of the C–Br bond.[6] Insight into the crystalline structure of these precisely halogenated polymers is also provided by this IR data. In this case, the significant peaks are those found at ~720 and ~1470 cm^{-1}, which correspond to the vibrational modes of the CH_2 sequences in PE analogues.[22] For **PE19F**, the doublets observed at 721–730 and 1463–1472 cm^{-1} are the same as observed in crystalline PE. The band at ~720 cm^{-1} corresponds to long *trans* CH_2 sequences and the band at 730 cm^{-1}, is associated with the rocking vibrations of CH_2 sequences of five or more carbons.[14,23] The IR spectra for **PE19Cl** and **PE19Br** are clearly different

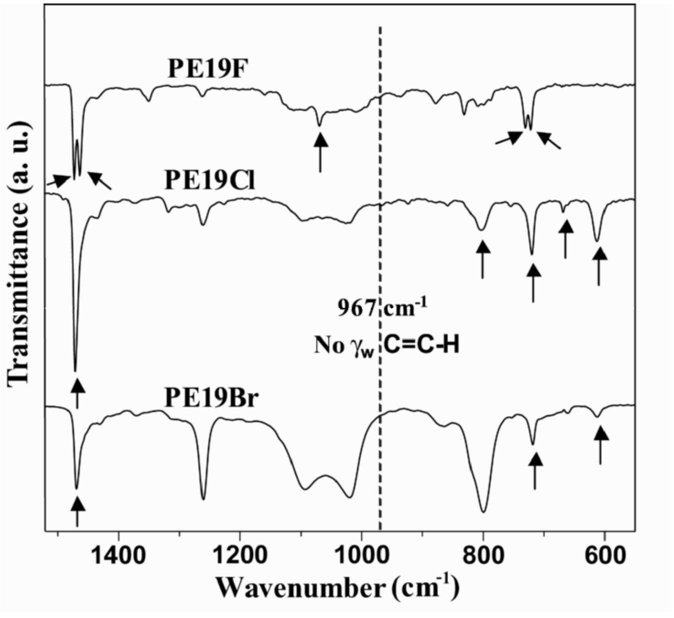

Figure 1. IR spectra for thin films of **PE19F**, **PE19Cl**, and **PE19Br** cast on KBr disks. (Reproduced from [19]. With permission.)

from that of the fluorinated analogue **PE19F** and pure PE, suggesting a distinct difference in the crystalline packing of these polymers. The Cl and Br polymers show a single peak rather than doublets at ~720 and ~1470 cm^{-1} suggesting that these polymers possess similar crystalline features, yet differ from **PE19F** or pure PE. Both WAXD and solid-state ^{13}C NMR studies of the crystalline structure, presented in the following sections support these results.

X-ray diffractograms of halogen containing ADMET samples cooled from the melt at 1°C/min are shown in Figure 2 together with the patterns of PE19O (with a C=O group on each and every 19th carbon) and of a linear PE narrow fraction in the same molecular weight range. All samples display very sharp diffraction peaks, except for the broader pattern of the brominated material. In contrast, random ethylene copolymers with the same type of branching having similar or lower branching levels are known to show much broader WAXD patterns.[13,20,24] Therefore, the sharp diffractograms in Figure 2 suggest a homopolymer rather than copolymer-like crystallization behavior. Also, it is evident that while substitution with O or F every 19th carbon does not alter the orthorhombic unit cell packing of linear PE, substitution with bulkier atoms leads to the formation of a different crystallographic phase.

Diffraction peaks at ~19° and ~22° for the Cl and Br containing samples were also found in similar precisely placed methyl-branched polymers and indexed as (010) and (100) diffractographic planes of a triclinic cell.[25] Therefore, the diffractograms of **PE19Cl** and **PE19Br** are assigned to triclinic structures. Compared to the orthorhombic packing displayed by PE and polymers with F and O substitutions, the triclinic pattern is a degeneration in the scale of symmetry supporting previous speculation[25] that a reduced order is needed to facilitate minimum spatial requirements to accommodate the bulky Cl, Br, or CH_3 groups between adjacent molecules in the crystal. The triclinic pattern is substantially different from a single diffraction pattern observed for methyl branched PE or for EVCs with the same content of side groups but randomly distributed.[13,15,16,20,24] In such systems single WAXD peaks were associated with defective orthorhombic or pseudohexagonal structures. Therefore, the progression of WAXD patterns in Figure 2 is clear evidence that both the *type and distribution* of the substituent has an impact on the chain ordering of branched or substituted PEs at the most fundamental level.

The 2θ values of the diffraction peaks, together with other characterization data, are summarized in Table 1 for PE and the ADMET precisely substituted polymers. Also listed are X van der Waals radii and C–X bond lengths. Inspection of these data allows evaluation of lattice expansions in

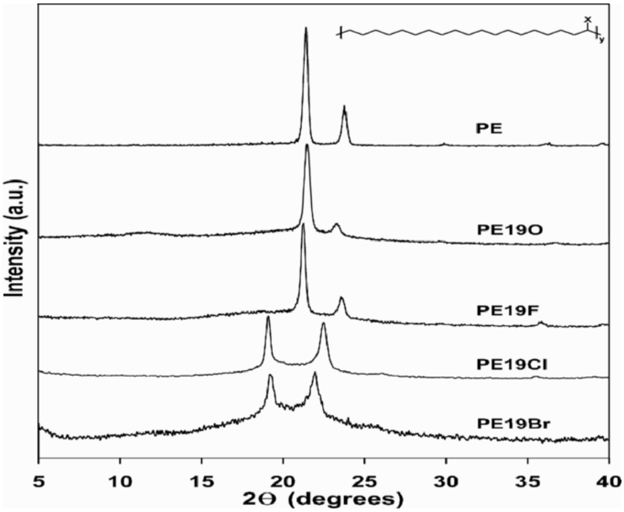

Figure 2. WAXD diffractograms of linear PE and ADMET precisely substituted PEs slowly cooled from the melt at ~1°/min. The pendant group (X = H, O, F, Cl, Br) is indicated in each pattern. (Reproduced from [19]. With permission.)

reference to geometric constraints imposed by the solute X in the adjoining matrix. Compared to the unsubstituted PE chain, the shift of 2θ (110) and 2θ (200) in the **PE19F** and **PE19O** patterns to lower angular values indicates the expansion of the orthorhombic lattice due to an increase in both van der Waals radius and bond length of C–F and C=O respectively. Similarly, the increase in the spacing of the triclinic (010) plane from 2θ = 22.47° (3.96 Å) for **PE19Cl** to 2θ = 21.95° (4.05 Å) for **PE19Br** is also explained by the increased radius and bond length of the Br atom. These angular shifts are as expected for the significant incorporation of side groups into the crystalline structure. Further, the sharp diffraction peaks indicate a strong correlation of diffractographic planes and highly organized crystalline structures.

The diffractograms of Figure 2 also indicate that there is a significant amorphous region in these systems that increase with the bulkiness of the substituent. To estimate the degree of crystallinity from the diffractograms, the WAXD patterns obtained at 150°C were scaled and subtracted from the room temperature patterns. Crystallinity levels obtained are listed in Table 1 and range from 83% for PE to ~ 40% for **PE19Br**. For comparison, random ethylene copolymers with the same level of methyl branching or chlorine pendant groups (~5.3 mol %), display much lower levels of crystallinity (~25%) with less organization.[13,26,27] In the random systems, one can then conclude that the initial selection of long methylene sequencesover sequences containing for example Cl or Br substituents, imposes additional constraints

Table 1. Crystalline data of precision ADMET polyolefins (PE19X) with general structure –[(CH2)18-CHX]$_y$–. Melting and crystallization temperatures and heat of fusions correspond to samples crystallized and melted at 10°C/min. (Reproduced from [19]. With permission.)

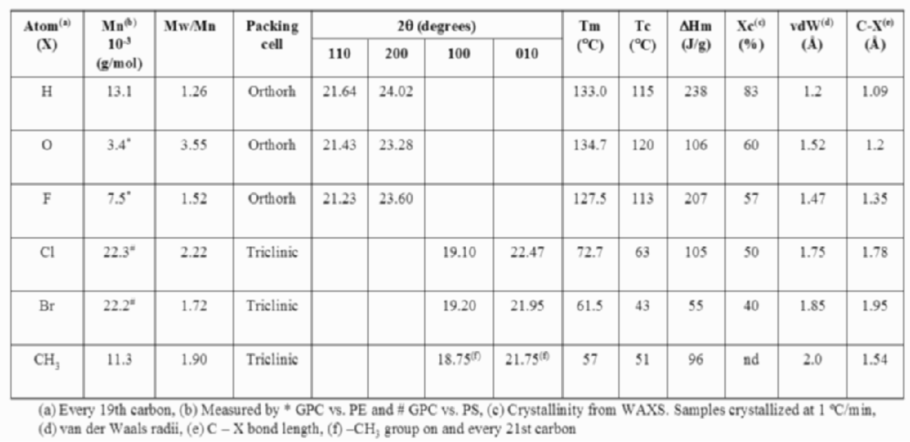

Atom$^{(a)}$ (X)	Mn$^{(b)}$ 10^{-3} (g/mol)	Mw/Mn	Packing cell	2θ (degrees)				Tm (°C)	Tc (°C)	ΔHm (J/g)	Xc$^{(c)}$ (%)	vdW$^{(d)}$ (Å)	C-X$^{(e)}$ (Å)
				110	200	100	010						
H	13.1	1.26	Orthorh	21.64	24.02			133.0	115	238	83	1.2	1.09
O	3.4*	3.55	Orthorh	21.43	23.28			134.7	120	106	60	1.52	1.2
F	7.5*	1.52	Orthorh	21.23	23.60			127.5	113	207	57	1.47	1.35
Cl	22.3$^{\#}$	2.22	Triclinic			19.10	22.47	72.7	63	105	50	1.75	1.78
Br	22.2$^{\#}$	1.72	Triclinic			19.20	21.95	61.5	43	55	40	1.85	1.95
CH_3	11.3	1.90	Triclinic			18.75$^{(f)}$	21.75$^{(f)}$	57	51	96	nd	2.0	1.54

(a) Every 19th carbon, (b) Measured by * GPC vs. PE and # GPC vs. PS, (c) Crystallinity from WAXS. Samples crystallized at 1 °C/min, (d) van der Waals radii, (e) C – X bond length, (f) –CH_3 group on and every 21st carbon

in the topology of the remaining melt for gathering additional sequences with the required length to propagate crystallization. Specifically, the crystallization is primarily driven by the selection of continuous crystallizable sequences longer than a critical value in the random systems, while shorter sequences remain uncrystallized. The lack of branching distribution in ADMET PEs with side groups on every 19th carbon, invokes a homopolymer-like crystallization with a driving force led by the accommodation of the side group in an all *trans* backbone packing conformation. This crystallization mode explains the sharp diffractograms.

The fact that precisely substituted ADMET polymers display relatively high levels of crystallinity suggest a crystalline state built on the basis of substitutional solid solutions.[28] In packing backbone sequences in all *trans* conformation, substitution of a H for O, F, Cl, or Br on each and every 19th carbon creates lattice distortions on levels proportional to the solute's van der Waals radius. As seen in Table 1, the orthorhombic lattice is preserved in this series up to a radius of ~1.6 Å, while bulkier atoms cause large lattice distortions to the point that correlated symmetry between crystallographic planes is only found within a different phase with significantly larger dimensions.[29] Relative to hydrogen, the discontinuity of isomorphic structures in this series occurs at a difference in van der Waals radius of ~30%. This is larger than the ~15% difference usually cited for the formation of isomorphic metallic solid solutions,[28] but not unexpected, taking into account the chain connectivity of polymer molecules and the weaker covalent bonding.

A further insight into the unique crystallization mode in this family of precisely substituted PEs is observed in their crystallization and melting behaviors as measured by differential scanning calorimetry (DSC) shown in Figure 3. The sharpness of the crystallization and melting traces are typical of the behavior of low molecular mass homopolymers, and they contrast with the much broader endotherms displayed by random ethylene copolymers of similar branching composition.[10,20,26] These thermodynamic features also point to a mechanism for ordering the precisely branched ADMET polymers that is not based on a partitioning of sequences in the crystallization process, observed typically in random copolymers.[7] In the random case, a richer melt in substituents is inevitable due to the chain's noncrystallizable short sequences; this feature leads to an inequality in partitioning of the substituent between the crystalline and noncrystalline regions. As a consequence, the composition of the melt coexisting with crystallites changes continuously during melting, leading to the broad endotherms usually observed in the random systems.[11,30]

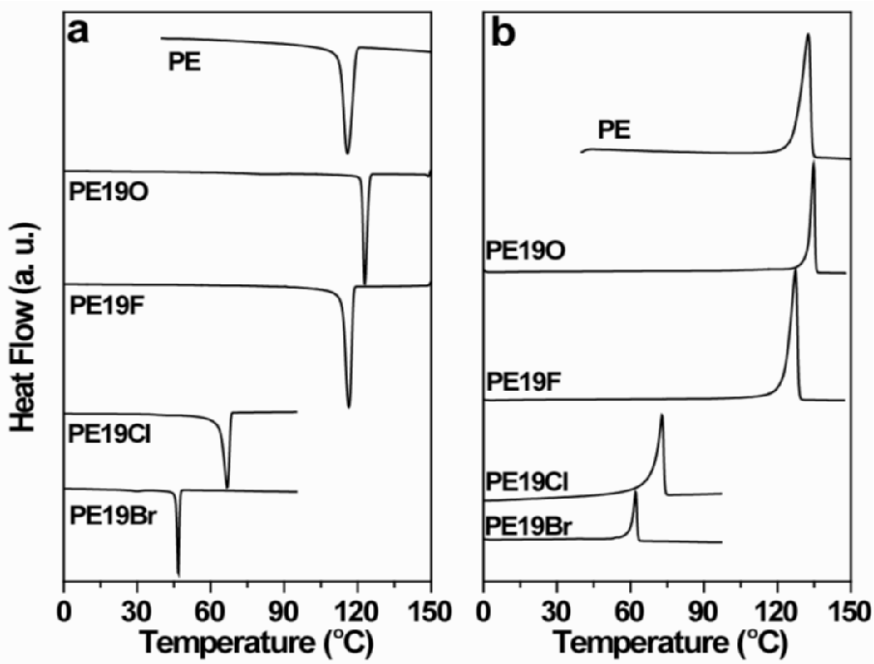

Figure 3. DSC exotherms (a) and endotherms (b) of linear PE and precisely substituted polyethylenes cooled from the melt at 10ºC/min and further heated at 10ºC/min. (Reproduced from [19]. With permission.)

The peak melting temperatures decrease dramatically and proportionally to the van der Waals radius in the series of halogenated polymers, as seen in

Figure 4. We observe that for similar van der Waals radii, shorter bond lengths increase the melting temperature as illustrated by the ~7° higher melting of **PE19O** compared to **PE19F**. Similarly, the melting temperature of **PE19CH$_3$**[27] is higher than predicted from the van der Waals radii due to a much shorter C–C bond length. The high heat of fusion of **PE19F** (Table 1) is associated with a high electronegativity of the F atom and its likelihood of increasing intermolecular secondary bonding compared to the other members of the series.

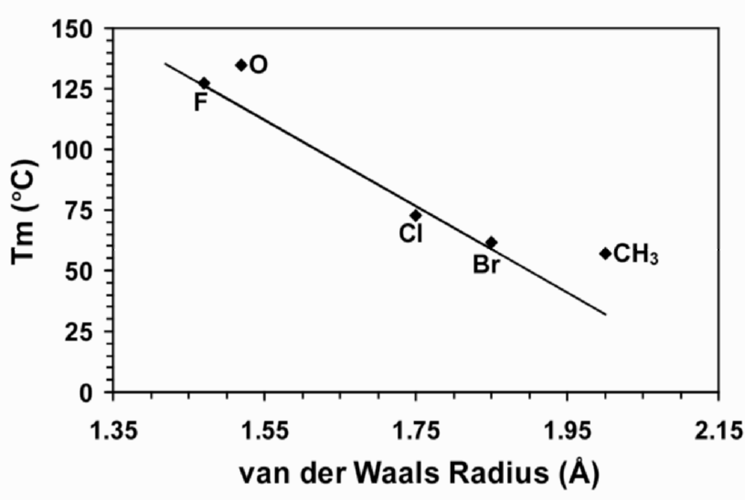

Figure 4. Peak melting temperatures of precisely substituted polyethylenes (PE19X) versus van der Waals radius of substituent (X). The linear regression was applied to halogenated samples. (Reproduced from [19]. With permission.)

The distribution of side groups among the different phases of the semicrystalline structure was probed by cross-polarized (CP) MAS NMR experiments that isolate the spectra of the crystalline regions.[31,32] Resonances in the crystalline spectra that are associated with the methine carbon or carbons adjacent to the methine group allow direct quantitative data on the content of these groups in the crystalline regions and, hence, on the partitioning of the side groups. Unfiltered CP MAS spectra, shown in Figure 5a reveals an increase of the intensity of the amorphous CH$_2$ resonance (~31 ppm) with the size of the substituent, reflecting a decrease of crystallinity from **PE19F** to **PE19Br**, in agreement with the WAXD data. Also of interest is the chemical shift corresponding to crystalline CH$_2$ of **PE19F**, observed at 33.1 ppm, a value that is very close to the all *trans* orthorhombic linear PE. This similarity in chemical shifts confirms that **PE19F** maintains the orthorhombic packing of the PE chain.

Resonances of carbons associated with the substituents are still observed in the filtered crystal spectra (Figure 5b) even after subtraction of most of the amorphous components. These include the methine (CHX ~65 ppm for Cl and Br and ~97 ppm for F), the α CH_2 (~ 40 ppm) and the β CH_2 (observed at 28.6 ppm for **PE19F**, at ~31.0 ppm for **PE19Cl** and buried within the main CH_2 resonance in the spectrum of **PE19Br**). These resonances confirm that all the types of halogen side groups are incorporated in the crystalline regions of these systems. The resolved character of the relatively sharp α CH_2 resonances and the resonance associated with the CHX in the crystalline spectra allow us to integrate these lines against the integrals of the main peaks and, thus, deduce the concentration of F, Cl, and Br groups in the crystal. Accounting for the larger experimental error associated with integration of broad CHX resonances, the values obtained for the concentration of halogen in the crystal from any of the resonances associated with the side groups are very similar to the concentration of halogen in the chain (5.3 mol %). Therefore, analyses of CP MAS spectra confirm the uniform distribution of the halogen in the semicrystalline structure and thus, the homopolymer crystallization behavior of these systems.

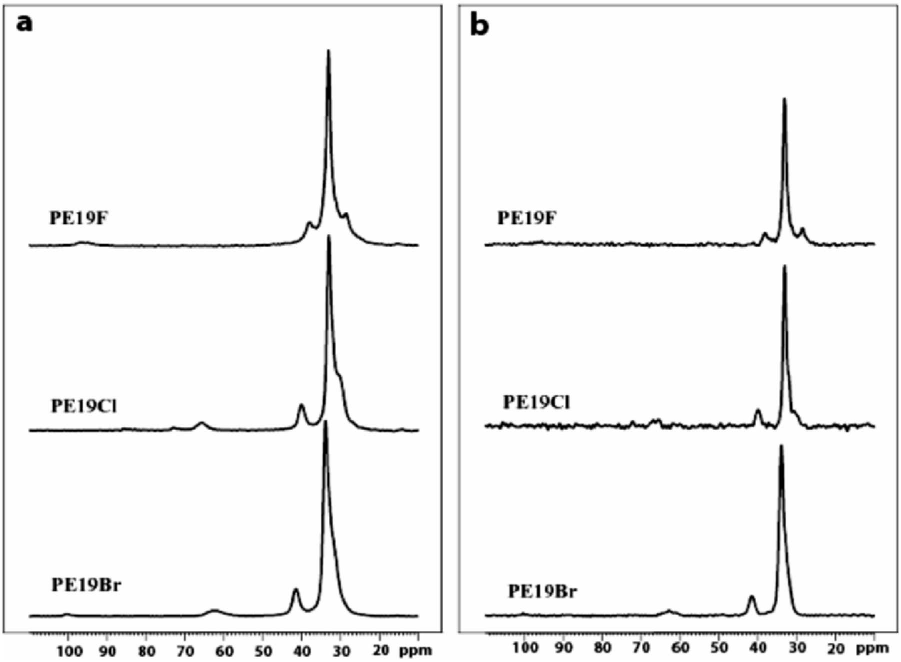

Figure 5. (a) Unfiltered ^{13}C NMR CP MAS spectra; and (b) ^{1}H spin locking filtered (crystalline) spectra of precision PE19X (X = F, Cl, Br) polyolefins. (Reproduced from [19]. With permission.)

3. Conclusions

The unique crystallization behavior of a series of precisely substituted polyolefins, with halogens (F, Cl, Br) on each and every 19th carbon, has been described. The very sharp diffraction patterns observed by WAXD and the narrow melting and crystallization peaks found by DSC for these polymers conform to a homopolymer-like crystallization. These observations contrast with much broader diffraction and melting peaks observed in ethylene copolymers with matched concentrations of randomly distributed side groups. In reference to the random copolymers, precisely substituted ADMET polymers display relatively high levels of crystallinity, as measured by WAXD, and a crystalline state built on the basis of substitutional solid solutions. The accommodation of O, F, Cl, or Br groups in the crystal creates lattice distortions on levels proportional to the solute's van der Waals' radius. The magnitude of the distortions is such that the PE orthorhombic lattice is only preserved up to a radius of ~1.6 Å (F, O substituents). Accommodation of bulkier substituents (Cl, Br) degenerates the correlated symmetry to a triclinic lattice with significantly larger dimensions. Direct solid-state ^{13}C NMR investigations of the crystalline and noncrystalline regions evidence a uniform partitioning of all of these substituents between the different phases. While crystallization of the random type is led by the selection of long crystallizable sequences, in these precision polyolefins it is governed by the accommodation of the side groups into the crystal. As such, both *type and distribution* of the substituent impact the chain ordering of branched and substituted PEs at the most fundamental level.

Acknowledgment

Funding of this work by the National Science Foundation, grant numbers DMR-0503876 and NSF 314110 is gratefully acknowledged. We gratefully acknowledge Anindya Ghosal for WAXS data and Riqiang Fu of the National High Magnetic Field Laboratory for SS NMR data. We also acknowledge URP student Kimberly Thompson for assistance with collection of DSC data, and Dr. Lisa Baugh at ExxonMobil for obtaining GPC data for PE19O and PE19F. Generous support from ARO for the acquisition of catalysts is also acknowledged.

References

[1] Mathot, V.B.F., Reynaers, H., Crystallization, Melting and Morphology of Homogeneous Ethylene Copolymers: Handbook of Thermal Analysis And Calorimetry, Vol. 3, Elsevier, Amsterdam, 2002, pp. 197–244.

[2] Feldman, D., Barbalata, A., Synthetic Polymers, Chapman & Hall, London, 1996, Chapter 2.

[3] Yang, H., Islam, M., Budde, C., Rowan, S.J., Ring-opening metathesis polymerization as a route to controlled copolymers of ethylene and polar monomers: synthesis of ethylene-vinyl chloride-like copolymers, J. Polym. Sci. Pol. Chem., 2003, 41:2107–2116.

[4] Walsby, N., Sundholm, F., Kallio, T., Sundholm, G., Radiation-grafted ion-exchange membranes: influence of the initial matrix on the synthesis and structure, J. Polym. Sci. Pol. Chem. 2001, 39:3008–3017.

[5] Tonelli, A.E., Conformational characteristics of poly(vinyl bromide) and ethylene-vinyl bromide copolymers, Macromolecules 1982, 15:290–293.

[6] Arroyo, A.N., Hiltner, A., Suspension bromination of high-density polyethylene, J. Appl. Polym. Sci. 1979, 23:1473–1485.

[7] Mandelkern, L., Crystallization of Polymers, 2 edn., Vol. 1, Cambridge University Press, Cambridge, 2002.

[8] Isasi, J.R., Haigh, J.A., Graham, J.T., Mandelkern, L., Alamo, R.G., Some aspects of the crystallization of ethylene copolymers, Polymer 2000, 41:8813–8823.

[9] Flory, P.J., Theory of crystallization in copolymers, T. Faraday Soc. 1955, 51:848–857.

[10] Alamo, R.G., Mandelkern, L., The crystallization behavior of random copolymers of ethylene, Thermochim. Acta 1994, 238:155–201.

[11] Crist, B., Howard, P.R., Crystallization and melting of model ethylene-butene copolymers, Macromolecules 1999, 32:3057–3067.

[12] Chen, H.Y., Chum, S.P., Hiltner, A., Baer, E., Comparison of semicrystalline ethylene-styrene and ethylene-octene copolymers based on comonomer content, J. Polym. Sci. Pol. Phy. 2001, 39:1578–1593.

[13] Stephens, C.H., Yang, H., Islam, M., Chum, S.P., Rowan, S.J., Hiltner, A., Baer, E., Characterization of polyethylene with partially random chlorine substitution, J. Polym. Sci. Pol. Phy. 2003, 41:2062–2070.

[14] Ver Strate, G.W., Wilchinsky, Z.W., Ethylene-propylene copolymers: degree of crystallinity and composition, J. Polym. Sci., Pol. Phy. Edit. 1971, 9:127–142.

[15] Hu, W., Sirota, E.B., Monoclinic crystallites in ethylene copolymers detected by solid-state NMR and X-ray diffraction, Macromolecules 2003, 36:5144–5149.

[16] de Ballesteros, O.R., Auriemma, F., Guerra, G., Corradini, P., Molecular organization in the pseudo-hexagonal crystalline phase of ethylene-propylene copolymers, Macromolecules 1996, 29:7141–7148.

[17] Sworen, J.C., Smith, J.A., Berg, J.M., Wagener, K.B., Modeling branched polyethylene: copolymers possessing precisely placed ethyl branches, J. Am. Chem. Soc. 2004, 126:11238–11246.

[18] Baughman, T.W., Wagener, K.B., Recent advances in ADMET polymerization, Adv. Polym. Sci. 2005, 176:1–42.

[19] Boz, E., Wagener, K.B., Fu, R., Ghosal, A., Alamo, R.G., synthesis and crystallization of precision ADMET polyolefins containing halogen, Macromolecules 2006, 39:4437–4447.

[20] Sworen, J.C., Smith, J.A., Wagener, K.B., Baugh, L.S., Rucker, S.P., Modeling random methyl branching in ethylene/propylene copolymers using metathesis chemistry: synthesis and thermal behavior, J. Am. Chem. Soc. 2003, 125: 2228–2240.

[21] Du Toit, F.J., Sanderson, R.D., Surface fluorination of polypropylene 1. Characterisation of surface properties, J. Fluorine Chem. 1999, 98:107–114.

[22] Stoeva, S., Structural and conformational changes in solid-phase chlorinated polyethylene, J. Appl. Polym. Sci. 2004, 94:189–196.

[23] Hagemann, H., Snyder, R.G., Peacock, A.J., Mandelkern, L., Quantitative infrared methods for the measurement of crystallinity and its temperature dependence: polyethylene, Macromolecules 1989, 22:3600–3606.

[24] Gomez, M.A., Tonelli, A.E., Lovinger, A.J., Schilling, F.C., Cozine, M.H., Davis, D.D., Structure and morphology of ethylene-vinyl chloride copolymers, Macromolecules 1989, 22:4441–4451.

[25] Lieser, G., Wegner, G., Smith, J.A., Wagener, K.B., Morphology and packing behavior of model ethylene/propylene copolymers with precise methyl branch placement, Colloid Polym. Sci. 2004, 282:773–781.

[26] Bowmer, T.N., Tonelli, A.E., Thermal transitions of ethylene-vinyl chloride copolymers Polymer 1985, 26:1195–1201.

[27] Smith, J.A., Brzezinska, K.R., Valenti, D.J., Wagener, K.B., Precisely controlled methyl branching in polyethylene via acyclic diene metathesis (ADMET) polymerization, Macromolecules 2000, 33:3781–3794.

[28] Callister, W.D., Materials Science and Engineering. An Introduction, Wiley, New York, 2003.

[29] Contrasting with the dimension of the “c” axis of orthorhombic crystals, 2.54 Å, the “c” axis of the triclinic cell corresponds to two full repeating units (>40 Å).

[30] Simanke, A.G., Alamo, R.G., Galland, G.B., Mauler, R.S., Wide-angle x-ray scattering of random metallocene-ethylene copolymers with different types and concentration of comonomer, Macromolecules 2001, 34:6959–6971.

[31] Alamo, R.G., VanderHart, D.L., Nyden, M.R., Mandelkern, L., morphological partitioning of ethylene defects in random propylene-ethylene copolymers, Macromolecules 2000, 33:6094–6105.

[32] Vander Hart, D.L., Perez, E. A carbon-13 NMR method for determining the partitioning of end groups and side branches between the crystalline and noncrystalline regions in polyethylene, Macromolecules 1986, 19:1902–1909.

SYNTHESIS OF NEW ELASTOMERS WITH CONTROLLED STRUCTURES BASED ON ALKYLENE OXIDES, GRAFTED BY ROMP

BOGDAN SPURCACIU[1], EMIL BUZDUGAN[1], CRISTIAN-ANDI NICOLAE[1], ILEANA DRAGUTAN[2], VALERIAN DRAGUTAN[2]*

[1]*National Institute of Research & Development for Chemistry and Petrochemistry (ICECHIM), 202 Spl. Independentei, Sect. 6, Bucharest, Romania*
[2]*Institute of Organic Chemistry of the Romanian Academy "C.D. Nenitescu"of the Romanian Academy, 202B Spl. Independentei, 060023 Bucharest, P.O. Box 35-108, Romania. *E-mail: vdragutan@yahoo.com*

Abstract: Poly(propylene oxide-*ran*-allyl glycidyl ether) (PPO-AGE) copolymers have been prepared using as initiating system an alkyl aluminum compound, controlled amounts of water and different organic compounds that act as cocatalysts, e.g. ethers, diols, phosphines, salicylic acid derivatives, and organozinc compounds. Among the investigated catalysts the most productive systems showed to be the ternary systems derived from triisobutylaluminum (TIBA) and water having $Zn(acac)_2$ as a third component. These copolymers have subsequently been grafted by ring-opening metathesis polymerization (ROMP) with cyclooctene in the presence of Grubbs first-generation ruthenium (Ru) catalyst to produce new comblike copolymers.

1. Introduction

Copolymerization is an important process providing access to new materials with tuneable physical, mechanical, and chemical properties, through adjustments to the ratio of individual components in the copolymer.[1] The established strategy to copolymers is a suitable combination of two or more mechanistically distinct polymerization processes in order to efficiently obtain a targeted product having optimized characteristics.[2] Polymerization reactions mostly applied in copolymer synthesis involve anionic,[3] cationic,[4] Ziegler–Natta,[5] metathesis polymerization (e.g. ROMP, ADMET),[6] group transfer,[7] and radical mechanisms (e.g. NMRP, ATRP).[8] These fundamental processes can be manipulated in precisely controlled ways to give either advanced polymer materials or well-characterized macromonomers with desired structures. When macromonomers arising from hydrophilic monomers are subsequently employed in a further polymerization step involving hydrocarbon monomers, amphiphilic copolymers are being created; the latter may organize into interesting supramolecular assemblies[9] and thereby have particular practical applications.

Y. İmamoğlu and V. Dragutan (eds.), Metathesis Chemistry: From Nanostructure Design to Synthesis of Advanced Materials, 347-353.

Owing mainly to the spectacular advance in well-defined metathesis-initiating systems,[10] ROMP has recently opened up enormous possibilities for commodity polymer synthesis. In this case ROMP behaves as a living process enabling synthesis of well-defined polymers with controlled molecular weights, polydispersities, and functionalities. By applying ROMP in tandem with one of the above-specified polymerization techniques, copolymers with special architectures and displaying a range of nanoscale morphologies can be accessed.[11–14]

In this paper we describe an efficient synthetic route to high molecular weight copolymers using a sequence of anionic ring-opening polymerization (ROP) of alkylene oxides and ruthenium (Ru)-catalyzed ring-opening metathesis polymerization (ROMP) of cycloolefins. In this protocol random copolymers obtained from propylene oxide (PO) and allyl glycidyl ether (AGE) are grafted by ROMP of cyclooctene at the pendant allyl units of the polyether backbone leading to comblike new copolymers.

Materials based on copolymers of alkylene oxides and modified by ROMP of cycloolefins possess valuable properties recommending them for special applications in the automotive industry (hoses, fittings, and complex assemblies), in the oil industry (drilling and oil processing), machine building, defence, aviation, and aeronautics.

2. Results and discussion

According to our approach, we conducted in a first reaction step the copolymerization of PO with AGE, in the presence of catalytic systems consisting of an alkyl aluminum (e.g. triisobutylaluminum [TIBA]), controlled amounts of water and different organic compounds that act as cocatalysts, e.g. ethers, diols, phosphines, salicylic acid derivatives, and organozinc compounds. Copolymers of type **1** having varying numbers of comonomer units in the chain have been obtained (Scheme 1).

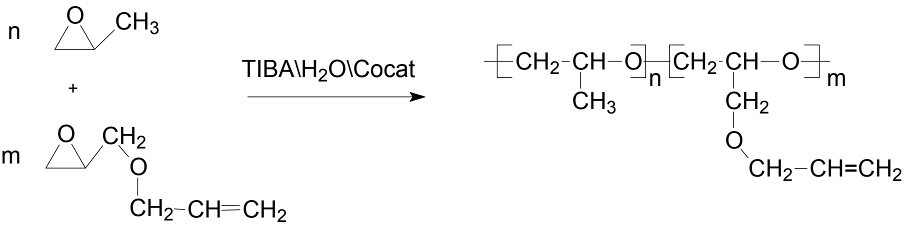

Scheme 1

Copolymerizations using an array of catalytic systems were carried out in toluene, at a monomer overall concentration of 100 g/800 mL solvent (Table 1). Comonomer ratio was PPO/AGE = 90/10 (wt/wt), with 30 mmol TIBA/100 g comonomers. Addition order of the catalytic components (TIBA/H_2O/Cocat) was essential to attain high yield and reproducibility.

Table 1. Catalytic systems (Catalyst 1–9) used in copolymerization reactions of propylene oxide with allyl glycidyl ether

Catalyst	Catalyst components	Molar ratio
Cat 1	TIBA:H_2O:Et_2O	1:0.5:0.25
Cat 2	TIBA:H_2O:MTBE	1:0.5:0.25
Cat 3	TIBA:H_2O:Dioxane	1:0.5:0.25
Cat 4	TIBA:H_2O:THF:1,4-Bu$(OH)_2$	1:0.5:0.2:0.2
Cat 5	TIBA:H_2O:DIPS	1:0.5:0.25
Cat 6	TIBA:H_2O:tri(di-*n*-butylamino)phosphine	1:0.5:0.25
Cat 7	TIBA:H_2O:trimorpholide of phosphorous acid	1:0.5:0.25
Cat 8	TIBA:H_2O:Zn$(acac)_2$	1:0.5:0.25
Cat 9	TIBA:H_2O:Zn$(DIPS)_2$	1:0.5:0.25

TIBA = triisobutylaluminum, MTBE = methyl *tert*-butyl ether, DIPS = diisopropyl salicylic acid

Among the investigated catalysts in PO-AGE copolymerization, the most productive systems, considering both copolymer yield and molecular mass, proved to be the ternary systems deriving from TIBA and water, and having as a third component Zn$(acac)_2$ (Cat 8) or Zn$(DIPS)_2$ (Cat 9). For molar ratios TIBA:H_2O:Zn = 1:0.5:0.25, the isolated yields were 94.5% and 83.7%, respectively, after 6 h reaction time (entry 8 and 9, Table 2).

Table 2. Poly(propylene oxide-*ran*-allyl glycidyl ether) copolymer (PPO-AGE) obtained with cat 1–9

Copolymer	Catalyst	Inherent visc. (dl/g)	Conversion (%)
PPOAGE 1	Cat 1	0.86	53.0
PPOAGE 2	Cat 2	0.79	27.2
PPOAGE 3	Cat 3	–	16.8
PPOAGE 4	Cat 4	1.09	48.5
PPOAGE 5	Cat 5	–	11.7
PPOAGE 6	Cat 6	1.17	62.4
PPOAGE 7	Cat 7	0.93	37.1
PPOAGE 8	Cat 8	1.21	94.5
PPOAGE 9	Cat 9	1.03	83.7

^{1}H NMR spectrum of poly(propylene oxide-*ran*-allyl glycidyl ether) (PPO-AGE) copolymer obtained with Cat 8 points out to a random copolymer with an AGE content of 10% (Figure 1).

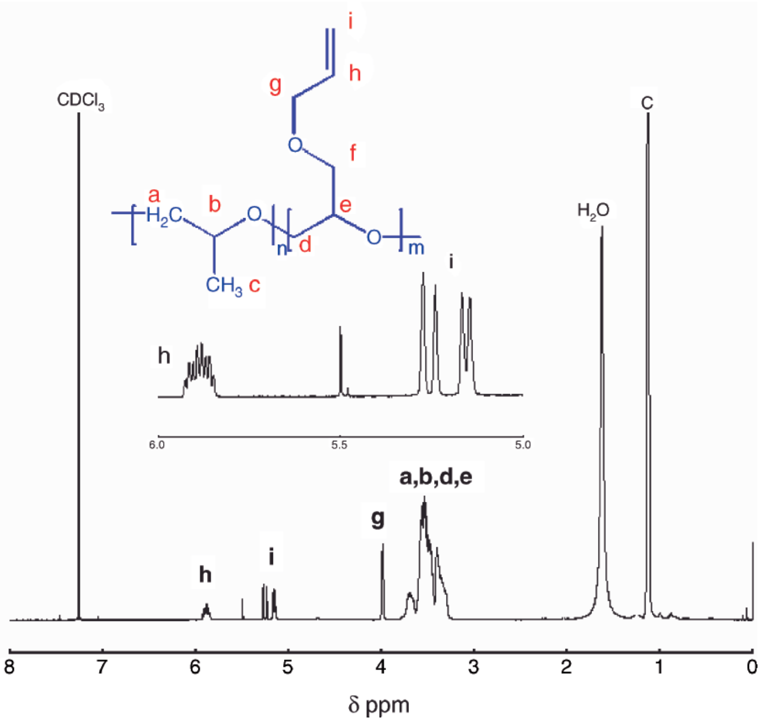

Figure 1. ^{1}H NMR spectrum of poly(propylene oxide-*ran*-allyl glycidyl ether) (10 mol % AGE).

Alkylene oxide copolymers of the elastomer type prepared according to our methodology exhibit low transition glass temperatures ($T_g < -35°C$) and diminished crystallinity resulting in increased physical–mechanical strength and resistance to various chemicals. These characteristic properties enable uses for parts of hoses and fittings functioning in agressive media, acids and bases, hydrocarbons, ozone, and flame.

In a second reaction step, modification of the pendant allylic groups of the PPO-AGE copolymer was achieved by ROMP with cyclooctene leading to graft copolymers (Scheme 2).

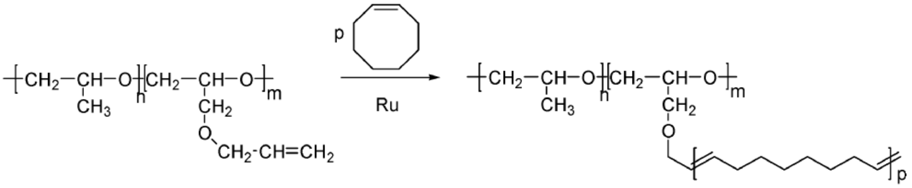

1 **2**

Scheme 2

The allyl unit of the PPO-AGE copolymer was used as a chain transfer agent in cyclooctene polymerization. The cyclooctene metathesis polymerization was carried out in a toluene–tetrahydrofuran (THF) mixture (5:1), using the benzylidene-bis(tricyclohexylphosphine)dichlororuthenium(II) catalyst (Grubbs I) (**3**). The following proportions between the reagents have been used: 0.8 g copolymer PPO-AGE (10% mol AGE) dissolved in 100 mL toluene and 10 mL THF, 0.1 g Ru catalyst and 20 mL cyclooctene. First, the Ru catalyst was added to the PPO-AGE copolymer solution, under inert atmosphere, and after 20 min cyclooctene has been added to start ROMP. Metathesis polymerization was completed within 22 h at 60°C, then the copolymer was precipitated with methanol. The resulted copolymer containing polyoctenamer grafts was characterized by ^{1}H NMR and GPC. ^{1}H NMR data evidenced that 40% of cyclooctene has been grafted on the binary PPO-AGE copolymer through a metathetic pathway while 60% homopolymerized to ungrafted polyoctenamer (Figure 2).

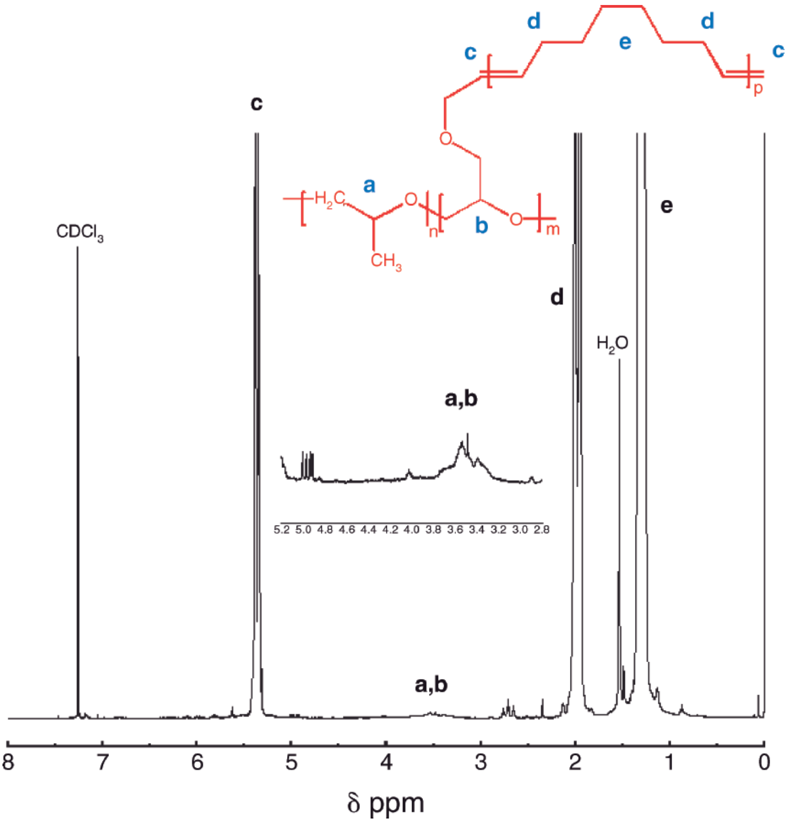

Figure 2. ^{1}H NMR spectrum of graft copolymer (propylene oxide-*ran*-allyl glycidyl ether)-cyclooctene.

Obviously, two distinct initiating and propagating Ru carbene species are responsible for the dual pathway by which ROMP of cyclooctene is proceeding. While initiation of the concurrently occurring process, cyclooctene homopolymerization, is promoted by the Ru–benzylidene **3**, grafting (through ROMP of cyclooctene) could be initiated by an immobilized Ru carbene **4**; the latter catalytically active species is generated by cross-metathesis of **3** with the pendant allyl group of the PPO-AGE **1** (Scheme 3).

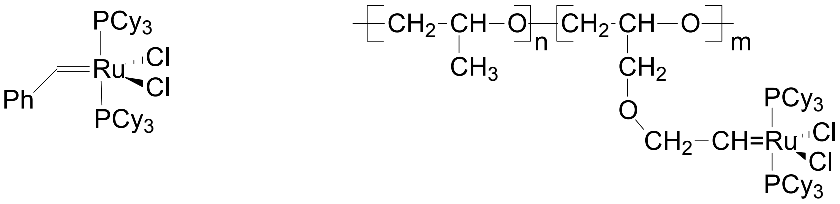

3 **4**

Scheme 3

In addition, the graft copolymer **2** may arise by competitive cross-metathesis of the PPO-AGE copolymer with the growing Ru-propagating species of the cyclooctene homopolymerization. The ratio between the two grafting processes depends essentially on the amount of Ru catalyst employed in this reaction.

Ongoing studies in our group focus on grafting other cycloolefins (norbornene, cyclododecene) onto the copolymer PPO-AGE by the ROMP approach. The unsaturated grafted block of polyalkenamer can be further hydrogenated using *p*-toluenesulfonylhydrazide as a mild hydrogenation agent to provide new products of wide utility.

3. Conclusions

In the present study PPO-AGE copolymers have been obtained using as initiators TIBA:H_2O and various cocatalysts, in a first step, and then grafted by ROMP with cyclooctene in the presence of Grubbs first-generation Ru catalyst, in a subsequent step. Future experiments will be directed at grafting other cycloolefins by ROMP onto PPO-AGE copolymer, and also at extending the same ROMP modification approach to copolymers prepared from epichlorohydrine–AGE and epichlorohydrine–PO–AGE.

References

[1] (a) Grubbs, R.H. (ed.), Handbook of Metathesis, Vol. 3, Wiley-VCH, Weinheim, 2003; (b) Dragutan, V., Streck, R., Catalytic Polymerization of Cycloolefins, Elsevier, Amsterdam, 2000.

[2] Khosravi, E., in: Grubbs, R.H. (ed.), Handbook of Metathesis, Vol. 3, Wiley-VCH, Weinheim, 2003, Chapter 3.3.

[3] Szwarc, M., Levy, M., Milkovich, R., J. Am. Chem. Soc. 1956, 78:2656.

[4] Matyjaszewski, K., Gaynor, S., Wang, J.-W., Macromolecules 1995, 28:2093.

[5] (a) Boor, J. Jr., Ziegler–Natta Catalysts and Polymerizations, Academic Press, New York, 1979; (b) Kaminsky, W., Bark, A., Dake, I., in: Keii, T., Soga, K. (eds), Catalytic Olefin Polymerization, Elsevier, Amsterdam, 1990, pp. 426–438.

[6] (a) Ivin, K.J., Mol, J.C., Olefin Metathesis and Metathesis Polymerization, Academic Press, London, 1987; (b) Dragutan, V., Balaban, A.T., Dimonie, M., Olefin Metathesis and Ring-Opening Polymerization of Cycloolefins, John Wiley, New York, 1985.

[7] (a) Webster, O.W., Sogah, D.Y., Group transfer and aldol group transfer polymerization, in: Comprehensive Polymer Science, Vol. 4, Pergamon Press, New York, 1988; (b) Webster, O.W., Sogah, D.Y., Recent advances in the controlled synthesis of acrylic polymers by group transfer polymerization, in: Fontanille, M., Guyot, A. (eds), Recent Advances in Mechanistic and Synthetic Aspects of Polymerization, D. Reidel Publishing Company, Dordrecht Holland, 1987, pp. 3–21.

[8] (a) Miura, Y., Sakai, Y., Taniguchi, I., Polymer 2003, 44:603; (b) Coca, S., Paik, H., Matyjaszewski, K., Macromolecules 1997, 30:6513.

[9] Miller, A.F., Richards, R.W., Macromolecules 2000, 33:7618.

[10] Grubbs, R.H. (ed.), Handbook of Metathesis, Vol. 1, Wiley-VCH, Weinheim, 2003.

[11] (a) Feast, W.J., Gibson, V.C., Johnson, A.F., Khosravi, E., Moshin, M.A., Polymer 1994, 35:3542; (b) Feast, W.J., Gibson, V.C., Johnson, A.F., Khosravi, E., Moshin, M.A., J. Mol. Catal. A. Chem. 1997, 115:37.

[12] Miller, A.F., Richards, R.W., Webster, J.R.P., Macromolecules 1997, 33:7618.

[13] (a) Herouguez, V., Gnanou, Y., Fontanille, M., Macromolecules 1996, 29:4459; (b) Herouguez, V., Gnanou, Y., Fontanille, M., Macromolecules 1997, 30:4791.

[14] Radano, C.P., Scherman, O.A., Stingelin-Stutzmann, N., Müller, C., Breiby, D.W., Smith, P., Janssen, R.A.J., Meijer, E.W., J. Am. Chem. Soc. 2005, 127:12502.

INVESTIGATION OF THE MICROSTRUCTURE OF METAL CATALYZED CYCLOPENTENE CO-NORBORNENE POLYMERS BY SPECTRAL METHODS

SEVIL ÇETİNKAYA,*[1] SOLMAZ KARABULUT,[2]
YAVUZ İMAMOĞLU[2]

*[1]*Kırıkkale University, Faculty of Science, Department of Chemistry, 71450 Kırıkkale, Turkey*
[2]*Hacettepe University, Department of Chemistry, 06800 Beytepe, Ankara, Turkey*

Abstract: For the first time, cyclopentene (CPE) has been copolymerized with the strained cycloolefin norbornene (NBE) using catalytic amounts of the electrochemically prepared metathesis catalyst. The microstructure of polymers was determined by ^{1}H NMR and ^{13}C NMR spectroscopy. The polymers were also characterized by differential scanning calorimetry and gel permeation chromatography (GPC) techniques.

1. Introduction

The recent advances in the copolymerization reactions are presented in terms of catalyst synthesis, catalytic activity, and polymer characteristics. A large variety of copolymers is synthesized by catalysis with organometallic complexes [1]. These catalysts have been divided into ill- and well-defined categories [2]. The development of new generation highly active and long lived metal–alkylidene initiators opens new possibilities in olefin metathesis and and its application to polymer synthesis. There are relatively few quantitative studies of copolymerization reaction of cyclopentene (CPE) with norbornene (NBE) initiated by ill- and well-defined metathesis catalysts [3–6]. Recently we reported a number of polymers synthesized using WCl_6-e-Al-CH_2Cl_2 catalyst system [7–10]. In this paper we describe the synthesis of ring-opening metathesis polymerization (ROMP) of CPE with NBE with the same catalyst.

2. Experimental

WCl_6 was purified by sublimation under nitrogen at about 200°C and kept under nitrogen atmosphere. NBE and CPE were supplied from Aldrich and used as received. Dichloromethane (Merck) was washed with concentrated H_2SO_4, water, an aqueous solution of Na_2CO_3 (5%, wt) and water again. It was dried over anhydrous $CaCl_2$ and then distilled over P_2O_5 under nitrogen. Tetrahydrofuran (THF) and methanol were supplied from Merck and used as received.

Y. İmamoğlu and V. Dragutan (eds.), Metathesis Chemistry: From Nanostructure Design to Synthesis of Advanced Materials, 355-360.

The catalysts were prepared according to previously described procedures [7–10]. Reactions were carried out in a flask equipped with a nitrogen gas inlet and a magnetic stirrer. A typical copolymerization reaction as follows: in copolymerization reactions, the mixture of equimolar amount of CPE and NBE (1.6 mmol) was used as a monomer solution. Then 1 mL of the catalytic solution was added to reactor. The mixture was kept at room temperature under vigorous stirring. The reaction was quenched by methanol addition after 24 h. The polymer was further purified to remove the catalytic residues by dissolving it in THF and reprecipitating it with methanol and drying it overnight in a vacuum at room temperature. Polymerization yield in percentage was calculated as the weight fraction of converted monomer over the total monomer.

^{1}H NMR and ^{13}C NMR spectra of the polymers were recorded with a Bruker GmbH 400 MHz high-performance digital Fourier transform–nuclear magnetic resonance (FT–NMR) spectrometer using $CDCl_3$ as solvent and tetramethylsilane as the reference. Average molecular weight (M_w) was determined by gel permeation chromatography (GPC). GPC analyses were performed with a Shimadzu LC–10ADVP liquid chromatograph equipped with a Shimadzu SPD–10AVP ultraviolet (UV) detector, relative to polystyrene standards. Samples were prepared in THF (%1) as eluent and passed through a μ-styragel column. A constant flow rate of 1 mL/min was maintained at 25°C. Glass transition temperature was measured by Shimadzu DSC-60 (10°C/min).

3. Results and discussion

In this work, copolymerization reaction of CPE with NBE was examined. Metathesis reaction of CPE with NBE resulted in the formation of co-CPE-NBE polymers (Scheme 1). A summary of the polymerization results is shown in Table 1.

The result obtained by GPC analysis showed that the molecular weight of CPE co-NBE polymer was 23,300. The CPE co-NBE polymer showed only one single glass transition at 9.2°C and this value is in between the T_g values of the two monomers [11]. One single T_g confirmed that no phase separated blocks of the monomers were built.

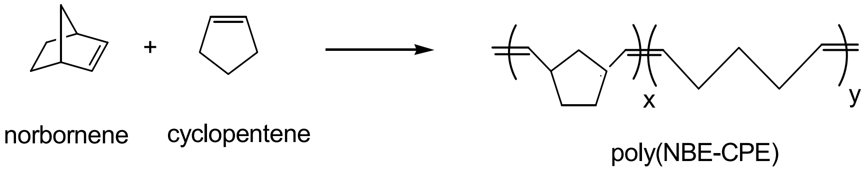

Scheme 1

Table 1. Characterization of copolymer synthesized by electrochemically produced W-based catalyst (catalyst/monomer$_{CPE}$/monomer$_{NBE}$ = 1:40:40)

Polymer	**Properties**	**Results**
CPE:NBE (1:1)	σ_c	0.36 (M_1M_1); 0.55 (M_2M_2)
	PDI	2.1
	T_g(ºC)	9.15
	M_w	23300
	Yield (%)	74

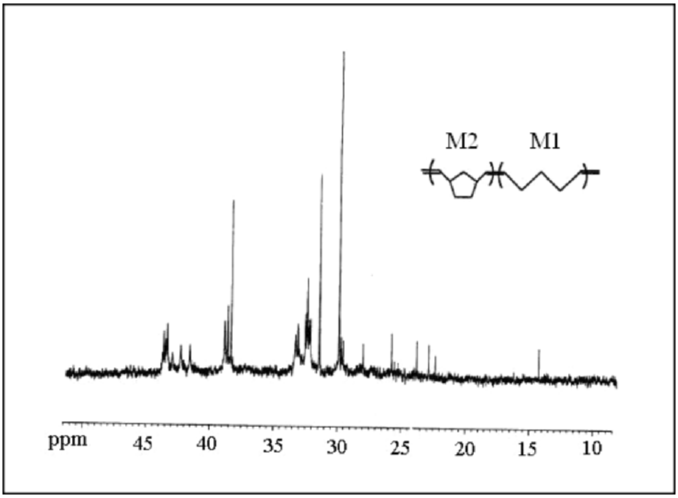

Figure 1. Olefinic region of the ^{13}C NMR spectrum of CPE co-NBE polymer.

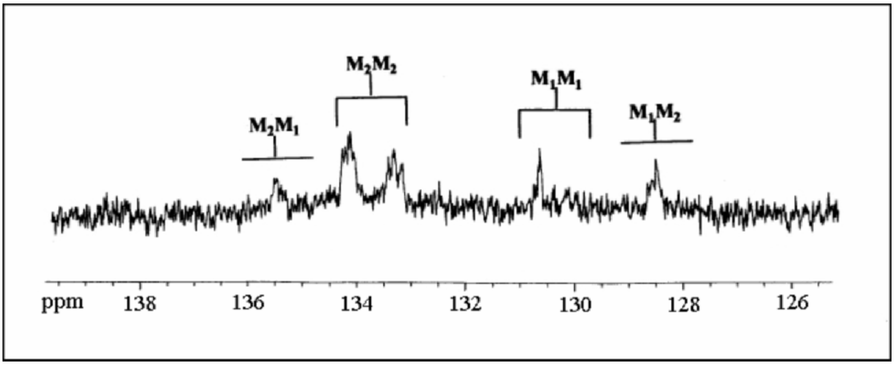

Figure 2. ^{13}C NMR spectrum of the nonolefinic carbons in CPE co-NBE polymer.

The ^{13}C NMR spectrum of polymer was recorded in $CDCl_3$ and assigned by comparison with literature data [1]. The ^{13}C NMR spectrum of the polymer obtained with electrochemically reduced tungsten-based active species is shown in Figures 1 and 2.

In copolymers of CPE (M_1) and NBE (M_2), the compositional dyads can be M_1M_1, M_1M_2, M_2M_1, or M_2M_2.

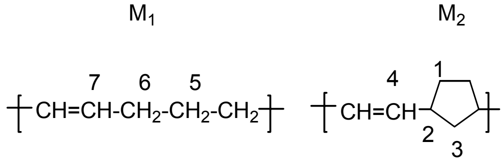

In the olefinic region of the copolymer of CPE and NBE, M_1M_2 and M_2M_1 heterodyads occured as well as M_1M_1 and M_2M_2 homodyads. All the resonances in the homodyads, M_1M_1 and M_2M_2 are the same as those assigned previously in detail for homopolymers [11]. The peak positions and assignments for CPE co-NBE polymers are listed in Tables 2 and 3. The *cis* contents of M_2M_2 and that of M_1M_1 in the copolymer are 55 % and 36 %, respectively. The mole fraction of the 1-pentenylene units in copolymer, F_1, was calculated from the area of the two upfield groups of peaks divided by total area as 0.30.

Table 2. Assignment of C^4 and C^7 lines in the ^{13}C NMR spectrum of CPE co-NBE polymer

Designation and assignment	**Peak position (ppm)**
4c/t (M_2M_1)	135.61
4c (M_2M_2)	134.22
4t (M_2M_2)	133.42
7c (M_1M_1)	130.20
7t (M_1M_1)	130.74
7c/t (M_1M_2)	128.60

Figure 3 shows the ^1H NMR spectrum of the obtained CPE co-NBE polymer. For CPE co-NBE polymer, signals were seen in the alkyl region as well as in the olefinic regions. ^1H NMR spectrum of CPE co- NBE polymer obtained by electrochemically produced catalyst is consistent with the ^1H NMR spectra of the copolymers in literature [12].

The Fourier transform infrared (FTIR) spectrum of the copolymer has the absorbency peaks corresponding to olefinic and aliphatic C–H vibrations as well as peaks for C=C vibrations at 1654 cm^{-1}. Content of the *cis* and *trans* products in the polymers were also estimated from the intensities of the $=CH_{trans}$

Table 3. Assignment of C^1, C^2, C^3, C^5, and C^6 lines in the ^{13}C NMR spectrum of CPE co-NBE polymer (M may be M_1 or M_2)

Designation and assignment	**Peak position (ppm)**
2tc (M_2M_2M)	43.82
2tt (M_2M_2M)	43.53
2cc (M_2M_2M)	39.05
2ct (M_2M_2M)	38.81
2tt (M_1M_2M)	43.67
2tc (M_1M_2M)	44.00
2cc (M_1M_2M)	38.54
2ct (M_1M_2M)	38.41
3 ($M_2M_2M_2$)	43.14
3 ($M_1M_2M_2$),($M_2M_2M_2$) or ($M_1M_2M_1$)	42.48
3 ($M_1M_2M_2$),($M_2M_2M_2$) or ($M_1M_2M_1$)	41.74
1cc (M_2M_2)	33.49
1ct (M_2M_2)	33.31
1cc (M_1M_2)	33.27
1ct (M_1M_2)	33.00
1tc (M_2M_2/M_1M_2)	32.75
1tt (M_2M_2/M_1M_2)	32.59
6tc (MM_1M_1/ MM_1M_2)	32.46
6tt (MM_1M_1/ MM_1M_2)	32.33
5cc ($M_1M_1M_1$)	30.10
5tc ($M_1M_1M_2$)	
5ct/tc ($M_2M_1M_2$)	
5ct/tc ($M_1M_1M_1$)	29.90
5ct ($M_1M_1M_2$)	
5tt ($M_1M_1M_1$/$M_1M_1M_2$/$M_2M_1M_2$)	29.77
6cc (MM_1M_2)	28.21

(966 cm^{-1}) and $=CH_{cis}$ (723 cm^{-1}) bands in the FTIR spectra. The relative intensities of the $=CH_{trans}$ at 966 cm^{-1} and the $=CH_{cis}$ at 723 cm^{-1} are nearly same for co-CPE–NBE polymer. ^1H NMR and FTIR analyses indicate that the unsaturation in the polymers is retained, which is an indication for the ring-opening metathesis mechanism [13].

5. Conclusion

In conclusion we have demonstrated that WCl_6-based electrochemically reduced catalyst is capable of producing copolymer from CPE with NBE. We documented a detailed microstructure analysis of the copolymer obtained by this catalyst.

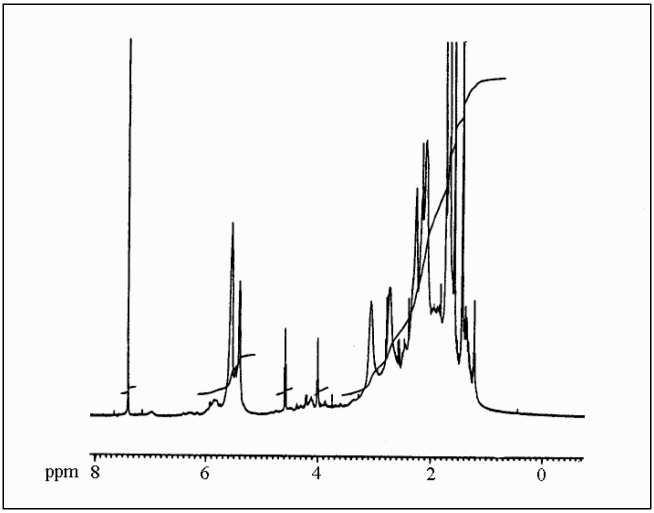

Figure 3. ^{1}H NMR spectrum of cyclopentene co-norbornene polymer.

References

[1] Ivin, K.J., Mol, J.C. (1997) Olefin Metathesis and Metathesis Polymerization, Academic Press, London.

[2] Claveria, J.P., Soula, R. (2003) Progg.Polym. Sci. 28, 619–662.

[3] Ivin, K.J., Lapienis, G., Rooney, J.J. (1982) Makromol. Chem. 193, 9.

[4] Ebrahimi, V.A., Carvill, A.G., Hamilton, J.G., Rooney, J.J., Tuffy, C. (1997) J. Mol. Catal. A.: Chem. 115, 85.

[5] Al Samak, B., Ebrahimi, V.A., Corry, D.G., Hamilton, J.G., Rigby, S., Rooney, J.J., Thompson, J.M. (2000) J. Mol. Catal. A: Chem. 160, 13.

[6] Ebrahimi, V.A., Rooney, J.J. (2004) J. Mol. Catal. A: Chem. 208, 115.

[7] Karabulut, S., Çetinkaya, S., Düz, B., İmamoğlu, Y. (2004) Appl. Organometal. Chem. 18, 375–379.

[8] Çetinkaya, S., Karabulut, S., Düz, B., İmamoğlu, Y. (2005) Appl. Organometal. Chem. 19, 347–351.

[9] Karabulut, S., Çetinkaya, S., İmamoğlu, Y. (2005) Appl. Organometal. Chem. 19, 997–1001.

[10] Çetinkaya, S., Karabulut, S., İmamoğlu, Y. (2005) Eur. Polym. J. 41, 467–474.

[11] Dounis, P., Feast, W.J., Kenwright, A.M. (1995) Polymer 14, 2787.

[12] Manivannan, R., Sundararajan, G., Kaminsky, W. (2000) J. Mol. Catal. 160, 85–95.

[13] Beerens, H., Wang, W., Verdonck, L., Verpoort, F. (2002) J. Mol. Catal. A: Chem. 3661, 1–7.

ADMET POLYMERIZATION ACTIVITIES OF ELECTROCHEMICALLY REDUCED W-BASED ACTIVE SPECIES FOR Ge- AND Sn-CONTAINING DIENES

SOLMAZ KARABULUT*, CEMIL AYDOGDU, BÜLENT DÜZ,
YAVUZ İMAMOĞLU

*Hacettepe University, Faculty of Science, Department of Chemistry, 06800 Beytepe, Ankara, Turkey. *E-mail: solmazk@hacettepe.edu.tr*

1. Introduction

In the last 20 years metal atom-containing polymers have become important classes of polymers [1]. Properties like high thermic stability, electric, and photo conductometry make them very interesting for producing films, fibers, and coating [2]. Many of these compounds can be synthesized by conventional methods [3]. For producing metal-containing polymers anionic, cationic, and radicalic polymerizations were used [4–6]. Metal-containing polymers were also synthesized via acyclic diene metathesis (ADMET) polymerization that is facilitated by Schrock's molybdenum alkylidene, or Grubbs' ruthenium carbene catalyst [7–9]. In 1979, Gilet and coworkers succeeded in synthesizing metathetically active species from electrochemical reduction of WCl_6 and $MoCl_5$ [10,11]. In the light of these works, we have showed that electrochemically generated tungsten-based active species (WCl_6-e^-–Al–CH_2Cl_2) catalyzes various metathesis-related reactions [12–16].

Indeed, we have recently observed high catalytic performance of WCl_6–e^-–Al–CH_2Cl_2 system in ADMET polymerization of metal-containing dienes [17,18]. In continuation of this work, we report in the present study the influence of reaction conditions on the catalytic performance of electrochemically generated tungsten-based active species for ADMET polymerization of germanium (Ge)- and tin (Sn)-containing monomers.

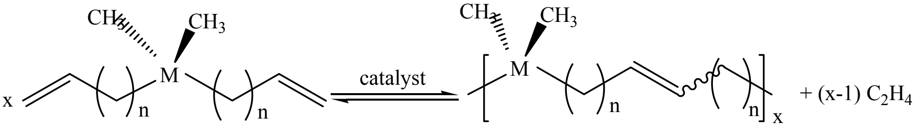

M= Ge **(1)**

M= Sn **(2)** n =3 x= 1,2,3,......

Y. İmamoğlu and V. Dragutan (eds.), Metathesis Chemistry: From Nanostructure Design to Synthesis of Advanced Materials, 361-365.

2. Results and discussion

A summary of ADMET polymerization of Ge- and Sn- containing polymer **(1)** and **(2)** in terms of polymerization conditions, polymer yield, and molecular weight is given in Table 1. It shows that the electrochemically reduced catalyst is an active system toward ADMET polymerization because quantitative yield for polymer **(1)** and **(2)** is 68% and 92% depending on the monomer to catalyst ratio and reaction time. The slightly higher *trans* polymers were obtained by this catalyst system with high yields in a short periods.

Table 1. A comparison of ADMET polymerization of Ge- and Sn-containing monomers by WCl_6–e$^-$–Al–CH_2Cl_2 catalyst systems

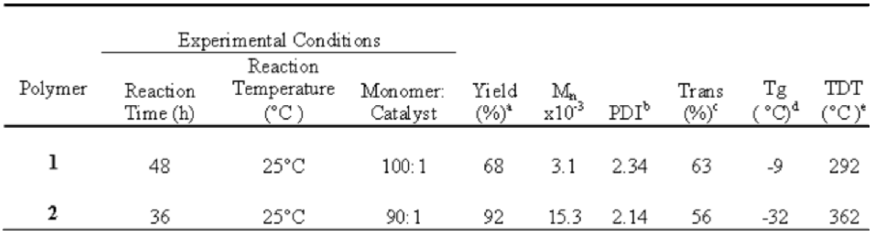

Polymer	Experimental Conditions								
	Reaction Time (h)	Reaction Temperature (°C)	Monomer: Catalyst	Yield (%)^a	M_n x10^{-3}	PDI^b	Trans (%)^c	Tg (°C)^d	TDT (°C)^e
1	48	25°C	100:1	68	3.1	2.34	63	-9	292
2	36	25°C	90:1	92	15.3	2.14	56	-32	362

[a]Determined by gravimetrically
[b]Determined by GPC, relative to polystyrene standard
[c]Calculated from ^{13}C NMR spectra
[d]Determined by DSC in N_2 atmosphere (heating rate: 10°C/min)
[e]Determined by TGA in Ar atmosphere (10% weight loss temperature)

The activity of a given catalyst system will be determined by both the concentration of the active species and the reaction period. For this aim, to optimize the reaction conditions, several experiments were performed by using different catalyst ratios and reaction time.

2.1 Effect of monomer concentration

In this part of the study, the effect of monomer concentration on the ADMET polymerization of Ge- and Sn-containing monomers was determined using these ranged from 20:1 to 150:1. Different amount of monomer was mixed with 2×10^{-2} mmol of catalyst. Polymerization reactions were carried out at room temperature under nitrogen atmosphere, for 36–48 h. Figure 1 shows the effect of monomer concentration on the yields of polymers **(1)** and **(2)**.

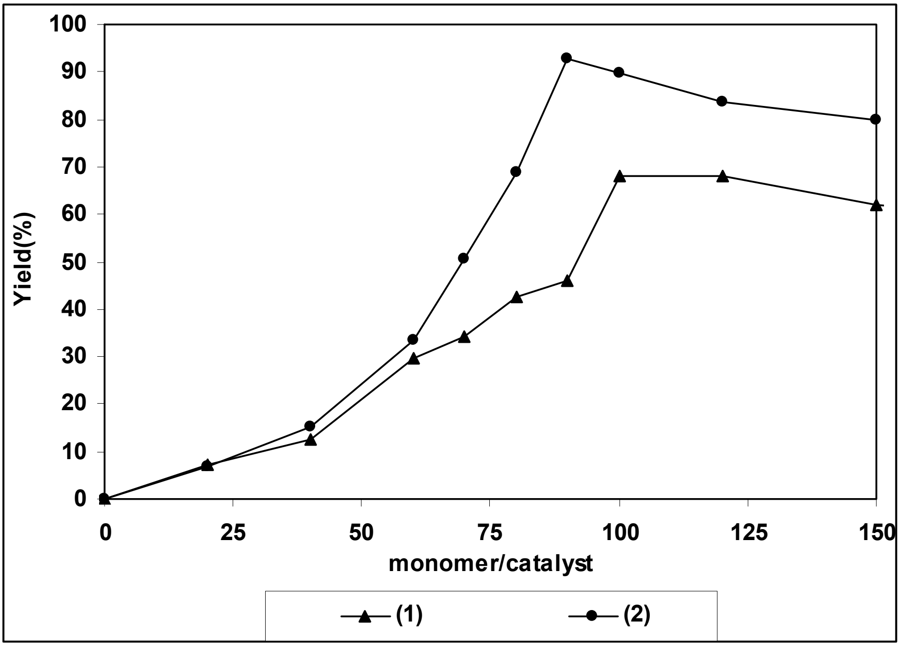

Figure 1. The effect of monomer concentration on the yield of the polymers **(1)** and **(2)** (reaction time: 36–48 h).

As the monomer to catalyst ratio was increased, yield of the polymer also increased reaching to a maximum value which is around 100:1 polymer **(1)** or 90:1 polymer **(2)**, and further increase of the ratio caused a decrease in the yield of the polymer. A maximum yield of 68% and 92% for polymer **(1)** and **(2)** was obtained. At high monomer concentrations deactivation of the active catalyst may occur which results in low yield of polymer.

2.2 Effect of reaction time

This group of experiments were performed for different reaction times (180–3200 min). The monomer to catalyst ratio was kept at 100:1 for polymer **(1)** or 90:1 for polymer **(2)**, and the reaction was quenched by the addition of methanol after a certain time from the start of reaction. Figure 2 shows the influences of different reaction times on the amount of polymers **(1)** and **(2)**. Polymerization yield first increased with time and almost reached a plateau value around 36–48 h.

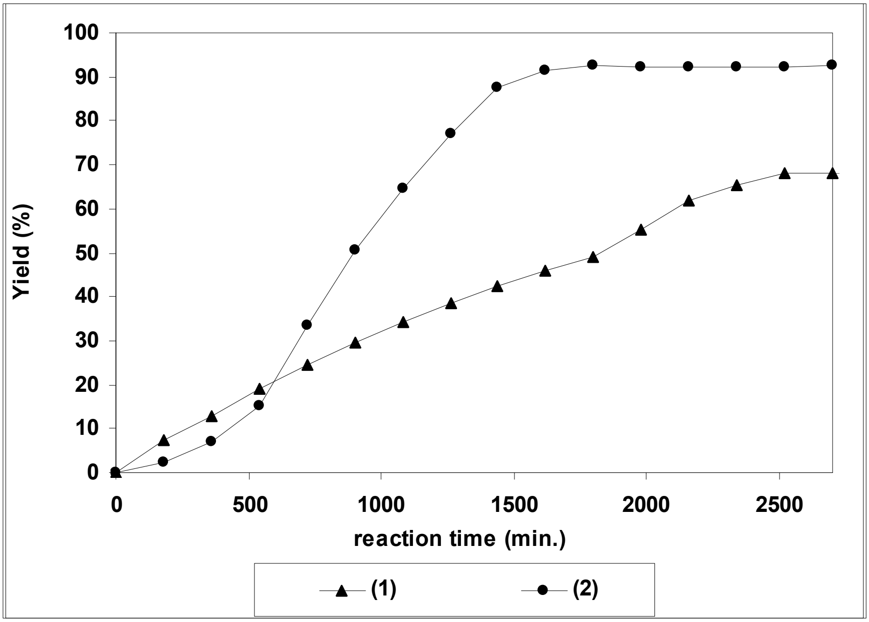

Figure 2. The effect of reaction time on the yield of the polymers **(1)** and **(2)** (monomer to catalyst ratio is 100:1 and 90:1).

3. Conclusion

The ADMET polymerization yield of Ge- **(1)** and Sn **(2)**-containing polymers reaches a maximum at a total monomer to catalyst ratio of about 100:1 and 90:1, respectively. Polymerization reaction completed at around 36–48 h.

Acknowledgment

This work financially supported by the Scientific and Technological Research Council of Turkey (project no: 104T344) and Hacettepe University Research Fund (project no: 04A601014).

References

[1] Sheats, J.E., Carraher, C.E., Pittman, C.U., Metal Containing Polymer Systems, Plenum Press, New York, 1985, p. 1.
[2] Bill, J., Aldringer, F., Adv. Mater. 1995, 7:775.
[3] Neuse, E.W., Adv. Macromol. Chem. 1968, 1:1.
[4] Hayashi, T., Uchimaru, Y., Reddy, N.P., Tanaka, M., Chem. Lett. 1992, 647.

[5] Brefort, J.L., Corriu, R.J.P., Gerin, C., Henner, B.J.L., J. Organometal. Chem. 1994, 133:464.

[6] Shoda, S., Iwata, S., Yajima, K., Yagi, K., Ohnishi, Y., Kobayashi, S., Tetrahedron 1997, 53:15281.

[7] Smith, D.W. Jr., Wagener, K.B., Macromolecules 1991, 24:6073.

[8] Wolfe, P.S., Gomez, F.J., Wagener, K.B., Macromolecules 1997, 30:14.

[9] Gomez, F.J., Wagener, K.B., J. Organomet. Chem. 1999, 59:2271.

[10] Gilet, M., Mortreux, A., Nicole, J., Petit, F., JCS Chem. Commun. 1979, 521.

[11] Gilet, M., Mortreux, A., Folest, J.C., Petit, F., J. Am. Chem. Soc. 1983, 105:3876.

[12] Düz, B., Pekmez, K., İmamoğlu, Y., Süzer, Ş., Yıldız, A., J. Organometal. Chem. 2003, 77:684.

[13] Karabulut, S., Çetinkaya, S., Düz, B., İmamoğlu, Y., Appl. Organomet. Chem. 2004, 18:375.

[14] Çetinkaya, S., Karabulut, S., İmamoğlu, Y., Appl. Organomet. Chem. 2005, 19:997.

[15] Çetinkaya, S., Karabulut, S., İmamoğlu, Y., Eur. Pol. J. 2005, 41:467.

[16] Dereli, O., Düz, B., Zümreoğlu, B.K., İmamoğlu, Y., Appl. Organomet. Chem. 2003, 17:23.

[17] Karabulut, S., Aydogdu, C., Düz, B., İmamoğlu, Y., J. Mol. Catal. 2006, 254:186.

[18] Karabulut, S., Aydogdu, C., Düz, B., İmamoğlu, Y., J. Inorg. Organomet. Polym. Mat. 2006, 16:115.

A STUDY ON THE REACTIVITY OF WCl_6–e^-–Al–CH_2Cl_2 WITH THE SILICON-CONTAINING DIENES

SOLMAZ KARABULUT* CEMIL AYDOGDU, BÜLENT DÜZ, YAVUZ İMAMOĞLU

*Hacettepe University, Faculty of Science, Department of Chemistry, 06800 Beytepe, Ankara, Turkey. *E-mail:solmazk@hacettepe.edu.tr*

1. Introduction

Although until the late 1980s very little information on effective metathesis conversion of organosilicon compounds had been reported, the use of molybdenum (Schrock) catalyst and ruthenium (Grubbs) carbene complexes as catalysts tolerating functional groups in substrates, have opened new synthetic opportunities in organosilicon chemistry. Silicon containing dienes undergo two types of metathetical transformation.

- Intramolecular ring-closing metathesis (RCM) leading to cyclic compounds [1,2]
- Intermolecular acyclic diene metathesis (ADMET) polymerization to yield linear polymers [3–6]

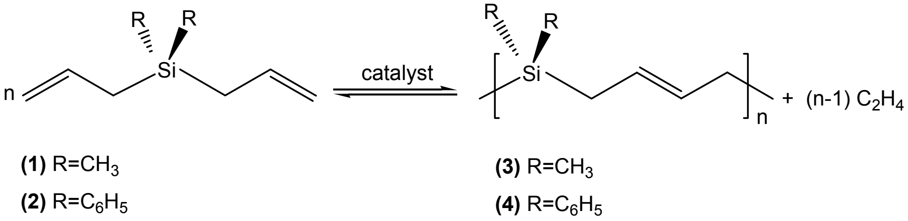

The goal of this study was to examine the effects of varying the pendant group on a common carbosilane backbone of Si-containing polymers that are obtained by ADMET in the presence of electrochemically reduced tungsten-based active species (WCl_6–e^-–Al–CH_2Cl_2).

The activity of a particular catalyst system is dependent on a number of factors including [7];

1. The proportions of the components
2. Pretreatment procedures, especially for catalysts supported on Al_2O_3 or SiO_2

Y. İmamoğlu and V. Dragutan (eds.), Metathesis Chemistry: From Nanostructure Design to Synthesis of Advanced Materials, 367-371.

3. The order in which the components are mixed
4. In the case where the olefin is added last, the period of incubation before adding the olefin

2. Experimental

WCl_6 was purified by sublimation from the more volatile impurities (WO_2Cl_2 and $WClO_4$) under nitrogen at about 200°C and kept under nitrogen atmosphere. Methylene chloride was washed with concentrated sulfuric acid, then with aqueous carbonate solution and water, followed by drying over calcium chloride. It was then distilled over P_2O_5 under nitrogen, kept under nitrogen. $CHCl_3$ and MeOH were supplied from Merck and used as received.

The electrochemical instrumentation consisted of an EGG–PAR Model 273 coupled with a PAR Model Universal Programmer. The measurements were carried out under a nitrogen atmosphere in a three-electrode cell having a jacket through which water from a constant-temperature bath was circulated. Exhaustive controlled potential experiments were carried out in an undivided cell with a macro working Pt foil electrode (2.0 cm^2) and an Al foil (2.0 cm^2) counter electrode. The reference electrode consisted of AgCl coated on an Ag wire in CH_2Cl_2/0.1M $TBABF_4$ that was also separated from the electrolysis solution by a sintered glass disc. Electrolysis was carried out without supporting electrolyte due to its deleterious effect on the catalyst system.

All manipulations involving polymerization reactions were carried out under pure and dry nitrogen. WCl_6 (0.2 g, 0.50 mmol) was introduced into the electrochemical cell containing CH_2Cl_2 (25 ml) and a red solution was observed. The electrodes were introduced into the deep red solution. Reductive electrolysis was done at +0.9V and electrolysis conducted for 3 h in reduced. The color of the solution darkened progressively. Aliquots from this catalytic solution were used in polymerization reactions.

All polymerization reactions were initiated in the bulk, at room temperature and under nitrogen atmosphere. A typical reaction was as follows: 1 mL of catalytic solution was taken with an automatic pipette from the cell and added to a certain amount of monomer in a Schlenk tube containing a magnetic stir bar. A rapid gelation was observed and stirring was continued until prevented by the viscosity increase. The reaction was quenched by methanol addition after several times to obtain polymers. The polymers formed were washed with methanol, dissolved in $CHCl_3$ and reprecipitated with methanol to remove the catalytic residues, dried, and weighed. The conversion of the polymerizations was determined gravimetrically.

3. Results and discussion

Polymerization data are summarized in Table 1. These results indicate that ADMET polymerization of monomer **(1)** and **(2)** using electrochemically reduced WCl_6-based catalyst proceeded with good selectivity to the silicon containing polymer **(3)** and **(4)** [8]. The GPC analysis of these polymers showed M_n values of 9100 polymer **(3)** and 4500 polymer **(4)**. The polydispersity indexes are 2.28 and 2.05, respectively, which well fit the step-growth mechanism of the ADMET polymerization.

Table 1. Comparison of ADMET polymerization of Si-containing monomers by WCl_6–e−–Al–CH_2Cl_2 catalyst systems

Polymer	Experimental Conditions			Yield (%)[a]	M_n $x10^{-3}$	PDI[b]	Trans (%)[c]	Tg (°C)[d]	TDT (°C)[e]
	Reaction Time (h)	Reaction Temperature (°C)	Monomer: Catalyst						
3	48	25	120:1	78	9.1	2.28	61	-48	290
4	51	25	120:1	71	4.5	2.05	60	16	315

[a] Determined by gravimetrically
[b] Determined by GPC, relative to polystyrene standard
[c] Calculated from ^{13}C NMR spectra
[d] Determined by DSC in N_2 atmosphere(heating rate: 10°C/min.)
[e] Determined by TGA in N_2 atmosphere (10 % weight loss temperature)

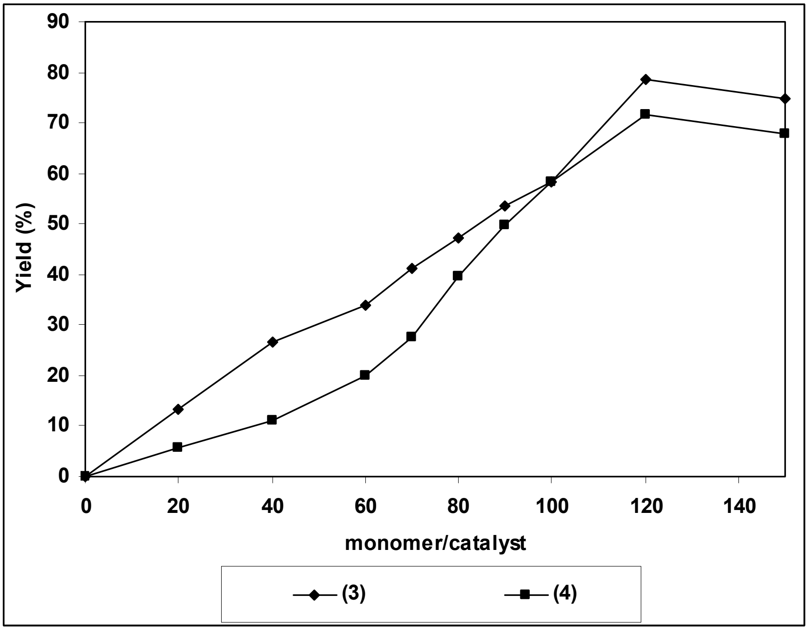

Figure 1. The effect of monomer concentration on the yield of the polymer **(3)** and **(4)** (reaction time: 48 h).

3.1 Effect of monomer concentration

A set of experiments were carried out in order to determine the optimum experimental conditions (monomer/catalyst ratio and polymerization time). Figure 1 shows the effect of monomer concentration on the yields of silicon containing polymers **(3)** and **(4)** synthesized by electrochemically produced tungsten-based catalyst. As the monomer/catalyst ratio was increased from 20:1 to 150:1, yield of the polymer also increased and reached a maximum yield at a monomer/catalyst ratio of about 120, and then decreases.

3.2 Effect of reaction time

Figure 2 displays the influence of reaction time on the polymerization yield for ADMET polymerization of monomer **(3)** and **(4)**. As monomer/catalyst ratio was 120:1, reaction was stopped by the addition of methanol after a certain time from the start of the reaction. Polymer yield increased with time and two distinct periods can be observed in the polymerization process. In the first period, a rapid increase with time is observed. In the second period, the polymer yield increased very slightly and tended to a constant value (at about 48 h reaction time) as a consequence of a significant decrease of the polymerization rate.

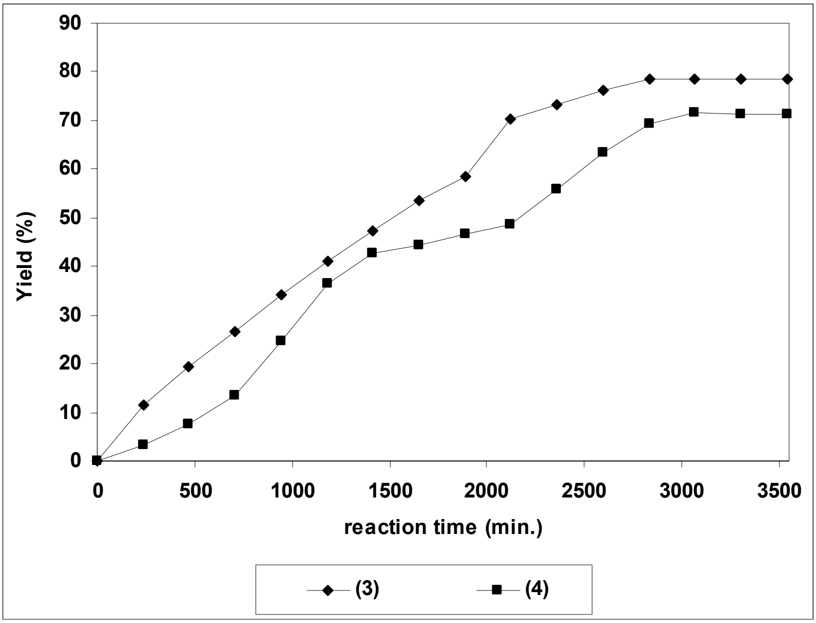

Figure 2. The effect of reaction time on the yield of the polymer **(3)** and **(4)** (monomer: catalyst ratio 120:1).

4. Conclusion

The optimum conditions for ADMET polymerization of silicon contaning dienes **(3)** and **(4)** are molar ratio of monomer/catalyst: 120:1 and about 48 h reaction time.

Acknowledgment

We thank the Scientific and Technological Research Council of Turkey (TUBITAK project no: 104T344) and Hacettepe University Research Fund.

References

[1] Marciniec, B., Coordin. Chem. Rev. 2005, 249(21–22):2374–2390.
[2] Pietraszuk, C., Marciniec, B., Rogalski, S., Fischer, H., J. Mol. Catal. A: Chem. 2005, 240(1–2):67–71.
[3] Smith, D.W., Jr., Wagener, K.B., Macromolecules 1991, 24:6073..
[4] Smith, D.W., Jr., Wagener, K.B., Macromolecules 1993, 26:1633.
[5] Zhang, X., Zhou, Q., Weber, W.P., Horvath, R.F., Chan, T.H., Manuel, G., Macromolecules 1988, 21:1563.
[6] Park, Y.T., Manuel, G., Weber, W.P., Macromolecules 1990, 23:1911.
[7] Ivin, K.J., Mol, J.C., Olefin Metathesis and Metathesis Polymerization, Academic Press, London, 1997.
[8] Karabulut, S., Aydogdu, C., Düz, B., İmamoğlu, Y., J. Inorg. Organomet. Polym. Mat., (in press).

PART IV. ADVANCED MATERIALS VIA METATHESIS AND RELATED CHEMISTRY

CATALYTIC CYCLOISOMERIZATION OF ENYNES INVOLVING VARIOUS ACTIVATION PROCESSES

CHRISTIAN BRUNEAU

CNRS-Université de Rennes1, Sciences Chimiques de Rennes, Catalyse et Organométalliques, Campus de Beaulieu, avenue du général Leclerc, 35042 Rennes Cedex, France; E-mail: christian.bruneau@univ-rennes1.fr

Abstract: The cycloisomerization of enynes can be performed with a variety of catalytic systems which operate according to various types of activation process. Metal catalysts showing different activation abilities can promote as the first step either oxidative coupling, triple bond insertion into metal-hydride bond, allylic activation, electrophilic activation, metal–vinylidene formation, and [2+2]-cycloaddition (metathesis). Depending on the nature of the enyne and the catalytic system, all these processes lead to a variety of cyclic compounds.

Keywords: enyne, cycloisomerization, metal catalysts

1. Introduction

Functionalized cyclic compounds are very important compounds because they are often part of the basic skeleton of useful biologically active products. Straightforward synthetic methods are therefore of great interest and many strategies focusing on efficiency and stereoselectivity have been proposed. Metal-catalyzed cycloisomerization represents a very interesting transformation as it proceeds with atom economy. In this respect, linear enynes, which are relatively easy to prepare starting substrates, have led to a variety of cyclic compounds with the help of transition metal and main group-metal catalysts able to provide a variety of activation processes. Several review articles have already been devoted to enyne transformations including cycloisomerization [1–3]. This paper is a non-exhaustive report on the metal-catalyzed cyclization of the simplest enynes containing only one triple and one double bond, with a special focus on enyne metathesis.

2. Cycloisomerization of enynes: various catalytic processes

2.1 Cycloisomerization via oxidative coupling

The coordination of both the triple and double bond of enynes to a metal centre is a common process in coordination chemistry (Scheme 1), and

Y. İmamoğlu and V. Dragutan (eds.), Metathesis Chemistry: From Nanostructure Design to Synthesis of Advanced Materials, 375-394.

metal-catalyzed transformations based on this activation have already been reported with various transition metals such as titanium, platinum, nickel, cobalt, rhodium, and ruthenium (Ru).

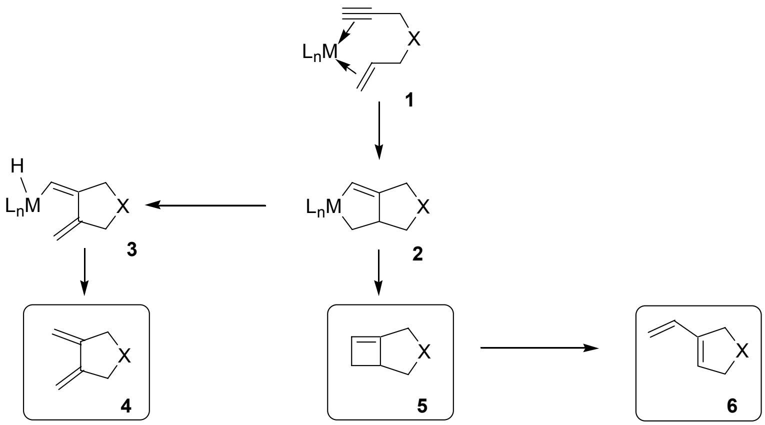

Scheme 1. Activation of enynes via oxidative coupling to a metal centre.

The formation of dienes of type **4** with β-H-elimination from **2** is favoured when there is no allylic substituent bearing hydrogen or subject to allylic activation at the external position of the double bond. This is mainly the case of enynes featuring a terminal double bond [4] but in some cases, even in the presence of an allylic branch, 1,3-dienes **4** are formed as illustrated by the cyclization of enyne **7** into diene **8** under palladium catalysis (Eq. 1) [5].

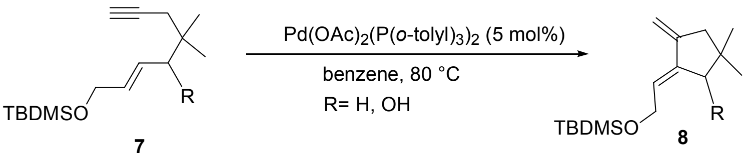

(1)

The direct reductive elimination from intermediates **2** leads to the formation of products **5** which present a very constrained structure. Usually, a conrotatory thermal opening leads to the formation of vinylcycloalkenes **6**. Only when the electrocyclic opening of the cyclobutene is not favoured, due to geometrical, steric or electronic reasons, the cyclobutene derivative can be isolated. This is the case with a substrate such as **9** which undergoes cycloisomerization via a formal [2+2] cycloaddition to give the polycyclic compound **10** (Eq. 2) [5].

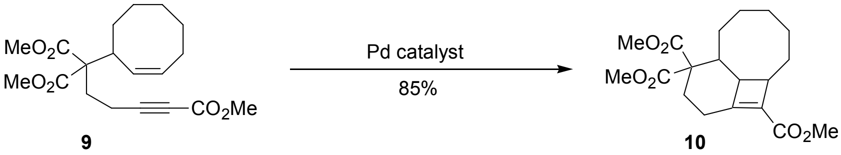

(2)

Most commonly, the cyclobutene opening takes place to form vinylcycloalkenes **6**, which present the same structural arrangement as the products resulting from enyne metathesis. This type of transformation has been initially observed with palladium catalysts [6,7]. When the starting enyne bears an allylic hydrogen at the external position of the double bond, the β-H–elimination of this hydrogen is favoured over the β-H-elimination of the ring junction hydrogen, and 1,4-dienes **12** are formed (Scheme 2). This is the most common cycloisomerization route involving oxidative coupling of both unsaturated bonds, which is proposed for a variety of metal catalysts such as palladium [7], Ru [8], rhodium [9], titanium [10], and cobalt [11].

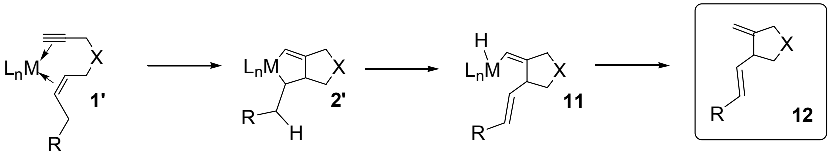

Scheme 2. 1,4-Dienes resulting from oxidative coupling to a metal centre.

It is interesting to note that the cycloisomerization leading to compounds of type **12** generates chiral molecules featuring one stereogenic centre. More information on the design of enantioselective catalytic systems will be given in Section 2.2.

2.2 Cycloisomerization via insertion of the triple bond into and M–H bond

Triple bonds are prone to insert into metal–hydride bonds to give metal-alkenyl species **14**. As shown in Scheme 3, the double bond can then insert into the metal-sp^{2}carbon to form intermediate **15** which liberates **16** after β-H–elimination.

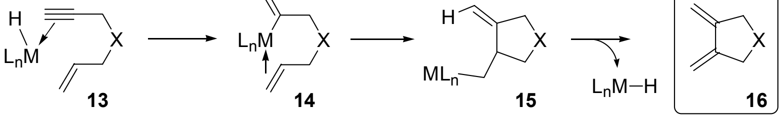

Scheme 3. 1,3-Dienes resulting from insertion of the triple bond into a metal–hydride bond.

This transformation is catalyzed by metal–hydride complexes such as $RuHCl(CO)(PPh_3)_3$ as shown in the cycloisomerization of **17** into **18** (Eq. 3) [12], but can also be promoted by in situ generated metal–hydride species resulting from the interaction of non-hydridic complexes with acidic co-reagent. This is illustrated by the cycloisomerization of allyl propargyl ethers **19** into dienes **20** in the presence of catalytic amounts of RuCp*Cl(COD) in acetic acid (Eq. 4) [13].

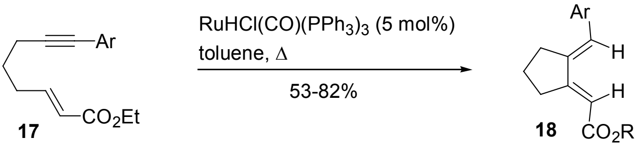

(3)

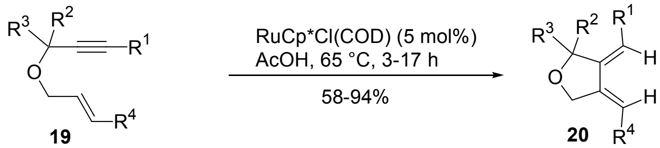

(4)

It is worth to note that the stereochemistry of compounds **18** and **20** is in agreement with the proposed mechanism. Other examples using palladium catalysts in acidic medium have also been reported [14].

In Scheme 4, the fate of the intermediate **15′** strongly depends on the nature of the substituents of the double bond. Here again, the presence of a hydrogen atom at the external allylic position favours the β-H–elimination from the exocyclic position. The resulting 1,4-diene **12** is the same compound as the one resulting from oxidative coupling process (Scheme 2). In fact, when reactions are carried out in protic solvent, it is sometimes difficult to distinguish which elemental steps are involved in the catalytic cycle.

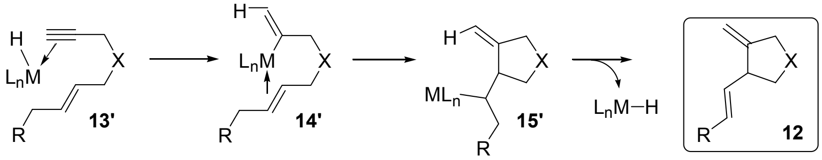

Scheme 4. 1,4-Dienes resulting from initial insertion of the triple bond into a metal–hydride bond.

The formation of chiral cyclic 1,4-dienes from cycloisomerization of 1,6-enynes and 1,7-enynes has triggered the search for enantioselective catalytic systems [15]. The first catalysts were based on palladium containing various types of optically pure ligands. Amidodiphosphanes such as **21** [16] and bisferrocenyldiphosphanes **22** [17] ligands were found to give satisfactory enantiomeric excesses associated with Pd(0) catalyst precursors.

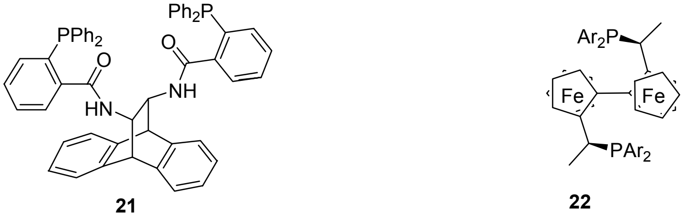

21

22

Figure 1. Chiral ligands for enantioselective cycloisomerization of enynes

The atropisomeric diphosphanes Binap, H_8-Binap, Segphos also led to very efficient and selective catalysts associated to $Pd(O_2CCF_3)_2$ [18] or $[Pd(MeCN)_4][BF_4]_2/HCO_2H$ [19]. In the presence of rhodium catalysts, depending on the nature of the starting enyne, several diphosphanes such as Me-Duphos, Binap, Biphemp were efficiently used [20].

2.3 Cycloisomerization involving first allylic activation

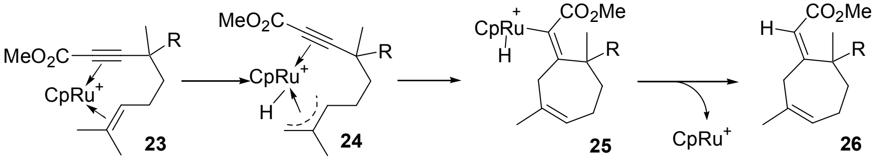

Scheme 5. Allylic C–H bond activation in ruthenium-catalyzed cycloisomerization of enynes.

The coordination of the triple and double bond to the Ru precursor $[RuCp(MeCN)_3][PF_6]$ after elimination of acetonitrile ligands promotes the formation of the allylic ligand in **24** via C–H bond activation rather than oxidative coupling. Further insertion of the triple bond into the Ru-carbon bond gives rise to the formation of the seven-membered ring **26** (Scheme 5) [21].

In the presence of a rhodium catalyst, when the enyne contains an halogen atom in allylic position, the allylic activation appears to take place first and the triple bond then inserts into the metal-halogen bond to form the cyclic diene **31** with halogen migration (Scheme 6) [22].

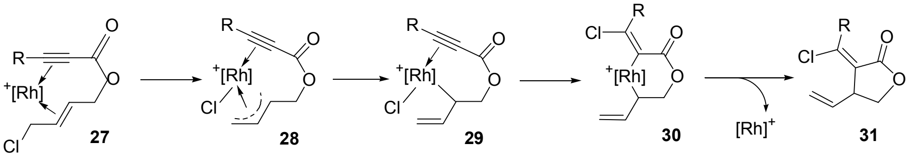

Scheme 6. Allylic C–Cl bond activation in rhodium-catalyzed cycloisomerization of enynes.

This transformation occurs only with halides but other leaving groups usually active for allylic activation such as carbonate or ester lead to the products resulting from oxidative coupling without leaving group migration.

2.4 Cycloisomerization involving electrophilic activation

The activation of the triple bond of enynes by an electrophilic and alkynophilic metal centre generates highly electrophilic species with cationic character, and triggers the nucleophilic attack of the double bond to the activated triple bond by an *exo*- or *endo-dig* cyclization pathway to form the ionic species **32** and **33**, respectively (Scheme 7) [23-27].

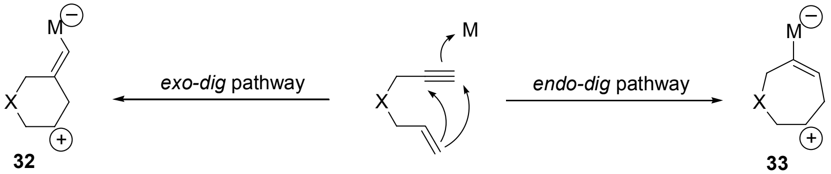

Scheme 7. General scheme for electrophilic activation of enynes.

2.4.1 Cycloisomerization into vinylcycloalkene derivatives

The most probable pathway for the formation of vinylcycloalkene derivatives involving electrophilic activation is the exo–dig cyclization (Scheme 8). The intramolecular rearrangement first leads to an organometallic intermediate **33** featuring a cyclopropane ligand. Several canonical forms can be envisaged and it is worth noting the congruence between the ionic form **33** and the carbenoid species **34**. From **35** and **36**, two different vinylcyclopentene isomers differing from the position of their substituents R^1 and R^2 can be formed. Depending on the nature of the starting enyne and the catalytic systems, both types of compounds have been isolated.

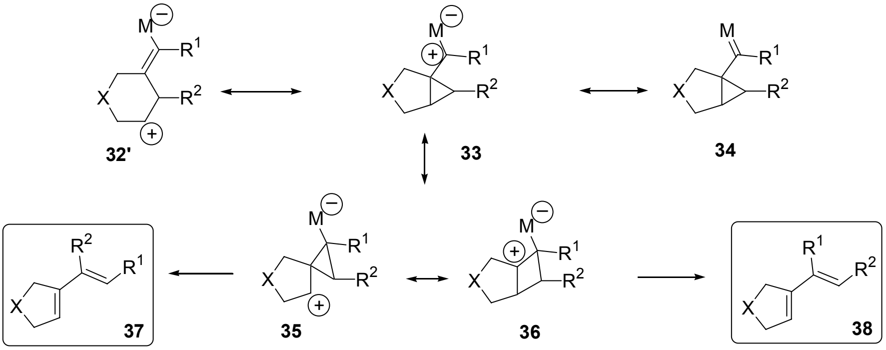

Scheme 8. Formation of vinylcycloalkenes via exo–dig cyclization.

Vinylcyclopentene derivatives of both types (**37** and **38**) depending on R^1, R^2, and X have been produced from a variety of electrophilic activators including transition metal catalysts such as $[RuCl_2(CO)_3]_2$ [28], platinum salts (mainly $PtCl_2$) [29-31], iridium [32], and gold [33], and main group salts such as $GaCl_3$ [34] and $InCl_3$ [35], most of them in apolar solvent. Stable bicyclic cyclobutene derivatives have been obtained from an intermediate of type **36** upon activation with gold catalysts [26], as well as $PtCl_2$ under CO [36].

2.4.2 Cycloisomerization into cyclopropane derivatives

When the propargylic position of the enyne bears an hydrogen and a bridging heteroatom able to stabilize cationic intermediate species such as **40**, the *endo–dig* pathway leads to the formation of cyclopropane derivatives (Scheme 9).

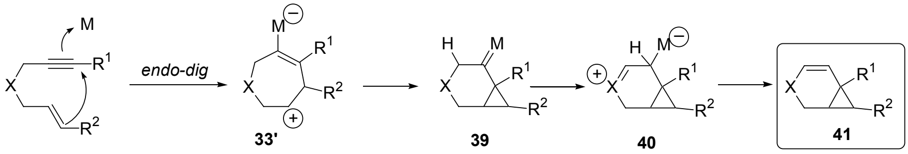

Scheme 9. Cycloisomerization into cyclopropane derivatives involving H-migration.

The 1,2-hydrogen migration has been confirmed by deuterium labelling experiments. This cycloisomerization was first shown from allyl propargyl ethers in the presence of $PtCl_4$ [37], and then from tosyl allyl propargyl amines catalyzed by $PtCl_2$ in toluene at 80°C [30,38] (Scheme 10), and $IrCl(COD)(PPh_3)_2/AgOTf$ [39].

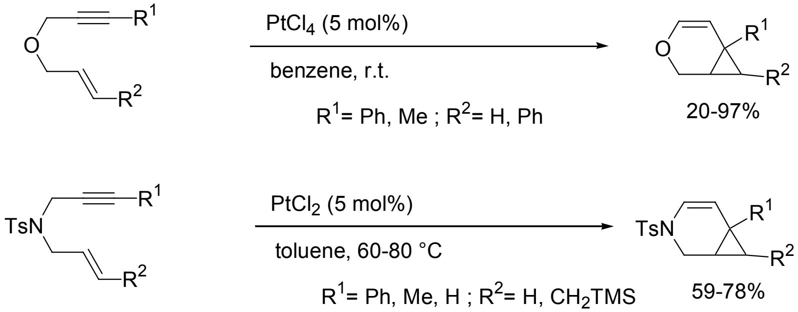

Scheme 10. Examples of cycloisomerization into [4.1.0]-heptene derivatives.

In the absence of any other functionality, this mechanism does not operate with platinum catalyst from 1,5-enynes. Recently, it has been shown that such 1,5-enynes with no heteroatom in the tether between the triple bond and the double bond could be efficiently performed by using a cationic gold catalyst to give [3.1.0]-hexene derivatives [40]. It implies cyclopropanation with 1,2-H-shift (Eq. 5), or alkyl shift with ring enlargement (Eq. 6).

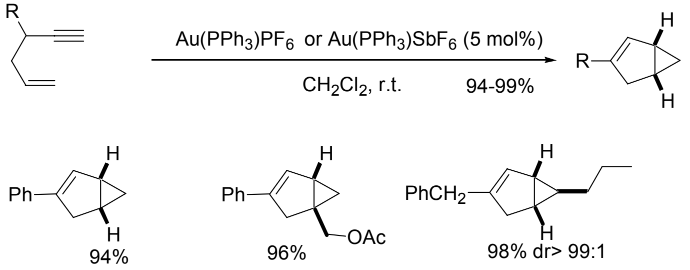

(5)

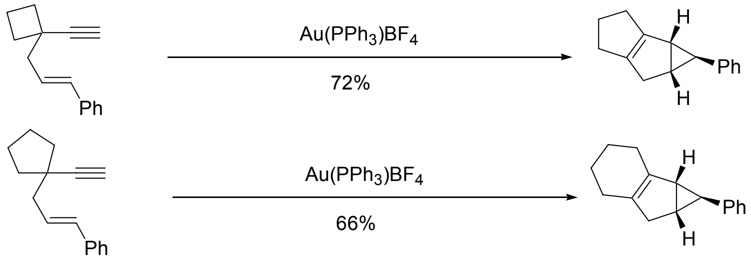

(6)

Functional 1,5-enynes containing a propargyl alcohol motive in their structure can be cycloisomerized in the presence of platinum and gold catalysts following the same endo–dig pathway and H-shift, to directly form [3.1.0]-hexanones (Eq. 7) [41,42].

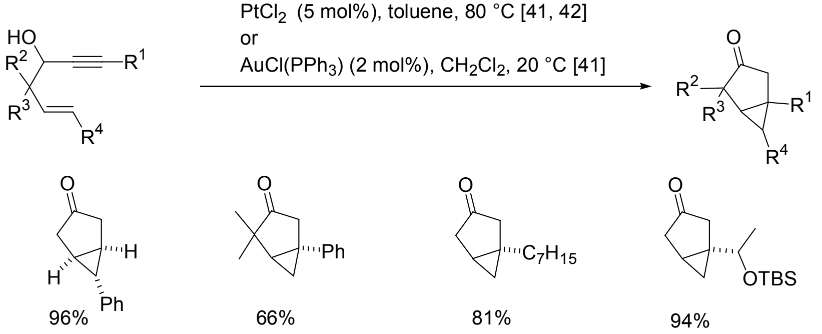

(7)

Very recently, a Cu(I)-catalyzed cycloisomerization of tertiary 5-en-1-yn-3-ols involving a 1,2-alkyl shift and leading to the stereoselective formation of polycyclic ketones was reported (Eq. 8) [43].

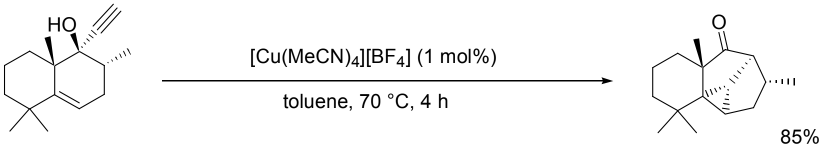

(8)

2.4.3 Cycloisomerization into alkylidenecycloalkene derivatives

As reported in Scheme 9, the *endo–dig* cyclization via electrophilic activation leads to a carbenoid intermediate **39** which lead to the formation of cyclopropane derivatives when a hydrogen migration can take place. Another possibity is the rearrangement of these intermediates into the cationic species **42**, which liberates the alkylidene cycloalkene **43** upon elimination of the metal (Scheme 11).

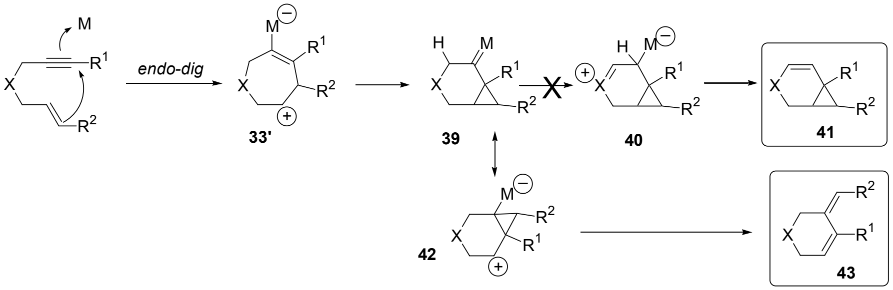

Scheme 11. Cycloisomerization of enynes into alkylidenecycloalkene derivatives.

This transformation has been shown from various types of enynes. It is worth noting that in most cases it is not selective and cyclopropane or vinylcycloalkene compounds resulting from the other mechanisms are often detected as accompanying products (Scheme 12) [33].

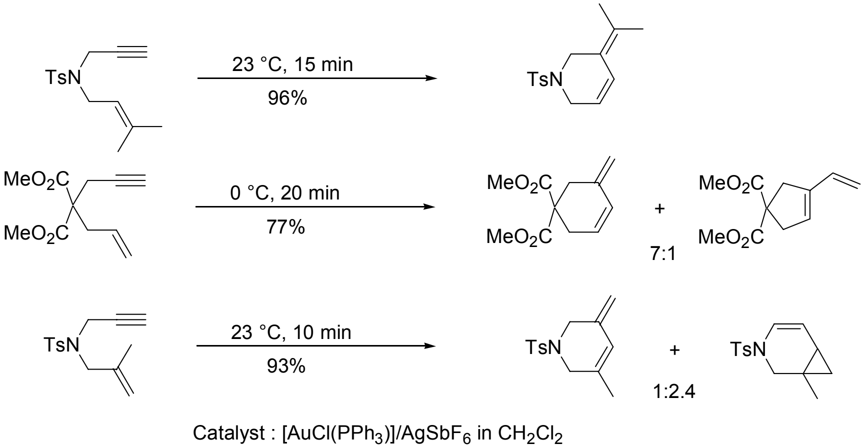

Scheme 12. Examples of formation of alkylidenecyclohexene derivatives from 1,6-enynes.

2.5 Cycloisomerization involving metal vinylidene intermediates

The formation of alkylidene cyclohexene derivatives from 1,6-enynes bearing a terminal triple bond has been carried out very efficiently with rhodium catalysts. Deuterium labelling experiments have shown that a rhodium

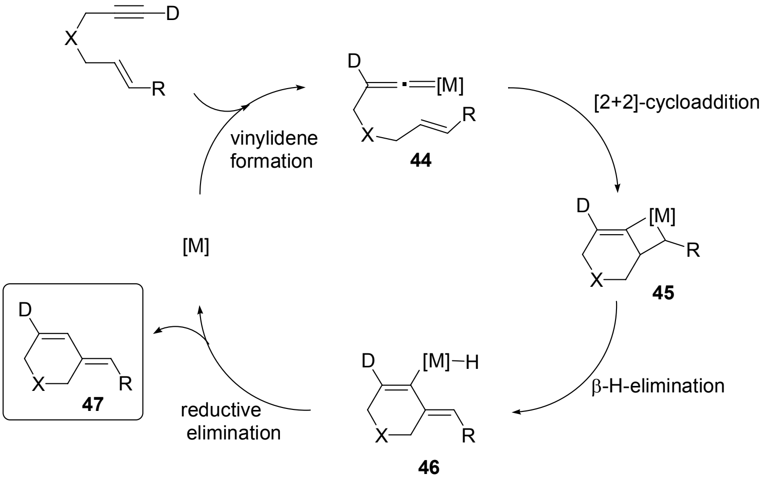

Scheme 13. Cycloisomerization into alkylidenecycloalkene derivatives via metal–vinylidene intermediates.

hydride or free-radical mechanism was unlikely and that the initial formation of a rhodium vinylidene species **44** was the most probable. Further [2+2]-cycloaddition to give **45**, followed by β-H–elimination (**46**) and reductive elimination closes the catalytic cycle and leads to **47** (Scheme 13) [44].

Thus, the use of $[RhCl(COD)]_2$ in the presence of tris(4-fluorophenyl)phosphine at 85°C led to the selective cycloisomerization of 1,6- and 1,7-enynes in good yields (Scheme 14) [44].

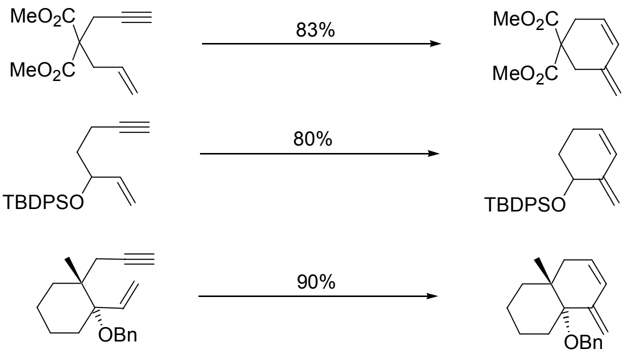

Catalyst : $[RhCl(COD)]_2$ (2.5-20 mol%)/ $P(4\text{-}FC_6H_4)_3$ (0-10%) in DMF, 85 °C, 24 h

Scheme 14. Examples of formation of methylenecyclohexene derivatives via metal–vinylidene intermediates.

2.6 Cycloisomerization involving metathesis

As for olefin metathesis, enyne metathesis is promoted by metal carbene precursors. After the initial work based on group 6 metal derivatives such as tungsten [45] or chromium [46], the development of enyne metathesis has known a great development with the introduction of the commercially available Ru catalysts [47,48]. The general mechanism involves a cascade of [2+2]-cycloadditions and retrocycloadditions and leads to conjugated dienes with an important skeleton rearrangement with creation of a carbon–carbon double bond and migration of the terminal alkene moiety to the terminal carbon of the triple bond. Two types of reaction pathways can be envisaged depending on the order of interaction of the triple bond or the double bond with the carbene complex, namely the Yne-then-ene pathway (Scheme 15) and the Ene-then-Yne pathway (Scheme 16). In addition, in both pathways, the orientation of the substrate with respect to the metal carbene bond provides two types of products (*endo* and *exo* modes) [49,50].

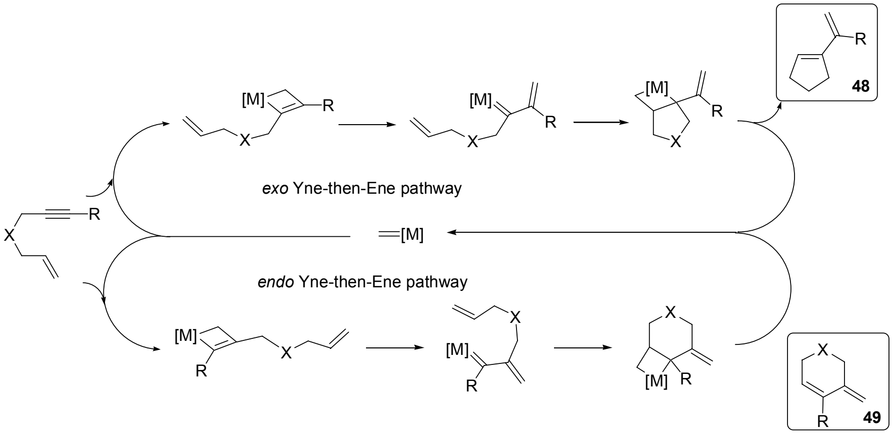

Scheme 15. Enyne metathesis: Yne-then-Ene pathways.

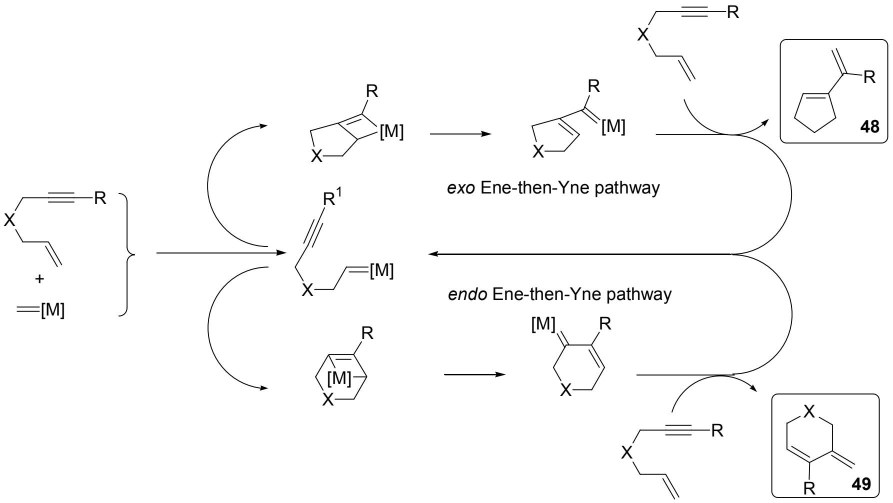

Scheme 16. Enyne metathesis: Ene-then-Yne pathways.

From the nature of the products which are formed, it is easy to identify which mode is involved. Several parameters including the nature of the catalyst (Eq. 9) [51,52], and the size of the formed ring (Eq. 10) [53] are crucial. On the other hand, it is often difficult to discriminate which type of pathway is involved. The Yne-then-Ene pathway has most often been proposed but recent results based on nuclear magnetic resonance (NMR) studies and C and H labelling are in favour of the other pathway [54,55].

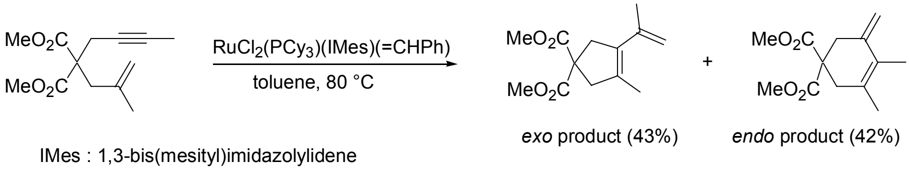

(9)

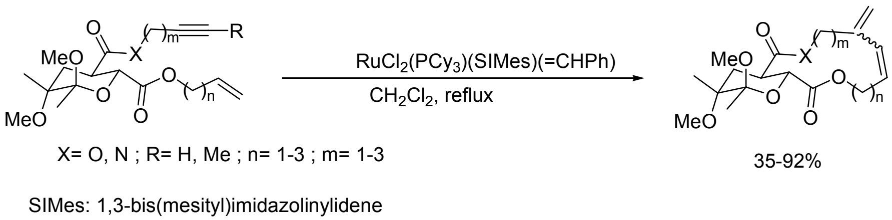

(10)

3. Cycloisomerization of allyl propargyl ethers

3.1 Metathesis with well-defined ruthenium–allenylidene catalysts

Allyl propargyl ethers are suitable 1,6-enyne substrates to give access to a variety of dihydrofuran derivatives upon cycloisomerization via metathesis reaction. The cationic $[RuCl(PCy_3)(p\text{-cymene})(C{=}C{=}C{=}CPh_2)][PF_6]$ complex (Eq. 11) promotes the transformation of a variety of allyl propargyl ethers at 80°C in toluene in satisfactory yields [56]. When the starting substrate bears an internal triple bond (**53**) or a highly substituted propargylic position (**54**), the reaction rate is decreased. It is also interesting to note that the dihydrofuran **55** is formed rather than the cyclopentene derivative resulting from cycloisomerization of the triple bond with the other more substituted double bond. The activation of the precatalyst by ultraviolet (UV) irradiation decreases the initiation period and the complete conversion of the enyne leading to compound **50** (isolated in 62% yield) was obtained after 1 h at 80°C, whereas without initial activation the complete conversion was reached after 6.5 h.

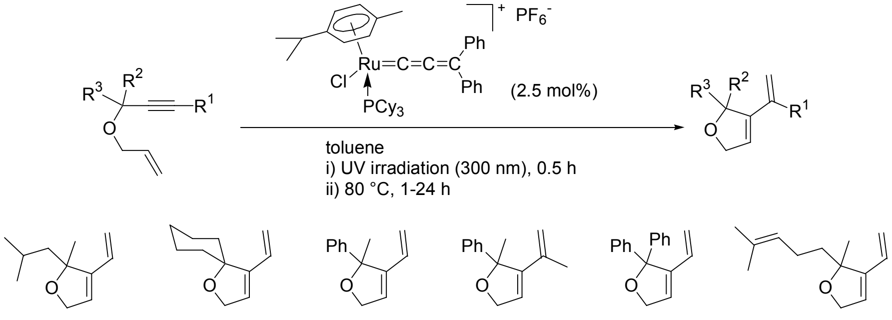

50 1 h (62%) **51** 1 h (63%) **52** 4 h (84%) **53** 24 h (83%) **54** 23 h (67%) **55** 1 h (74%)

(11)

3.2 Cycloisomerization of allyl propargyl ethers with in situ generated catalysts

3.2.1 Experimental results

The development of *N*-heterocyclic carbene (NHC) ligands in catalysis associated to a variety of metal precursors has provided impetus to create new olefin and enyne metathesis catalysts based on the $RuCl_2(PCy_3)(=CHPh)$ model. The generation of new catalysts by mixing a Ru precursor, a NHC source, and a base to produce a variety of catalytic systems was at the origin of our investigations. Thus, a mixture of $[RuCl_2(p\text{-cymene})]_2$, bis(mesityl)imidazolium chloride, and Cs_2CO_3 as a base in the ratio 1:2:4 (catalysts **A**) provided an efficient catalytic system for the cycloisomerization of allyl propargyl ethers (Eq. 12) [57]. Compounds **56–60** were obtained in good yields within reaction times depending on the structure of the starting enyne with various substitution patterns.

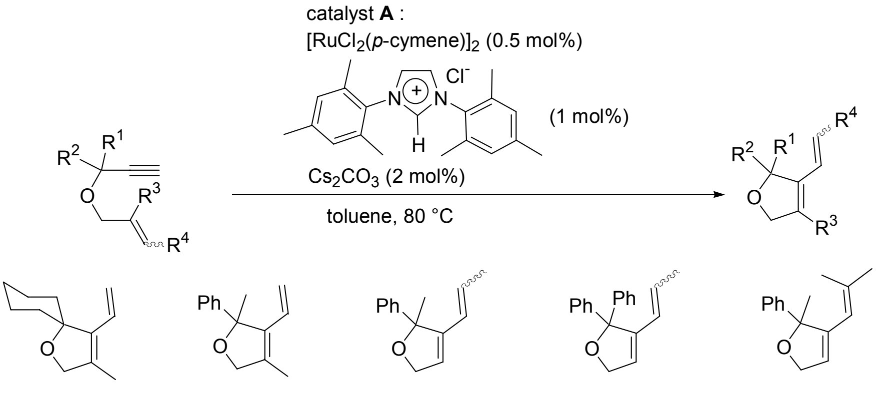

56 0.5 h (86%) **57** 1.5 h (75%) **58** 2 h (61%) **59** 15 h (52%) **60** 25 h (16%)

(12)

The more favourable steric and electronic properties of imidazolidinylidene ligands reported for Grubbs type catalysts [58,59] led us to test the activity of catalyst **B** (Eq. 13) generated from the same Ru source and the same base but in the presence of bis(mesityl)imidazolinium chloride as carbene precursor.

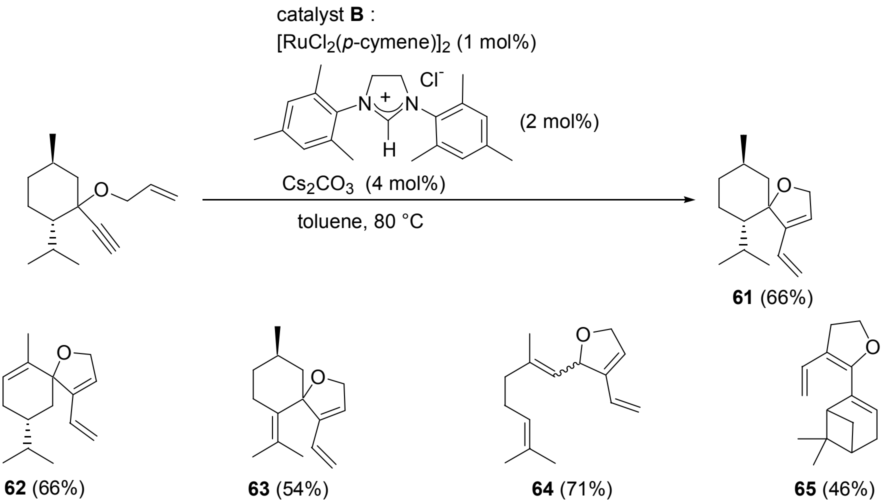

(13)

Starting from terpenoid derivatives, featuring a carbonyl group such as (-)-menthone, (-)-carvone, (+)-pulegone, *cis*- and *trans*-citral, and (-)-myrtenal, the addition of first lithium acetylide to form a propargylic alcohol, and then reaction with allyl bromide after deprotonation with NaH, led to modified terpenoid derivatives containing the allyl propargyl ether motive. Their treatment with the in situ generated catalyst **B** led to the formation of the spirocyclic compounds **61–63**, and the cyclic compounds **64–65** in satisfactory to good yields (Eq. 13) [60]. When a vinyl group was first added to the keto group of (-)-carvone and the corresponding allylic alcohol was etherified by a propargyl group, the resulting allyl propargyl ether compound was cycloisomerize into product **66** in 61% yield under our typical conditions with catalyst **B** (Eq. 14). In this compound, the added five carbon atoms have the isoprenoid arrangement, and **66** is thus a new non-natural sesquiterpenoid.

With the objective of increasing the ring size of the cycloisomerized products, a silicon atom was introduced in the allylic branch by preparing allylsilyl ethers from the same terpenoid substrates. In addition, upon cyclization, this type of substrate generate Si-O-containing rings, which are useful intermediates for further chemical transformations via selective ring cleavage [61–63].

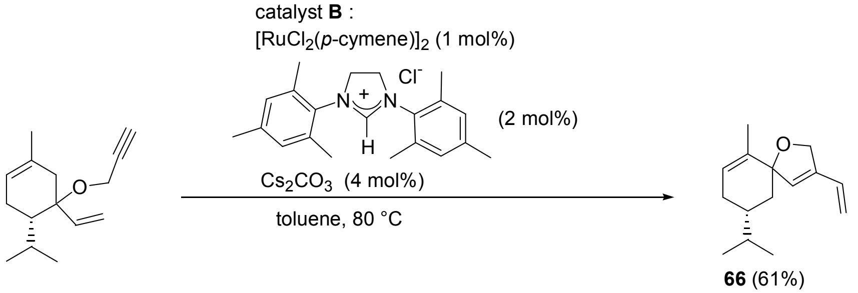

(14)

We had already shown that the catalytic system **B** was able to perform the cycloisomerization of simple allyl propargyl ethers [64], and its utilization to the terpenoid derivatives was also efficient for the formation of the six-membered heterocycles **67–70** incorporating a Si-O bond (Eq. 15) [65].

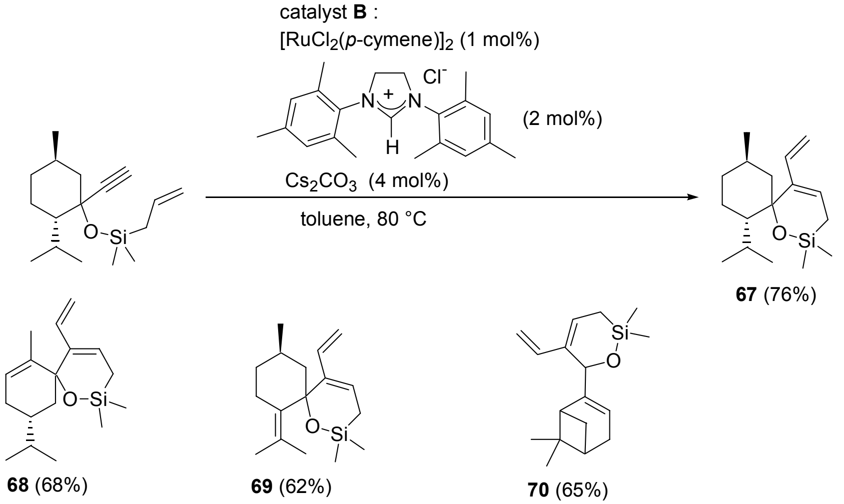

(15)

3.2.2 Mechanistic investigation

The catalysts precursors **A** and **B** contain no Ru carbene at the outset of the reaction. Thus, the question arises whether the cycloisomerization of the allyl propargyl ethers reported above proceeds via a metathesis pathway or another type of mechanism (see Section 2). To try to answer this question, a catalytic transformation of dienes was attempted with the catalytic system **B**. A complete conversion of the starting dienes into the cycloisomerization methylenecycloalkane derivatives **71–74**, isolated in 64–88%, was observed

(Eq. 16) [66,67]. The cyclopentene derivatives resulting from RCM were not detected and compounds **71–74** probably resulted from initial oxidative coupling process (Section 2.1).

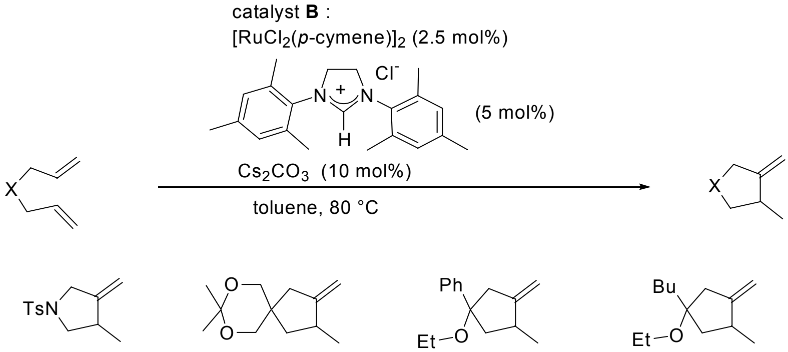

71 1 h (88%) **72** 8 h (64%) **73** 8 h (85%) **74** 5.5 h (78%)

(16)

The addition of a terminal alkyne to a Ru precursor with the objective of creating a metathesis catalyst is a known strategy. It has already been used by Grubbs to generate an efficient metathesis catalyst from [RuCl$_2$(*p*-cymene)]$_2$, a NHC and *tert*-butylacetylene [68]. Indeed, when the reaction was performed with the catalytic system **B**, under the same conditions but with an acetylene atmosphere instead of an inert gas atmosphere, an active alkene metathesis catalyst was generated, and no cycloisomerization was observed. The metathesis products **75–78** were thus formed in 68–82% yield (Eq. 17) [66,67]. To understand this change of catalytic activity, the fast formation of a Ru vinylidene, precursor of Ru carbene species, is proposed [69].

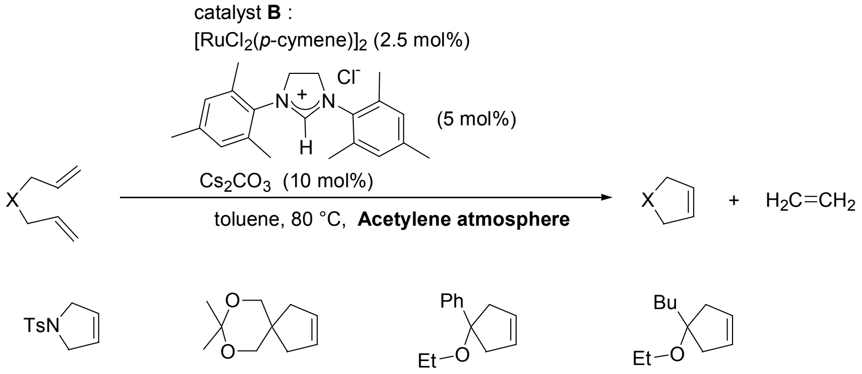

75 2.5 h (76%) **76** 8 h (72%) **77** 16 h (68%) **78** 16 h (82%)

(17)

4. Conclusion

The preparation of catalytic systems from $[RuCl_2(p\text{-cymene})]2$, a NHC source and a base, represents a very simple and practical method as it avoids the synthesis of well-defined Ru complexes which sometimes require strict experimental conditions. A large number of catalytic systems can be produced by mixing various Ru sources and carbene precursors. We have shown that the activity of the resulting catalysts can be tuned by a slight modification of the experimental conditions. Thus, it is easy to transform an enyne cycloisomerization catalyst into a metathesis catalyst by addition of a catalytic amount of terminal alkyne.

References

[1] Aubert, C., Buisine, O., Malacria, M. (2002) Chem. Rev. 102:813.

[2] Lloyd-Jones, G.C. (2003) Org. Biomol. Chem. 1:215.

[3] Zhang, Z., Zhu, G., Tong, X., Wang, F., Xie, X., Wang, J., Jiang, L. (2006) Curr. Org. Chem. 10:1457.

[4] (a) Trost, B.M., Lautens, M., Chan, C., Jebaratnam, D.J., Mueller, T. (1991) J. Am. Chem. Soc. 113:636; (b) Trost, B.M., Hipskind, P.A., Chung, J.Y.L., Chan, C. (1989) Angew. Chem. Int. Edit. 28:1502; (c) Kezuka, S., Okado, T., Niou, E., Takeuchi, R. (2005) Org. Lett. 7:1711.

[5] Trost, B.M., Chung, J.Y.L. (1985) J. Am. Chem. Soc. 107:4586.

[6] Trost, B.M., Yanai, M., Hoogsteen, K. (1993) J. Am. Chem. Soc. 115:5294.

[7] Trost, B.M., Tanoury, G.J. (1988) J. Am. Chem. Soc. 110:1636.

[8] Trost, B.M., Toste, F.D. (2002) J. Am. Chem. Soc. 124:5025.

[9] Cao, P., Wang, B., Zhang, X. (2000) J. Am. Chem. Soc. 122:6490.

[10] Sturla, S.L., Kablaoui, N.M., Buchwald, S.L. (1999) J. Am. Chem. Soc. 121:1976.

[11] (a) Cruciani, P., Stammler, R., Aubert, C., Malacria, M. (1996) J. Org. Chem. 61:2699; (b) Renaud, J.L., Petit, M., Aubert, C., Malacria, M. (1997) Synlett. 931.

[12] Nishida, N., Adachi, N., Onozuka, K., Matsumura, H., Mori, M. (1998) J. Org. Chem. 63:9158.

[13] Le Paih, J., Rodriguez, D.C., Dérien, S., Dixneuf, P.H. (2000) Synlett. 95.

[14] (a) Trost, B.M., Lee, D.C., Rise, F. (1989) Tetrahedron Lett. 30:651; (b) Trost, B.M., Romero, D., Rise, F. (1994) J. Am. Chem. Soc. 116:4268.

[15] Fairlamb, I.J.S. (2004) Angew. Chem. Int. Edit. 43:1048.

[16] Trost, B.M., Czeskis, B.A. (1994) Tetrahedron Lett. 35:211.

[17] Goeke, A., Sawamura, M., Kuwano, R., Ito, Y. (1996) Angew. Chem. Int. Edit. 35:662.

[18] Hatano, M., Terada, M., Mikami, K. (2001) Angew. Chem. Int. Edit. 40:249.

[19] Hatano, M., Mikami, K. (2003) J. Am. Chem. Soc. 125:4704.

[20] (a) Cao, P., Zhang, X. (2000) Angew. Chem. Int. Edit 39:4104; (b) Lei, A., He, M., Zhang, X. (2002) J. Am. Chem. Soc. 124:8198; (c) Lei, A., Waldkirch, J.P., He, M., Zhang, X. (2002) Angew. Chem. Int. Edit. 41:4526; (d) Hashmi, A.S.K., Haufe, P., Rivas Nass, A. (2003) Adv. Synth. Catal. 345:1237.
[21] Trost, B.M., Toste, F.D. (1999) J. Am. Chem. Soc. 121:9728.
[22] Tong, X., Li, D., Zhang, Z., Zhang, X. (2004) J. Am. Chem. Soc. 126:7601.
[23] Mendez, M., Mamane, V., Fürstner, A. (2003) Chemtracts-Org. Chem. 16:397.
[24] Anorbe, L., Dominguez, G., Prez-Castells, J. (2004) Chem. Eur. J. 10:4938.
[25] Echavarren, A.M., Nevado, C. (2004) Chem. Soc. Rev. 33:431.
[26] Nieto-Oberhuber, C., Lopez, S., Jimenez-Nunez, E., Echavarren, A.M. (2006) Chem. Eur. J. 12:5916.
[27] Bruneau, C. (2005) Angew. Chem. Int. Edit. 44:2328.
[28] Chatani, N., Morimoto, T., Muto, T., Murai, S. (1994) J. Am. Chem. Soc. 116:6049.
[29] Chatani, N., Furukawa, N., Sakurai, H., Murai, S. (1996) Organometallics 15:901.
[30] Fürstner, A., Szillat, H., Stelzer, F. (2000) J. Am. Chem. Soc. 122:6785.
[31] Oi, S., Tsukamoto, I., Miyano, S., Inoue, Y. (2001) Organometallics 20:3704.
[32] Chatani, N., Inoue, H., Morimoto, T., Muto, T., Murai, S. (2001) J. Org. Chem. 66:4433.
[33] Nieto-Oberhuber, C., Munoz, M.P., Bunuel, E., Nevado, C., Cardenas, D.J., Echavarren, A.M. (2004) Angew. Chem. Int. Edit. 43:2402.
[34] Chatani, N., Inoue, H., Kotsuma, T., Murai, S. (2002) J. Am. Chem. Soc. 124:10294.
[35] Miyanohana, Y., Chatani, N. (2006) Org. Lett. 8:2155.
[36] Fürstner, A., Davies, P.W., Gress, T. (2005) J. Am. Chem. Soc. 127:8244.
[37] Blum, J., Beer-Kraft, H., Badrieh, Y. (1995) J. Org. Chem. 60:5567.
[38] Nevado, C., Ferrer, C., Echavarren, A.M. (2004) Org. Lett. 6:3191.
[39] Shibata, T., Kobayashi, Y., Maekawa, S., Toshida, N., Takagi, K. (2005) Tetrahedron 61:9018.
[40] Luzung, M.R., Markham, J.P., Toste, F.D. (2004) J. Am. Chem. Soc. 126:10858.
[41] Mamane, V., Gress, T., Krause, H., Fürstner, A. (2004) J. Am. Chem. Soc. 126:8654.
[42] Harrak, Y., Blaszykowski, C., Bernard, M., Cariou, K., Mainetti, E., Mouriès, V., Dhimane, A-L., Fensterbank, L., Malacria, M. (2004) J. Am. Chem. Soc. 126:8656.
[43] Fehr, C., Farris, I., Sommer, H. (2006) Org. Lett. 8:1839.
[44] Kim, H., Lee, C. (2005) J. Am. Chem. Soc. 127:10180.
[45] Katz, T.J., Sivacec, T.M. (1985) J. Am. Chem. Soc. 107:737.
[46] Watanuki, S., Ochifuji, N., Mori, M. (1994) Organometallics 13:4129.
[47] Mori, M. (1998) Top. Organomet. Chem. 1:133.
[48] Storm Poulsen, C., Madsen, R. (2003) Synthesis 1.
[49] Mori, M., Kitamura, T., Sato, Y. (2001) Synthesis 654.
[50] Sashuk, V., Grela, K. (2006) J. Mol. Catal. A: Chem. 257:59.
[51] Mori, M., Sakakibara, N., Kinoshita, A. (1998) J. Org. Chem. 63:6082.
[52] Kitamura, T., Sato, Y., Mori, M. (2001) Chem. Commun. 1258.

[53] Hansen, E.C., Lee, D. (2004) J. Am. Chem. Soc. 126:15074.
[54] Hoye, T.R., Donaldson, S.M., Vos, T.J. (1999) Org. Lett. 1:277.
[55] Lloyd-Jones, G.C., Margue, R.G., de Vries, J.G. (2005) Angew. Chem. Int. Edit. 44:7442.
[56] Picquet, M., Bruneau, C., Dixneuf, P.H. (1998) Chem. Commun. 2249.
[57] Ackermann, L., Bruneau, C., Dixneuf, P.H. (2001) Synlett 397.
[58] Scholl, M., Ding, S., Lee, C.W., Grubbs, R.H. (1999) Org. Lett. 1:953.
[59] Smulik, J.A., Diver, S.T. (2000) Org. Lett. 2:2271.
[60] Le Nôtre, J., Bruneau, C., Dixneuf, P.H. (2002) Eur. J. Org. Chem. 3816.
[61] Evans, P.A., Murthy, V.S. (1998) J. Org. Chem. 63:6768.
[62] Hoye, T.R., Promo, M.A. (1999) Tetrahedron. Lett. 40:1429.
[63] Grimm, J.B., Lee, D. (2004) J. Org. Chem. 69:8967.
[64] Sémeril, D., Cléran, M., Jimenez Perez, A., Bruneau, C., Dixneuf, P.H. (2002) J. Mol. Catal. A: Chem. 190:9.
[65] Le Nôtre, J., Acosta Martinez, A., Dixneuf, P.H., Bruneau, C. (2003) Tetrahedron 59:9425.
[66] Sémeril, D., Bruneau, C., Dixneuf, P.H. (2001) Helv. Chim. Acta. 84:3335.
[67] Sémeril, D., Bruneau, C., Dixneuf, P.H. (2002) Adv. Synth. Catal. 344:585.
[68] Louie, J., Grubbs, R.H. (2001) Angew. Chem. Int. Edit. 40:247.
[69] Katayama, H., Ozawa, F. (2004) Coord. Chem. 248:1703.

ROMP, ROP, AND ADDITION POLYMERIZATION OF SILICON-CONTAINING CYCLIC MONOMERS AS A WAY TO NEW MEMBRANE MATERIALS

MARIA L. GRINGOLTS, NIKOLAI V. USHAKOV, YULIA V. ROGAN, KIRYLL L. MAKOVETSKII, YURI P. YAMPOLSKII, EUGENE SH. FINKELSHTEIN

A.V. Topchiev Institute of Petrochemical Synthesis, Russian Academy of Sciences, 29, Leninskii prospect, 119991 Moscow, Russia. E-mail: fin@ips.ac.ru

Abstract: The presented paper is a summary of our results on synthesis and polymerization of silyl-containing norbornenes and norbornadienes via ring-opening metathesis polymerization (ROMP) and addition processes as well as ring-opening polymerization (ROP) of silacyclobutanes and disilacyclobutanes. The synthesis of heterochain and carbochain polymer families with regularly varied substituents at Si atom and various number and location $Si(CH_3)_3$-substituents has been realized. Systematic study of gas transport parameters of polycarbosilanes series of different classes allowed us to find out real correlations between features of chemical polymer structure and its gas separation characteristics.

Keywords: ROMP, addition polymerization, silicon containing norbornenes, silacyclobutanes, disilacyclobutanes.

1. Introduction

The possibility of gas transport through nonporous polymeric membranes is one of the basic phenomena of polymer materials [1]. It is based on "solution–diffusion" concept. It means that the presence of microscopic open pores or capillaries is not necessary for mass transfer through polymeric films. On the other hand, closed porosity or the presence of free-volume elements within a polymer matrix is required for gas permeation in the polymers considered for use as materials for gas separation membranes.
The permeation process includes three stages: (1) sorption of gas by polymer film; (2) diffusion of the sorbed gas molecules; and (3) their subsequent desorption at the other side of the membrane as permeated gas.

The following equation holds for the flux J of an individual gas through the film:

$$J = P(\Delta p/l)$$

where Δp is the pressure difference across the membrane; l is the film thickness.

Y. İmamoğlu and V. Dragutan (eds.), Metathesis Chemistry: From Nanostructure Design to Synthesis of Advanced Materials, 395-411.

The coefficient of proportionality or permeability coefficient P can be presented as follows:

$$P = DS$$

where D is the diffusion coefficient and S is the solubility coefficient. According to these equations it is clear that P depends upon two factors:

1. A thermodynamic term, S, that determines the number of gas molecules sorbed into the polymer (the driving force of the mass transfer)
2. A kinetic or mobility term, D, that characterizes the mobility of gas molecules as they diffuse through the polymer

A widely used and accepted unit for P is: 1 Barrer = 10^{-10} cm^3 (STP) cm/(cm^2·s·cm Hg).

Another key parameter of membranes is selectivity in gas separation defined as follows:

$$\alpha_{\mathrm{AB}} = \frac{P_{\mathrm{A}}}{P_{\mathrm{B}}}$$

where P_{A} and P_{B} are the permeability coefficients of gases A and B (if more permeable gas is taken as A, α_{AB} > figure1).

The selectivity can be expressed as follows:

$$\alpha_{\mathrm{AB}} = \left(\frac{D_{\mathrm{A}}}{D_{\mathrm{B}}}\right)\left(\frac{S_{\mathrm{A}}}{S_{\mathrm{B}}}\right) = \alpha_{\mathrm{AB}}^{\mathrm{D}} \cdot \alpha_{\mathrm{AB}}^{\mathrm{S}}$$

There is a trade-off existing between permeability and selectivity: for the majority of polymers higher permeability corresponds to lower permselectivity and vice versa.

As a rule, glassy polymers are suitable for separation of light gases such as He, H_2, O_2, N_2, and CO_2. In this case permeation rate is defined by the size of gas molecule: in the diffusivity controlled process smaller molecules permeate faster through polymeric film.

Rubbery polymers provide solubility-controlled permeation. In this case, e.g. hydrocarbon gases can be separated according to their molecular mass and solubility in membrane film: heavier gases have a better solubility, so they permeate faster under the action of larger driving force.

There are, however, some exceptions, when glassy polymers demonstrate membrane properties more characteristic for rubbery ones, i.e. the permeation is defined by solubility of permeating gases.

As a typical representative of the first type of behavior one can mention glassy poly(vinyltrimethyl silane), of the second one it is rubbery poly(dimethylsiloxane), and, of the third one is poly(trimethylsilyl propyne) [2]:

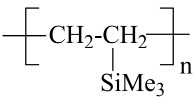

$$\left[CH_2-\underset{SiMe_3}{\underset{|}{CH_2}} \right]_n$$

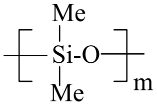

$$\left[\overset{Me}{\overset{|}{\underset{Me}{\underset{|}{Si}}}}-O \right]_m$$

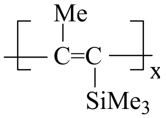

$$\left[\overset{Me}{\overset{|}{C}}=\underset{SiMe_3}{\underset{|}{C}} \right]_x$$

It is clear that peculiarities of polymer structure such as rigidity of the main chain and the presence and size of side groups play important roles. Some glassy polymers having bulky organosilicon side groups, such as in poly(vinyltrimethyl silane) and poly(trimethylsilyl propyne) reveal high permeability, sometimes even higher than that in rubbers [2].

This work is devoted to systematic study of gas transport parameters of polycarbosilanes obtained from silicon-containing cyclic monomers. This approach allowed us to synthesize carbochain and heterochain polymer families with regularly varied substituents at Si atom. On the other hand, such research on polymer series of different classes leads to basic correlations and helps one to understand relationships between features of polymer chemical structure and its gas separation characteristics.

2. Synthesis of monomers

Four types of organosilicon cyclic compounds were used as monomers for preparation of polycarbosilanes having different main chains:

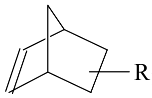

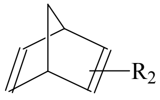

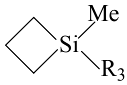

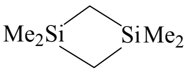

R_1 and R_2: Si-containing substituents
R_3: Alk-, Ar-, or Si-containing groups

Norbornenes and norbornadienes derivatives were synthesized by Diels–Alder condensation of cyclopentadiene and corresponding dienophile as a key reaction [3–6]:

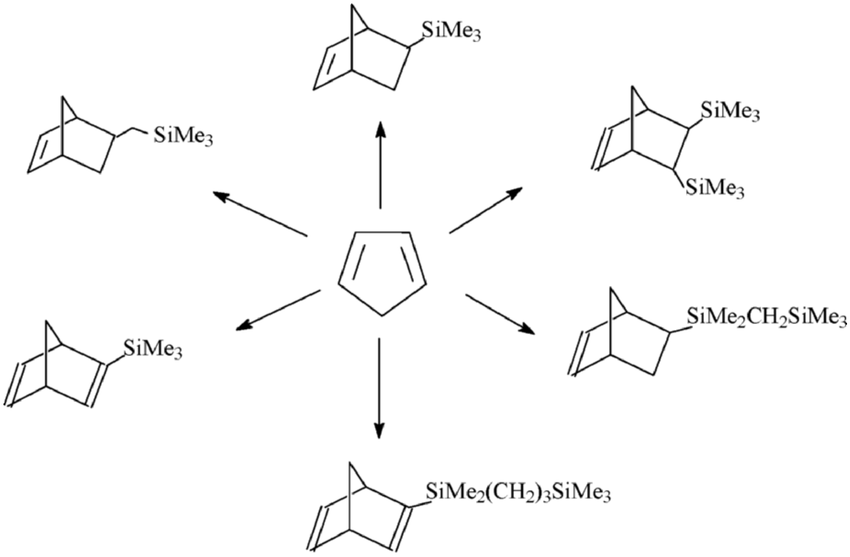

Scheme 1

Four-membered silacyclobutanes and disilacyclobutanes were prepared from accessible organosilicon raw materials according to well-studied reliable techniques [7–13].

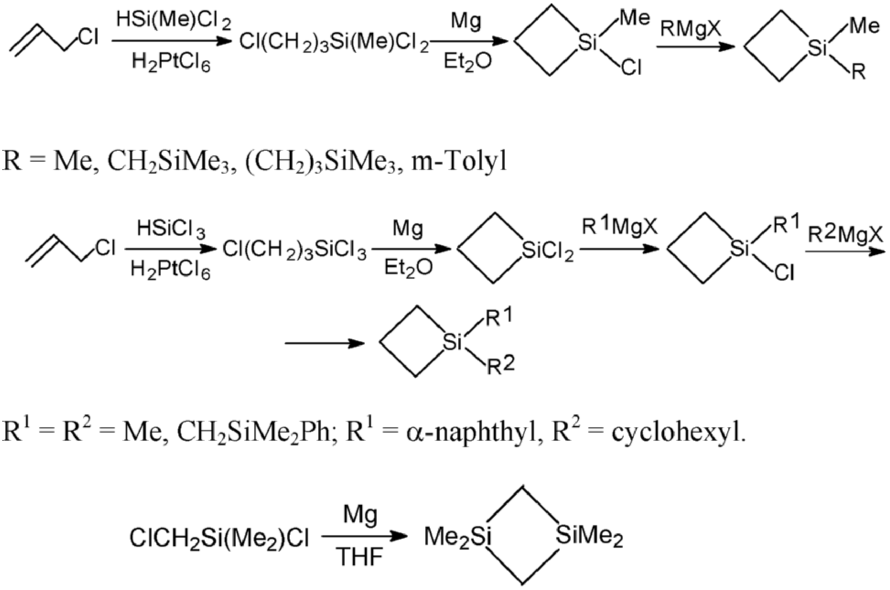

R = Me, CH$_2$SiMe$_3$, (CH$_2$)$_3$SiMe$_3$, m-Tolyl

R^1 = R^2 = Me, CH$_2$SiMe$_2$Ph; R^1 = α-naphthyl, R^2 = cyclohexyl.

Scheme 2

3. Glassy ROMP polycarbosilanes for separation of light gases

Ring-opening metathesis polymerization (ROMP) of silicon-containing norbornenes and norbornadienes (Scheme 3 and Table 1) proceeded much more slowly than in the case of unsubstituted norbornene. Nevertheless, even classical poor characterized Ru or W catalyst systems proved to be active in these reactions. We used various catalysts to obtain polymers with different content of *cis*- and *trans*-double bonds.

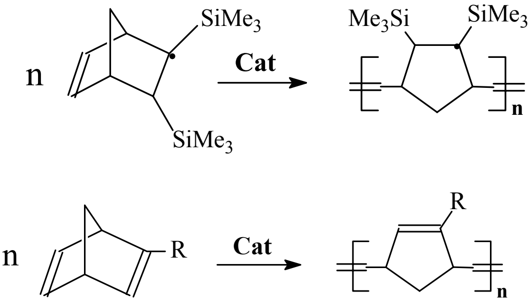

R= $-SiMe_3$, $-SiMe_2(CH_2)_3SiMe_3$, $-SiCl_3$

Scheme 3

Table 1. ROMP of silicon-containing norbornenes and norbornadienes

Monomer	Catalyst	[M]/[cat] m/m	Solvent	T °C	τ, h	Yield, %	Mw	Mw/ Mn	*Cis,* %
[14,15] 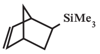	$RuCl_3{\cdot}3H_2O$	160	C_2H_5OH, PhCl	60	15	84	(2,4)**	-	-
	$RuCl_2(PPh_3)_3$	180	PhCl	60	15	63	(1,5)**	-	-
	$Cl_2Ru(=CHPh)(PCy_3)_2$	720	PhCl	25	21	98	356000	2,4	-
	WCl_6/TMDSB*	1000	$PhCH_3$	20	2	99	(4,0)**	-	
[16] 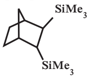	$RuCl_3$	80	C_2H_5OH, PhCl	75	12	73	633000	1,7	5
	$RuCl_2(PPh_3)_3$	80	PhCl	75	26	83	452500	2,0	9
	WCl_6/ TMDSB	50	$PhCH_3$	20	2	93	291400	3,1	54
[14] 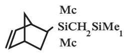	$WCl_6/PhC{\equiv}CH$	750	$PhCH_3$	20	3	81	(2,0)**	-	-
[16] 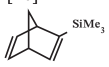	WCl_6/TMDSB	250	$PhCH_3$	20	10	70	539000	3,1	-
[16] 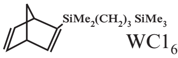	$WC1_6$/TMDSB	92	$PhCH_3$	20	48	50	318700	4,0	43

* TMDSB: 1,1,3,3-tetramethyldisilacyclobutane

** [η], dL/g, toluene, 30°C

The investigation of gas permeability of the obtained polymers gave an opportunity to find out some correlations between polymer structure and its properties (Table 2). Introduction of $SiMe_3$ pendant groups in ROMP polynorbornenes substantially increases permeability coefficients for light gases. At the same time the permselectivity for some gas pairs also increases, while in the majority of cases an increase in permeability is accompanied by reduced permselectivity and vice versa. It should be noted that *cis* or *trans* content in the obtained polycyclopentylenevinylenes did not exert some influence on the gas transport parameters [17].

The double bond in five-membered ring of the main chain does not cause noticeable changes in gas permeability. An interesting negative effect was observed for polynorbornene containing two silicon atoms in the same side group ($Si(CH_3)_2CH_2Si(CH_3)_3$). It is likely related with self-plasticization caused by long pendant group: T_g of this polymer decreased down to 24°C, whereas

Table 2. Gas transport parameters of glassy polycarbosilanes

	Tg (°C)	P, Barrer						α=Pi/Pj				
		H_2	O_2	N_2	CO_2	CH_4	C_2H_6	H_2/N_2	H_2/CH_4	O_2/N_2	CO_2/CH_4	CH_4/C_2H_6
1	31	21	2,8	1,5	15,4	2,5	1,4	14,4	8,6	1,9	6,3	1,8
2	113	140	30	7,2	89	17	7	19,4	8,2	4,2	5,2	2,4
3	108	81	20	4,9	64	8,5	4,5	16,5	9,5	4,1	7,5	1,9
4	24	73	16	3,7	67	8,5	10	19,7	8,6	4,3	7,9	0,85
5	5			R	U	B	B	E	R	Y		
6	167	375	95	25	445	45	30	15	8,3	3,8	9,9	1,5
7	150	-	44	11	-	-	-	-	-	-	4	-

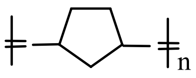

1

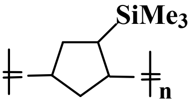

2

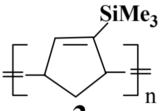

3

4

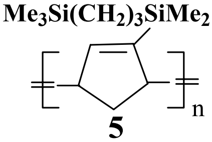

5

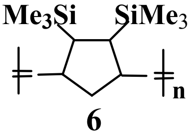

6

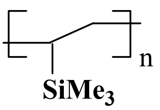

7

the glass transition temperature of poly(trimethylsilylnorbornene) is in the range of 101–113°C. Polynorbornadiene with a long substituent shows even lower glass transition temperature 5°C, which is typical for rubbers.

Entirely different result was observed for the polymer containing two adjacent $Si(CH_3)_3$ groups, attached to different sites within repeat unit. Introduction of the second $Si(CH_3)_3$ group in the polynorbornene main chain is accompanied by approximately the same increase in permeability as for the first $Si(CH_3)_3$ group. It is rather uncommon case when a significant increase in permeability with no reduction of permselectivity is observed. The highest T_g of this polymer indicates more rigidity of its structure. Probably the increased permeability means that more rigid chains of this polymer cannot be packed efficiently and larger free volume is responsible for high permeability. So, we can use the polymers with rigid chains as another way of constructing high permeable materials. The search for rigid structure polymers prompted us to study addition polymerization of silyl-containing norbornenes (see Section 4).

4. Rubbery ROP polysilalkylenes for separation of hydrocarbons

The separation of hydrocarbon mixtures C_1–C_4 can be realized with polymeric films in which gas transport is mainly determined by thermodynamic factors, i.e. solubility coefficients. Membranes based on elastomers, for example, weakly cross-linked polydimethylsiloxane with the highest permeability coefficients [18] among rubbers, are used presently for this purpose. At the same time, Si–O bonds are known to possess a noticeable chemical activity [19], which can limit the sphere of practical use of polysiloxane-based membrane materials.

For the separation of natural and casing-head gases, it seemed of interest to study heterochain polycarbosilanes viz., polysilmethylenes and polysiltrimethylenes containing Si–C bonds in the main chain

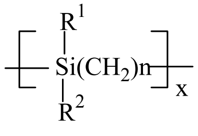

$$\left[-\overset{R^1}{\underset{R^2}{Si}}(CH_2)_n - \right]_x \qquad n=1,3$$

It is known that these substances are chemostable and thermostable elastomers with low glass transition temperatures [12]. Since low gas transition temperatures cause, as a rule, higher permeability coefficients, the rubbery [20,21] polysilmethylenes and polysiltrimethylenes seem to be potential membrane materials for separation of gaseous hydrocarbons according to molecular masses.

The purpose of this part of the work is to obtain new polycarbosilane polymers and systematically study their gas separation properties.

Polysilmethylenes (P1) and a series of polysiltrimethylenes (P2–P7) with different substituents at the silicon atom were synthesized by thermal and catalytic polymerization of monomers M1–M7 (Scheme 4).

Silacyclobutane monomers with various substituents at the Si atom are much more accessible than Si-substituted disilacyclobutanes. Correspondingly, the related siltrimethylene polymers are also more accessible.

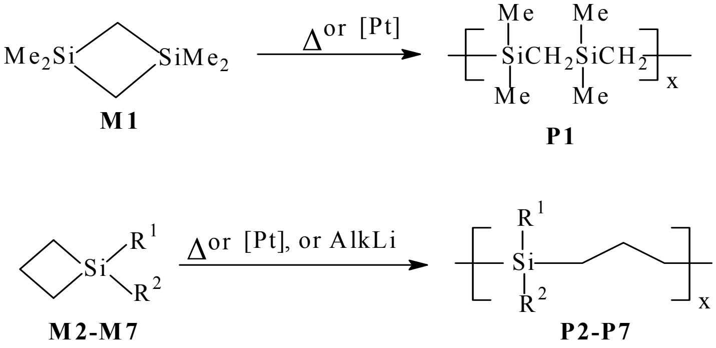

Scheme 4

Compound	R^1	R^2
M2, P2	Me	Me
M3, P3	CH_2SiMe_2Ph	CH_2SiMe_2Ph
M4, P4	Me	CH_2SiMe_3
M5, P5	Me	$(CH_2)_3SiMe_3$
M6, P6	Me	m-Tolyl
M7, P7	α-Naphthyl	Cyclohexyl

Therefore, series of polysiltrimethylenes were studied for ascertainment of correlation between polymer membrane properties and their structure. According to the Scheme 4 ring-opening polymerization (ROP) performed both by thermal and catalytic initiation [22–24]. As a result families of polysiltrimethylenes bearing different groups at Si atom (P2–P7) as well as the polysilmethylene (P1) were prepared.

The permeability for hydrocarbon gases was studied on the synthesized polysilalkylenes supported by polysulfone and polyamide porous hollow fibers (Table 3).

The permeability of the membranes, $Q = P/l$ (P is the permeability coefficient and l is the efficient thickness of the selective layer) depends on the thickness of the selective layer, pore size in the polymer support, degree of penetration of the membrane material into pores, and resistance in the porous sublayer. In the first approximation, for the series of membranes of the same type, the permeability can characterize, more or less correctly the transport properties of a polymer in the selective layer.

We found that polydimethylsilmethylene (P1) possesses high gas permeability combined with high selectivity for the butane–methane pair (α ~40). The physicochemical properties of polysiltrimethylenes and polydimethylsilmethylene and their gas-separation characteristics with respect to methane and butane are presented in Table 3.

Table 3. Permeability of polymers and ideal separation factors for composite hollow fiber membranes (20°C)

	Mol.W. (M_w/M_n)	T_g, ^oC	Hollow Fiber	$P/l(l/m^2\ h\ atm)$		$P/l(l/m^2\ h\ atm)$		α C_4H_{10}/CH_4
				O_2	N_2	C_4H_{10}	CH_4	
P1	357000 (3.43)	-92	PSF	79.6	39.8	3650	94.0	38.8
P1	1600000 (1.13)	-92	PA	55.1	20.5	2219	61.4	36.1
P2	1400000 (1.16)	-75	PA	14.1	5.79	457	16.8	27.2
P3	1200000 (2.4)	-36	PA	71.9	29.9	1294	85.1	15.2
P4	1650000 (1.14)	-51	PA	5.04	2.0	194	6.91	28.1
P5	1420000 (1.2)	-46	PA	8.26	3.56	118	4.5	26.2
P6	760000 (1.44)	-25	PA	4.15	1.85	76.4	4.36	17.5
P7	270000 (2.53)	47.5	PA	4.37	1.38	7.4	6.1	1.2

PSF – membrane supported by polysulfone hollow fibers; PA – membrane supported by polyamide hollow fibers

However, it turned out to be that even a high-molecular weight sample of P1 (M_w up to 1×10^6) forms no free-standing films. The selectivity of polydimethylsiltrimethylene P2 (β ~27) is somewhat lower. At the same time, this crystalline polymer exhibited well film-forming properties. Due to the "magic" trimethylsilyl groups located at some distances from the Si atom of the main chain in polymers P4 and P5, these polysiltrimethylenes retain high selectivities for the butane–methane pair (α 28.1 and 26.2), respectively and remain elastomers with glass transition temperatures of –51°C and –46°C, respectively. However, the permeability with respect to butane for the best of these polymers (P4) was almost 20-fold lower than that for P1. The selectivity with respect to hydrocarbons was more than twofold smaller for polysiltrimethylene with two bulky substituents (P3) (T_g = –36°C) and (P6) (T_g = –25°C). Finally, the selectivity and permeability decrease sharply for the glassy polymer with bulky cyclohexyl and α-naphthyl groups (P7) (T_g = +47.5°C).

Table 4. Permeability coefficients of polysilalkylenes at 25°C: homopolymeres and statistical copolymers

Polymer	*P*/Barrer*											
	O_2	N_2	CH_4	C_2H_6			C_3H_8			n-C_4H_{10}		
				$p \to 0$	$\Delta p \to 0$	$\Delta p \to 0.4$	$p \to 0$	$\Delta p \to 0$	$\Delta p \to 0.4$	$p \to 0$	$\Delta p \to 0$	$\Delta p \to 0.4$
P1[a]	99	40	130	-	345	364	-	434	837	-	1361	2807
P2[b]	9.5	3.0	8.4	10.6	-	26	13.5	-	37	14.3	-	240
CP3 (50/50)[a]	69	27	90	-	239	265	-	295	636	-	753	1748
CP3 (75/25)[b]	104	39	113	310	-	335	449	-	547	1163	-	2340
P1 **	100	45	130	-	390	-	-	850	-	-	-	-

*1 Barrer = $10^{-11} cm^3(n.c.) cm^{-2} s^{-1} Torr^{-1}$.

[a] Voumetric measurements at a pressure behind the membrane of 1 atm.

[b] Mass spectrometric measurements at a pressure behind the membrane of 10^{-3} Torr.

**- [34]

So, membrane parameters to hydrocarbon gases became worse when elastomers acquired thermoplastic properties. At the same time, the selectivity with respect to oxygen and nitrogen of glassy polysiltrimethylene P7 is somewhat higher. Polydimethylsilmethylene (P1) is the most promising polymer for use as a material separating hydrocarbon gases (Table 4).

It should be mentioned that the modern technology of gas separation on porous hollow-fiber membranes requires small amounts of a supported polymeric material, which holds promise for the practical use of comparatively expensive polysilmethylenes and polysiltrimethylenes.

The further studies of polydimethylsilmethylene (P1) were aimed at eliminating its main disadvantage: poor mechanical characteristics which prevent the formation of stable films. A solution of this problem has been achieved by copolymerization of dimethylsilacyclobutane and tetramethyldisilacyclobutane in the presence of Pt catalyst [13] (Scheme 5).

Both homopolymers (P1) and (P2) had high permeability and selectivity with respect to hydrocarbon gases. On the other hand the homopolymer (P2) possesses a high degree of crystallinity; therefore, one can expect a decrease in the fluidity of the copolymer with statistical distribution of units P1 and P2. It seemed promising to combine the valuable properties of P1, first of all, high selectivity to hydrocarbon gases, with the film-forming ability of P2.

We synthesized for the first time the corresponding copolymers by copolymerization of methyl derivatives of monosilacyclobutane and disilacyclobutane (M2 and M1) (Scheme 5). The process can be thermally or catalytically initiated.

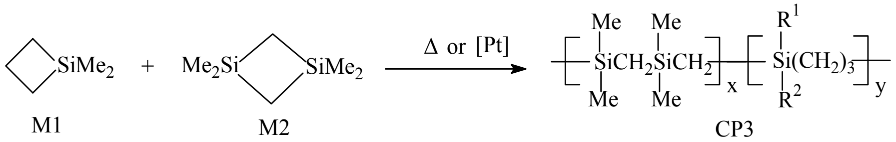

Scheme 5

The copolymerization of M1 and M2 occurs successfully at 7–15°C at a monomer to catalyst ratio of 10^4:1. We confirmed that the copolymerization produces real copolymers (CP3) with statistical unit distribution. This unambiguously followed from the presence of only one glass transition point in the differential scanning calorimetry (DSC) curves for each copolymer (no melting peaks), while the specially prepared mixtures of P1 and P2 with the same compositions show two glass transition points of both homopolymers. The compositions of copolymers CP3 were determined by ^{1}H NMR spectroscopy from the ratio of integral intensities of signals for the protons of the "integral" methylene groups of the siltrimethylene units (δ ~1.33 in $CDCl_3$) and signals for the protons of the methyl groups at the silicon atom (δ – 0.28÷0.06). Some properties of the prepared copolymers CP3 of different compositions are presented in Table 5.

Table 5. Properties of copolymers M1 with M2

Copolymer	x/y	M_w	M_w/M_n	T_g (°C)
	80/20	740,000	1.43	–83
CP3	75/25	210,000	1.87	–79.5
	50/50	88,500	2.1	–76.5

The copolymers had good film-forming properties and high gas transport parameters. This especially concerns to the 1:1 copolymer. In this case, the

selectivity (α) with respect to the butane–methane pair is ~20 combined with high permeability. It is most likely that such a happy situation where the copolymer acquires valuable properties of both homopolymers is explained by the fact that the homopolymers have similar chemical nature.
Statistical copolymers CP3 obtained at the relatively high content of P1 units have an amorphous structure and rather low T_g. In this case, the permeability coefficients differ slightly from the coefficients for P1 and, finally, demonstrate perfect film-forming properties. The permeability coefficients P for n-alkanes C_1–C_4 and air components are presented in Table 4.

4. Glassy addition Si-containing polynorbornenes for separation of hydrocarbons

Addition polymerization of norbornene and its derivatives proceeds with opening the double bond. It leads to completely saturated polymers with bicyclic repeat units (Scheme 6). Addition polynorbornene possessing rigid structure is characterized with glass transition temperature higher than its destruction temperature, which is 350°C.

We studied a behavior of 5-trimethylsilyl-2-norbornene under the conditions of addition polymerization initiated by some Ni- and Pd-containing catalytic systems. The catalysts of this type have already demonstrated high activity in addition polymerization of norbornene and its alkyl derivatives [25,26]. The known Pd-containing catalytic systems: $\{(\eta^3\text{-allyl})Pd(SbF_6)\}$ [27] and σ,π-bicyclic complex $[NB(OMe)PdCl]_2$ [28] turned out to be practically inactive in polymerization of 5-trimethylsilyl-2-norbornene. On the contrary, Ni-based complexes displayed a real activity in respect to this monomer. As a result saturated cyclolinear polymers were formed according to Scheme 6 of addition polymerization. The absence of any unsaturation in these polymers was confirmed by both infrared (IR) (no bands in 1620–1680 cm^{-1} region) and ^1H NMR spectroscopy (no signals at 5–6 ppm).

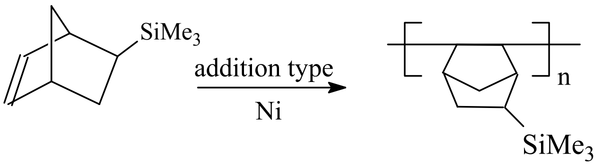

Scheme 6

Some details of polymerization process are represented in Table 6. Addition poly(5-trimethylsilyl-2-norbornenes) were obtained with the yields up to 80%. All of them were completely soluble in aromatic solvents. Among the Ni-based catalytic systems presented in Table 6.

Table 6. Addition polymerization of 5-trimethylsilylnorbornene

Catalyst	[M]/[cat] mol/mol	Time, h	Polymer yield, %	Conversion of isomers %[a]		Mw[b]	Mw/Mn
				exo	endo		
(π-$C_5H_9NiCl)_2$/ $Et_3Al_2Cl_3$ Al/Ni=3	600	48	56	83	28	41000	1,7
	1000	120	8	15	1	-	-
(π-$C_5H_9NiCl)_2$/ MAO MAO/Ni=100	600	96	80	98	61	104000	1,8
	1000	19	64	100	28	152000	1,7
$(Nph)_2Ni$ / MAO MAO/Ni=100	600	27	63	86	40	248000	2,4
	1000	24	56	69	27	260000	2,0
	1500	24	55	-	-	263000	2,9
	3000	24	32	40	24	277000	2,9
$(PPh_3)_4Ni$ / Et_2OBF_3 B/Ni=300	600	27	12	-	-	20000	1,7
	1000	24	1,4	-	-	-	-

[a] Determined by GLC of final reaction mixture

[b] Determined by GPC relative to polystyrene standards, $T = 20°C$

Table 6, Ni(II)naphtenate–methylaluminoxane (MAO) and (π-$C_5H_9NiCl)_2$–MAO were more active. Polymers prepared in the presence of Ni(II)naphtenate–MAO catalyst had the highest molecular weights and demonstrated better film-forming properties. They did not show any glass transition up to 340°C (DSC). Gas–liquid chromatography (GLC) analysis of the final polymerization mixtures indicated that in the course of the reaction *exo*-conformer was consumed much faster than *endo*-form independently of the type of catalytic system employed. It should be noted that polymerization of 5-trimethylsilyl-2-norbornene proceeded substantially slower than that of unsubstituted norbornene.

Copolymerization of 5-trimethylsilyl-2-norbornene with 5-*n*-hexyl-2-norbornene (HexNB)was another way which was used for improving film-forming properties (Scheme 7). It is known that incorporation of long-pendant substituent should plasticize the polymer. Addition copolymer of 5-trimethylsilyl-2-norbornene ($SiMe_3NB$) with HexNB synthesized in the presence of Ni(II)naphtenate–MAO with yields 60–70% contained about 40–50% of the units with *n*-hexyl substituent [29,30]. GPC analysis confirmed the formation of copolymers by demonstrating unimodal and rather narrow molecular mass distribution for all the polymers obtained in this study. So, the copolymer with higher molecular weight (M_w = 440,000) and better film-forming properties was obtained.

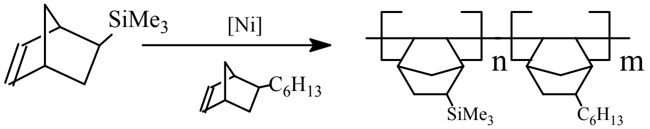

Scheme 7

Table 7 presents permeability coefficients of addition polynorbornenes with different side groups including $SiMe_3$ substituent synthesized in this work and those described earlier. It is seen that poly(5-trimethylsilyl-2-norbornene) is characterized by much higher gas permeability coefficients than other polynorbornenes. So, an increase in the *P* values due to replacement of CH_3 by

Table 7. Gas-transport parameters of addition polynorbornenes

Polymer	P, Barrer						$\alpha=P_i/P_j$			
	T_g °C	O_2	N_2	CO_2	CH_4	C_4H_{10}	O_2/N_2	CO_2/CH_4	H_2/CH_4	C_4H_{10}/CH_4
8	>350	6,9	1,5	33,6	2,6	-	4,6	12,9	16	-
9*)	>380	502	89,2	396	30,3	-	3,7	13,1	16,6	-
10	>340	780	297	4350	790	21846	2,6	5,5	2,1	22
11	>340	60	19	330	48	-	3,2	6,9	3,4	-
12*)	280	20	6,9	84	18,7	-	2,9	4,5	3,0	-
13	>260	9000	6600	27000	15500	80050	1,4	1,7	1,0	5,2

**[32]

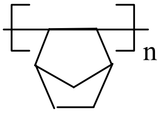

8

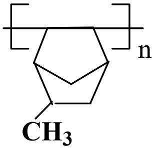

9

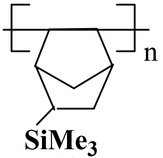

10

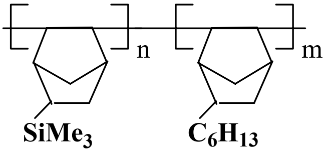

11

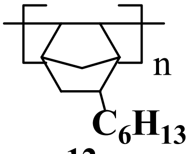

12

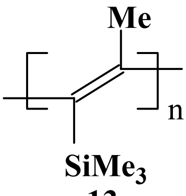

13

$Si(CH_3)_3$ substituent can be as large as two orders. The copolymer of $SiMe_3NB$ and HexNB characterized by lower gas permeability coefficients than homopolymer of $SiMe_3NB$, but higher, than homopolymer of HexNB. Permselectivity or separation factors $\alpha(M_1/M_2) = P(M_1)/P(M_2)$ are compared in Table 7 for addition poly(5-trimethylsilylnorbornene) and some other polymers. It is seen that in the most cases addition poly(5-trimethylsilyl-2-norbornene) is more permselective than high permeability polymer polytrimethylsilylpropyne (PTMSP).

An interesting peculiarity that can be potentially important from the practical viewpoint is solubility-controlled selectivity of some high permeability, high free-volume polymers revealed in separation of hydrocarbons according their molecular mass. As permeability coefficients can be presented as the product $P = DS$, the variations of the P values for the series of penetrants can be ascribed to corresponding trends of the D and S values [31].

In conventional glassy polymers, size sieving or mobility selectivity, which is determined by the variations of the diffusion coefficients, prevails, so the separation factors, reveal higher permeation rates of lighter components, e.g. $\alpha(C_4H_{10}/CH_4)$, <1. On the other hand, in rubbers the diffusion coefficients only weakly depend on the penetrant size, so the opposite inequality $\alpha(C_4H_{10}/CH_4) > 1$ is valid, because the solubility coefficient become a parameter more sensitive to penetrant size and properties. It is important that in some high free-volume glassy polymers (first and foremost, PTMSP) also solubility-controlled permeation behavior is observed [33].

Acknowledgment

This work was supported by RFBI Project 05-03-32369.

References

[1] Yampolskii, Yu.P., Pinnau, I., Freeman, B.D. (2006) Materials Science of Membranes for Gas and Vapor Separation, Wiley, New York, p. 1.
[2] Plate, N.A., Yampolskii, Yu.P. (1994) In: Paul, D.R., Yampolskii, Yu.P. (eds), Polymeric Gas Separation Membranes, CRC Press, Boca Raton, FL, 1994, p. 155.
[3] Cunico, R.F. (1971) J. Org. Chem. 36:929.
[4] Finkelshtein, E.Sh., Makovetskii, K.L., Yampolskii, Yu.P., Portnykh, E.B., Ostrovskaya, I.Ya., Kaliuzhnyi, N.E., Pritula, N.A., Gol'berg, A.I., Yatsenko, M.S., Plate, N.A. (1991) Makromol. Chem. 192:1.
[5] Finkelshtein, E.Sh. (1995) Polym. Sci. Ser. B 37:185.

[6] Rogan, Ju.V., Gringolts, M.L., Ushakov, N.V., Yampol'skii, Yu.P., Finkelshtein, E.Sh. (2003) In: İmamoğlu, Y., Bencze, L. (eds), Novel Metathesis Chemistry: Well-Defined Initiator Systems for Specialty Chemical Synthesis, Tailored Polymers and Advanced Material Applications, Kluwer Academic, Dordrecht, p. 341.

[7] Finkelshtein, E.Sh., Ushakov, N.V., Pritula, N.A., Andreev, E.A., Plate, N.A. (1992) Izv. Akad. Nauk SSSR, Ser. Khim. 41:223 [Bull. Russ. Acad. Sci., Div. Chem. Sci. 1992, 41:185 (Eng. Trans.)].

[8] Vdovin, V.M., Nametkin, N.S., Grinberg, P.L. (1963) Dokl. Akad. Nauk SSSR 150:799 [Dokl. Chem. USSR 1963].

[9] Kriner, W.A. (1964) J. Org. Chem. 29:1601.

[10] Ushakov, N.V., Vdovin, V.M. (1978) Izv. Akad. Nauk SSSR, Ser. Khim. 27:1686 [Bull. Russ. Acad. Sci., Div. Chem. Sci. 1978, 27:1868 (Eng. Trans.)].

[11] Nametkin, N.S., Ushakov, N.V., Vdovin, V.M. (1974) J. Gen. Chem. USSR 44:1970.

[12] Ushakov, N.V., Finkelshtein, E.Sh., Babich, E.D. (1995) Vysokomol. Soedin. Ser. A 37:470 [Polym. Sci. Ser. A 1995, 37:3209 (Eng. Trans.)].

[13] Finkelshtein, E.sh., Ushakov, N.V., Krasheninnikov, E.G., Yampolskii, Yu.P. (2004) Russ. Chem. Bull., Int. Ed. 53:1.

[14] Portnykh, E.B., Makovetskii, K.L., Ostrovskaya, I.Ya., Bespalova, N.B., Yampolskii, Yu.P. (1998) Synthesis of membrane materials by ROMP of norbornenes, in: İmamoğlu, Y. (ed.), Metathesis Polymerization of Olefins and Polymerization of Alkynes, Kluwer Academic, Dordrecht, pp. 189–199.

[15] Makovetskii, K.L., Finkelshtein, E.Sh., Ostrovskaya, I.Ya., Portnykh, E.B., Gorbacheva, L.I., Golberg, A.I., Ushakov, N.V., Yampolskii, Yu.P. (1992) J. Mol. Catal. 76:107.

[16] Finkelshtein, E.Sh., Gringolts, M.L., Ushakov, N.V., Lakhtin, V.G., Soloviev, S.A., Yampolskii, Yu.P. (2003) Polymer 44:2843.

[17] Yampolskii, Yu.P., Finkelshtein, E.Sh., Makovetskii, K.L., Bondar, V.I., Shantarovich, V.P. (1996) J. Appl. Polym. Sci. 62:349.

[18] Plate, N.A., Yampolskii, Yu.P. (1994) In: Paul, D.R., Yampolskii, Yu.P. (eds), Polymeric Gas Separation membranes, CRC Press, Boca Raton, FL, p. 155.

[19] Voronkov, M.G., Mileshkevich, V.P., Yuzhelevskii, Yu.A. (1976) Siloxanovaya svyaz [Siloxane Bond] Nauka Novosibirsk (in Russian).

[20] Van Amerongen, G.J. (1964) Rubber Chem. Technol. 37:1065.

[21] Yampolskii, Yu.P., Durgar'yan, S.G., Nametkin, N.S. (1982) Vysokomol. Soedin. Ser. A:536 [Polym. Sci. Ser. A 1995, 24 (Eng. Trans.)].

[22] Kriner, W.A. (1966) J. Pol. Sci. 4:444.

[23] Nametkin, N.S., Vdovin, V.M., Zav'alov, V.I. (1965) Izv. Akad. Nauk SSSR Ser. Khim. 1448 [Bull. Acad. Sci. USSR Div. Chem. Sci. 1965:14 (Eng. Trans.)].

[24] Radugina, Yu.E., Sakharova, I.N., Avilov, G.V., Uspenskii, V.I., Nametkin, N.S., Kargin, V.A., Vdovin, V.M., Ushakov, N.V., Zav'alov, V.I., Zelenaya, A.V. (1973) Autors Certificate 225015 USSR; Byul. Izobret. [Invention Bulletin] 1973,10 (in Russian); Radugina, Yu.E., Sakharova, I.N., Avilov, G.V., Uspenskii, V.I., Nametkin, N.S., Kargin, V.A., Vdovin, V.M., Ushakov, N.V., Pushchevaya, K.S., Zav'alov, V.I., Zelenaya, A.V. Autors Certificate 228525 USSR; Byul. Izobret. [Invention Bulletin] 1973:5 (in Russian).

[25] Janiak, C., Lassahn, P.G. (2001) J. Mol. Cat. A 166:193.

[26] Makovetsky, K.L. (1999) Polym. Sci. Ser. B 41:269.

[27] Mathew, J.P., Reinmuth, A., Melia, J., Swords, N., Risse, W. (1996) Macromolecules 29:2755.

[28] Green, M., Hancock, R. (1967) J. Chem. Soc. A:2054.

[29] Finkelshtein, E.Sh., Makovetskii, K.L., Gringolts, M.L., Rogan, Y.V., Golenko, T.G., Lakhtin, V.G., Filatova, M.P. (2006) J. Mol. Cat. 257:9.

[30] Finkelshtein, E.Sh., Makovetskii, K.L., Gringolts, M.L., Rogan, Yu.V., Golenko, T.G., Starannikova, L.E., Yampolskii, Yu.P., Shantarovich, V.P., Suzuki, T. (2006) Macromolecules 39:7022.

[31] Freeman, B., Pinnau, I. (1997) Trends Polym. Sci. 5:167.

[32] Dorkenoo, K.D., Pfromm, P.H., Rezac, M.E. (1998) J. Polym. Sci. Part B: Polym. Phys. 36:797.

[33] Merkel, T.C., Bondar, V., Nagai, K., Freeman, B.D. (2000) J. Polym. Sci. Part B: Polym. Phys. 38:273.

[34] Stern, S.A., Shah, V.M., Hardy, B.J. (1987) J. Polym. Sci. Part B: Polym. Phys. 25:1263.

POLYDIPHENYLACETYLENE WITH SCHIFF BASE END GROUPS: SYNTHESIS AND CHARACTERIZATION

RADOSTINA KALINOVA, CHRISTO JOSSIFOV

Institute of Polymers, Bulgarian Academy of Sciences, Acad. G. Bonchev str. 103A, 1113 Sofia, Bulgaria

Abstract: The carbonyl–olefin exchange reaction is a new reaction between carbonyl group and olefin double bond, which has a formal similarity with the olefin metathesis – one carbon atom in the latter is replaced with an oxygen atom. Till now the new reaction is performed successfully only when the two functional groups (carbonyl group and olefin double bond) are in one molecule and are conjugated. The α,β-unsaturated carbonyl compounds (substituted propenones) are the compounds with such a structure. They polymerize giving substituted polyacetylenes. The chain propagation step of this polymerization is in fact the carbonyl–olefin exchange reaction.[1] The question arises: is it possible the carbonyl–olefin exchange reaction to take place when the two functional groups are not in one molecule and are not conjugated, and could this reaction become an alternative of the existing carbonyl olefination reactions?

1. Introduction

Rigid polymers with conjugated main chain (polyacetylenes, polyphenylenes, polyphenylene vinylenes, polypyrrole, polythiophene, polyaniline) are a research topic of high activity.[1] "Conjugation and no end" was originally an idealized concept, but it turned out that only short segments with effective conjugation length exists even in very long, fully conjugated chains without any structural deficiencies. Thus optical, electrical, and optoelectrical properties of high molecular weight polymers are nearly the same as the properties of oligomers with a sufficient chain length. The effect of end-groups on the bulk material properties is low to negligible in the case of high molecular weight polymers. However, this effect can be fairly pronounced in short-chain polymers. It is clear that the mechanical and thermal stability of the oligomers is rather poor. It is interesting to incorporate well-defined oligomers into a polymeric chain in order to create polymers with isolated electroactive and photoactive moieties, i.e. to synthesize rod-coil or segmented conjugated polymers.[2] These materials combine the good mechanical properties and processability of high molecular weight polymers with the interesting and tunable electrical, electrochemical, and optoelectrical properties of the conjugated polymers.[3]

Y. İmamoğlu and V. Dragutan (eds.), Metathesis Chemistry: From Nanostructure Design to Synthesis of Advanced Materials, 413-420.

The polymeric Schiff bases are interesting group of conjugated polymers having carbon–nitrogen double bonded units in the main chain, capable of protonation and complexation. They have been studied intensively owing to their properties: good thermal stability, mechanical strength, nonlinear optical properties, ability to form metal chelates, semiconducting properties, environmental stability, and fiber-forming properties, which are associated mainly with their conjugated backbone and the presence of imine sites.[4] These polymers could become new materials suitable for use in polymer electronics, especially in view of a recent discovery that the photoluminescence of conjugated polymers containing basic sites in the main chain can be strongly modified by protonic (acid–base) doping.[5]

The polymeric Schiff bases are synthesized mainly by a polycondensation reaction between a diamine or hydrazine and a dialdehyde or diketone, and have the general structure (Scheme 1):

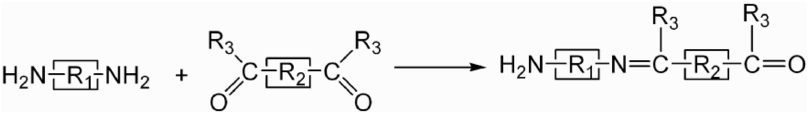

1 **2**

Here R_1, R_2 can be aryl or alkyl, R_3 can be aryl, alkyl or H

Scheme 1

These polymers are also named polyazomethines or polyazines when diamines and hydrazine, respectively, are used in a reaction between dialdehyde compounds and polyketamines or polyketazines when diketones are used as dicarbonyl compounds in reaction with diamine or hydrazine. The interest in this class of polymers has been renewed in the last few years because aromatic polyazomethines and poly(*p*-phenylenevinylene), the first electroluminescent polymer, are isoelectronic as well as the polyazin, synthesized from glioxal and hydrazine, is a nitrogen containing analogue of polyacetylene.

When R_1 and R_2 in Scheme 1 are aryls, then fully conjugated polymers are obtained. A major drawback of such polymers is their limited solubility in most organic solvents. High molecular weight polymers cannot be obtained because the growing macromolecular chain comes out of solution during the polycondensation at low polymerization degree. There are some general methods used to improve the solubility of the polymeric Schiff bases, such as: Insertion of flexible spacer between main chain aromatic rings (the result is segmented poly(Schiff bases)); introduction of pendant groups, i.e. aromatic or alkyl substituents, onto the polymer chain; introduction of structural irregularities as kinks, bents, crankshaft-shaped units, etc.

All that said above evokes the following idea: if **2** in Scheme 1 is any conjugated oligomer possessing carbonyl end groups, and **1** is any aliphatic diamine, the result would be a segmented conjugated polymer possessing carbon–nitrogen double bonded units in the main chain. Such a product would combine the properties of both the conjugated polymer and the soft segment with the properties of the Schiff bases.

The present paper reports the results of our first attempts in realization of this idea.

2. Result and discussion

In the last decade a new synthetic route to oligomeric polydiphenylacetylene has been developed on the bases of carbonyl–olefin exchange reaction and reductive coupling of conjugated dicarbonyl compounds.[5] The oligomers thus prepared are well soluble, stable in air, and they still possess the physical properties of the conjugated polymers. This approach provides the possibility to synthesize polydiphenylacetylenes with different end groups[6,7] (Scheme 2). Their photoluminescent and photoelectrical properties have been investigated.[8]

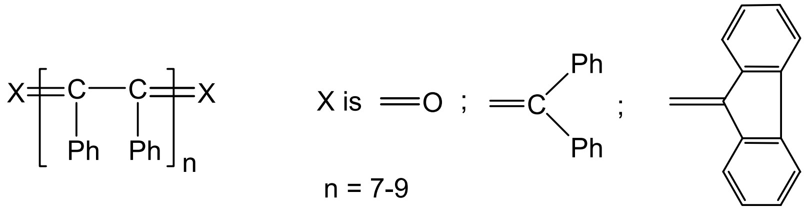

Scheme 2

The oligomeric polydiphenylacetylene possessing carbonyl end groups (P1) was obtained via polymerization of benzil under the influence of the Friedel–Crafts olefin metathesis catalytic system $WCl_6 + AlCl_3$ (Scheme 3).

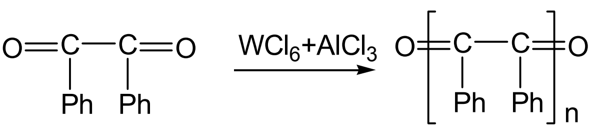

(P1)

Scheme 3

The monomer and the oligomer are very convenient for the realization of our idea.

Generally the polycondensation reactions of diamines with dicarbonyl compounds have some disadvantages, among them the requirement of meeting specific reaction conditions. That is why we have tried to copolymerize some diamines (1,4-diaminobutane, 1,6-diaminohexane, and poly(propylene glycol)bis(2-aminopropylether)) with molecular weight 2000) with benzil (Chart 1) and with polydiphenylacetylene with carbonyl end groups (Chart 2) varying the solvent (ethanol, tetrahydrofuran, *N*,*N*-dimethylformamide, cyclohexanol, or in bulk), the temperature (80–160°C), time (1–48 h) and the catalyst (*p*-toluenesulphonic acid, tin chloride, or without catalyst).

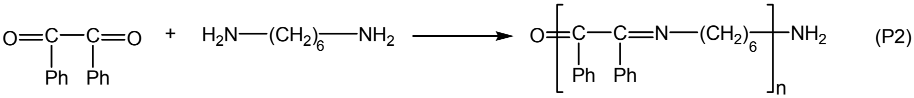

Chart 1. Synthesis of poly(Schiff base) from benzil.

Experimental conditions: t = 80°C, τ = 4 h, t =100°C, τ = 21 h, t =120°C, τ = 24 h, solvent: chlorobenzene, catalyst: $ZnCl_2$, yield: 62%, Mw = 1295

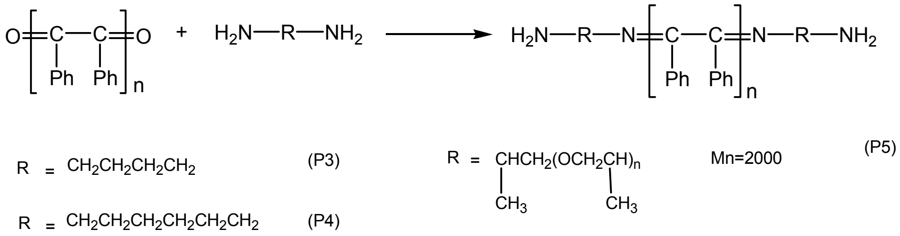

Chart 2. Synthesis of polydiphenylacetylene with Schiff base end groups.

Experimental conditions: P3 and P4: t =100°C, τ = 24h, Mw(P4)= 2513, P5: t = 100°C, τ = 24 h, t = 160°C, τ = 24 h, no solvent, Mw = 6899.

The optimal reaction conditions are given in the charts. The best solvent for polycondensation of benzil with diamines is chlorobenzene. Surprisingly the presence of acid catalysts does not improve substantially the yield of the products. According to the gel permeation chromatography (GPC), infrared (IR), and ^{1}H nuclear magnetic resonance (NMR) analyses the products thus obtained are oligomers, containing carbonyl, amine end C=N groups, (Figure 1).

Unlike benzil polydiphenylacetylene does not react with the diamines in any of the above mentioned solvents. We have succeeded in performing this reaction in bulk at higher temperatures.

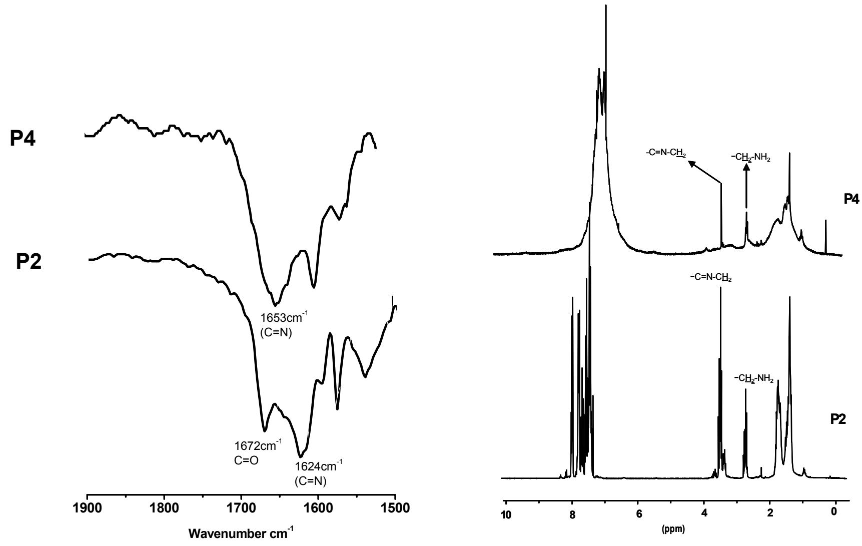

Figure1. IR and ^{1}H NMR spectra of P2 and P4.

The difference between the reactivity of the carbonyl groups of benzil and oligomeric polydiphenylacetylene is understandable. As a general rule the reactivity of bis-carbonyl compounds decreases in the order:

dialdehyde >diketone > quinone.

Because of the conjugation with the polyacetylene main chain the reactivity of the carbonyl end groups should be closer to those of the quinones.

When P1 was condensed with diamines the molecular weight of the products, measured by GPC Waters 244 apparatus with refractometer and ultraviolet–visible (UV–Vis) detectors and ultrastiragel columns, is almost equal to the sum of the conjugated oligomer and two amine molecules. In addition there are no carbonyl absorbances in IR spectra of the products (Figure 1). On the grounds of these facts we consider that polydiphenylacetylenes possessing Schiff base end groups are obtained.

The reaction products are isolated following the next procedure:

The reaction mixture was cooled down, dissolved in chloroform and precipitated in methanol. The powder was redissolved in chloroform, reprecipitated in methanol and dried under vacuum for 8 h. The yields were reasonable >50%. The structure of the reaction products was proved by IR and ^{1}H NMR analysis. During the reaction the intensities of the peaks for –CO and –NH_2 groups in IR spectra (1672 cm^{-1} and 3334 cm^{-1}, respectively) diminish and those for C=N (1624 cm^{-1}) group increase (Figure 2).

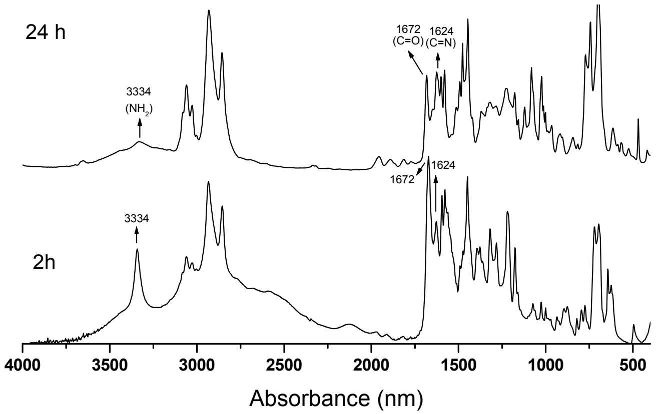

Figure 2. IR spectra taken at different stages of progress of the reaction between benzyl and 1,6-diaminohexane.

The products of the polycondensation of benzil with diamines have negligible photoluminescent properties even in solution, while the polydiphenylacetylenes with Schiff end groups exhibit photoluminescence comparable or higher than that of the starting polydiphenylacetylene (Figure 3).

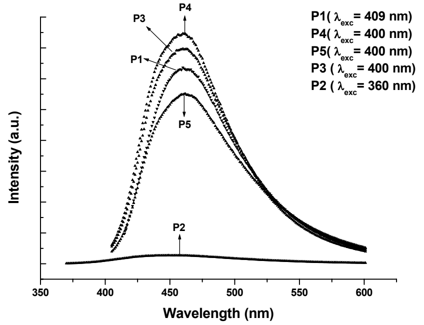

Figure 3. PL spectra of polydiphenylacetelene containing different Schiff base end groups in chloroform (concentration 0.02 g/L).

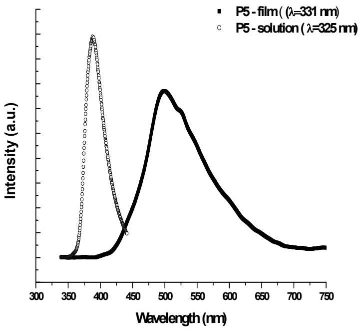

Figure 4. PL spectra of P5 sample in chloroform (concentration 0.02 g/L) and in film.

One of the latter newly synthesized products (P5) is photoluminescent not only in solution but in film as well (Figure 4). It is stable and amorphous up to 300°C, as the differential scanning calorimetry (DSC) analyses show (Figure 5).

Therefore it meets some of the basic requirements for electroluminescent polymers.

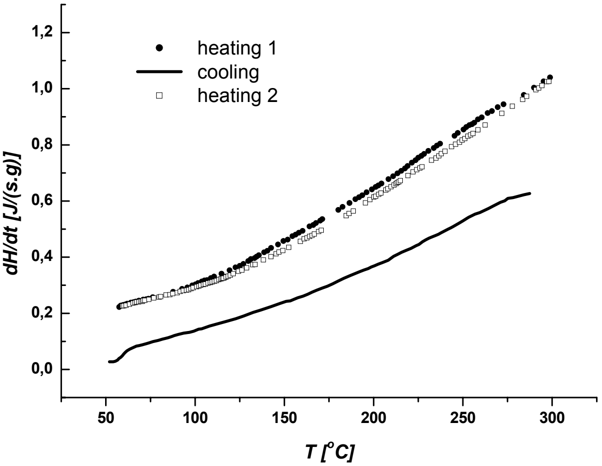

Figure 5. DSC curves of P5 sample, registered at a heating and cooling rate of 10°C min^{-1}

3. Conclusion

We have succeeded in synthesizing polydiphenylacetylene with Schiff base end groups with different length and structure. Their photoluminescent properties have been investigated. It is clear that better experimental conditions (proper solvent or solvent mixture, proper catalyst, etc.) are necessary for the preparation of poly(Schiff bases) with a similar structure. This is the aim of our future investigations.

Acknowledgments

The financial support of this work by the National Science Fund of the Bulgarian Ministry of Education and Science, project X-1413, is gratefully acknowledged

References

[1] Skotheim, T.A., Elsenbaumer, R.L., Reynolds, J.R., Handbook of Conducting Polymers, 2nd edn., Marcel Dekker, New York, 1998.
[2] Schopov, I., Sinigerski, V., Macromol. Symp. 1997, 121:35–51.
[3] Paul, L.B., Andrew, B.H., Arno K., Donald, D.C.B., Adam, R.B., Richard, H.F., Chem. Comm. 1992, 32–34.
[4] Grigoras, M., Catanescu, C., J. Macromol. Sci; Part C. Polym. Rev. 2004, C44:131.

[5] Iwan, A., Sek, D., Rannou, P., Kasperczyk, J., Janeczek, H., Mazurak Z., Pron, A., Sunth. Met. 2004, 143:331–339.
[6] Jossifov, C, in: Khosravi, E., Szymanska-Buzar, T. (eds) Ring Opening Metathesis Polymerization and Related Chemistry, NATO Science Series, II/56, 2002, pp. 425–436.
[7] Jossifov, C., Europ. Polym J. 1998, 34:883–885.
[8] Pavlik, M., Pfleger, J., Jossifov, C., J. Vohlidal, Macromol. Symp. 2004, 212:555–562.
[9] Pfleger, J., Pavlik, M., J. Vohlidal, React. Functional Polym. 2005, 65:79–91.

TWO-WAY INTRAMOLECULAR TRANSFER OF CHIRALITY IN ORGANOCOBALT COMPLEXES

CLAUDIA ZUCCHI[1], DAVIDE TURRINI[1], ROLAND BOESE[2],
LAJOS BENCZE[3], ROBERT KURDI[3], GEORG FRÁTER[4],
LUCIANO CAGLIOTI[5], GYULA PÁLYI[1]

[1]*Department of Chemistry, University of Modena and Reggio Emilia, Via Campi 183, I-41100 Modena, Italy*
[2]*Institute of Inorganic Chemistry, University of Essen, Universitätsstrasse 5-7, D-45117 Essen, Germany*
[3]*Müller Laboratory, Department of Organic Chemistry, University of Veszprém, Egyetem-utca 10, H-8200 Veszprém, Hungary*
[4]*Givaudan Roure Research Ltd., Überlandstrasse 138, CH-8600 Dübendorf, Switzerland*
[5]*Department of Chemistry and Technology of Biologically Active Compounds, University "La Sapienza" Roma, P.zale Moro 5, I-00185 Roma, Italy*

Abstract: $R^1OC(O)CH_2Co(CO)_3PR^2_3$ complexes (R^1 = *S*-EtOC(O)CH(CH_3), R^2 = Ph a; R^1 = (1S,2R,5S)-2-isopropyl-5-methylcyclohexyl, R^2 = Ph, b; R^1 = (1R,2S,5R)-2-isopropyl-5-methylcyclohexyl, R^2 = Ph, c; R^1 = isopropyl, R^2_3 = Ph_2{(1S,2S,5R)-2-isopropyl-5-methylcyclohexyl}, d) were prepared and characterised by analyses including IR, ^1H NMR, $^{13}C\{^1H\}$ NMR spectra, as well as by x-ray diffraction structure determination. Principles of self-organisation of chiral conformations were deduced from the structural data.

Keywords: alkylcobalt carbonyls, cooperative phenomena, intramolecular, chirality, conformations

1. Introduction

Preparation of new chiral compounds, with the aid of chiral auxiliaries is one of the central issues of present day organic chemistry. This goal has not only practical implications in pharmaceutical, fragrance/odour, or materials chemistry, but is also of crucial importance in fields such as theoretical biology or physical organic chemistry.

Transfer of the chiral information from one reactant or group to the product often proceeds through chiral (intermediary) conformers. In spite of the great importance of the aspects listed above, systematic efforts at the exploration of the mechanisms leading to such chiral conformations have dealt mostly with problems of bidentate ligands, while for the more "elementary" case of monodentate ligands, much less observations have been reported.

Y. İmamoğlu and V. Dragutan (eds.), Metathesis Chemistry: From Nanostructure Design to Synthesis of Advanced Materials, 421-439.

Our groups are exploring these mechanisms using mononuclear and dinuclear organocobalt complexes.

In the mononuclear series, complexes of the $ROC(O)CH_2Co(CO)_3PPh_3$ type, with R = achiral alkyl,[9f,h,i] (racemic) *sec*-butyl[9e] and glucosil groups[9g] were studied. The particular self-organisation of these complexes is due to the concerted rotation of more groups around some single bonds, which opens relatively low activation energy paths 9i which are asymmetric in the two possible directions. As a consequence of this situation transmission of chiral information though the achiral fragments of these molecules was observed. These (thermal) processes are reversible and free of errors, yielding, therefore, always racemates. Experience with the (R, S) *s*-Bu[9e] and glucosyl[9g] derivatives indicated that the study of complexes with centres of chirality in the ester group or in the phosphine ligand may lead to interesting new effects governing the self-organisation processes which are acting in the intramolecular transmission of the chiral information.

We present here preparative and structural studies on alkylcobalt carbonyl phosphine complexes with centres of configurational chirality in the alkyl- or in the phosphine ligand.

2. Experimental

All operations were performed according to the standard Schlenk techniques. Starting materials were of commercial origin, with the exception of *S*-2-bromoacetoxypropionic acid ethyl ester, the bromoacetate of D-menthol [(1S, 2R, 5S)-2-isopropyl-5-methylcyclohexanol] and L-menthol [(1R, 2S, 5R)-2-isopropyl-5-methylcyclo-hexanol] as well as of dicobalt octacarbonyl, which were prepared according to published procedures.

Infrared (IR) spectra were recorded with a Bruker IFS 113V Fourier Transform Infrared (FT-IR) spectrometer. ^1H NMR, and $^{13}C\{^1H\}$ NMR, and $^{31}P\{^1H\}$ NMR spectra were obtained with a Bruker DPX-200 and an AMX-400 instrument.

The x-ray diffraction experiments were performed using a Siemens P4 x-ray four-circle diffractometer with Mo–Kα radiation at room temperature (r.t.). SHELXTL-Plus programs and an SGI IRIS Indigo computer were used for calculations. Atomic scattering factors were taken from SHELXTL and the literature as well as the correction for anomalous dispersion.

The alkylcobalt tricarbonyl *tert*–phosphine complexes 3a–d were prepared according to variants of the procedures described in a published method.

(Scheme 1), using ion metathesis (1), ligand-promoted carbonylation (2), and thermal decarbonylation (3) steps in a one-pot mode.

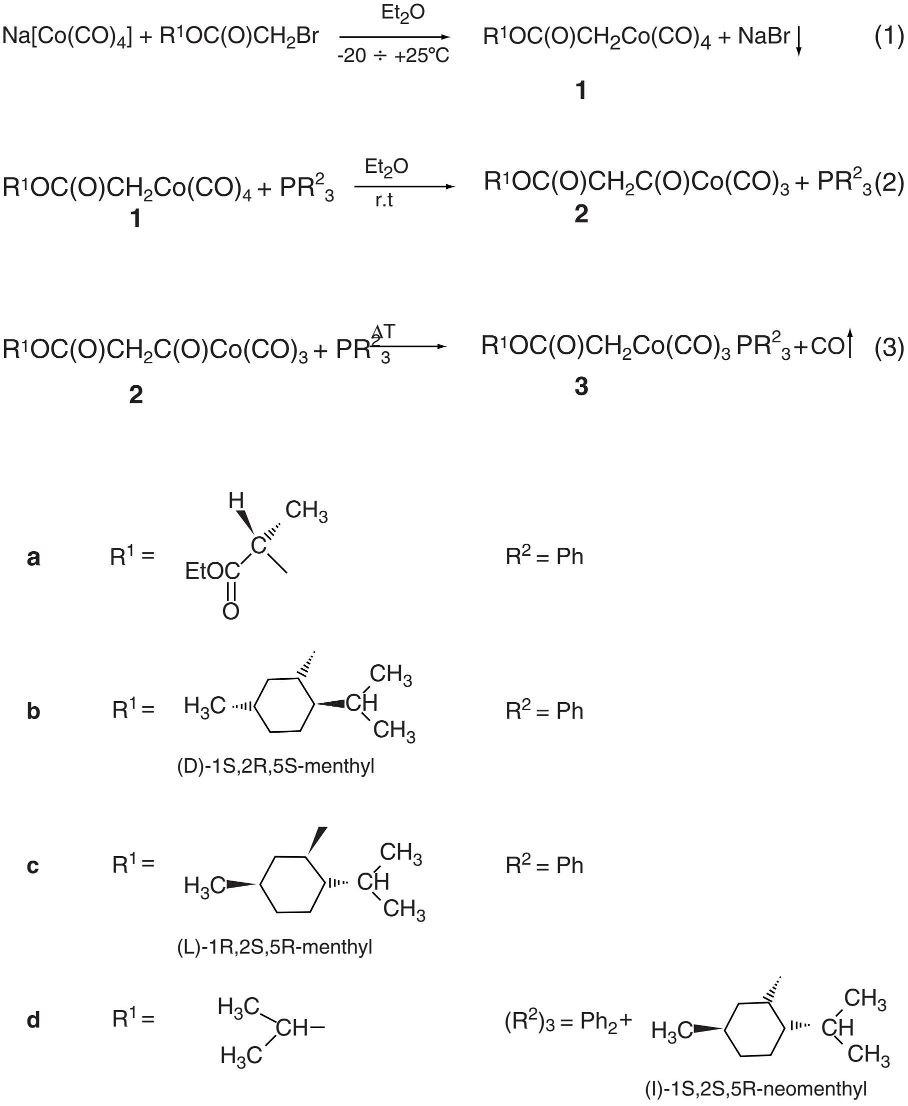

Scheme 1

2.1 Preparation of (*S*)-EtOC(*O*)C(H)(CH_3)OC(*O*)CH_2Co(CO)$_3$$PPh_3$ (3a)

A solution of Na[Co(CO)$_4$] (2 mmol, prepared by Na/Hg reduction of $Co_2(CO)_8$, 342 mg, 1.0 mmol) in 30 mL of dry Et_2O was filtered into a 100 mL Schlenk vessel under an Ar atmosphere. This solution was cooled to –30°C, and then, while stirred, *S*-2-bromoacetoxypropionic acid ethyl ester (478 mg, 2 mmol) was added at once. Immediately after this, the formation of a white precipitate (NaBr) started and the (originally colourless) solution turned gradually yellow then brown. The stirring was continued for 2 h at –30°C and then the reaction mixture was left to warm to r.t. The stirring was continued for an additional 1 h at r. t. After this period a liquid sample was taken for spectroscopic analysis. The IR *v* (C–O) spectrum showed the complete disappearance of the strong, broad band of $[Co(CO)_4]$- at ~1900 cm^{-1} and the emergence of a new band system compatible with an $XCo(CO)_4$-type complex.[17a,] This complex was characterised as R1OC(O)CH2Co(CO)4 [R1 = $EOC(O)CH(CH_3)$–] (1a) on the basis of its IR and NMR spectra (Table 1). Complex 1 was not isolated.

Table 1. IR *v* (C–O) data in *n*-hexane (cm^{-1}), ^1H NMR and $^{13}C\{^1H\}$ NMR spectra in $CDCl_3$ (δ, (ppm), J (Hz)) of complexes **1**

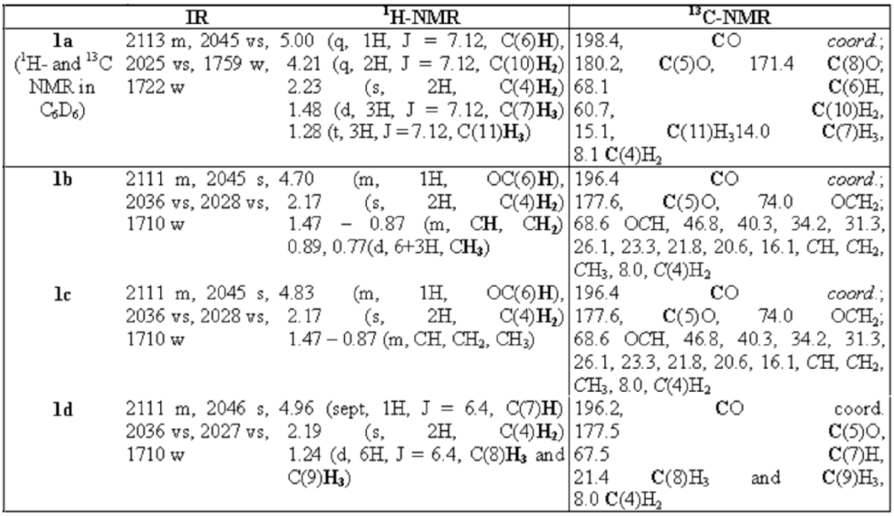

	IR	^1H-NMR	^{13}C-NMR
1a (^1H- and ^{13}C NMR in C_6D_6)	2113 m, 2045 vs, 2025 vs, 1759 w, 1722 w	5.00 (q, 1H, J = 7.12, C(6)**H**), 4.21 (q, 2H, J = 7.12, C(10)$\mathbf{H_2}$) 2.23 (s, 2H, C(4)$\mathbf{H_2}$) 1.48 (d, 3H, J = 7.12, C(7)$\mathbf{H_3}$) 1.28 (t, 3H, J = 7.12, C(11)$\mathbf{H_3}$)	198.4, **C**O *coord.*; 180.2, **C**(5)O, 171.4 **C**(8)O; 68.1 **C**(6)H, 60.7, **C**(10)H_2, 15.1, **C**(11)$H_3$14.0 **C**(7)H_3, 8.1 **C**(4)H_2
1b	2111 m, 2045 s, 2036 vs, 2028 vs, 1710 w	4.70 (m, 1H, OC(6)**H**), 2.17 (s, 2H, C(4)$\mathbf{H_2}$) 1.47 – 0.87 (m, CH, CH_2) 0.89, 0.77(d, 6+3H, CH_3)	196.4 **C**O *coord.*; 177.6, **C**(5)O, 74.0 O*C*H_2; 68.6 OCH, 46.8, 40.3, 34.2, 31.3, 26.1, 23.3, 21.8, 20.6, 16.1, *C*H, *C*H_2, *C*H_3, 8.0, *C*(4)H_2
1c	2111 m, 2045 s, 2036 vs, 2028 vs, 1710 w	4.83 (m, 1H, OC(6)**H**), 2.17 (s, 2H, C(4)$\mathbf{H_2}$) 1.47 – 0.87 (m, CH, CH_2, CH_3)	196.4 **C**O *coord.*; 177.6, **C**(5)O, 74.0 O*C*H_2; 68.6 OCH, 46.8, 40.3, 34.2, 31.3, 26.1, 23.3, 21.8, 20.6, 16.1, *C*H, *C*H_2, *C*H_3, 8.0, *C*(4)H_2
1d	2111 m, 2046 s, 2036 vs, 2027 vs, 1710 w	4.96 (sept, 1H, J = 6.4, C(7)**H**) 2.19 (s, 2H, C(4)$\mathbf{H_2}$) 1.24 (d, 6H, J = 6.4, C(8)$\mathbf{H_3}$ and C(9)$\mathbf{H_3}$)	196.2, **C**O coord. 177.5 **C**(5)O, 67.5 **C**(7)H, 21.4 **C**(8)H_3 and **C**(9)H_3, 8.0 **C**(4)H_2

The reaction mixture was then filtered and to the filtrate, while stirred at r.t. under an Ar atmosphere, $P(C_6H_5)_3$ (514 mg, 2 mmol) was added in one portion. The stirring was then continued for additional 8 h. After 2 h the colour of the brown solution turned gradually light yellow and gas evolution (CO) was observed. After this period, a sample was taken, which was analysed by IR spectroscopy in the C–O stretching range (2200–1600 cm^{-1}). The only detectable metal carbonyl species showed a *v* (C–O) band system characteristic for an $XCo(CO)_3L$-type complex[18–20], and it was attributed to $R_1OC(O)CH_2Co(CO)_3PPh_3$ 3a. Then the reaction mixture was filtered and the solvent was evaporated at r.t. and reduced pressure. The crude product (673 mg, 60.9%) was then recrystallised from diethyl ether/*n*-hexane (liquid diffusion) providing light yellow crystals (473 mg, 42.8%). Complexes 3b–d were prepared similarly. The products 3 were characterised by elemental analyses (Table 2), IR, ^{1}H NMR, ^{13}C{^{1}H} NMR , and ^{31}P{^{1}H} NMR (Table 3), and x-ray diffraction (Tables 4 and 5).

Table 2. Elemental analyses of complexes **3**

Compd.	**Formula**	**Mol. weight**	**Composition (%)**	
			Found	**Calculated**
3a	$C_{28}H_{26}O_7CoP$	564.32	C 59.7; H 4.7	C 59.59; H 4.64
3b	$C_{33}H_{36}O_5CoP$	602.52	C 65.8; H 6.1; Co 10.0; P 5.1	C 65.78; H 6.02; Co 9.78; P 5.14
3c	$C_{33}H_{36}O_5CoP$	602.52	C 66.1; H 6.2	C 65.78; H 6.02
3d	$C_{30}H_{38}O_5CoP$	559.43	C 63.4; H 6.9	C 63.38; H 6.74

Table 3. IR *v* (C–O) spectra in *n*-hexane (cm^{-1}), ^{1}H NMR, ^{13}C{^{1}H} NMR, and ^{31}P{^{1}H} NMR in CDCl$_3$ (δ in ppm, J in Hz) of complexes **3**

	IR	**^{1}H NMR**	**^{13}C{^{1}H} NMR** (J_{C-P})	**^{31}P{^{1}H} NMR**
3a	2052 vw, 1982 s, 1971 s, 1754 w, 1705 w	7.58–7.55 (m, C**H** *arom.*); 4.93 (q, 1H, *J* = 7.12, C(6)**H**); 4.17 (q, 2H, *J* = 7.12, C(10)**H**$_2$); 2.234 ($^3J_{HP}$ = 3.34) 1.42 (d, 3H, *J* = 7.12, C(7)**H**); 1.26 (t, 3H, *J* = 7.12, C(11)**H**)	198.4 (d, 22.25) **C**O *coord.*; 180.1, **C**(5)O, 171.4 **C**(8)O; 133.0 (d, 47.87), 132.9 (d, 10.91), 130.9 (d, 2.36), 128.7 (d, 10.55), **C**$_6$H$_5$ in PPh$_3$; 68.1 **C**(6)H; 60.7 **C**(10)H$_2$; 16.8 **C**(11)H$_3$; 14.0 **C**(7)H$_3$; 4.1 (d, 16.06) **C**(4)H$_2$	57.63
3b	2050 vw, 1984 s, 1975 s, 1702 w		198.7 (d, 21.54) **C**O *coord.*; 180.4 **C**(5)O; 133.2 (d, 46.281), 132.9 (d, 11.067), 130.8 (d, 2.012), 128.6 (d, 11.07), **C**$_6$H$_5$ in PPh$_3$; 68.1 O**C**H; 72.73 O**C**H$_2$; 47.1, 40.5, 34.3, 31.2, 25.9, 23.3, 22.1, 20.8, 16.2 **C**H, **C**H$_2$, **C**H$_3$; 5.620 (d, 17.054) **C**H$_2$–Co	
3c	2050 vw, 1985 s, 1975 s, 1701 w		198.7 (d, 21.54) **C**O *coord.*; 180.4 **C**(5)O; 133.2 (d, 46.281), 132.9 (d, 11.067), 130.8 (d, 2.012), 128.6 (d, 11.07), **C**$_6$H$_5$ in PPh$_3$; 68.1 O**C**H; 72.73 O**C**H$_2$; 47.1, 40.5, 34.3, 31.2, 25.9, 23.3, 22.1, 20.8, 16.2 **C**H, **C**H$_2$, **C**H$_3$; 5.620 (d, 17.054) **C**H$_2$–Co	
3d	2046 vw, 1981 s, 1966 s, 1706 w			

Table 4. Experimental parameters of the X-ray diffraction of compounds **3**

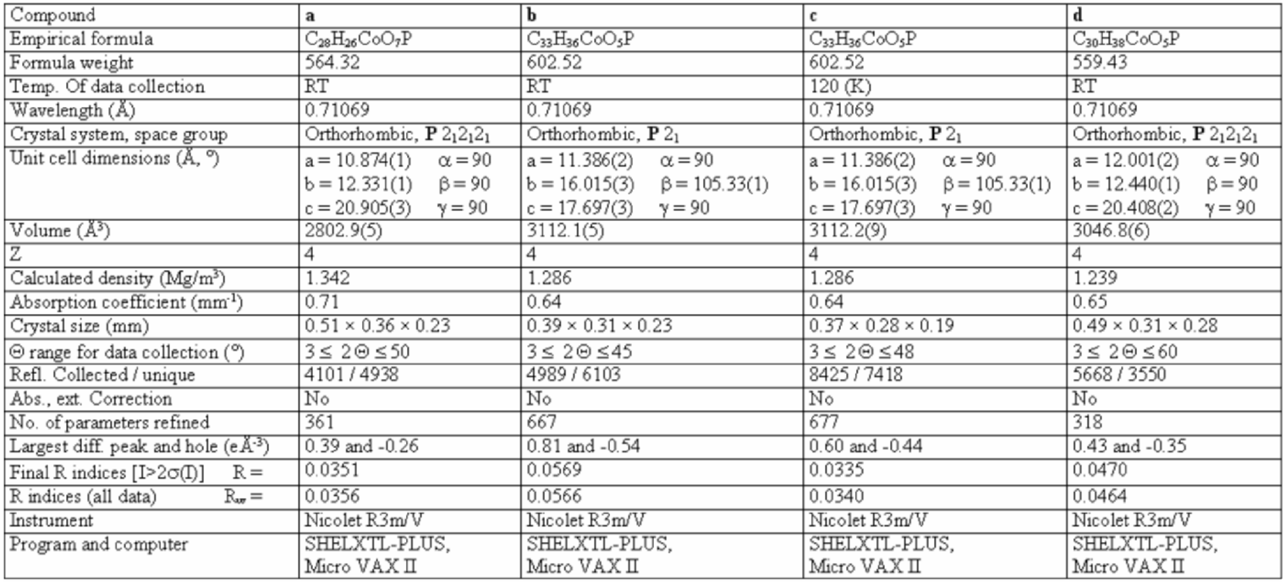

Compound	**a**	**b**	**c**	**d**
Empirical formula	$C_{28}H_{26}CoO_7P$	$C_{33}H_{36}CoO_5P$	$C_{33}H_{36}CoO_5P$	$C_{30}H_{38}CoO_5P$
Formula weight	564.32	602.52	602.52	559.43
Temp. Of data collection	RT	RT	120 (K)	RT
Wavelength (Å)	0.71069	0.71069	0.71069	0.71069
Crystal system, space group	Orthorhombic, **P** $2_12_12_1$	Orthorhombic, **P** 2_1	Orthorhombic, **P** 2_1	Orthorhombic, **P** $2_12_12_1$
Unit cell dimensions (Å, °)	a = 10.874(1) α = 90 b = 12.331(1) β = 90 c = 20.905(3) γ = 90	a = 11.386(2) α = 90 b = 16.015(3) β = 105.33(1) c = 17.697(3) γ = 90	a = 11.386(2) α = 90 b = 16.015(3) β = 105.33(1) c = 17.697(3) γ = 90	a = 12.001(2) α = 90 b = 12.440(1) β = 90 c = 20.408(2) γ = 90
Volume ($Å^3$)	2802.9(5)	3112.1(5)	3112.2(9)	3046.8(6)
Z	4	4	4	4
Calculated density (Mg/m^3)	1.342	1.286	1.286	1.239
Absorption coefficient (mm^{-1})	0.71	0.64	0.64	0.65
Crystal size (mm)	0.51 × 0.36 × 0.23	0.39 × 0.31 × 0.23	0.37 × 0.28 × 0.19	0.49 × 0.31 × 0.28
Θ range for data collection (°)	$3 \leq 2\Theta \leq 50$	$3 \leq 2\Theta \leq 45$	$3 \leq 2\Theta \leq 48$	$3 \leq 2\Theta \leq 60$
Refl. Collected / unique	4101 / 4938	4989 / 6103	8425 / 7418	5668 / 3550
Abs., ext. Correction	No	No	No	No
No. of parameters refined	361	667	677	318
Largest diff. peak and hole ($eÅ^{-3}$)	0.39 and -0.26	0.81 and -0.54	0.60 and -0.44	0.43 and -0.35
Final R indices [$I>2\sigma(I)$] R =	0.0351	0.0569	0.0335	0.0470
R indices (all data) R_w =	0.0356	0.0566	0.0340	0.0464
Instrument	Nicolet R3m/V	Nicolet R3m/V	Nicolet R3m/V	Nicolet R3m/V
Program and computer	SHELXTL-PLUS, Micro VAX II	SHELXTL-PLUS, Micro VAX II	SHELXTL-PLUS, Micro VAX II	SHELXTL-PLUS, Micro VAX II

The absolute structure was established by refining eta: **a** = 1.0356(32); **b** = 1.122(60); **c** = 1.039(27); **d** = 0.991(49); see: Rogers, D. *Acta Cryst.* **1981**, *A37*, 734-741.

Table 5. Selected bond length (Å) and bond angle (°) values of compounds **3** Bond lengths (Å)

	3a	**3b**	**3c**	**3d**
Co–P	2.207(1)	2.213(3)	2.215(1)	2.239(1)
Co–C(1)	1.782(4)	1.776(10)	1.791(5)	1.778(5)
Co–C(2)	1.792(4)	1.789(9)	1.779(4)	1.786(5)
Co–C(3)	1.773(4)	1.802(10)	1.827(3)	1.779(5)
Co–C(4)	2.078(3)	2.088(10)	2.077(5)	2.078(4)
C(1)–O(1)	1.137(5)	1.149(12)	1.146(6)	1.138(6)
C(2)–O(2)	1.123(5)	1.144(11)	1.148(5)	1.132(7)
C(3)–O(3)	1.132(5)	1.126(12)	1.132(6)	1.141(6)
C(4)–C(5)	1.467(4)	1.496(14)	1.495(7)	1.472(8)
C(5)–O(5)	1.207(5)	1.175(12)	1.198(6)	1.218(7)
C(5)-O(6)	1.353(5)	1.379(10)	1.368(5)	1.333(7)
O(6)–C(6)	1.433(5)	1.453(11)	1.449(5)	
P–C(16)	1.828(3)	1.826(6)	1.827(3)	1.859(4)
P–C(22)	1.831(3)	1.822(5)	1.816(3)	1.834(3)
P–C(28)	1.823(3)	1.819(6)	1.827(3)	1.834(3)
Co′–P′		2.209(3)	2.208(2)	
Co′–C(1)		1.799(10)	1.803(5)	
Co′–C(2′)		1.792(8)	1.795(4)	
Co′–C(3′)		1.783(10)	1.790(5)	
Co′–C(4′)		2.065(11)	2.080(5)	

Bond angles (°)

	3a	**3b**	**3c**	**3d**
P–Co–C(1)	93.7(1)	92.8(4)	92.7(2)	92.0(2)
P–Co–C(2)	90.1(1)	90.1(4)	90.4(2)	95.5(2)
P–Co–C(3)	93.5(1)	93.4(3)	93.6(2)	91.0(1)
C(1)–Co–C(2)	118.4(2)	119.6(5)	120.7(2)	116.5(2)
C(1)–Co–C(3)	116.6(2)	114.2(4)	113.8(2)	120.5(3)
C(2)–Co–C(3)	124.5(2)	125.8(4)	125.1(2)	122.4(3)
P–Co–C(4)	179.1(1)	176.8(2)	177.0(1)	175.4(2)
C(1)–Co–C(4)	87.0(1)	87.8(4)	87.2(2)	85.0(2)
C(2)–Co–C(4)	89.0(2)	87.0(4)	87.0(2)	89.0(2)
C(3)–Co–C(4)	86.8(2)	89.2(4)	89.2(2)	87.6(2)
Co–P–C(16)	115.7(1)	114.9(2)	115.0(1)	112.8(1)
Co–P–C(22)	114.8(1)	113.6(2)	114.1(1)	109.9(1)
Co–P–C(28)	114.2(1)	113.7(2)	113.7(1)	116.0(1)

3. Results and discussion

In the course of previous studies with alkylcobalt carbonyl *tert*-phosphine complexes, similar to type 3, we discovered:

(a) The alkyl (ester) and phosphine ligands develop chiral conformations even with achiral groups.[9b–d]

(b) These conformations are generated in a concerted manner, radically reducing (with achiral groups in the ester to 50%) the number of "statistically possible" conformations.[9f]

(c) This selection rule emerges as a consequence of asymmetry in the rotational barriers of the ester group,[9i] leading to "molecular clockwork" arrays.

(d) The "selection" (orientation) of the ester position is transmitted by a clockwork-like mechanism to the rest of the molecule, leading to concertedness between the (chiral) conformations of the phosphine and those of the alkyl ester ligand.[9f,i]

(e) Introduction of one centre of chirality into the ester-alkyl group, in the form of a flexible, apolar, non-bulky group (*s*-Bu) results in an even more radical reduction of the (statistically possible) conformers (by 75%).[9e]

(f) Introduction of a bulky, polar group into the ester fragment (diacetone-D-glucofuranosyl rest) causes, the formation of only one chiral conformer; however, due to the bulkiness, this form is much less ordered than the former complexes.[9g]

(g) Effects (d) and (e) are strengthened by a C–H…O hydrogen bridge interaction in the ester group between the α-CHn group and the ester carbonyl–O.[9f,g]

The essential effects leading to these results are summarised in Scheme 2.

The basis of the selection of the structure of the compounds studied in this paper was to find out, how these principles work using compounds with (i) a flexible ester "alkyl" group with polar fragments and one centre of chirality (3a); (ii) flexible apolar (not too bulky) alkyl groups with more (3) stereogenic units (3b,c); and (iii) (configurationally) chiral group in the phosphine ligand (3d).

The preparative access to these molecules was developed on the basis of earlier experience with similar compounds,[9,17] using a one-pot variant, without isolation or detailed characterisation of intermediates 1 and 2. High yields of complexes **3** were obtained without attempt at optimisation of the yield. No cobalt carbonyl species other than complex **3** were detected after reactions (1)–(3) were completed (Scheme 1). Spectroscopic analysis of the reaction mixture during the reaction and immediately after did not reveal isomers (equatorial) other than characterised in the end products **3a**–**d** (c.f. [18]). X-ray crystal and molecular structure determination was performed with complexes **3a**, **b**, **c**, and **d**.

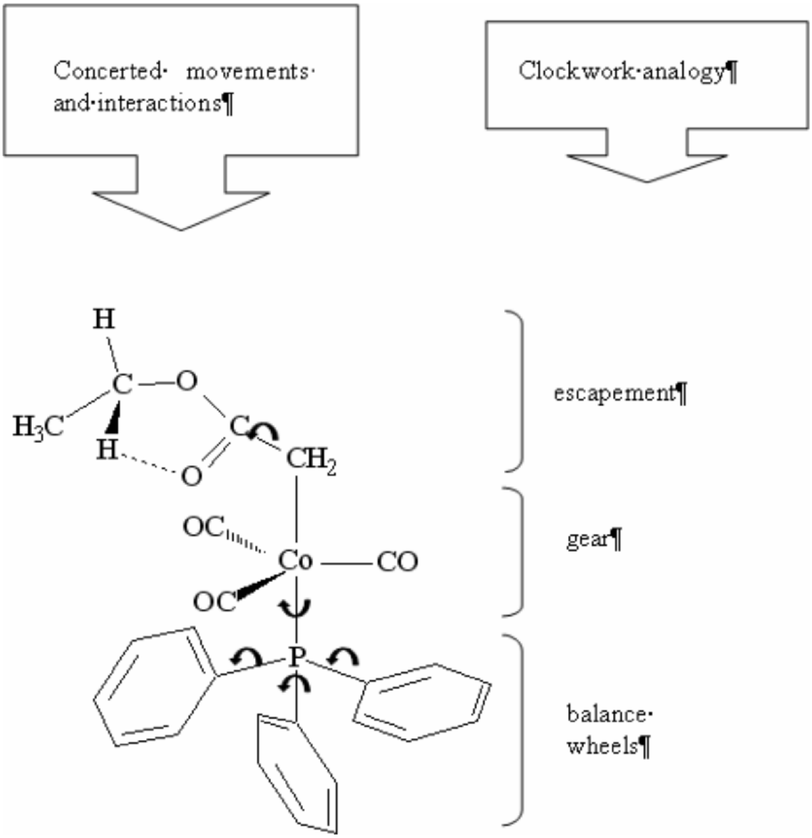

Scheme 2

The overall molecular structure of complex **3** shows a trigonal bipyramidal (TBP) array with the non-carbonyl ligands in axial (*trans*) positions and the carbonyls in a slightly bent equatorial plane, turning its concave face towards the alkyl ligand. This picture is similar to the geometry of several other $XCo(CO)_3L$ type complexes.[9,17,18,19b,20,22] The preferential development of the *trans*-(bis-axial) TBP geometry in complex **3** is a fortunate circumstance for the analysis of the mechanisms of the interaction of the conformations of ligands in the two opposite positions on the metal.

The crystal lattice of complexes **3a** and **d** contains only one conformer of each of these complexes (both are $P2_12_12_1$ phases), while **3b** and **c** both form $P2_1$ phases, with two independent molecules (each) in these lattices. All complexes contain four molecules in the elementary cell.

A comparison of the behaviour of complexes **3a** and **d** with that of the **3**, R = achiral alkyl,[9h] (R, S)*s*-Bu[9e] and glucosyl[9g] derivatives, gives a strong indication for the supposition that the "racemates" of the conformational isomers of the ester and phosphine groups are "resolved" by the introduction of permanent centres of chirality into the ligands. This, however, does not lead necessarily to the formation of only one isomer (conformer). If the steric conditions permit, additional (diastereomeric) forms develop, as in the case of the two menthylester derivatives **3b** and **c**. The loss of helicity in the phosphine ligand at the glucosyl derivative[9g] as well as the development of the two diastereomers (each) in the menthylester complexes **3b** and **c** indicates that the presence of more centres of configurational chirality does not necessarily promote the formation of a "more chiral" product. This is a problem that one encounters in preparative (empirical) attempts in terms of observing more or less "efficiency" of additives used for the induction of chirality.

The individual features of the structural details of complexes **3a**, **b**, **c**, and **d** require some comments.

The structure of complex **3a** (Figure 1) is primarily characterised by the remarkable non-equivalence of the (ligand) carbonyl angles OC–Co–CO: 125.8°, 118.0°, and 115.5°. The broadest of these angles is certainly due to the bulkiness of the organic ligand, which is organised in a very particular manner. First of all, it is to be noted that in this long, flexible organic ligand, with six6 σ-bonds that could generate new conformers, only one conformer develops in the $P2_12_12_1$ phase. This conformer is characterised by a very symmetric orientation with respect to the rest of the molecule, as it can be seen through the dihedral angle between the main axis of the "lactic acid" fragment and the anti-CO ligand: –178.3° (almost a straight line). Other interesting features are the short (ester) carbonyl-O vs. α- (alkyl) C distances (C10–O8, 269.4 pm) indicative of the formation of C (sp^3) H vs. >C=O hydrogen bonds, similarly as has been found with other three derivatives with (ester)–α–CH groups.[9e,g,h] The H-bridging generates a new centre of chirality on C10 (Figure 1). It is a highly interesting feature of this structure that this new centre of chirality on C10 is generated only in one enantiomeric form ("R"). The phosphine ligand in complex **3a** shows only one helical conformation (M), where the phenyl ring orientations are somewhat different from those observed at the achiral, alkyl[9h], and *s*-Bu[9e] derivatives. The difference is mostly in the orientation of the C16–C21 ring, which is more "steep" than usual. This can be caused by an additional H-bridge interaction between the C17 and O8 atoms (C17–O8 distance 269 pm, C17–H17–O8 angle 152.2°), which may be one of the factors contributing to the stabilisation of the astonishingly selective organisation of the conformation in the ester fragment of complex **3a**. An additional "through-space" intramolecular interaction can be identified between the C5 and the Co atoms. This "enforced" interaction (distance 293.9 pm) renders the C5 atom tetracoordinated, with four different substituents (Co, O5, O6, C4) and, therefore, generates a new centre of chirality on this atom. Since in the $P2^12^12^1$ phase, the C5, O5, O6 carboxyl group turns only its si-face towards the Co atom, the new centre of chirality will be (with quantitative enantioselectivity) of *S* configuration. This kind of intramolecular interaction a was detected by x-ray structural studies in some analogous molecules[9,17a] as well as analysed by MO calculations[23c,d] that showed that a considerable electron density transfer occurs between the C5, O5, O6, and the Co atoms. These particular interactions lead to a dramatic diminution of the number of "statistically" possible conformers. Regarding only P and M for the PPh3 ligand, si or re (towards Co) for the C5-centred ester group, as well as "R" or "S" for the C10 atom, this gives eight combinations and only one (12.5%), in 100% enantiomeric yield, gets realised under the influence of the permanent *S* configuration on C6 with the aid of the supramolecular forces.

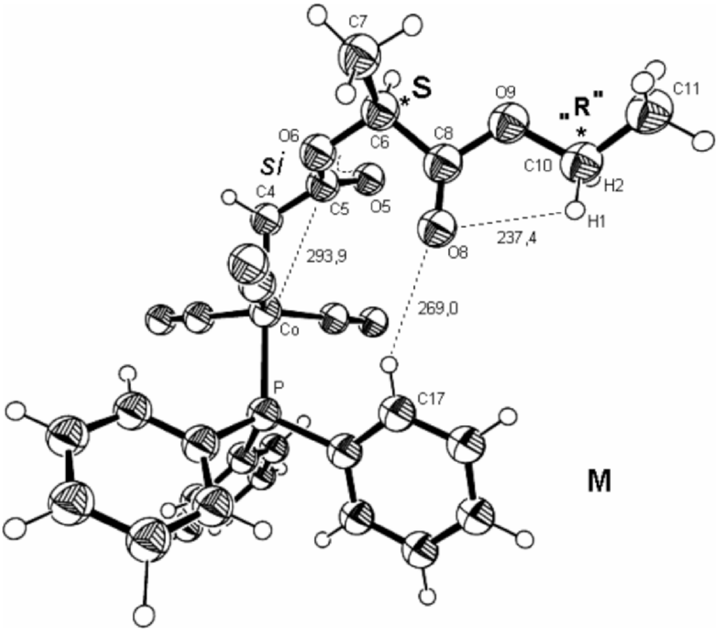

Figure 1. ORTEP drawing of the x-ray crystal structure of complex **3a**.

The considerations described earlier in this paper on the structure of complex **3a** are reflecting the situation in the condensed $P2_12_12_1$ phase. Since most of the reactions where alkylcobalt carbonyls are important intermediates are displayed in solution or vapour phase[18], we made an attempt at exploring whether the highly interesting structural features observed in the crystalline phase are to be taken into account in the solution and/or gas phase. The results are as follows:

(a) `The IR *v* (C–O) frequencies of both "organic" carbonyl groups observed in apolar solvents (Table 3) are compatible with C–H…O and =O…C interactions.

(b) The ABX-type signal observed for the CH$_2$ group directly linked to the Co atom in the 1H NMR spectrum represents an additional proof for the "survival" of the chiral conformation detected in the crystalline phase. The fact that this ABX-type splitting can be observed also in apolar solvent (Table 1, benzene-d$_6$) gives, according to our experience 9e an additional indication that the chiral conformation in complex **3** is particularly stable.

(c) The solution CD spectrum of complex **3a** shows bands at λ = … nm. These are absent in the CD spectrum of the *S*-2-bromoacetoxypropionic acid ethyl ester precursor. These bands can be assigned to transitions involving Co *d*-orbitals,[9a,10] giving thus a support for the chiral perturbation of the Co atom[9a,23] as deduced from the crystal phase data.

(d) Energy decomposition analyses of the ligand bonding energies performed in the means of Ziegler's extended transition state method using the Amsterdam density functional (ADF) program attribute substantial (8–10 kcal/mol) bond energy for the Co–C5 (O5, O6) coordination.[23d] The model structures with distorted Co–C4–C5–O6 dihedral angels rapidly re-establish their natural angle (±90) when optimised by QM semi-empirical PM3(tm) parameter set of SPARTAN 5.1 or molecular mechanical calculations. The substantial driving force observed in this isolated monomolecular event rules out the assumption attributing this highly selective self organisation to solid phase intermolecular forces.

The x-ray structure of the menthylester complexes **3b** and **c** provided an entirely new and highly interesting picture. This is characterised by the fact that both compounds (in P2$_1$ phases) appear as pairs of diastereomers each of which are characterised by the different orientations of the 5-methyl group ((farther from ↑ or closer to ↓ the Co atom) or (↓,↑: the 5-Me group of the menthyl fragment lies in or farther away from the equatorial plane) as well as by enantiomeric configurations developing in the rest of the molecules (Figure 2). The combinations found experimentally in the crystalline phase are **L**↑*re***P**, **L**↓*si***M**, and **D**↓*re***P**, **D**↑*si***M**, while the 12 combinations are completely lacking. This is the first instance when diastereomer pairs are found to form the unit cells of compounds **3**.

One of the most interesting feature of these structures is the fact, that each of the enantiomers appear separately in different crystals: the chiral **L**↑*re***P** molecule is in the elementary cell of **3b**, while its enantiomer **D**↑*si***M** is in the lattice of complex **3c**.

Both complexes 3b and 3c develop H bonding between the alkyl-α-H atom and the sp^2 O atom of the carboxyl group. The 5-membered, H-bonded, non-planar rings thus formed show enantiomeric configurations characterised by exactly the same bond lengths, bond angles and equal dihedral angles (with opposite signs) as shown in Figure 3 and Table 6. Since the C6 atom in the menthyl group is already chiral, the H-bonding does not generate a new centre of chirality as it was observed at the "outer" ester group of complex 3a (this work) as well as at the ethyl and *n*-propylester derivatives in earlier studies.[9h,i] It is worth to note that the distances and angles around the C–H…O bridge show an excellent agreement between the enantiomers in different crystals (Table 6).

Table 6. Selected geometric data of menthyloxycarbonylmethyl–cobalt–tricarbonyl–triphenylphosphine complexes (**3b**, **c**) (From x-ray files TIYXAA (L-menthyl-); TIYWUT (D-mentil-) (L: 1R, 2S, 5R; D: 1S, 2R, 5S)

	L↑re(**R**)**P**	L↓si(**S**)**M**	D↓re(**R**)**P**	D↑si(**S**)**M**
3b				
Co–C–C=O, deg	–94	89.3	–89.9	93.3
Ester ring				
αH–O=, pm	230.6	239.4	239.8	229.1
αC–O=, pm	273.0	269.2	269.6	272.7
H–O=C, deg	82.4	80.9	80	82.5
C–H–O=, deg	105.9	97.4	97.5	106,7
3c				
O=C–O–C, deg	–3.1	–13.9	15.3	4.9
C–O–C–H, deg	–5	40.9	–41.5	4,1
O–C–H–O=, deg	6.5	–32	33.6	–6.5
H–O=C–O, deg	4.7	–3.0	1.9	–5.9
O=C–C–H, deg	–7.4	26.7	–26.4	8.1
C–H–O=C , deg	–8.1	27.2	–26.7	8.9
Co–C .....C_5–C_{Me} deg	127	9	–9.3	–127.9

L↑*re***P**; **L**↓*si***M**; (↓,↑: the 5-Me group of the menthyl fragment lies in or farther away from the equatorial plane)

The "enforced" vicinity of the carboxylic C5 and the Co, i.e. the Co—C5(O5, O6) coordination reproduces the C5–Co distances rather efficiently (3b 296.2 pm; 3c 296.9 pm.). This effect generates new centres of chirality on C5 (*si*→**S** and *re*→**R**) and on the Co atom. The chiral perturbation of the metal

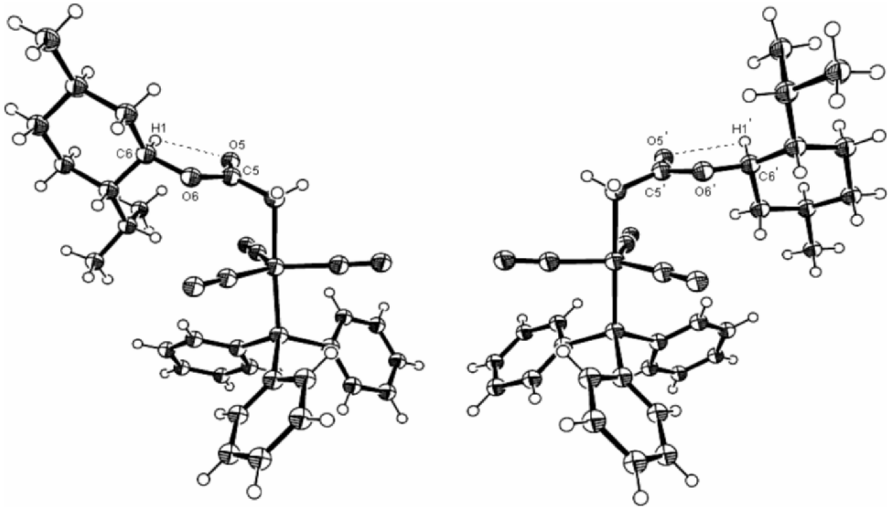

Figure 2. Thermal ellipsoids are shown at the 90% probability level for the diastereomers of complex **3c**.

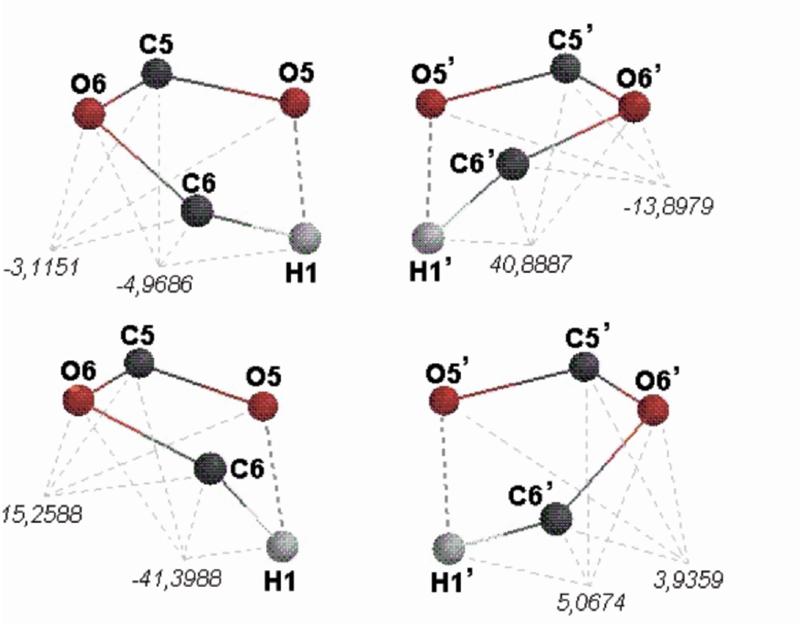

Figure 3. Enantiomeric conformations in different crystals. Comparison of the conformations of the H-bonded rings in complexes **3b** and **c**.

atom is reflected also in the low-energy CD bands of complexes **3c** and **d**.[9a] The CD activity as well as the ABX-type signal of the α-CH2 groups in the

1H NMR spectra of these complexes provide important hints at the "survival" of the supramolecular effects also in the solution phase.

Compound **3d** was synthesised to test the effect of a chiral organic rest in the phosphine ligand. The x-ray structure of complex **3d** shows a bis-axial TBP overall geometry which is similar to the previous complexes **3a**, **b**, and **c** (see also refs. [9,17a,20]). In the chiral $P2_12_12_1$ phase the elementary cells contain four identical chiral molecules. These are characterised by the following structural features:

(a) The autosolvation-type interaction between the carboxyl-C sp^2 atom and the Co seems to be justified again by the relatively short C5–Co distance (295.1 pm). The carboxyl group is turned with its reside towards the Co atom, and acquires *R* configuration by its interaction with the metal.

(b) The bulky neo-menthyl group has heavily distorted the structure of the phosphine ligand especially the arrangement of the two phenyl blades with their corresponding torsion angles of –72.5 and –12.6°. The helicity is nearly collapsed but it is still possible to assign the *P* configuration and the average of the corresponding dihedral angles is about the ideal value, –46.5°. This *re*P configuration is the "diastereomer" of the triphenyl phosphine analogue[9c] (siP, reM, Figure 4).

(c) One of the (O)C–Co–C(O) angles opens up to 123.6° to accommodate a bulky menthyl group and capitalising on the occasion the ester group organises itself also into this segment eclipsing with the menthyl group. The two isopropyl groups are found in surprisingly close vicinity to each other.

(d) Nevertheless, this closely packed molecular structure is energetically (by about 2 kcal/mol) more favourable than the possible three (reM, siP, and siM) others.[27] The chiral alkyl (neo-menthyl) group introduced into the phosphine ligand is inducing the inversion of the coordinated ester fragment from si to re and achieving a 100% enantioselection with respect to the possible stereoisomers.

(e) Similarly to other esters containing α-CH units (**3b**, **c**, refs. [9e–I]) H-bonding between the C7 and O5 atoms can be identified.

(f) The existence of the chiral conformer (found in the $P2_12_12_1$ phase) also in solution phase gains support from the low-energy CD bands[9a] and from the well-resolved ABX-type H^1 NMR band of the (Co)–CH_2 group of complex **3d**. The fundamental difference between the conformations of complexes **3b** and **c** vs. complex **3d** is rooted in the difference between the rotational freedoms of the (otherwise very similar) organic groups bearing central chirality, in **3b** and **c** with respect to **d**.

4. Conclusions

Most of our earlier studies on the mechanism of the intramolecular transfer of chiral information concerned the recognition and self-organisation of conformationally invertable stereogenic units. The origin, and the major driving force of these phenomena are the new coordination type of the prochiral ester group of the compounds **3** that may be influenced significantly by the structure of corresponding alkoxide group. The stereoselectivity of the self-organisation of these compounds may be fundamentally enhanced by the introduction of a permanent configurational chirality in the alkoxide group. The behaviour of compound **3a**, as well as of (R, S) *s*-BuOC(O)CH$_2$Co(CO)$_3$PPh$_3$,[9e] shows clearly that only one centre of configurational chirality is sufficient to generate the lowest possible number (one) of chiral conformations. Some sort of the combined effect of the various structural characteristics is transferred from the ester group to the *trans* axial ligand determining its energetically most favourable helical configuration. Due to this combined steric effect more centres of chirality, as in the case of compounds **3b** and **c** do not necessarily lead to the development of "more chiral" conformations. Even more, under certain conditions (e.g. steric repulsion) may produce "less chiral" states, as was recently observed with the glucose-ester-derived analogue of complex **3**.[9g] Now, this time we demonstrate that introducing a chiral hydrocarbon group into the distant *trans* axial position, the chiral induction is efficiently channelled in the molecule the other way around, as well.

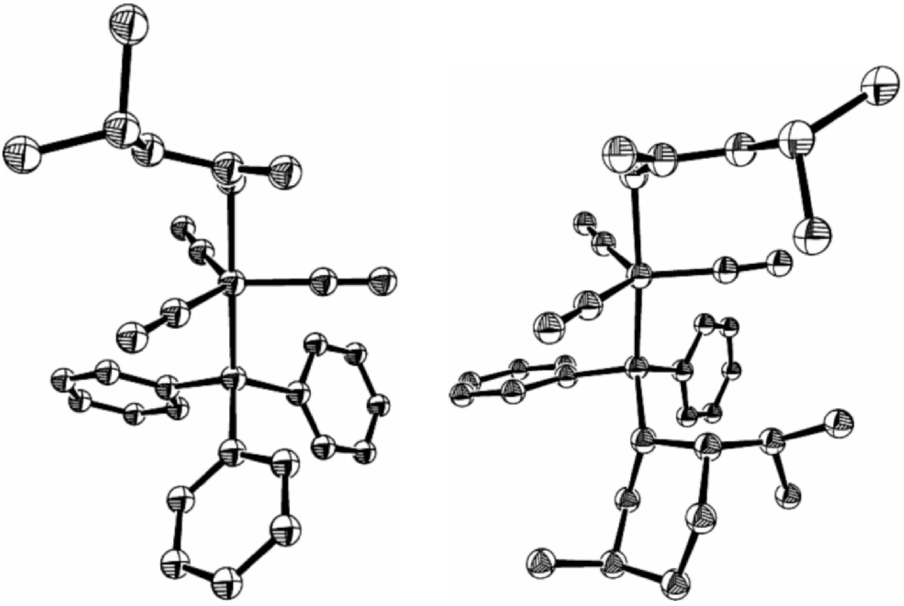

Figure 4. Comparison of the structures of complex **3d** and iPrOC(O)CH^{2}Co(CO)^{3}PPh^3.

The result is convincing: the intramolecular transmission of the chiral information is a two-way process and providing an easily accessible model of the transition state and for the mechanism of chiral phosphine induced metal catalysed asymmetric syntheses.

The results described in this paper and in some previous reports[9,10] seem to support our initial hopes that a systematic study of the development of chiral conformations in transition metal complexes might produce some useful principles for the "engineering" of sufficient systems for enantioselective catalysis. We believe, in this respect, it is not enough to develop chiral ligands, but it is also necessary to study the active complex(es) of the catalytic cycle. Our groups are working on the analysis of additional suitable models in this respect.

Acknowledgement

We acknowledge financial support of this work by the [Italian] Ministry of the University and Research (MURST ex60%), the [Italian] National Research Council (CNR, Rome), the [Hungarian] OTKA program (contract No.: T016326 and T035221) and the Deutsche Akademische Austauschdienst.

References

[1] (a) Hanessian, S., Total Synthesis of Natural Products: The Chiron Approach, Pergamon Press, Oxford, 1983; (b) Brunner, H., Zettlmeier, W., Handbook of Enantioselective Catalysis, Vol. I and II, VCH, Weinheim, 1993; (c) Sheldon, R.A., Chirotechnology, Marcel Dekker, New York, 1993; (d) Ojima, J. (ed.), Catalytic Asymmetric Synthesis, VCH, New York, 1993; (e) Gawley, R.E., Aubé, J., Principles of Asymmetric Synthesis, Pergamon Press/Elsevier, Oxford, 1996; (f) Stephenson, G.R. (ed.), Advanced Asymmetric Synthesis, Blackie Academic & Professional/Chapman & Hall, London, 1996; (g) Feringa, B.L., van Delden, R.A., Angew. Chem. Int. Edit. 1999, 38:3418–3438.

[2] (a) Simonyi, M., Adv. Drug Res. 1997, 30:73–110; (b) Stinson, S.C., Chem. Eng. News 1998 (Sept. 21):83–104; 1999 (Oct. 11):101–120; 2000 (May 8):59–70; 2000 (July 10):63–80; 2000 (Oct. 23):55–78; 2001 (Oct. 1):79–97; (c) Jacoby, M., ibid. 2002 (Mar. 25):43–46; (d) Maureen Rouhi, A., ibid. 2002 (June 10):43–50; 2002 (June 10):51–57.

[3] (a) Fráter, G., Bajgrowitz, J.A., Kraft, P., Tehtrahedron 1998, 54:7633–7703 [Tetrahedron Rep. No. 456]; (b) Kraft, P., Bajgrowitz, J.A., Denis, C., Fráter, G., Angew. Chem. Int. Edit. 2000, 39:2980–3010.

[4] (a) Mandelkern, L., Acc. Chem. Res. 1990, 23:380; (b) Okomoto, Y., Nakano, T., Chem. Rev. 1994, 94:349; (c) Long, N.J., Angew. Chem. Int. Edit. 1995, 34:21; (d) Green, M.M., Jha, S.K., Mullers, B., Park, J.-W., Schultz, G., Kremers, J., Polym. Mater. Sci. Eng. 1996, 75:450; (e) Green, M.M., Park, J.-W.,

Sato, T., Teramoto, A., Lifson, S., Selinger, R.L.B., Selinger, J.V., Angew. Chem. Int. Edit. 1999, 38:3138–3154.

[5] (a) Keszthelyi, L., Quart. Rev. Biophys. 1995, 28:473–507; (b) Cline, D., Comments Nucl. Part. Phys. 1997, 22:131–154; (c) Markó, L., Diss. Savariensis 1998, 24:1–64; (d) Pályi, G., Zucchi, C., Caglioti, L., in: Pályi, G., Zucchi, C., Caglioti, L. (eds), Advances in BioChirality, Elsevier, Amsterdam, 1999, pp. 3–12; (e) Keszthelyi, L., ibid, pp. 99–103; (f) Pályi, G., Zucchi, C., Hajdu, C., Atti Memorie, Acc. Naz. Sci. Lett. Arti Modena 2000, 316(8/2):389–415; (g) Keszthelyi, L., in: Pályi, G., Zucchi, C., Caglioti, L. (eds), Fundamentals of Life, Elsevier, Paris, 2002, pp. 379–387.

[6] (a) Szabó-Nagy, A., Keszthelyi, L., in: Pályi, G., Zucchi, C., Caglioti, L. (eds), Advances in BioChirality, Elsevier, Amsterdam, 1999, pp. 367–376; (b) Zanasi, R., Lazzeretti, P., Ligabue, A., Soncini, A., ibid., pp. 377–385; (c) Szabó-Nagy, A., Keszthelyi, L., Proc. Natl. Acad. Sci. USA 1999, 96:4252–4255; (d) Inoue, Y., Tsuneishi, H., Hakushi, T., Tai, A., J. Am. Chem. Soc. 1997, 119:472–478.

[7] Dodziuk, H., Tetrahedron Asymm. 1992, 3:43–50; (b) Idem, Modern Conformational Analysis, VCH, New York, 1995.

[8] Some leading references: (a) Mislow, K., Acc. Chem. Res. 1976, 9:26–33; (b) Iwamura, H., Mislow, K., ibid. 1988, 21:175–182; (c) Polowin, J., Mackie, S.C., Baird, M.C., Organometallics, 1992, 11:3724–3730; (d) Garner, S.E., Orpen, A.G., J. Chem. Soc. Dalton Trans. 1993, 533–541; (e) Mayer, H.A., Kaska, W.C., Chem. Rev. 1994, 94:1239; (f) Nandi, N., Bagchi, B., J. Am. Chem. Soc. 1996, 118:11208–11216; (g) Lucero, M.J., Houk, K.N., ibid. 1997, 119:826–827; (h) Vacek, J., Michl, J., New J. Chem. 1997, 21:1259–1268.

[9] (a) Galamb, V., Pályi, G., Kajtár, M., Inorg. Chim. Acta 1981, 55:L113–L114; (b) Pályi, G., Zucchi, C., Bartik, T., Boese, R., J. Organomet. Chem. Conf., 1st (Nov. 4–5, 1993, München Germany), Abstract p. 183; (c) Pályi, G., Zucchi, C., Bartik, T., Herbrich, T., Kriebel, C., Boese, R., Sorkau, A., Fráter, G., Atti Accad. Sci. Bologna, Rend. Cl. Sci. Fis. 1992/1993, 281(14/10):159–167; (d) Pályi, G., Alberts, K., Bartik, T., Boese, R., Fráter, G., Herbrich, T., Herfurth, A., Kriebel, C., Sorkau, A., Tschoerner, C.M., Zucchi, C., Organometallics 1996, 15:3253–3255; (e) Szabó, M.J., Szilágyi, R.K., Bencze, L., Boese, R., Caglioti, L., Zucchi, C., Pályi, G., Enantiomer 2000, 5:215–219; (f) Bencze, L., Boese, R., Pályi, G., Szabó, M.J., Szilágyi, R.K., Zucchi, C., Magyar Kém. Folyóirat 2001, 56:215–219; (g) Zucchi, C., Tiddia, S., Boese, R., Tschoerner, C.M., Bencze, L., Pályi, G., Chirality 2001, 13:458–164; (h) Zucchi, C., Boese, R., Alberts, K., Herbrich, T., Tóth, G., Bencze, L., Pályi, G., Eur. J. Inorg. Chem. 2001, 2297–2304; (i) Bencze, L., Szilágyi, R.K., Szabó, M.J., Boese, R., Zucchi, C., Pályi, G., in: Pályi, G., Zucchi, C., Caglioti, L. (eds), Fundamentals of Life, Elsevier, Paris, 2002, pp. 451–471.

[10] (a) Kajtár, M., Kajtár-Miklós, J., Váradi, G., Horváth, I.T., Zucchi, C., Pályi, G., Ital. Phys. Soc., Conf. Proc. 1994, 48 (Non-linear dynamics):219–226; (b) Kajtár, M., Kajtár-Miklós, J., Giacomelli, G., Gaál, G., Váradi, G., Horváth, I.T., Zucchi, C., Pályi, G., Tetrahedron Asymm. 1995, 6:2177–2194; (c) Pini, A., Ph.D. thesis, University of Modena, Modena, 1997.

[11] Shriver, D.F., Drezdzon, M.A., Manipulation of Air Sensitive Compounds, 2nd edn., Wiley, New York, 1986.

[12] Fráter's group (citation here)

[13] Szabó, P., Markó, L., Bor, G., Chem. Technol. (Berlin) 1961, 13:549–550.

[14] Cromer, D.T., Mann, J.B., Acta Cryst. 1968, 24A:321–324.

[15] $\Delta f'$, $\Delta f''$ from: Cromer, D.T., Liberman, D.J., Chem. Phys. 1970, 53:1891–1898.

[16] (a) Galamb, V., Pályi, G., Cser, F., Furmanova, M.G., Struchkov, Yu.T., J. Organomet. Chem. 1981, 209:183–195; (b) Galamb, V., Pályi, G., in: Eisch, J.J., King, R.B. (eds), Organometallic Syntheses, Vol. 3, Elsevier, Amsterdam, 1986, pp. 142–146.

[17] Reviews: (a) Galamb, V., Pályi, G., Coord. Chem. Rev. 1984, 59:203–238; (b) Kovács, I., Ungváry, F., Coord. Chem. Rev. 1997, 161:1–32.

[18] (a) Markó, L., Bor, G., Almásy, G., Szabó, P., Brennstoff. Chem. 1963, 44:184–187; (b) Bor, G., Inorg. Chim. Acta 1967, 1:81–92; (c) Nagy-Magos, Z., Bor, G., Markó, L., J. Organomet. Chem. 1968, 14:205–210.

[19] (a) Galamb, V., Pályi, G., J. Chem. Soc., Chem. Commun. 1982, 487–488; (b) Galamb, V., Pályi, G., Ungváry, F., Markó, L., Boese, R., Schmid, G., J. Am. Chem. Soc. 1986, 108:3344–3351; (c) Galamb, V., Pályi, G., Boese, R., Schmid, G., Organometallics 1987, 6:861–867; (d) Somlyai-Haász, J., Haász, F., Galamb, V., Benedetti, A., Zucchi, C., Pályi, G., Krümmling, T., Happ, B., Bartik, T., J. Organomet. Chem. 1991, 419:205–217; (e) Zucchi, C., Pályi, G., Galamb, V., Sámpár-Szerencsés, E., Markó, L., Li, P., Alper, H., Organometallics 1996, 15:3222–3231; (f) Zucchi, C., Cornia, A., Boese, R., Kleinpeter, E., Alper, H., Pályi, G., J. Organomet. Chem. 1999, 586:61–69.

[20] Spectroscopic or/and preparative identification of the supposed acyl-type intermediate 2 (Scheme 1) was beyond the scope of the present study.

[21] (a) Röper, M., Krüger, C., J. Organomet. Chem. 1988, 339:159-164; (b) Tasi, M., Pályi, G., Organometallics 1985, 4:1523–1528; (c) Bartik, T., Krümmling, T., Krüger, C., Markó, L., Boese, R., Schmid, G., Vivarelli, P., Pályi, G., J. Organomet. Chem. 1991, 421:323–333.

[22] (a) Pályi, G., Transition Met. Chem. 1977, 2:273–275; (b) Pályi, G., Kovács-Toplak, M., Váradi, G., Atti Accad. Sci. Bologna, Rend. Cl. Sci. Fis. 1978, 266(13/5):139–146; (c) Bencze, L., Szabó, M.J., Szilágyi, R.K., Pályi, G., NATO ASI: Metal-Ligand Interactions in Chemistry, Physics and Biology (Sept. 1–12, 1998, Cetraro, Italy), Abstract p. 33; (d) Szabo, M.J., Szilagyi, R.K., Bencze, L. (2002) (submitted for publication).

[23] (a) Ziegler, T., Rauk, A., Inorg. Chem. 1979, 18:1558; (b) Ziegler, T., Rauk, A., Inorg. Chem. 1979, 18:1755.

[24] (a) Stewart, J.J.P., J. Comput. Chem. 1989, 10:209–220; 221–264; (b) Cundari, T.R., Deng, J., J. Chem. Info. Comput. Sci. 1999, 39:376–381.

[25] SPARTAN 5.3, Wavefunction, Inc., 18401 Von Karman, Suite 370, Irvine, CA 92715, USA.

[26] Bencze, L., Kurdi, R., in: Lakshinarayanan (ed.), Nanomachines: Concerted Development of Chiral Conformations in an Oxo-Catalyst Intermediate in NanoComputing – Technology Trends, Allied Publishers Limited, New Delhi, 2001.

[27] Horváth, I.T., International Conference On Molecular Engineering in Homogeneous Catalysis (Oct. 16–17, 1998, Veszprém, Hungary) Abstracts pp. 13–16.

NANOMOLECULAR SWITCHES OPERATED BY CLOCKWORK MECHANISM

LAJOS BENCZE, ROBERT KURDI

University of Veszprém, Müller (Computational Chemistry) Laboratory, Egyetem utca 10, H-8200, P.O. Box 158 8201, Veszprem, Hungary; E-mail: ben016@almos.vein.hu

Abstract: Crystalline phases of the flexible complexes ROC(O)CH2Co(CO)3PPh3 contain enantiomeric pairs of chiral conformers characterized by two forms of the PPh3 ligand of opposed helical chirality, each of which is accompanied by only one conformation of the ester fragment. While the interconversion amongst enantiomers is very fast its stereoselectivity is very high as well: no diastereomers have been detected so far.

A member of this family, [(etoxycarbonyl)methyl]cobalt tricarbonyl triphenylphosphine (I) was chosen as a model to study the mechanism of the highly specific selection of the si,M and re,P enantiomers found in the crystalline phase.

The results of semi-empirical calculations, molecular graphical studies, molecular mechanical (MM) conformation analyses on the Et ester derivative I, show that correlated motions of coaxial rotors, coupled bevel gear-like rotors with different periodicity and the first example of a coupled conrotation identified in a molecular system provide the mechanism of the inversion. These dynamic gearing, originating mainly in non-bonded interactions, govern the preferred spatial disposition and carry far-reaching conformational information through the molecular system. The partial rotation of the ester group and its impact on the coupled structural elements are identical to those of the escapement wheel in a clock. The Co(CO)3 rotor acts as an anchor, its two carbonyl ligands form a OC–Co–CO fork which functions as pellet. The role of the third coordinated carbonyl of this "molecular anchor", also assisted by the other two, is to convey the impulse to the phenyl rings, thus acting as a balance-wheel flipping over to their phase enantiomeric configuration. Both the macroscale and (here) molecular scale escapements transform into their phase isomeric (mirror image) configuration when their action is completed.

According to our knowledge, the present system represents the most complete molecular level analogue of a mechanical clockwork.

Extensive preparative and theoretical studies on the [(alkoxycarbonyl)methyl]cobalt tricarbonyl triphenyl–phosphine type molecules are aimed at providing new molecular building blocks for design and synthesis of nanoscale components for nanomechanical structures.

Y. İmamoğlu and V. Dragutan (eds.), Metathesis Chemistry: From Nanostructure Design to Synthesis of Advanced Materials, 441-452.

Keywords: concerted rotations, clockwork, conformation analysis, organocobalt complex, force field, stereo inversion.

1. Introduction

Cogwheels, ratchets, brakes, switches, even propellers, and their various gear-like cogging combinations have been applied in the development of the earliest appliances, such as: watermills, windmills, and mechanical clocks. Analogies are also numerous at the molecular level where motion is the norm, and spontaneous free rotation around single bonds thus a rule, not an exception. Several examples have become known in the last 3 decades of crowded molecular systems, where correlated rotation of two or more groups became energetically more feasible than the independent rotation around a single bond [1]. While the phenomenon of the concerted torsion may be interpreted as resulting from orbital symmetry control [2], the coupled disrotation of chemical rotors awakes a strong image of mashed cogwheels in motion [3]. The coupling mechanisms are conceived in order for these dynamic gearing to create principally non-bonded interactions between tightly intermeshed groups, as might be expected for sterically crowded molecules. It is here that the analogy between chemical and mechanical gears is most aptly applied. These effects govern preferred spatial disposition of the bulky groups in a molecule, which could carry far-reaching conformational information through the molecular system and may be responsible for many important stereochemical consequences. This paper presents quantum mechanical (QM) semi-empirical and MM conformational studies on correlated structure changes of an [(alkoxycarbonyl)methyl]cobalt tricarbonyl triphenylphosphine compound [4,5], whose highly selective enantiomeric rearrangements seem to be closely related to the actions of some man-made mechanical devices. Members of the set of the aforementioned compounds have been synthesized for entirely different purposes [6]. In course of the investigation of the structure of EtOC(O)CH2Co(CO)3(PPh3) (I) a coupled conrotation in a molecular system was recognized. The presence of a branched skeleton, series of flexible bonds, coaxial rotors, and coupled rotors with different periodicity are elements of this previously unobserved molecular motion.

The identification of the elementary steps of these molecular events may be generalized and might help elucidate the basis for correlated internal rotations in other molecules of stereochemical interest, particularly in intermediates and transition states of enantioselective catalysis. In addition, the phenomenon discussed here could provide new ideas for the design of sophisticated nanotechnological devices.

2. Experimental

2.1 Structural features of [(alkoxycarbonyl)methyl]cobalt tricarbonyl triphenylphosphine complexes

The flexible ROC(O)CH2Co(CO)3PR′3 complexes develop a quite peculiar architecture exhibited clearly in the crystalline phase and also in solution [7]. In the absence of (configurational) centres of chirality, the unit cell (Z = 2 or 4) contains always one (or occasionally two) pair(s) of chiral enantiomeric molecules, related by a centre of symmetry. If stereogenic centre(s) is (are) present either in the (ester) alkyl moiety or in the phosphine ligand, individual (non-centrosymmetric) molecules with chiral conformations are formed. A survey of the published alkyl- and acyl-cobalt carbonyl structures [8] showed that this behaviour is quite general in the self-organization of these (and actually also other) transition metal complexes in the crystalline phase.

This kind of behaviour is well demonstrated by the crystal structure of the complex I (Figure 1), which was chosen for more detailed analysis.

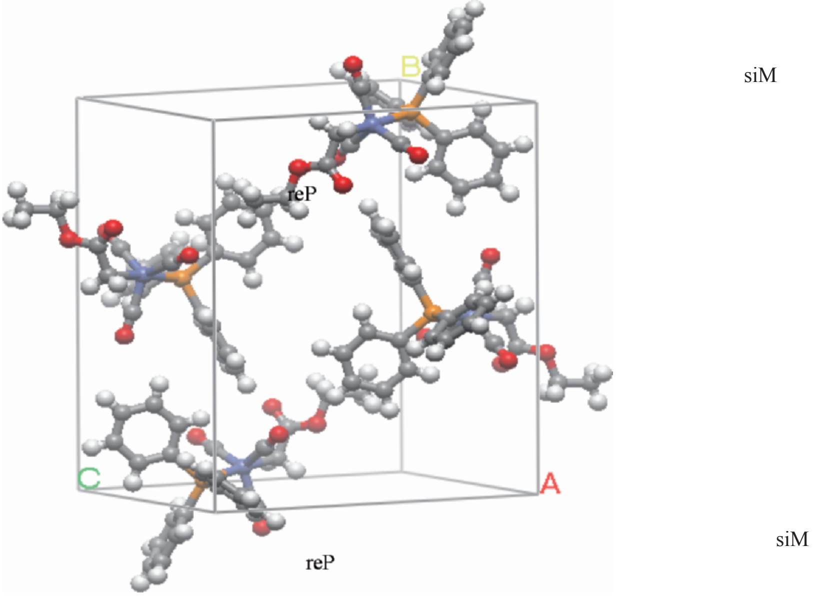

Figure 1. The unit cell of crystal structure of molecule I (monoclinic; space group = P21/n; a = 9.435Å; b = 18.105Å; c = 14.373Å; α= 90.00°; β= 103.62°; γ= 90.00°).

The unit cell of complex I contains two pairs of enantiomeric molecules. The asymmetric unit of the crystal contains one molecule, while the other three molecules are defined by the P21/n space group. The ester fragment is always quasi-parallel oriented to the approximate plane of the Co(CO)3 group (defined by the three carbonyl carbon atoms). The plane to plane angle is less than 25°. Other possible conformations of this group allowed by the rotation around the Csp2–Csp3 bond are not populated. The enantiomeric conformers, P and M (Scheme 1), of the PPh3 ligand are accompanied by only one conformer of the EtOC(O)(CH2...Co) group (re and si, resp., avoiding statistically equivalent and sterically possible combinations such as, e.g. (P)–PR3/(si)–COOR, and (M)–PR3/(re)–COOR. These forms were not detected yet, not even in solution. The coordination of the enantiotopic faces of the carboxylic group to the Co atom [9] gives rise to R (from re) and S (from si) asymmetric centres located on the carboxylic carbon.

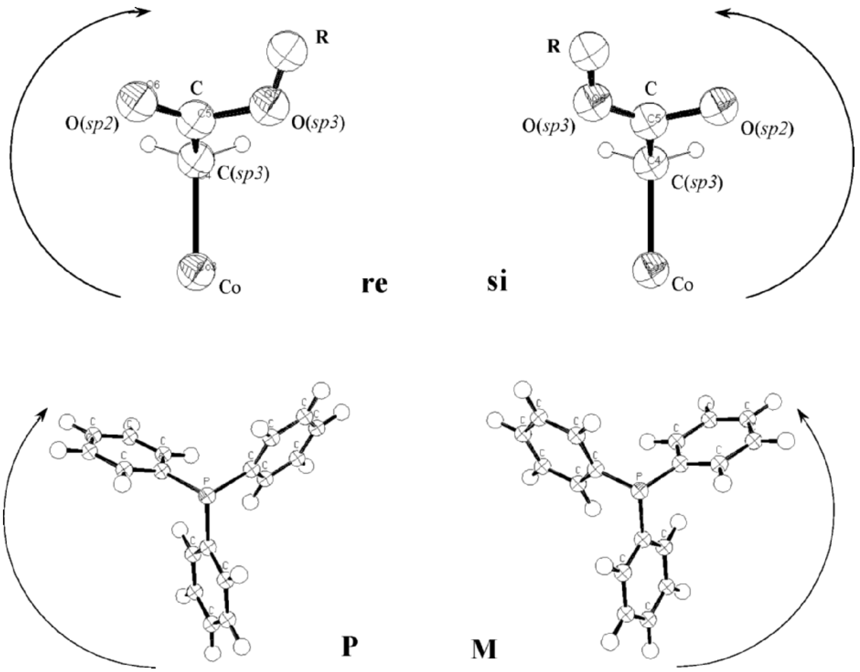

Scheme 1. The stereogenic units in ROC(O)CH2Co(CO)3PR′3 complexes.

2.2 Modelling studies

PM3 [10] parameter set gives quite reasonable equilibrium geometries for cobalt containing complexes as it is incorporated in the programme Spartan [11]. We scanned the PES for possible stereoisomers by one- and two-dimensional, rigid conformational analyses as it is provided by the programme Spartan. Starting from the solid state equilibrium structure, continuous rotations were carried out in both positive and negative directions using the step size 5° until the first maximum was reached. The energy of each step was calculated without relaxation of the internal coordinates.

The conformational drivers defined within complex I are summarized in Scheme 2 for the si,M isomer. The torsion ω1 describes the motion of the ester group relative to the equatorial plane of the complex (i.e. a plane defined by the three carbon atoms of the terminal CO ligands). If $\omega_1 = 0$ deg., the plane of the ester group and the equatorial plane are perpendicular and if $\omega_1 = 90°$., they are parallel to each other. The torsions ω_2 and ω_3 are coaxial drivers and determine the location of the ester group and triphenylphosphine ligand, respectively, relative to the equatorial carbonyl groups. The torsions ω_4 define the relative position of the phenyl rings to the equatorial plane. If they are zero, the rings are perpendicular to the equatorial plane. The equilibrium geometry of the isomer si,M can be exactly described in terms of ω_1/ω_4 dihedral angles as +75°/–45° and the re,P isomer as –75°/+45°.

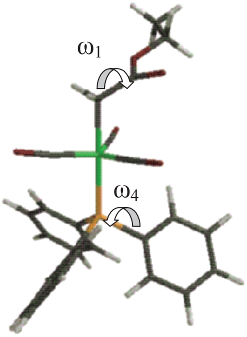

Scheme 2. Confromation drivers ω_1, ω_4.

The complex EtOC(O)CH2Co(CO)3PPh3 (I) is composed of three major moieties, the acetic acid derived ester fragment, the central Co(CO)3 group and the triphenylphosphine ligand. These moieties are linked together via two twistable single bonds, Co–C(H2) and P–Co. The C(H2)–C(O) and the P–Car bonds, whose rotations are directly involved in the chiral inversions, are far from each other with the cobalt atom in between.

If no "supramolecular" effects are involved, the information from one stereogenic region to the next should be transferred through these bonds. In order to describe the complete mechanism of the molecular synchronous inversion accurately, the simultaneous rotation of eight flexible bonds should be followed in which more than 80 significant torsion interactions are involved.

Our efforts failed to find the transition state and the saddle region of the intramolecular inversion in modelling the inversion of complex I. Contrary to the preparative chemical observations, diastereomerization was favoured over inversion and no stability differences were observed for diastereomers. Uncertainties of calculation culminated in the vicinity of the transition region.

Nevertheless, the main features of the correlated torsional changes were exhibited all over the intramolecular motions and the complex system strongly resembled a mechanical clockwork.

An empirical molecular mechanical force field was created and used (within the Cerius2 Open Force Field) in the next stage often studies. X-ray structural data of 25 [(alkoxycarbonyl)methyl]cobalt tricarbonyl triphenylphosphine complexes were used for parameterization of the force field. Conformational grid method with full relaxation was used starting from the solid state equilibrium structure. Two dihedral angles (ω_1 and ω_4) were resorted to incremental group driving calculation. Continuous rotations were carried out using the step size 1°. Steric energy surfice is shown in Figure 2.

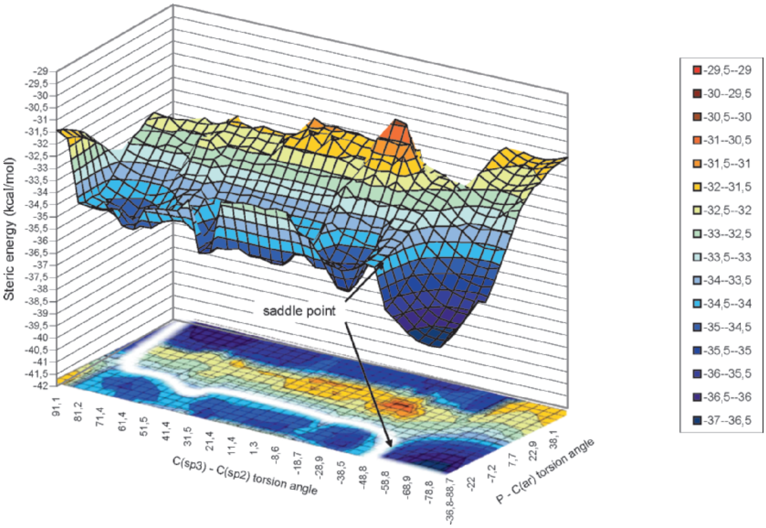

Figure 2. Conformational study, steric energy surfices.

3. Results and discussion

3.1 The mechanism of the molecular inversion

The results of the MM conformational analysis have verified the earlier assumptions. The tendency of the correlated σ-bond rotations are so strong that driven rotation of only two distant σ-bonds provided the necessary driving force to flip the si,M structure to its re,P enantiomer and vice verse in a clockwork manner through well-demonstrated trjectorias.

The mechanism of molecular inversion of the si,M isomer in terms of intramolecular movements and interactions within complex I can be described as follows: the inversion starts as the Csp2 atom of the ester group (a pseudo symmetry centre) gets inverted by flipping in a semicircle over the equatorial plane. For the anticlockwise rotation of the ester group around the Csp3–Csp2 axis (ω_1), the repulsion energy between the ester carbonyl oxygen and the nearest carbonyl ligand sharply increases, starting from the energy minimum (Figure 2). The carbonyl oxygen of the ester group penetrates into the plane of the corresponding OC–Co–CO angle pushing the closest carbonyl ligand and the rest of the Co(CO)3 rotor with it to a anticlockwise rotation. The transition state region is reached at about ±43°. Beyond the transition state the ester group rotates freely to occupy its phase enantiomeric position (i.e. the reconfiguration), close to the next carbonyl ligand of the same OC–Co–CO fork. The movement is terminated there.

Due to the repulsive forces between the two rotors (ester group and equatorial carbonyl ligands) both are rotating anticlockwise. The correlated geometric change by partial rotation around single bonds (occasionally denoted as gear effect) involves coupled rotation of groups in vicinal positions. These adjacent groups behave like interlocking rotors in a synchronous rotation [12]. This motion is analogous to those of the rotors in “internal gears” of wheels with teeth cut on the outside, moving in the internal hollow of a cylinder with teeth cut in to its inner surface, where the motion is conrotatory. This is in sharp contrast to the gear-meshing effects within other highly crowded systems.

The chore of the equatorial carbonyls is forced to twist into the direction that opens the way for the rotation of the aromatic rings through an edge-wise engagement. The synchronous and correlated twist of the single bonds involved in this process, significantly diminishes the overall barrier.

During the inversion, the shaft of the EtOC(O)CH2- rotor (ω_2) is simply rocking by ±16° about the centre of the potential energy well from one staggered position (equilibrium) to the next, i.e. the C(O)OR group never leaves the staggered region, marked by two carbonyl ligands, in which the inversion has commenced [13].

The inversion of the triphenylphosphine ligand is effected through the twist of the P–Car axes (ω_4) by ±90°. In our model the ortho-H atoms of the phosphine ligand and the terminal carbonyl ligands are in a complex bevel gear engagement in which a three-toothed wheel, the Co(CO)3 rotor is dragging three, two-toothed wheels (the phenyl rotors), or vice versa in a correlated disrotatory motion. A schematic model of intramolecular motions in the molecular escapement mechanism with parallel Csp3–Csp2, Co–P, and Car–P arbours is shown in Figure 3.

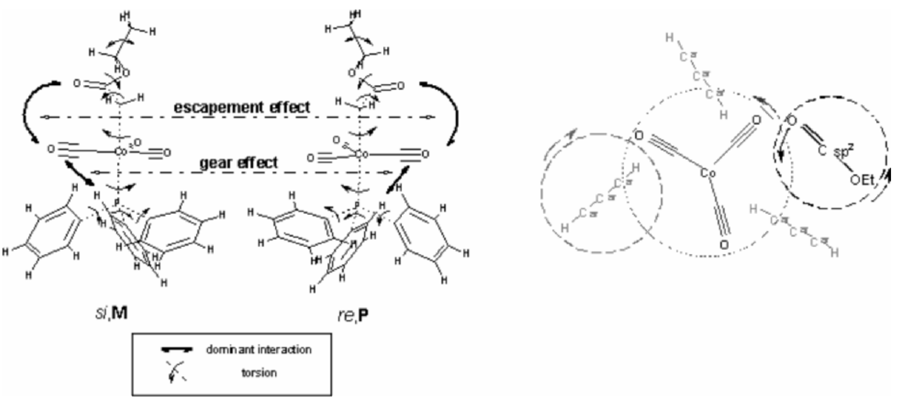

Figure 3. Schematic models of intramolecular motions and molecular escapment mechanism.

3.2 Macromechanical analogy

The creation and control of movement are fundamental aspects of machineries at both macroscopic and microscopic levels as stimulated also by imaginative ideas of Feynman over 40 years ago [14]. Much of the current interest in this field is focused on searching or constructing molecular scale analogues of macroscopic devices, in part because of the intellectual challenge, and also due to their potential applications in nanotechnology [15].

Several examples that may be considered mechanical molecular devices have been reported including the rotaxane based molecular shuttle [16], the chiroptical molecular switch [17], light-activated bianthrone molecules [18], molecular brakes [19], molecular ratchets [20], molecular propellers [21], and conformationally invertable columnar mesophases [22].

Complex I shows much more than a coupled rotation: here a long train of interlocking rotors is involved in a correlated motion as it was demonstrated above. In a normal gear engagement, the intermeshing tooth wheels rotate in opposite directions all over the train of wheels transferring the potential and/or kinetic energy from one end to the other. Concerning the relative motional direction of some interlocking rotor pairs, complex I can be related rather to a mechanical clockwork, than to a gear-type system, however. As in a molecular scale replica of the traditional clockwork mechanism, the motion of the central dihedral angles (rotors) is limited to a pendulum like partial rotation.

A usual train of timekeeping clock consists of five interlocking wheels and pinions [23] (see Scheme S2 for a graphical illustration). The main spring driving directly the great wheel provides power transmitted through the center pinion for the rest of the going train, ending by the escape wheel. The latter one is the first component of the escapement, the mechanism which releases the strain stored in the main spring or driving weight of the clock at regular intervals of time, maintaining a balance (or pendulum) in oscillation. The term escapement is emphasizing the unique features of this mechanistic unit compared to the normal gear tooth wheel engagement of the train of wheels, characterized by phase dependent alternating con- or disrotating (anchor and anchor-wheel) and a disrotating (anchor and balance) arbour pair combination. The escape wheel in its clockwise rotation is lifting the pellet of the anchor and pushing the latter into a partial clockwise rotation. The impulse is transferred by the anchor to the balance wheel swinging it to an opposite direction against the (hair) spring. Partial rotations of the anchor and the balance result in phase isomer states: in the extreme positions of the anchor and the balance both are in phase enantiomeric position just like their combinations. Formation of diastereomeric combinations would be malfunction; result of gear slippage that is to be avoided with several installed technical means (e.g. barriers).

Inversion of the si,M enantiomer of complex I displays close analogy to one period of the anchor escapement motions. The partial rotation of the ester group and its impact on the coupled elements are identical to those of the escapement wheel in a clock. The Co(CO)3 rotor acts as an anchor and the two carbonyl ligands of the OC–Co–CO fork function as pellets [24].

The role of the third terminal carbonyl of this “molecular anchor” is to convey the impulse to the phenyl rings acting as balance wheels flipping over to their phase enantiomeric configuration. (The application of such triple balance is unknown in macromechanical devices, so far). While both of the macroscale and molecular scale escapement transform into their phase isomeric configuration when their action is completed, the escapement-wheel is inverted only in the latter one to its phase enantiomer providing complete mirror image repetition of the former cycle.

4. Conclusion

The intramolecular transfer of chiral information in [(alkoxycarbonyl)methyl]-cobalt tricarbonyl triphenylphosphine complexes was investigated by semi-empirical quantum chemical and MM calculations. The phenomenon was interpreted in terms of interactions between the (prochiral) carboxyl group and the cobalt tricarbonyl moiety transmitting the dissymmetric induction to the chiral enantiomeric conformers of the PPh3 group through synchronous, correlated rotations of a series of σ-bonds.

Results of molecular graphical studies, stability calculations, rigid and relaxed conformation analyses have allowed, for the first time, the recognition of correlated motions of coaxial rotors, coupled bevel gear-like rotors with different periodicity, and a coupled conrotation within a molecular system. Our modelling studies revealed that the highly stereoselective interconversion of si,M and re,P enantiomeric forms of the [(etoxycarbonyl)methyl]cobalt tricarbonyl triphenylphosphine complex represents a strong analogy to macromechanical devices.

According to our knowledge the present system represents the most complete molecular analogue of a mechanical clockwork.

Extensive preparative and theoretical studies on the [(alkoxycarbonyl)methyl]-cobalt tricarbonyl triphenyl-phosphine type molecules are aimed at providing new molecular building blocks for design and synthesis of nanoscale components for nanomechanical structures.

Our studies in this area have also resulted in the first indication of a permanent one way rotation in a molecular system [25].

References

[1] (a) Mislow, K., Acc. Chem. Res. 1976, 9:26; (b) Iwamura, H., Mislow, K., Acc. Chem. Res. 1988, 21:175 and references therein.

[2] (a) Hoffmann, R.J., J. Am. Chem. Soc. 1978, 100:6274 and ibid. 1979, 101:3456; (b) Edidin, R.T., Northon, J.R., Mislow, K., Organometallics 1982, 1:3456.

[3] (a) Cozzi, F., Guenzi, A., Johnson, C.A., Mislow, K., Hounshell, W.D., Blount, J.F., J. Am. Chem. Soc. 1981, 103:957; (b) Johnson, C.A., Guenzi, A., Mislow, K., J. Am. Chem. Soc. 1981, 103:6240.

[4] Galamb, V., Pályi, G., Kajtár, M., Inorg. Chim. Acta 1981, 55, L113.

[5] (a) Pályi, G., Zucchi, C., Bartik, T., Herbrich, T., Kriebel, C., Boese, R., Sorkau, A., Fráter, G., AttiAccad. Sci. Ist. Bologna, Cl: Sci., Fis., Mem. 1992/93, 281(14,10):159; (b) Pályi, G., Alberts, K., Bartik, T., Boese, R., Fráter, G., Herbrich, T., Herfurth, A., Kriebel, C., Sorkau, A., Tschoerner, C.M., Zucchi, C., Organometallics 1996, 15:3253; (c) Galamb, V., Palyi, G., Cser, F., Furmanova, M.G., Struchkov, Yu.T., J. Organomet. Chem. 1981, 209:183; (d) Bartik, T., Krummling, T., Happ, B., Sieker, A., Marko, L., Boese, R., Ugo, R., Zucchi, C., Palyi, G., Catal. Lett. 1993, 19:383.

[6] (a) Galamb, V., Pályi, G., Coord. Chem. Rev. 1984, 59:203; (b) Kovács, I., Ungváry, F., ibid, 1997, 161:1.

[7] Zucchi, C., et al., submitted for publication, 2000.

[8] (a) Tasi, M., Pályi, G., Organometallics 1982, 4:1523; (b) Pályi, G., Zucchi, C., unpublished data, 1998; (c) Milstein, D., Huckaby, J.L., J. Am. Chem. Soc. 1982, 104:615; (d) Galamb, V., Pályi, G., Ungváry, F., Markó, L., Boese, R., Schmid, G., J. Am. Chem. Soc. 1986, 108:3344; (e) Galamb, V., Pályi, G., Boese, R., Schmid, G., Organometallics 1987, 6:861; (f) Wilford, F.B., Powell, H.M., J. Chem. Soc. A 1967, 2092; (g) Leigh, J.S., Whitmire, K.H., Acta Crys. C (Cr.Str.Commm.) 1989, 45:210; (h) Bartik, T., Krummling, T., Kruger, C., Markó, L., Boese, R., Schmid, G., Vivarelli, P., Pályi, G., J. Organometal. Chem. 1991, 421:323; (i) MacMeil, J.H., Chiverton, A.C., Fortrier, S., Baird, M.C., Hynes, R.C., Williams, A.J., Preston, K.F., Ziegler, T., J. Am. Chem. Soc. 1991, 113:9834; (j) Ungváry, F., Kovács, I., Hammerschmitt, B., Cordier, G., Organometallics 1993, 113:2849.

[9] The existence of a coordinative interaction between the Co atom and the carbonyl group of the ester moiety is supported by quantum chemical calculations: (a) Bencze, L., Szabó, M.J., Szilágyi, R.K., Pályi, G., NATO ASI: Metal-Ligand Interactions in Chemistry, Physics and Biology, Cetraro, Calabria, Italy, 1–12 September 1998, Abstract No. 28., p. 33.; (b) Szabo, M.J., Szilagyi, R.K., Zucchi, C., Bencze, L., submitted for publication, 2000.

[10] (a) Stewart, J.J.P., J. Comput. Chem. 1989, 10:209; (b) Stewart, J.J.P., J. Comput. Chem. 1989, 10:221.

[11] SPARTAN 4.0, Wavefunction, Inc., 18401 Von Karman, Suite 370, Irvine, California 92715.

[12] (a) Lindén, A., Roussel, C., Liljefors, T., Chanon, M., Carter, E.R., Mezger, J., Sandström, J., J. Am. Chem. Soc. 1976, 98:253; (b) Iroff, L.D., J. Comput. Chem. 1980, 1:76.

[13] The actual range of the motion is somewhat broader (~45–60°) in the vicinity of the transition state of ω_1, but the Co(CO)3 rotor recoils as the carbonyl oxygen of the –COOEt rotor has emerged over its plane at the end of the inversion. This sort of recoiling phenomenon is well known in horology, as well. Recoil escapement most commonly found in pendulum clocks, first used in the last quarter of the 17th century, but it is just almost the same in anchor (e.g. Brockot escapement) clocks: each tooth of the escape wheel, after it comes to rest is pressed backward by the pellets 33c.

[14] Feynman, R.P., in: Miniaturization Gilbert H.D. (ed.) Reinhold, New York, 1961, p. 282.

[15] (a) Rebek, J., Jr., Acc. Chem. Res. 1984, 17:258; (b) Mislow, K., Chemtracts Org. Chem. 1989, 2:151; (c) Evans, D.H., Fitch, A., J. Am. Chem. Soc. 1984, 106:3039; (d) Kilvay, K.V., Siegel, J.S., J. Am. Chem. Soc. 1991, 113:2332; (e) Lehn, J.-M., Supramolecular Chemistry VCH, Weinheim, 1995; (f) Ball, P.G., Garvin, L., Nature 1992, 355:761; (g) Feringa, B.L., Jager, W.F., de Lange, B., Tetrahedron 1993, 49:8267; (h) Willner, I., Willner, B., Adv. Mater. 1995, 17:587; (i) Kawai, S.H., Gilat, S.L., Lehn, J.-M., J. Chem. Soc. Chem. Commun. 1994, 8:1011.

[16] (a) Anelli, P.L., Shton, P.R., Ballardini, R., Balzani, V., Delgado, M., Gandolfi, M.T., Goodnov, T.T., Kaifer, A.E., Philp, D., Pietraszkiewicz, M.,

Prodi, L., Reddington, M.V., Slawin, A.M.Z., Spencer, N., Stoddart, J.F., Vincent, C., Williams, J.D., J. Am. Chem. Soc. 1994, 114:193; (b) Bradley, D., Science 1993, 259:890.

[17] Feringa, B.L., Jager, W.F., de Lange, B., Meijer, E.W., J. Am. Chem. Soc. 1991, 113:5468.

[18] Jorgenson, M., Lerstrup, K., Fredeiksen, P., Bjornholm, T., Sommer-Larsen, P., Schaumburg, K., Brunfeldt, K., Bechgaard, K., J. Org. Chem. 1993, 58:2785.

[19] Kelly, T.R., Bowyer, M.C., Bhaskar, K.V., Bebbington, D., Garcia, A., Lang, F., Kim, M.H., Jette, M.P., J. Am. Chem. Soc. 1994, 116:3657.

[20] Kelly, T.R., Tellitu, I., Sestelo, J.P., Angew. Chem. Int. Edit. 1997, 36:1866.

[21] Finocchiaro, P., Gust, D., Mislow, K., J. Am. Chem. Soc. 1974, 96:3198.

[22] (a) Malthete, J., Collet, A., Nouv. J. Chim. 1895, 9:151; (b) Malthete, J., Collet, A., J. Am. Chem. Soc. 1987, 19:7544; (c) Spielberg, N., Sakar, M., Luz, Z., Poupko, R., Billard, J., Zimmerman, H., Liq. Cryst. 1993, 15:311; (d) Cometti, G., Dalcanale, E., DuVosel, A., Levelut, A.-M., J. Chem. Soc. Chem. Commun. 1990, 163; (e) Zheng, H., Carroll, P., Swager, T.M., Liq. Cryst. 1993, 14:1421; (f) Tantravong, S., Styring, P., Goodby, J.W., J. Mater. Chem. 1993, 3:1209; (g) Giroud-Godquim, A., Maitlis, P.M., Angew. Chem. Int. Edit. 1991, 30:375; (h) Chandrasekhar, S., Liquid Crystals, Cambridge University Press, New York, 1992; (i) Chandrasekhar, S., Liq. Cryst. 1993, 14:3; (j) Hudson, S.A., Maitlis, P.M., Chem. Rev. 1993, 93:861.

[23] (a) Britten, F.J., The Watch and Clock Maker's Handbook, Dictionary and Guide, 11th edn., Antique Collectors' Club Ltd., Woodbridge, Suffolk, 1976; (b) Britten, F.W., Horological Hints and Helps, 4th edn., Antique Collectors' Club Ltd., Woodbridge, Suffolk, 1996; (c) The Country Life International Dictionary of Clocks, Consultant Smith A. (ed.), Country Life Books, The Hamilton Publishing Group, London, 1979.

[24] The most accurate analogue of this escapement action is the Brocot-escapement seen frequently in the front of the dial of 19th century French–American clocks. In the Brocot-escapement, the pellets are made from cylindrical pins and the impulse is given on the quarter circular face from the highest point of the lower lip of the pellet.

[25] Manuscript in preparation.

COPOLYMERIZATION OF ETHYLENE WITH NORBORNENE AND ITS FUNCTIONAL DERIVATIVES CATALYZED BY NICKEL COMPLEXES WITH PHOSPHORYLIDE LIGANDS

VICTOR I. BYKOV, VITALII A. DRONOV, TAMARA A. BUTENKO,
EUGENE SH. FINKELSHTEIN, KIRYL L. MAKOVETSKII

Topchiev Institute of Petrochemical Synthesis, Russian Academy of Sciences,
Leninsky prospect 29, Moscow 119991, Russia

Abstract: The addition polymerization of norbornene and its derivatives has been carried out in the presence of a nickel complex or carboxylate and an electron acceptor to obtain amorphous polymers with bicyclic units. Norbornene copolymers with conjugated dienes or ethylene cannot be obtained with these catalysts because of rapid chain transfer reactions. Norbornene can be copolymerized with ethylene under mild conditions in the presence of nickel phosphorylide chelates without using any cocatalyst. In most cases, the backbone of the resulting copolymer consists of alternating comonomer units. The new catalysts allow ethylene to be copolymerized with norbornene derivatives containing ester substituents.

Keywords: addition copolymerisation, ethylene, norbornene, functional derivatives of norbornene, nickel phosphorylide catalysts.

1. Introduction

High-molecular weight addition polymers of monocyclic olefins (cyclobutene and cyclopentene) and norbornene derivatives, whose backbone contains of cyclic units, were for the first time synthesized by Kaminsky and his colleagues [1] in the late 1980s. Polymerization was carried out in the presence of catalysts consisting of an *ansa*-zirconocene and methylalumoxane. Later, palladium [2] and nickel [3] complexes were applied to the addition polymerization of norbornene. Since then, a variety of catalysts based on transition metals (Ni, Pd, Co, Cr, Zr, and Ti) have been developed for this process. Amorphous saturated norbornene polymers containing bicyclic units are interesting because they combine remarkable properties: chemical and thermal stability, high transparence, low hygroscopicity, and good mechanical and dielectric characteristics [4]. However, the addition polymers of norbornene have a high glass transition temperature (T_g) close to their decomposition temperature (~400°C). Therefore, they cannot be processed by conventional methods. Therefore, it is necessary to introduce flexible units into the very rigid polynorbornene chain and thereby to reduce T_g. The

Y. İmamoğlu and V. Dragutan (eds.), Metathesis Chemistry: From Nanostructure Design to Synthesis of Advanced Materials, 453-460.

copolymerization of ethylene with norbornene leads to predominantly amorphous materials with relatively high glass transition temperatures, exhibiting numerous useful physical properties, such as high optical transparency, low birefringence, and low moisture absorption. These properties are very interesting for application in optics, especially for laser optical devices like CDs, DVDs, and optical lenses. Their high thermal stability (e.g. compared with polycarbonate) combined with low dissipating and dielectric loss factors makes copolymers suitable also for microelectronic applications. The properties of the copolymers depend strongly on the comonomer combination and comonomer contents.

The first success in this approach was norbornene–ethylene copolymerization in the presence of zirconocene catalysts [5]. Later, this method was refined and commercialized by researchers of Hoechst AG [6]. At present, norbornene–ethylene copolymers are manufactured by Ticona GmbH. (trademark Topas) [7].

Here, we report norbornene–ethylene copolymerization in the presence of specific nickel catalysts. Furthermore, we present some unpublished results concerning norbornene homopolymerization.

2. Experimental

Norbornene (Aldrich) was distilled in flowing argon. Norbornene solutions were stored in an argon atmosphere over sodium wire in Schlenk flasks. 5-Hexylnorbornene (BF Goodrich) was distilled in vacuo. Ethylaluminum sesquichloride, bis(cyclooctadiene) nickel, methyldiphenylphosphine, dimethylphenylphosphine (all from Aldrich), triphenylphosphine (Fluka), and acetylmethylenetriphenylphosphorane (Fluka) were used as received. Bis(π-pentenylnickel chloride) was obtained from pentenyl chloride and $Ni(CO)_4$ by the Fischer method [8]. Benzoylmethylenetriphenylphosphorane, $PPh_3 = CHC(O)Ph$, was synthesized from PPh_3 and phenacyl bromide by a procedure described in [9].

The solvents were purified by standard methods used in organometallic chemistry. All manipulations involved in the preparation of norbornene solutions and catalysts and in the charging of components into the reactor were made in an oxygen- and water-free argon atmosphere. Copolymerization was carried out in a 80 mL stainless steel reactor fitted with a magnetic stirrer.

The composition of resulting copolymers was determined by ^1H NMR spectroscopy in $CDCl_3$. NMR spectra were recorded on a Bruker Model MSL-300 spectrometer. Infrared (IR) spectra of the ylides and copolymers synthesized were recorded on a Specord M-82 spectrophotometer. Differential scanning calorimetry (DSC) studies were carried out using a Mettler calorimeter (heating rate, 20 K/min). The molecular weight distribution of copolymers was determined by gel permeation chromatography on a Waters chromatograph.

3. Results and discussion

Initially, we tested in norbornene polymerization nickel π-allyl complexes, which are known to be effective in the stereospecific polymerization of dienes. π-Pentenylnickel chloride appeared to be almost ineffective: only small amounts of liquid norbornene oligomers were detected. However, complexes obtained by reacting π-pentenylnickel chloride with various electron acceptors, such as nickel trichloroacetate, ether–BF_3 complex, and particularly alkylaluminum chlorides, effectively catalyzed the addition polymerization of norbornene. Later, it was found that the nickel π-allyl complex can be replaced with a nickel carboxylate or a nickel bis chelate. In all cases, we prepared saturated amorphous polymers with a relatively high molecular weight and a high T_g value. These polymers are well soluble in chlorinated arenes (chlorobenzene and dichlorobenzene) and cyclohexane and are insoluble in toluene and chloroform. Furthermore, we synthesized addition polymers of some norbornene derivatives (*endo*-dicyclopentadiene, *exo*-dicyclopentadiene, *endo,exo*-tetracyclododecene, and 5-substituted alkylnorbornenes). The activity of these monomers depends strongly on their conformation: the *exo* conformers polymerize much more rapidly than the *endo* conformers, particularly in the case of dicyclopentadiene. In 72 h dicyclopentadiene containing ~97% *endo* conformer is polymerized into a low-molecular weight polymer with M_w = 2800 in 55% yield. By contrast, specially synthesized *exo*-dicyclopentadiene polymerizes nearly as rapidly as norbornene. In this case, the yield of amorphous polymer is 75% in 1.5 h. This polymer has M_w =130,000 and is readily soluble in toluene and chloroform. Like polynorbornene, it does not vitrify up to decomposition temperature (~400°C).

Our attempts to copolymerize norbornene with conjugated dienes (butadiene and isoprene) or ethylene have been unsuccessful. With dienes, we obtained semiliquid polymers with M_w = 4000–6000 and M_n =1800–2500 that consisted mainly of norbornene units and contained only one or two diene units. Copolymerization with ethylene resulted in only low-molecular weight polynorbornene with terminal vinyl groups because of chain transfer occurring at a high rate.

In searching for norbornene–ethylene copolymerization catalysts, we looked at nickel phosphorylide complexes. Keim et al. [10] reported the ylide complex I as an effective catalyst for ethylene oligomerization.

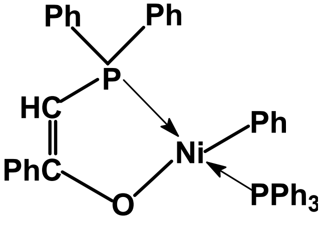

I

The phosphine ligand ensures chain transfer and the formation of C_8–C_{30} ethylene oligomers. Later, it was found that replacing PPh_3 in **I** for a weakly bonded ligand, such as pyridine, results in high-molecular weight polyethylene rather than oligomers [11].

We assumed that such complexes can initiate norbornene–ethylene copolymerization as well. The pyridine-containing complex **II**

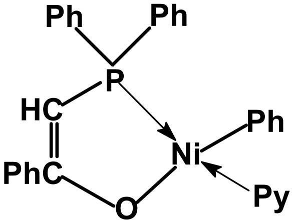

II

was synthesized by reacting equimolar amounts of benzoylmethylenetriphosphorane and $(\pi\text{-}C_8H_{12})_2Ni(0)$ in the presence of pyridine. At room temperature, this complex was almost inactive in norbornene homopolymerization. In contrast, norbornene–ethylene copolymerization in toluene in the presence of **II** occurred even at low temperatures (Table 1) and did not require any cocatalyst. The use of nickel phosphorylide complexes in norbornene–ethylene copolymerization was patented by us together with BF Goodrich people [12].

Unlike polynorbornene, the copolymers obtained with complex **II** are readily soluble in ordinary organic solvents. According to DSC data, the copolymers are amorphous and show only one phase transition, specifically, a glass transition at 125–150°C. They have a comparatively low molecular weight (usually $M_w \leq 2 \times 10^4$) and a unimodal molecular weight distribution. Equimolar amounts of $(\pi\text{-}C_8H_{12})_2Ni(0)$ added to the catalyst allow the molecular weight to be somewhat increased. The composition of the copolymers was derived from ^1H NMR data, making use of the fact that the signals between

Table 1. Copolymerization of norbornene (NB) and ethylene in the presence of complex **II**

№	T °C	Ethylene pressure, atm	Time, h	Copolymer yield, % based on NB	T_g, °C	NB content in copolymer, mol.%	$M_w \times 10^3$	M_w/M_n
1	20	20	3	138	75	34	16.8	2.0
2	20	5	3.5	115	99	42	15.1	2.0
3	20	1	6	18	144	57	13.8	1.8
4*	50	5	4	24	153	59	7.4	2.6
5**	20	5	4	87	125	51	32.5	1.6
6	20	5	4	44	125	51	21.1	1.7
7	80	5	4	45	126	51	5.1	3.0

*Copolymerization in norbornene melt

With addition of the equimolar amount of $(C_8H_{12})_2Ni(0)$ to complex **II

1.7 and 2.4 ppm are from two types of protons in the norbornene unit. As a rule, these copolymers contained 40–50 mol % of norbornene units. Raising the polymerization temperature to 50–70°C reduces both activity of the catalyst and molecular weight of the copolymer.

In some experiments, the catalyst was prepared in situ by charging the reactor with solutions of the ylide and $(\pi\text{-}C_8H_{12})_2Ni(0)$ in the presence of norbornene. In this case, norbornene served as a weakly bonded ligand. In order to study effect of a structure of the complex on catalytic activity and on properties of the copolymer, we synthesized a series of ylides with substituents in different positions in the ylide structure. A series of nickel complexes with general formula **III** was obtained in situ from these ylides, and these complexes were tested in norbornene–ethylene copolymerization.

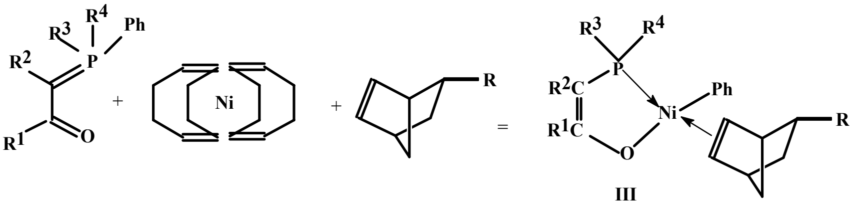

III

R^1= OEt	**R^1= Ph**	**R^1= Ph; Me; H**
R^2=H	**R^2=H**	**R^2=H; SO_3Na**
R^3=Ph, R^4=Ph	**R^3=Me, R^4=Ph** **R^3=Me, R^4=Me**	**R^3=Ph, R^4=Ph**
Inactive	**Low active**	**Active**

The nickelylide complexes show different activities. High yields of copolymers with moderate molecular weights can be obtained with a complex prepared from benzoylmethyltriphenylphosphorane or acetylmethyltriphenylphosphorane.

It should be noted that the successive replacement of phenyl groups at the phosphorus atom by methyl groups causes a considerable decrease in catalytic activity and, at the same time, increases the proportion of norbornene units in the resulting copolymers from 40–58 to 60–70 mol %. This is accompanied by an increase in T_g. Spectroscopic data indicate the presence of norbornene–norbornene dyads in these copolymers.

In order to increase the molecular weight of the copolymers, we carried out norbornene–ethylene copolymerization at lower catalyst concentrations (Table 2). Although copolymerization in this case is much slower at room temperature, it affords large amounts of copolymers with molecular weights up to 10^5.

Table 2. Copolymerization of norbornene (NB) and ethylene at 20°C in toluene with catalyst **III** ($R^1 = R^2 = R^4 = Ph$, and $R^3 = H$) obtained in situ

No.	Ethylene pressure (atm)	NB:Ni (mol/mol)	Time (h)	Copolymer yield based on NB (%)	T_g (°C)	NB content in copolymer (mol %)	$M_w \times 10^3$	M_w/M_n
1	20	300:1	20	36	146	58	27.6	1.7
2	5	800:1	20	24	143	57	89.3	1.6
3	1	2000:1	70	50	138	55	99.4	2.2
4	5	3000:1	20	54	132	53	95.5	3.2
5	5	6000:1	40	46	125	51	93.0	2.9

The ylide catalysts **III** were also used in the synthesis of ethylene–hexylnorbornene copolymers and ternary copolymers of ethylene, norbornene, and substituted norbornenes containing hexyl or trimethylsilyl groups (Table 3).

The nickel phosphorylide complexes allow ethylene to be copolymerized with functionalized norbornenes. We synthesized copolymers of ethylene and norbornene with ester substituents, namely, 5-methylcarboxy and 5-*tert*-butylcarboxy groups. The copolymer yields 40–60% were achieved in 5–6 days. The copolymers have molecular weight of M_w = 17,100–20,000 and

Table 3. Binary and ternary copolymers of ethylene, norbornene, and 5-hexylnorbornene or 5-trimethylsilylnorbornene prepared in the presence of catalyst **III** (R1, R2, R4 = Ph; R3 = H) at 20°C (toluene is used as a solvent)

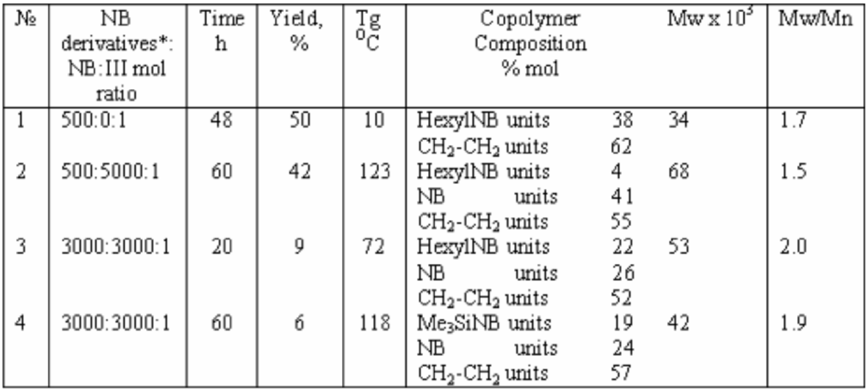

№	NB derivatives*: NB:III mol ratio	Time h	Yield, %	Tg °C	Copolymer Composition % mol		Mw x 10^3	Mw/Mn
1	500:0:1	48	50	10	HexylNB units CH_2-CH_2 units	38 62	34	1.7
2	500:5000:1	60	42	123	HexylNB units NB units CH_2-CH_2 units	4 41 55	68	1.5
3	3000:3000:1	20	9	72	HexylNB units NB units CH_2-CH_2 units	22 26 52	53	2.0
4	3000:3000:1	60	6	118	Me_3SiNB units NB units CH_2-CH_2 units	19 24 57	42	1.9

Ethylene pressure 14 atm

*In experiments 1–3, 5-hexylnorbornene was used as a norbornene derivative; in experiment 4, 5-trimethylsilylnorbornene was used

polydispersity index (PDI) = 1.7–2.0. The composition of the ethylene–carboxynorbornene copolymers were determined by ^{1}H NMR and ^{13}C NMR spectroscopy. The polymers were found to contain 30–46 mol % bicyclic units, and their T_g were 51–117°C. The copolymers of ethylene with functionalized norbornenes cannot be obtained with zirconocene catalysts.

It was noted that norbornene–ethylene copolymers, obtained in the presence of the nickel ylide catalysts, can contain comonomer units in nearly equimolar proportions. The mechanism of the formation of these copolymers can be viewed as follows. The norbornene molecule coordinated with the Ni atom cannot insert itself into the Ni–phenyl or Ni–norbornyl bond for steric reasons, while the insertion of ethylene into these bonds takes place readily. This leads to copolymers in which comonomer units alternate with a high degree of regularity.

Thus, we demonstrate that norbornene–ethylene copolymers can be synthesized using comparatively simple nickel phosphorylide complexes. Although these copolymerization catalysts are less active than the systems based on zirconocene and methylalumoxane, they do not require any cocatalyst (e.g. alumoxane, which is an expensive chemical). Moreover, the lower oxophility of nickel in the ylide catalysts allows ethylene to be copolymerized with functionalized norbornenes.

Acknowledgments

This work was supported by the Presidium of the Russian Academy of Sciences through the Fundamental Problems of the Physics and Chemistry of Nanosized Systems and Nanomaterials Program, and by the Support of Leading Scientific Schools Program.

References

[1] Kaminsky, W., Bark, A., Daeke, I., Proceedings Of the International Symposium on Recent Developments in Olefin Polymerization Catalysis, Amsterdam, 1990, p. 425.
[2] Mehler, C., Risse, W., Makromol. Chem., Rapid Commun. 1991, 12(5):255.
[3] Makovetskii, K.L., Gorbacheva, L.I., Golenko, T.G., Ostrovskaya, I.Ya., Vysokomol. Soedin., Ser. A 1996, 38(3):435.
[4] Makovetskii, K.L., Vysokomol. Soedin., Ser. B 1999, 41(9):1525.
[5] Kaminsky, W., Bark, A., Arndt, M., Makromol. Chem., Macromol. Symp. 1991, 47:83.
[6] Cherdron, H., Breckner, M.-J., Osan, F., Angew. Makromol. Chem. 1994, 223(4011):121.
[7] Chem. Eng. 2000, 107(11):25.
[8] Fischer, E.O., Buerger, C., Z. Naturforsch., B: Anorg. Chem. Org. Chem. Biochem. Biol. 1961, 16(1):77.
[9] Ramirez, F., Dershowitz, S., J. Org. Chem. 1957, 22(1):43.
[10] Keim, W., Kowaldt, F.H., Goddard, R., Krueger, C., Angew. Chem. Int. Edit. 1978, 17(6):466.
[11] Klabunde, U., Ittel, S.D., J. Mol. Catal. 1987, 41(2):123.
[12] Makovetskii, K.L., Finkelshtein, E.Sh., Bykov, V.I., Bagdasaryan, A.Kh., Goodall, B.L., Benedict, G.M. US Patent 5929181, 1999.

CARBONYL–OLEFIN EXCHANGE REACTION: PRESENT STATE AND OUTLOOK

CHRISTO JOSSIFOV, RADOSTINA KALINOVA

Institute of Polymers, Bulgarian Academy of Sciences, Acad.G. Bonchev str. 103A, 1113 Sofia, Bulgaria

Abstract: The carbonyl–olefin exchange reaction (COER) is a new reaction between carbonyl group and olefin double bond, which has a formal similarity with the olefin metathesis (OM) – one carbon atom in the latter is replaced with an oxygen atom. Till now the new reaction is performed successfully only when the two functional groups (carbonyl group and olefin double bond) are in one molecule and are conjugated. The α,β-unsaturated carbonyl compounds (substituted propenones) are the compounds with such a structure. They polymerize giving substituted polyacetylenes. The chain propagation step of this polymerization is in fact the COER. The question arises: is it possible the COER to take place when the two functional groups are not in one molecule and are not conjugated, and could this reaction became an alternative of the existing carbonyl olefination reactions?

Keywords: carbon–carbon bond formation reactions, carbonyl–olefin exchange reaction, olefin metathesis, reductive coupling of carbonyl compounds, carbonyl olefination, conjugated polymers

1. Introduction

In studying the evolution of organic chemistry and grasping its essence, one comes quickly to the conclusion that no other type of reaction has a role in shaping this domain of science more important than that of carbon–carbon bonds forming reactions. The Grignard, Diels–Alder, and Wittig reactions are but three prominent examples of such processes.

In the last quarter of the 20th century a new family of C–C forming reactions based on transition metal catalysts evolved as powerful tools in synthesis. Palladium-catalyzed cross-coupling reactions (Heck, Stile, Suzuki)[1] and metathesis of olefins, enynes, and alkynes[2] have had a profound impact on the art of total synthesis.

The present paper deals with a new carbon–carbon double bond formation reaction, discovered at the Institute of Polymers, Bulgarian Academy of Sciences.

Y. İmamoğlu and V. Dragutan (eds.), Metathesis Chemistry: From Nanostructure Design to Synthesis of Advanced Materials, 461-470.

2. Carbonyl–olefin exchange reaction: present state

In 1983 was published the first paper of the series "Carbonyl-olefin exchange reaction (COER). A new route to conjugated polymers".[3] We have shown in this paper that treatment of an α,β-unsaturated carbonyl compound 1,3-diphenylprop-2-en-one (chalkone) with WCl_6 results in the formation of polyphenylacetylene and benzaldehyde (Eq. 1).

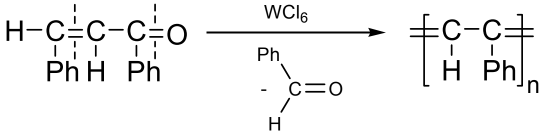

(1)

Using the same procedure several differently substituted α,β-unsaturated carbonyl compounds were polymerized thus obtaining substituted polyacetylenes (polyphenylacetylene, polydiphenylacetylene, polymethylacetylene, polycamphor etc.).[4,5] The general scheme of these transformations can be represented as follow (Eq. 2).

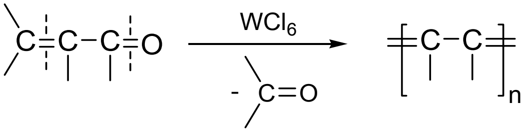

(2)

The single C–C bond can be a part of a cycle as well.

The chain propagation step of this polymerization process can be described as a cleavage of the double bonds and generation of new ones. The final result is a redistribution of atoms (C and O) connected with double bonds (Eq. 3).

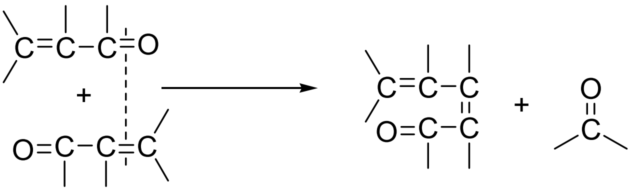

(3)

This is a new reaction. We named it COER. There is a formal similarity between the schemes of the olefin metathesis (OM) and COER. One carbon atom in the scheme of OM is replaced with oxygen atom (Eq. 4)

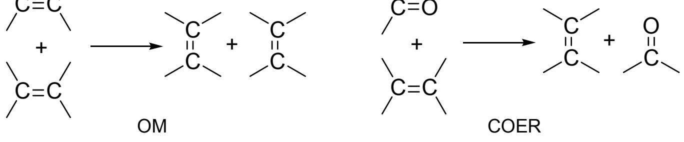

(4)

The dimer obtained via COER (Eq. 3) (the first step in Eq. 2) possesses a carbonyl and olefin end groups and is able to undergo further similar transformations resulting into chain propagation. Every step is accompanied by the evolution of a low molecular weight product. The dimer formation was proved by comparing the gel permeation (GP) chromatogram of the reaction mixture to that of an authentic sample prepared separately.[6,7] The dimer polymerizes under the influence of WCl_6 giving again substituted polyacetylene and carbonyl compound. All these facts show that the polymerization of α,β-unsaturated carbonyl compounds is a step process and a true polycondensation reaction.

The results of the investigations on the α,β-unsaturated carbonyl compounds polymerization can be described shortly as follow:

1. The reaction can be carried out either without solvents or in aromatic solvents. Better results are obtained in chlorobenzene.[8]
2. The yield and molecular weight rise with the quantity of WCl_6 (up to ratio monomer : WCl_6 = 1:1), with the temperature (up to 120°C) and with the time. It should be mentioned that with an equimolar amount of WCl_6 the reaction takes place even at ambient temperature.
3. During the reaction the transition metal changes its degree of oxidation.[9]
4. The more substituted the propenone is, the higher is the yield of the polymer.[4]
5. The polyacetylenes are obtained as complexes containing up to 40 mol % WCl_6, which is in accordance with the fact that several conjugated polymers can be partially oxidized ("doped") with WCl_6.[10] In order to obtain pure polymer it is necessary to treat the stable complex with concentrated sodium hydroxide.
6. Some of the low molecular weight carbonyl compounds (benzaldehyde, acetophenone), formed in the main reactions, interact with WCl_6 evolving HCl. Others (benzophenone) do not react with WCl_6. In the latter cases higher yields of polymers (up to 100%) can be achieved using lower amounts of WCl_6 (WCl_6: monomer < 1:1).

The polymerization of α,β-unsaturated carbonyl compounds is very similar to the Friedel–Crafts synthesis of aromatic ketones, where the catalyst forms a complex with the reaction products and therefore is necessarily to be used in equimolecular amount. In order to avoid the WCl_6 consumption via doping of polyacetylenes we tried to perform COER with highly substituted olefins (tetraphenylethylene, stylbene, 1,1-diphenylethylene) and simple carbonyl compounds (benzophenone, terephthalaldehyde) using WCl_6 as catalyst. In these cases the two functional groups are in different molecules and the results should be new olefins and new carbonyl compounds, not a conjugated polymer. The gas chromatography (GC) analyses show that the desired products appear in the reaction mixture but in very low quantities.[11] Most probably WCl_6 is not a good catalyst for COER in general. It is active only when the two functional groups are in one molecule and are conjugated.

WCl_6 is a representative of the classical catalytic systems for OM.[12] Because of this and because of the formal similarity between COER and OM we looked among the above mentioned systems for a more effective catalyst for COER. We were not able to promote COER when the two functional groups are not conjugated, but we have found that some of them are active in the polymerization of α,β-unsaturated carbonyl compounds.[13] The best results are obtained when so called Friedel–Crafts metathesis catalytic systems (transition metal halides or oxohalides + Lewis acids) are used. Performing these investigations we ran into very striking unexpected results: Using $WOCl_4$ (alone or in combination with $AlCl_3$ as cocatalyst) as a catalyst for polymerization of 1,2,3,3-tetraphenylprop-2-en-1-one, the yield of polydiphenylacetylene was higher than the expected one with regard to the stoichiometry presented in Eq. 3 (Table 1).[13]

Table 1. Experimental results from the polymerization of 1,2,3,3-tetraphenylprop-2-en-1-one mediated by $WOCl_4$ + $AlCl_3$

Experiments[a]	**1**	**2**	**3**
$WOCl_4$ in g	0.66	0.60	0.016
$AlCl_3$ in g	–	0.28	0.10
Polymer yield in g	0.94	0.86	0.95

[a]Reaction conditions: monomer 1,2,3,3-tetraphenylprop-2-en-1-one (1g); solvent: chlorobenzene; time: 8 h; temperature: 90°C; theoretical yield of oligomeric and polymeric products according to Scheme 3 – 0.49 g.

When $AlCl_3$ is used as cocatalyst, the polymer has more pronounced carbonyl infrared (IR) absorption than that of the polymer obtained with $WOCl_4$ alone, both polymers having almost the same molecular weight. This phenomenon could be explained assuming that the polymer molecules possess different end groups. Traces of molecular oxygen, benzophenone, tetraphenylethylene, and benzyl were identified among the reaction products.[14] Quantitative transformation of the monomer can be achieved even with catalytic amounts of $WOCl_4$ (Table 1, Exp. 3). All these results can be described with Eq. 5.[15]

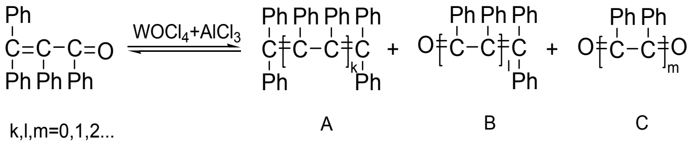

(5)

A(k=0) - tetraphenylethylene
A(l=0) - benzophenone
A(m=1) - benzil
A(m=0) - molecular oxygen

Obviously several double bond formation reactions have taken place simultaneously and these reactions should be catalytic ones. We presume these are: COER (Eq. 6), OM (Eq. 7), and reductive coupling (RC) of carbonyl compounds, accompanied with molecular oxygen evolution (Eq. 8).

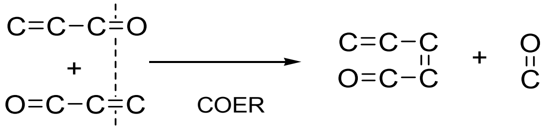

(6)

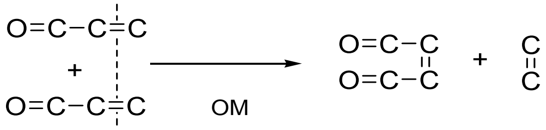

(7)

(8)

In the case of 1,2,3,3-tetraphenylprop-2-en-1-one polymerization the new double bonds are always the same (polydiphenylacetylene repeating unit) regardless of the type of the reaction. The low molecular weight products, however, are different – carbonyl compound, olefin and molecular oxygen, respectively. The only polymer formation reaction is the COER (the dimer and the oligomer products possess carbonyl and olefin end groups). The other two reactions give dimers or double the molecular weights of the oligomers obtained via COER. The higher yield than stoichiometry of COER allows, could be explained by the participation of all double bonds (not only the end-ones) and the low molecular weight products in the reactions under discussion, i. e. by accepting these reactions are reversible. One example explaining the benzil formation is given in Eq. 9

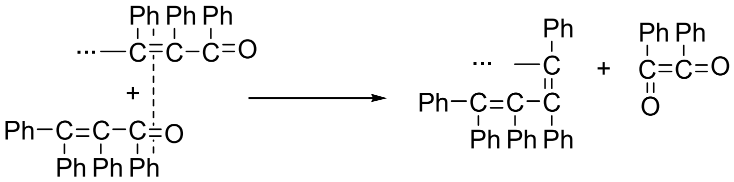

(9)

If this explanation is correct one can suggest that the above mentioned reactions could run separately. In proving this assumption we have succeeded unprecedentedly to carry out reductive coupling polymerization of the conjugated dicarbonyl compound benzil under the influence of the Friedel–Crafts metathesis catalytic system $WCl_6 + AlCl_3$.[16] In this case the quantity of the transition metal compound is less than the quantity of the Ti reagent used for

McMury reaction. The very new moment here is the absence of reducing agent. The result is polydiphenylacetylene with carbonyl end groups. If this reaction proceeds in the presence of tetraphenylethylene the polymer obtained has olefin end groups, which is a result of COER between the carbonyl end groups and the olefin tetraphenylethylene (Eq. 10).

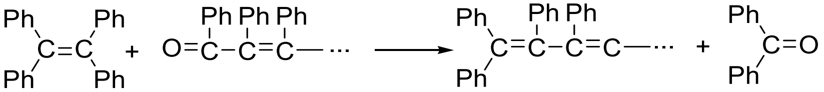

(10)

Thus we succeeded for the first time to perform COER when the two functional groups (olefin and carbonyl) are not in the same molecule.[16,17] The carbonyl group in this case however is again conjugated. If the double bond of the olefin is included into a cycle the cycloolefins could copolymerize with conjugated dicarbonyl compounds. We succeed indeed for the first time in copolymerizing benzyl, terephthalaldehyde, and benzoquinon with cycloolefins (cyclopentene, cyclooctene, norbornene).[18,19,20] The result of this copolymerizations are oligomer products possessing conjugated blocks, originating from the dicarbonyl compounds, connected with soft segments, originating from the cycloolefins. The latter, however, do not contain unconjugated olefin double bonds. These facts show that the situation is more complicated than we have expected.

In summary we explained our unexpected experimental results accepting that the three double bond formation reactions (COER, OM an RC) can take place simultaneously. This could be possible if some kind of relationship between these reactions exists. What could be the relation? To answer the question we should discuss each of the reactions separately.

The reductive coupling of carbonyl compounds (Eq. 11) by transition metal complexes is an important method for carbonyl olefination.[21]

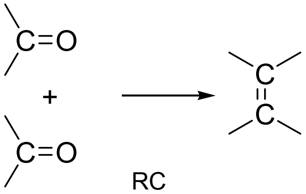

(11)

The reaction running under the influence of reduced Ti reagents is known as McMurry reaction. The driving force of this reaction is the formation of the Ti=O bonds. The species containing such bonds are no more active. That is why the quantity of the reagent is high – usually 2 mol for 1 mol carbonyl compound. The mechanism of this reaction is too obscure. However there is a strong supports that it follows a carbene mechanism[22] when the system $WCl_6 + LiAlH_4$ (a representative of the classical catalytic systems for OM) is used.

The carbene mechanism of the OM in all its variants (ROM, ROMP, RCM, ADMET) is well documented. Numerous heterogeneous and homogeneous catalytic systems are known to initiate this reaction. The classical systems consist of compound of transition metal (especially from groups VI or VII of the periodic system, W, Mo and Re being the most active) alone or in combination with organometal compounds (Ziegler–Natta type) or with Lewis acids (Friedel–Crafts type). These systems have a lot of drawbacks: side reactions (alkylation, isomerization, cyclization, addition across the double bond) can occur during OM; they suffer from a limited substrate scope – they are not tolerant toward some functional groups; it is difficult to describe the generation and the structure of the active carbene complexes; the proper degree of oxidation of the transition metal atom is still under discussion.[23]

All these drawbacks are overcome by synthesizing well defined carbene complexes (Fisher, Osborn, Grubbs, Schrock, Hoveida, etc.). This has led to a much better understanding of the mechanism, to preparation of a new family of block copolymers through the use of “living” systems and to an explosion of applications in the synthesis of biologically active compounds. In 2005 the OM turned to be a Nobel Prize winning topic in Chemistry.

Having in mind the carbene mechanism of the OM and the existence of strong supports for carbene mechanism of the RC of the carbonyl compounds we launched the hypothesis about the carbene mechanism of the COER thus underlying the relation between these three reactions. The hypothesis is based on the existence of common catalytic systems and on the fact that the transition metal carbene complexes can take part in many [2 + 2] metathesis reactions between multiply bonded compounds.[24] These reactions may be represented in shorthand form by the Eq. 12.

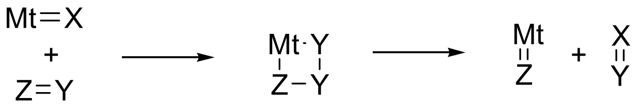

$$\begin{matrix}Mt=X\\+\\Z=Y\end{matrix} \longrightarrow \begin{matrix}Mt\cdot Y\\|\quad\;|\\Z-Y\end{matrix} \longrightarrow \begin{matrix}Mt\\\|\\Z\end{matrix} + \begin{matrix}X\\\|\\Y\end{matrix} \qquad (12)$$

Mt is a transition metal.

Many reactions can be envisaged using this scheme. For some of them (OM (X = Y = Z = C) and carbonyl olefination via Wittig-like reaction of the transition metal carbene complexes[25] (Z = O, X = Y = C)) the validity of Eq. 12 is well documented. For others (X = O, Y = Z = C) it is only suggested.[26,27] The other combinations are still unknown reactions.

The carbene mechanism of COER according to our hypothesis consists of forward (Z = O, X = Y = C) and backward (X = O, Y = Z = O) Wittig-like reactions.[28] A transition metal–carbene complex reacts with a carbonyl compound generating an olefin and transition metal oxo-complex. Then the oxo-complex reacts with another olefin generating a new carbonyl compound and regenerating the transition metal–carbene complex. It is known that oxo-alkylidene complexes can be generated via oxidative addition reaction between some tungsten complexes with carbonyl compounds.[29]

There are, however, a few papers describing OM catalyzed by nontransition elements,[30] platinum- and acid-catalyzed enyne metathesis,[31] and acid catalyzed olefination of benzaldehyde with an olefin.[32] The reported mechanisms of these transformations do not include participation of carbene species. Because WCl_6 is a Lewis acid itself a noncarbene mechanism of COER cannot be ruled out.

3. Conclusion

It is well known that the transition metal compounds are able to promote many reactions and that it is difficult to make one of them to prevail over the others. It is even more difficult to elucidate the mechanism of a new reaction mediated by these compounds. The use of well defined transition metal complexes is a well established way to overcome these difficulties. There are numberless ligands that facilitate tuning the reactivity of a given metal. Almost all the reactions discovered during the last quarter of the 20th century are illustrations of this strategy. In addition some of the well defined transition metal complexes are able to mediate different reactions. For example, the carbene complexes accelerate the Kharash reaction and atom transfer radical polymerization[33] and the Mn and Cr salen complexes accelerate the cyclopropanation and epoxidation of olefins.[34] We believe that it would be possible to synthesize transition metal complexes able to catalyze the COER when the two functional groups are not in one molecule and are not conjugated. It is worth working in this direction. If such complexes will be synthesized, then the COER will be an alternative to some of the existing carbon–carbon bond formation reactions, especially to the carbonyl olefination reactions (Wittig, Peterson, Julia, etc. reactions).

Acknowledgments

The financial support of this work by the National Science Fund of the Bulgarian Ministry of Education and Science, project X-1413, is gratefully acknowledged.

References

[1] Nicolaou, K.C., Bulger, P.G., Sarlah, D., Angew. Chem. Int. Edit, 2005, 44:4442–4489 and the references there in.
[2] Grubbs, R.H. (ed.) Handbook of Metathesis, Vols 1–3, Wiley-VCH, Weinheim, 2003.
[3] Schopov, I., Jossifov, C., Macromol. Chem., Rapid Commun. 1983, 4:659–662.
[4] Schopov, I., Mladenova, L., Macromol. Chem., Rapid Commun.1985, 6:659–663.
[5] Schopov, I., Mladenova, L., Synthetic Metals 1992, 48:249–258.
[6] Schopov, I. Acta Polymerica. 1988, 39:91–94.
[7] Schopov, I, Mladenova, L., Macromol. Chem 1989, 190:1483–1488.
[8] Schopov, I, Mladenova, L., Kovachev, G., Macromol. Chem 1988, 189: 1787–1792.
[9] Jossifov, C., Schopov, I., Eur. Polym. J 1993:621–623.
[10] Shirakawa, H., Kobayashi, T., J. Phys. C3 1983, 44:3.
[11] Unpublished results.
[12] Dragutan, V., Balaban, A.T., Dimonie, M. (eds) Olefin Metathesis and Ring-Opening Polymerization of Cyclo-Olefins, Editura Academiei Bucuresti/Wiley, Chichester, 1985.
[13] Jossifov, C., Schopov, I., Macromol. Chem. 1991, 192:857–861.
[14] Jossifov, C., Schopov, I., Macromol. Chem. 1991, 192:863–866.
[15] Jossifov, C., Eur. Polym. J. 1993, 29:9–13.
[16] Jossifov, C., Eur.Polym. J. 1998, 34:883–885.
[17] Pavlic, M., Pfleger, J., Jossifov, C., Vohlidal, J., Macromol. Symp. 2004, 211:555–562.
[18] Jossifov, C., J. Mol. Cat. A: Chem. 1998, 135:263–267.
[19] Jossifov, C, Ilieva, O., J. Mol. Cat. A: Chem. 2002, 190:235–239.
[20] Unpublished results.
[21] Takeda, T. (ed.) Modern Carbonyl Olefination, Wiley-VCH Verlag, 2004, pp. 223–285.
[22] Fujiwara, Y., Ishikawa, R., Akyama, F., Teranishi, S., J. Org. Chem. 1978, 43:2477–2480.
[23] Katz, T., Angew. Chem. Int. Edit. 2005, 44:3010–3019.
[24] Ivin, K.J., Mol, J.C. (eds), Olefin Metathesis and Metathesis Polymerization, Academic Press, San Diego/London/Boston/New York/Sydney/Tokyo/Toronto, 1997, p. 82.
[25] Takeda, T. (ed.) Modern Carbonyl Olefination, Wiley-VCH, Verlag, 2004, pp. 151–199.
[26] Sharpless, K.B., Teranishi, A.Y., Backvall, J. –E., J. Am. Chem. Soc. 1977, 99:3120–3128.
[27] McGarrigle, E.M., Gilheany, D.G., Chem. Rev. 2005, 105:1563–1602.
[28] Jossifov, C., in: Khosravi E., Szymanska-Buzar, T. (eds) Ring Opening Metathesis Polymerization and Related Chemistry, NATO Science Series, II/56, 2002, pp. 425–436.
[29] Bryan, J.C., Mayer, J.M., J. Am, Chem. Soc. 1990, 112:2298–2308.
[30] Ivin. K.J, Mol, J.C. (eds), Olefin Metathesis and Metathesis Polymerization, Academic Press, San Diego/London/Boston/New York/Sydney/Tokyo/Toronto, 1997, p. 12.

[31] Furstner, A., Szillat, H., Gabor, B., Mynott, R., J. Am. Chem. Soc. 1998, 120:8305–8314.
[32]. Van Schaik, H.-P, Vijen, R-J., Bickelhaupt, F., Angew. Chem. Int. Edit. 1994, 33:1611–1612.
[33] Simal, F., Demonceau, A., Noels, A.F., Tetrahedron Lett. 1999, 40:5689–5693.
[34] Katsuki, T., Adv. Synth. Catal. 2002, 344:131–147 and references therein.

IMMOBILIZATION OF METAL NANOPARTICLES IN SURFACE LAYER OF SILICA MATRICES

KSENIIA KATOK, VALENTIN TERTYKH, VICTOR YANISHPOLSKII

Institute of Surface Chemistry of National Academy of Sciences of Ukraine,
17 General Naumov Str., 03164 Kyiv-164, Ukraine

Abstract: Gold and silver nanoparticles were obtained by in situ reduction with silicon hydride groups grafted to the mesoporous MCM-41 silica surface. Nickel-, cobalt-, and iron-containing silicas were synthesized by chemisorption of appropriate metal acetylacetonates with following reduction in the acetylene atmosphere. Such metal-containing MCM-41 matrices have been applied for preparation of carbon nanostructures at pyrolytic decomposition of acetylene. From transmission electron microscopy (TEM) data a lot of carbon nanotubes were formed, namely tubes with external diameter of 10-35 nm for Ni-, 42–84 nm for Co-, and 14–24 nm for Fe-containing silicas. In the metal absence on the silica surface low yield of nanotubes (up to 2%) was detected.

Keywords: MCM-41 silica, surface silicon hydride groups, gold and silver in situ reduction, nickel, cobalt, and iron acetylacetonates, acetylene pyrolysis, carbon nanotubes

1. Introduction

Manufacturing composites that contain monodispersed nanodimensional clusters of metals would have potential use in heterogeneous catalysis,[1] surface-enhanced Raman scattering,[2] and other fields, where surface properties of materials and interfacial phenomena are important.

One of possible approaches to such a controlled synthesis is use of porous matrices that confine growth of nanoparticles. But particle size depends also on the method of supporting, conditions of metal ions reduction at a surface and stabilization of the formed nanoparticles in order to prevent their aggregation.

For preparation of supported metal nanoparticles the chemically modified ordered mesoporous silica of MCM-41 type was applied in this work. The surface of such matrix contained chemically bound groups possessing reducing properties towards metals which are allocated after hydrogen in the electromotive series. For this purpose we have also used the volatile metal-containing compounds (acetylacetonates of iron-, nickel-, and cobalt), which

Y. İmamoğlu and V. Dragutan (eds.), Metathesis Chemistry: From Nanostructure Design to Synthesis of Advanced Materials, 471-481.

can react with silanol groups with following chemisorption on the silica surface. Both these approaches can allow to obtain metal nanoparticles in the close vicinity to the appropriate surface compounds and, thus, to fulfill definite anchorage (immobilization) of the formed nanoclusters. It is expedient to use obtained iron-, nickel-, and cobalt-containing mesoporous silicas as catalysts in pyrolytic synthesis of carbon nanostructures. As known, interest to carbon nanotubes is caused by potential opportunities of their use as scanning probes[3] and sensors,[4] as active elements of field emitters,[5] as matrice templates for preparation of nanocomposites.[6]

2. Experimental

Synthesis of ordered mesoporous silica, such as MCM-41, was carried out according to recommendations[7] in a reaction mixture with a molar ratio of reagents 1.0TEOS:0.52CTMABr:16NH_3:39H_2O in the following way. Cetyltrimethylammonium bromide (8.3 g) (CTMABr, Aldrich) was introduced into aqueous ammonia (25 wt%, 126 mL), then tetraethoxysilane (9 g) (TEOS) was added and the mixture was heated at 70°C under stirring before formation of the gel structure. The sample obtained was calcined at 540 C for 6 h in air. Structural characteristics of silica were studied by nitrogen ad(de)sorption measurements at 77 K (Micromeritics ASAP-2000 system).

2.1 Preparation of gold- and silver-containing silica matrices

Reducing reagents immobilized on the external surface of ordered mesoporous silicas were used for in situ reduction of nanoparticles of gold or silver at the interaction with corresponding salt solutions in the mild conditions. For this, silica matrix was modified with triethoxysilane in the presence of acetic acid with the object of producing grafted silicon hydride groups (≡SiH) on the silica surface. Then modified silica was impregnated with chloroauric acid or silver nitrate solutions at room temperature and was dried for 24 h in an oven at 150°C.

Presence of silicon hydride groups grafted to the silica surface was confirmed by Fourier transform infrared (FTIR) spectra data (NEXUS FT-IR) Nanoparticles of metals were recorded using x-ray powder diffraction (DRON-4-07, CuK$_\alpha$-radiation). Ultraviolet–visible (UV–Vis) spectra of metal-containing composites were recorded on Carl Zeiss Jena spectrophotometer.

2.2 Preparation of nickel-, cobalt-, and iron-containing mesoporous silica matrices for synthesis of carbon nanotubes

Other efficient methods for producing catalysts that can be used to synthesize carbon nanostructures have been developed. The syntheses of carbon nanotubes were carried out by two routes: (a) chemisorption of volatile acetylacetonates of nickel, cobalt on ordered mesoporous silicas at 150°C, reduction nanoparticles of appropriate metals with H_2 at 450°C, and pyrolysis of acetylene at 700°C; (b) MCM-41 modification with $Ni(acac)_2$ $Co(acac)_2$, or $Fe(acac)_2$, reduction of chemisorbed metal complexes with C_2H_2, and pyrolysis at 700°C (in situ reduction). During pyrolysis of acetylene a deposition of decomposition products of black color on silica matrices is observed. The synthesized composite was treated with solution of hydrofluoric acid at the ambient temperature for removal silica phases. In the result insoluble carbon fraction was obtained for application in the following study. Carbon nanotubes were identified using transmission electron microscope (JEM-1OOCXII, Japan).

3. Results and discussion

The sorption isotherms of nitrogen on synthesized silica recorded at 77 K provide information about the mesostructure of the material (Figure 1a).

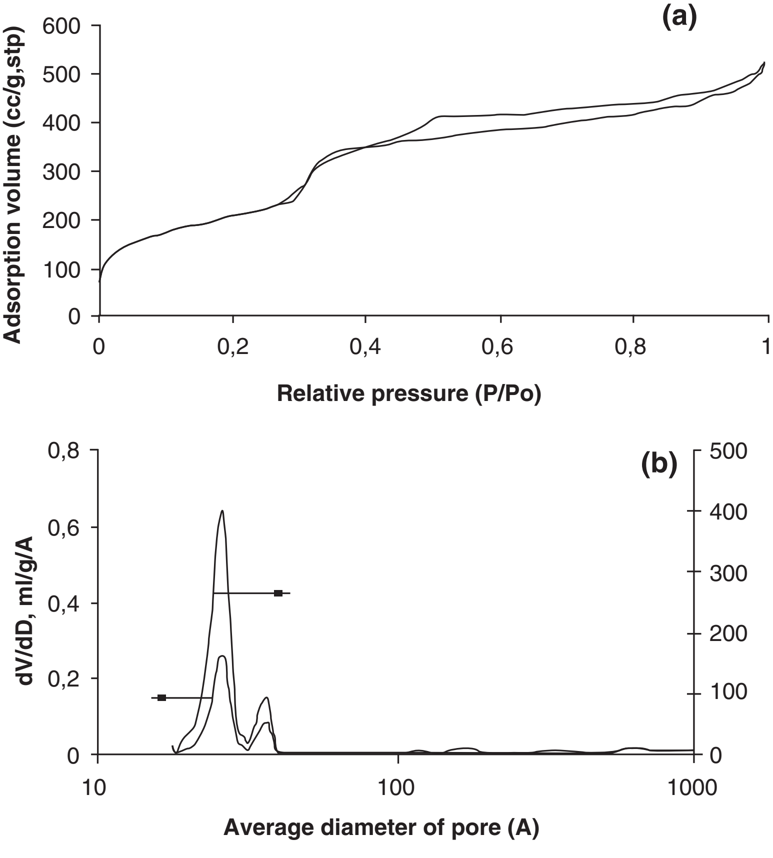

Figure 1. Ad(de)sorption isotherm of nitrogen at 77 K (a) and pore size distribution (b) for the synthesized MCM-41 silica.

Specific surface area of the sample determined from the linear part of the BET equation[8] (at $P/P_s = 0.03–0.20$) is 905 m^2/g. The specific volume of pores calculated from the BET equation (desorption branch of the isotherm of nitrogen) reaches a value of 0.87 cm^3/g (at $P/P_s = 0.98$); average diameter of pores determined by the Barret–Joyner–Halenda method[9] is about 39 Å.

3.1 Nanoparticles of gold and silver formed by in situ reduction

Ordered mesoporous silica MCM-41 with silicon hydride groups in the grafted modifying layer were used for synthesis of noble metal nanoparticles. In the IR spectrum of the silica (Figure 2, curve 1), a sharp band is observed in the region of O–H vibration at 3750 cm^{-1}, which originates from isolated OH groups of the silica surface. In the spectrum of the silicon hydride-containing silicas (Figure 2, curve 2) this band is absent and, a broad band is seen at 2240 cm^{-1} indicating evidence for the fact that attachment of ≡SiH groups occurred. Also strong narrow adsorption bands at 1390 and 2976 cm^{-1} relating to deformation vibrations of the C–H bonds in CH_2 group are observed. Decrease of intensity of adsorption band 2240 cm^{-1} relating to ≡SiH groups and appearance of adsorption band of silanol groups 3750 cm^{-1} as a result of reduction noble nanoparticles in surface layer of silica matrices is observed.

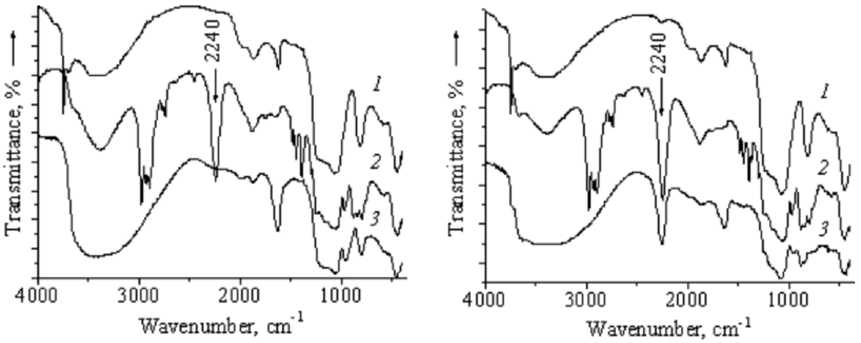

Figure 2. FTIR spectra: 1 – initial MCM-41 silica, 2 – MCM-41 with grafted ≡SiH groups, 3 – MCM-41 with reduced nanoparticles of silver (*left*) and gold (*right*).

Fig. 3 shows the low-angle X-ray diffraction patterns of the calcined porous host silica MCM-41 curve 1, after modification with triethoxysilane – sample MCM-H curve 2 and the calcined sample MCM-41–Ag contained 2.0 wt% Ag curve 3. The x-ray powder diffractogram of the initial MCM-41 silica sample exhibits (100), (110), and (200) reflections in a low angle range of 2θ=2–8°, which is characteristic of the hexagonal ordered structure. The peak appearing at low angle ($2\theta = 2.6°$) corresponds to (100) plane of MCM-41 indicating ordered pore structure of MCM-41, which suggests that the hexagonal pore structure of MCM-41 should be retained after being incorporated with Au (Ag). However, the fact that peak intensity for the low-angle reflections decreases in Ag/MCM-41 sample shows that the formation of Ag clusters inside the channels leads to the loss of ordered structure, which is consistent with the observations in literature.[10]

In the high-angle region at $2\theta = 30–90°$, typical peaks of face-centered cubic structure of metallic gold are observed, which are ascribed to (111), (200), and (220) diffractions. The crystallite sizes of nanoparticles were determined by Scherrer equation[11]:

$$D = \frac{0.9\lambda}{\beta\cos\theta},$$

where λ is the x-ray wavelength in nm, β is the intrinsic peak width in radians (2θ), θ is Bragg angle, and 0.9 is the Scherrer constant. Average diameters of formed nanoparticles accordingly to this equation fall within the range of 20-30 nm for gold and 25–28 nm for silver.

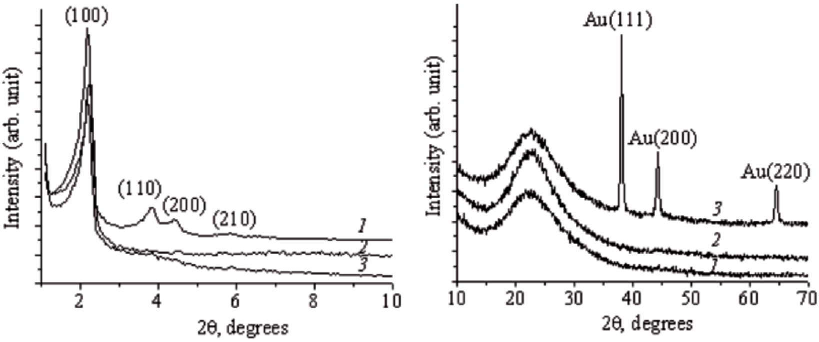

Figure 3. XRD patterns of: *1* – initial MCM-41 silica, *2* – modified with triethoxysilane MCM-H, *3* – MCM-41 with incorporated nanoparticles of silver.

Dimensions of formed nanoparticles is succeeded to control depending on concentration of metal-containing compounds in solution that is accompanied by the changes in the color of samples, registered in UV–Vis spectra.

After treatment of the MCM–H materials with $HAuCl_4$ solution for 24 h, it was observed that all materials had attained a deep pink color, evidently due to the presence of Au nanoparticles in the cavities of the silica matrix. Au nanoparticles, due to their surface plasmon vibrations, have a characteristic absorption band in the visible region of the electromagnetic spectrum at

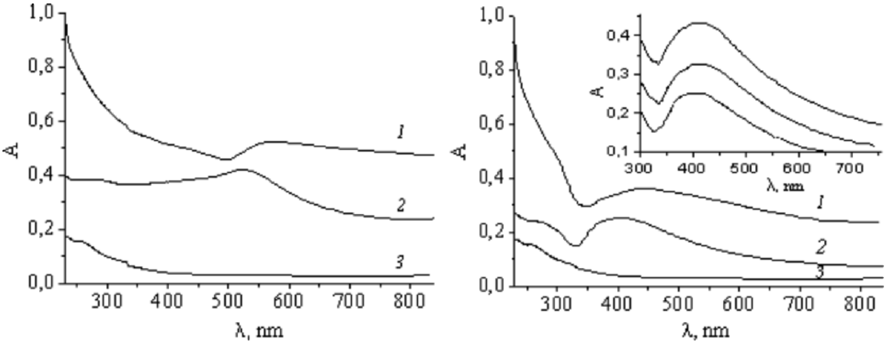

Figure 4. UV–Vis spectra recorded on (A) Au-colloid (a), MCM–Au (b), MCM–H (c); (B) Ag-colloid (a), MCM–Ag (b), MCM–H (c).

about 520–550 nm, which is responsible for the striking violet to pink range of colors of the nanoparticles depending upon the particle size.[12,13]

Figure 4 shows the UV–Vis spectra recorded on the (a) colloid gold, (b) MCM–Au materials, and (c) modified silica MCM–H. 30 mg of metal-containing composites were dissolved in 5 mL solution of 5 M sodium hydroxide for measuring of UV–Vis spectra of colloid gold. A strong absorption at approxmately 540 nm is observed for colloid gold and gold-containing silica. It demonstrated that the $AuCl_4^-$ ions have been totally reduced into gold clusters.

The absorption band at about 540 nm was due to the surface plasmon resonance of the Au nanoparticles. The appearance of the plasmon band indicates that the colloidal Au particles have reduced in the silica matrices by grafted silicon hydride groups.[14] It was found that the surface plasmon band increased in intensity with growth of particle sizes. In general, the intensity enhancement of absorption band results from increase of metal particles size, combining with band shift.[15]

The absorption peaks at about 400 nm due to the surface plasmon resonance effect could be seen to be blue-shifted with the decrease in size of silver nanoparticles (inset of Figure 4). The blue-shift is attributed to contraction of the lattice induced by surface stress,[16] effect of surface potential,[17] changes of optical interband transitions between the discrete energy levels, changes of electron band structure etc. Besides the above effects, deviation from perfect spherical shape, and irregular size distribution would profoundly effect the large inhomogeneous broadening.[18] This resonance is absent in modified silica MCM–H (Fig. 4A, curve c) sample as expected. Its UV–Vis spectrum did not show any absorbance in this visible region. At the decreasing dimension of metal nanoparticles changes in the samples color were observed.

Thus a number of metallized composites, which contain highly dispersed metals namely gold and silver on their surface by reduction of corresponding ions of metal from its solutions over silica matrices were obtained.

3.2 Nanoparticles of nickel, cobalt, and iron embedded in mesoporous silica matrices in synthesis of carbon nanotubes

In order to provide the homogeneous catalyst deposition, silicas were treated with volatile cobalt(II), nickel(II), and iron(II) acetylacetonates at the moderate temperatures. At these conditions acetylacetonates of metals are chemisorbed on the silica surface due to reaction with surface silanol groups with eliminating one of ligands.

After chemisorption of acetylacetonates of the iron-subgroup metals on the mesoporous support, IR spectra of the appropriate surface compounds were recorded. The IR spectra of the $Co(acac)_2$, MCM-41, and corresponding cobaltous complexes anchored on the MCM-41 surface are shown in Figure 5. According to the papers by Nakamoto et al.[19] and Dismukes et al.[20] asymmetric and symmetric stretching vibrations of the chelate group (C=C) and (C=O + CH) in $Co(acac)_2$ appear at 1570–1575 and 1460–1513 cm^{-1}, respectively. In our case in the spectrum of silica after treatment with $Co(acac)_2$ these absorption bands are observed at 1546 and 1481 cm^{-1} (Figure 2). Absorption bands at 1562 and 1430 cm^{-1} in the spectrum of the modified silica could provide evidence for the fact that the chelate ring structure of the bound ligands is retained. According to Mazurenko et al.,[21] the ring-opening reaction for pure $Cr(acac)_3$ occurs at 280°C and is accompanied by an increase in the intensity of the absorption bands at 1780 and 1800 cm^{-1}. Since the above-mentioned absorption bands for the supported cobalt-containing complex in this frequency range were not observed, it is possible to assume that the ring-opening reaction does not proceed under the experiment conditions. These observations are in agreement with the data published by Kenvin et al.[22] that made a conclusion that no ring-opening process occurred for $Fe(acac)_3$ and $Mn(acac)_3$ after removal of one or two of acetylacetonate ligands as a result of reaction with silanol groups of the silica surface.

The removal of the ligands from metal complexes supported on silica was studying in air by thermogravimetric technique. The destruction of the residual ligands of acetylacetonates (after interaction with silanol groups) occurred at about 445°C (Figure 6). As a result, formation of complex oxides of the corresponding metals (cobalt and iron) had occurred on the silica surface.

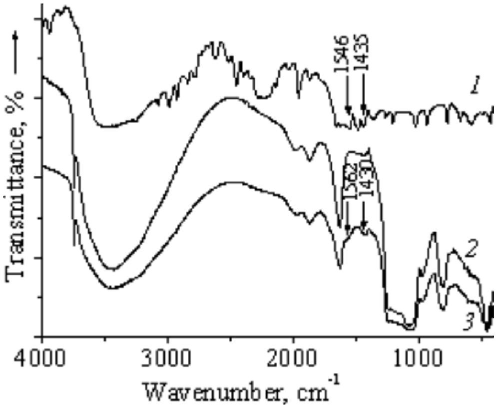

Figure 5. FTIR spectra: 1 – Co(acac)$_2$; 2 – MCM-41 modified with Co(acac)$_2$; 3 – MCM-41.

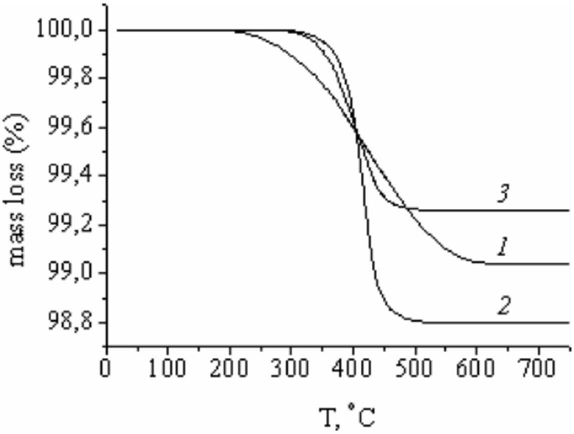

Figure 6. TG curves of Ni(acac)$_2$ (1), Co(acac)$_2$ (2), and Fe(acac)$_2$ (3) complexes supported on the MCM-41 surface.

Application of matrices with the supported metals as catalysts enabled us to attain rather high content of carbon nanostructures (20–30% of the process product). Content of nanotubes in pyrolytic deposition was determined by subtraction of the mass of amorphous carbon from the mass of resulting product (amorphous carbon plus nanotubes). According to electron microscopic data, in the methods of obtaining of carbon nanostructures with reduction nanoparticles of metals in atmosphere of hydrogen a lot of nanotubes were formed with external diameters in the range 35–52 nm for the cobalt catalyst

(Figure 7a) and, 10–35 nm for the nickel catalyst (Figure 7b). Formation of small quantities of carbon fibres of diameter of 50–70 nm was also observed.

In the use of acetylene as a source of carbon and as a reducer of metals in the second case, electron microscopy data provided evidence for formation of nanotubes with an external diameter of 42–84 nm in the case of the cobalt

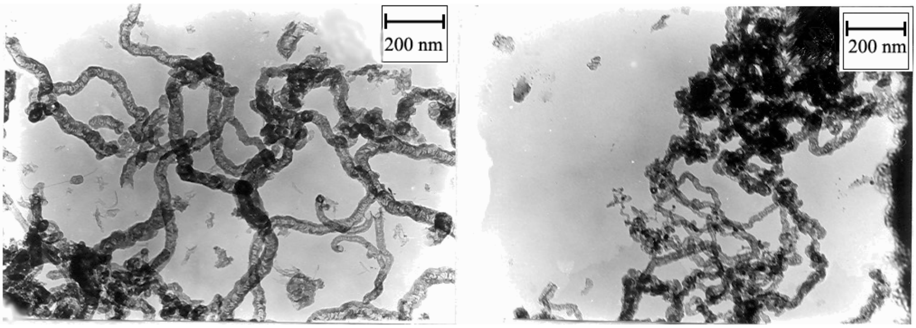

Figure 7. TEM micrographs of carbon nanotubes obtained on MCM-41 matrices with (a) cobalt and (b) nickel catalysts prepared by reduction in hydrogen.

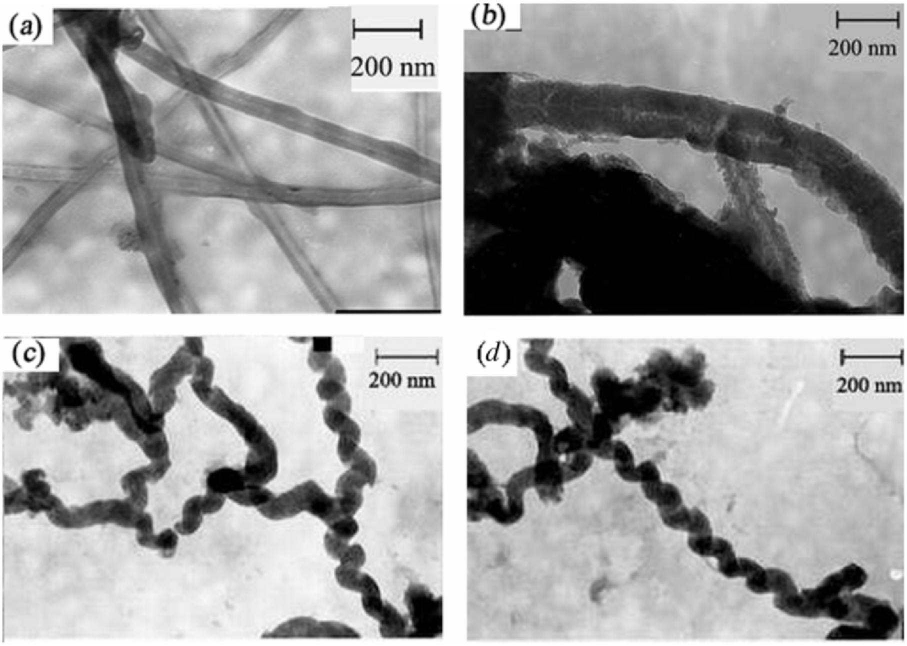

Figure 8. TEM micrographs of carbon nanotubes obtained on MCM-41 matrices with cobalt (a), iron (b), catalysts and carbon nanofibers obtained with nickel (c,d) catalyst, prepared by reduction in acetylene.

catalyst (Figure 8a) and 14–200 nm in the case of the iron catalyst (Figure 8b). Formation of carbon fibres, with diameters in the range 80–110 nm, for the nickel catalyst (Figure 8c,d) were also observed. Observation of presence of nanofibers with large diameter for the nickel catalyst (Figure 8d) is depended with enhanced dimensions of reduced nanoparticles of metal. Comparison of nanotubes growth using the cobalt catalysts by two methods show that nanotubes in Figure 7a are more curved. Catalysts that were prepared in an atmosphere of acetylene (without reduction with hydrogen) (Figure 8a) promote formation of more aligned nanotubes. Here it is noted that in the absence of a catalyst on such matrices small yields (up to 2%) of carbon nanotubes were obtained.[23]

4. Summary

Thus, a number of metallized composites, which contain highly dispersed metals, namely gold and silver, on their surface by reduction of corresponding ions of metal from its solutions over chemically modified silica matrices were obtained. Such an approach allow us to regulate size of the immobilized nanoclusters by varying in the concentration of corresponding metal in contrast to common reduction in the hydrogen atmosphere.

Pyrolysis of acetylene on the surface of MCM-41 silicas containing metallic catalysts has been studied. Application of matrices with the supported metals as catalysts enabled us to attain rather high yields of carbon nanostructures (20–30% of the process product). The electron microscopy data provided evidence for formation of nanotubes with an external diameter of 42–84 nm in the case of the cobalt catalyst and 14–200 nm in the case of the iron catalyst. Formation of carbon fibers with diameters in the interval 80–110 nm for the nickel catalyst was also observed. In the absence of a catalyst on such matrices small yields (up to 2%) of carbon nanotubes were attained.

References

[1] Bandyopadhyay, M., Korsak, O., van den Berg, M.W.E., Grunert, W., Birkner, A., Li, W., Schuth, F., Gies, H., Micropor. Mesopor. Mat. 2006, 89:158–163.

[2] Palpant, B., Saviot, L., Lerme J., Prevel B., Pellarin M., Duval E., Perez A., Broyer M., Eur. Phys. J. 1999, D 9:585–589.

[3] Wong, S., Joselevich, E., Woolley, A.T., Cheung, C.L., Lieber, C.M., Nature 1998, 394:52–54.

[4] Kong, J., Franklin, N.R., Zhou, C.W., Chapline, M.G., Peng, S., Cho, K.J., Dai, H.J., Science 2000, 287:622–625.

[5] Nilsson, L., Groening, O., Emmenegger, C., Kuettel, O., Schaller E., Schlapbach, L., Kind, H., Bonard, J.-M., Kern, K., Appl. Phys. Lett. 2000, 76:2071–2073.
[6] Schadler, L.S., Giannaris, S.C., Ajayan, P.M., Appl. Phys. Lett. 1998, 73:3842.
[7] Pavlenko, A.N., Yanishpolskii, V.V., Tertykh V.A., Il'in, V.G., Leboda, R., Skubiszewska-Zieba, J., Chem. Phys. Techn. Surf. 2002, 7–8:19–22.
[8] Gregg, S.J., Sing, K.S.W., Adsorption, Surface Area and Porosity, Acadamic Press, London, 1982.
[9] Barrett, E.P., Joyner, L.J., Halenda, P.P., J. Am. Chem. Soc. 1951, 73:373–380.
[10] Zhao, X.G., Shi, J.L., Hu, B., Zhang, L.X., Hua, Z.L., Mater. Lett. 2004, 58:2152–2156.
[11] Genie, A., Radiographic Imaging of Crystals, State publisher of physico-mathematical literature, Moscow, 1961 (in Russian).
[12] Underwood, S., Mulvaney, P., Langmuir 1994, 10:3427–3430.
[13] Link, S., El-Sayed, M.A., J. Phys. Chem. B. 1999, 103:4212–4217.
[14] Hulteen, J.C., Patrissi, C.J., Miner, D.L., Crosthwait, E.R., Oberhauser, E.B., Martin, C.R., J. Phys. Chem. B. 1997, 101:7727–7731.
[15] Fornasiero, D., Grieser, F., J. Colloid Interface Sci. 1991, 141:168–179.
[16] Cai, W., Hofmeister, H., Dubiel, M., Eur. Phys. J. D. 2001, 13:245–253.
[17] Cocchini, F., Bassani, F., Surf. Sci. 1985, 156:851–858.
[18] Gans, R., Ann. Physik. 1912, 342:881–900.
[19] Nakamoto, K., McCarthy, P.J., Ruby, A., Martell, A.E., J. Am. Chem. Soc. 1961, 83:1066–1069.
[20] Dismukes, J.P., Jones, L.H., Bailar, J.C., Jr., J. Phys. Chem. 1961, 65:792–795.
[21] Mazurenko, E.A., Gerasimchuk, A.I., Zheleznova, L.I., Volkov, S.V., Koord. Khimiya 1987, 13:1313.
[22] Kenvin, J.C., White, M.G., Mitchell, M.B., Langmuir 1991, 7:1198–1205.
[23] Brichka, S.Ya., Prikhod'ko, G.P., Ogenko, V.M., Tertykh, V.A., Pavlenko, A.N., Yanishpolskii, V.V., Ukr. Khim. Zhurn. 2004, 70:76.

CATALYTIC ALKENE METATHESIS IN IONIC LIQUIDS

CEDRIC FISCHMEISTER

Catalyse et Organométalliques UMR 6226:CNRS-Université de Rennes1, Institut Sciences Chimiques de Rennes. Campus de Beaulieu 35042 Rennes, France. E-mail: cedric.fischmeister@univ-rennes1.fr
Phone: + 33 2 23 23 59 98. Fax: + 33 2 23 23 69 39

Abstract: Olefin metathesis has found a tremendous number of application in the past 25 years. Immobilisation of olefin metathesis (pre)catalysts in room temperature ionic liquids (RTILs) offers the opportunity to recover and reuse the catalyst and also to reduce the level of ruthenium (Ru) contaminants in the products.

Keywords: olefin metathesis, ruthenium catalysts, ionic liquids, catalyst recycling.

1. Introduction

Although alkene metathesis is a catalytic reaction discovered about 50 years ago [1], it has found only during the last 15 years a leading role in synthetic methodology due to its power to break and make carbon–carbon double bonds according to the general equation :

$$R^1HC{=}CHR^1 + R^2HC{=}CHR^2 \rightleftharpoons 2\ R^1HC{=}CHR^2$$

The tremendous impact of olefin metathesis on synthetic chemistry has only been possible with the elaboration of well-defined organometallic complexes in particular the very active molybdenum complexes prepared by the Schrock group [2] and the robust ruthenium (Ru) complexes elaborated by the Grubbs group [3]. The early proposal of the olefin mechanism by Chauvin was a determining step for the development of these catalysts [4]. Alkene metathesis has acquired a key role in the formation of functional cyclic and macrocyclic molecules via ring-closing metathesis (RCM), cross-metathesis (CM), or enyne metathesis reactions [5, 6]. Useful applications have also been found in material science via the ring-opening metathesis polymerisation (ROMP) of cyclic olefins, or acyclic dienes metathesis (ADMET) reactions [7]. More recently asymmetric ring-closing metathesis (ARCM) and related transformations have been developed and several chiral complexes synthesised [8]. Ru complexes, in particular those of the second generation (Figure 1), combine high activity and stability towards functional groups and can be manipulated without specific precautions.

Y. İmamoğlu and V. Dragutan (eds.), Metathesis Chemistry: From Nanostructure Design to Synthesis of Advanced Materials, 483-501.

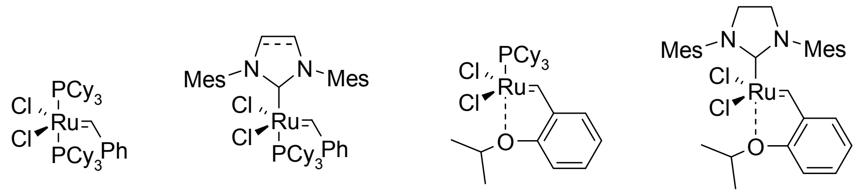

Grubbs 1st Gen. Grubbs 2nd Gen. Hoveyda1st Gen. Hoveyda 2nd Gen.

1, [9] **2**, [10] **3**, [11] **4**, [12]

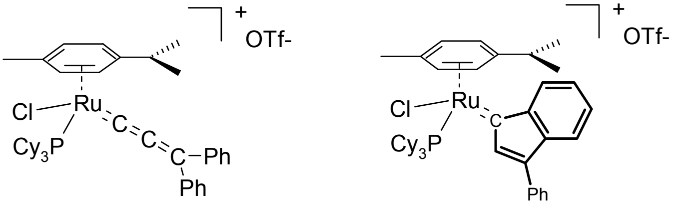

Dixneuf Dixneuf

5, [13] **6**, [14]

Figure 1. Catalyst precursors.

However, for most applications catalysts loading higher than 1 mol% are required raising two problems which are the cost of the targeted transformations and contamination of the products in particular when olefin metathesis is employed for the synthesis of biologically active molecule. Classical purification by column chromatography is the most used method to remove Ru residues but it requires large amounts of solvents and does not allow recycling of the catalyst. Hoveyda type catalysts **3** and **4** are described as very robust complexes that can be purified by column chromatography. Recently, Grela has used this property and prepared a Ru catalyst that can be separated and recovered by column chromatography [15]. Several alternative methods have been developed to decrease as much as possible the level of Ru contaminants. Grela [16] and Fogg [17] have prepared complexes with high affinity for silica. Chemical treatment [18], sequential treatment by activated carbon and chromatography [19], and Ru scavengers have also been used [20]. Catalysts immobilisation combine the possibility to both recycle the catalysts and decrease the amount of organometallic residues in the products. Immobilisation on a support [21] or in non-conventional solvents [22] such as water [23], super critical CO_2 [24], and perfluoroalkanes [25] have been described. Among these solvents, ionic liquids (ILs) are probably those that have attracted much attention in recent years. Alkene metathesis in RTILs appeared recently in 1995 and was quickly developed during the last 10 years. The goal of this review is to present the main achievements of olefin metathesis in RTILs.

2. Olefin metathesis in ionic liquids

2.1 What are Ionic liquids ?

Room temperature ionic liquids (RTILs) are salts with low melting points (<100°C) [26]. They are sometimes considered as green solvents since they are non-volatile, non-flammable [27], have a high thermal stability, and are so far considered as non-toxic although very little is known about their toxicity [28]. The cations are essentially nitrogen based, i.e. ammonium, pyridinium, and imidazolium. The latter is the most employed (Figure 2) and a variety of anions can be used (PF_6^-, BF_4^-, NTf_2^-, OTf^-, etc.). Thus, a judicious combination of the cation/anion pair will confer specific properties to the IL in terms of polarity, hydrophilicity, or lipophilicity. Having in mind the influence of solvents on the course of a chemical reaction in particular in terms of efficiency and selectivity, it is not surprising that RTILs have known impressive developments as solvents for chemical synthesis in the past few years.

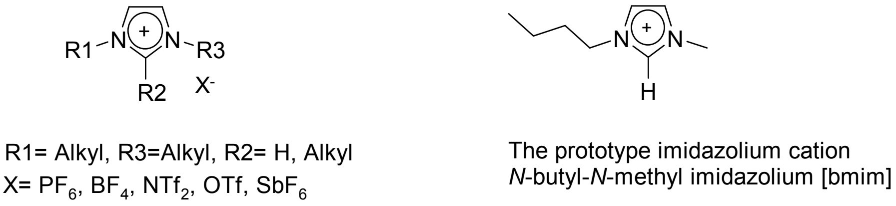

Figure 2. Imidazolium cations.

Furthermore, RTILs are able to dissolve organic, organometallics, and inorganic compounds, and they are immiscible with most of the organic solvents depending on the nature of the cation/anion pair. They are thus candidates as reaction media for the immobilisation of organometallic catalysts allowing a facile separation of the catalyst and the products and of course catalyst recovery. To the best of our knowledge only a few industrial process involving RTILs are currently operating among which is the nickel catalysed dimerisation of butene (Difasol process, IFP) or the BASF "Basil" acid scavenging process. Several reviews have covered the area of catalysis in RTILs [29]. We will emphasize here on the achievements of olefin metathesis in RTILs in several research groups including ours.

2.2 Neutral pre-catalysts

Most of the research performed on olefin metathesis in ILs has been done with Ru-based catalysts although the very first olefin metathesis in ILs was reported in 1995 with a tungsten catalyst [30]. In 2000, Bayer AG patented the use of Ru and molybdenum catalysts for olefin metathesis in ILs [31].

Shortly after Buijsman et al. [32] reported the use of Grubbs catalysts **1** and **2** in [bmim][X] and mixtures of RTILs for the RCM of various substrates (Scheme 1). This study aimed at using the IL in order to decrease the amount of Ru residue in the product.

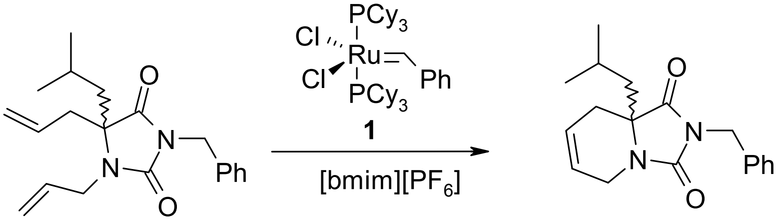

Scheme 1. RCM in [bmim][PF_6] with Grubbs catalyst **1**.

A reference reaction was performed with 5 mol% of catalyst at 50°C in dichloromethane giving a quantitative conversion after 1 h and the Ru-contaminant was found to be 1.7 µg/mg (1700 ppm) after purification by column chromatography on silica gel. When this reaction was performed in [bmim][PF_6] under the same experimental conditions, the conversion was almost quantitative (98%) after 24 h. The reaction product was easily extracted with diethyl ether and the Ru contaminant was found to be 3.2 µg/mg (3200 ppm). The reuse of the IL containing the catalyst was attempted but after 20 h and the conversion reached only 15%. Due to the very low level of Ru in the product, the authors concluded on catalyst decomposition to explain this poor recycling. Better results were obtained by using the Grubbs second-generation catalyst **2** under similar conditions, the Ru contaminant level being as low as 1.6 µg/mg (1600 ppm) which is comparable to the level obtained after purification by column chromatography. Attempts to recycle catalysts **1** and **2** in the IL showed a loss of activity with the number of cycle (74% conversion for the third run with catalyst **2**).

In 2002, Kiddle et al. showed that Ru catalysed olefin metathesis in [bmim][BF_4] or dichloromethane could be accelerated upon microwave heating [33]. For instance, the RCM of diethyl diallylmalonate under microwave was complete in 15 s in [bmim][BF_4] when using the Grubbs second-generation catalyst **2** (Scheme 2).

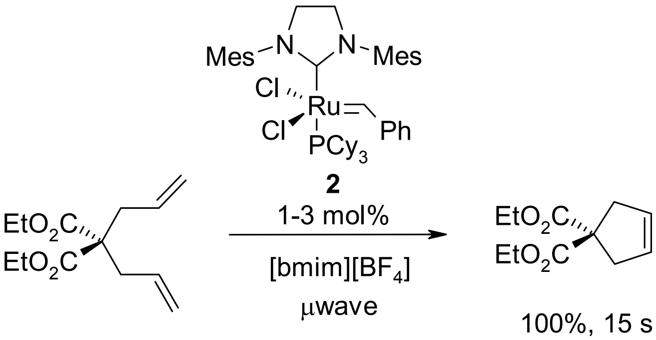

Scheme 2. RCM in [bmim][BF$_4$] under microwave with Grubbs II catalyst **2**.

More recently, in 2006, the beneficial use of RTILs in olefin metathesis was reported by two groups. Tang et al. showed that the second-generation Grubbs catalyst **2** was able to perform olefin CM in [bmim][PF$_6$] and [bmim][BF$_4$] [34]. Stilbene was prepared from styrene in yields comparable to those obtained in dichloromethane (Scheme 3).

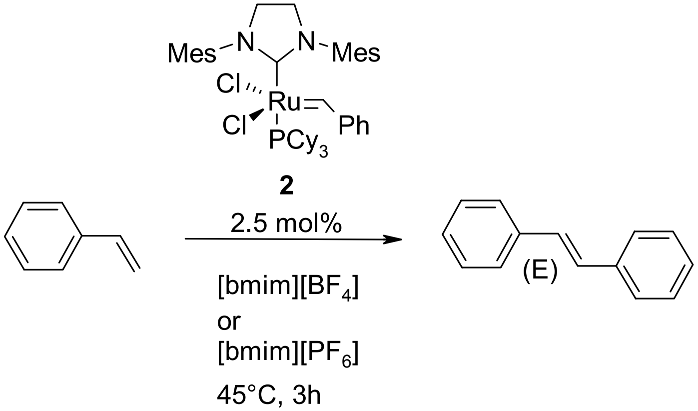

Scheme 3. Styrene self-metathesis in RTILs.

After extraction of the organic products with diethyl ether the IL containing the catalyst could be reused several times with, however, a little drop in the isolated yields (Table 1).

Table 1. Stilbene synthesis. Recycling of catalyst **2**

Solvent	Cycle	Yield (%)
DCM	1	81
[bmim][BF_4]	1	74
[bmim][BF_4]	2	61
[bmim][BF_4]	3	54
[bmim][BF_4]	4	48
[bmim][PF_6]	1	85
[bmim][PF_6]	2	82
[bmim][PF_6]	3	79
[bmim][PF_6]	4	75

Reactions performed with 2.5 mol% of catalyst at 45°C for 3 h.

It was clearly demonstrated that the catalyst was partially extracted by diethyl ether (not quantified) and the results were slightly improved by using petroleum ether. The same year (2006) the use of Ru catalysts for the self-metathesis of 1-octene in RTILs was reported by a researcher from the University of Johannesburg and Sasol Technology Ltd. (Scheme 4) [35].

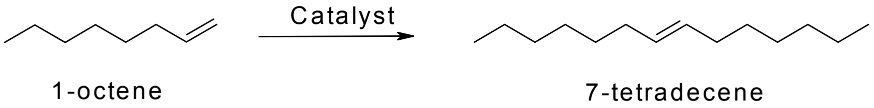

Scheme 4. Selective 1-octene self-metathesis.

The first-generation Grubbs catalyst **1** and the Sasol PhobCat catalyst [Cl_2(Phoban-Cy)$_2$Ru=CHPh] were not very active for the above-mentioned reaction and were subject to significant catalyst leaching (up to 72%). The second-generation Grubbs catalyst **2** showed a better selectivity in ILs than in a solventless reaction (Table 2).

Table 2. Compared selectivity for 1-octene self-metathesis

Solvent	Conversion of 1-octene	Selectivity toward 7-tetradecene
Solventless	99	70
[bmim][PF_6]	99	95

Grubbs catalyst **2** (0.01 mol%), 60°C, 5 h.

The second-generation Hoveyda catalyst **4** showed good solubility in RTILs with concomitant lower leaching. It was used to test the influence of the [bmim] counteranion and the alkyl group on the imidazolium cation. Contrary to the results reported by Tang on stilbene synthesis, the BF_4^- anion provided here the best result in terms of activity, 92% conversion vs 80% for PF_6^-, and 47% for NTf_2^-. In all three cases the selectivity toward 7-tetradecene was almost identical (95–98%) and higher than that obtained in solventless conditions (91%). The influence of the alkyl chain length of the imidazolium cation is also very pronounced and shorter chains provided the best conversions (Table 3).

Table 3. Influence of the alkyl chain length

Solvent	**Conversion of 1-octene**	**Selectivity towards 7-tetradecene**
Solventless	93	91
[emim][NTf$_2$][a]	90	98
[bmim][NTf$_2$][a]	47	98
[hmim][NTf$_2$][a]	13	99

Hoveyda catalyst **4** (0.02 mol%), 40°C.

[a] e = ethyl, b = butyl, h = hexyl.

It is noteworthy that IL media provide much better selectivity than solventless reaction. This better selectivity observed in RTILs "is believed to be due to a lack of solubility of the metathesis product in the polar ionic medium, which would limit contact of that compound with the catalyst" hence avoiding isomerisation reactions. Finally catalyst **4** was found to be moderately recyclable with 79% conversion for the first run and 69% conversion for the second run.

2.3 Ionic precatalysts : the allenylidene ruthenium pre-catalyst

Cationic Ru–allenylidene complexes (Scheme 5) have been discovered in 1998 in the Dixneuf's group [13]. They exhibit a reactivity which is comparable with that of the Grubbs first-generation catalyst **1**. Their ionic character prompted us to investigate their use in RTILs since good solubility and compatibility could be foreseen in such media. Our two first articles appeared in that field in 2002.

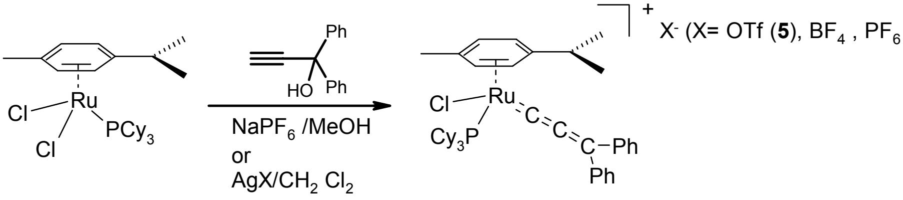

Scheme 5. Cationic Ru–allenylidene complexes [Ru$^+$][X$^-$].

As expected, the complexes displayed a very good solubility and affinity for RTILs as shown in Figure 3.

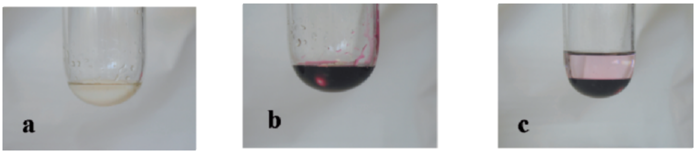

Figure 3. Solubility of **5** in [bmim][PF_6].

a: [bmim][PF_6]; **b**: **5** in [bmim][PF_6]; **c**: **b** + toluene after 10 min stirring.
In toluene the activity and selectivity of these Ru–allenylidene catalysts is dependant on the nature of the anion (Scheme 6). The triflate anion provides the best activity and selectivity for the RCM product *a,* whereas the tetrafluoroborate complex is less active and gives a mixture of the three products *a*, *b*, and *c*.

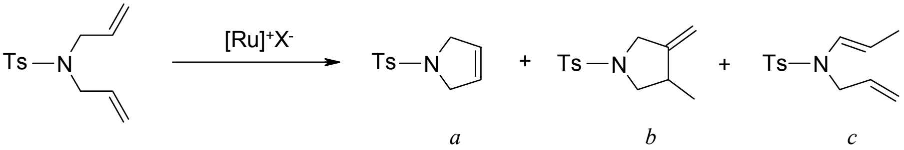

Scheme 6. Selectivity of Ru–allenylidene catalysts.

This transformation was investigated in various RTILs with pre-catalyst **5**, the organic product being extracted with toluene at the end of the reaction (Table 4) [36].

Table 4. Influence of the IL anion on activity and selectivity

Entry	Solvent	Time	Conv. (%)	a (%)	B (%)	c (%)
1	Toluene	20 min	100	100		
2	[bmim][OTf]	2 h 30 min	100	97	3	
3	[bmim][OTf]	18 h[a]	100	100		
4	[bmim][BF_4]	5 h	60	23	31	6
5	[bmim][NTf_2]	5 h	53	31	18	4
6	[bmim][PF_6]	5 h	85	83	2	

Pre-catalyst **5** (2.5 mol%), 80°C.
[a]Room temperature.

As shown by these results the reaction rate is slowed and the nature of the IL anion influences the selectivity. This is explained by anion exchange between the catalyst and the IL. As a consequence when using the more active catalyst (OTf anion) it is necessary to operate in [bmim][OTf] or [bmim][PF_6] to ensure high activity and selectivity. When operating at 80°C the catalyst recycling was not possible due to complete decomposition of the catalyst. Thus lower temperature (room temperature) and longer reaction time (18 h) have been used. Under these conditions two consecutive cycles provided good to reasonable conversions (100% and 86%), but a drop in activity was observed for the third run (33%). It is likely that the reaction time required at room temperature was too long and that catalyst had decomposed after the two first cycles (36 h reaction time). In addition, it was found later that toluene was not the best solvent for extracting the organic product since it also extracted some complex (not quantified). This first study showed the possibility to use the ionic Ru-allenylidene complex in RTILs. However, for a more efficient catalyst recycling shorter reaction time are required. With the same catalyst **5** it has been possible to prepare polymers in RTILs [37]. Norbornene was thus polymerised in a biphasic mixture of [bdmim][PF6] and toluene (Scheme 7).

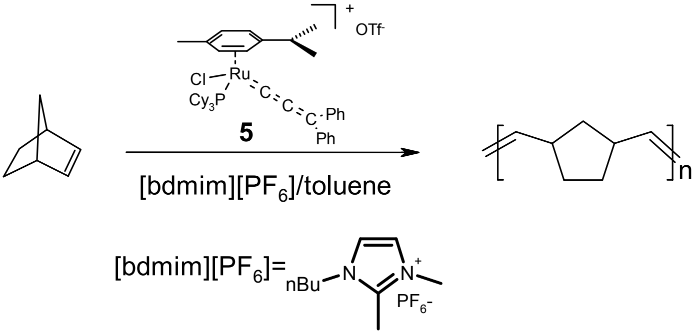

Scheme 7. ROMP of norbornene with pre-catalyst **5**.

The [bdmim] anion was used to prevent carbene formation at the C2 carbon atom and the biphasic system was necessary to solubilise the polymer formed during the reaction. Indeed, polymerisation in pure [bdmim][PF_6] was possible but exceedingly long time was necessary to extract the polymer from the IL which was detrimental to the catalyst lifetime. Thus, under the biphasic conditions, four cycles were possible with good polymer yields. The increase in the average molecular weights with cycles may be explained by a diminution of the catalytic active sites (Table 5).

Table 5. ROMP of norbornene: catalyst recycling

Cycle	Time (h)	Polymer yield (%)	Mn (g mol^{-1})[a]	PD*i*
1	0.5	96	113,800	1.9
2	0.5	99	168,100	1.9
3	0.5	98	206,700	1.8
4	0.5	97	–	–
5	0.5	64	–	–
6	0.5	27	303,000	1.5

[a]Measured by GPC calibrated with polystyrene standards and polymer dissolved in THF.

After the sixth cycle, the IL was directly reloaded with fresh catalyst and a new recycling sequence started. Again the first five cycles provided very good polymer yields. The neutral Grubbs first and second-generation catalyst **1** and **2** have been evaluated for the polymerisation of norbornene in [bdmim][PF_6] under the same conditions. None of the two provided results was as good as with the ionic allenylidene showing the advantage of using an ionic catalyst for such an application. Indeed, the Grubbs catalysts were not very soluble in the media and very likely quickly extracted. In addition, it has been shown by others [32, 35] that the first-generation Grubbs catalyst exhibits a modest stability in IL media.

2.4 Immobilised pre-catalysts

Following the results with neutral and ionic precatalysts, it became obvious that immobilisation of neutral catalysts was the solution for an efficient catalyst recycling. Several groups have worked in this direction by modifying the stable and recyclable Hoveyda catalysts **3** and **4**. In 2003, Mauduit and Guillemin reported the synthesis of an IL supported Hoveyda type catalyst **7** [38]. The synthesis was performed in nine steps starting from the commercially available methyl-3(4-hydrophenyl)propionate. Complex **7** was obtained in 32% overall yield (Scheme 8).

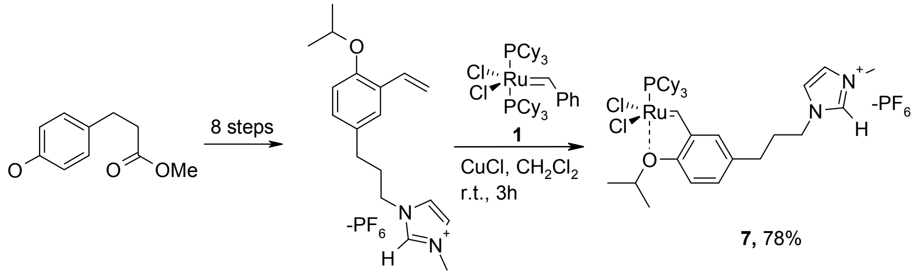

Scheme 8. Ionic liquid tagged Hoveyda catalyst.

With this complex **7** it was possible to run efficiently ten consecutives RCM of *N,N*-diallyltosylamide by extracting the product with toluene at the end of each cycle. The excellent catalyst stability in this media was demonstrated since the ninth run was performed following a “3-month aging” of the catalyst. The neutral catalyst **3** was not recyclable under the same conditions since the conversion dropped to 29% from the third run due to catalyst extraction (Table 6).

Table 6. Catalyst recycling with catalyst **7**

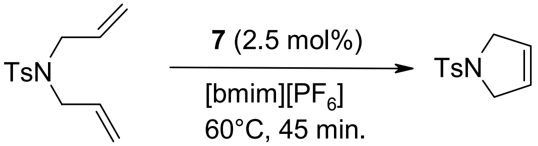

	Cycle (% conv.)									
Catalyst	1	2	3	4	5	6	7	8	9	10
7	>98	>98	>98	>98	>98	96	92	92	92	95
3	>98	40	29							

The ionic catalyst in [bmim][PF_6] was found to be efficient for the RCM of various substrates with good recyclability except for sterically demanding olefins (Scheme 9).

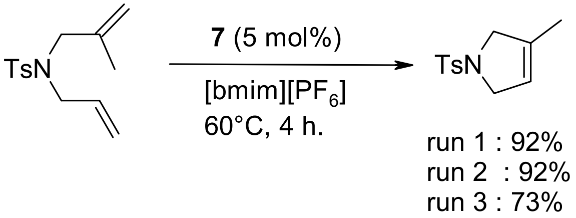

Scheme 9. RCM in [bmim][PF_6]. Sterically demanding substrate.

In this case, higher catalyst loading (5 mol%) and longer reaction time (4 h) were necessary to ensure 92% conversion. The same conversion was obtained on the second cycle but because of this, more drastic conditions, the conversion dropped to 73% on the third run due to catalyst decomposition. For these reasons a second-generation Hoveyda catalyst **8** was prepared by replacing the phosphine ligand by *N*-Heterocyclic carbene (Scheme 10) [39].

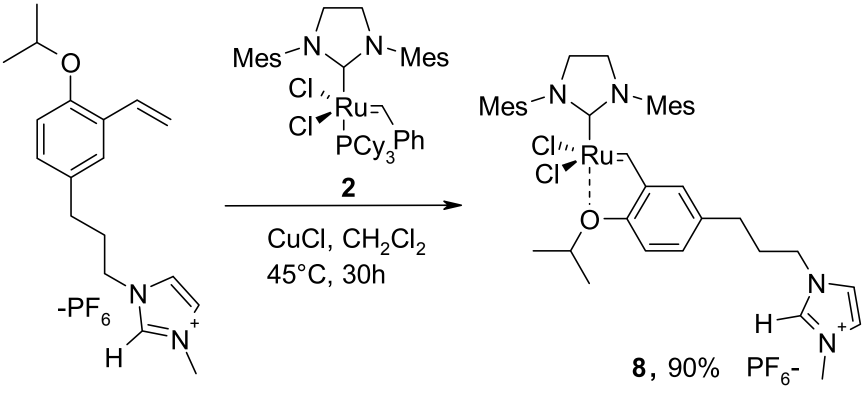

Scheme 10. Ionic liquid tagged Hoveyda catalyst.

With this catalyst the RCM of the sterically demanding substrate (see Scheme 9) was attempted. The recycling results were slightly improved with a conversion of 68% obtained on the fourth cycle but milder conditions were undoubtedly necessary to ensure a better recycling. Optimised conditions were found by using a biphasic media [bmim][PF_6]/toluene (25:75) at room temperature for 3 h. Under these conditions up to eight runs were performed with conversions better than 95%. Furthermore the Ru content of the product was measured for each cycle and found to be between 2.3 and 16.9 ppm, which is among the lowest values obtained after an olefin metathesis reaction.

The Yao group reported very similar Hoveyda-type ionically tagged complexes, a first-generation **9** in 2003 [40] and a second-generation **10** in 2005 [41]. The main difference with the Mauduit and Guillemin complexes **7** [38] and **8** [39] concerns the anchorage of the ionic arm which is performed via an alkoxy instead of an alkyl linkage. The first-generation catalyst **9** was synthesised in nine steps from 2,5-dihydroxybenzaldehyde and obtained in 30% overall yield (Scheme 11).

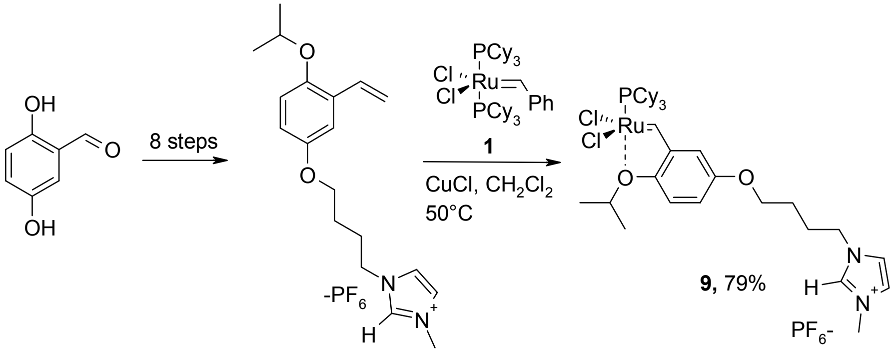

Scheme 11. Ionic liquid tagged Hoveyda catalyst.

This catalyst was used in a mixture of [bmim][PF_6] and dichloromethane (1:9; v/v). It showed much better recycling capabilities than the neutral version of the first-generation Grubbs and Hoveyda catalyst (Table 7). After each run, dichloromethane was evaporated and the organic product extracted with diethyl ether.

Table 7. Catalyst **9** activity and recycling

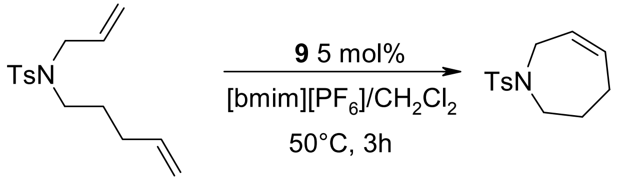

Catalyst	Cycle (% conv.)									
	1	2	3	4	5	6	7	8	9	10
1	>98	54	41[a]							
3	>98	75	37[a]							
9	>98	>98	97	96	95	94	92	92	91	90

All reactions were performed at 50°C for 3 h
[a] 6 h.

The stability of the catalyst was demonstrated by consecutively running the RCM of various substrates with good conversion with the same catalyst. A second-generation-type catalyst **10** was elaborated by ligand exchange with **2** (Scheme 12).

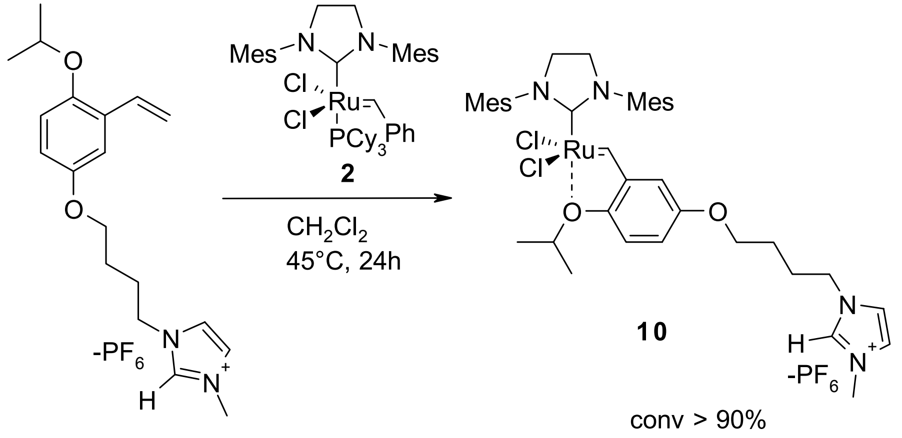

10

Scheme 12. Ionic liquid tagged Hoveyda catalyst.

With this new catalyst it has been possible to run 17 cycles of *N,N*-diallyltosylamide RCM with a conversion of 90% for the 17th run. A more sterically demanding substrate bearing a disubstituted olefin was also efficiently transformed with this catalyst and six cycles performed with very good conversions (Table 8).

Table 8. Catalyst **10** activity and recycling

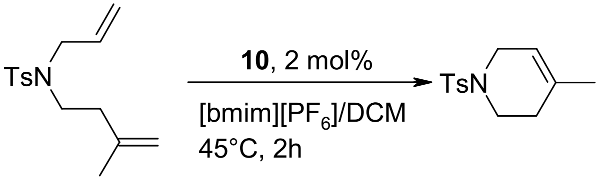

Cycle	1	2	3	4	5	6
Conv. %	96	96	95	93	91	90

A substrate with two disubstituted olefins was also efficiently ring closed and the catalyst reused for two additional runs with identical activity (Scheme 13).

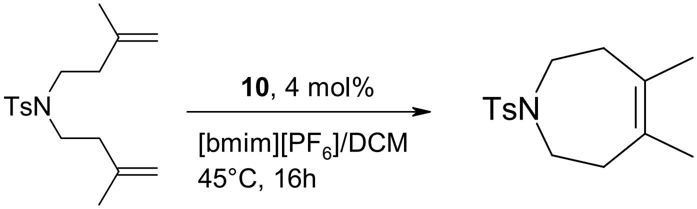

Scheme 13. RCM of sterically hindered diene with catalyst **10.**

For this transformation, more drastic conditions were necessary (4 mol% of catalyst, 16 h at 45°C). However, even after 32 h of operation at 45°C the catalyst remained active for further RCM transformations.

In our group two types of ionic catalysts have been developed [42]. Initially complex **11** synthesis requiring only five steps was considered in order to link the ionic chain to the ortho oxygen of the benzylidene ligand. The desired complex **11** was then obtained in 50% overall yield (Scheme 14).

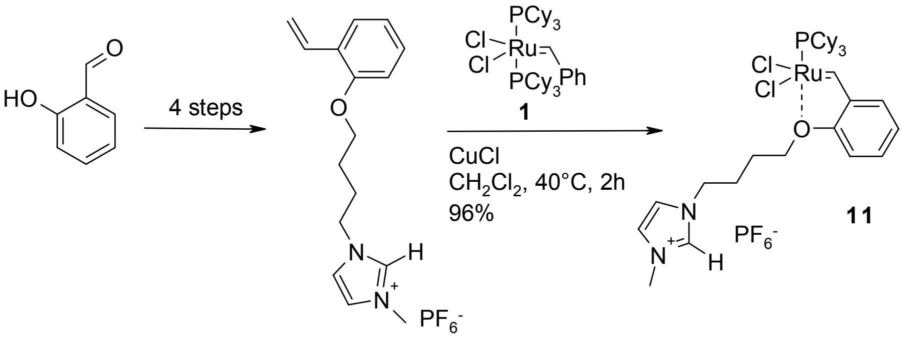

Scheme 14. Ionic liquid tagged Hoveyda type catalyst **11**.

This catalyst was evaluated for the RCM of *N,N*-diallyltosylamide in [bmim][NTf_2] and [bmim][PF_6]. In both cases, good conversions were obtained on the first cycle but the activity dropped during the forthcoming cycles (Table 9).

Table 9. Influence of the IL anion on the activity and recycling of **11**

[bmim][X]	Cycle (% conv.)		
X =	1	2	3
NTf_2	90	89	75
PF_6	90	85	60

Hoveyda-type catalyst **11**, 2.5 mol% catalyst, 45 min, 60°C

These results showed the dramatic influence of the steric hindrance on the alkoxy substituent. This influence was observed in the original work by Hoveyda [11]. Since the isopropoxy coordinating group seemed to be necessary, we considered the synthesis of a "sterically activated" catalyst by introducing the ionic tag at the ortho-position of the isopropoxy substituent. Indeed, Blechert showed that the introduction of a substituent at the ortho-position of the isopropoxy substituent dramatically increased the catalyst activity [43]. Thus, catalyst **12** was prepared in six steps from the commercially available 2,3-dihydroxybenzaldehyde (Scheme 15).

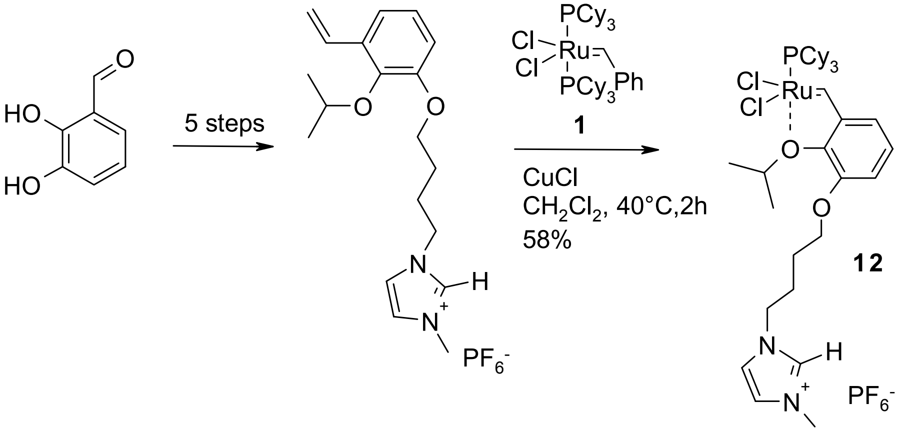

Scheme 15. Ionic liquid tagged Blechert catalyst **12**.

As expected this catalyst was found to be more active than **11** allowing the RCM of *N,N*-diallyltosylamide in [bdmim][PF_6] at room temperature. However, this catalyst was found to be difficult to recycle since the conversion dropped after the first cycle (Table 8). This poor recycling can be explained by the steric hindrance of the ligand that disfavours its recoordination (“release and return” or “boomerang” mechanism) [11]. This is corroborated by the low yield (58%) obtained for the complex synthesis whereas it is 91% for the non-congested complex **11**. The repeatability of the experiment was checked and found to be very good (Table 10).

Table 10. Reproducibility of RCM reaction in RTILs

	Cycle (conv. %)		
	1	2	3
First sequence	89	77	46
Second sequence[a]	85	79	42

[a] New batches of RTIL and catalyst

Finally the activity and recycling of catalysts **11** and **12** have been compared to catalysts **1**, **2**, and **3** for the RCM of diallyl diethylmalonate under mild conditions (Table 11).

Table 11. Comparison of catalyst activity and recycling

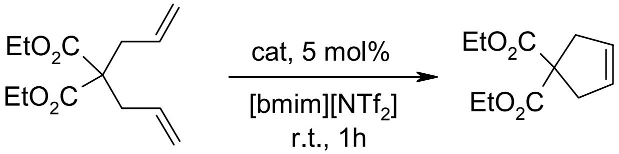

Catalyst	**Cycle (conv. %)**					
	1	**2**	**3**	**4**	**5**	**6**
1	4	0				
2	35	10				
3	31	11	5			
11	24	22	22	16	14	9
12	53	39	23	8		

Under these conditions the catalyst **12** was still the more active on its first use but its activity decreased more rapidly than the less reactive catalyst **11**. However, the benefit of immobilising the catalysts was again proved since the neutral catalysts **1**, **2** and **3** were almost not recyclable (Table 9).

3. Conclusions

ILs have attracted much attention in the recent years as alternative media for organic and catalytic reactions. They can improve the activity or selectivity of certain reactions with regards to conventional organic solvents. When used as solvents for olefin metathesis reactions these improvements are sometimes observed but the most important feature is the facility for separating the reaction product and the catalyst especially with ionic catalysts when they have been suitably designed and modified to be efficiently immobilised in these media. As a result the metal content in the extracted product is usually extremely low without classical column chromatography purification and without employing any sophisticated techniques or reagents. Finally, when the catalyst is stable enough it can be reused several times (up to 17 times) thus decreasing the cost of the targeted reactions.

References

[1] (a) Banks R.L., Bailey G.C. (1964) Ind. Eng. Chem. Process Res. Dev. 3:170; (b) Eleuterio HS. (1963) US Patent 3,074, 918, 13:30; (c) Calderon N. (1972) Acc. Chem. Res. 5:127. For an historical review see: Astruc D. (2005) New J. Chem. 29:42 and references therein.

[2] (a) Schrock R.R., Murdzek J.S., Bazan G.C., Robbins J., Di Mare M., O'Regan M. (1990) J. Am. Chem., Soc. 112:3875. (b) Schrock R.R. (2004) J. Mol. Catal A: Chem. 213:21.

[3] (a) Nguyen S.T., Johnson L.K., Grubbs R.H., Ziller J.W. (1992) J. Am. Chem. Soc. 114:3974; (b) Trnka T.M., Grubbs R.H. (2001) Acc. Chem. Res. 34:18; (c) Grubbs R.H. (2004) Tetrahedron 60:7117.

[4] Hérisson J.L., Chauvin Y. (1971) Makromol. Chem. 141:161.

[5] (a) Grubbs R.H. (ed.) (2003) Handbook of Metathesis Volume 1, 2, 3 Wiley-VCH, Weinheim; (b) Connon S. J., Blechert S. (2004) Recent Advances in Alkene Metathesis. In: Bruneau C., Dixneuf PH. (eds) Chapter 4, Springer, Berlin/Heidelberg, p. 93.

[6] For recent general reviews on olefin metathesis, see: (a) Fürstner, A. (2000) Angew. Chem., Int. Edit. 39:3012; (b) Maier, M. E. (2000) Angew. Chem., Int. Edit. 39:2073.

For a review on olefin cross-metathesis reactions, see: Connon S.J., Blechert S. (2003) Angew. Chem. Int. Edit. 42:1900.

For review on enyne metathesis, see: (a) Diver ST., Giessert AJ. (2004) Chem. Rev. 104:1317; (b) Poulsen C. S., Madsen R. (2003) Synthesis 1:1.

For a review on olefin metathesis in total synthesis, see: Nicolaou K.C., Bulger P.G., Sarlah D. (2005) Angew. Chem. Int. Edit. 44:4490.

[7] For a review on olefin metathesis polymerisation, see: Buchmeiser M.R. (2000) Chem. Rev. 100:1565. For a review on ADMET polymerisation, see: Schwendeman J.E., Church A.C., Wagener K.B. (2002) Adv. Synth. Catal. 344:597.

[8] (a) Hoveyda A.H., Schrock R.R. (2001) Chem. Eur. J. 7:945; (b) Schrock R.R., Hoveyda A.H. (2003) Angew. Chem. Int. Edit. 42:4592; (c) Lee A-L., Malcolmson S.J., Puglis A., Schrock R.R., Hoveyda A.H. (2006) J. Am. Chem. Soc. 128:5153; (d) Funk T.W., Berlin J.M., Grubbs R.H. (2006) J. Am. Chem. Soc. 128:1840.

[9] Schwab P., France M.B., Ziller J.W., Grubbs R.H. (1995) Angew. Chem. Int. Edit. 34:2039.

[10] (a) Huang J., Nolan S.P., Petersen J.L. (1999) J. Am. Chem. Soc. 121:2674; (b) Scholl M., Trnka T.M., Morgan J.P., Grubbs R.H. (1999) Tetrahedron Lett. 40:2247; (c) Weskamp T., Kohl F.J., Hieringer W., Gleich D., Herrmann

W.A. (1999) Angew. Chem., Int. Edit. 38:2416; (d) Scholl M., Ding S., Lee C.W., Grubbs R.H. (1999) Org. Lett. 1:953.

[11] (a) Harrity J.P.A., La D.S., Cefalo D.R., Visser M.S., Hoveyda A.H. (1998) J. Am. Chem. Soc. 120:2343; (b) Kingsbury J.S., Harrity J.P.A., Bonitatebus P.J., Hoveyda A.H. (1999) J. Am. Chem. Soc. 121:791; (c) Kingsbury J.S., Hoveyda A.H. (2005) J. Am. Chem. Soc. 127:4510.

[12] (a) Garber S.B., Kingsbury J.S., Gray B.L., Hoveyda A.H. (2000) J. Am. Chem. Soc. 122:8168; (b) Gessler S., Randl S., Blechert S. (2000) Tetrahedron Lett. 41:9973.

[13] (a) Fürstner A., Picquet M., Bruneau C., Dixneuf P.H. (1998) Chem. Commun. 1315; (b) Picquet M., Bruneau C., Dixneuf P.H. (1998) Chem. Commun. 2249; (c) Fürstner A., Liebl M., Lehmann C.W., Piquet M., Kunz R., Bruneau C., Touchard D., Dixneuf P. (2000) Chem. Eur. J. 6:1847; (d) Castarlenas R., Fischmeister C. Bruneau C. Dixneuf P.H. (2004) J. Mol. Catal A: Chem. 213:31.

[14] (a) Castarlenas R., Dixneuf P. (2003) Angew. Chem. Int. Edit. 42:4524; (b) Castarlenas R., Vovard C., Fischmeister C., Dixneuf P. (2006) J. Am. Chem. Soc. 128:4079.

[15] Michrowska A., Gulaski L., Grela K. (2006) Chem. Commun. 841.

[16] Michrowska A., Gulaski L., Kaczmarska Z., Mennecke K., Kirschning A., Grela K. (2006) Green Chem. 8:685.

[17] Conrad J.C., Parnas H.H., Snelgrove J.L., Fogg D.E. (2005) J. Am. Chem. Soc. 127:11882.

[18] (a) Paquette L.A., Schloss J.D., Efremov I., Fabris F., Gallou F., Méndez-Andino J., Yang F. (2000) Org. Lett. 2:1259; (b) Ahn Y.M., Yang K.L., Georg G.I. (2001) Org. Lett. 3:1411.

[19] Cho J.H., Kim M. (2003) Org. Lett. 5:531.

[20] (a) McEleney K., Allen D.P., Holliday A.E., Crudden C.M. (2006) Org. Lett. 8:2663; (b) Westhus M., Gonthier E., Brohm D., Breinbauer R. (2004) Tetrahedron Lett. 45:3141; (c) Maynard H.D., Grubbs R.H., (1999) Tetrahedron Lett. 40:4137.

[21] (a) Buchmeiser M.R. (2004) New J. Chem. 28:549; (b) Elias X., Pleixats R., Wong Chi Man M., Moreau J.J.E. (2006) Adv. Synth. Catal. 348:751; (b) Mennecke K., Grela K., Kunz U., Kirschning A. (2006) Synthesis 19:2498; (c) Fischer D., Blechert S. (2005) Adv. Synth. Catal. 347:1329.

[22] (a) Cornils B., Herrmann W.A., Horvath I.T., Leitner W., Mecking S., Olivier-Bourbigou H., Vogt D. (eds) (2005) Multiphase Homogeneous Catalysis, 1st edn, Wiley-VCH, Weinheim; (b) Andrade C.K.Z., Alves L.M. (2005) Curr. Org. Chem., 9:195.

[23] (a) Hong S.H., Grubbs R.H. (2006) J. Am. Chem. Soc., 128:3508; (b) Saoud M., Romerosa A., Perruzini M. (2000) Organometallics, 19:4005.

[24] (a) Fürstner A., Ackerman L., Beck K., Hori H., Koch D., Langeman K., Liebl M., Six C., Leitner W., (2001) J. Am. Chem. Soc. 123:9000; (b) Leitner W. (2004) Pure Appl. Chem. 76:635; (c) Jessop P.G., Ikariya T., Noyori R. (1999) Chem. Rev. 99:475.

[25] (a) Correa da Costa R., Gladysz J.A. (2006) Chem. Commun. 2619; (b) Matsugi M., Curran D.P., (2005) J. Org. Chem. 70:1636; (c) Yao Q., Zhang

Y. (2004) J. Am. Chem. Soc. 126:75; (d) Horvath I.T., Rabai J., (1994) Science 266:72; (e) Horvath I.T. (1998) Acc. Chem. Res. 31:641.

[26] (a) Wasserscheid P. Welton T. (eds) (2007) Ionic Liquids in Synthesis, 2nd edn, Wiley-VCH, Weinheim; (b) Earle M.J., Seddon K.R. (2000) Pure Appl. Chem. 72:1391; (c) Davis. JH. Jr., Fox PA. (2003) Chem. Commun. 1209; (d) Ludwig R. (2006) Chem. Phys. Chem. 7:1415.

[27] Ionic liquids are almost always reported as non-flammable compounds. A series of flammable ILs has recently been reported: Smiglak M., Reichert W.M., Holbrey J.D., Wilkes J.S., Sun L., Trasher J.S., Kirichenko K., Singh S., Katrizky A.R., Rogers R.D., (2006) Chem. Commun. 2554.

[28] (a) Couling D.J., Berrot R.J., Docherty K.M., Dixon J.N.K., Maginn E.J. (2006) Green Chem. 8:82; (b) Stotle L., Arning J., Bottin-Weber U., Matzke M., Stock F., Thiele K., Uerdingen M., Welz-Biermann U., Jasturff B., Ranke J. (2006) Green Chem. 8:621; (c) Pretti C., Chiappe C., Pieraccini D., Gregori M., Abramo F., Monni G., Intorre L. (2006) Green Chem. 8:238; (d) Ciniecka-Roslonkiewicz A., Pernak J., Kubis-Feder J., Ramani A., Robertson A.J., Seddon K.J., (2005) 7:855; (e) Swatlowski R.P., Holbrey J.D., Memonm S.B., Caldwell G.A., Caldwell K.A., Rogers R.D. (2004) Chem. Commun. 668; (f) Garcia M.T., Gatherhood N., Scammels P.J. (2005) Green. Chem. 7:9.

[29] (a) Welton T. (2004) Coord. Chem. Rev. 248:2459; (b) Dupont J., de Souza R.F., Suarez P.A.Z. (2002) Chem. Rev. 102:3667; (c) Olivier-Bourbigou H., Magna L. (2002) J. Mol. Catal. A:Chem. 182:419; (d) Zhao D, Wu M., Kou Y., Min E. (2002) Catal. Today 74:157; (e) Sheldon R. (2001) Chem. Commun. 2399; (f) Wasserscheid P., Keim W. (2000) Angew. Chem. Int. Edit. 39:3772; (g) Welton T. (1999) Chem. Rev. 99:2071.

[30] Chauvin Y., Olivier-Bourbigou H. (1995) Chemtech. 9:26.

[31] Gürtler C., Jautelat M. (2000) EP 1035093 A2.

[32] Buijsman RC., van Vuuren E., Sterrenburg J.G. (2001) Org. Lett. 3:3785.

[33] Mayo K.G., Nearhoof E.H., Kiddle J.J. (2002) Org. Lett. 4:2002.

[34] Ding X., Lv X., Hui B., Chen Z., Xiao M., Guo. B., Tang W. (2006) Tetrahedron Lett. 47:2921.

[35] Williams D.B.G., Ajam M., Ranwell A. (2006) Organometallics 25:3088.

[36] Sémeril D., Olivier-Bourbigou H., Bruneau C., Dixneuf P.H. (2002) Chem. Commun. 146.

[37] Csihony S.z., Fischmeister C., Bruneau C., Horváth I.T., Dixneuf P.H. (2002) New J. Chem. 26:1667.

[38] Audic N., Clavier H., Mauduit M., Guillemin J.C. (2003) J. Am. Chem. Soc. 125:9248.

[39] (a) Clavier H., Audic N., Mauduit M., Guillemin J.C. (2004) Chem. Commun. 2282; (b) Clavier H., Audic N., Guillemin J.C., Mauduit M. (2005) J. Organomet. Chem. 690:3585.

[40] Yao Q., Zhang Y. (2003) Angew. Chem. Int. Edit. 42:3395.

[41] Yao Q., Sheets M. (2005) J. Organomet. Chem. 690:3577.

[42] Thurier C., (2004) Ph.D. thesis, University Rennes 1

[43] Wakamatsu H., Blechert S. (2002) Angew. Chem. Int. Edit. 41:2403.

SUBJECT INDEX